The Molecular Mechanism of Progesterone Receptor in Regulating Gene Expression in Mouse Granulosa Cells during Ovulation

Doan Thao Dinh

Robinson Research Institute, Research Centre for Reproductive Health,
Discipline of Obstetrics and Gynaecology, Adelaide Medical School,
Faculty of Health Sciences, University of Adelaide, Australia

A thesis submitted to the University of Adelaide in fulfilment of the requirements for admission to the degree of Doctor of Philosophy

February 2020

Abstract

The process of ovulation is critical for successful fertilisation and pregnancy. Of utmost importance is the progesterone receptor (PGR), which regulates various biological processes preceding pregnancy including ovulation, oviductal oocyte/embryo transportation and embryo implantation. How PGR can achieve divergent reproductive roles is still poorly understood. This thesis aims to explore the molecular mechanisms that allow for highly specialised PGR ovulatory functions through describing the PGR cistrome and transcriptome in mouse peri-ovulatory granulosa cells when PGR is highly induced and active. In addition, the relationship between PGR and other transcription factors, especially RUNX1, as well as isoform-specific actions were also determined.

As PGR acts through direct binding to the PGR response element (PRE), differences in PGR chromatin targets can influence PGR actions. Characterisation of the PGR cistrome using chromatin immunoprecipitation – sequencing (ChIP-seq) showed striking distinctions in preferential PGR targets in peri-ovulatory granulosa cells compared to the uterus. Granulosa PGR favourably interacted with transcriptionally active promoters and had few mutual chromatin targets with uterine PGR. Interestingly, motif analysis of PGR peaks identified specific patterns in the degree of PRE occupancy and the enrichment of distinct non-canonical motifs, suggesting that PGR interacts with other transcription factors in a context-specific manner.

Motif analysis of PGR peaks in granulosa cells implied a number of potential protein partners such as the JUN/FOS, LRH1, and RUNX families. The physical interaction of these proteins with PGR in mouse peri-ovulatory granulosa cells was confirmed through proximity ligation assay. Among these, RUNX was a granulosa-specific factor and thus potentially important in granulosa-specific PGR roles. RUNX1 displayed context-specific chromatin binding properties as shown through RUNX1 ChIP-seq of mouse foetal and adult granulosa cells before and after the LH surge. In peri-ovulatory granulosa cells, PGR/RUNX1 interaction was specifically hCG-induced, RUNX1 shared mutual targets and non-canonical binding motifs with PGR that resulted in the regulation of mutual ovulatory genes. This indicates a close

interplay between PGR and RUNX1 in granulosa cells during ovulation, likely in conjunction with other modulators.

The PGR-A and PGR-B isoforms play distinct roles in different biological contexts, with PGR-A being prominent in peri-ovulatory granulosa cells. To further assess the specific roles of PGR-A and PGR-B during ovulation, transcriptomes of peri-ovulatory granulosa cells from mice lacking both isoforms (PGRKO), PGR-A (AKO) or PGR-B (BKO) were obtained through RNA-seq. More than 600 differentially expressed genes were identified in PGRKO and AKO with few identified in BKO. Mutual PGR/RUNX1 direct binding was important in the regulation of these genes. PGRKO and AKO transcriptomes shared nearly half of their genes with little similarities with the BKO transcriptome. The transcriptomic data supports the key physiological roles of PGR-A in ovulation.

Altogether, this study provides the first description of the PGR cistrome, interactome and transcriptome in granulosa cells. A unique cooperation between PGR, especially PGR-A, and specific transcription factors, especially RUNX1, in a mutual transcription complex leads to the specification of PGR ovulatory action in granulosa cells. Such understanding in tissue-specific PGR actions is crucial for the development of novel contraceptives targeting ovulation.

Declaration

I certify that this work contains no material which has been accepted for the award of any other degree or diploma in my name, in any university or other tertiary institution and, to the best of my knowledge and belief, contains no material previously published or written by another person, except where due reference has been made in the text. In addition, I certify that no part of this work will, in the future, be used in a submission in my name, for any other degree or diploma in any university or other tertiary institution without the prior approval of the University of Adelaide and where applicable, any partner institution responsible for the joint-award of this degree.

I acknowledge that copyright of published works contained within this thesis resides with the copyright holder(s) of those works.

I also give permission for the digital version of my thesis to be made available on the web, via the University's digital research repository, the Library Search.

Doan Thao Dinh

February 2020

Acknowledgements

I would like to sincerely thank my panel of supervisors, Professor Darryl Russell, Professor Rebecca Robker and Dr James Breen for giving me the opportunity to undertake this PhD project. Darryl, thank you for giving me the opportunity to work in such an exciting field, for your constant guidance and unwavering support throughout the years and for having more faith in me than I do myself sometimes. For these, I cannot thank you enough. To Becky, thank you for reminding me the importance of what I am doing when I lose my head in the maze of biology, for your boundless support, guidance, encouragement and feedback. To Jimmy, thank you for introducing and guiding me to the scary and fascinating world of bioinformatics, for your support and for sparkling new ideas. Thank you all for the many exciting opportunities to really push myself and learn how to be resilient in the face of difficulties. And thanks to Dr Hannah Brown for introducing me to the Robinson Research Institute and the opportunities to take part in the exciting researches conducted here, thank you for your enthusiasm and constant support throughout my early career.

I would like to acknowledge the support of the University of Adelaide and the National Health and Medical Research Council for my scholarship and for grant funding. I would also like to thank the University of Adelaide Graduate Centre, the Robinson Research Institute, the Endocrine Society and the Society for Reproductive Biology for opportunities to present my work interstate and internationally. Thank you to the staff at the School of Medicine, the Robinson Research Institute, the Laboratory Animal Service and Adelaide Microscopy for your resources and assistance throughout my studies.

Thank you Alka for your support and guidance, for challenging my ways of thinking and for your kind friendship. To Sonja, Laura and Macarena, thank you for all your help in the lab, your critical comments and discussions. To Franco, Humphrey, Barbara and Karina, thank you for the collaboration opportunities and for sharing your fascinating works. Many thanks to present and past members of the Russell/Robker research groups, Adrian, Atsushi, Carl, Catherine, David, Eryk, Haley, Minnu, Takashi, Tasman, Tim and Yasmyn, for being a constant source of inspiration and for your support. Thank you Monica, Nicole, Qianhui, Tiffany, Megan and Darren for your friendship and encouragement throughout the years.

To my best friends Nhu, Tuan, Anh Vu and Mai, thank you for staying by my side through thick and thin, even though there is usually an ocean keeping us apart. Thank you Noko, Tsuki, Susan, Dung, Giang, Susan, Helen, Tracy and Eric for being a dear friend and for your support through good and bad times. To other volunteers at the Adelaide Visitor Information Centre, thank you for your kind words and support. More than anyone, I would like to thank all of my family members for their endless encouragement, especially my parents. It would be impossible for me to be where I am today without your love, support, encouragement and understanding. Thank you to my sister Lan, her husband Binh and my niece Duong for their constant support and for being there for our family in my absence. To dear Sammy, thank you for being with me since I was twelve and you have never failed to cheer me up even in the darkest of times. Thank you all!

Publications arising during PhD candidature

Dinh, D.T., Breen, J., Akison, L.K. *et al.* Tissue-specific progesterone receptor-chromatin binding and the regulation of progesterone-dependent gene expression. *Sci Rep* **9,** 11966 (2019). https://doi.org/10.1038/s41598-019-48333-8

Abstracts arising from this thesis

2019

Dinh, D.T., Breen, J., Akison, L.K., DeMayo, F.J., Brown, H.M., Robker, R.L., Russell, D.L., Context is all - Progesterone receptor-chromatin binding properties and implications on tissue-specific gene expression in mouse reproductive tissues, Lorne Genome 2019, Lorne, Australia **(poster)**

Dinh, D.T., Breen, J., Akison, L.K., DeMayo, F.J., Brown, H.M., Robker, R.L., Russell, D.L., Context-Specific Chromatin Binding Properties of Progesterone Receptor and Consequential Effects on Gene Expression in Mouse Reproductive Tissues, ENDO 2019, Endocrine Society, New Orleans, USA **(oral)**

Outstanding Abstract award

Dinh, D.T., Nicol, B., Rodriguez, K., Breen, J., Robker, R.L., Yao, H.H, Russell, D.L., RUNX1 as a potential co-regulator of progesterone receptor in mouse peri-ovulatory granulosa cells, The Australian Society for Medical Research (ASMR) Conference 2019, Adelaide, Australia **(oral)**

Dinh, D.T., Nicol, B., Rodriguez, K., Breen, J., Robker, R.L., Yao, H.H, Russell, D.L., RUNX1 as a potential co-regulator of progesterone receptor in mouse peri-ovulatory granulosa cells, The Endocrine Society of Australia - Society for Reproductive Biology - Asia & Oceania Thyroid Association (ESA-SRB-AOTA) 2019, Sydney, Australia **(oral)**

Dinh, D.T., Nicol, B., Rodriguez, K., Breen, J., Robker, R.L., Yao, H.H, Russell, D.L., RUNX1 as a tissue-specific coregulator of progesterone receptor action in ovulation, Annual Florey Postgraduate Conference 2019, Adelaide, Australia **(poster)**

Adelaide Medical School prize

Dinh, D.T., Nicol, B., Rodriguez, K., Breen, J., Robker, R.L., Yao, H.H, Russell, D.L., RUNX1 as a tissue-specific coregulator of progesterone receptor action in ovulation, Robinson Research Institute (RRI) Symposium 2019, Adelaide, Australia **(poster)**

Best Student Poster award

2018

Dinh, D.T., Breen, J., Akison, L.K., DeMayo, F.J., Brown, H.M., Robker, R.L., Russell, D.L., Context is all – Progesterone receptor-chromatin binding properties and tissue-specific gene expression in mouse reproductive tissues, The Endocrine Society of Australia - Society for Reproductive Biology (ESA-SRB) 2018, Adelaide, Australia **(poster)**

Dinh, D.T., Breen, J., Akison, L.K., DeMayo, F.J., Brown, H.M., Robker, R.L., Russell, D.L., Context is all – Progesterone receptor-chromatin binding properties and tissue-specific gene expression in mouse reproductive tissues, The Australian Society for Medical Research (ASMR) Conference 2018, Adelaide, Australia **(oral)**

Dinh, D.T., Breen, J., Akison, L.K., DeMayo, F.J., Brown, H.M., Robker, R.L., Russell, D.L., Context is all – Progesterone receptor-chromatin binding properties and tissue-specific gene expression in mouse reproductive tissues, Annual Florey Postgraduate Conference 2019, Adelaide, Australia **(poster)**

Table of contents

Abstract II
Declaration IV
Acknowledgements V
Publications arising during PhD candidature VII
Abstracts arising from this thesis VIII
Table of contents X
List of figures XVI
List of tables XVIII
List of appendices XIX
Abbreviations XX
CHAPTER 1 Literature review 1
1.1 THE OVARY 1
1.1.1 The oocyte 3
1.1.2 Somatic cells 3
1.1.3 The oestrous cycle 5
1.2 OVULATION 6
1.2.1 Molecular regulation of ovulation 6
1.2.1.1 The LH-induced signalling cascade 6
1.2.1.2 Key master transcription factors 7
(a) CREB 7
(b) CEBPβ 8
(c) CBP/p300-CITED4 9
1.2.1.3 The role of non-coding RNA 12
1.2.2 Physiological aspects of ovulation 13
1.2.2.1 COC expansion and oocyte functions 13
1.2.2.2 Tissue remodelling 15
1.2.2.3 Vasoconstriction and muscular contraction 16
1.2.3 Dysregulation of ovulation and targets for contraception 17
1.3 PROGESTERONE RECEPTOR 18
1.3.1 PGR structure 18
1.3.2 PGR functions in the ovary 22

1.3.2.1 Studies on PGRKO mouse model 22
1.3.2.2 Target genes of PGR in ovulation 23
1.3.2.3 Isoform-specific roles of PGR in ovulation 24
1.3.3 PGR functions in the oviduct 24
1.3.4 PGR functions in the uterus 25
1.3.5 PGR functions in mammary tissues and other reproductive functions 27
1.3.6 PGR functions in other tissues and non-reproductive cancer 28
1.3.7 Molecular mechanism of PGR action 30
1.3.7.1 Ligand-dependent and -independent molecular mechanisms 30
1.3.7.2 Regulation of PGR isoforms 32
1.3.7.3 Co-regulators of PGR 32
(a) SRC 33
(b) c-SRC 34
(c) *Sra1* 35
(d) JUN/FOS 36
(e) SP1/SP3 38
1.3.7.4 PGR action at enhancers 43
1.4 RUNX TRANSCRIPTION FACTOR 43
1.4.1 Structure of RUNX proteins 43
1.4.2 RUNX functions in the ovary 46
1.4.2.1 RUNX1 46
1.4.2.2 RUNX2 46
1.4.2.3 RUNX3 47
1.4.2.4 CBFβ 48
1.4.3 RUNX functions in other reproductive tissues 49
1.4.4 Molecular mechanisms of RUNX 50
1.4.4.1 Transcriptional co-regulators of RUNX 50
1.4.4.2 RUNX action on enhancers 52
1.5 HYPOTHESIS & AIMS 53
1.5.1 Main hypothesis 53
1.5.2 Specific hypotheses and aims 54
1.6 REFERENCES 57
CHAPTER 2 PGR interacts with transcriptionally active chromatin to regulate target gene expression during ovulation 82
2.1 INTRODUCTION 82

2.2 MATERIALS & METHODS....84
2.2.1 Animals....84
2.2.2 Peri-ovulatory time course experiment....84
2.2.2.1 Time course sample collection....84
2.2.2.2 mRNA level quantification....85
2.2.2.3 Protein level quantification....86
2.2.3 ChIP-seq....86
2.2.3.1 Experiment....86
2.2.3.2 Bioinformatics analysis....87
2.2.4 ChIP-qPCR....91
2.2.5 Microarray data....92
2.3 RESULTS....92
2.3.1 The expression of PGR in peri-ovulatory granulosa cells....92
2.3.2 PGR-dependent transcriptome in peri-ovulatory granulosa cells....94
2.3.3 Characteristics of PGR chromatin-binding properties in peri-ovulatory granulosa cells....96
2.3.3.1 Quality control of PGR ChIP-seq....96
2.3.3.2 Assessing robustness and selection of consensus PGR binding sites....96
2.3.3.1 PGR preference for transcriptionally active promoters in granulosa cells....99
2.3.3.2 Functional consequences of the PGR cistrome....102
2.3.3.3 PGR interacts with PRE as well as non-canonical chromatin motifs....104
2.4 DISCUSSION....109
2.5 REFERENCES....112
CHAPTER 3 Tissue-specific PGR cistromes and consequences on PGR-regulated transcriptomes in the reproductive tract....116
3.1 INTRODUCTION....116
3.2 MATERIALS & METHODS....118
3.2.1 Animals....118
3.2.2 ChIP-seq....118
3.2.2.1 Experiment....118
3.2.2.2 Bioinformatics analysis....119
3.2.3 Microarray analysis....119
3.3 RESULTS....119
3.3.1 PGR regulates specific transcriptomes in granulosa cells, oviduct and uterus 119
3.3.2 Characteristics of PGR chromatin-binding properties in progesterone-responsive uterus....125

3.3.3 Distinctions between PGR cistrome in granulosa cells vs uterus 131
3.4 DISCUSSION 137
3.5 REFERENCES 140
CHAPTER 4 Potential co-regulators of PGR in granulosa cells 142
4.1 INTRODUCTION 142
4.2 MATERIALS & METHODS 145
4.2.1 Animals 145
4.2.2 Tissue collection 145
4.2.3 Granulosa cell culture and treatment 145
4.2.4 Cell line culture and treatment 146
4.2.5 Immunofluorescence 146
4.2.5.1 Tissue sections 146
4.2.5.2 Cell cultures 147
4.2.6 Proximity Ligation Assay 147
4.2.7 RNA co-immunoprecipitation 148
4.3 RESULTS 149
4.3.1 Expression of PGR and other transcription factors in peri-ovulatory follicles 149
4.3.2 Validation of the PLA methodology in tissues and cell culture 152
4.3.3 Interaction of PGR and co-partners in peri-ovulatory granulosa cells 154
4.3.4 Interaction of PGR and non-coding RNA in peri-ovulatory granulosa cells ... 160
4.4 DISCUSSION 164
4.5 REFERENCES 168
CHAPTER 5 RUNX1 chromatin interaction in granulosa cells specialisation and regulation of follicle functions during pre- and peri-ovulation 172
5.1 INTRODUCTION 172
5.2 MATERIALS & METHODS 174
5.2.1 Animals 174
5.2.2 Peri-ovulatory time course experiment 175
5.2.2.1 mRNA level quantification 175
5.2.2.2 Protein level quantification 175
5.2.3 ChIP-seq experiments 175
5.2.3.1 Adult mouse granulosa cell collection 175
5.2.3.2 Foetal granulosa cells 176
5.2.3.3 Bioinformatics analysis 176
5.3 RESULTS 177

5.3.1 RUNX transcription factors are induced in granulosa cells during ovulation . 177
5.3.2 Characteristics of RUNX1 cistromes in granulosa cells in different developmental contexts 181
5.3.2.1 Assessing robustness and selection of consensus RUNX1 binding sites 181
5.3.2.2 Mutual and context-specific RUNX1 binding sites in granulosa cells 182
5.3.2.3 RUNX1 regulates different pathways in a context-specific manner 185
5.3.2.4 RUNX1 binds to different motifs in foetal and adult granulosa cells 189
5.3.3 Distinct RUNX1 cistromes in granulosa cells in response to the LH surge 191
5.3.3.1 RUNX1 preferably binds transcriptionally active promoters before and after the LH surge 191
5.3.3.2 RUNX1 interacts with RUNT as well as non-canonical sequence motifs ... 194
5.4 DISCUSSION 196
5.5 REFERENCES 201
CHAPTER 6 The functional and physical interaction between PGR and RUNX1 in ovulatory gene regulation 204
6.1 INTRODUCTION 204
6.2 MATERIALS & METHODS 206
6.2.1 Animals 206
6.2.2 ChIP-seq experiments 206
6.2.3 Proximity ligation assay 206
6.3 RESULTS 207
6.3.1 Interaction between RUNX1 and the PGR transcription machinery on a chromatin level 207
6.3.1.1 RUNX1 shares occupancy of promoters with PGR 207
6.3.1.2 RUNX1 and PGR functional similarities in peri-ovulatory granulosa cells 212
6.3.2 The physical interaction between RUNX1 and PGR is highly dynamic in the peri-ovulatory window 215
6.4 DISCUSSION 218
6.5 REFERENCES 222
CHAPTER 7 PGR regulates isoform-specific transcriptomes in granulosa cells 225
7.1 INTRODUCTION 225
7.2 MATERIALS & METHODS 227
7.2.1 Animals and breeding strategy 227
7.2.2 Genotyping of PGRKO mouse strains 229
7.2.2.1 PGRKO genotyping 229
7.2.2.2 AKO genotyping 230

7.2.2.3 BKO strain....230
7.2.3 Western blot....233
7.2.4 RNA-sequencing....233
7.2.4.1 Tissue sample collection and RNA extraction....233
7.2.4.2 Sequencing....233
7.2.4.3 Bioinformatics analysis....233
7.3 RESULTS....236
7.3.1 PGR protein expression in PGRKO, AKO and BKO ovaries....236
7.3.2 PGR isoform-specific transcriptomes....238
7.3.2.1 Granulosa cell gene expression changes in PGRKO mice....238
7.3.2.2 Granulosa cell gene expression changes in AKO mice....241
7.3.2.3 Granulosa cell gene expression changes in BKO mice....244
7.3.2.4 Unique patterns of gene regulation that are isoform-specific....247
7.3.3 Combined analysis of transcriptomes regulated by ovulatory stimulus, PGR-regulated transcriptomes and PGR bound cistromes....253
7.4 DISCUSSION....256
7.5 REFERENCES....261
CHAPTER 8 Conclusions & future directions....265
8.1 INTRODUCTION....265
8.2 MAIN FINDINGS....267
8.2.1 PGR binds chromatin and regulates downstream gene expression in a tissue-specific manner....267
8.2.2 PGR interacts with a selective group of co-regulators in peri-ovulatory granulosa cells especially RUNX1....268
8.2.3 PGR-A and PGR-B regulate different transcriptomes in granulosa cells....269
8.2.4 Overall conclusion of thesis....270
8.3 REMAINING QUESTIONS & FUTURE STUDIES....272
8.4 SIGNIFICANCE OF THIS STUDY....276
8.5 REFERENCES....278
APPENDIX....282

List of figures

Figure 1.1 Ovarian structure and the hypothalamic-pituitary-ovarian axis. 2
Figure 1.2 Molecular pathways in the peri-ovulatory follicle before and after the LH surge. 11
Figure 1.3 Structure of the PGR protein. 21
Figure 1.4 Ligand-dependent molecular pathway of PGR. 31
Figure 1.5 Structure of RUNX proteins. 45
Figure 2.1 Bioinformatics workflow for the analysis of ChP-seq data. 88
Figure 2.2 PGR mRNA and protein are induced by the LH surge in granulosa cells. 93
Figure 2.3 PGR-dependent differentially expressed genes in PGRKO vs PGR+/- peri-ovulatory granulosa cells. 95
Figure 2.4 Validation of PGR ChIP-seq through ChIP-qPCR. 98
Figure 2.5 PGR associates with transcriptionally active promoters in granulosa cells. 101
Figure 2.6 Consequence of PGR binding on PGR-dependent gene expression and peri-ovulatory transcriptome. 103
Figure 2.7 PGR binding properties to the canonical PRE motif in granulosa cells. 105
Figure 2.8 Properties of PGR-binding motifs in granulosa cells. 108
Figure 3.1 Differences in PGR-regulated transcriptome in granulosa cells, oviduct and uterus. 122
Figure 3.2 Canonical pathway analysis of DEG in the uterus, oviduct and granulosa cells. 124
Figure 3.3 Correlation between PGR binding sites in uteri treated with P4 or vehicle control. 127
Figure 3.4 Properties of PGR-binding motifs the uterus. 130
Figure 3.5 Correlation between PGR binding sites in granulosa cells vs uterus. 133
Figure 3.6 Functional consequence of PGR cistrome in uterus and granulosa cells. 134
Figure 3.7 Properties of PGR-binding sequences in tissue-specific binding sites. 136
Figure 4.1 Immunofluorescent detection of PGR and transcription markers in ovarian sections. 150
Figure 4.2 Immunofluorescent detection CBFβ, RUNX1 and RUNX2 in ovarian sections. 151
Figure 4.3 Dynamics of PGR/H3K27ac interaction in R5020-treated T47D cells. 153
Figure 4.4 Proximity ligation assay in ovarian sections. 155
Figure 4.5 Immunofluorescent detection of PGR and associated transcriptional markers in cultured granulosa cells treated with hCG and R5020. 156
Figure 4.6 Interaction between PGR and RUNX members in granulosa cells treated with hCG and R5020. 157

Figure 4.7 Interaction between PGR and bZIP (JUN/FOS) members and LRH1 in granulosa cells treated with hCG and R5020. 159
Figure 4.8 The expression of non-coding RNA and in peri-ovulatory granulosa cells. 162
Figure 4.9 Interaction between PGR and RNA partners in granulosa cells. 163
Figure 5.1 RUNX / CBFβ mRNA and protein are induced by the LH surge in granulosa cells. 180
Figure 5.2 Correlation between RUNX1 binding sites in different biological contexts 184
Figure 5.3 Gene categories associated with RUNX1 binding throughout ovarian folliculogenesis. 188
Figure 5.4 Identity of context-specific RUNX1-binding motifs. 190
Figure 5.5 LH-dependent RUNX1 chromatin binding properties. 193
Figure 5.6 Changing identity of RUNX1 binding motifs in response to LH ovulatory signal. 195
Figure 6.1 PGR and RUNX1 shared mutual chromatin targets in peri-ovulatory granulosa cells. 208
Figure 6.2 Transcription factor-specific chromatin binding properties of PGR and RUNX1 cistrome. 211
Figure 6.3 Consequences of RUNX1 binding on gene expression. 214
Figure 6.4 LH-dependent dynamic PGR / RUNX interactions in response to ovulatory stimulus. 217
Figure 7.1 Strategies for KO generation. 232
Figure 7.2 Bioinformatics workflow for RNA-seq analysis. 235
Figure 7.3 Expression of PGR-A and PGR-B proteins in granulosa cells of animals from each strain. 237
Figure 7.4 Genes differentially regulated in the absence of both PGR isoforms in ovulatory granulosa cells. 240
Figure 7.5 Genes differentially regulated in the absence of PGR-A in ovulatory granulosa cells. 243
Figure 7.6 Genes differentially regulated in the absence of PGR-B in ovulatory granulosa cells. 246
Figure 7.7 Correlation between PGR isoform-specific transcriptomes. 249
Figure 7.8 Isoform-specific transcriptome in relation to ovulatory genes and ovulatory transcription factors. 255
Figure 8.1 Summary of the thesis. 266
Figure 8.2 Schematic conclusion to the thesis, in regards to specialised PGR action in the ovary and the female reproductive tract. 271

List of tables

Table 1.1 List of transcription regulators that form protein-protein interaction with PGR.....40

Table 2.1 Mouse allocation per stimulation time point for the time course experiment. 85

Table 2.2 Tools used for bioinformatics analysis of ChIP-seq data 89

Table 2.3 Position weight matrix for the PRE/NR3C motif from HOMER Motif Database that was used for the identification of the motif map. 90

Table 5.1 Position weight matrix for the RUNT motif HOMER Motif Database that was used for the identification of the motif map. 177

Table 7.1 Tools used for bioinformatics analysis of RNA-seq data. 236

Table 7.2 Upstream regulators of PGRKO / AKO / BKO DEGs. 251

List of appendices

Appendix 1 List of primers used for qPCR, ChIP-qPCR and RIP-qPCR. 282

Appendix 2 List of primary and secondary antibodies used in Western blot. 283

Appendix 3 List of antibodies used in ChIP and RIP. 283

Appendix 4 Summary of ChIP-seq datasets, including library size, sequence length, alignment stats and peak counts 284

Appendix 5 List of differentially expressed genes in PGRKO vs PGR+/- granulosa cells identified through microarray. 285

Appendix 6 Reproducibility and correlation of PGR ChIP-seq replicates. 286

Appendix 7 List of differentially expressed genes in 8h vs 0h post-hCG granulosa cells identified through RNA-seq. 288

Appendix 8 List of differentially expressed genes in PGRKO vs PGR+/- oviduct identified through microarray 315

Appendix 9 List of differentially expressed genes in PGRKO vs PGR+/+ uterus identified through microarray 316

Appendix 10 List of antibodies used for immunofluorescence and PLA 317

Appendix 11 RUNX1 ChIP-seq reproducibility and correlation of biological replicates for RUNX1 0h, RUNX1 6h and RUNX1 E14.5. 318

Appendix 12 Summary of RNA-seq-seq datasets, including library size, sequence length, alignment stats, gene count and DEG count 320

Appendix 13 List of differentially expressed genes identified in RNA-seq PGRKO vs WT granulosa cells identified through RNA-seq. 322

Appendix 14 List of differentially expressed genes identified in RNA-seq AKO vs WT granulosa cells identified through RNA-seq. 329

Appendix 15 List of differentially expressed genes identified in RNA-seq BKO vs WT granulosa cells identified through RNA-seq. 338

Appendix 16 List of PGRKO and AKO DEGs with PGR and/or RUNX1 binding. 340

Abbreviations

Abbreviation	Full term
ABCB1B	ATP-binding Cassette, sub-family B
ABCC4	ATP Binding Cassette Subfamily C Member 4
ABHD2	Abhydrolase Domain-containing protein 2
AD	Activation Domain
ADAM8 / ADAM17	ADAM Metallopeptidase Domain 8 / 17
ADAMTS1	ADAM Metallopeptidase With Thrombospondin Type 1 Motif 1
AF	Transactivation Function
AKO	PGA-A knockout
ALOX12E	Arachidonate 12-Lipoxygenase, Epidermal-type
AP-1	Activator Protein
APLN	Apelin
AR	Androgen Receptor
AREG	Amphiregulin
ATAC-seq	Assay for Transposase-Accessible Chromatin - sequencing
ATGR2	Angiotensin II Receptor Type 2
BHMT	Betaine-Homocysteine S-Methyltransferase
BKO	PGR-B knockout
BMI	Body mass index
BMP15	Bone Morphogenetic Protein 15
bp	base pair
BSA	Bovine serum albumin
BTC	Betacellulin
BTEB1 (KLF9)	Basic Transcription Element-Binding protein 1
bZIP	Basic Leucine Zipper
cAMP	Cyclic Adenosine Monophosphate
CBAF1	CBA x C57BL/6 F1
CBFα / CBFβ	Core Binding Factor α / β
CBP	CREB-Binding Protein
CCND1	Cyclin D1
CD4 / CD28	Cluster of Differentiation 4 / 28
CDK2	Cyclin A / Cyclin-Dependent Kinase-2

CDKN1A	Cyclin Dependent Kinase Inhibitor 1A
CEBPα / CEBPβ	CCAAT-enhancer-binding proteins α / β
c-FOS	Fos Proto-Oncogene, AP-1 Transcription Factor Subunit
CGA	Glycoprotein Hormones, Alpha Polypeptide
cGMP	Cyclic Guanosine Monophosphate
CITED1 / CITED4	Cbp/p300-interacting Transactivator 1 / 4
c-JUN / JUNB / JUND	Jun / JunB / JunD Proto-Oncogene
CLDN11	Claudin 11
COC	Cumulus Oocyte Complex
COL10A1	Collagen Type X Alpha 1 Chain
CP2	Transcription factor CP2
CREB	cAMP Response Element-Binding Protein
CSN2	β Casein
c-SRC	Proto-oncogene tyrosine-protein kinase
CTCF	CCCTC-binding Factor
CTNNB1	Catenin β 1
CTSL	Cathepsin L
CUEDC2	CUE Domain Containing 2
CXCL12	C-X-C motif Chemokine 12
CXCR4	C-X-C Motif Chemokine Receptor 4
CYP11A1	Cytochrome P450 Family 11 Subfamily A Member 1
CYP19	Cytochrome P450 Family 19
DBD	DNA Binding Domain
DEG	Differentially Expressed Gene
DES	Desmin
DICER	Double-stranded RNA (dsRNA) Endoribonuclease
DMRT1	Doublesex And Mab-3 Related Transcription Factor 1
dpc	Days Post Coitum
E6-AP	E6-Associated Protein
eCG	Equine Chorionic Gonadotropin
EDN1 / EDN2 / EDN3	Endothelin 1 / 2 / 3
EFNB2	Ephrin B2
EGF1	Early Growth Response 1
EGF-like	Epidermal Growth Factor-like
EGFR	Epidermal Growth Factor Receptor
EGR1	Early Growth Response 1
eIF4b	Eukaryotic translation Initiation Factor 4B

ERBB2	Erb-B2 Receptor Tyrosine Kinase 2
EREG	Epiregulin
ERK1/2	Serine/threonine Kinase 1 / 2
ER-α (ESR1) / ER-β (ESR2)	Oestrogen Receptor α / β
ETS	E26 Transformation-Specific
F3	Tissue Factor
FABP6	Fatty Acid Binding Protein 6
FAIRE-seq	Formaldehyde-Assisted Isolation of Regulatory Elements - sequencing
FAK/CAS	Focal Adhesion Kinase / Crk-associated Substrate
FGF2	Fibroblast Growth Factor 2
FOXL2	Forkhead Box L2
FOXO1 / FOXO3	Forkhead Box O1 / 3
FRA1 / FRA2	Fos-Related Antigen 1 / 2
FSH	Follicle Stimulating Hormone
FSHB	FSH Subunit B
FSHR	FSH Receptor
GABP	GA-Binding Protein
GAPDH	Glyceraldehyde 3-Phosphate Dehydrogenase
GAS5	Growth Arrest Specific 5
GATA1 / GATA2 / GATA4 / GATA6	GATA Binding Protein 1 / 2 / 4 / 6
GATAD2B	GATA Zinc Finger Domain Containing 2B
GdA	Guanine Deaminase
GDF9	Growth Differentiation Factor 9
GIOT1	Gonadotropin-Inducible Ovary Transcription Repressor 1
GJA1	Gap Junction Alpha-1
GnRH	Gonadotropin-Releasing Hormone
GR	Glucocorticoid Receptor
GREAT	Genomic Regions Enrichment of AnnoTation
GVBD	Germinal Vesicle BreakDown
h	hour
H2A / H3 / H4	Histone 3 / 4
H3K27ac	Histone 3 Lysine 27 Acetylation
HA	Hyaluronan
HAPLN1	Hyaluronan And Proteoglycan Link Protein 1
HAS2	Hyaluronan Synthase 2

HAT	Histone Acetyltransferase
hCG	Human Chorionic Gonadotropin
HDAC	Histone Deacetylase
HIF	Hypoxia-Inducible Factor
HIST1H2AO / HIST1H4M / HIST1H4N	Histone cluster 1, H2ao / H4m / H4n
HMG1	High Mobility Group box 1
hnRNP	Heterogeneous Nuclear Ribonucleoprotein
HOMER	Hypergeometric Optimization of Motif EnRichment
HP1G	Heterochromatin Protein 1 Gamma
HSD2B11	11β-Hydroxysteroid dehydrogenase type-2
HSD3B1	3beta-Hydroxysteroid Dehydrogenase/delta(5)-delta(4)isomerase type I
HSP56 / HSP90	Heat Shock Protein 56 / 90
i.p	intraperitoneally
ID	Inhibitory Domain
IDR	Irreproducibility Discovery Rate
IGFBP3	Insulin Like Growth Factor Binding Protein 3
IHH	Indian Hedgehog
IL6	Interleukin 6
INHBA	Inhibin A
IP	immunoprecipitation
IP3	Inositol triphosphate
IPA	Ingenuity Pathway Analysis
ITGA8	Integrin Subunit Alpha 8
IVF	In vitro Fertilisation
IVM	In Vitro Maturation
IαI	Inter-α-Inhibitor
JAB1	Jun Activation Domain-Binding Protein 1
JDP1 / JDP2	Jun Dimerization Protein 1 / 2
kb	kilobase
KISS1	Kisspeptin 1
KLF	Kruppel Like Factor
KO	Knockout
LBD	Ligand Binding Domain
LH	Luteinising Hormone
LHB	Luteinizing Hormone Subunit Beta
LHCGR (LHR)	Luteinizing Hormone/Choriogonadotropin Receptor

LIF	Leukaemia Inhibitory Factor
lncRNA	long non-coding RNA
LRH1	Liver Receptor Homolog 1
MAPK	Mitogen-Activated Protein Kinase
miRNA	micro RNA
mTOR	Mammalian Target of Rapamycin
MMP	Matrix Metallopeptidase
MR	Mineralocorticoid Receptor
mSIN3A	transcriptional regulator, SIN3A
MT1A / MT2	Metallothionein 1A / 2
MTHFD2	Methylenetetrahydrofolate Dehydrogenase 2
MYB / MYC	MYB / MYC Proto-Oncogene
MYH11	Myosin Heavy Chain 11
MYOCD	Myocardin
ncRNA	non-coding RNA
NEAT1	Nuclear Enriched Abundant Transcript 1
NF-κB	Nuclear Factor Kappa-light-chain-enhancer of activated B cells
NMTS	Nuclear Matrix Targeting Signal
NOTCH2	Notch Receptor 2
NPPC	Natriuretic Peptide C
NR3C3	Nuclear Receptor subfamily 3 group C member 3
NR5A2	Nuclear Receptor Subfamily 5 Group A Member 2
OSP	Osteopontin
OXCT2	3-Oxoacid CoA-Transferase 2
p300	E1A Binding Protein P300
P4	Progesterone
P450ssc	P450 side chain cleavage
p54	Tumour Protein 54
PBS	Phosphate Buffered Saline
PCA	Principal Component Analysis
PCNA	Proliferating Cell Nuclear Antigen
PCOS	Polycystic Ovarian Syndrome
PDE3A	Phosphodiesterase 3A
PER1	Period Circadian Regulator 1
PGC-1α	Peroxisome proliferator-activated receptor Gamma Coactivator 1-alpha
PGE2	Prostaglandin E2

PGR	Progesterone Receptor
PGRKO	total PGR knockout
PI3K/AKT/PKB	Phosphoinositide 3-kinase / Protein Kinase B
PIAS3	Protein Inhibitor Of Activated STAT 3
PKA / PKC	Protein Kinase A / C
PLA	Proximity Ligation Assay
PLC	Phospholipase C
POLL / POLE4	DNA Polymerase Lambda / Epsilon 4
PPARγ	Peroxisome Proliferator Activated Receptor Gamma
PRE / NR3C	Progesterone receptor Response Element
PRLR	Prolactin Receptor
PTGDS	Prostaglandin D2 Synthase
PTGES	Prostaglandin E Synthase
PTGS1 / PTGS2	Prostaglandin-Endoperoxide Synthase 1 / 2
PTX3	Pentraxin 3
RCOR1	REST Corepressor 1
REST	RE1/-Silencing Transcription factor
RGCC	Regulator Of Cell Cycle
RHD	Runt Homolog Domain
RHOX5	Reproductive Homeobox 5
RIP	RNA co-immunoprecipitation
RMST	Rhabdomyosarcoma 2 Associated Transcript
RNY1	Ro60-associated Y1
RUNX	Runt-related transcription factor
SERPINA1	Serpin Family A Member 1
SF-1	Steroidogenic Factor 1
SGK	Serum/Glucocorticoid Regulated Kinase
siRNA	small interfering RNA
SKI	SKI Proto-Oncogene
SLCO2A1	Solute Carrier Organic Anion Transporter Family Member 2A1
SLP	Sex-Limited Protein
SNAI2	Snail Family Transcriptional Repressor 2
SNAP25	Synaptosome Associated Protein 25
snoRNA	Small Nucleolar RNA
snRNA	Small Nuclear RNA
SNRNP70	Small Nuclear Ribonucleoprotein U1 Subunit 70

SOX2 / SOX9 / SOX12	SRY-Box Transcription Factor 2 / 9 / 12
SP1 / SP3	Specificity Protein 1 / 3
SRA1 / SRAP	Steroid receptor RNA Activator 1 (Protein)
SRC1 / SRC2 / SRC3	Steroid Receptor Coactivator 1 / 2 / 3
StAR	Steroidogenic Acute Regulatory Protein
STAT3 / STAT5	Signal Transducer And Activator Of Transcription 3 / 5
SUMO-1	Small Ubiquitin-related MOdifier 1
SWI/SNF	SWItch/Sucrose Non-Fermentable
TAD	Topologically Associating Domain
TCR	T-cell Receptor
TEL (ETS6)	ETS Variant Transcription Factor 6
TES	Transcription End Site
TGFβ	Transforming Growth Factor β 1
TIMP	Metallopeptidase Inhibitor 1
TLR2 / TLR4	Toll-Like Receptor 2 / 4
TMEM100	Transmembrane Protein 100
TNFAIP6	TNF Alpha Induced Protein 6
TNFSF11 (RANKL)	TNF Superfamily Member 11 (Receptor Activator of Nuclear factor-κB ligand)
TSS	Transcription Start Site
TWIST1	Twist-related protein 1
UBC	Ubiquitin C
UBE2F / UBE2M	Ubiquitin Conjugating Enzyme E2F / E2M
VDR	Vitamin D Receptor
VEGF	Vascular Endothelial Growth Factor
WNT	Wingless-related integration site
WT	Wild-type
XIST	X Inactive Specific Transcript
YAP1	Yes Associated Protein 1
ZBTB1 / ZBTB16 (PLZF)	Zinc Finger And BTB Domain Containing 1 / 16 (Promyelocytic Leukaemia Zinc Finger)
ZFAS1	ZNFX1 Antisense RNA 1

CHAPTER 1 Literature review

Unique among all systems within the female body, the ovary is the only organ in which germ cells are developed and is thus aptly responsible for ensuring female reproductive success. In support of oocyte development are a host of ovarian somatic cells that cooperate with one another and with the oocyte to drive various ovarian functions. Among many critical ovarian functions is oocyte maturation and ovulation, during which mature oocytes are released from the confinement of the follicle (and the ovary) into the oviduct where fertilisation can occur. A number of biological processes, mediated by a complex network of signalling pathways and their resultant target genes, contribute to the success of ovulation. Chief among these factors is progesterone receptor (PGR), a steroid nuclear receptor of undisputable importance in determining ovulation. Outside of the ovary, PGR is also highly involved in distinct biological processes throughout the female reproductive tract prior to pregnancy. Exactly how these diverse roles are achieved remains to be answered.

1.1 THE OVARY

The ovarian follicle is composed of female germ cells (oocytes) and somatic cells (mural granulosa cells, cumulus cells and theca cells), with the complex interactions between each of these compartment being vital for ovarian functions. The main purposes of the ovary are to generate viable oocytes and reproductive hormones, with the ultimate goal to enable fertilisation and development as well as supporting potential pregnancy. A number of biological events occur within the ovary in preparation for these goals, including the formation of follicles each containing an oocyte and its supporting network of somatic cells, oocyte development and maturation, ovulation and the formation of the corpus luteum (CL) (Figure 1.1A). Events happening in the ovary are orchestrated by hormones produced by the hypothalamus and pituitary that in turn receive feedback from ovarian signals. All of these are under strict timely control, the rhythmic nature of which results in the oestrous (or menstrual) cycle.

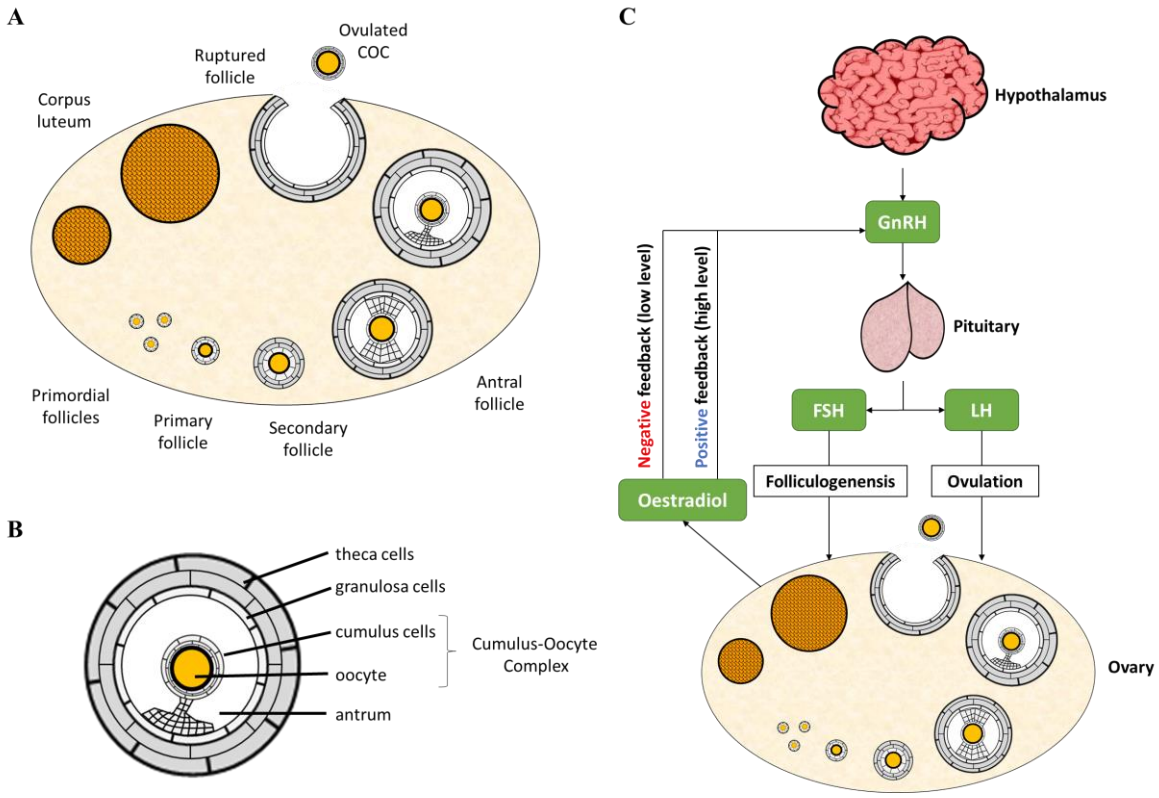

Figure 1.1 Ovarian structure and the hypothalamic-pituitary-ovarian axis.

(A) Schematic of follicular development in the ovary in an oestrous cycle. From bottom left, anti-clockwise: follicle activation (primordial to primary follicle), folliculogenesis (primary – secondary – antral follicle progression), oocyte maturation (pre-ovulatory follicle), ovulation and corpus luteum formation **(B)** Structure of the pre-ovulatory follicle, including oocyte and somatic cell components **(C)** The hypothalamic-pituitary-ovarian axis and effects on the oestrous cycle. During pro-oestrus, FSH released from the anterior pituitary in response to hypothalamus-secreted GnRH promotes follicle development in the ovary, which in turn produces oestradiol acting as a negative feedback to GnRH at low level and positive feedback to GnRH when oestradiol level peaks. This also triggers the spike in LH production which induces ovulatory pathways in the ovary and results in ovulation.

1.1.1 The oocyte

The most important cell in the ovary, and arguably the entire female body, is the female germ cell or oocyte, for it bears the genetic material required for the creation of the next generation. It is one of the largest cells in the body and contains nutrients as well as other factors in support of its growth, maturation and development prior to embryo implantation.

Oocytes are created during oogenesis from primordial germ cells [1]. This process involves the migration of germ cells to the genital ridge and the proliferation of these germ cells by mitosis in the foetal ovary. In the developing ovary, unlike in testis, cell division is arrested early in prenatal development when the oocyte enters meiosis which is then arrested at the diplotene stage of the first meiotic prophase, as illustrated in Bury *et al.*, 2016 [2]. During this arrested phase the oocyte still generates abundant mRNA that is required for later stages of oocyte maturation and early embryo development, during which the oocyte is transcriptionally quiet [3]. Meiotic arrest is sustained by the high level of cAMP in the oocyte, which is maintained by endogenous and exogenous cAMP production in the surrounding granulosa and cumulus cells [4] and can last for up to 40 years in humans. Oocyte development is sporadically initiated in a small number of oocytes each day and the resumption of meiosis I in the oocyte is triggered by the LH surge [5]. This involves the progression to meiosis II in oocyte, during which germinal vesicle breakdown (GVBD) and the formation of the first polar body also occur. By the time of ovulation, the oocyte is arrested at metaphase of the second meiotic division, a secondary arrest which is sustained until fertilisation triggers the extrusion of the second polar body and formation of the female pronucleus [6].

1.1.2 Somatic cells

In the ovary, each oocyte is normally packaged into a multicellular structure called the ovarian follicle in which the oocyte is enclosed in somatic cells (Figure 1.1B). At birth in humans or shortly after birth in mice, oocytes are contained within primordial follicles in which oocytes are surrounded by a layer of flat un-differentiated pre-granulosa cells, the differentiation of which produces granulosa cells that proliferate rapidly [7]. Concurrently, the follicle grows, the oocyte increases in size and an additional layer of cells known as theca cells are recruited and differentiated from the ovarian stromal compartment. Within the peri-ovulatory follicle, granulosa cells can be categorised as either cumulus cells, which are immediately surrounding the oocyte, or mural granulosa cells (referred to from now on as granulosa cells) which line the

wall (hence the term mural) of the follicle. While both cell types share the same origin, each is under the control of different paracrine factors that result in different gene expression profiles as well as ovarian functions that are disparate essential roles in ovulation [8].

Granulosa cells start out as progenitor somatic cells that are recruited to surround the oocyte during early follicle formation in the first 4 days postnatal in the mouse [9]. These cells are derived from either the mesonephros or the ovarian cortex [1]. During the early stage of follicle development, granulosa cells display morphological changes and turn more cuboidal [10]. This is followed by proliferation, resulting in multiple layers of granulosa cells which is then defined as the secondary follicle stage. The divergence of granulosa-cumulus cell specification occurs in the third stage, where the fluid-filled space known as the antrum is formed within the follicle, creating a physical separation between cumulus cells and mural granulosa cells. During folliculogenesis and ovulation, the two granulosa cell lineages have shared as well as distinct functions. Granulosa cells are responsible for the production of oestradiol and progesterone in response to follicle-stimulation hormone (FSH) and luteinising hormone (LH) signalling [11]. Cumulus cells, on the other hand, are essential for supplying the oocyte with nutrients and signalling molecules via specialised gap junctions, thereby promoting oocyte growth and developmental competence [10]. During ovulation, cumulus expansion, a process of rapid extensive extracellular matrix production, is important for ovulation. These two somatic cell lineages are also important in maintaining meiotic I arrest in oocytes prior to the LH surge through sustaining the cAMP build-up within the oocyte [4].

Throughout all stages of development, the oocyte and somatic cells maintain interaction through a network of paracrine factors which is vital for follicular development, oocyte maturation and ovulation. The most important oocyte signalling factors are members of the TGFβ family, notably GDF9 and BMP15, which work in synergy to promote cumulus-specific gene expression, including genes controlling metabolic pathways and cumulus expansion [12]. Knockout (KO) mouse models of these factors show compromised ovarian functions, including developmental arrest at the primary follicle stage (GDF9 KO), impaired ovulation and fertilisation (BMP15 KO or double GDF9/BMP15 KO) [10]. Reciprocally, somatic-secreted factors are also vital for oocyte functions, especially oocyte maturation [4]. Prior to the LH surge, cGMP and cAMP synthesised in granulosa and cumulus cells are diffused into the oocyte via gap junctions where they maintain high cAMP concentration, which inactivates oocyte meiosis-promoting factor and thereby suppresses meiotic resumption. Upon the LH surge,

epidermal growth factor-like (EGF-like) factors including amphiregulin (AREG), epiregulin (EREG) and BTC are produced by granulosa cells through various signalling pathways and inhibits the production of cGMP and cAMP. The resulting drop in cAMP in the oocyte releases the block on meiotic progression, ultimately resulting in GVBD and oocytes completing the final stage of maturation.

Aside from granulosa cells, theca cells also support oocyte development principally through steroidogenesis. During follicle development, progenitor theca cells are recruited to the external side of the follicle basement membrane, upon which these cells differentiate and proliferate, resulting in the theca layer surrounding the externa of the follicle. During folliculogenesis, LH-responsive theca cells produce androgens, which are then taken up by granulosa cells as the precursor for oestradiol and progesterone synthesis [1]. The production of oestradiol in the ovary is thus dependent on granulosa cells and theca cells (the two-cell two-gonadotrophin model) and is illustrated in Patel *et al.*, 2015 [13].

1.1.3 The oestrous cycle

The oestrous cycle (or menstrual cycle in human) is under the control of the hypothalamic-pituitary-ovarian axis. This involves the stringent cross-control of reproductive hormones produced at these organs in a dose-dependent manner, which leads to distinct ovarian functions at different time points, such as folliculogenesis, oocyte maturation, ovulation and CL formation. The coordination of these processes is critical for fertilisation and pregnancy success. A schematic of the cycling hormone pathways in the female reproductive cycle is shown in Figure 1.1C.

Gonadotropin-releasing hormone (GnRH) neurons in the hypothalamus secretes GnRH in a pulsative manner under the influence of other reproductive hormones [14]. In turn, circulating GnRH stimulates the release of two pituitary hormones, FSH and LH, from gonadotropic cells in the anterior pituitary. Such hormone productions are dependent on the frequency of the GnRH pulse, with FSH being continuously released whereas LH production is rapidly induced by the GnRH surge and thus contributes to differences in the effect of FSH and LH on granulosa and theca cells in the ovary. Specifically, prior to the ovulation-inducing LH surge, FSH is the main factor to influence ovarian functions through the activation of protein kinase pathways in granulosa cells that results in the regulation of proliferation and cell survival [15]. In response to

pituitary hormone signalling, the ovary, itself an endocrine organ, produces oestradiol and inhibins to regulate GnRH, FSH and LH in feedback loops. Prior to the LH surge, oestradiol synthesis in granulosa cells is directly triggered by FSH [14]. Similarly, FSH also promotes the expression of inhibin A and inhibin B [16]. As granulosa cells lack the receptor for LH (LHR) at this point, circulating LH indirectly promotes granulosa oestradiol synthesis through inducing androgen production in LHR-expressed theca cells which is then converted into oestradiol in granulosa cells. The resultant oestradiol and inhibin act in a negative feedback loop on the hypothalamus to regulate GnRH and consequentially LH production, while at the same time promotes the expression of LHR on the surface of granulosa cell, making them LH-responsive. Eventually, the build-up of ovarian oestradiol production switches on the positive feedback loop that promotes GnRH secretion, which acts on the pituitary to induce LH production (LH surge). Consequently, this leads to various parallel events culminating in the release of the mature oocyte into the oviduct, or ovulation.

1.2 OVULATION

The events of ovulation begin with the LH surge originating from the pituitary gland as a result of oestradiol production by the ovary, which acts to increase GnRH expression in the hypothalamus and sensitise the pituitary to GnRH action. Together these processes lead to the rising release of LH culminating in the LH surge. This results in a number of physiological responses in the ovary in preparation for the release of the mature oocyte into the oviduct and potential fertilisation, embryo development and implantation, as illustrated in Russell & Robker, 2019 [17]. In the ovary, a multifaceted interplay between different components of the pre-ovulatory follicle has to be coordinated as meiotic resumption in oocyte and preparation for follicle rupture are initiated following the LH surge. The result is the release of the mature oocyte into the oviduct, where further oocyte development and fertilisation can occur, as well as the formation of the CL which maintains progesterone production during pregnancy.

1.2.1 Molecular regulation of ovulation

1.2.1.1 The LH-induced signalling cascade

A signalling cascade begins with the LH surge in the ovary (Figure 1.2). LH binding to membrane LHR on granulosa and theca cells leads to the activation of the G-protein coupled complex followed by the activation of adenylate cyclase (AC) which synthesises cAMP, the

second messenger that activates protein kinase A (PKA). The LH surge also leads to the activation of the Serine/Threonine Kinase 1 / 2 (ERK1/2) signalling pathway [18]. The disruption of any of these components is detrimental to ovulation, as shown in various KO models in which the elimination of LHR, PKA or ERK1/2 results in the complete abolition of LH effect on oocyte maturation, cumulus-oocyte complex (COC) expansion, ovulation and luteinisation [19,20]. A number of transcription factors are subsequently induced by this pathway, including CBP-CITED4 and CEBPβ, which act as master transcription factors in regulating downstream processes [21,22]. Notable among the genes responding to LH is PGR, a key ovulatory transcription factor that by its own merit is responsible for the expression of various ovarian functions, including tissue remodelling, muscle contraction and steroidogenesis, all of which are vital for ovulation [23]. Details on the role of PGR in ovulation as well as other reproductive functions are discussed in detail in section 1.3. At the same time, LHR-associated phospholipase C (PLC) is also activated which in turn activates other protein kinases, such as PKB and PKC [4], that has also been linked to the induction of downstream transcription factors crucial for the regulation of ovulatory genes, namely PGR [24] and JUN/FOS transcription factors [25].

1.2.1.2 Key master transcription factors

A consequence of the LH surge is the activation of a number transcriptional pathways through different signalling cascades. These are activated in parallel to each other with considerable convergence in target genes. Throughout the peri-ovulatory window myriads of transcription factors are initiated and are crucial for the regulation of various biological responses to the LH surge, ultimately leading to ovulation. The majority of these transcription factors are downstream of three known master transcription factors: cAMP Response Element-Binding Protein (CREB), CCAAT-enhancer-binding proteins β (CEBPβ) and CREB-Binding Protein (CBP)-CITED4. Discussed below are these key transcription factors and their importance in the regulation of downstream ovulatory processes, with a focus on studies in mice where most research has been done:

(a) CREB

CREB is one of the first transcription factors to be activated by the LH surge and plays a vital role in transcriptional regulation during ovulation. In granulosa cells, CREB phosphorylation is rapidly triggered by the LH surge through PKA signalling [26]. The inhibition of CREB

activation leads to defects in reproduction, as shown in a transgenic mouse model with a mutation in CREB phosphorylation site that renders it inactive [27]. Female mice with this mutation are subfertile due to the disruption of the oestrous cycle, especially affecting LH peaking, suggesting a role of CREB in the positive feedback loop responsible for sustaining LH production. CREB also regulates the expression of a suite of downstream target genes that are important in various biological events in granulosa cells, including steroidogenesis (*StAR* [28], *Inhba* [29]), COC expansion (EGF-like factors [26] and *Egf1* [30]) and circadian clock (*Per1* [31]). Importantly, CREB is also involved in the regulation of other transcription factors that are LH-induced such as c-FOS [32], a member of the JUN/FOS family also with diverse roles in ovulation (reviewed in section 1.3.7.3). Another important role of CREB is in the regulation of prostaglandin-endoperoxide synthase 2 (PTGS2) and prostaglandin E2 (PGE2) which are inflammatory factors important for COC expansion and ovulation [33]. The activity of CREB in gene regulation often requires interaction with other transcription factors, such as SF-1 in regulating *Giot1* and *Cyp19* [34], SP1/SP3 in the expression of *Ctsl* [35] and CBP/p300 in regulating *Inhba* [29].

(b) CEBPβ

CEBPβ, together with CEBPα, are two transcription factors that are induced by LH through the PKA/ERK1/2 pathway in granulosa cells, as shown through a lack of CEBPα/β expression in ERK1/2 KO mice [22]. Both proteins are expressed in granulosa and cumulus cells of antral follicles and are highly upregulated in granulosa cells by 4-8 h after stimulation with human chorionic gonadotropin (hCG). Not only are CEBPα/β induced by the LH surge, it has been shown that the expression of CEBPα/β in human breast cancer cell is also influenced by the PGR agonist R5020 and interestingly, an interaction between PGR and CEBPα/β has been described in progestin-treated breast cancer cell line, suggesting potential mutual actions between these two transcription factors in peri-ovulatory granulosa cells [36]. However, while there is a regression of CEBPα expression in post-ovulatory granulosa cells, CEBPβ level remains high in the luteal phase and may also contribute to CL function [22].

In granulosa cells, the role of CEBPβ is deemed more important than CEBPα in ovulatory processes, as shown through granulosa-specific single KO models of either CEBPα or CEBPβ [22]. CEBPα KO female mice display no abnormal reproductive phenotypes; however, the ablation of CEBPβ leads to reduced ovulation and double KO of both proteins results in

complete sterility. This indicates that while CEBPβ is the more prominently functional transcription factor in granulosa cells, CEBPα does have additional roles on granulosa functions. In these mice, while there are no defects observed in oocyte maturation, there is a loss of cumulus cell integrity and a lack of vascularisation, follicle rupture and luteal formation. As one of the first transcription factors to be initiated by the LH surge, CEBPβ is involved in a number of biological events in granulosa cells in preparation for ovulation and luteinisation through regulating the expression of luteal cell genes (*Abcb1b, Prlr, StAR, Bhmt)* and genes involved in vascularisation (*Apln*) and COC expansion (*Has2*). Interestingly, other ovulatory transcription factors, such as *Runx2,* is also found to be regulated by CEBPβ in granulosa cells, illustrating the role of CEBPβ as an upstream regulator of the subsequent transcriptional cascade in response to the LH surge.

(c) CBP/p300-CITED4

CBP/p300 refers to the CBP/p300 coactivator family composed of two members, CBP and p300, with similar protein structures and functions. While the nomenclature for these two proteins are often used interchangeably or in combination, CBP and p300 in fact possess unique acetylation properties [37]. However, due to the ambiguous nature of publications on CBP/p300, here the term CBP/p300 is used to address both proteins. CBP/p300 is a generic transcription modulator that regulates gene expression through various means. CBP/p300 possesses histone acetyltransferase (HAT) enzymatic activity and can act on different classes of histones, including H2A, H2B, H3 and H4, as well as other transcriptional activators such as steroid receptor coactivator (SRC) proteins which themselves have additional HAT activity [38]. CBP/p300 does not possess a DNA binding domain (DBD) and cannot directly interact with DNA, instead it is tethered to specific target sites through interactions with other transcription factors. In breast cancer, the recruitment of CBP/p300 and other HAT proteins to target chromatin sites is driven by PGR, which subsequently leads to histone/protein acetylation and thereby creates open chromatin regions to which RNA Polymerase II (Pol II) and the basal transcriptional machinery bind in preparation for transcription [39]. Additionally, CBP/p300 can also facilitate transcriptional elongation by Pol II beyond the first nucleosome and the TSS [40].

CBP/p300 plays a role in various aspects of ovarian functions, including pre- and post-LH roles. In granulosa cells, CBP/p300 is involved in the ERK1/2 signalling pathway activated in response to the LH surge, but is however independent of CREB [26]. CBP/p300, acting in

conjunction with its binding partner CITED4, is responsible for the transcriptional regulation of extracellular matrix genes that are critical for cumulus expansion, such as *Has2*, *Ptx3* and *Tnfaip6* [17]. CBP/p300 also acts in conjunction with other co-factors in steroidogenesis, including CEBPβ and GATA4 with implications in the regulation of *StAR* [41] and with Specificity Protein 1 (SP1) in regulating *Cyp11a1* expression [42]. CBP/p300 also plays a role in follicular growth in which it is involved in the nuclear receptor subfamily 5 group A (NR5A) transcription complex that regulates the granulosa expression of *Inhba* [43].

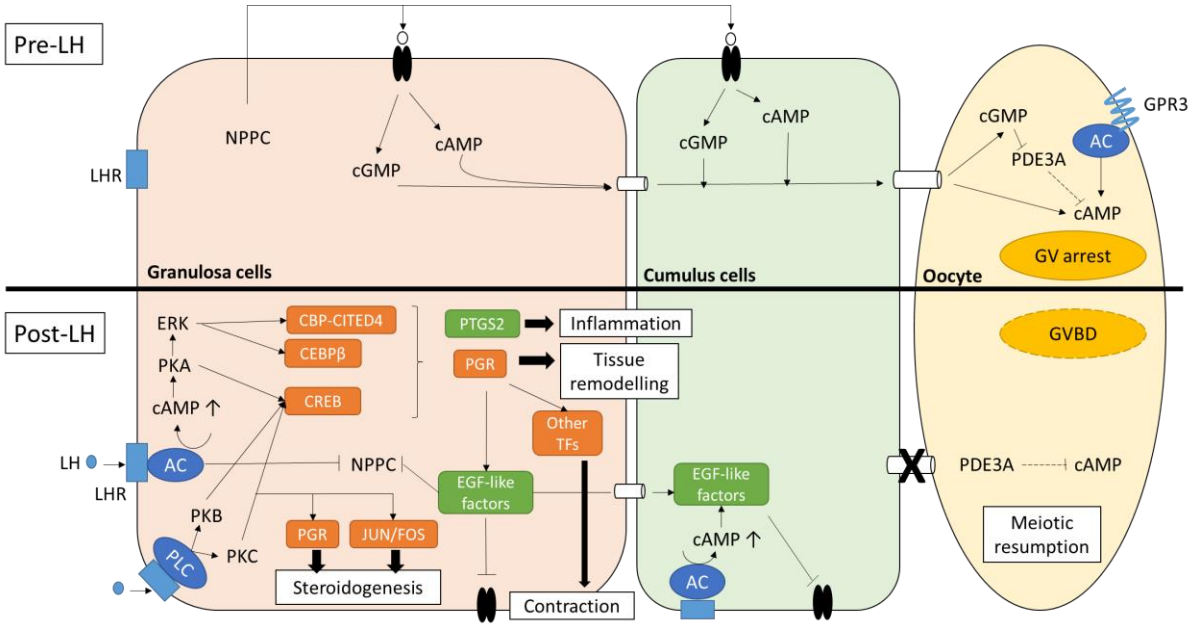

Figure 1.2 Molecular pathways in the peri-ovulatory follicle before and after the LH surge.

Before the LH surge occurs, NPPC-triggered cGMP and cAMP production in granulosa and cumulus cells leads to the inhibition of PDE3A and a build-up of cAMP level in the oocyte, which maintains high cAMP concentration and thus meiotic arrest in the oocyte. Upon the LH surge, cAMP/PKA/ERK1/2 and other protein kinase signalling pathways are activated in granulosa and cumulus cells, which lead to the induction of various transcription factors (CBP-CITED4, CEBPβ, CREB, etc.). Subsequently, downstream target genes are upregulated and have roles in COC expansion, steroidogenesis, muscle contraction, inflammation and tissue remodelling in the follicle. EGF-like factors produced from these pathways also block the production of cGMP and cAMP in somatic cells and promote the degradation of cAMP in the oocyte, resulting in meiotic resumption.

1.2.1.3 The role of non-coding RNA

Previously regarded as 'junk RNA' due to the lack of an encoded protein sequence and their low level of expression, within the past two decades studies demonstrating the roles of non-coding RNA (ncRNA) in gene regulation have exploded with the development of modern transcriptomic techniques that allow for detailed dissection of low-abundant ncRNA. These include short ncRNA like micro RNA (miRNA), which bind complementary mRNA sequence and facilitate mRNA degradation, thereby acting as a post-transcriptional suppressor [44]; as well as long non-coding (lncRNA), which can interact with various protein, DNA and RNA targets and have extensive roles in protein modification, transcriptional and translational regulation [45]. One of the first discovered lncRNA, Steroid receptor RNA Activator (*Sra1*), is a classic example of a ncRNA that forms complexes with the transcriptional machinery including steroid receptors and is discussed in more detail in section 1.3.7.3. These ncRNA have now been linked to diverse roles which are just beginning to be unravelled in the context of reproduction and particularly in ovulation.

Studies on the ovarian transcriptome using different methods have indicated a number of ncRNA that are associated with poor oocyte development and pregnancy outcome [46-48], with different lncRNA profiles associated to different follicular components [49]. In contrast, other lncRNA play a supportive role in female reproduction, such as promoting ovulation [50] and luteinisation of granulosa cells after ovulation [51]. Of particular interest is *Gas5*, a lncRNA that is induced in stress or nutrient deprivation conditions through the inhibition of the mTOR pathway [52]. Recently *Gas5* has been highlighted as a suppressor of glucocorticoid receptor (GR) transactivation functions, achieved through the RNA hairpin structure of the *Gas5* exon 11-12 that competes with the canonical DNA target of GR in binding the GR DBD [53]. Similarly, *Gas5* can also regulate other steroid receptors (SR), including PGR, androgen receptor (AR) and mineralocorticoid receptor (MR), although the impact of such interactions has not been studied in detail. *Gas5* is present in various parts of the ovary, including granulosa cells at various stages of follicle development [54], cumulus cells in associating with pregnancy outcomes [55] as well as COCs in response to lipotoxic conditions (Russell lab, unpublished observation), which suggests potential roles of *Gas5* in oocyte maturation and possibly in response to stress.

Not only are lncRNA involved in ovarian functions but the presence of specific miRNA is also critical for ovulation [56]. The regulatory role of miRNA in female reproduction can be observed

through a reproductive tissue-specific KO mouse model that targets DICER, the enzyme required for miRNA biogenesis [57]. Female DICER KO mice display multiple reproductive defects, including impaired ovulation, decreased oocyte and embryo integrity and defective development of the Müllerian duct, ultimately resulting in sterility. In particular, oocyte-specific DICER KO leads to abnormal chromosomal and spindle morphologies, cell fragmentation and defective cell division. In granulosa cells, the expression of a specific subset of miRNA is regulated by the LH surge and studies on an alternative KO model conclude that steroidogenesis and luteal vascularisation are abrogated when miRNA/siRNA biogenesis is abolished. The efficacy of LH action in granulosa cells can also be modulated by miRNA, such as *miRNA-200b* and *miRNA*-429, which promote the expression of LHR [58]. While miRNA can theoretically target multiple mRNA sequences, miRNA activities in the ovary are highly specialised, with specific miRNA having discreet roles at its cellular targets. In granulosa cells, for instance, *miRNA-224* and *miRNA-383* are involved in various granulosa functions, including cell proliferation, differentiation and steroidogenesis; whereas in the COC, *miRNA-224* is involved in COC expansion [59]. Other short ncRNA, such as endogenous siRNA, may also play a role in oocyte development [57].

In general, while there is an association between ncRNA and reproductive outcomes, exactly what is entailed in such reproductive functions is still largely unknown, especially regarding the impact of these ncRNA on ovulatory factors in granulosa cells and transcription factors in particular. While post-transcriptional regulatory action of miRNA is relatively well-described, the activities of lncRNA are much more convoluted, as ncRNA can partake in various molecular mechanisms. Further investigations into the roles of miRNA and lncRNA will be beneficial in understanding the complex interplay between different protein and ribonucleotide factors in the regulation of ovulation.

1.2.2 Physiological aspects of ovulation

1.2.2.1 COC expansion and oocyte functions

COC activation refers to the meiotic resumption of oocyte and modifications in cumulus gene expression and the accompanying cumulus layers in peri-ovulatory follicles in prompt response to the LH surge. This response in the COC is initiated by EGF-like factors secreted from granulosa cells after the LH-surge. A number of important processes and physiological changes occur during this event. Meiotic resumption occurs in the oocyte, leading to the extrusion of

the first polar body and the second meiotic arrest at MII stage. At the same time, the surrounding cumulus cell layers expand and increase in mass as well as gaining additional migratory and invasive properties which are necessary for ovulation.

The expansion of the COC matrix is the result of the production and accumulation of hyaluronan (HA), a vital component of the extracellular matrix, around cumulus cells [60]. The synthesis of HA requires the induction of the *Has2* gene which is regulated by FSH and prostaglandins as well as EGF-like factors [61,62]. Other specific extracellular matrix proteins also interact with HA, including IαI, which infiltrates the follicle from serum at the time of ovulation and aides in the organisation of the COC matrix; TNFAIP6 and PTX3, which form a complex that promotes HA-IαI binding [63,64]. Another important factor is versican, a proteoglycan produced by granulosa cells which is cleaved by ADAM metallopeptidase with thrombospondin type 1 motif 1 (ADAMTS1) and plays a role in the COC extracellular matrix through HA binding [65]. The disruption of these proteins can have detrimental effects on extracellular matrix formation and ovulation. For instance, ADAMTS1 KO female mice exhibit defective tissue remodelling and vascularisation, altered COC matrix and are overall subfertile [66]. The ablation of TNFAIP6 and PTX3 also results in impaired COC matrix formation and sterility in female mice [67].

As cumulus cells and oocytes do not express LHR, COC expansion is initiated by paracrine factors that are produced in granulosa cells in response to LH signalling [68]. Most important among these are EGF-like factors, including AREG, EREG and BTC which are downstream of a number of factors including PTGS2/PGE2 [69] and PGR [23] that are themselves upregulated by the LH-induced PKA/CREB signalling pathway. After protein synthesis, these factors diffuse to cumulus cells in which they suppress further production of cGMP and cAMP, resulting a decline in cAMP build-up in the oocyte and ultimately triggering meiotic resumption [4]. KO mouse models of AREG and EREG show a reduction in COC activation, with double KO of both AREG and EREG having an accumulative effect [62]. Such phenotype is also displayed in rats treated with an inhibitor for EGFR, the shared receptor for these factors [70]. However, in each of these cases GVBD is not completely eliminated, suggesting a level of redundancy among EGF-like factors as well as the importance of other factors in initiating oocyte maturation. The interaction between oocyte and its surrounding somatic cells is not unidirectional as oocyte can also reciprocally signal to cumulus cells through specific proteins. Classic examples are GDF9 and BMP15 which are secreted by the oocyte and are necessary

for the cumulus activation response [71]. This highlights the importance of cell-cell communication in the ovulation process, not only between somatic cells but also between somatic cells and the oocyte.

1.2.2.2 Tissue remodelling

Follicle rupture, in which the mature oocyte is released from the peri-ovulatory follicle into the oviduct at the follicle apex, is the most important event during ovulation. For this to occur, the physical cellular barrier of the follicle, composed of granulosa cells, the follicular basal membrane, theca layers and the ovarian surface epithelium needs to be thinned and broken down. A number of events happen concurrently during this tissue remodelling process which involves the apoptosis of surface epithelial cells, the proteolytic degradation of extracellular matrix layers and the basement membrane, the involvement of immune cells, the migration of theca cells from the apex, neovascularisation and luteinisation of granulosa cells.

First to undergo degradation during the peri-ovulatory window is the follicular basement membrane, which is composed of extracellular matrix substrates including collagen, laminin and proteoglycans. These degradation process has been ascribed to the action of a number of proteolytic enzymes, included in which are matrix metalloproteases (MMP) with collagenase properties. Among the many members of this family, MMP1, MMP2 and MMP9 are the most involved in ovulation. MMP1 is localised to the apex of the follicle during ovulation with increasing concentration [72]. At the same time, MMP2 and MMP9 are also increased in granulosa cells and theca cells, respectively, the activity of which leads to the degradation of collagen at the site of follicle rupture [73]. Other MMP proteins are also associated with ovulation, including MMP14, MMP16 [74] and MMP19 [75], although their roles are less well-known. MMP proteins are regulated by inhibitory proteins (TIMP), which are also expressed in the ovary during ovulation, indicating that a fine balance between MMP and TIMP needs to be achieved to fine-tune MMP protease activity [73]. Other proteases also contribute to the degradation process, such as plasmin and plasminogen activators [76], ADAMTS1 [66] and cathepsin L [77]. Proteolysis is also required for activating EGF-like factors through cleaving of their precursors, thus making it necessary for COC expansion and for coordinating different biological processes between granulosa and cumulus cells [78].

Another contributor to the proteolytic activities in the ovary are immune cells, which infiltrate the ovary as part of the inflammatory response triggered by ovulatory cues. Leukocytes release additional chemokines and cytokines to further recruit other immune cells to the site and eventually resulting in the release of proteases by the built-up leukocyte population [79]. Macrophages are the main leukocytes to be recruited to the ovary [80], but other immune cells such as neutrophils and T-lymphocytes are also recruited to the theca and medulla layers of the ovary, the inhibition which can result in ovulation failure [81]. Important leukocyte-secreted factors include nitric oxide and reactive oxygen species which likely mediate vasoconstriction, circulating leukocyte attraction and prostaglandin production [82]. Conversely, granulosa and cumulus cells can themselves produce immune factors. These include interleukin 6 (IL6), which has a role in COC expansion [83]; LIF and its receptor which act in support of IL6 in promoting ovulation [84] and TLR2/4, which promote sperm capacitation and fertilisation in the oviduct [85].

Another important part of the tissue remodelling process is the generation of new vasculature around the peri-ovulatory follicle, which is necessary for the formation of the CL from the ovulated follicle by providing nutrients and hormones to the developing CL [86]. The angiogenesis process in granulosa cells requires the expression of vascular endothelial growth factor (VEGF), which is expressed in granulosa and theca cells, as well as luteal cells post-ovulation [87]. The expression of VEGF is reliant on progesterone, as shown by downregulation of VEGF in sows treated with the PGR antagonist RU486 [86]. In turn, the proper development of follicular vascularity is important for luteal blood flow and progesterone production [88]. Disruption of VEGF in macaque monkeys leads to abnormal ovarian functions, particularly abnormal oestrous cycle length due to dysregulation of steroidogenesis [88]. Another important mitogen factor is FGF2, which is associated with hypoxia-inducible factor 1 subunit alpha (HIF1α) in early-phase CL and the suppression of FGF2 results in luteal deficiency [89].

1.2.2.3 Vasoconstriction and muscular contraction

During ovulation, it is essential that follicle rupture happens at the apex of the follicle to allow for the release of the oocyte into the oviduct. Apart from proteolytic enzymatic actions, precisely-timed muscle contraction as well as vasocontraction at the apex are also required for this to occur [90]. The key factor for contraction during ovulation are endothelin proteins, specifically EDN2, which is highly expressed in granulosa cells and theca cells at the time of

ovulation [90]. EDN2 is regulated by PGR, as shown in a lack of EDN2 expression in PGRKO mice [91], which is likely through the activity of intermediary transcription factors HIF [92] and peroxisome proliferator activated receptor gamma (PPARγ) [93]. EDN2 KO mouse models that are specific to the ovary or granulosa cells have confirmed the importance of EDN2 in ovulation, with KO female mice displaying impaired follicle rupture and fertility [94]. It has been shown that EDN2 is responsible for ovarian follicular contraction as well as vasodilation, with contraction of ovarian tissues triggered by treatment with EDN2; vice versa, blocking endothelin using antagonists leads to anovulation [90,91,95]. Other factors, such as prostaglandins, are also involved in determining the spatial orientation of follicle rupture, as shown in treatment with prostaglandin inhibitor in rats that leads to spatially random ruptured follicles [96].

1.2.3 Dysregulation of ovulation and targets for contraception

It is clear that the success of reproduction is dependent on ovulation, which is itself under the strict modulation of endocrine and ovarian paracrine network. Irregularities in this process can lead to anovulation and infertility in women. Ovulation disorders are one of the leading causes of infertility, accounting for 25% of cases [97]. The most clinically relevant disorders for anovulation are in polycystic ovarian syndrome (PCOS) and obesity. PCOS, characterised by aberrant androgen production and hyperinsulinemia, is highly associated with anovulation, resulting in a 70-80% infertility rate in PCOS women [98]. The mechanisms under which PCOS can affect ovulation is still largely unclear; but it is likely that multiple factors, including dysregulation of neuroendocrine [99] and metabolic [100] pathways, that lead to abnormalities in reproductive functions ranging from folliculogenesis to ovulation. Evidences have also indicated a link between high BMI and anovulatory infertility, with cases of insensitivity to gonadotropin also observed in obese infertility patients [101]. Genetic mouse models and diet studies have shown that obesity has an effect on folliculogenesis, ovulation [102], embryo [103] and foetal development potential [104,105]. Multiple factors are likely to contribute to the effect of obesity on anovulation. This includes mitochondria dysfunction, metabolic stress and lipotoxic-induced apoptosis [106]. A conclusion on the exact mechanisms is still under investigation.

On the other hand, a further understanding in the regulatory mechanisms of ovulation can also allow for finely tuned control of the ovulation process, a key goal of female contraception. The main ingredients of currently existing hormonal contraception are oestrogens and progestins

which act to blunt gonadotropin secretion through artificially elevated progestin level, thus maintaining low FSH and LH levels and preventing follicle development and ovulation [107]. However, as such therapies are based on the disruption of essential hormones that are involved in diverse biological processes throughout the body, considerations need to be given to potential side effects. The evidence for many undesirable effects of progestin contraception has been obtained in subsequent observations and studies, these include thromboembolism, breast and uterine cancer risks and depression. Currently-used oral contraceptives have existed since the 1960s with unfortunately little genuine change in the technology since its implementation; clearly, the improvement of the current technology and the development of alternative contraceptive means are vital. However, the advancement of such methods is constrained by our limited understanding on the specific mechanisms of ovulation in which a multitude of ovulatory factors are required, many of which are also prominent in other tissues, most importantly PGR and oestrogen receptor (ER). The fact that these transcription factors are able to modulate different molecular targets and biological processes in different tissue contexts points to distinct tissue-specific molecular mechanisms at play, however such distinction between their ovarian functions and other tissue types have not been examined in detail. A deeper understanding in the precise mechanisms at play will be vital in the development of novel contraceptives specifically targeting ovulation.

1.3 PROGESTERONE RECEPTOR

Progesterone, together with other hormones including androgens and oestradiol, belongs to a group of sex steroids that has shown profound importance in the regulation and maintenance of the normal reproductive physiology. Traditionally referred to as ‘pregnancy hormone’, in the last twenty years evidence has shown that progesterone is more involved in the regulation of female reproductive potential than initially assumed. The main mode of action of progesterone is through its nuclear transcription factor receptor PGR, which is present in the uterus, oviduct, and mammary gland. Most importantly, PGR is expressed in the ovary and has major roles in ovulation.

1.3.1 PGR structure

PGR belongs to the nuclear receptor subfamily 3 group C (NR3C) and is encoded by the *PGR* gene consisting of 8 exons in human (or 9 exons in mouse). These are translated into four main

domains in PGR, with exon 2 to 8 being fundamental to PGR structure and functions, while transcription from different promoters gives rise to various transcript variants [108]. There are also G/C rich regions embedded within the promoter of *PGR* which have been characterised as SP1/SP3 binding sites and shown to be crucial in *PGR* transcriptional regulation [109,110].

The receptor structure in general is made up of four distinctive domains [111] (Figure 1.3). The DBD, which is highly conserved between species, is located in the centre of the molecule and comprises two zinc finger elements that facilitate receptor binding to the canonical DNA motif PGR response element (PRE/NR3C), the consensus sequence of which is 5'-GTTACAAACTGTTCT-3', but most importantly, must contain the palindrome ACAnnnTGT. Located at the C-terminal of the receptor is the ligand binding domain (LBD) which interacts with ligands, such as progesterone and R5020, and supports dimerisation of two PGR units. This region is also known as ligand-dependent transactivation function-2 (AF-2) domain. Also aiding transactivation is a short variable hinge region between the LBD and DBD which is important in stabilising the association between the inactive receptor and the heat shock protein complex as well as the bidirectional shuttling of ligand-bound PGR in and out of the nucleus [112]. The most variable region of the receptor is the N-terminal region, which contains additional ligand-independent AF-1 and AF-3 and is critical in the specificity of PGR activity [113]. An inhibitory function (IF) domain is also located in the N-terminus between AF-3 and AF-1 and is important for suppressing PGR activities through blocking the transactivation function of AF-1 and AF-2 [114,115]. The PGR protein also includes an IKEE sequence in the N-terminal that is targeted by SUMO-1 for sumoylating modifications and is important for PGR auto-inhibition.

Translation from alternative start sites results in two main ligand-binding PGR isoforms, termed PGR-A and PGR-B [116]. PGR-B is the full-length isoform that possesses an additional 164 amino acid in the N terminus (and thus the AF-3 domain). This addition to the transactivation region of the B isoform is critical in mediating the specificity in progesterone regulatory function by allowing PGR-B to bind to exclusive co-activators. This also grants PGR-B the unique ability to evade the inactivation effect by antagonists (RU486 and ZK112993) through sumoylation mechanism [114]. PGR-A, the other main isoform of PGR, lacks the first 164 amino acids seen in the B-isoform, thus has weaker transactivation properties than PGR-B and is unable to form AF-3 specific interactions with co-regulators [117]. However, PGR-A can regulate specific downstream gene expression especially in the context of reproductive

tissues and can act as a trans-repressor to PGR-B [118]. Two other truncated isoforms, termed PGR-C and PGR-M, have also been identified. PGR-C, which has been identified in the uterus in different species, lacks one of the zinc fingers in the DBD but retains the full LDB. This renders the C-isoform incapable of binding DNA, however it can still interact with other PGR isoforms [119-121]. Similarly in PGR-M, which has only been identified in humans and not mice, is transcribed from exon 4-8 of the human *PGR* gene, thus lacking the N-terminal and DBD [122,123]. Instead, it consists of the hinge and LBD capped with a 16-amino acid sequence encoded by the distal third intron that is unique to this isoform.

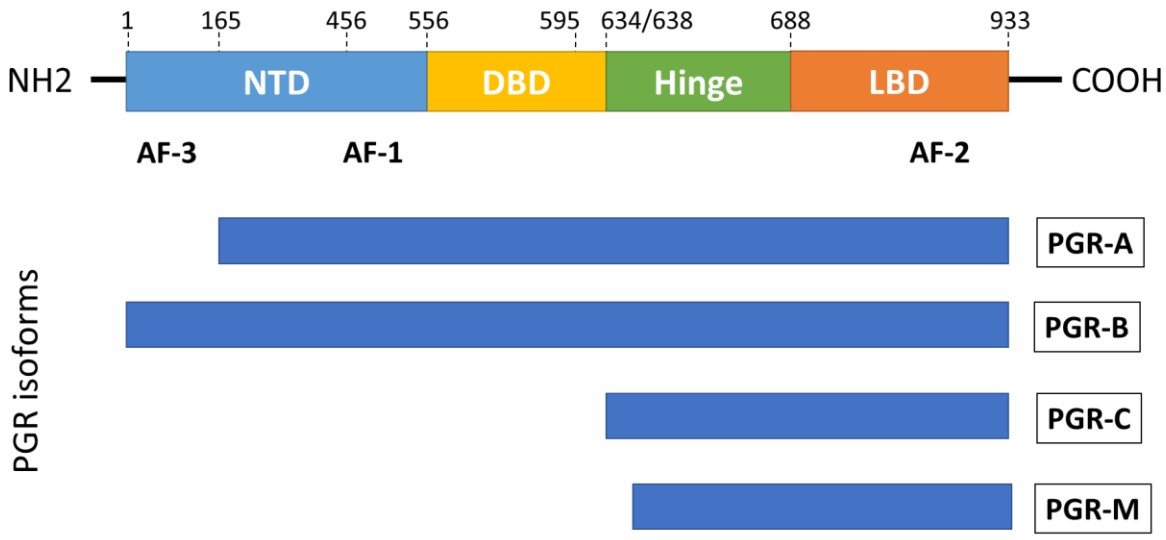

Figure 1.3 Structure of the PGR protein.

The PGR protein is composed of different domains (from N- to C-terminus): NTD with transactivation properties and containing two AF regions (AF-3 and AF-1), DBD that binds DNA, hinge region that stabilises the PGR-HSP inactive complex and plays a role in PGR shuttling between cellular compartments, LBD which interacts with ligands and has a role in dimerisation of PGR monomers, also contains another transactivation function domain (AF-2). Transcription from different TSS leads to the formation of four functional isoforms: full-length PGR-B, PGR-A without the first 165 amino acid (and thus AF-3), PGR-C without the NTD and DBD and PGR-M which is yet more truncated.

1.3.2 PGR functions in the ovary

In the rodent ovary, PGR is exclusively expressed in granulosa cells of peri-ovulatory follicles [124,125]. In granulosa cells of mice [125], human [126] and other species [127,128] PGR is transiently induced in mature follicles in response to the LH surge and declines during oestrous. The expression of PGR can also be induced by forskolin, cAMP or FSH treatment of cultured granulosa cells [129]. PGR mRNA level reportedly peaks at 4 h post-LH treatment *in vitro* [130] and gradually declines within 24 h, which matches the pattern observed *in vivo* [131]. PGR protein level is the highest at 5-7 h post-LH surge and there is a strong preference for the enrichment of isoform A compared to B.

1.3.2.1 Studies on PGRKO mouse model

Progesterone is a key factor in mammalian ovulation, especially in follicle rupture. It has been well-established that inhibition of progesterone by PGR antagonist R486 results in ovulation suppression in rodents [130,132] and humans [133] . Treatment with PGR antagonists also promotes apoptosis as well as DNA damage. Research on PGRKO mouse models has shed more light on the role of PGR in female reproduction. Homozygous female PGRKO mice are shown to be infertile when crossed with wild-type (WT) male mice [134]. Subsequent histological assessment shows that in contrast to the typical characteristics of the WT ovary, the ovary of super-ovulated PGRKO mice contains a large number of unruptured mature follicles and an absence of CL. This PGRKO phenotype is preserved even when PGRKO ovary is grafted into WT females, while WT ovary transplanted into PGRKO mice still ovulates normally (Akison and Robker, unpublished data), demonstrating that anovulation in PGRKO mice is due to defects arising from the lack of PGR in the ovary and not other organs. Interestingly, the retained oocytes are still fully matured and capable of being fertilised and developing into normal pups [135]. This result is supported by previous observations that PGR level is relatively low in cumulus cells and shows that the absence of PGR is important in follicular rupture but not for oocyte maturation. In addition, granulosa cells in these follicles are able to differentiate into a luteal phenotype with the P450ssc enzyme marker. Although the role of PGR in oocyte maturation has been disclaimed, other studies challenge this idea and show that PGR might be involved in oocyte development at least to some degree. There have been reports of PGRKO oocytes being less capable of undergoing maturation in mouse, assessed through the rate of germinal vesicle breakdown in pre-ovulatory follicles [136] as well as limited evidence in humans suggesting a correlation between cumulus cell-expressing PGR and IVF outcomes [137]. On the

other hand, studies on bovine follicles are less conclusive. While inhibiting progesterone by the antagonist RU486 could improve blastocyst rate in bovine IVF in one study [138], others show that COCs treated with RU486 and trilostane have poorer embryo development [139].

As stated above, the role of PGR in ovulation has also been confirmed in most vertebrate species. Of note is a PGRKO zebrafish model in which female KO fish also show oocyte entrapment in the ovary and infertility [140]. Interestingly, analysis of the PGR-dependent transcriptome in this zebrafish model shows that in pre-ovulatory follicular cells PGR is responsible for the regulation of a number of genes [141], including *Zbtb16, Runx1* and RUNX1-regulated ovulatory genes (*Ptgs2, Rgcc* [142,143]) . However, since there is no clear cumulus-granulosa specification in fish follicles and the expression of PGR in piscine pre-ovulatory somatic-oocyte complex was not described, it is hard to determine whether PGR holds exclusive granulosa functions like in mammals. Still, the fact that PGRKO results in similar phenotype across different species indicates a high level of conservation in PGR function at this primary level of fertility control.

1.3.2.2 Target genes of PGR in ovulation

While PGR acts as a transcription factor through binding a consensus response element within the genome, in a range of cell types, the transcriptomic profile is very tissue-specific. In the ovary specifically, PGR has been linked to the regulation of a wide range of genes, some of which have been confirmed to be key factors in ovulation. For instance, *Adamts1* is a PGR-regulated gene in ovary and ADAMTS1 KO mice have a severely reduced rate of ovulation due to follicle rupture failure [66,144,145]. Another group of proteins, endothelin, is also induced by PGR and is linked to ovulation in rodents [90,94]. AREG and EREG, both being upregulated in the presence of PGR, play an important role in cumulus expansion and meiotic resumption in response to LH signal [61,62,70]. PGR also supports granulosa cell survival by upregulating PCNA and downregulating caspase-3. Other genes, such as *Ctsl*, *Pparg* and *Hif1a*, are highly up-regulated by PGR and might be of importance in oocyte development [35,77,92,93]. In other tissues, however, PGR affects very different sets of genes, suggesting that different key transcriptional regulatory mechanisms are at play in ensuring PGR specificity.

1.3.2.3 Isoform-specific roles of PGR in ovulation

Both PGR-A and PGR-B are induced by LH stimulation in the pre-ovulatory follicle; however, the two isoforms do not have the same level of expression. In granulosa cells, the A:B ratio remains at 2:1 throughout the ovulatory cascade, suggesting that while both may have an effect on ovulation, the role might predominantly require the A isoform [125]. Interestingly, this ratio differs in other tissues, which might help to explain the differences in the function of PGR between tissue types. PGR isoforms also have distinct temporal distribution in the ovary [132,146]. While both isoforms are found in theca cells, granulosa cells and luteal cells, PGR-A is only found upon the LH surge and during CL formation, whereas PGR-B is found at all stages of development [146]. The generation of KO mouse model targeting PGR-A and PGR-B separately allows for an opportunity to dissect the function of each isoform. PRAKO mice exhibit a similar anovulatory phenotype as total PGRKO mice, with gonadotropin-stimulated mice failing to ovulate, although the impairment is less complete than total PGRKO phenotype [147]. In contrast, ovulation is normal in PRBKO mice undergoing the same treatment [148]. Interestingly, it has also been shown that PGR-A has the ability to specifically repress PGR-B activity in the breast [114] and uterus [149], which further emphasises the importance of tissue specific A:B ratio and how that might affect PGR functions.

It is clear that PGR plays an important role in the ovary; still, much is still unknown about the mechanism under which PGR itself is regulated, especially in the reproductive tract. Furthermore, PGR is responsible for the regulation of genes that are unique to the ovary, and while the PGR-regulated ovulatory gene profile has been identified, it is still unknown how PGR achieves tissue specificity and whether elements controlling the activity of PGR are involved in the process. The interaction between PGR and other coactivators has been addressed in previous studies; however, none has focused on characterising potential PGR partners in the ovary. Considering how differently PGR behaves between cell types, it is necessary to actively investigate the regulatory mechanism for PGR in the ovary.

1.3.3 PGR functions in the oviduct

In the oviduct, PGR is expressed mostly in the epithelial and muscle cells and is dependent on the oestrous cycle stage. It is generally constitutively expressed at high level until just prior to ovulation when there is a decline in PGR expression [125,150-153]. This pattern of expression is highly conserved between species, as observed in humans, bovine and mice. Differential

expression of the two main PGR isoforms in a spatial manner has also been observed in the mouse oviduct, where PGR-A is found mostly in stromal cells and PGR-B in epithelial cells, with each isoform having a distinct pattern of expression through the oestrous cycle, indicating possible distinct functions in each cell type [146]. PGR-C isoform has also been found in the bovine oviduct during the follicular phase, suggesting a specific role for the C-isoform [119].

In rodents, carefully timed treatment with the PGR antagonists RU486 or ZK98734 during the period of embryo transport through the oviduct leads to premature embryo entrance into the uterus [154,155]. This is the result of progesterone-modulated ciliary functions, shown in a reduced beat frequency in oviducal cilia in human Fallopian epithelial tissues [156]. Thus, PGR is likely acting as a modulator to the transport of oocyte and embryo post-ovulation, likely to promote fertilisation and early embryo development in an intra-oviductal microenvironment, and also perhaps acting in favour of sexual selection by promoting sperm competition [157]. While this is difficult to portray *in vivo* and the PGRKO mouse model shows no gross morphological difference between WT and KO animals, microarray analysis has identified a number of genes that are dependent on the expression of PGR in the oviduct, including known PGR-dependent genes such as *Adamts1* and *Zbtb16* [152]. Other genes that are associated with cell movement and migration were also identified, including *Itga8*, as well as genes important for muscle functions (*Myocd, Des, Atgr2*), oviductal epithelial cell secretion (*Edn3*) and embryo implantation (*Prlr*). However, since PGRKO females are anovulatory, it is unclear whether PGR deficiency in the oviduct has any physiological impact on fertilisation and embryo development. A tissue-specific KO model will be required for further investigations.

1.3.4 PGR functions in the uterus

In the mouse and human uterus, PGR is expressed in the epithelial, stromal and muscle cells, and unlike in the ovary, PGR is constantly expressed regardless of the presence of progesterone [125]. Similar to the ovary, both of the main PGR isoforms are expressed in the uterus, with PGR-A holding important reproductive functions and PGR-B being less critical for uterine functions [147,148]. The expression of PGR-A, but not PGR-B, is inducible by oestradiol treatment [147]. PRAKO mice do not show the normal inhibition of proliferation of the uterine epithelium after progesterone treatment, indicating that the A-isoform is important for mediating differentiation and hyperplasia in the uterus.

PGR has profound roles in the uterus from the pre-implantation window up to parturition. The early impact of PGR on uterine preparation for pregnancy is shown in PGRKO mouse models. In total PGRKO female mice there is a lack of decidualisation in the uterus in response to artificial stimulation as well as a lack of proliferation inhibition in response to progesterone treatment [134]. Analysis of the PGR cistrome in human endometrial stroma indicates that PGR chromatin binding is promoted in the presence of ligand [158]. Further analyses of PGR-dependent transcriptomes in mouse and human uterine tissues have identified various downstream targets, including GATA2, a transcription factor of import in embryo implantation [159-161].

During parturition, the onset of labour is signalled by a decrease in PGR activity through a drastic drop in progesterone level, which is observed in non-human animals [162]. However, in human, circulating progesterone level remains elevated up to birth and rather than a systematic decline in progesterone level, uterine progesterone is metabolised at a local level, which leads to a decrease in ligand-dependent PGR activity and parturition induction [163]. In rodents, artificial disruption of PGR activity through RU486 treatment is sufficient to initiate myometrial contraction and induce a labour state whereas progesterone treatment can prolong pregnancy. Progesterone withdrawal in the uterus is necessary to induce labour, which involves a change in PGR functions in response to progesterone. During this process, there is a shift in the expression dynamics of different PGR isoforms, with PGR-A known to be significantly upregulated in the uterine myometrium obtained from in-labour women, which dramatically increases the PGR-A:PGR-B ratio [149]. PGR-C has also been reported to be upregulated in human myometrium during parturition [120]. During labour, while PGR-B level remains unchanged, there is a significant induction of PGR-A, resulting in an increase in PGR-A:PGR-B ratio [164]. Oddly enough, in cultured human myometrial cells PGR-A is not reported to have transactivation functions in response to progesterone treatment, instead it is PGR-B that responds to progesterone treatment in reporter assays [164,165]. However, PGR-A has a repressive action on PGR-B activity, as seen in a lack of progesterone-induced response in the reporter assay when PGR-A is present, indicating that PGR activities in the uterus are likely a result of PGR-A controlling PGR-B actions in a hormone-dependent manner. In myometrium, each isoform can have specific intracellular localisation that is reliant on the presence of ligands [163]. In the presence of progesterone, PGR-A is found to translocate from the nucleus into the cytoplasm, whereas ligand-bound PGR-B shows a reversed shuttling direction. As progesterone decline is a hallmark of parturition initiation, the nuclear activity of PGR-A and

loss of nuclear PGR-B activity might be proven important for labour. Current theories propose a shift in PGR isoform activation and action. In a pre-labour state, high systemic and local progesterone level promotes ligand-dependent PGR-B transactivation and trans-repression activities, most likely through the recruitment of transcriptional activator or repressor complexes to target genes. Upon progesterone withdrawal at term, PGR-A gains ligand-independent nuclear functions and suppresses the activity of PGR-B, leading to an upregulation of contraction and inflammation genes that are required for the initiation of parturition [166,167].

1.3.5 PGR functions in mammary tissues and other reproductive functions

The interrelationship between PGR isoforms as well as distinct isoform functions have been extensively studied in the context of normal and cancerous mammary tissues, where each PGR isoform is involved in normal mammary development as well as cancer progression. Unlike in the female reproductive tract, PGR-B is of great importance in normal mammary development. Female mice that have ablated B-isoform show impaired ductal development as a result of reduced ductal sidebranching [148], which leads to decreased lactation. Conversely, excessive PGR-B expression leads to inappropriate alveolar growth [168]. While PGR-A KO mice do not display mammary abnormalities, it has been shown to also play a role in the ductal development. A and B isoforms display distinctive temporal expression pattern in mouse mammary tissue, with PGR-A being the predominant form pre-pregnancy and PGR-B playing a major role in alveologenesis during pregnancy [169]. Thus, the tight regulation of each isoform is crucial for normal mammary development and functions during puberty and pregnancy. In mammary tumour, such precise activities are disrupted with a leaning towards aberrant PGR-A expression, which was shown in a transgenic mouse model where overexpression of the A isoform leads to ductal hyperplasia and loss of structural integrity, the hallmarks of cancer development [170]. A shift in the otherwise 1:1 isoform ratio also results in poorer prognostic outcome in breast cancer patients [171].

Within the cell, PGR isoforms also show different spatial expression patterns, with PGR-A mostly localised to the nucleus while PGR-B is shuttled between the cytoplasm and nucleus, suggesting that PGR-B has both nuclear and extra-nuclear functions in breast cancer cells [172]. Such differences in compartmentalisation patterns between the two isoforms also allows for interaction with unique co-regulators and affects downstream gene expression. An example of this is shown for the regulation of *Ccnd1* by PGR-B through interaction with c-SRC in a PRE-

independent manner, while at the same time a PRE-possessing gene, *Sgk*, is exclusively regulated by nuclear PGR-A [173]. More broadly, PGR-A and PGR-B modulate specific transcriptomes in breast cancer in a ligand-dependent as well as ligand-independent manner [171,174]. It has been shown using T47D cells expressing either isoform that in the presence of ligands PGR-B has stronger transactivation functions than PGR-A, resulting in unique transcriptomes being regulated by each isoform [175]. Such enhanced transactivation is ascribed to the extra AF-3 domain that is only present in the B isoform. Subsequent studies have also shown PGR-A to play a prominent trans-repressive role to PGR-B in the context of breast cancer through interaction with the PGR-B N-terminal IKEE sequence [114].

While the literature on PGR in mammary tissue is extensive, there are fundamental differences in PGR characteristics in the breast versus the reproductive tract, not just in the predominant isoform but also in the temporal pattern of expression in response to reproductive markers (oestrous cycle and pregnancy). This makes PGR actions in these two contexts highly distinctive and it would be amiss to assume ovarian or uterine PGR mechanisms and actions to be the same as in mammary tissues, making it necessary to study the action of PGR in its appropriate contexts.

1.3.6 PGR functions in other tissues and non-reproductive cancer

While the majority of PGR function is in the female reproductive system, evidence has emerged for potential PGR roles in other organs. This includes cardiac mitochondrial functions, where the truncated PGR-M isoform has been identified to play a role [123]. In mice, the *Pgr* gene lacks the distal intron 3 which encodes the unique amino acid sequence found in human PGR-M and is thus reported to not express PGR-M [176]. To circumvent this, a transgenic mouse model that expresses human PGR-M exclusively in the heart has been generated for studies on PGR-M function. As the metabolic profile of these transgenic mice is not fully described, it is uncertain whether the presence of PGR-M (or lack thereof) is crucial for vital metabolic functions. However, an elevation in genes responsible for mitochondrial functions has been observed in this mouse model. Knockdown of PGR-M in T47D cells results in the repression of progesterone-induced promotion of mitochondrial membrane potential, whereas HeLa cells treated with R5020 show an increase in oxygen consumption and thus cellular respiration when transfected with PGR-M [123]. PGR-M has also been found to interact with mitochondrial membrane proteins, for which the unique PGR-M amino acid sequence is shown to be crucial.

Introducing PGR-M through genome editing into a mouse model artificially prone to heart failure is shown to be protective of cardiac dysfunctions in male mice, indicating a possible sex-specific protective role of PGR-M in heart diseases [176].

Steroid receptors play a big role in osteogenesis and have profound implications on bone-related diseases. Among these, the role of ER have been extensively studied [177]; however, increasing evidence has also pointed to a role for PGR. PGR is present in osteoblast cells in bones and increasing evidence has indicated a role of PGR in osteogenesis, as shown in various PGRKO mouse studies [178-180]. In particular, PGR acts upon selective areas on the skeleton and results in an accumulation of bone mass, which together with oestradiol likely affects bone development during puberty in females and results in the sexual differences in bone mass and the higher risk of osteoporosis and other related diseases in females.

PGR is expressed in different parts of the brain, including hypothalamus, hippocampus and synapses [181]. Most notably, in the hypothalamus, PGR participates in the mediation of the feedback loop that regulates the oestrous cycle. The role of PGR in the hypothalamic-pituitary-ovarian axis has been shown through a *Kiss*-cre PGRKO mouse model that specifically knockdown PGR in kisspeptin neurons [182]. Female KO mice exhibit abnormal oestrous cycling and subfertility. There is reduced LH production in response to exogenous oestradiol stimulation and subsequently lower ovulation rate. This is likely a functional consequence to the cooperation between PGR, kisspeptin and ER-α, all of which are shown to colocalise in kisspeptin neurons. A role for PGR in the regulation of sexual behaviour has also been implicated in PGRKO female mice in which KO females fail to display the typical lordosis reflex in response to male mice [134]. Isoform-specific knockout mouse models points to PGR-A having a more important role in sexual behaviours, both in the presence and absence of ligand [183]. Sexual dimorphism in PGR isoform-specific activities is also observed in different parts of the brain. In rats, there is a predominance of PGR-A as opposed to PGR-B that is observed in the hypothalamus, preoptic area, hippocampus and olfactory bulbs in females but not in males, which might have implications on gender-specific sexual behaviours, oxytocin receptor and somatostatin activities [184].

1.3.7 Molecular mechanism of PGR action

1.3.7.1 Ligand-dependent and -independent molecular mechanisms

As a ligand-binding transcription factor, the main function of PGR involves regulating gene expression through direct DNA binding in a ligand-dependent manner (Figure 1.4). Newly translated PGR proteins reside in the cytoplasm in an inactive state that is maintained in the absence of ligands through interaction with heat shock proteins [185]. However, when ligands are present, binding between ligand and PGR facilitates conformational change in PGR that leads to the release of PGR from the multiprotein complex, translocation of the ligand-bound PGR into the nucleus and dimerisation with other PGR units. The canonical pathway of PGR involves recruitment of the PGR dimer to the canonical PRE motif leading to the induction or repression of specific PGR-regulated genes depending on the interactions with co-activators or co-repressors. The influence of PGR is not only restricted to genes with known PRE. In recent years, it has been shown that some of the PGR-regulated genes in granulosa cells not only lack the PRE sequence but instead possess distinct G/C-rich regions located in their promoters that bind SP1 and SP3 transcription factors [186]. Further investigation has shown that the removal of these SP1/SP3 binding sites significantly reduces the effect of PGR as an inducer. It is now suggested that the interaction between PGR and these SP1/SP3 sites, either directly or indirectly, is important in the regulation of target genes. Interestingly, these SP1/SP3 sites are also present in the promoter region of the *PGR* gene itself, implying that PGR is capable of auto-regulation.

In specific tissue context, PGR is capable of acting in a ligand-independent manner through a number of different mechanisms. Ligand-independent PGR has been shown to be activated by dopamine in the mouse brain and PGR can be activated through phosphorylation by a cAMP-dependent PKA pathway or by CDK2, which can then act as a transcription factor through chromatin binding [187]. PGR is also capable of non-transcriptional regulatory roles, for example by activating the Src/Ras/Raf/mitogen-activated protein kinase (MAPK) signalling cascade in the cytoplasm [173,188]. However, ligand dependent activity of PGR in these tissues still has specific and physiologically important effects [160].

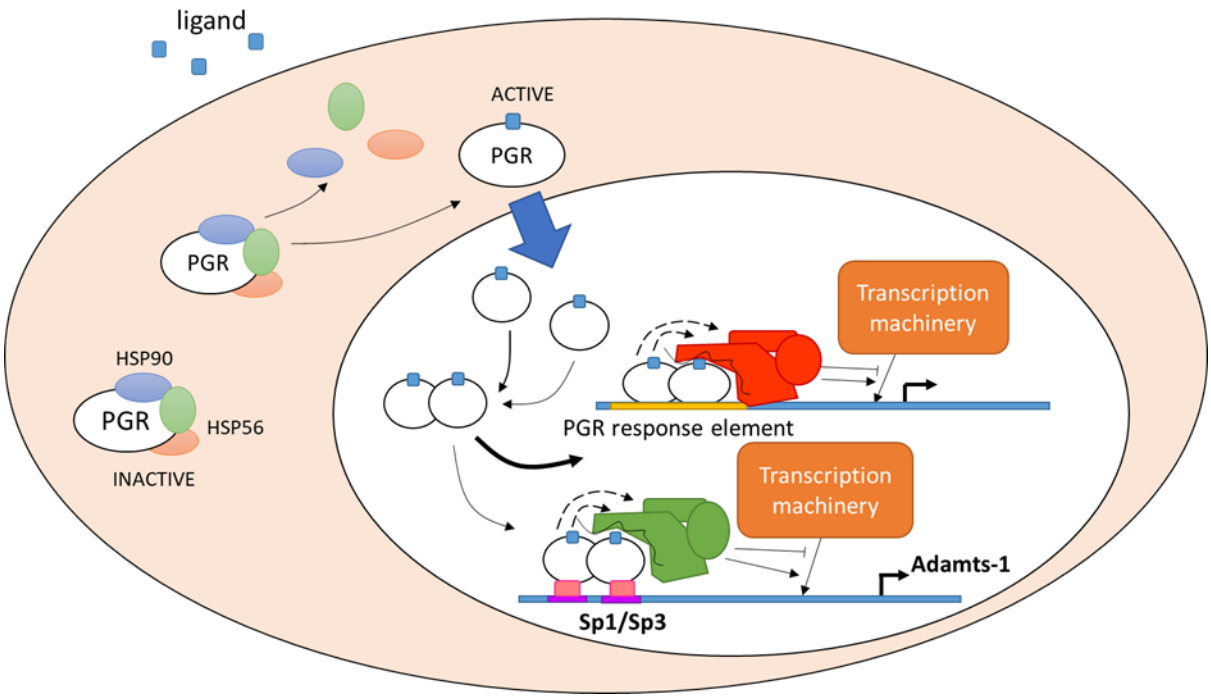

Figure 1.4 Ligand-dependent molecular pathway of PGR.

In the absence of ligands, PGR is retained in an inactive complex containing HSP56 and HSP90 in the cytoplasm. Upon ligand binding, the inactive complex is disassociated and PGR translocate into the nucleus where it dimerises with other PGR monomers. The PGR dimer acts as a transcription factor through binding the consensus PGR response element at target DNA, recruiting other components of the transcription machinery and regulating downstream gene expression. Alternatively, in genes such as *Adamts1,* PGR can also be tethered to non-canonical target genes through binding sites for other transcription factors such as SP1 and SP3.

1.3.7.2 Regulation of PGR isoforms

In general, PGR-B has higher transcriptional activity than PGR-A, as seen through reporter assays in different cellular contexts [117]. This is due to the additional presence of AF-3 in the B-isoform, specifically the LxxLL amino acid motifs in AF-3 which interacts with class I coactivators and can by itself promote gene expression in reporter assays [189]. While the transactivation function of PGR-A is comparatively weaker than PGR-B, it has been shown that PGR-A is capable of regulating the activity of PGR-B. In the uterus during labour, PGR-A can repress PGR-B transactivation action in response to progesterone [164]. The mechanism of this regulation is unlikely to be through PGR-A mediating the expression of PGR-B, for exogenous addition of PGR-A does not alter PGR-B level [165]. Instead, PGR-A binds to the N-terminal IKEE sequence of PGR-B to regulate its transactivation functions [114]. This has important physiological implications, notably in the induction of parturition in the uterus as well as the isoform-driven functions of PGR in different breast cancer subtypes. The truncated PGR-C isoform has also been shown to repress PGR-B transactivation through direct binding and interfering with PGR-B binding to target PRE [120]. The trans-repressive role of PGR-A also applies to other steroid nuclear receptors as PGR-A can also suppress the transactivation of GR and AR in a ligand-dependent manner [118]. Other steroid receptors in turn have also been shown to regulate PGR expression, with the complex interplay between PGR and ER-α in mammary tissues being particularly of interest [190,191]. Recently, it has also been determined that GR is capable of influencing the canonical genomic actions of PGR [192]. GR and PGR are shown to be part of the same transcription complex that binds target chromatin sites in breast cancer cells in a ligand-dependent manner and can either hinder or promote PGR binding at choice target genes, indicating an additional layer of PGR regulation in mammary carcinoma.

1.3.7.3 Co-regulators of PGR

Like other steroid receptors, PGR has no intrinsic chromatin remodelling capability, rather, the nuclear receptors work in conjunction with other members of the transcription complex in order to exercise its transcriptional regulatory functions. Traditionally, protein partners of PGR and other NR3C were determined through exploratory yeast two-hybrid systems using steroid receptors as bait as well as *in vitro* protein pull-down. Using these, a number of partners of potential functional importance was identified, including SRC, c-SRC and *Sra1*. A large body of work are based in the context of breast cancer and particularly breast cancer cell line models, where various PGR co-regulators have been implicated as fundamental determinants in PGR

activities in tumorigenesis and subsequent prognostic outcomes. More recent studies, taking advantages of immunoprecipitation techniques, were able to investigate *in vivo* interactions between PGR and its binding partners. A number of co-regulators have also been identified in the uterus where PGR plays an important role in uterine receptivity to embryo implantation and parturition. However, while the importance of PGR in ovulation is indisputable, its mechanism, including the involvement of other transcription regulators to form the regulatory complex in the ovary remains unexplored. Many transcription factors, previously associated with PGR in other biological contexts, are expressed in the reproductive tract including ovary and are involved in reproductive processes, making them likely potential partners for PGR in this context. A list of known interactors of PGR is shown in Table 1.1, and following are some of the most well-studied co-modulators of PGR with important implications on PGR activities, especially in the context of PGR reproductive functions.

(a) SRC

One of the most well-known co-regulators of steroid receptors is the aptly-named steroid receptor coactivator (SRC) family. Among the earliest coactivator groups to be discovered, this includes three members SRC-1, SRC-2 and SRC-3 which have all been indicated to interact with different steroid receptor members involving the highly conserved LxxLL motif in their AF domains [193]. PGR has been shown to form interactions with all three SRC members in various cell line models [181,194-197]. While the interaction between PGR and SRC members has not been illustrated in reproductive tissues, it is important to note that SRC proteins have been shown to play an important role in female reproduction in studies independent to PGR.

SRC-1 and SRC-3 are capable of binding PGR in a ligand-dependent manner, which has been shown *in vitro* [198] and *in vivo* in breast cancer [197,199]. Studies in *in vitro* system have shown that the LBD of PGR interacts with SRC-1, upon such binding SRC-1 can enhance the transactivation of PGR [194]. This ability to promote PGR transactivation can be explained by the HAT activity of SRC-1, which has a preference for acetylation of H3 and H4 [200]. Furthermore, SRC-1 can also interact with other HAT proteins both *in vitro* and *in vivo*, thus promoting the recruitment of other histone modifiers to target acetylation sites for additional chromosomal modifications in preparation for transcription. One such example is CBP/p300, which can act in synergy with SRC-1 to promote PGR and ER transactivation of gene expression *in vitro* [201]. Recent exciting work on the synergy of the ER/SRC/CBP interaction

has further elucidate the relationship between different components of the nuclear receptor-related transcription complex. Using a combination of cryogenic electron microscopy and 3D modelling, Yi *et al.* have illustrated the order of recruitment of ER coactivators at target chromatins, in which SRC-3 proteins act as linkage between ER and CBP/p300 that in turn acetylates nearby histones and facilitates transcription [202].

The role of the SRC family in reproduction has been investigated using a number of KO animal models. SRC-1 KO mice are shown to be fertile; however, KO females display a failure to mount a decidualisation response to artificial stimulation and leads to a reduction in ductal development in mammary tissues, similar to what is observed in total PGR and PGR isoform-specific KOs [203]. This points to the possible role of SRC-1 as a PGR coactivator in different tissue contexts. SRC-1 can also influence the level of PGR expression, as has been shown in the uterus [199,204]. In the mouse ovary, SRC-3 is found in oocytes yet not in granulosa cells, however SRC-3 KO animals do exhibit lower ovulation rate that is not a result from entrapped oocytes [205]. The fact that SRC-3 is not found in a typical PGR-occupied cellular compartment and the difference in phenotype shows that the effect of SRC-3 on fertility is unlikely due to interaction with PGR in the ovary and more likely because of an independent role in oocyte development. In mammary tissues, SRC-3 plays a role in the regulation of PGR expression and the ablation of SRC-3 leads to a reduction in ductal sidebranching, a phenotype commonly seen in PRBKO female mice [199,205]. Thus, this indicates a functional similarity between SRC-3 and PGR-B and suggesting SRC-3 to be a specific B-isoform co-modulator. It remains undetermined whether SRC-1, 2 or 3 mediate PGR function in granulosa cells.

(b) c-SRC

Not to be confused with the previously discussed SRC, c-SRC is not a transcription factor but is instead a non-receptor tyrosine kinase belonging to the SRC kinase family that is active outside of the nucleus. c-SRC is known to interact with various steroid receptors through distinct domains and while it is unlikely that c-SRC has a role on PGR transcriptional functions through DNA interaction, c-SRC is highly involved in various processes in the ovary, especially in folliculogenesis, oocyte maturation and ovulation where PGR action is crucial. Thus, it is worth taking a further look at the relationship between PGR and c-SRC and its implications on unexplored non-transcriptional roles of PGR in granulosa cells and ovulation.

As the name suggests, c-SRC phosphorylates tyrosine residues of target proteins [206]. The activation of c-SRC involves auto-phosphorylation at specific tyrosine or through interaction with FAK/CAS [207]. Thus, c-SRC is involved in an array signalling pathways, including but not limited to MAPK, PI3K/AKT and FAK pathways [208,209]. c-SRC is also capable of interacting with other SR, including ER, AR and GR; in the case of PGR in particular, the interaction with c-SRC is dependent on the DBD of PGR [210] and occurs outside of the nucleus [173]. More importantly, while both PGR-A and PGR-B can form interaction with c-SRC *in vitro* [210], c-SRC is exclusively extra-nuclear and thus readily forms interaction with PGR-B and not PGR-A in breast cancer cells, leading to isoform-specific transcriptional functions [173].

Due to its involvement in various signalling pathways, the role of c-SRC in the ovary is many-fold. Phenotypically, the ablation of s-SRC leads to infertility in both male and female mice and SRCKO females exhibit impaired follicular development, have less antral follicles and increased atretic follicles compared to WT littermates [211]. These mice also fail to ovulate but can mount a partial ovulatory response if given exogenous gonadotropin. On a molecular level, inhibiting c-SRC activity interferes with the PI3K-PKC-ERK1/2 pathway and results in primordial follicle developmental arrest [212]. In granulosa cells, activated c-SRC is involved in the PI3K-AKT signalling cascade that results in granulosa cell proliferation [68]. Phosphorylated c-SRC can also act in conjunction with ADAM17 to activate the EGFR pathway, thereby promoting gene expression that is important for luteinisation in granulosa cells (*Cyp11a1* and *Hsd3b1*) and COC maturation and expansion in cumulus cells (*Has2* and *Tnfaip6*) [213]. The role of c-SRC in other reproductive tissues is less known, although an interaction between ER-α and c-SRC has been shown to affect the growth of uterine leimyoma cells [214] while c-SRC is known to regulate the expression and phosphorylation of AR in prostate cancer [208]. It is unknown what the relationship between c-SRC and PGR is in the reproductive tract, especially the ovary where the non-transcriptional role of PGR remains unexplored.

(c) *Sra1*

The name of steroid receptor RNA activator, or *Sra1*, reflects the history of discovery for this long non-coding RNA co-activator. Originally discovered in an attempt to identify potential steroid receptor partners through yeast two-hybrid screening, *Sra1* was found to have no typical protein coding gene structure and subsequently shown to act as a generic steroid receptor coactivator important in the transactivation property of PGR as well as other SR, including GR,

AR and ER [215,216]. The AF-1 domain of PGR is shown to be important for *Sra1* regulatory effect and *Sra1* has also been found in the SRC-1 dependent transcription complex. Subsequently, a short functional protein encoded by *Sra1* has also been discovered (termed SRAP), making this the first case of a dual functional RNA/protein encoding gene [217].

Relevant to PGR action, *Sra1* is found to be upregulated in tumours in the breast, uterus and ovary [218]. Transgenic mice expressing human *Sra1* are shown to be subfertile and exhibit a dysregulation in breast development, with aberrant ductal development and a hyperplasia phenotype that are precursors to tumorigenesis, suggesting a role for *Sra1* in controlling the proliferation and developmental rate in mammary tissues [218]. The addition of *Sra1* also leads to a significantly higher level of ligand-dependent PGR expression in mammary glands. There has been no report of *Sra1* and SRAP in physiologically normal female reproductive tissues, thus it is unknown whether they regulate PGR reproductive functions under normal circumstances. While the role of *Sra1* and SRAP in reproduction remains elusive, they have been linked to a number of reproductive disorders, including cervical cancer [219], ovarian endometriosis [220] and polycystic ovarian syndrome [221].

(d) JUN/FOS

JUN and FOS proteins belong to the activator protein 1 (AP-1) transcription factor family, a large group of transcription factors that form interactions with target DNA through a basic Leucine zipper (bZIP) domain and are known to form homodimers as well as heterodimers with other AP-1 transcription factors. The AP-1 family plays a role in various biological contexts, and in respect to the female reproductive tract, JUN/FOS proteins have been shown to be involved both in ovarian and uterine processes.

In rodents, JUN/FOS proteins have been shown to be expressed in granulosa cells in a specific manner. JUN proteins, including c-JUN and JUNB are induced with forskolin treatment *in vitro* while JUND is maintained at a high level even without treatment [222]. FOS proteins, such as c-FOS, FRA1 and FRA2 are also induced by ovulatory cues in granulosa cells, whereas FOSB is downregulated in the presence of forskolin. *In vivo* granulosa cells show an induction of JUNB, JUND and FRA2 by hCG stimulation, with proteins being upregulated 4 h post-hCG. In human, JUNB, JUND and FOS but not c-JUN is present in granulosa cells of antral follicles [223]. However, all four proteins are detectable at a protein level in granulosa cells by 12 h post-

hCG stimulation. Interestingly, among these four proteins, FOS has also been shown to be PGR-regulated in granulosa cells. PGR binding is found at the promoter region of FOS and treatment with PGR antagonist leads to a specific suppression in FOS expression.

JUN/FOS transcription factors have been linked to steroidogenesis in the ovary. In the KGN human granulosa tumour cell line, JUN proteins repress the ovarian-specific expression of *Cyp19a1* through binding the canonical CREB motif in the proximal promoter, thereby supporting the attenuation of oestradiol synthesis in granulosa cells and the transition into a differentiated state in response to ovulatory cues [224]. c-FOS has been shown to be involved in the negative regulation of *StAR* in rat ovaries through direct binding to AP-1 binding sites in its promoter region [225]. In rat granulosa cells, FOS is found to interact with AP-1 binding sites in the promoter of *Ptges, Slco2a1* and *Abcc4* which are involved in prostaglandin production in granulosa cells. However, whether such binding leads to a FOS-dependent transcription of these genes remains unexplored. Other members of the JUN/FOS family, such as JDP2, are associated with the strict regulation of FSH, the disruption of which can lead to early reproductive cessation [226]. While the importance of JUN/FOS members in ovulation still remains to be explored, it has been shown in *Caenorhapditis elegans* that JUN/FOS are vital for ovulation [227]. Transgenic *C. elegans* that lack JUN/FOS are anovulatory with entrapped eggs in the ovary. This is a result of the JUN/FOS influence on the IP3 signalling pathway that is responsible for ovulation. Recently, very high enrichment of the AP-1 binding sites, canonically recognised by JUN/FOS transcription factors, was observed in open chromatin regions in peri-ovulatory mouse granulosa cells, indicates the important transcriptional regulatory role of JUN/FOS during ovulation [228].

A number of JUN/FOS members have been identified to form interactions with PGR, most notably in the uterus. In human myometrial cell lines, PGR has been shown to interact with members of the JUN/FOS family in an isoform-specific manner. Both A- and B-isoforms form physical interaction with c-JUN, JUNB, JUND, c-FOS and PGR-A also forms preferential interaction with FRA1 and FRA2 [163]. Such interactions have specific impacts on the regulation of gene expression in the uterus during labour. For example, the presence of the JUNB/JUND leads to a repression of the PGR-regulated expression of *Gja1* likely through interaction with the target chromatin at AP-1 binding sites in its promoter, which is reversed in the presence of the FRA2/JUND heterodimer. Overall, in the context of the pre-labour uterus, PGR-B acts in conjunction with JUN proteins to recruit the p54/mSin3A/HDAC repressor complex to target

genes, thereby suppressing the expression of genes that are fundamental for labour induction. Using different PGR constructs, it has been shown that two JUN dimerization proteins, JDP1 and JDP2, can interact with the PGR DBD regardless of the presence of ligands [229,230]. However, in the presence of R5020, JDP-PGR interaction can enhance PGR-mediated transactivation through specifically promoting the AF-1 domain function.

(e) SP1/SP3

SP1 and SP3 belong to the Kruppel like factor (KLF) transcription factor family that possess a zinc finger DNA binding domain and bind G/C-rich sequences known as G/C-boxes at target promoters. SP1/SP3 are responsible for the regulation of gene expression both in normal and cancer cells. In the normal ovary, SP1/SP3 are responsible for gene expression regulation at different stages, including but not restricted to *Adamts1* [186], *Nr5a2* [231], *Rhox5* [232], *Ctsl* [35], *Ereg* [233], *Igfbp3* [234], *Egr1* [30] and *Notch2* [235]. SP1/SP3 are ubiquitously expressed and in the majority of cases, SP1/SP3 manifest their transcriptional functions through interaction with other transcription factors, including SF-1, PGC-1α, GABP, CBP/p300 and PGR, indicating a role of SP1/SP3 as a general pioneer factor for other transcription factors. Physiologically, this has an impact on steroidogenesis and follicle rupture during ovulation; however, as SP1/SP3 are vital in various tissues and developmental contexts, the specific role for SP1/SP3 in ovarian development and ovulation have not been directly examined through global knockout models. A recent study using an SP1 knockout model in cultured mouse perinatal ovaries however has indicated an important role of SP1 in the development of primordial follicles, especially through regulating the activities of forkhead box L2 (FOXL2), a critical factor in early folliculogenesis consistent with a pioneer function regulating granulosa-specific chromatin structure [235].

SP1/SP3 are known to act as a recruiter of other transcription factors through direct protein-protein interaction to target promoters that harbour SP1/SP3 binding G/C-boxes, thereby regulating downstream gene expression. This interaction has been illustrated in the ovarian context, in the regulation of *Lhcgr* via SP1/SP3 interaction with GATA4 in human luteal cells [236] and the collaboration between SP1 and ER-α in regulating *Mmp19* in mouse granulosa cells [237]. In respect to PGR transcriptional regulatory function, a number of PGR target genes have been shown to possess SP1/SP3 binding sites yet lack the canonically recognised PRE motif in their proximal promoter regions. These include the classic PGR target gene *Adamts1*, which

contains three distinct SP1/SP3 motifs within 1000 bp upstream of its TSS [186]. Through reporter assays, it has been shown that these SP1/SP3 sites are vital for the transcriptional regulatory role of PGR on *Adamts1* expression. Similarly, in other genes, such as *Cdkn1a*, *Snap25* and *GdA*, the presence of SP1/SP3 binding sites in the promoter region has been shown to be important for PGR-dependent transcriptional regulation of said genes [238,239]. Remarkably, PGR can also regulate its own expression in a progestin-dependent manner through interaction with SP1/SP3 binding motifs in the *PGR* proximal promoter region, as described in human endometrial stromal cells [240]. While the direct interaction between PGR and SP1 was hypothesised but not demonstrated in these instances, it has been shown in a separate study in T47D and ZR-75 breast cancer cell lines that SP1 and PGR co-bind SP1/SP3 sites in the promoter region of *F3* gene to promote its activation [241].

A recurring mode of trans-regulation can be observed in many PGR-binding co-modulators, that is, their ability to regulate the expression of PGR in different cellular contexts. This has been identified in the transcriptional regulation of PGR by JUN/FOS transcription factors in breast cancer cells [242,243] as well as by SP1/ER-α in breast cancer cells [109] and peri-ovulatory granulosa cells [110]. Perhaps this is a self-sustaining mechanism in which members of the protein complex are inducible by their potential protein partners, thereby helping sustaining the transcription complex and thus downstream gene expression. This would be of special interest in malignancy and would require further investigations.

Table 1.1 List of transcription regulators that form protein-protein interaction with PGR

Factor	Biological consequence	Biological context	Methods of identification	Ref
BTEB1	promotes PGR-B transactivation	Uterus	Mammalian 2-hybrid	[244]
	promotes PGR-A inhibition of PGR-B	Uterus	co-immunopreci-pitation (IP)	[244,245]
CBP/p300	promotes progestin-dependent tumour growth and proliferation	Breast cancer	FLAG IP	[195]
c-JUN, JUNB, JUND, c-FOS	maintains progestin-dependent repression of parturition, interacts with PGR in the hypothalamus	Uterus	co-IP[246]	[246]
		Uterus	Proximity ligation assay (PLA)	[163]
		In vitro	GST pulldown	[181]
c-SRC	regulates the cytoplasmic Src/Erk pathway in cancer, interacts with and promotes PGR-B transactivation, interacts with PGR in the hypothalamus	in vitro	GST pulldown	[210,181]
		Breast cancer	co-IP	[210]
		Yeast system	Yeast 2-hybrid	[210]
		In vitro	GST pulldown	[190,181]
CUEDC2	promotes PGR ubiquitination and degradation	Breast cancer	GST pulldown	[247]
		Breast cancer	co-IP	[247]
E6-AP	depending on contexts, can promote PGR ubiquitination and degradation or acts as PGR coactivator, promotes PGR-B transactivation	Yeast system	Yeast 2-hybrid	[248]
		Breast cancer	co-IP	[249]
ERBB2	forms a complex together with STAT3, regulates progestin-dependent cell cycle progression	Breast cancer	IF	[39]
		Breast cancer	co-IP	[39]
ERK-2	regulates the Src/Erk pathway in cancer	Breast cancer	co-IP	[250]
ER-α	promotes progestin-dependent tumour growth and proliferation, regulates the Src/Erk pathway in cancer, promotes PGR-B transactivation	Yeast system	Yeast 2-hybrid	[190]
		in vitro	GST pulldown	[190]
		Breast cancer	co-IP	[190,191,251]
		Breast cancer	co-IF	[191]
FOXO1	Interacts with PGR in the hypothalamus and influences energy metabolism	In vitro	GST pulldown	[181]
FRA1, FRA2, JUND	interacts with unliganded PGR-A to promote parturition	Uterus	PLA	[163]

GATAD2B	promotes PGR-regulated expression of pro-inflammatory genes and induces parturition	Uterus	co-IP	[252]
		Uterus	PLA	[252]
GR	Shares mutual target DNA with PGR and can promote or hinder PGR-DNA binding in a ligand-dependent manner	Breast cancer	Co-IP	[192]
		Breast cancer	Co-IF	[192]
		Breast cancer	Sequential ChIP	[192]
HMG1	promotes PGR-DNA binding through DNA conformational change	Breast cancer	co-IP	[253]
HP1G / HDAC1	forms a repressive complex	Breast cancer	co-IP	[254]
HSP90 / HSP56	interacts with ligand-free PGR to maintain PGR tertiary folded state	Yeast system	Yeast 2-hybrid	[255]
JAB1	promotes PGR transactivation, stabilise PGR/SRC-1 interaction	Yeast system	Yeast 2-hybrid	[256]
		Mammalian cell system	Mammalian 2-hybrid	[256]
		in vitro	GST pulldown	[256]
JDP1 / JDP2	promotes PGR transactivation	in vitro	GST pulldown	[229,230]
		Mammalian cell system	co-IP	[229]
NF-KB	represses PGR transactivation	in vitro	GST pulldown	[257]
PIAS3	sumoylates PGR and represses PGR transactivation	Yeast system	Yeast 2-hybrid	[258]
		in vitro	GST pulldown	[258]
		Mammalian cell system	co-IP	[258]
		Mammalian cell system	IF	[258]
PSF / P54nrb / mSIN3A / HDAC1	maintains progestin-dependent repression of parturition through PGR transactivation	Uterus	co-IP	[246]
		Uterus	FLAG IP	[259]
		in vitro	GST pulldown	[260]
		in vitro	GST pulldown	[259]
		Uterus	PLA	[163]
SP1	promotes progestin-dependent tumour growth and proliferation	Breast cancer	Co-IP	[195,241]
SRC-1	promotes progestin-dependent tumour growth and proliferation	Yeast system	Yeast 2-hybrid	[194,241]
		In vitro	GST pulldown	[181,194]
		Breast cancer	FLAG IP	[181,194,195]
		Breast cancer	co-IP	[195,197]

SRC-2	mediates PGR transactivation	in vitro	GST pulldown	[181,194,196,197]
		Mammalian cell system	IF	[5,188]
SRC-3	promotes progestin-dependent tumour growth and proliferation	Breast cancer	FLAG IP	[195-197]
STAT3	regulates progestin-dependent cell cycle progression	Breast cancer	co-IP	[195,261]
		Breast cancer	Co-IF	[181,196,197,261]
SUMO-1	sumoylates PGR and promotes PGR transactivation	Breast cancer	NI-NTA precipitation	[261,262]

1.3.7.4 PGR action at enhancers

Traditionally described only in the context of proximal promoters, the transcriptional role of steroid receptors and PGR in particular has been extended to the regulation through distal enhancer elements in the genome, which has been previously described for various steroid receptors [263,264]. In the context of PGR, the focus on enhancer activation stems from cistromic studies in mammary cells in which PGR is found to mainly occupy regions that are distal to gene boundaries [265-268]. Subsequently, the functional impact of such interaction between PGR and various enhancer sites has been identified, which can have permissive or suppressive effects on downstream gene expression. For example, PGR is recruited to the enhancer of *Hsd2b11* through co-binding with STAT5A and promotes the expression of 11β-HSD2 [269]. In contrast, PGR interacts with the upstream enhancer of *Csn2* in the presence of ligand as a competitive measure to suppress PRL/glucocorticoid-induced expression of β-casein [270]. In the uterus, PGR enrichment is also found in distal intergenic regions and is critical in transcriptional regulation, such as in the induction of *Ihh* by PGR in conjunction with GATA2 [160,271]. In other reproductive tissues, such as granulosa cells and oviducts, the involvement of PGR in modulating enhancer functions remains unknown.

1.4 RUNX TRANSCRIPTION FACTOR

The Runt-related Transcription Factor (RUNX) family, historically referred to as Core Binding Factor Alpha (CBFA) and more familiarly known as Acute Myeloid Leukaemia (AML) factor in the respective cancer contexts, consists of three known members: RUNX1 (CBFA2/AML1), RUNX2 (CBFA1/AML3) and RUNX3 (CBFA3/AML2), with high level of structural conservation between members of the family as well as between different species [272]. RUNX transcription factors are most well-known as oncogenic factors in acute myeloid leukaemia and other cancer types; however, evidence has shown them to also play a role in female reproduction.

1.4.1 Structure of RUNX proteins

RUNX1, RUNX2 and RUNX3 are encoded by three separate genes, with RUNX1 and RUNX3 being closer homologs to one another than to RUNX2 [272]. In each of the three RUNX genes, the utilisation of two separate promoters that are either distal or proximal gives rise to two major variants, RUNX type I and type II, which are reported to have different expression

pattern and roles in tissue-specific contexts. Aside from these two main variants, there are a number of other lesser-known RUNX isoforms, the compositions as well as functions of which are still poorly understood.

The molecular structure of the RUNX proteins is highly conserved, with homologs identified in both invertebrate and vertebrate animal groups and contains a number of functional domains that are shared between all three RUNX proteins [273] (Figure 1.5). On the N terminus is the runt homolog domain (RHD), so named due to its homology with the *Drosophila* runt gene, and is responsible for binding to the canonical RUNT DNA motif as well as for hetero-dimerisation with CBFβ, the RUNX canonical dimerising protein partner which lacks DNA binding capacity. The presence of CBFβ is highly important for ensuring the affinity between RUNX and target DNA as well as for stabilising the RUNX complex, even though CBFβ by itself does not interact with target DNA. Downstream of the RHD are a number of functional domains, including two AF domains (AD) important for the transcriptional regulatory function of RUNX and a putative inhibitory domain (ID) that bind co-repressors. A nuclear matrix-targeting signal (NMTS) domain is involved in nuclear matrix attachment and localisation of RUNX in nuclear subdomains, with an additional replication activation domain within the NMTS that is associated with the DNA replication machinery. At the C-terminal end of RUNX is a VWRPY site which binds the co-repressors from the Groucho/TLE family. In RUNX2, an extra glutamine/alanine-rich (QA) site is found at the N-terminus, which acts as an additional transactivation domain.

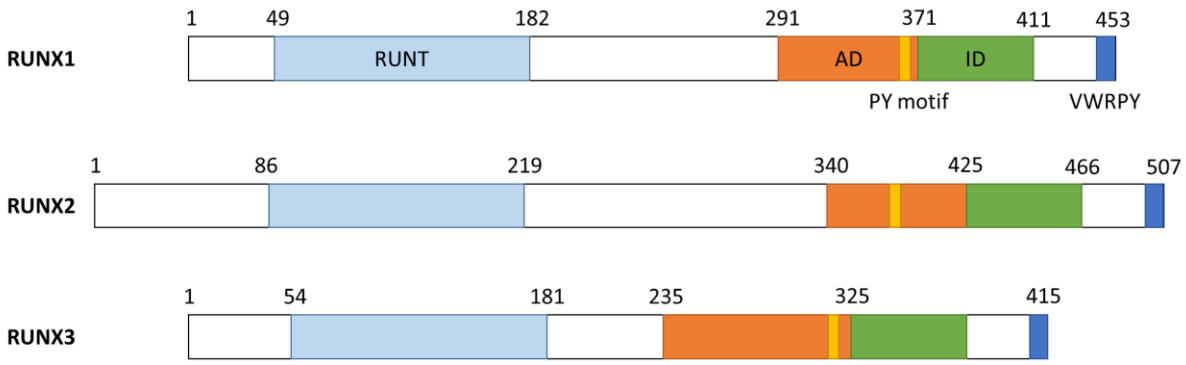

Figure 1.5 Structure of RUNX proteins.

RUNX1, RUNX2 and RUNX3 share the majority of important domains (from N- to C-terminus): RHD that binds the RUNT motif at target DNA, AD with transactivation properties, NMTS domain is important for nuclear localisation of RUNX, ID which binds co-repressors and a VWRPY site that binds additional co-repressors. RUNX2 has an additional glutamine/alanine-rich site at the N-terminus which contains another transactivation domain and RUNX3 has a shortened hinge region.

1.4.2 RUNX functions in the ovary

1.4.2.1 RUNX1

The ovarian expression of RUNX1 has been identified in a number of species in association with granulosa cell functions. In the rat ovary, RUNX1 is absent in primary and secondary follicles, but in antral follicles RUNX1 is expressed at a basal level and is induced by hCG stimulation up until the luteinisation of granulosa cells [143,274]. RUNX1 is detectable in granulosa cells of peri-ovulatory follicles in human [275] and is also present in the theca layer independent of the LH surge. The RUNX1 pattern of expression is replicable in an *in vitro* culture system in which the level of RUNX1 translation is induced by hCG as well as forskolin and phorbol myristate acetate [143,276]. Further investigation showed that a number of intracellular molecular pathways following the LH surge, including PKA/adenylate cyclase and MAPK pathways, are important for the upregulation of RUNX1. In the goat ovary, RUNX1 is expressed in oocytes, granulosa cells as well as theca cells at different stages of follicle development.

In rat and goat granulosa cells, RUNX1 is involved in the LH-regulated production of progesterone and oestradiol through regulating the expression of *Cyp11a1*, which encodes an enzyme that catalyses the conversion of cholesterol to pregnenolone, the precursor to progesterone. RUNX1 also induces the expression of *Ptgs2* in peri-ovulatory rat granulosa cells through direct binding to RUNT sequences in its promoter [277]. RUNX1 also regulates *Hapln1* and *Rgcc* which are genes shown to be upregulated in peri-ovulatory granulosa cells, although their ovulatory roles remain speculative [278]. Unlike for PGR and other ovulatory factors, which benefited from studies on KO mouse models, the historical lack of a viable RUNX1 KO model has prevented attempts to study the ovulatory role of RUNX1 in a summative way. While recent attempts have been made to generate tissue-specific RUNX1 KO and data are emerging in the field, thus far a global characterisation of RUNX1-dependent ovarian transcriptome and cistrome have not been described in detail.

1.4.2.2 RUNX2

Like RUNX1, RUNX2 is highly expressed in rat and mouse granulosa cells of antral follicles as well as CL arisen from ovulated follicles [275]. RUNX2 is also found to be upregulated in rat COCs in response to hCG stimulation. In human, RUNX2 is also expressed in peri-ovulatory

granulosa cells and an increase in RUNX2 expression in cumulus cells is also associated with poor pregnancy success in infertility patients [279].

In rat granulosa cells, RUNX2 is responsible for the regulation of a number of peri-ovulatory genes, including *Ptgs2* and *Ptgds* (which are involved in prostagladin synthesis), *Fabp6* (the ablation of which in granulosa cells leads to a reduction in ovulation in mice) [280], *Acbc1a, Rgcc* and *Mmp13* [275]. Interestingly, RUNX2 is also a regulator of RUNX1, as indicated in the binding of RUNX2 at the *Runx1* promoter in granulosa cells and the induction of known RUNX1 targets *Ptgs2* and *Tnfaip6* when there is a loss of RUNX2 *in vitro* [281]. RUNX2 is also capable of binding to the *Ptgs2* promoter region known to be targeted by RUNX1, suggesting a redundant mechanism between RUNX1 and RUNX2. Remarkably, heterozygous deletion of RUNX2 in the context of CBFβ ablation resulted in infertility in female KO mice which was not achievable in single CBFβ KO. However, ovulation still occurred albeit at a lower rate, suggesting that RUNX2 regulates multiple processes that are important for successful pregnancy. Similar to RUNX1, global RUNX2 ablation proves lethal and cannot be used for reproductive studies, thus the specific role of RUNX2 in ovulation still remains to be explored.

1.4.2.3 RUNX3

Like the other two RUNX transcription factors, RUNX3 has also been identified in the mouse ovary, specifically in granulosa cells [282]. Unlike RUNX1 and RUNX2, RUNX3 is present in follicles at all stages of development, although whether RUNX3 can be further induced by the LH surge has not been examined. However, this difference in expression pattern likely explains the distinct role of RUNX3 in the ovary and female reproduction, which is evidenced in studies on the RUNX3 KO mouse model. While the standard global RUNX3 KO on a C57BL/6 mouse genetic background is proven to diminish the vitality of *in utero* foetuses and newborn pups [283,284], a global RUNX3 KO model on a BALB/c background is shown to produce viable offspring and thus was used to examine the importance of RUNX3 on female fertility [285]. Due to somatic defects associated with RUNX3, the long-term fecundity of RUNX3 KO mice has not been reported. While ovulation in RUNX3 KO females can be induced by exogenous hormone stimulation, naturally cycling RUNX3 KO females do display a classic anovulatory phenotype, with developed antral follicles but no CL observed. The normal phenotype can be restored through cross-transplanting WT and KO ovaries, in which ovulation is observable in KO-to-WT ovaries and ovulation failure occurs in WT-to-KO ovarian transplants. This implies a dysregulation of the hypothalamic-pituitary-ovarian axis and negative feedback loop, which

can be explained by the influence of RUNX3 in the production of reproductive hormones in the hypothalamus during the oestrous cycle, where RUNX3 is normally present [282]. RUNX3 deficiency leads to an alteration in the expression of *Fshb*, *Lhb* and *Cga* in the pituitary, demonstrating a role of RUNX3 in FSH and LH production [282,286]. This results in a decrease in ovarian levels of *Cyp11a1*, *Cyp19a1*, *Fshr* and *Lhcgr*, which has implications for steroidogenesis in the ovary, shown as a repression in oestradiol- and progesterone-induced proliferation in ovarian epithelial cells. Other than regulating the oestrous cycle, RUNX3 is also involved in folliculogenesis by regulating the expression of activins and inhibins in the ovary, leading to a reduction in follicle number at all stages and an increase in atresia.

1.4.2.4 CBFβ

Unlike RUNX proteins which are upregulated and nuclear localised in granulosa cells, the level of CBFβ remains unchanged throughout ovulation and is reported to be present in both the nuclear and cytoplasmic compartment of granulosa cells [275]. However, as the dimerisation of RUNX proteins with CBFβ is crucial for effective DNA binding of RUNX and the ablation of CBFβ still results in viable offspring, CBFβ has been targeted as an indirect way to investigate RUNX functions in knockout mouse models. The role of CBFβ in the ovary has been well documented through two granulosa cell-specific CBFβ KO mouse models, with CBFβ deletion in the ovary being conditional in granulosa cell by using *Cyp19a1* and *Esr2*-cre transgenic models, which are expressed in granulosa cells from the FSH-dependent secondary follicle stage [274,287]. In both conditional KO models, CBFβ KO females were subfertile compared to WT littermates and while some ovulation still occurred at a lower rate, these mice failed to form proper CL after ovulation. Female KO mice also exhibited abnormal oestrous cycles, reduced vascularisation of the ovary and reduced circulating progesterone level in response to the LH surge. Microarray analysis of CBFβ KO granulosa cells showed that the absence of CBFβ lead to changes in the expression of genes responsible for ovulation, luteal formation and steroidogenesis (eg *Edn2, Ptgs1, Lhcgr*), which likely accounted for the reduced ovulation rate. Interestingly, the ablation of CBFβ resulted in an increase in RUNX1 transcriptional and translational levels, whereas the level of RUNX2 was unaffected. Unlike RUNX1 and RUNX2 which localise in the nucleus, CBFβ could be found in both the nuclear and cytoplasmic compartments, suggesting that CBFβ can hold non-transcriptional functions independent of RUNX1 and RUNX2 [275].

1.4.3 RUNX functions in other reproductive tissues

Apart from its role in ovulatory granulosa cells, RUNX1 is also known to be important in the female-specific commitment in foetal gonad differentiation, best known to be regulated by the master transcription factor FOXL2. RUNX1 is expressed in female gonads of a number of vertebrates, including human, mouse, turtle and fish [288,289]. Studies on tissue-specific KO mouse models have shown that RUNX1 works closely with the female-determinant FOXL2 at a functional as well as chromatin binding level, shown through colocalisation in foetal granulosa cells and mutual chromatin targets and downstream regulated genes which are important for granulosa cell functions [286]. Not just in the gonads, RUNX1 is also involved in the cell fate commitment of epithelial cells in the Müllerian duct, the precursor for the female reproductive tract [290].

In the male gonad, RUNX2 is found to be present in the testis and sperm, however does not seem to play a role in sperm motility [291]. The presence of RUNX2 in mammary epithelial cells is important in the regulation of lactation through direct transcriptional regulation of b-casein [292]. RUNX2 also regulates the expression of *Cldn11* in mammary epithelial cells, which is important in the normal differentiation of the mammary gland. While RUNX2 is normally upregulated by the LH surge, an overexpression of RUNX2 has been detected in cumulus cells of PCOS patients [279] where it represses the expression of *Cyp11a1* and *Cyp19a1* [293].

All three RUNX proteins are expressed in the uterus during early pregnancy. Curiously, they all have a very similar pattern of expression in the uterus, being detectable in luminal, glandular epithelium and stromal cells of the uterus of female mice and is especially induced by decidualisation and at embryo implantation [294-297]. In ovariectomised mouse uterus the RUNX1 mRNA level is acutely responsive to oestradiol treatment but has a delayed response to progesterone treatment [295]. Here, RUNX1 is responsible for the regulation of genes involved in decidualisation, especially in the remodelling of the extracellular matrix (*Mmp2*, but not *Mmp9*) and angiogenesis (*Ptgs2* and *Ptges*). RUNX2 is also involved in angiogenesis in mouse uterus through regulating *Ptgs2* and *Vegf* and in extracellular matrix (*Mmp9)*, likely through an association with CEBPβ [296]. RUNX3 has a gradual response to oestradiol treatment, whereas progesterone has no effect on RUNX3 expression [294]. RUNX3 KO female mice are shown to have poorly-developed uterus that are lighter in weight and in glandular development [285]. RUNX3 ablation also leads to altered TGF expression in the uterus [298]. These data highlight a

recurrent theme, in which RUNX members are shown to possess distinct expression profiles and roles in the same tissue type, alluding to distinct regulatory mechanisms for each RUNX member.

1.4.4 Molecular mechanisms of RUNX

All three members of the RUNX family act as transcription factors to regulate downstream gene expression. RUNX proteins share the same basic molecular mechanism at the chromatin level, where all three RUNX proteins bind the canonical RUNT motif (5′-PuACCPuCA-3′) at target DNA sites. Such interaction can occur in proximity to the target TSS within the promoter regions or can be more distal to the genebody and even within the genebody, for example in intronic regions [299]. The transcriptional activity of RUNX is highly dependent on the interaction with myriads of other transcriptional modulators in a cell-specific manner. Aside from direct DNA binding, RUNX can also exert influence on a number of important signalling pathways. For instance, all three RUNX are involved in the regulation of the Wnt/β-catenin pathway [300] as well as the TGFβ-regulated signalling cascade [273].

The molecular mechanisms of each of the RUNX proteins have been studied at some length, especially in the context of cancer and development. As all RUNX proteins share similar key domains, including RHD and AD/NMTS that are prime targets for co-modulator binding, it is likely that the three RUNX transcription factors share a number of mutual co-regulators. However, not only have mutual molecular pathways identified in these three proteins, a number of distinct mechanisms have also been discovered for each protein, suggesting that RUNX proteins possess a level of redundancy as well as specificity depending on the biological context.

1.4.4.1 Transcriptional co-regulators of RUNX

The bulk of literature on RUNX mechanisms is in the context of carcinoma and development, in which areas RUNX members historically play prominent roles. As previously discussed for PGR, such interactions are often highly cell-specific and cannot be inferred for all biological contexts. However, as a number of known co-modulators of RUNX are concurrently expressed in granulosa cells during ovulation, it is reasonable to expect a level of similarities in co-modulator dependent RUNX regulatory mechanisms and if this is not the case, it would be of interest to investigate the specificity of such interactions in the context of reproduction.

Like other transcription factors, the roles of RUNX proteins are reliant on interactions with various co-modulators in a context-specific manner. In the context of osteoblast functions, where RUNX proteins have prominent roles, interactions with other transcription factors such as TWIST1 [301], CEBPβ [302], c-JUN and c-FOS [303] are important in RUNX transcriptional regulatory functions. In megakaryocytes, the interaction between RUNX1 and GATA1 promotes cell differentiation [304]. In lymphocytes, the RUNX interactome, including members of the T-box [305] and ETS families [303], is involved in cell fate determination and differentiation. Interestingly, members of the GATA and JUN/FOS family have been show to play important roles in ovulation, including GATA4, GATA6 [306], c-JUN and c-FOS, among other JUN/FOS members [223]. It would be of interest to investigate the interaction between RUNX and these transcription factors in the context of female reproduction. While RUNX proteins play various roles in different parts of the female reproductive tract, the role of the relevant interactomes have not been discussed in any of these tissue types, rendering the tissue-specific underlying mechanisms of RUNX poorly understood.

There is evidence for RUNX roles in regulating SR-induced gene expression. RUNX1 and RUNX2 have been shown to interact with AR and GR at the *Slp* enhancer element *in vitro*, suggesting a role of RUNX proteins in regulating hormone-induced transcription [307]. Such interaction is through the DBD that is typical of all SR, thus it is likely that RUNX can also form physical interactions with other SR. Subsequent studies have elucidated the impact of such interactions, such as the synergistic regulation of *Snai2* by AR and RUNX2 in prostate cancer [308], the trans-sequestering effect of AR and RUNX2 on each other in osteoblasts [309] and functional links between AR and RUNX1 in epididymis epithelial cells [310]. RUNX also plays a role in ER-α functions, as shown in bones [311] and breast cancer [312].

Not only can RUNX proteins act as pioneer factors through direct tethering other transcription factors to novel target chromatins but can also exert their influence through promoting chromosomal conformational changes, allowing for the formation of open chromatin spaces that are available for the occupancy of other transcription factors. In support of this, evidence has indicated the cooperation between RUNX1 and RUNX2 with the SWI/SNF chromatin remodelling complex. RUNX1 shares mutual chromatin binding sites with SWI/SNF components at genes that are important in haematopoiesis and has a role in the recruitment of the SWI/SNF complex to such binding sites, therefore exhibiting a recruiter function [303]. In leukaemia cell lines the presence of RUNX1 is also important in maintaining chromatin

accessibility, as shown in reduced histone 3 lysine 27 acetylation (H3K27ac) markers at RUNX1 binding targets [313]. For RUNX2, interaction with SWI/SNF is observed in osteoblast and dependent on the co-biding of CEBPβ .

Whilst RUNX proteins are mainly known for activation functions, RUNX can also interact with a number of co-repressors in order to suppress specific gene expression. One such co-repressors is the Groucho/TLE/Grg (TLE) family through the VWRPY motif at the C-terminus of RUNX. TLE proteins are ubiquitous repressors that are employed by various transcription factors and specifically the interaction of RUNX2 with TLE leads to the repression of RUNX2-regulated promoters [314]. Additionally, RUNX1 also interacts with mSin3A, a stabilising component of the HDAC complex, resulting in the expression of RUNX1-modulated genes. RUNX can also form interaction with various HDAC proteins, including HDAC1-4 and HDAC6 in various biological contexts [303,314]. Such interactions result in transcriptional suppression of target genes through various means, either from altering the open chromatin state, modifying nearby transcription modulators or preventing RUNX from binding target DNA. In one example observed in the SAOS-2 osteosarcoma cell line, RUNX2 is shown to repress rRNA synthesis through recruiting the histone acetyltransferase HDAC1 to target rRNA repeats, leading to the deacetylation of the upstream regulator UBF which is important for the expression of rRNA genes [315]. In another, HDAC4-RUNX2 interaction in chondrocytes blocks RUNX2 from accessing target DNA, thereby inhibiting RUNX2 transcriptional activities [316]. Other co-repressors of RUNX include CoAA [317], the Polycomb repressor complex [318] and SKI [319]. In other instances, interactions with other transcription factors that are not global transcription suppressors can also have a repressive effect on RUNX transactivation activities. For example, FOXP3 can bind RUNX1 at its ID region to inhibit RUNX1 action in T-lymphocytes; similarly, interaction between RUNX2 and SOX9 promotes degradation of RUNX2 in mesenchymal stem cells [303]. Furthermore, there are cases where one co-factor can have multiple specific effects on RUNX activities, such as YAP1, which acts as a repressor to RUNX2 [314] but can enhance transcriptional activator when binding to RUNX3 [320].

1.4.4.2 RUNX action on enhancers

Apart from its role at target promoters, RUNX can also exert influence on gene expression through distal enhancer elements. This has been described in various haematopoietic cell lines in which RUNX1 regulates the expression of *Cebpa* [321], *Myb* and *Myc* [313], *Cd4* [322] and members

of the *Tcr* family [323]. In natural killer T cell precursor cells, RUNX1 also interacts with specific enhancer loci in the introns of *Zbtb16* in order to regulate its expression [324]. Similarly, RUNX2 can direct the expression of *Col10a1* in chondrocytes [325], *Snai2* in prostate cancer [308] and *Mmp13* in osteoblasts [326] through binding their respective upstream enhancers.

1.5 HYPOTHESIS & AIMS

1.5.1 Main hypothesis

The process of ovulation, regulated by various regulatory elements acting in coordination with one another, is critical for successful fertilisation and pregnancy. The expression of PGR in mural granulosa cells is especially essential for ovulation in which PGR acts as a master transcription factor for various downstream biological processes that are necessary for ovulation to occur. Elsewhere in the female reproductive tract, PGR is vital for the coordination of a number of reproductive processes occurring prior to and during pregnancy, including the transportation of oocytes and embryos, the preparation for embryo implantation and the regulation of labour. Although much is known about the physiological consequence of PGR activity in reproductive tissues, exactly how these unique roles are achieved on a molecular level in a tissue-specific manner is not understood. Combining the fact that PGR can target chromatin through binding diverse motifs and that PGR is known to cooperate with many transcription factors in different tissue settings, it is likely that partnerships with unique co-regulators allow PGR to achieve tissue-specific chromatin binding and gene regulatory patterns. This study aims to discover finely-tuned contextual PGR-chromatin interactions and tissue-specific roles of PGR, specifically in the ovulating ovary, in combination with comparisons across the reproductive tract, to understand the shared and unique activities of PGR. The refined mechanistic understanding of ovulation and PGR action will identify new targets for contraceptive and cancer therapeutics, while also reveal novel approaches for the management of ovulatory infertility.

Thus, the main hypothesis of this thesis is that:

Progesterone receptor interacts with other transcription factors in tissue-specific complexes to target unique chromatin sites in different reproductive tissues, leading to tissue-specific gene expression and hence pleiotropic regulation of reproductive functions.

1.5.2 Specific hypotheses and aims

Hypothesis 1: The PGR cistrome in different reproductive tissues possesses unique patterns that are important to the regulation of tissue-specific genes and functions

PGR is essential for various functions in the female reproductive tract, especially ovulation in the ovary. To perform these diverse roles, PGR regulates highly divergent gene sets in each organ. It is likely that a fundamental divergence between PGR functions in each tissue is due to differences in PGR-chromatin binding patterns, but this has not been directly investigated.

To address this hypothesis, the aims were to:

- Characterise the PGR cistrome in peri-ovulatory granulosa cells through PGR chromatin immunoprecipitation – sequencing (ChIP-seq)
- Define the active chromatin landscape in peri-ovulatory granulosa cells through H3K27ac ChIP-seq
- Characterise the relationship between PGR cistrome and the active chromatin landscape along with the PGR-dependent granulosa cell transcriptome identified through microarray and the complete ovulatory gene expression profile during ovulation identified through RNA-seq
- Identify tissue-specific characteristics of PGR regulation in mouse reproductive tissues through comparison of PGR-bound cistromes in ovary and uterus

The results for this hypothesis are in Chapter 2 and 3.

Hypothesis 2: PGR interacts with a selective group of co-regulators in granulosa cells during ovulation

Analysis of the PGR cistrome indicated possible interaction between PGR and other transcription factors in granulosa cells and that selective interaction between PGR and tissue-specific co-regulators could explain how PGR achieve unique roles in reproductive tissues. PGR and other NR3C receptors are also known to interact with other transcription factors in other cell types. Furthermore, a number of ncRNA has also been identified as regulators to PGR and NR3C receptor function. However, the transcription complex containing PGR in granulosa cells has never been investigated.

To address this hypothesis, the aims were to:

- Identify transcription factors that are present in the PGR transcription complex in peri-ovulatory granulosa cells through proximity ligation assay

- Confirm the presence of ncRNA partners in the PGR transcription complex in peri-ovulatory granulosa cells through RNA co-immunoprecipitation

The results for this hypothesis are in Chapter 4.

Hypothesis 3: RUNX1 is a co-regulator of PGR in peri-ovulatory granulosa cells

Results from Hypotheses 1 and 2 indicated a possible role of RUNX1 as a PGR co-regulator. While RUNX1 regulates gene expression in granulosa cells during ovulation, the overall RUNX1-dependent transcriptome has never been previously described. It is likely that RUNX1 and PGR share similar chromatin binding properties and this interaction may be a part of the mechanism for unique chromatin-binding and specific ovulatory functions for each transcription factor, which in turn affects the granulosa cell transcriptome.

To address this hypothesis, the aims were to:

- Characterise the properties of RUNX1 cistromes in different developmental stages through comparative analysis of RUNX1 cistrome in adult and foetal granulosa cells, especially differences in RUNX1 target chromatin before and after the LH surge
- Identify similarities between PGR and RUNX1 chromatin binding properties in peri-ovulatory granulosa cells through comparative analysis of PGR and RUNX1 ChIP-seq and their consequence on ovulatory gene expression profile
- Investigate the dynamics of the interaction between PGR and RUNX1 in response to ovulatory cues through proximity ligation assay

The results for this hypothesis are in Chapter 5 and 6.

Hypothesis 4: PGR isoforms mediate distinctive regulation of genes in granulosa cells during ovulation

PGR consists of two main isoforms, PGR-A and PGR-B, which can have different expression pattern and are responsible for various unique roles in different tissue contexts. While both are present in the reproductive tract, PGR-A is the only one known to be essential for ovulation while PGR-B plays a lesser role in the reproductive tract. However, the specific roles of PGR isoforms on gene expression in peri-ovulatory granulosa cells have not been previously investigated in detail.

To address this hypothesis, the aims were to:

- Identify the unique roles of PGR isoforms in the peri-ovulatory transcriptome through comparative analysis of PGRKO, AKO and BKO vs WT RNA-seq

- Investigate the relationship between PGR and RUNX1 cistrome on isoform-specific cistromes

The results for this hypothesis are in Chapter 7.

1.6 REFERENCES

1 Richards, J. S. in *Vitamins and Hormones* Vol. 107 (ed Gerald Litwack) 1-25 (Academic Press, 2018).

2 Bury, L., Coelho, P. A. & Glover, D. M. in *Current Topics in Developmental Biology* Vol. 120 (ed Melvin L. DePamphilis) 125-171 (Academic Press, 2016).

3 Virant-Klun, I., Knez, K., Tomazevic, T. & Skutella, T. Gene expression profiling of human oocytes developed and matured in vivo or in vitro. *BioMed research international* **2013** (2013).

4 Prochazka, R., Blaha, M. & Nemcova, L. Significance of epidermal growth factor receptor signaling for acquisition of meiotic and developmental competence in mammalian oocytes. *Biol Reprod* **97**, 537-549, doi:10.1093/biolre/iox112 (2017).

5 Liang, C.-G., Su, Y.-Q., Fan, H.-Y., Schatten, H. & Sun, Q.-Y. Mechanisms Regulating Oocyte Meiotic Resumption: Roles of Mitogen-Activated Protein Kinase. *Molecular Endocrinology* **21**, 2037-2055, doi:10.1210/me.2006-0408 (2007).

6 Yesilaltay, A., Dokshin, G. A., Busso, D., Wang, L., Galiani, D., Chavarria, T., Vasile, E., Quilaqueo, L., Orellana, J. A., Walzer, D., Shalgi, R., Dekel, N., Albertini, D. F., Rigotti, A., Page, D. C. & Krieger, M. Excess cholesterol induces mouse egg activation and may cause female infertility. *Proceedings of the National Academy of Sciences* **111**, E4972-E4980, doi:10.1073/pnas.1418954111 (2014).

7 Rimon-Dahari, N., Yerushalmi-Heinemann, L., Alyagor, L. & Dekel, N. in *Molecular Mechanisms of Cell Differentiation in Gonad Development* (ed Rafal P. Piprek) 167-190 (Springer International Publishing, 2016).

8 Borgbo, T., Povlsen, B. B., Andersen, C. Y., Borup, R., Humaidan, P. & Grøndahl, M. L. Comparison of gene expression profiles in granulosa and cumulus cells after ovulation induction with either human chorionic gonadotropin or a gonadotropin-releasing hormone agonist trigger. *Fertility and Sterility* **100**, 994-1001.e1002, doi:https://doi.org/10.1016/j.fertnstert.2013.05.038 (2013).

9 Nicol, B. & Yao, H. H. C. Building an Ovary: Insights into Establishment of Somatic Cell Lineages in the Mouse. *Sexual Development* **8**, 243-251, doi:10.1159/000358072 (2014).

10 Uyar, A., Torrealday, S. & Seli, E. Cumulus and granulosa cell markers of oocyte and embryo quality. *Fertility and sterility* **99**, 979-997, doi:10.1016/j.fertnstert.2013.01.129 (2013).

11 Diaz, F. J., Wigglesworth, K. & Eppig, J. J. Oocytes determine cumulus cell lineage in mouse ovarian follicles. *Journal of Cell Science* **120**, 1330-1340, doi:10.1242/jcs.000968 (2007).

12 Monsivais, D., Matzuk, M. M. & Pangas, S. A. The TGF-β Family in the Reproductive Tract. *Cold Spring Harb Perspect Biol* **9**, a022251, doi:10.1101/cshperspect.a022251 (2017).

13 Patel, S., Zhou, C., Rattan, S. & Flaws, J. A. Effects of Endocrine-Disrupting Chemicals on the Ovary1. *Biology of Reproduction* **93**, doi:10.1095/biolreprod.115.130336 (2015).

14 Padmanabhan, V. & Cardoso, R. C. Neuroendocrine, autocrine, and paracrine control of follicle-stimulating hormone secretion. *Molecular and Cellular Endocrinology* **500**, 110632, doi:https://doi.org/10.1016/j.mce.2019.110632 (2020).

15 Casarini, L. & Crépieux, P. Molecular Mechanisms of Action of FSH. *Frontiers in Endocrinology* **10**, doi:10.3389/fendo.2019.00305 (2019).

16 Welt, C. & Schneyer, A. in *The Ovary (Third Edition)* (eds Peter C. K. Leung & Eli Y. Adashi) 95-105 (Academic Press, 2019).

17 Russell, D. L. & Robker, R. L. in *The Ovary (Third Edition)* (eds Peter C. K. Leung & Eli Y. Adashi) 217-234 (Academic Press, 2019).
18 Duffy, D. M., Ko, C., Jo, M., Brannstrom, M. & Curry, T. E., Jr. Ovulation: Parallels With Inflammatory Processes. *Endocrine Reviews* **40**, 369-416, doi:10.1210/er.2018-00075 (2018).
19 Pakarainen, T., Zhang, F.-P., Nurmi, L., Poutanen, M. & Huhtaniemi, I. Knockout of Luteinizing Hormone Receptor Abolishes the Effects of Follicle-Stimulating Hormone on Preovulatory Maturation and Ovulation of Mouse Graafian Follicles. *Molecular Endocrinology* **19**, 2591-2602, doi:10.1210/me.2005-0075 (2005).
20 Fan, H. Y., Liu, Z., Shimada, M., Sterneck, E., Johnson, P. F., Hedrick, S. M. & Richards, J. S. MAPK3/1 (ERK1/2) in ovarian granulosa cells are essential for female fertility. *Science* **324**, 938-941, doi:10.1126/science.1171396 (2009).
21 Zhang, Y.-L., Xia, Y., Yu, C., Richards, J. S., Liu, J. & Fan, H.-Y. CBP-CITED4 is required for luteinizing hormone-triggered target gene expression during ovulation. *Molecular Human Reproduction* **20**, 850-860, doi:10.1093/molehr/gau040 (2014).
22 Fan, H.-Y., Liu, Z., Johnson, P. F. & Richards, J. S. CCAAT/Enhancer-Binding Proteins (C/EBP)-α and -β Are Essential for Ovulation, Luteinization, and the Expression of Key Target Genes. *Molecular Endocrinology* **25**, 253-268, doi:10.1210/me.2010-0318 (2011).
23 Kim, J., Bagchi, I. C. & Bagchi, M. K. Control of ovulation in mice by progesterone receptor-regulated gene networks. *Molecular Human Reproduction* **15**, 821-828, doi:10.1093/molehr/gap082 (2009).
24 Henríquez, S., Kohen, P., Muñoz, A., Godoy, A., Orge, F., Strauss, J. F. & Devoto, L. In-vitro study of gonadotrophin signaling pathways in human granulosa cells in relation to progesterone receptor expression. *Reproductive BioMedicine Online* **35**, 363-371, doi:https://doi.org/10.1016/j.rbmo.2017.06.011 (2017).
25 Chen, D.-b. & Davis, J. S. Epidermal growth factor induces c-fos and c-jun mRNA via Raf-1/MEK1/ERK-dependent and -independent pathways in bovine luteal cells. *Molecular and Cellular Endocrinology* **200**, 141-154, doi:https://doi.org/10.1016/S0303-7207(02)00379-9 (2003).
26 Wang, Y., Hao, X., Yang, J., Li, J. & Zhang, M. CREB activity is required for luteinizing hormone-induced the expression of EGF-like factors. *Molecular reproduction and development* **83**, 1116-1127, doi:10.1002/mrd.22753 (2016).
27 Miller, R. S., Wolfe, A., He, L., Radovick, S. & Wondisford, F. E. CREB Binding Protein (CBP) Activation Is Required for Luteinizing Hormone Beta Expression and Normal Fertility in Mice. *Molecular and cellular biology* **32**, 2349-2358, doi:10.1128/mcb.00394-12 (2012).
28 Clem, B. F., Hudson, E. A. & Clark, B. J. Cyclic adenosine 3',5'-monophosphate (cAMP) enhances cAMP-responsive element binding (CREB) protein phosphorylation and phospho-CREB interaction with the mouse steroidogenic acute regulatory protein gene promoter. *Endocrinology* **146**, 1348-1356, doi:10.1210/en.2004-0761 (2005).
29 Ito, M., Park, Y., Weck, J., Mayo, K. E. & Jameson, J. L. Synergistic activation of the inhibin α-promoter by steroidogenic factor-1 and cyclic adenosine 3′, 5′-monophosphate. *Molecular Endocrinology* **14**, 66-81 (2000).
30 Russell, D. L., Doyle, K. M. H., Gonzales-Robayna, I., Pipaon, C. & Richards, J. S. Egr-1 Induction in Rat Granulosa Cells by Follicle-Stimulating Hormone and Luteinizing Hormone: Combinatorial Regulation By Transcription Factors Cyclic Adenosine 3′,5′-Monophosphate Regulatory Element Binding Protein, Serum Response Factor, Sp1, and Early Growth Response Factor-1. *Molecular Endocrinology* **17**, 520-533, doi:10.1210/me.2002-0066 (2003).

31 He, P.-J., Hirata, M., Yamauchi, N., Hashimoto, S. & Hattori, M.-a. Gonadotropic regulation of circadian clockwork in rat granulosa cells. *Molecular and Cellular Biochemistry* **302**, 111-118, doi:10.1007/s11010-007-9432-7 (2007).

32 Sassone-Corsi, P., Visvader, J., Ferland, L., Mellon, P. L. & Verma, I. M. Induction of proto-oncogene fos transcription through the adenylate cyclase pathway: characterization of a cAMP-responsive element. *Genes & Development* **2**, 1529-1538, doi:10.1101/gad.2.12a.1529 (1988).

33 Fang, L., Chang, H.-M., Cheng, J.-C., Leung, P. C. K. & Sun, Y.-P. Nitric Oxide and cGMP Induce COX-2 Expression and PGE2 Production in Human Granulosa Cells Through CREB Signaling Pathway. *The Journal of Clinical Endocrinology & Metabolism* **100**, E262-E269, doi:10.1210/jc.2014-2886 (2015).

34 Carlone, D. L. & Richards, J. S. Evidence that functional interactions of CREB and SF-1 mediate hormone regulated expression of the aromatase gene in granulosa cells and constitutive expression in R2C cells. *The Journal of Steroid Biochemistry and Molecular Biology* **61**, 223-231, doi:https://doi.org/10.1016/S0960-0760(97)80016-7 (1997).

35 Sriraman, V. & Richards, J. S. Cathepsin L Gene Expression and Promoter Activation in Rodent Granulosa Cells. *Endocrinology* **145**, 582-591, doi:10.1210/en.2003-0963 (2004).

36 Nacht, A. S., Ferrari, R., Zaurin, R., Scabia, V., Carbonell-Caballero, J., Le Dily, F., Quilez, J., Leopoldi, A., Brisken, C., Beato, M. & Vicent, G. P. C/EBPalpha mediates the growth inhibitory effect of progestins on breast cancer cells. *EMBO J* **38**, e101426, doi:10.15252/embj.2018101426 (2019).

37 Henry, R. A., Kuo, Y. M. & Andrews, A. J. Differences in specificity and selectivity between CBP and p300 acetylation of histone H3 and H3/H4. *Biochemistry* **52**, 5746-5759, doi:10.1021/bi400684q (2013).

38 Edwards, D. P. The Role of Coactivators and Corepressors in the Biology and Mechanism of Action of Steroid Hormone Receptors. *Journal of Mammary Gland Biology and Neoplasia* **5**, 307-324, doi:10.1023/a:1009503029176 (2000).

39 Béguelin, W., Díaz Flaqué, M. C., Proietti, C. J., Cayrol, F., Rivas, M. A., Tkach, M., Rosemblit, C., Tocci, J. M., Charreau, E. H., Schillaci, R. & Elizalde, P. V. Progesterone receptor induces ErbB-2 nuclear translocation to promote breast cancer growth via a novel transcriptional effect: ErbB-2 function as a coactivator of Stat3. *Molecular and cellular biology* **30**, 5456-5472, doi:10.1128/MCB.00012-10 (2010).

40 Boija, A., Mahat, D. B., Zare, A., Holmqvist, P.-H., Philip, P., Meyers, D. J., Cole, P. A., Lis, J. T., Stenberg, P. & Mannervik, M. CBP Regulates Recruitment and Release of Promoter-Proximal RNA Polymerase II. *Molecular Cell* **68**, 491-503.e495, doi:https://doi.org/10.1016/j.molcel.2017.09.031 (2017).

41 Silverman, E., Yivgi-Ohana, N., Sher, N., Bell, M., Eimerl, S. & Orly, J. Transcriptional activation of the steroidogenic acute regulatory protein (StAR) gene: GATA-4 and CCAAT/enhancer-binding protein β confer synergistic responsiveness in hormone-treated rat granulosa and HEK293 cell models. *Molecular and Cellular Endocrinology* **252**, 92-101, doi:https://doi.org/10.1016/j.mce.2006.03.008 (2006).

42 Shih, M.-C. M., Chiu, Y.-N., Hu, M.-C., Guo, I.-C. & Chung, B.-c. Regulation of steroid production: Analysis of Cyp11a1 promoter. *Molecular and Cellular Endocrinology* **336**, 80-84, doi:https://doi.org/10.1016/j.mce.2010.12.017 (2011).

43 Weck, J. & Mayo, K. E. Switching of NR5A Proteins Associated with the Inhibin a-Subunit Gene Promoter Following Activation of the Gene in Granulosa Cells. (2006).

44 Huang, Y., Shen, X. J., Zou, Q., Wang, S. P., Tang, S. M. & Zhang, G. Z. Biological functions of microRNAs: a review. *Journal of Physiology and Biochemistry* **67**, 129-139, doi:10.1007/s13105-010-0050-6 (2011).

45 Cheng, J.-T., Wang, L., Wang, H., Tang, F.-R., Cai, W.-Q., Sethi, G., Xin, H.-W. & Ma, Z. Insights into Biological Role of LncRNAs in Epithelial-Mesenchymal Transition. *Cells* **8**, 1178 (2019).

46 Xu, X.-F., Li, J., Cao, Y.-X., Chen, D.-W., Zhang, Z.-G., He, X.-J., Ji, D.-M. & Chen, B.-L. Differential Expression of Long Noncoding RNAs in Human Cumulus Cells Related to Embryo Developmental Potential:A Microarray Analysis. *Reproductive Sciences* **22**, 672-678, doi:10.1177/1933719114561562 (2015).

47 Li, J., Cao, Y., Xu, X., Xiang, H., Zhang, Z., Chen, B., Hao, Y., Wei, Z., Zhou, P. & Chen, D. Increased New lncRNA–mRNA Gene Pair Levels in Human Cumulus Cells Correlate With Oocyte Maturation and Embryo Development. *Reproductive Sciences*, doi:10.1177/1933719115570911 (2015).

48 Yerushalmi, G. M., Salmon-Divon, M., Yung, Y., Maman, E., Kedem, A., Ophir, L., Elemento, O., Coticchio, G., Dal Canto, M., Mignini Renzinu, M., Fadini, R. & Hourvitz, A. Characterization of the human cumulus cell transcriptome during final follicular maturation and ovulation. *Molecular Human Reproduction* **20**, 719-735, doi:10.1093/molehr/gau031 (2014).

49 Battaglia, R., Vento, M. E., Borzì, P., Ragusa, M., Barbagallo, D., Arena, D., Purrello, M. & Di Pietro, C. Non-coding RNAs in the Ovarian Follicle. *Frontiers in Genetics* **8**, doi:10.3389/fgene.2017.00057 (2017).

50 Liu, K.-S., Li, T.-P., Ton, H., Mao, X.-D. & Chen, Y.-J. Advances of Long Noncoding RNAs-mediated Regulation in Reproduction. *Chin Med J (Engl)* **131**, 226-234, doi:10.4103/0366-6999.222337 (2018).

51 Nakagawa, S., Shimada, M., Yanaka, K., Mito, M., Arai, T., Takahashi, E., Fujita, Y., Fujimori, T., Standaert, L., Marine, J.-C. & Hirose, T. The lncRNA Neat1 is required for corpus luteum formation and the establishment of pregnancy in a subpopulation of mice. *Development* **141**, 4618-4627, doi:10.1242/dev.110544 (2014).

52 Pickard, M. R. & Williams, G. T. Molecular and Cellular Mechanisms of Action of Tumour Suppressor GAS5 LncRNA. *Genes* **6**, 484-499 (2015).

53 Hudson, W. H., Pickard, M. R., de Vera, I. M., Kuiper, E. G., Mourtada-Maarabouni, M., Conn, G. L., Kojetin, D. J., Williams, G. T. & Ortlund, E. A. Conserved sequence-specific lincRNA-steroid receptor interactions drive transcriptional repression and direct cell fate. *Nat Commun* **5**, 5395, doi:10.1038/ncomms6395 (2014).

54 Ernst, E. H., Nielsen, J., Ipsen, M. B., Villesen, P. & Lykke-Hartmann, K. Transcriptome Analysis of Long Non-coding RNAs and Genes Encoding Paraspeckle Proteins During Human Ovarian Follicle Development. *Frontiers in Cell and Developmental Biology* **6**, doi:10.3389/fcell.2018.00078 (2018).

55 Gebhardt, K. M., Feil, D. K., Dunning, K. R., Lane, M. & Russell, D. L. Human cumulus cell gene expression as a biomarker of pregnancy outcome after single embryo transfer. *Fertility and Sterility* **96**, 47-52.e42, doi:http://dx.doi.org/10.1016/j.fertnstert.2011.04.033 (2011).

56 Hourvitz, A., Ophir, L., Yung, Y., Orvieto, R. & Yerushalmi, G. M. Characterization of the human ovulatory non-coding transcriptome reveals mirnas as new regulators of the ovulatory cascade. *Fertility and Sterility* **104**, e135, doi:10.1016/j.fertnstert.2015.07.418 (2015).

57 Fitzgerald, J. B., George, J. & Christenson, L. K. in *Non-coding RNA and the Reproductive System* (eds Dagmar Wilhelm & Pascal Bernard) 79-93 (Springer Netherlands, 2016).

58 Hasuwa, H., Ueda, J., Ikawa, M. & Okabe, M. MiR-200b and miR-429 Function in Mouse Ovulation and Are Essential for Female Fertility. *Science* **341**, 71-73, doi:10.1126/science.1237999 (2013).

59 Robles, V., Valcarce, D. G. & Riesco, M. F. Non-coding RNA regulation in reproduction: Their potential use as biomarkers. *Non-coding RNA Research* **4**, 54-62, doi:https://doi.org/10.1016/j.ncrna.2019.04.001 (2019).

60 Yokoo, M. & Sato, E. Physiological function of hyaluronan in mammalian oocyte maturation. *Reprod Med Biol* **10**, 221-229, doi:10.1007/s12522-011-0093-6 (2011).

61 Shimada, M., Hernandez-Gonzalez, I., Gonzalez-Robayna, I. & Richards, J. S. Paracrine and Autocrine Regulation of Epidermal Growth Factor-Like Factors in Cumulus Oocyte Complexes and Granulosa Cells: Key Roles for Prostaglandin Synthase 2 and Progesterone Receptor. *Molecular Endocrinology* **20**, 1352-1365, doi:10.1210/me.2005-0504 (2006).

62 Hsieh, M., Lee, D., Panigone, S., Horner, K., Chen, R., Theologis, A., Lee, D. C., Threadgill, D. W. & Conti, M. Luteinizing Hormone-Dependent Activation of the Epidermal Growth Factor Network Is Essential for Ovulation. *Molecular and cellular biology* **27**, 1914-1924, doi:10.1128/mcb.01919-06 (2007).

63 Rugg, M. S., Willis, A. C., Mukhopadhyay, D., Hascall, V. C., Fries, E., Fülöp, C., Milner, C. M. & Day, A. J. Characterization of Complexes Formed between TSG-6 and Inter-α-inhibitor That Act as Intermediates in the Covalent Transfer of Heavy Chains onto Hyaluronan. *Journal of Biological Chemistry* **280**, 25674-25686, doi:10.1074/jbc.M501332200 (2005).

64 Camaioni, A., Klinger, F. G., Campagnolo, L. & Salustri, A. The Influence of Pentraxin 3 on the Ovarian Function and Its Impact on Fertility. *Frontiers in Immunology* **9**, doi:10.3389/fimmu.2018.02808 (2018).

65 Russell, D. L., Ochsner, S. A., Hsieh, M., Mulders, S. & Richards, J. S. Hormone-Regulated Expression and Localization of Versican in the Rodent Ovary. *Endocrinology* **144**, 1020-1031, doi:10.1210/en.2002-220434 (2003).

66 Brown, H. M., Dunning, K. R., Robker, R. L., Boerboom, D., Pritchard, M., Lane, M. & Russell, D. L. ADAMTS1 Cleavage of Versican Mediates Essential Structural Remodeling of the Ovarian Follicle and Cumulus-Oocyte Matrix During Ovulation in Mice1. *Biology of Reproduction* **83**, 549-557, doi:10.1095/biolreprod.110.084434 (2010).

67 Fülöp, C., Szántó, S., Mukhopadhyay, D., Bárdos, T., Kamath, R. V., Rugg, M. S., Day, A. J., Salustri, A., Hascall, V. C., Glant, T. T. & Mikecz, K. Impaired cumulus mucification and female sterility in tumor necrosis factor-induced protein-6 deficient mice. *Development* **130**, 2253-2261, doi:10.1242/dev.00422 (2003).

68 Shimada, M. & Yamashita, Y. The Key Signaling Cascades in Granulosa Cells during Follicular Development and Ovulation Process. *Journal of Mammalian Ova Research* **28**, 25-31, doi:10.1274/jmor.28.25 (2011).

69 Niringiyumukiza, J. D., Cai, H. & Xiang, W. Prostaglandin E2 involvement in mammalian female fertility: ovulation, fertilization, embryo development and early implantation. *Reprod Biol Endocrinol* **16**, 43-43, doi:10.1186/s12958-018-0359-5 (2018).

70 Ashkenazi, H., Cao, X., Motola, S., Popliker, M., Conti, M. & Tsafriri, A. Epidermal Growth Factor Family Members: Endogenous Mediators of the Ovulatory Response. *Endocrinology* **146**, 77-84, doi:10.1210/en.2004-0588 (2005).

71 Paulini, F. & Melo, E. O. The Role of Oocyte-Secreted Factors GDF9 and BMP15 in Follicular Development and Oogenesis. *Reproduction in Domestic Animals* **46**, 354-361, doi:10.1111/j.1439-0531.2010.01739.x (2011).

72 Hulboy, D. L., Rudolph, L. A. & Matrisian, L. M. Matrix metalloproteinases as mediators of reproductive function. *Molecular Human Reproduction* **3**, 27-45, doi:10.1093/molehr/3.1.27 (1997).
73 Curry, T. E., Jr., Song, L. & Wheeler, S. E. Cellular Localization of Gelatinases and Tissue Inhibitors of Metalloproteinases During Follicular Growth, Ovulation, and Early Luteal Formation in the Rat1. *Biology of Reproduction* **65**, 855-865, doi:10.1095/biolreprod65.3.855 (2001).
74 Puttabyatappa, M., Jacot, T. A., Al-Alem, L. F., Rosewell, K. L., Duffy, D. M., Brännström, M. & Curry, T. E., Jr. Ovarian Membrane-Type Matrix Metalloproteinases: Induction of MMP14 and MMP16 During the Periovulatory Period in the Rat, Macaque, and Human1. *Biology of Reproduction* **91**, doi:10.1095/biolreprod.113.115717 (2014).
75 Hagglund, A. C., Ny, A., Leonardsson, G. & Ny, T. Regulation and localization of matrix metalloproteinases and tissue inhibitors of metalloproteinases in the mouse ovary during gonadotropin-induced ovulation. *Endocrinology* **140**, 4351-4358, doi:10.1210/endo.140.9.7002 (1999).
76 Liu, Y.-X., Liu, X.-M., Nin, L.-F., Shi, L. & Chen, S.-R. Serine protease and ovarian paracrine factors in regulation of ovulation. *Front Biosci (Landmark Ed)* **18**, 650-664 (2013).
77 Robker, R. L., Russell, D. L., Espey, L. L., Lydon, J. P., O'Malley, B. W. & Richards, J. S. Progesterone-regulated genes in the ovulation process: ADAMTS-1 and cathepsin L proteases. *Proc Natl Acad Sci U S A* **97**, 4689-4694 (2000).
78 Light, A. & Hammes, S. R. LH-Induced Steroidogenesis in the Mouse Ovary, but Not Testis, Requires Matrix Metalloproteinase 2- and 9-Mediated Cleavage of Upregulated EGF Receptor Ligands. *Biol Reprod* **93**, 65, doi:10.1095/biolreprod.115.130971 (2015).
79 Oakley, O. R., Kim, H., El-Amouri, I., Patrick Lin, P.-C., Cho, J., Bani-Ahmad, M. & Ko, C. Periovulatory Leukocyte Infiltration in the Rat Ovary. *Endocrinology* **151**, 4551-4559, doi:10.1210/en.2009-1444 (2010).
80 Wu, R., Van der Hoek, K. H., Ryan, N. K., Norman, R. J. & Robker, R. L. Macrophage contributions to ovarian function. *Human Reproduction Update* **10**, 119-133, doi:10.1093/humupd/dmh011 (2004).
81 Van der Hoek, K. H., Maddocks, S., Woodhouse, C. M., van Rooijen, N., Robertson, S. A. & Norman, R. J. Intrabursal Injection of Clodronate Liposomes Causes Macrophage Depletion and Inhibits Ovulation in the Mouse Ovary1. *Biology of Reproduction* **62**, 1059-1066, doi:10.1095/biolreprod62.4.1059 (2000).
82 Basini, G. & Grasselli, F. Nitric oxide in follicle development and oocyte competence. *Reproduction* **150**, R1-R9 (2015).
83 Liu, Z., de Matos, D. G., Fan, H.-Y., Shimada, M., Palmer, S. & Richards, J. S. Interleukin-6: An Autocrine Regulator of the Mouse Cumulus Cell-Oocyte Complex Expansion Process. *Endocrinology* **150**, 3360-3368, doi:10.1210/en.2008-1532 (2009).
84 Murphy, M. J., Halow, N. G., Royer, P. A. & Hennebold, J. D. Leukemia Inhibitory Factor Is Necessary for Ovulation in Female Rhesus Macaques. *Endocrinology* **157**, 4378-4387, doi:10.1210/en.2016-1283 (2016).
85 Shimada, M., Yanai, Y., Okazaki, T., Noma, N., Kawashima, I., Mori, T. & Richards, J. S. Hyaluronan fragments generated by sperm-secreted hyaluronidase stimulate cytokine/chemokine production via the TLR2 and TLR4 pathway in cumulus cells of ovulated COCs, which may enhance fertilization. *Development* **135**, 2001-2011, doi:10.1242/dev.020461 (2008).

86 Mauro, A., Martelli, A., Berardinelli, P., Russo, V., Bernabò, N., Di Giacinto, O., Mattioli, M. & Barboni, B. Effect of Antiprogesterone RU486 on VEGF Expression and Blood Vessel Remodeling on Ovarian Follicles before Ovulation. *PLOS ONE* **9**, e95910, doi:10.1371/journal.pone.0095910 (2014).

87 Tamanini, C. & De Ambrogi, M. Angiogenesis in Developing Follicle and Corpus Luteum. *Reproduction in Domestic Animals* **39**, 206-216, doi:10.1111/j.1439-0531.2004.00505.x (2004).

88 Fraser, H. M., Wilson, H., Rudge, J. S. & Wiegand, S. J. Single Injections of Vascular Endothelial Growth Factor Trap Block Ovulation in the Macaque and Produce a Prolonged, Dose-Related Suppression of Ovarian Function. *The Journal of Clinical Endocrinology & Metabolism* **90**, 1114-1122, doi:10.1210/jc.2004-1572 (2005).

89 Woad, K. J. & Robinson, R. S. Luteal angiogenesis and its control. *Theriogenology* **86**, 221-228, doi:https://doi.org/10.1016/j.theriogenology.2016.04.035 (2016).

90 Ko, C., Gieske, M. C., Al-Alem, L., Hahn, Y., Su, W., Gong, M. C., Iglarz, M. & Koo, Y. Endothelin-2 in Ovarian Follicle Rupture. *Endocrinology* **147**, 1770-1779, doi:10.1210/en.2005-1228 (2006).

91 Palanisamy, G. S., Cheon, Y.-P., Kim, J., Kannan, A., Li, Q., Sato, M., Mantena, S. R., Sitruk-Ware, R. L., Bagchi, M. K. & Bagchi, I. C. A Novel Pathway Involving Progesterone Receptor, Endothelin-2, and Endothelin Receptor B Controls Ovulation in Mice. *Molecular Endocrinology* **20**, 2784-2795, doi:10.1210/me.2006-0093 (2006).

92 Kim, J., Bagchi, I. C. & Bagchi, M. K. Signaling by hypoxia-inducible factors is critical for ovulation in mice. *Endocrinology* **150**, 3392-3400, doi:10.1210/en.2008-0948 (2009).

93 Kim, J., Sato, M., Li, Q., Lydon, J. P., DeMayo, F. J., Bagchi, I. C. & Bagchi, M. K. Peroxisome Proliferator-Activated Receptor γ Is a Target of Progesterone Regulation in the Preovulatory Follicles and Controls Ovulation in Mice. *Molecular and cellular biology* **28**, 1770-1782, doi:10.1128/mcb.01556-07 (2008).

94 Cacioppo, J. A., Lin, P.-C. P., Hannon, P. R., McDougle, D. R., Gal, A. & Ko, C. Granulosa cell endothelin-2 expression is fundamental for ovulatory follicle rupture. *Scientific reports* **7**, 817-817, doi:10.1038/s41598-017-00943-w (2017).

95 Migone, F. F., Cowan, R. G., Williams, R. M., Gorse, K. J., Zipfel, W. R. & Quirk, S. M. In vivo imaging reveals an essential role of vasoconstriction in rupture of the ovarian follicle at ovulation. *Proceedings of the National Academy of Sciences* **113**, 2294-2299, doi:10.1073/pnas.1512304113 (2016).

96 Gaytan, F., Bellido, C., Gaytan, M., Morales, C. & Sanchez-Criado, J. E. Differential effects of RU486 and indomethacin on follicle rupture during the ovulatory process in the rat. *Biol Reprod* **69**, 99-105, doi:10.1095/biolreprod.102.013755 (2003).

97 Wang, R., Kim, B. V., van Wely, M., Johnson, N. P., Costello, M. F., Zhang, H., Ng, E. H. Y., Legro, R. S., Bhattacharya, S., Norman, R. J. & Mol, B. W. J. Treatment strategies for women with WHO group II anovulation: systematic review and network meta-analysis. *BMJ* **356**, j138, doi:10.1136/bmj.j138 (2017).

98 Melo, A. S., Ferriani, R. A. & Navarro, P. A. Treatment of infertility in women with polycystic ovary syndrome: approach to clinical practice. *Clinics (Sao Paulo)* **70**, 765-769, doi:10.6061/clinics/2015(11)09 (2015).

99 Walters, K. A., Gilchrist, R. B., Ledger, W. L., Teede, H. J., Handelsman, D. J. & Campbell, R. E. New Perspectives on the Pathogenesis of PCOS: Neuroendocrine Origins. *Trends in Endocrinology & Metabolism* **29**, 841-852, doi:https://doi.org/10.1016/j.tem.2018.08.005 (2018).

100 Franks, S., Stark, J. & Hardy, K. Follicle dynamics and anovulation in polycystic ovary syndrome. *Human Reproduction Update* **14**, 367-378, doi:10.1093/humupd/dmn015 (2008).
101 Mitchell, A. & Fantasia, H. C. Understanding the effect of obesity on fertility among reproductive-age women. *Nursing for women's health* **20**, 368-376 (2016).
102 Kannan, S. & Bhaskaran, R. S. Sustained obesity reduces litter size by decreasing proteins regulating folliculogenesis and ovulation in rats - A cafeteria diet model. *Biochemical and Biophysical Research Communications* **519**, 475-480, doi:https://doi.org/10.1016/j.bbrc.2019.09.025 (2019).
103 Han, L., Ren, C., Li, L., Li, X., Ge, J., Wang, H., Miao, Y.-L., Guo, X., Moley, K. H., Shu, W. & Wang, Q. Embryonic defects induced by maternal obesity in mice derive from Stella insufficiency in oocytes. *Nature Genetics* **50**, 432-442, doi:10.1038/s41588-018-0055-6 (2018).
104 Fabian, D., Babelova, J., Cikos, S. & Sefcikova, Z. Overweight negatively affects outcome of superovulation treatment in female mice. *Zygote* **25**, 751-759, doi:10.1017/s0967199417000648 (2017).
105 Wu, L. L., Russell, D. L., Wong, S. L., Chen, M., Tsai, T.-S., St John, J. C., Norman, R. J., Febbraio, M. A., Carroll, J. & Robker, R. L. Mitochondrial dysfunction in oocytes of obese mothers: transmission to offspring and reversal by pharmacological endoplasmic reticulum stress inhibitors. *Development* **142**, 681-691, doi:10.1242/dev.114850 (2015).
106 Wu, L. L.-Y., Dunning, K. R., Yang, X., Russell, D. L., Lane, M., Norman, R. J. & Robker, R. L. High-Fat Diet Causes Lipotoxicity Responses in Cumulus–Oocyte Complexes and Decreased Fertilization Rates. *Endocrinology* **151**, 5438-5445, doi:doi:10.1210/en.2010-0551 (2010).
107 Frye, C. A. An overview of oral contraceptives: mechanism of action and clinical use. *Neurology* **66**, S29-36, doi:10.1212/wnl.66.66_suppl_3.s29 (2006).
108 Misrahi, M., Venencie, P.-Y., Saugier-Veber, P., Sar, S., Dessen, P. & Milgrom, E. Structure of the human progesterone receptor gene. *Biochimica et Biophysica Acta (BBA) - Gene Structure and Expression* **1216**, 289-292, doi:https://doi.org/10.1016/0167-4781(93)90156-8 (1993).
109 Petz, L. N. & Nardulli, A. M. Sp1 Binding Sites and An Estrogen Response Element Half-Site Are Involved in Regulation of the Human Progesterone Receptor A Promoter. *Molecular Endocrinology* **14**, 972-985, doi:10.1210/mend.14.7.0493 (2000).
110 Sriraman, V., Sharma, S. C. & Richards, J. S. Transactivation of the Progesterone Receptor Gene in Granulosa Cells: Evidence that Sp1/Sp3 Binding Sites in the Proximal Promoter Play a Key Role in Luteinizing Hormone Inducibility. *Molecular Endocrinology* **17**, 436-449, doi:10.1210/me.2002-0252 (2003).
111 Bourguet, W., Germain, P. & Gronemeyer, H. Nuclear receptor ligand-binding domains: three-dimensional structures, molecular interactions and pharmacological implications. *Trends in Pharmacological Sciences* **21**, 381-388, doi:https://doi.org/10.1016/S0165-6147(00)01548-0 (2000).
112 Guiochon-Mantel, A., Delabre, K., Lescop, P. & Milgrom, E. Nuclear localization signals also mediate the outward movement of proteins from the nucleus. *Proceedings of the National Academy of Sciences* **91**, 7179-7183, doi:10.1073/pnas.91.15.7179 (1994).
113 Tanos, T., Rojo, L. J., Echeverria, P. & Brisken, C. ER and PR signaling nodes during mammary gland development. *Breast Cancer Research* **14**, 210, doi:10.1186/bcr3166 (2012).

114 Abdel-Hafiz, H., Takimoto, G. S., Tung, L. & Horwitz, K. B. The Inhibitory Function in Human Progesterone Receptor N Termini Binds SUMO-1 Protein to Regulate Autoinhibition and Transrepression. *Journal of Biological Chemistry* **277**, 33950-33956, doi:10.1074/jbc.M204573200 (2002).

115 Hovland, A. R., Powell, R. L., Takimoto, G. S., Tung, L. & Horwitz, K. B. An N-terminal Inhibitory Function, IF, Suppresses Transcription by the A-isoform but Not the B-isoform of Human Progesterone Receptors. *Journal of Biological Chemistry* **273**, 5455-5460, doi:10.1074/jbc.273.10.5455 (1998).

116 Kastner, P., Krust, A., Turcotte, B., Stropp, U., Tora, L., Gronemeyer, H. & Chambon, P. Two distinct estrogen-regulated promoters generate transcripts encoding the two functionally different human progesterone receptor forms A and B. *The EMBO Journal* **9**, 1603-1614, doi:10.1002/j.1460-2075.1990.tb08280.x (1990).

117 Tung, L., Shen, T., Abel, M. G., Powell, R. L., Takimoto, G. S., Sartorius, C. A. & Horwitz, K. B. Mapping the Unique Activation Function 3 in the Progesterone B-receptor Upstream Segment: TWO LXXLL MOTIFS AND A TRYPTOPHAN RESIDUE ARE REQUIRED FOR ACTIVITY. *Journal of Biological Chemistry* **276**, 39843-39851, doi:10.1074/jbc.M106843200 (2001).

118 Vegeto, E., Shahbaz, M. M., Wen, D. X., Goldman, M. E., O'Malley, B. W. & McDonnell, D. P. Human progesterone receptor A form is a cell- and promoter-specific repressor of human progesterone receptor B function. *Molecular Endocrinology* **7**, 1244-1255, doi:10.1210/mend.7.10.8264658 (1993).

119 Ulbrich, S. E., Kettler, A. & Einspanier, R. Expression and localization of estrogen receptor α, estrogen receptor β and progesterone receptor in the bovine oviduct in vivo and in vitro. *The Journal of Steroid Biochemistry and Molecular Biology* **84**, 279-289, doi:https://doi.org/10.1016/S0960-0760(03)00039-6 (2003).

120 Condon, J. C., Hardy, D. B., Kovaric, K. & Mendelson, C. R. Up-Regulation of the Progesterone Receptor (PR)-C Isoform in Laboring Myometrium by Activation of Nuclear Factor-κB May Contribute to the Onset of Labor through Inhibition of PR Function. *Molecular Endocrinology* **20**, 764-775, doi:10.1210/me.2005-0242 (2006).

121 Chen, C., Opazo, J. C., Erez, O., Uddin, M., Santolaya-Forgas, J., Goodman, M., Grossman, L. I., Romero, R. & Wildman, D. E. The human progesterone receptor shows evidence of adaptive evolution associated with its ability to act as a transcription factor. *Mol Phylogenet Evol* **47**, 637-649, doi:10.1016/j.ympev.2007.12.026 (2008).

122 Saner, K. J., Welter, B. H., Zhang, F., Hansen, E., Dupont, B., Wei, Y. & Price, T. M. Cloning and expression of a novel, truncated, progesterone receptor. *Molecular and Cellular Endocrinology* **200**, 155-163, doi:https://doi.org/10.1016/S0303-7207(02)00380-5 (2003).

123 Dai, Q., Shah, A. A., Garde, R. V., Yonish, B. A., Zhang, L., Medvitz, N. A., Miller, S. E., Hansen, E. L., Dunn, C. N. & Price, T. M. A truncated progesterone receptor (PR-M) localizes to the mitochondrion and controls cellular respiration. *Mol Endocrinol* **27**, 741-753, doi:10.1210/me.2012-1292 (2013).

124 Ismail, P. M., Li, J., DeMayo, F. J., O'Malley, B. W. & Lydon, J. P. A Novel LacZ Reporter Mouse Reveals Complex Regulation of the Progesterone Receptor Promoter During Mammary Gland Development. *Molecular Endocrinology* **16**, 2475-2489, doi:10.1210/me.2002-0169 (2002).

125 Teilmann, S. C., Clement, C. A., Thorup, J., Byskov, A. G. & Christensen, S. T. Expression and localization of the progesterone receptor in mouse and human reproductive organs. *J Endocrinol* **191**, 525-535, doi:10.1677/joe.1.06565 (2006).

126 Robker, R. L., Akison, L. K. & Russell, D. L. Control of oocyte release by progesterone receptor-regulated gene expression. *Nuclear Receptor Signaling* **7**, nrs.07012, doi:10.1621/nrs.07012 (2009).
127 Cassar, C. A., Dow, M. P. D., Pursley, J. R. & Smith, G. W. Effect of the preovulatory LH surge on bovine follicular progesterone receptor mRNA expression. *Domestic Animal Endocrinology* **22**, 179-187, doi:https://doi.org/10.1016/S0739-7240(02)00124-8 (2002).
128 Słomczyńska, M., Krok, M. & Pierściński, A. Localization of the progesterone receptor in the porcine ovary. *Acta Histochemica* **102**, 183-191, doi:https://doi.org/10.1078/S0065-1281(04)70027-6 (2000).
129 García, V., Kohen, P., Maldonado, C., Sierralta, W., Muñoz, A., Villarroel, C., Strauss Iii, J. F. & Devoto, L. Transient expression of progesterone receptor and cathepsin-l in human granulosa cells during the periovulatory period. *Fertility and Sterility* **97**, 707-713.e701, doi:http://dx.doi.org/10.1016/j.fertnstert.2011.12.039 (2012).
130 Natraj, U. & Richards, J. S. Hormonal regulation, localization, and functional activity of the progesterone receptor in granulosa cells of rat preovulatory follicles. *Endocrinology* **133**, 761-769, doi:10.1210/en.133.2.761 (1993).
131 Park, O.-K. & Mayo, K. E. Transient Expression of Progesterone Receptor Messenger RNA in Ovarian Granuiosa Cells after the Preovulatory Luteinizing Hormone Surge. *Molecular Endocrinology* **5**, 967-978, doi:doi:10.1210/mend-5-7-967 (1991).
132 Shao, R., Markström, E., Friberg, P. A., Johansson, M. & Billig, H. k. Expression of Progesterone Receptor (PR) A and B Isoforms in Mouse Granulosa Cells: Stage-Dependent PR-Mediated Regulation of Apoptosis and Cell Proliferation1. *Biology of Reproduction* **68**, 914-921, doi:10.1095/biolreprod.102.009035 (2003).
133 Gemzell-Danielsson, K., Berger, C. & P.G.L, L. Emergency contraception — mechanisms of action. *Contraception* **87**, 300-308, doi:https://doi.org/10.1016/j.contraception.2012.08.021 (2013).
134 Lydon, J. P., DeMayo, F. J., Funk, C. R., Mani, S. K., Hughes, A. R., Montgomery, C. A., Jr., Shyamala, G., Conneely, O. M. & O'Malley, B. W. Mice lacking progesterone receptor exhibit pleiotropic reproductive abnormalities. *Genes Dev* **9**, 2266-2278 (1995).
135 Robker, R. L. & Richards, J. S. in *Ovulation* 121-129 (Springer, 2000).
136 Shimada, M., Nishibori, M., Yamashita, Y., Ito, J., Mori, T. & Richards, J. S. Down-Regulated Expression of A Disintegrin and Metalloproteinase with Thrombospondin-Like Repeats-1 by Progesterone Receptor Antagonist Is Associated with Impaired Expansion of Porcine Cumulus-Oocyte Complexes. *Endocrinology* **145**, 4603-4614, doi:10.1210/en.2004-0542 (2004).
137 Hasegawa, J., Yanaihara, A., Iwasaki, S., Otsuka, Y., Negishi, M., Akahane, T. & Okai, T. Reduction of progesterone receptor expression in human cumulus cells at the time of oocyte collection during IVF is associated with good embryo quality. *Human Reproduction* **20**, 2194-2200, doi:10.1093/humrep/dei005 (2005).
138 Silva, C. C. & Knight, P. G. Effects of androgens, progesterone and their antagonists on the developmental competence of in vitro matured bovine oocytes. *J Reprod Fertil* **119**, 261-269 (2000).
139 Aparicio, I. M., Garcia-Herreros, M., O'Shea, L. C., Hensey, C., Lonergan, P. & Fair, T. Expression, Regulation, and Function of Progesterone Receptors in Bovine Cumulus Oocyte Complexes During In Vitro Maturation. *Biology of reproduction* **84**, 910-921, doi:10.1095/biolreprod.110.087411 (2011).
140 Zhu, Y., Liu, D., Shaner, Z. C., Chen, S., Hong, W. & Stellwag, E. J. Nuclear progestin receptor (pgr) knockouts in zebrafish demonstrate role for pgr in ovulation but not in

rapid non-genomic steroid mediated meiosis resumption. *Frontiers in endocrinology* **6**, 37-37, doi:10.3389/fendo.2015.00037 (2015).

141 Liu, D. T., Brewer, M. S., Chen, S., Hong, W. & Zhu, Y. Transcriptomic signatures for ovulation in vertebrates. *General and Comparative Endocrinology* **247**, 74-86, doi:https://doi.org/10.1016/j.ygcen.2017.01.019 (2017).

142 Liu, J., Park, E.-S. & Jo, M. Runt-related transcription factor 1 regulates luteinized hormone-induced prostaglandin-endoperoxide synthase 2 expression in rat periovulatory granulosa cells. *Endocrinology* **150**, 3291-3300 (2009).

143 Jo, M. & Curry, T. E., Jr. Luteinizing Hormone-Induced RUNX1 Regulates the Expression of Genes in Granulosa Cells of Rat Periovulatory Follicles. *Molecular Endocrinology* **20**, 2156-2172, doi:10.1210/me.2005-0512 (2006).

144 Mittaz, L., Russell, D. L., Wilson, T., Brasted, M., Tkalcevic, J., Salamonsen, L. A., Hertzog, P. J. & Pritchard, M. A. Adamts-1 Is Essential for the Development and Function of the Urogenital System1. *Biology of Reproduction* **70**, 1096-1105, doi:10.1095/biolreprod.103.023911 (2004).

145 Shindo, T., Kurihara, H., Kuno, K., Yokoyama, H., Wada, T., Kurihara, Y., Imai, T., Wang, Y., Ogata, M., Nishimatsu, H., Moriyama, N., Oh-hashi, Y., Morita, H., Ishikawa, T., Nagai, R., Yazaki, Y. & Matsushima, K. ADAMTS-1: a metalloproteinase-disintegrin essential for normal growth, fertility, and organ morphology and function. *The Journal of Clinical Investigation* **105**, 1345-1352, doi:10.1172/jci8635 (2000).

146 Gava, N., Clarke, C. L., Byth, K., Arnett-Mansfield, R. L. & deFazio, A. Expression of Progesterone Receptors A and B in the Mouse Ovary during the Estrous Cycle. *Endocrinology* **145**, 3487-3494, doi:10.1210/en.2004-0212 (2004).

147 Mulac-Jericevic, B., Mullinax, R. A., DeMayo, F. J., Lydon, J. P. & Conneely, O. M. Subgroup of Reproductive Functions of Progesterone Mediated by Progesterone Receptor-B Isoform. *Science* **289**, 1751-1754, doi:10.1126/science.289.5485.1751 (2000).

148 Mulac-Jericevic, B., Lydon, J. P., DeMayo, F. J. & Conneely, O. M. Defective mammary gland morphogenesis in mice lacking the progesterone receptor B isoform. *Proceedings of the National Academy of Sciences* **100**, 9744-9749, doi:10.1073/pnas.1732707100 (2003).

149 Mesiano, S., Chan, E.-C., Fitter, J. T., Kwek, K., Yeo, G. & Smith, R. Progesterone Withdrawal and Estrogen Activation in Human Parturition Are Coordinated by Progesterone Receptor A Expression in the Myometrium. *The Journal of Clinical Endocrinology & Metabolism* **87**, 2924-2930, doi:10.1210/jcem.87.6.8609 (2002).

150 Saruhan, B. G., Sağsoz, H., Akbalik, M. E. & Ketani, M. A. Distribution of estrogen receptor α and progesterone receptor B in the bovine oviduct during the follicular and luteal phases of the sexual cycle: an immunohistochemical and semi-quantitative study. *Biotechnic & Histochemistry* **86**, 315-325, doi:10.3109/10520295.2010.494473 (2011).

151 Shao, R., Norström, A., Weijdegård, B., Egecioglu, E., Fernandez-Rodriguez, J., Feng, Y., Stener-Victorin, E., Brännström, M. & Billig, H. Distinct Expression Pattern of Dicer1 Correlates with Ovarian-Derived Steroid Hormone Receptor Expression in Human Fallopian Tubes during Ovulation and the Midsecretory Phase. *The Journal of Clinical Endocrinology & Metabolism* **96**, E869-E877, doi:10.1210/jc.2010-2353 (2011).

152 Akison, L. K., Boden, M. J., Kennaway, D. J., Russell, D. L. & Robker, R. L. Progesterone receptor-dependent regulation of genes in the oviducts of female mice. *Physiological Genomics* **46**, 583-592, doi:10.1152/physiolgenomics.00044.2014 (2014).

153 Bylander, A., Gunnarsson, L., Shao, R., Billig, H. & Larsson, D. G. J. Progesterone-mediated effects on gene expression and oocyte-cumulus complex transport in the mouse fallopian tube. *Reprod Biol Endocrinol* **13**, 40-40, doi:10.1186/s12958-015-0038-8 (2015).
154 Vinijsanun, A. & Martin, L. Effects of progesterone antagonists RU486 and ZK98734 on embryo transport, development and implantation in laboratory mice. *Reprod Fertil Dev* **2**, 713-727, doi:10.1071/rd9900713 (1990).
155 Fuentealba, B., Nieto, M. & Croxatto, H. B. Ovum transport in pregnant rats is little affected by RU486 and exogenous progesterone as compared to cycling rats. *Biol Reprod* **37**, 768-774, doi:10.1095/biolreprod37.4.768 (1987).
156 Mahmood, T., Saridogan, E., Smutna, S., Habib, A. M. & Djahanbakhch, O. The effect of ovarian steroids on epithelial ciliary beat frequency in the human Fallopian tube. *Human Reproduction* **13**, 2991-2994, doi:10.1093/humrep/13.11.2991 (1998).
157 Holt, W. V. & Fazeli, A. Sperm selection in the female mammalian reproductive tract. Focus on the oviduct: Hypotheses, mechanisms, and new opportunities. *Theriogenology* **85**, 105-112, doi:https://doi.org/10.1016/j.theriogenology.2015.07.019 (2016).
158 Kommagani, R., Szwarc, M. M., Vasquez, Y. M., Peavey, M. C., Mazur, E. C., Gibbons, W. E., Lanz, R. B., DeMayo, F. J. & Lydon, J. P. The Promyelocytic Leukemia Zinc Finger Transcription Factor Is Critical for Human Endometrial Stromal Cell Decidualization. *PLoS genetics* **12**, e1005937-e1005937, doi:10.1371/journal.pgen.1005937 (2016).
159 Jeong, Y.-J., Choi, H.-W., Shin, H.-S., Cui, X.-S., Kim, N.-H., Gerton, G. L. & Jun, J. H. Optimization of real time RT-PCR methods for the analysis of gene expression in mouse eggs and preimplantation embryos. *Molecular reproduction and development* **71**, 284-289, doi:10.1002/mrd.20269 (2005).
160 Rubel, C. A., Lanz, R. B., Kommagani, R., Franco, H. L., Lydon, J. P. & DeMayo, F. J. Research resource: Genome-wide profiling of progesterone receptor binding in the mouse uterus. *Molecular endocrinology* **26**, 1428-1442 (2012).
161 Mazur, E. C., Vasquez, Y. M., Li, X., Kommagani, R., Jiang, L., Chen, R., Lanz, R. B., Kovanci, E., Gibbons, W. E. & DeMayo, F. J. Progesterone Receptor Transcriptome and Cistrome in Decidualized Human Endometrial Stromal Cells. *Endocrinology* **156**, 2239-2253, doi:10.1210/en.2014-1566 (2015).
162 Zakar, T. & Hertelendy, F. Progesterone withdrawal: key to parturition. *Am J Obstet Gynecol* **196**, 289-296, doi:10.1016/j.ajog.2006.09.005 (2007).
163 Nadeem, L., Shynlova, O., Matysiak-Zablocki, E., Mesiano, S., Dong, X. & Lye, S. Molecular evidence of functional progesterone withdrawal in human myometrium. *Nature Communications* **7**, 11565, doi:10.1038/ncomms11565 (2016).
164 Merlino, A. A., Welsh, T. N., Tan, H., Yi, L. J., Cannon, V., Mercer, B. M. & Mesiano, S. Nuclear Progesterone Receptors in the Human Pregnancy Myometrium: Evidence that Parturition Involves Functional Progesterone Withdrawal Mediated by Increased Expression of Progesterone Receptor-A. *The Journal of Clinical Endocrinology & Metabolism* **92**, 1927-1933, doi:10.1210/jc.2007-0077 (2007).
165 Dong, X., Challis & Lye, S. Intramolecular interactions between the AF3 domain and the C-terminus of the human progesterone receptor are mediated through two LXXLL motifs. **32**, 843, doi:10.1677/jme.0.0320843 (2004).
166 Pabona, J. M. P., Zhang, D., Ginsburg, D. S., Simmen, F. A. & Simmen, R. C. M. Prolonged Pregnancy in Women Is Associated With Attenuated Myometrial Expression of Progesterone Receptor Co-Regulator Krüppel-Like Factor 9. *The Journal*

of Clinical Endocrinology & Metabolism **100**, 166-174, doi:10.1210/jc.2014-2846 (2015).

167 Wu, S.-P., Li, R. & DeMayo, F. J. Progesterone Receptor Regulation of Uterine Adaptation for Pregnancy. *Trends in Endocrinology & Metabolism* **29**, 481-491, doi:https://doi.org/10.1016/j.tem.2018.04.001 (2018).

168 Shyamala, G., Yang, X., Cardiff, R. D. & Dale, E. Impact of progesterone receptor on cell-fate decisions during mammary gland development. *Proceedings of the National Academy of Sciences* **97**, 3044-3049, doi:10.1073/pnas.97.7.3044 (2000).

169 Aupperlee, M. D., Smith, K. T., Kariagina, A. & Haslam, S. Z. Progesterone Receptor Isoforms A and B: Temporal and Spatial Differences in Expression during Murine Mammary Gland Development. *Endocrinology* **146**, 3577-3588, doi:10.1210/en.2005-0346 (2005).

170 Lange, C. A., Sartorius, C. A., Abdel-Hafiz, H., Spillman, M. A., Horwitz, K. B. & Jacobsen, B. M. in *Innovative Endocrinology of Cancer* (eds Lev M. Berstein & Richard J. Santen) 94-111 (Springer New York, 2008).

171 Singhal, H., Greene, M. E., Zarnke, A. L., Laine, M., Al Abosy, R., Chang, Y.-F., Dembo, A. G., Schoenfelt, K., Vadhi, R., Qiu, X., Rao, P., Santhamma, B., Nair, H. B., Nickisch, K. J., Long, H. W., Becker, L., Brown, M. & Greene, G. L. Progesterone receptor isoforms, agonists and antagonists differentially reprogram estrogen signaling. *Oncotarget* **9**, 4282-4300, doi:10.18632/oncotarget.21378 (2017).

172 Bellance, C., Khan, J. A., Meduri, G., Guiochon-Mantel, A., Lombès, M. & Loosfelt, H. Progesterone receptor isoforms PRA and PRB differentially contribute to breast cancer cell migration through interaction with focal adhesion kinase complexes. *Molecular biology of the cell* **24**, 1363-1374, doi:10.1091/mbc.E12-11-0807 (2013).

173 Boonyaratanakornkit, V., McGowan, E., Sherman, L., Mancini, M. A., Cheskis, B. J. & Edwards, D. P. The Role of Extranuclear Signaling Actions of Progesterone Receptor in Mediating Progesterone Regulation of Gene Expression and the Cell Cycle. *Molecular Endocrinology* **21**, 359-375, doi:10.1210/me.2006-0337 (2007).

174 Khan, J. A., Bellance, C., Guiochon-Mantel, A., Lombès, M. & Loosfelt, H. Differential regulation of breast cancer-associated genes by progesterone receptor isoforms PRA and PRB in a new bi-inducible breast cancer cell line. *PloS one* **7**, e45993-e45993, doi:10.1371/journal.pone.0045993 (2012).

175 Kariagina, A., Aupperlee, M. D. & Haslam, S. Z. Progesterone receptor isoform functions in normal breast development and breast cancer. *Crit Rev Eukaryot Gene Expr* **18**, 11-33, doi:10.1615/critreveukargeneexpr.v18.i1.20 (2008).

176 Dai, Q., Likes, C. E., III, Luz, A. L., Mao, L., Yeh, J. S., Wei, Z., Kuchibhatla, M., Ilkayeva, O. R., Koves, T. R. & Price, T. M. A Mitochondrial Progesterone Receptor Increases Cardiac Beta-Oxidation and Remodeling. *Journal of the Endocrine Society* **3**, 446-467, doi:10.1210/js.2018-00219 (2019).

177 Seeman, E. Invited Review: Pathogenesis of osteoporosis. *Journal of Applied Physiology* **95**, 2142-2151, doi:10.1152/japplphysiol.00564.2003 (2003).

178 Rickard, D. J., Iwaniec, U. T., Evans, G., Hefferan, T. E., Hunter, J. C., Waters, K. M., Lydon, J. P., O'Malley, B. W., Khosla, S., Spelsberg, T. C. & Turner, R. T. Bone Growth and Turnover in Progesterone Receptor Knockout Mice. *Endocrinology* **149**, 2383-2390, doi:10.1210/en.2007-1247 (2008).

179 Yao, W., Dai, W., Shahnazari, M., Pham, A., Chen, Z., Chen, H., Guan, M. & Lane, N. E. Inhibition of the Progesterone Nuclear Receptor during the Bone Linear Growth Phase Increases Peak Bone Mass in Female Mice. *PLOS ONE* **5**, e11410, doi:10.1371/journal.pone.0011410 (2010).

180 Zhong, Z. A., Kot, A., Lay, Y. A. E., Zhang, H., Jia, J., Lane, N. E. & Yao, W. Sex-Dependent, Osteoblast Stage-Specific Effects of Progesterone Receptor on Bone Acquisition. *Journal of Bone and Mineral Research* **32**, 1841-1852 (2017).

181 Acharya, K. D., Nettles, S. A., Sellers, K. J., Im, D. D., Harling, M., Pattanayak, C., Vardar-Ulu, D., Lichti, C. F., Huang, S., Edwards, D. P., Srivastava, D. P., Denner, L. & Tetel, M. J. The Progestin Receptor Interactome in the Female Mouse Hypothalamus: Interactions with Synaptic Proteins Are Isoform Specific and Ligand Dependent. *eNeuro* **4**, ENEURO.0272-0217.2017, doi:10.1523/ENEURO.0272-17.2017 (2017).

182 Gal, A., Lin, P.-C., Cacioppo, J. A., Hannon, P. R., Mahoney, M. M., Wolfe, A., Fernandez-Valdivia, R., Lydon, J. P., Elias, C. F. & Ko, C. Loss of Fertility in the Absence of Progesterone Receptor Expression in Kisspeptin Neurons of Female Mice. *PLOS ONE* **11**, e0159534, doi:10.1371/journal.pone.0159534 (2016).

183 Mani, S. K., Reyna, A. M., Chen, J. Z., Mulac-Jericevic, B. & Conneely, O. M. Differential Response of Progesterone Receptor Isoforms in Hormone-Dependent and -Independent Facilitation of Female Sexual Receptivity. *Molecular Endocrinology* **20**, 1322-1332, doi:10.1210/me.2005-0466 (2006).

184 Guerra-Araiza, C., Coyoy-Salgado, A. & Camacho-Arroyo, I. Sex differences in the regulation of progesterone receptor isoforms expression in the rat brain. *Brain Research Bulletin* **59**, 105-109, doi:https://doi.org/10.1016/S0361-9230(02)00845-6 (2002).

185 Li, X. & O'Malley, B. W. Unfolding the Action of Progesterone Receptors. *Journal of Biological Chemistry* **278**, 39261-39264, doi:10.1074/jbc.R300024200 (2003).

186 Doyle, K. M. H., Russell, D. L., Sriraman, V. & Richards, J. S. Coordinate Transcription of the ADAMTS-1 Gene by Luteinizing Hormone and Progesterone Receptor. *Molecular Endocrinology* **18**, 2463-2478, doi:10.1210/me.2003-0380 (2004).

187 Mani, S. & Oyola, M. Progesterone Signaling Mechanisms in Brain and Behavior. *Frontiers in Endocrinology* **3**, doi:10.3389/fendo.2012.00007 (2012).

188 Fu, X.-D., Flamini, M., Sanchez, A. M., Goglia, L., Giretti, M. S., Genazzani, A. R. & Simoncini, T. Progestogens regulate endothelial actin cytoskeleton and cell movement via the actin-binding protein moesin. *Molecular Human Reproduction* **14**, 225-234, doi:10.1093/molehr/gan010 (2008).

189 Wang, L., Lonard, D. M. & O'Malley, B. W. The Role of Steroid Receptor Coactivators in Hormone Dependent Cancers and Their Potential as Therapeutic Targets. *Hormones and Cancer* **7**, 229-235, doi:10.1007/s12672-016-0261-6 (2016).

190 Ballaré, C., Uhrig, M., Bechtold, T., Sancho, E., Di Domenico, M., Migliaccio, A., Auricchio, F. & Beato, M. Two domains of the progesterone receptor interact with the estrogen receptor and are required for progesterone activation of the c-Src/Erk pathway in mammalian cells. *Molecular and cellular biology* **23**, 1994-2008, doi:10.1128/mcb.23.6.1994-2008.2003 (2003).

191 Giulianelli, S., Vaqué, J. P., Soldati, R., Wargon, V., Vanzulli, S. I., Martins, R., Zeitlin, E., Molinolo, A. A., Helguero, L. A., Lamb, C. A., Gutkind, J. S. & Lanari, C. Estrogen Receptor Alpha Mediates Progestin-Induced Mammary Tumor Growth by Interacting with Progesterone Receptors at the Cyclin D1/MYC Promoters. *Cancer Research* **72**, 2416-2427, doi:10.1158/0008-5472.can-11-3290 (2012).

192 Ogara, M. F., Rodríguez-Seguí, S. A., Marini, M., Nacht, A. S., Stortz, M., Levi, V., Presman, D. M., Vicent, G. P. & Pecci, A. The glucocorticoid receptor interferes with progesterone receptor-dependent genomic regulation in breast cancer cells. *Nucleic Acids Research* **47**, 10645-10661, doi:10.1093/nar/gkz857 (2019).

193 York, B. & O'Malley, B. W. Steroid Receptor Coactivator (SRC) Family: Masters of Systems Biology. *Journal of Biological Chemistry* **285**, 38743-38750, doi:10.1074/jbc.R110.193367 (2010).
194 Onate, S., Tsai, S., Tsai, M.-J. & O Malley, B. Sequence and characterization of a coactivator for the steroid hormone receptor superfamily. *Science* **270**, 1354, doi:10.1126/science.270.5240.1354 (1995).
195 Owen, G. I., Richer, J. K., Tung, L., Takimoto, G. & Horwitz, K. B. Progesterone Regulates Transcription of the p21 WAF1 Cyclindependent Kinase Inhibitor Gene through Sp1 and CBP/p300. *Journal of Biological Chemistry* **273**, 10696-10701, doi:10.1074/jbc.273.17.10696 (1998).
196 Voegel, J. J., Heine, M. J., Zechel, C., Chambon, P. & Gronemeyer, H. TIF2, a 160 kDa transcriptional mediator for the ligand-dependent activation function AF-2 of nuclear receptors. *The EMBO journal* **15**, 3667-3675 (1996).
197 Amazit, L., Roseau, A., Khan, J. A., Chauchereau, A., Tyagi, R. K., Loosfelt, H., Leclerc, P., Lombès, M. & Guiochon-Mantel, A. Ligand-Dependent Degradation of SRC-1 Is Pivotal for Progesterone Receptor Transcriptional Activity. *Molecular Endocrinology* **25**, 394-408, doi:10.1210/me.2010-0458 (2011).
198 Liu, Z., Wong, J., Tsai, S. Y., Tsai, M.-J. & O'Malley, B. W. Steroid receptor coactivator-1 (SRC-1) enhances ligand-dependent and receptor-dependent cell-free transcription of chromatin. *Proceedings of the National Academy of Sciences* **96**, 9485-9490, doi:10.1073/pnas.96.17.9485 (1999).
199 Han, S. J., DeMayo, F. J., Xu, J., Tsai, S. Y., Tsai, M.-J. & O'Malley, B. W. Steroid Receptor Coactivator (SRC)-1 and SRC-3 Differentially Modulate Tissue-Specific Activation Functions of the Progesterone Receptor. *Molecular Endocrinology* **20**, 45-55, doi:10.1210/me.2005-0310 (2006).
200 Spencer, T. E., Jenster, G., Burcin, M. M., Allis, C. D., Zhou, J., Mizzen, C. A., McKenna, N. J., Onate, S. A., Tsai, S. Y., Tsai, M.-J. & O'Malley, B. W. Steroid receptor coactivator-1 is a histone acetyltransferase. *Nature* **389**, 194-198, doi:10.1038/38304 (1997).
201 Li, X., Wong, J., Tsai, S. Y., Tsai, M.-J. & O'Malley, B. W. Progesterone and Glucocorticoid Receptors Recruit Distinct Coactivator Complexes and Promote Distinct Patterns of Local Chromatin Modification. *Molecular and cellular biology* **23**, 3763-3773, doi:10.1128/mcb.23.11.3763-3773.2003 (2003).
202 Yi, P., Wang, Z., Feng, Q., Chou, C. K., Pintilie, G. D., Shen, H., Foulds, C. E., Fan, G., Serysheva, I., Ludtke, S. J., Schmid, M. F., Hung, M. C., Chiu, W. & O'Malley, B. W. Structural and Functional Impacts of ER Coactivator Sequential Recruitment. *Mol Cell* **67**, 733-743 e734, doi:10.1016/j.molcel.2017.07.026 (2017).
203 Shimizu, A., Maruyama, T., Tamaki, K., Uchida, H., Asada, H. & Yoshimura, Y. Impairment of Decidualization in SRC-Deficient Mice1. *Biology of Reproduction* **73**, 1219-1227, doi:10.1095/biolreprod.105.041616 (2005).
204 Han, S. J., Jeong, J., DeMayo, F. J., Xu, J., Tsai, S. Y., Tsai, M.-J. & O'Malley, B. W. Dynamic Cell Type Specificity of SRC-1 Coactivator in Modulating Uterine Progesterone Receptor Function in Mice. *Molecular and cellular biology* **25**, 8150-8165, doi:10.1128/mcb.25.18.8150-8165.2005 (2005).
205 Xu, J., Liao, L., Ning, G., Yoshida-Komiya, H., Deng, C. & O'Malley, B. W. The steroid receptor coactivator SRC-3 (p/CIP/RAC3/AIB1/ACTR/TRAM-1) is required for normal growth, puberty, female reproductive function, and mammary gland development. *Proceedings of the National Academy of Sciences* **97**, 6379-6384, doi:10.1073/pnas.120166297 (2000).

206 Bjorge, J. D., Jakymiw, A. & Fujita, D. J. Selected glimpses into the activation and function of Src kinase. *Oncogene* **19**, 5620-5635, doi:10.1038/sj.onc.1203923 (2000).
207 Aleshin, A. & Finn, R. S. SRC: A Century of Science Brought to the Clinic. *Neoplasia* **12**, 599-607, doi:https://doi.org/10.1593/neo.10328 (2010).
208 Varkaris, A., Katsiampoura, A. D., Araujo, J. C., Gallick, G. E. & Corn, P. G. Src signaling pathways in prostate cancer. *Cancer Metastasis Rev* **33**, 595-606, doi:10.1007/s10555-013-9481-1 (2014).
209 Homsi, J., Cubitt, C. & Daud, A. The Src signaling pathway: a potential target in melanoma and other malignancies. *Expert Opinion on Therapeutic Targets* **11**, 91-100, doi:10.1517/14728222.11.1.91 (2007).
210 Boonyaratanakornkit, V., Scott, M. P., Ribon, V., Sherman, L., Anderson, S. M., Maller, J. L., Miller, W. T. & Edwards, D. P. Progesterone Receptor Contains a Proline-Rich Motif that Directly Interacts with SH3 Domains and Activates c-Src Family Tyrosine Kinases. *Molecular Cell* **8**, 269-280, doi:https://doi.org/10.1016/S1097-2765(01)00304-5 (2001).
211 Roby, K. F., Son, D.-S., Taylor, C. C., Montgomery-Rice, V., Kirchoff, J., Tang, S. & Terranova, P. F. Alterations in reproductive function in Src tyrosine kinase knockout mice. *Endocrine* **26**, 169-176, doi:10.1385/ENDO:26:2:169 (2005).
212 Du, X.-Y., Huang, J., Xu, L.-Q., Tang, D.-F., Wu, L., Zhang, L.-X., Pan, X.-L., Chen, W.-Y., Zheng, L.-P. & Zheng, Y.-H. The proto-oncogene c-src is involved in primordial follicle activation through the PI3K, PKC and MAPK signaling pathways. *Reproductive Biology and Endocrinology* **10**, 58, doi:10.1186/1477-7827-10-58 (2012).
213 Yamashita, Y., Okamoto, M., Ikeda, M., Okamoto, A., Sakai, M., Gunji, Y., Nishimura, R., Hishinuma, M. & Shimada, M. Protein Kinase C (PKC) Increases TACE/ADAM17 Enzyme Activity in Porcine Ovarian Somatic Cells, Which Is Essential for Granulosa Cell Luteinization and Oocyte Maturation. *Endocrinology* **155**, 1080-1090, doi:10.1210/en.2013-1655 (2014).
214 Zhu, Y., Zhang, T., Xie, S., Tu, R., Cao, Y., Guo, X., Zhou, J., Zhou, X. & Cao, L. Gestrinone inhibits growth of human uterine leiomyoma may relate to activity regulation of ERα, Src and P38 MAPK. *Biomedicine & Pharmacotherapy* **66**, 569-577, doi:https://doi.org/10.1016/j.biopha.2012.02.003 (2012).
215 Agoulnik, I. U. & Weigel, N. L. Coactivator selective regulation of androgen receptor activity. *Steroids* **74**, 669-674, doi:https://doi.org/10.1016/j.steroids.2009.02.007 (2009).
216 Lanz, R. B., Razani, B., Goldberg, A. D. & O'Malley, B. W. Distinct RNA motifs are important for coactivation of steroid hormone receptors by steroid receptor RNA activator (SRA). *Proceedings of the National Academy of Sciences* **99**, 16081-16086, doi:10.1073/pnas.192571399 (2002).
217 Cooper, C., Vincett, D., Yan, Y., Hamedani, M. K., Myal, Y. & Leygue, E. Steroid receptor RNA activator bi-faceted genetic system: Heads or Tails? *Biochimie* **93**, 1973-1980, doi:https://doi.org/10.1016/j.biochi.2011.07.002 (2011).
218 Lanz, R. B., Chua, S. S., Barron, N., Söder, B. M., DeMayo, F. & O'Malley, B. W. Steroid receptor RNA activator stimulates proliferation as well as apoptosis in vivo. *Molecular and cellular biology* **23**, 7163-7176 (2003).
219 Eoh, K. J., Paek, J., Kim, S. W., Kim, H. J., Lee, H. Y., Lee, S. K. & Kim, Y. T. Long non-coding RNA, steroid receptor RNA activator (SRA), induces tumor proliferation and invasion through the NOTCH pathway in cervical cancer cell lines. *Oncol Rep* **38**, 3481-3488, doi:10.3892/or.2017.6023 (2017).

220 Lin, K., Zhan, H., Ma, J., Xu, K., Wu, R., Zhou, C. & Lin, J. Silencing of SRA1 Regulates ER Expression and Attenuates the Growth of Stromal Cells in Ovarian Endometriosis. *Reproductive Sciences* **24**, 836-843, doi:10.1177/1933719116670036 (2017).

221 Li, Y., Zhao, W., Wang, H., Chen, C., Zhou, D., Li, S., Zhang, X., Zhao, H., Zhou, D. & Chen, B. Silencing of LncRNA steroid receptor RNA activator attenuates polycystic ovary syndrome in mice. *Biochimie* **157**, 48-56, doi:https://doi.org/10.1016/j.biochi.2018.10.021 (2019).

222 Sharma, S. C. & Richards, J. S. Regulation of AP1 (Jun/Fos) factor expression and activation in ovarian granulosa cells. Relation of JunD and Fra2 to terminal differentiation. *J Biol Chem* **275**, 33718-33728, doi:10.1074/jbc.M003555200 (2000).

223 Choi, Y., Rosewell, K. L., Brännström, M., Akin, J. W., Curry Jr, T. E. & Jo, M. FOS, a Critical Downstream Mediator of PGR and EGF Signaling Necessary for Ovulatory Prostaglandins in the Human Ovary. *The Journal of Clinical Endocrinology & Metabolism* **103**, 4241-4252 (2018).

224 Ghosh, S., Wu, Y., Li, R. & Hu, Y. Jun proteins modulate the ovary-specific promoter of aromatase gene in ovarian granulosa cells via a cAMP-responsive element. *Oncogene* **24**, 2236-2246, doi:10.1038/sj.onc.1208415 (2005).

225 Shea-Eaton, W., Sandhoff, T. W., Lopez, D., Hales, D. B. & McLean, M. P. Transcriptional repression of the rat steroidogenic acute regulatory (StAR) protein gene by the AP-1 family member c-Fos. *Molecular and Cellular Endocrinology* **188**, 161-170, doi:https://doi.org/10.1016/S0303-7207(01)00715-8 (2002).

226 Jonak, C. R., Lainez, N. M., Roybal, L. L., Williamson, A. D. & Coss, D. c-JUN Dimerization Protein 2 (JDP2) Is a Transcriptional Repressor of Follicle-stimulating Hormone β (FSHβ) and Is Required for Preventing Premature Reproductive Senescence in Female Mice. *Journal of Biological Chemistry* **292**, 2646-2659, doi:10.1074/jbc.M116.771808 (2017).

227 Hiatt, S. M., Duren, H. M., Shyu, Y. J., Ellis, R. E., Hisamoto, N., Matsumoto, K., Kariya, K.-i., Kerppola, T. K. & Hu, C.-D. Caenorhabditis elegans FOS-1 and JUN-1 Regulate plc-1 Expression in the Spermatheca to Control Ovulation. *Molecular Biology of the Cell* **20**, 3888-3895, doi:10.1091/mbc.e08-08-0833 (2009).

228 Bianco, S., Bellefleur, A.-M., Beaulieu, É., Beauparlant, C. J., Bertolin, K., Droit, A., Schoonjans, K., Murphy, B. D. & Gévry, N. The Ovulatory Signal Precipitates LRH-1 Transcriptional Switching Mediated by Differential Chromatin Accessibility. *Cell Reports* **28**, 2443-2454.e2444, doi:https://doi.org/10.1016/j.celrep.2019.07.088 (2019).

229 Wardell, S. E., Boonyaratanakornkit, V., Adelman, J. S., Aronheim, A. & Edwards, D. P. Jun Dimerization Protein 2 Functions as a Progesterone Receptor N-Terminal Domain Coactivator. *Molecular and cellular biology* **22**, 5451-5466, doi:10.1128/mcb.22.15.5451-5466.2002 (2002).

230 Hill, K. K., Roemer, S. C., Jones, D. N. M., Churchill, M. E. A. & Edwards, D. P. A Progesterone Receptor Co-activator (JDP2) Mediates Activity through Interaction with Residues in the Carboxyl-terminal Extension of the DNA Binding Domain. *Journal of Biological Chemistry* **284**, 24415-24424, doi:10.1074/jbc.M109.003244 (2009).

231 Kawabe, S., Yazawa, T., Kanno, M., Usami, Y., Mizutani, T., Imamichi, Y., Ju, Y., Matsumura, T., Orisaka, M. & Miyamoto, K. A novel isoform of liver receptor homolog-1 is regulated by steroidogenic factor-1 and the specificity protein family in ovarian granulosa cells. *Endocrinology* **154**, 1648-1660, doi:10.1210/en.2012-2008 (2013).

232 MacLean, J. A., II, Rao, M. K., Doyle, K. M. H., Richards, J. S. & Wilkinson, M. F. Regulation of the Rhox5 Homeobox Gene in Primary Granulosa Cells: Preovulatory

Expression and Dependence on SP1/SP3 and GABP1. *Biology of Reproduction* **73**, 1126-1134, doi:10.1095/biolreprod.105.042747 (2005).

233 Sekiguchi, T., Mizutani, T., Yamada, K., Yazawa, T., Kawata, H., Yoshino, M., Kajitani, T., Kameda, T., Minegishi, T. & Miyamoto, K. Transcriptional Regulation of the Epiregulin Gene in the Rat Ovary. *Endocrinology* **143**, 4718-4729, doi:10.1210/en.2002-220440 (2002).

234 Ongeri, E. M., Verderame, M. F. & Hammond, J. M. Follicle-Stimulating Hormone Induction of Ovarian Insulin-Like Growth Factor-Binding Protein-3 Transcription Requires a TATA Box-Binding Protein and the Protein Kinase A and Phosphatidylinositol-3 Kinase Pathways. *Molecular Endocrinology* **19**, 1837-1848, doi:10.1210/me.2004-0487 (2005).

235 Cai, H., Liu, B., Wang, H., Sun, G., Feng, L., Chen, Z., Zhou, J., Zhang, J., Zhang, T., He, M., Yang, T., Guo, Q., Teng, Z., Xin, Q., Zhou, B., Zhang, H., Xia, G. & Wang, C. SP1 governs primordial folliculogenesis by regulating pregranulosa cell development in mice. *Journal of Molecular Cell Biology*, doi:10.1093/jmcb/mjz059 (2019).

236 Convissar, S., Winston, N. J., Fierro, M. A., Scoccia, H., Zamah, A. M. & Stocco, C. Sp1 regulates steroidogenic genes and LHCGR expression in primary human luteinized granulosa cells. *The Journal of Steroid Biochemistry and Molecular Biology* **190**, 183-192, doi:https://doi.org/10.1016/j.jsbmb.2019.04.003 (2019).

237 Nalvarte, I., Töhönen, V., Lindeberg, M., Varshney, M., Gustafsson, J.-Å. & Inzunza, J. Estrogen receptor β controls MMP-19 expression in mouse ovaries during ovulation. **151**, 253, doi:10.1530/rep-15-0522 (2016).

238 Gao, J., Mazella, J., Seppala, M. & Tseng, L. Ligand activated hPR modulates the glycodelin promoter activity through the Sp1 sites in human endometrial adenocarcinoma cells. *Molecular and Cellular Endocrinology* **176**, 97-102, doi:https://doi.org/10.1016/S0303-7207(01)00450-6 (2001).

239 Shimada, M., Yanai, Y., Okazaki, T., Yamashita, Y., Sriraman, V., Wilson, M. C. & Richards, J. S. Synaptosomal-Associated Protein 25 Gene Expression Is Hormonally Regulated during Ovulation and Is Involved in Cytokine/Chemokine Exocytosis from Granulosa Cells. *Molecular Endocrinology* **21**, 2487-2502, doi:10.1210/me.2007-0042 (2007).

240 Tang, M., Mazella, J., Gao, J. & Tseng, L. Progesterone receptor activates its promoter activity in human endometrial stromal cells. *Molecular and Cellular Endocrinology* **192**, 45-53, doi:https://doi.org/10.1016/S0303-7207(02)00111-9 (2002).

241 Bravo, M. L., Pinto, M. P., Gonzalez, I., Oliva, B., Kato, S., Cuello, M. A., Lange, C. A. & Owen, G. I. Progesterone regulation of tissue factor depends on MEK1/2 activation and requires the proline-rich site on progesterone receptor. *Endocrine* **48**, 309-320, doi:10.1007/s12020-014-0288-9 (2015).

242 Petz, L. N., Ziegler, Y. S., Schultz, J. R. & Nardulli, A. M. Fos and Jun Inhibit Estrogen-Induced Transcription of the Human Progesterone Receptor Gene through an Activator Protein-1 Site. *Molecular Endocrinology* **18**, 521-532, doi:10.1210/me.2003-0105 (2004).

243 Matthews, J., Wihlén, B. r., Tujague, M., Wan, J., Ström, A. & Gustafsson, J.-A. k. Estrogen Receptor (ER) β Modulates ERα-Mediated Transcriptional Activation by Altering the Recruitment of c-Fos and c-Jun to Estrogen-Responsive Promoters. *Molecular Endocrinology* **20**, 534-543, doi:10.1210/me.2005-0140 (2006).

244 Zhang, D., Zhang, X.-L., Michel, F. J., Blum, J. L., Simmen, F. A. & Simmen, R. C. M. Direct Interaction of the Krüppel-like Family (KLF) Member, BTEB1, and PR Mediates Progesterone-Responsive Gene Expression in Endometrial Epithelial Cells. *Endocrinology* **143**, 62-73, doi:10.1210/endo.143.1.8590 (2002).

245 Zhang, X.-L., Zhang, D., Michel, F. J., Blum, J. L., Simmen, F. A. & Simmen, R. C. M. Selective Interactions of Krüppel-like Factor 9/Basic Transcription Element-binding Protein with Progesterone Receptor Isoforms A and B Determine Transcriptional Activity of Progesterone-responsive Genes in Endometrial Epithelial Cells. *Journal of Biological Chemistry* **278**, 21474-21482, doi:10.1074/jbc.M212098200 (2003).

246 Xie, N., Liu, L., Li, Y., Yu, C., Lam, S., Shynlova, O., Gleave, M., Challis, J. R. G., Lye, S. & Dong, X. Expression and Function of Myometrial PSF Suggest a Role in Progesterone Withdrawal and the Initiation of Labor. *Molecular Endocrinology* **26**, 1370-1379, doi:10.1210/me.2012-1088 (2012).

247 Zhang, P.-J., Zhao, J., Li, H.-Y., Man, J.-H., He, K., Zhou, T., Pan, X., Li, A.-L., Gong, W.-L., Jin, B.-F., Xia, Q., Yu, M., Shen, B.-F. & Zhang, X.-M. CUE domain containing 2 regulates degradation of progesterone receptor by ubiquitin-proteasome. *The EMBO journal* **26**, 1831-1842, doi:10.1038/sj.emboj.7601602 (2007).

248 Nawaz, Z., Lonard, D. M., Smith, C. L., Lev-Lehman, E., Tsai, S. Y., Tsai, M.-J. & O'Malley, B. W. The Angelman Syndrome-Associated Protein, E6-AP, Is a Coactivator for the Nuclear Hormone Receptor Superfamily. *Molecular and cellular biology* **19**, 1182-1189, doi:10.1128/mcb.19.2.1182 (1999).

249 Ramamoorthy, S., Dhananjayan, S. C., Demayo, F. J. & Nawaz, Z. Isoform-Specific Degradation of PR-B by E6-AP Is Critical for Normal Mammary Gland Development. *Molecular Endocrinology* **24**, 2099-2113, doi:10.1210/me.2010-0116 (2010).

250 Migliaccio, A., Piccolo, D., Castoria, G., Di Domenico, M., Bilancio, A., Lombardi, M., Gong, W., Beato, M. & Auricchio, F. Activation of the Src/p21ras/Erk pathway by progesterone receptor via cross-talk with estrogen receptor. *The EMBO journal* **17**, 2008-2018, doi:10.1093/emboj/17.7.2008 (1998).

251 Mohammed, H., Russell, I. A., Stark, R., Rueda, O. M., Hickey, T. E., Tarulli, G. A., Serandour, A. A., Birrell, S. N., Bruna, A., Saadi, A., Menon, S., Hadfield, J., Pugh, M., Raj, G. V., Brown, G. D., D'Santos, C., Robinson, J. L. L., Silva, G., Launchbury, R., Perou, C. M., Stingl, J., Caldas, C., Tilley, W. D. & Carroll, J. S. Progesterone receptor modulates ERα action in breast cancer. *Nature* **523**, 313, doi:10.1038/nature14583 (2015).

252 Chen, C.-C., Montalbano, A. P., Hussain, I., Lee, W.-R. & Mendelson, C. R. The transcriptional repressor GATAD2B mediates progesterone receptor suppression of myometrial contractile gene expression. *Journal of Biological Chemistry* **292**, 12560-12576, doi:10.1074/jbc.M117.791350 (2017).

253 Oñate, S. A., Prendergast, P., Wagner, J. P., Nissen, M., Reeves, R., Pettijohn, D. E. & Edwards, D. P. The DNA-bending protein HMG-1 enhances progesterone receptor binding to its target DNA sequences. *Molecular and cellular biology* **14**, 3376-3391, doi:10.1128/mcb.14.5.3376 (1994).

254 Vicent, G. P., Nacht, A. S., Zaurin, R., Font-Mateu, J., Soronellas, D., Le Dily, F., Reyes, D. & Beato, M. Unliganded progesterone receptor-mediated targeting of an RNA-containing repressive complex silences a subset of hormone-inducible genes. *Genes & development* **27**, 1179-1197 (2013).

255 Beato, M., Herrlich, P. & Schütz, G. Steroid hormone receptors: Many Actors in search of a plot. *Cell* **83**, 851-857, doi:https://doi.org/10.1016/0092-8674(95)90201-5 (1995).

256 Chauchereau, A., Georgiakaki, M., Perrin-Wolff, M., Milgrom, E. & Loosfelt, H. JAB1 interacts with both the progesterone receptor and SRC-1. *J Biol Chem* **275**, 8540-8548, doi:10.1074/jbc.275.12.8540 (2000).

257 Kalkhoven, E., Wissink, S., van der Saag, P. T. & Burg, B. v. d. Negative Interaction between the RelA(p65) Subunit of NF-B and the Progesterone Receptor. *Journal of Biological Chemistry* **271**, 6217-6224, doi:10.1074/jbc.271.11.6217 (1996).

258 Man, J.-H., Li, H.-Y., Zhang, P.-J., Zhou, T., He, K., Pan, X., Liang, B., Li, A.-L., Zhao, J., Gong, W.-L., Jin, B.-F., Xia, Q., Yu, M., Shen, B.-F. & Zhang, X.-M. PIAS3 induction of PRB sumoylation represses PRB transactivation by destabilizing its retention in the nucleus. *Nucleic Acids Research* **34**, 5552-5566, doi:10.1093/nar/gkl691 (2006).

259 Dong, X., Yu, C., Shynlova, O., Challis, J. R. G., Rennie, P. S. & Lye, S. J. p54nrb Is a Transcriptional Corepressor of the Progesterone Receptor that Modulates Transcription of the Labor-Associated Gene, Connexin 43 (Gja1). *Molecular Endocrinology* **23**, 1147-1160, doi:10.1210/me.2008-0357 (2009).

260 Dong, X., Shylnova, O., Challis, J. R. G. & Lye, S. J. Identification and Characterization of the Protein-associated Splicing Factor as a Negative Co-regulator of the Progesterone Receptor. *Journal of Biological Chemistry* **280**, 13329-13340, doi:10.1074/jbc.M409187200 (2005).

261 Proietti, C. J., Béguelin, W., Flaqué, M. C. D., Cayrol, F., Rivas, M. A., Tkach, M., Charreau, E. H., Schillaci, R. & Elizalde, P. V. Novel role of signal transducer and activator of transcription 3 as a progesterone receptor coactivator in breast cancer. *Steroids* **76**, 381-392, doi:https://doi.org/10.1016/j.steroids.2010.12.008 (2011).

262 Chauchereau, A., Amazit, L., Quesne, M., Guiochon-Mantel, A. & Milgrom, E. Sumoylation of the Progesterone Receptor and of the Steroid Receptor Coactivator SRC-1. *Journal of Biological Chemistry* **278**, 12335-12343, doi:10.1074/jbc.M207148200 (2003).

263 Greulich, F., Hemmer, M. C., Rollins, D. A., Rogatsky, I. & Uhlenhaut, N. H. There goes the neighborhood: Assembly of transcriptional complexes during the regulation of metabolism and inflammation by the glucocorticoid receptor. *Steroids* **114**, 7-15, doi:https://doi.org/10.1016/j.steroids.2016.05.003 (2016).

264 Groner, A. C. & Brown, M. Role of steroid receptor and coregulator mutations in hormone-dependent cancers. *The Journal of Clinical Investigation* **127**, 1126-1135, doi:10.1172/JCI88885 (2017).

265 Clarke, C. L. & Graham, J. D. Non-Overlapping Progesterone Receptor Cistromes Contribute to Cell-Specific Transcriptional Outcomes. *PLOS ONE* **7**, e35859, doi:10.1371/journal.pone.0035859 (2012).

266 Yin, P., Roqueiro, D., Huang, L., Owen, J. K., Xie, A., Navarro, A., Monsivais, D., Coon V, J. S., Kim, J. J., Dai, Y. & Bulun, S. E. Genome-Wide Progesterone Receptor Binding: Cell Type-Specific and Shared Mechanisms in T47D Breast Cancer Cells and Primary Leiomyoma Cells. *PLOS ONE* **7**, e29021, doi:10.1371/journal.pone.0029021 (2012).

267 Ballaré, C., Castellano, G., Gaveglia, L., Althammer, S., González-Vallinas, J., Eyras, E., Le Dily, F., Zaurin, R., Soronellas, D., Vicent, Guillermo P. & Beato, M. Nucleosome-Driven Transcription Factor Binding and Gene Regulation. *Molecular Cell* **49**, 67-79, doi:https://doi.org/10.1016/j.molcel.2012.10.019 (2013).

268 Ceballos-Chávez, M., Subtil-Rodríguez, A., Giannopoulou, E. G., Soronellas, D., Vázquez-Chávez, E., Vicent, G. P., Elemento, O., Beato, M. & Reyes, J. C. The Chromatin Remodeler CHD8 Is Required for Activation of Progesterone Receptor-Dependent Enhancers. *PLOS Genetics* **11**, e1005174, doi:10.1371/journal.pgen.1005174 (2015).

269 Subtil-Rodríguez, A., Millán-Ariño, L., Quiles, I., Ballaré, C., Beato, M. & Jordan, A. Progesterone Induction of the 11β-Hydroxysteroid Dehydrogenase Type 2 Promoter in

Breast Cancer Cells Involves Coordinated Recruitment of STAT5A and Progesterone Receptor to a Distal Enhancer and Polymerase Tracking. *Molecular and cellular biology* **28**, 3830-3849, doi:10.1128/mcb.01217-07 (2008).

270 Buser, A. C., Obr, A. E., Kabotyanski, E. B., Grimm, S. L., Rosen, J. M. & Edwards, D. P. Progesterone Receptor Directly Inhibits β-Casein Gene Transcription in Mammary Epithelial Cells Through Promoting Promoter and Enhancer Repressive Chromatin Modifications. *Molecular Endocrinology* **25**, 955-968, doi:10.1210/me.2011-0064 (2011).

271 Rubel, C. A., Wu, S.-P., Lin, L., Wang, T., Lanz, R. B., Li, X., Kommagani, R., Franco, H. L., Camper, S. A., Tong, Q., Jeong, J.-W., Lydon, J. P. & DeMayo, F. J. A Gata2-Dependent Transcription Network Regulates Uterine Progesterone Responsiveness and Endometrial Function. *Cell reports* **17**, 1414-1425, doi:10.1016/j.celrep.2016.09.093 (2016).

272 Levanon, D. & Groner, Y. Structure and regulated expression of mammalian RUNX genes. *Oncogene* **23**, 4211-4219, doi:10.1038/sj.onc.1207670 (2004).

273 Mevel, R., Draper, J. E., Lie-a-Ling, M., Kouskoff, V. & Lacaud, G. RUNX transcription factors: orchestrators of development. *Development* **146**, dev148296 (2019).

274 Wilson, K., Park, J., Curry, J. T. E., Mishra, B., Gossen, J., Taniuchi, I. & Jo, M. Core Binding Factor-β Knockdown Alters Ovarian Gene Expression and Function in the Mouse. *Molecular Endocrinology* **30**, 733-747, doi:10.1210/me.2015-1312 (2016).

275 Park, E.-S., Lind, A.-K., Dahm-Kähler, P., Brännström, M., Carletti, M. Z., Christenson, L. K., Curry, T. E., Jr. & Jo, M. RUNX2 Transcription Factor Regulates Gene Expression in Luteinizing Granulosa Cells of Rat Ovaries. *Molecular Endocrinology* **24**, 846-858, doi:10.1210/me.2009-0392 (2010).

276 Gao, K., Wang, P., Peng, J., Xue, J., Chen, K., Song, Y., Wang, J., Li, G., An, X. & Cao, B. Regulation and function of runt-related transcription factors (RUNX1 and RUNX2) in goat granulosa cells. *The Journal of Steroid Biochemistry and Molecular Biology* **181**, 98-108, doi:https://doi.org/10.1016/j.jsbmb.2018.04.002 (2018).

277 Park, E.-S., Choi, S., Muse, K. N., Curry, T. E., Jr. & Jo, M. Response Gene to Complement 32 Expression Is Induced by the Luteinizing Hormone (LH) Surge and Regulated by LH-Induced Mediators in the Rodent Ovary. *Endocrinology* **149**, 3025-3036, doi:10.1210/en.2007-1129 (2008).

278 Liu, J., Park, E.-S., Curry, T. E., Jr. & Jo, M. Periovulatory expression of hyaluronan and proteoglycan link protein 1 (Hapln1) in the rat ovary: hormonal regulation and potential function. *Mol Endocrinol* **24**, 1203-1217, doi:10.1210/me.2009-0325 (2010).

279 Huang, X., Hao, C., Shen, X., Zhang, Y. & Liu, X. RUNX2, GPX3 and PTX3 gene expression profiling in cumulus cells are reflective oocyte/embryo competence and potentially reliable predictors of embryo developmental competence in PCOS patients. *Reproductive Biology and Endocrinology* **11**, 109, doi:10.1186/1477-7827-11-109 (2013).

280 Duggavathi, R., Siddappa, D., Schuermann, Y., Pansera, M., Menard, I. J., Praslickova, D. & Agellon, L. B. The fatty acid binding protein 6 gene (Fabp6) is expressed in murine granulosa cells and is involved in ovulatory response to superstimulation. *J Reprod Dev* **61**, 237-240, doi:10.1262/jrd.2014-139 (2015).

281 Park, E.-S., Park, J., Franceschi, R. T. & Jo, M. The role for runt related transcription factor 2 (RUNX2) as a transcriptional repressor in luteinizing granulosa cells. *Molecular and Cellular Endocrinology* **362**, 165-175, doi:https://doi.org/10.1016/j.mce.2012.06.005 (2012).

282 Ojima, F., Saito, Y., Tsuchiya, Y., Kayo, D., Taniuchi, S., Ogoshi, M., Fukamachi, H., Takeuchi, S. & Takahashi, S. Runx3 transcription factor regulates ovarian functions and ovulation in female mice. *J Reprod Dev* **62**, 479-486, doi:10.1262/jrd.2016-005 (2016).

283 Inoue, K.-i., Ozaki, S., Shiga, T., Ito, K., Masuda, T., Okado, N., Iseda, T., Kawaguchi, S., Ogawa, M., Bae, S.-C., Yamashita, N., Itohara, S., Kudo, N. & Ito, Y. Runx3 controls the axonal projection of proprioceptive dorsal root ganglion neurons. *Nature Neuroscience* **5**, 946-954, doi:10.1038/nn925 (2002).

284 Li, Q.-L., Ito, K., Sakakura, C., Fukamachi, H., Inoue, K.-i., Chi, X.-Z., Lee, K.-Y., Nomura, S., Lee, C.-W., Han, S.-B., Kim, H.-M., Kim, W.-J., Yamamoto, H., Yamashita, N., Yano, T., Ikeda, T., Itohara, S., Inazawa, J., Abe, T., Hagiwara, A., Yamagishi, H., Ooe, A., Kaneda, A., Sugimura, T., Ushijima, T., Bae, S.-C. & Ito, Y. Causal Relationship between the Loss of RUNX3 Expression and Gastric Cancer. *Cell* **109**, 113-124, doi:https://doi.org/10.1016/S0092-8674(02)00690-6 (2002).

285 Sakuma, A., Fukamachi, H., Ito, K., Ito, Y., Takeuchi, S. & Takahashi, S. Loss of Runx3 affects ovulation and estrogen-induced endometrial cell proliferation in female mice. *Molecular reproduction and development* **75**, 1653-1661, doi:10.1002/mrd.20904 (2008).

286 Ojima, F., Saito, Y., Tsuchiya, Y., Ogoshi, M., Fukamachi, H., Inagaki, K., Otsuka, F., Takeuchi, S. & Takahashi, S. Runx3 regulates folliculogenesis and steroidogenesis in granulosa cells of immature mice. *Cell and Tissue Research* **375**, 743-754, doi:10.1007/s00441-018-2947-2 (2019).

287 Lee-Thacker, S., Choi, Y., Taniuchi, I., Takarada, T., Yoneda, Y., Ko, C. & Jo, M. Core binding factor β expression in ovarian granulosa cells is essential for female fertility. *Endocrinology* **159**, 2094-2109 (2018).

288 Nef, S., Schaad, O., Stallings, N. R., Cederroth, C. R., Pitetti, J.-L., Schaer, G., Malki, S., Dubois-Dauphin, M., Boizet-Bonhoure, B., Descombes, P., Parker, K. L. & Vassalli, J.-D. Gene expression during sex determination reveals a robust female genetic program at the onset of ovarian development. *Developmental Biology* **287**, 361-377, doi:https://doi.org/10.1016/j.ydbio.2005.09.008 (2005).

289 Nicol, B., Grimm, S. A., Chalmel, F., Lecluze, E., Pannetier, M., Pailhoux, E., Dupin-De-Beyssat, E., Guiguen, Y., Capel, B. & Yao, H. H. C. RUNX1 maintains the identity of the fetal ovary through an interplay with FOXL2. *Nature communications* **10**, 5116 (2019). <https://doi.org/10.1038/s41467-019-13060-1>.

290 Terakawa, J., Serna, V. A., Nair, D., Sato, S., Kawakami, K., Radovick, S., Maire, P. & Kurita, T. SIX1 cooperates with RUNX1 and SMAD4 in cell fate commitment of Müllerian duct epithelium. *bioRxiv*, 427351, doi:10.1101/427351 (2018).

291 Jeong, J.-H., Jin, J.-S., Kim, H.-N., Kang, S.-M., Liu, J. C., Lengner, C. J., Otto, F., Mundlos, S., Stein, J. L., van Wijnen, A. J., Lian, J. B., Stein, G. S. & Choi, J.-Y. Expression of Runx2 transcription factor in non-skeletal tissues, sperm and brain. *J Cell Physiol* **217**, 511-517, doi:10.1002/jcp.21524 (2008).

292 Inman, C. K. & Shore, P. The Osteoblast Transcription Factor Runx2 Is Expressed in Mammary Epithelial Cells and Mediates osteopontin Expression. *Journal of Biological Chemistry* **278**, 48684-48689, doi:10.1074/jbc.M308001200 (2003).

293 Zhang, C.-l., Wang, H., Yan, C.-y., Gao, X.-f. & Ling, X.-j. Deregulation of RUNX2 by miR-320a deficiency impairs steroidogenesis in cumulus granulosa cells from polycystic ovary syndrome (PCOS) patients. *Biochemical and Biophysical Research Communications* **482**, 1469-1476, doi:https://doi.org/10.1016/j.bbrc.2016.12.059 (2017).

294 Bai, Z.-K., Guo, B., Tian, X.-C., Li, D.-D., Wang, S.-T., Cao, H., Wang, Q.-Y. & Yue, Z.-P. Expression and regulation of Runx3 in mouse uterus during the peri-implantation period. *Journal of Molecular Histology* **44**, 519-526, doi:10.1007/s10735-013-9501-z (2013).

295 Bai, Z.-K., Li, D.-D., Guo, C.-H., Yang, Z.-Q., Cao, H., Guo, B. & Yue, Z.-P. Differential expression and regulation of Runx1 in mouse uterus during the peri-implantation period. *Cell and Tissue Research* **362**, 231-240, doi:10.1007/s00441-015-2174-z (2015).

296 Guo, C.-H., Yue, Z.-P., Bai, Z.-K., Li, D.-D., Yang, Z.-Q. & Guo, B. Runx2 acts downstream of C/EBPβ to regulate the differentiation of uterine stromal cells in mice. *Cell and Tissue Research* **366**, 393-401, doi:10.1007/s00441-016-2412-z (2016).

297 Wall, E. H., Hewitt, S. C., Liu, L., Rio, R. d., Case, L. K., Lin, C.-Y., Korach, K. S. & Teuscher, C. Genetic control of estrogen-regulated transcriptional and cellular responses in mouse uterus. *The FASEB Journal* **27**, 1874-1886, doi:10.1096/fj.12-213462 (2013).

298 Tsuchiya, Y., Saito, Y., Taniuchi, S., Sakuma, A., Maekawa, T., Fukamachi, H., Takeuchi, S. & Takahashi, S. Runx3 Expression and Its Roles in Mouse Endometrial Cells. *Journal of Reproduction and Development* **58**, 592-598, doi:10.1262/jrd.2012-066 (2012).

299 Otto, F., Lübbert, M. & Stock, M. Upstream and downstream targets of RUNX proteins. *Journal of Cellular Biochemistry* **89**, 9-18, doi:10.1002/jcb.10491 (2003).

300 Otálora-Otálora, B. A., Henríquez, B., López-Kleine, L. & Rojas, A. RUNX family: Oncogenes or tumor suppressors (Review). *Oncology reports* **42**, 3-19, doi:10.3892/or.2019.7149 (2019).

301 Bialek, P., Kern, B., Yang, X., Schrock, M., Sosic, D., Hong, N., Wu, H., Yu, K., Ornitz, D. M., Olson, E. N., Justice, M. J. & Karsenty, G. A Twist Code Determines the Onset of Osteoblast Differentiation. *Developmental Cell* **6**, 423-435, doi:https://doi.org/10.1016/S1534-5807(04)00058-9 (2004).

302 Young, D. W., Hassan, M. Q., Pratap, J., Galindo, M., Zaidi, S. K., Lee, S.-h., Yang, X., Xie, R., Javed, A., Underwood, J. M., Furcinitti, P., Imbalzano, A. N., Penman, S., Nickerson, J. A., Montecino, M. A., Lian, J. B., Stein, J. L., van Wijnen, A. J. & Stein, G. S. Mitotic occupancy and lineage-specific transcriptional control of rRNA genes by Runx2. *Nature* **445**, 442-446, doi:10.1038/nature05473 (2007).

303 Chuang, L. S. H., Ito, K. & Ito, Y. RUNX family: Regulation and diversification of roles through interacting proteins. *International Journal of Cancer* **132**, 1260-1271, doi:10.1002/ijc.27964 (2013).

304 Elagib, K. E., Racke, F. K., Mogass, M., Khetawat, R., Delehanty, L. L. & Goldfarb, A. N. RUNX1 and GATA-1 coexpression and cooperation in megakaryocytic differentiation. *Blood* **101**, 4333-4341 (2003).

305 Cruz-Guilloty, F., Pipkin, M. E., Djuretic, I. M., Levanon, D., Lotem, J., Lichtenheld, M. G., Groner, Y. & Rao, A. Runx3 and T-box proteins cooperate to establish the transcriptional program of effector CTLs. *The Journal of Experimental Medicine* **206**, 51-59, doi:10.1084/jem.20081242 (2009).

306 Bennett, J., Wu, Y.-G., Gossen, J., Zhou, P. & Stocco, C. Loss of GATA-6 and GATA-4 in Granulosa Cells Blocks Folliculogenesis, Ovulation, and Follicle Stimulating Hormone Receptor Expression Leading to Female Infertility. *Endocrinology* **153**, 2474-2485, doi:10.1210/en.2011-1969 (2012).

307 Ning, Y.-M. & Robins, D. M. AML3/CBFα1 Is Required for Androgen-specific Activation of the Enhancer of the Mouse Sex-limited Protein (Slp) Gene. *Journal of Biological Chemistry* **274**, 30624-30630, doi:10.1074/jbc.274.43.30624 (1999).

308 Little, G. H., Baniwal, S. K., Adisetiyo, H., Groshen, S., Chimge, N.-O., Kim, S. Y., Khalid, O., Hawes, D., Jones, J. O., Pinski, J., Schones, D. E. & Frenkel, B. Differential Effects of RUNX2 on the Androgen Receptor in Prostate Cancer: Synergistic Stimulation of a Gene Set Exemplified by SNAI2 and Subsequent Invasiveness. *Cancer Research* **74**, 2857-2868, doi:10.1158/0008-5472.can-13-2003 (2014).

309 Kawate, H., Wu, Y., Ohnaka, K. & Takayanagi, R. Mutual transactivational repression of Runx2 and the androgen receptor by an impairment of their normal compartmentalization. *The Journal of Steroid Biochemistry and Molecular Biology* **105**, 46-56, doi:https://doi.org/10.1016/j.jsbmb.2006.11.020 (2007).

310 Yang, R., Browne, J. A., Eggener, S. E., Leir, S.-H. & Harris, A. A novel transcriptional network for the androgen receptor in human epididymis epithelial cells. *Molecular Human Reproduction* **24**, 433-443, doi:10.1093/molehr/gay029 (2018).

311 McCarthy, T. L., Chang, W.-Z., Liu, Y. & Centrella, M. Runx2 Integrates Estrogen Activity in Osteoblasts. *Journal of Biological Chemistry* **278**, 43121-43129, doi:10.1074/jbc.M306531200 (2003).

312 Stender, J. D., Kim, K., Charn, T. H., Komm, B., Chang, K. C. N., Kraus, W. L., Benner, C., Glass, C. K. & Katzenellenbogen, B. S. Genome-Wide Analysis of Estrogen Receptor α DNA Binding and Tethering Mechanisms Identifies Runx1 as a Novel Tethering Factor in Receptor-Mediated Transcriptional Activation. *Molecular and cellular biology* **30**, 3943-3955, doi:10.1128/mcb.00118-10 (2010).

313 Choi, A., Illendula, A., Pulikkan, J. A., Roderick, J. E., Tesell, J., Yu, J., Hermance, N., Zhu, L. J., Castilla, L. H., Bushweller, J. H. & Kelliher, M. A. RUNX1 is required for oncogenic Myb and Myc enhancer activity in T-cell acute lymphoblastic leukemia. *Blood* **130**, 1722-1733, doi:10.1182/blood-2017-03-775536 (2017).

314 Westendorf, J. J. Transcriptional co-repressors of Runx2. *Journal of Cellular Biochemistry* **98**, 54-64, doi:10.1002/jcb.20805 (2006).

315 Ali, S. A., Dobson, J. R., Lian, J. B., Stein, J. L., van Wijnen, A. J., Zaidi, S. K. & Stein, G. S. A RUNX2–HDAC1 co-repressor complex regulates rRNA gene expression by modulating UBF acetylation. *Journal of Cell Science* **125**, 2732-2739, doi:10.1242/jcs.100909 (2012).

316 Vega, R. B., Matsuda, K., Oh, J., Barbosa, A. C., Yang, X., Meadows, E., McAnally, J., Pomajzl, C., Shelton, J. M., Richardson, J. A., Karsenty, G. & Olson, E. N. Histone Deacetylase 4 Controls Chondrocyte Hypertrophy during Skeletogenesis. *Cell* **119**, 555-566, doi:https://doi.org/10.1016/j.cell.2004.10.024 (2004).

317 Li, X., Hoeppner, L. H., Jensen, E. D., Gopalakrishnan, R. & Westendorf, J. J. Co-activator activator (CoAA) prevents the transcriptional activity of Runt domain transcription factors. *Journal of Cellular Biochemistry* **108**, 378-387, doi:10.1002/jcb.22263 (2009).

318 Yu, M., Mazor, T., Huang, H., Huang, H.-T., Kathrein, K. L., Woo, A. J., Chouinard, C. R., Labadorf, A., Akie, T. E., Moran, T. B., Xie, H., Zacharek, S., Taniuchi, I., Roeder, R. G., Kim, C. F., Zon, L. I., Fraenkel, E. & Cantor, A. B. Direct recruitment of polycomb repressive complex 1 to chromatin by core binding transcription factors. *Molecular cell* **45**, 330-343, doi:10.1016/j.molcel.2011.11.032 (2012).

319 Feld, C., Sahu, P., Frech, M., Finkernagel, F., Nist, A., Stiewe, T., Bauer, U.-M. & Neubauer, A. Combined cistrome and transcriptome analysis of SKI in AML cells identifies SKI as a co-repressor for RUNX1. *Nucleic Acids Research* **46**, 3412-3428, doi:10.1093/nar/gky119 (2018).

320 Chuang, L. S. H. & Ito, Y. RUNX3 is multifunctional in carcinogenesis of multiple solid tumors. *Oncogene* **29**, 2605-2615, doi:10.1038/onc.2010.88 (2010).

321 Guo, H., Ma, O., Speck, N. A. & Friedman, A. D. Runx1 deletion or dominant inhibition reduces Cebpa transcription via conserved promoter and distal enhancer sites to favor monopoiesis over granulopoiesis. *Blood* **119**, 4408-4418, doi:10.1182/blood-2011-12-397091 (2012).

322 Kojo, S., Yasmin, N., Muroi, S., Tenno, M. & Taniuchi, I. Runx-dependent and silencer-independent repression of a maturation enhancer in the Cd4 gene. *Nature communications* **9**, 3593-3593, doi:10.1038/s41467-018-05803-3 (2018).

323 Rodríguez-Caparrós, A., García, V., Casal, Á., López-Ros, J., García-Mariscal, A., Tani-ichi, S., Ikuta, K. & Hernández-Munain, C. Notch Signaling Controls Transcription via the Recruitment of RUNX1 and MYB to Enhancers during T Cell Development. *The Journal of Immunology* **202**, 2460-2472, doi:10.4049/jimmunol.1801650 (2019).

324 Mao, A.-P., Ishizuka, I. E., Kasal, D. N., Mandal, M. & Bendelac, A. A shared Runx1-bound Zbtb16 enhancer directs innate and innate-like lymphoid lineage development. *Nature Communications* **8**, 863, doi:10.1038/s41467-017-00882-0 (2017).

325 Amano, K., Densmore, M., Nishimura, R. & Lanske, B. Indian Hedgehog Signaling Regulates Transcription and Expression of Collagen Type X via Runx2/Smads Interactions. *Journal of Biological Chemistry* **289**, 24898-24910, doi:10.1074/jbc.M114.570507 (2014).

326 Meyer, M. B., Benkusky, N. A., Onal, M. & Pike, J. W. Selective regulation of Mmp13 by 1,25(OH)2D3, PTH, and Osterix through distal enhancers. *The Journal of Steroid Biochemistry and Molecular Biology* **164**, 258-264, doi:https://doi.org/10.1016/j.jsbmb.2015.09.001 (2016).

CHAPTER 2 PGR interacts with transcriptionally active chromatin to regulate target gene expression during ovulation

2.1 INTRODUCTION

Progesterone (P4) is an essential reproductive hormone produced by the ovarian follicular granulosa cells immediately prior to ovulation. Progesterone has diverse pleiotropic roles and plays a primary role in controlling fertility as the essential mediator of ovulation [1]. Progesterone mainly functions through the direct binding and activation of its target receptor PGR, a nuclear receptor that has profound importance in the regulation and maintenance of normal female reproductive physiology. PGR belongs to the 3-Ketosteroid receptor family and includes two isoforms, PGR-A and PGR-B, both of which are present in most PGR-positive cells. However, PGR-A is more important for ovarian and uterine functions whereas PGR-B plays the main role in the mammary gland [2,3].

In reproductive tissues, PGR shows distinct functions that are highly dependent on the tissue context, revealed in studies on PGRKO mouse models [4]. In the pre-ovulatory ovary, PGR is expressed exclusively in granulosa cells in response to the ovulatory LH-surge [5]. Treatment with RU486, a PGR antagonist, results in ovulation suppression in rodents [6,7] and humans [8]. PGRKO female mice are infertile due to complete anovulation with the corpus luteum containing the entrapped oocyte [4]. The role of PGR on oocyte development is more unclear - oocytes from KO mice that have undergone IVM are capable of fertilisation and, following uterine transfer, developing into normal pups [9]. However, *in vitro* studies in other mammalian species, have shown that PGR antagonist treatment has detrimental effects on cumulus expansion [10]. The ovulatory role of PGR is also critical in primates and humans as illustrated by PGR antagonist or gene knockdown [11]. In the ovary, PGR is responsible for the induction of genes that are critical for ovulation, such as *Adamts1, Edn2* and *Pparg* in granulosa cells [12-14]. PGR also plays a number of roles in the reproductive tract including oocyte and embryo transport in the oviduct and decidualisation in the uterus [4], which are achieved through regulating specific genes [15-17]. Although PGR regulates large suites of genes in many reproductive tissues, the transcription-modulating effect of PGR is highly tissue-specific.

Previous studies on PGR-dependent transcriptome profile have been performed independently however, and there has been no direct comparative investigation across different target tissues.

The canonical PGR-dependent transcriptional regulation is most well-studied in breast cancer in which PGR is a ligand-dependent nuclear transcription factor [18]. Upon binding P4, activated PGR translocates into the nucleus and binds to regulatory motifs, most often containing the PRE/NR3C motif. The canonical PRE/NR3C motif is an inverted palindrome, but it is recognised that the PRE/NR3C motif can vary depending on neighbouring transcription factor binding or other chromatin modifiers [19]. The influence of PGR is also not uniquely restricted to genes with known PRE/NR3C, as interaction between PGR and other transcription factors can recruit PGR to non-consensus motifs [20,21]. This has been reported in the ovary for PGR-induced *Adamts1* which does not have PRE/NR3C in the defined regulatory region but possesses G/C-rich regions in the proximal promoter region that bind to SP1/SP3 co-mediators [22]. An interaction between PGR and SP1/SP3 at these sites has been proposed as a mechanism for PGR-mediated gene regulation.

Previous studies on PGR action have largely focused on identifying PGR-regulated genes using targeted reporter assays or genomic screening [22-24], which does little to explain the selective and tissue-dependent action of PGR on the genome. Recent studies have begun to define the molecular pathway of PGR action in the reproductive tract, assisted by improved genome-wide molecular technologies [16,25,26]. However, no studies have yet investigated the molecular pathway involving PGR in the ovary or how the specialised physiological roles in different reproductive organs are achieved through the same receptor signalling mechanism. An understanding of the mechanism responsible for the diversity in PGR action between different target tissues may reveal key details of PGR functions; considering how differently PGR functions between cell types, including normal versus cancerous cells, it is valuable to actively investigate these contrasting regulatory mechanisms. In this chapter, the PGR chromatin-binding cistrome was characterised in relation to the open chromatin landscape defined by H3K27ac in peri-ovulatory granulosa cells through PGR ChIP-seq. The impact of PGR binding on transcription regulation was investigated through comparison with the PGR-dependent transcriptome obtained from microarray analysis of PGRKO granulosa cells, as well as the gene expression profile during ovulation, identified through RNA-seq of granulosa cells pre- and post-LH.

2.2 MATERIALS & METHODS

2.2.1 Animals

CBA x C57BL/6 F1 (CBAF1) mice were obtained from The University of Adelaide, Laboratory Animal Services. All mice were maintained in 12 h light /12 h dark conditions and given water and rodent chow *ad libitum*. All experiments were approved by The University of Adelaide Animal Ethics Committee and were conducted in accordance with the Australian Code of Practice for the Care and Use of Animals for Scientific Purposes (ethics no m/2015/075).

2.2.2 Peri-ovulatory time course experiment

2.2.2.1 Time course sample collection

A total of 69 mice were used for three replicates of the experiment. Samples were collected from mice that were either not stimulated, equine chorionic gonadotropin (eCG)-stimulated or eCG + hCG-stimulated for 4, 6, 8, 10, or 12 h. The allocation of mice according to these time points is listed in Table 2.1. For eCG-stimulated samples, female CBAF1 mice at 3 weeks of age were administered intraperitoneally (i.p) 5 IU eCG (Lee Biosolutions, Maryland Heights, MO, USA). For eCG + hCG-stimulated samples, mice were injected with 5 IU hCG (Merck, Sharp and Dohme) 46 h post-eCG and sacrificed according to allocation plan. Mice were culled by cervical dislocation and whole ovaries were dissected and placed in αMEM media. For obtaining RNA and protein, ovaries were punctured using 26G needle and the COC and granulosa cells (GC) released from ovaries were pooled together, transferred into 1.5ml tubes, briefly centrifuged to remove excess media and snap frozen in liquid nitrogen. All samples were stored at -80^{o}C prior to use.

Table 2.1 Mouse allocation per stimulation time point for the time course experiment.
The number of mice shown below is for one replicate (total 69 mice for three replicates).

Time point	Mice	Ovaries	Ovaries for RNA	Ovaries for Protein
Unstimulated	5	10	4	6
eCG 46 h	3	6	3	3
eCG + hCG 4h	3	6	3	3
eCG + hCG 6 h	3	6	3	3
eCG + hCG 8 h	3	6	3	3
eCG + hCG 10 h	3	6	3	3
eCG + hCG 12 h	3	6	3	3
Total number	**23**	**46**	**Total mice (3 replicates)**	**69**

2.2.2.2 mRNA level quantification

RNA from COC/GC collected from the time course collection was purified using RNeasy Mini Kit and accompanying protocol (Qiagen, Hilden, Germany). Briefly, cells were lysed in 350 µl lysis buffer with added β-mercaptoethanol and the lysate was applied to spin column for purification. RNA was treated with DNase I while on column and eluted with 15 µl H_2O. Final RNA concentration was measured using the Nanodrop 2000 Spectrophotometer (Thermo Fisher). cDNA from purified RNA was synthesised using the Superscript III First-Strand kit and accompanying protocol (Thermo Fisher). 500 ng of purified RNA was used per reaction. To confirm that there was no genomic DNA contamination, 'no reverse transcriptase' negative controls were included. The reaction was conducted in a GeneAmp PCR System 9700 (Applied Biosystems, Thermo Fisher) at the following setting: 25^{o}C for 10 minutes, 50^{o}C for 50 minutes, 85^{o}C for 5 minutes, 4^{o}C to cool. Then, 2 U RNAse H were added to each sample for RNA digestion and the samples were incubated for a further 20 minutes at 37^{o}C. cDNA was then diluted in H_2O for a final concentration of 5 ng/µl. cDNA was stored at -20^{o}C for short term or -80^{o}C for long term prior to use.

RT-qPCR for gene expression analysis was done using Taqman assays (Appendix 1) and Gene Expression Mastermix (Thermo Fisher). The following components were included per every 10 µl reaction: 5 µl Mastermix, 0.25 µl Taqman assay, 3.75 µl H_2O and 1 µl cDNA. The reaction was run in a QuantStudio 12K Flex Real-Time PCR System (Thermo Fisher) and the thermal cycle setting was as follows: 50^{o}C for 2 minutes, 95^{o}C for 10 minutes, [95^{o}C for 15 seconds, 60^{o}C for 1 minute] x 40 cycles. Controls included the absence of cDNA (H_2O control) or reverse transcriptase ('-RT' control). Each reaction was run in technical triplicates. The

quantification of gene expression was presented as the relative expression of three replicates normalised to the unstimulated sample, with *Rpl19* as the housekeeping gene, using the delta delta C_T formula. Data normality was confirmed using the Shapiro-Wilk test due to the small number of data points. Statistical significance was determined through one-way ANOVA with Tukey test for multiple comparison.

2.2.2.3 Protein level quantification

Lysate was prepared from COC/GC pooled from 3 ovaries by adding 100 µl LDS Sample Buffer 4x (Thermo Fisher), 1 µl β-mercaptoethanol and 1 µl benzonase, then incubated for 10 minutes at 65^{o}C for cell lysis and protein denaturation. Western blot was performed using pre-set Bolt 4-12% Bis-Tris Plus gels (Thermo Fisher) in MES running buffer (Thermo Fisher) in a Bolt Mini Gel Tank (Thermo Fisher). For each well, 5-10 µl denatured lysate was loaded and 5 µl of Precision Plus protein standard (Bio-Rad, Gladesville, NSW, Australia) was used as the protein ladder. Electrophoresis was at 165 V for 40 minutes at room temperature or until the loading dye had run off the gel. Protein from the gel was transferred onto nitrocellulose membrane in a standard transfer sandwich at 15 V for 35 minutes at room temperature. Protein loading was confirmed by Ponceau S staining for 5 minutes and prior to blocking the stain was removed by incubating with phosphate buffered saline (PBS). The membrane was blocked in Odyssey Blocking buffer for 1 h at room temperature or overnight at 4^{o}C. Primary and secondary antibodies were prepared accordingly to Appendix 2 and membrane was stained for at least 1 h at room temperature on constant rotation (from secondary antibody incubation onwards, the membrane container was kept in the dark throughout incubation). Membrane was washed three times with PBS + 0.05% Tween-20 (pH 7.4) after each incubation and finally rinsed briefly with PBS before imaging. For fluorescent detection, the membrane was imaged using the LiCor Odyssey 9120 Imaging System (LiCor, Lincoln, NE, USA) with accompanying software. Statistical significance was determined through two-way ANOVA with Tukey test for multiple comparison.

2.2.3 ChIP-seq

2.2.3.1 Experiment

Super-ovulation in 21-day old CBAF1 female mice was induced by injecting mice i.p with 5 IU eCG and 5 IU hCG 46 h post-hCG. Mice were culled and dissected at 6 h post-hCG for whole ovary extraction. Granulosa cells collected from punctured ovaries were snap frozen in

liquid nitrogen and shipped in liquid nitrogen to Active Motif (Carlsbad, CA, USA) for ChIP-seq. Two samples from at least 5 mice with a minimum of $1x10^7$ cells were used for PGR ChIP (both replicates) and H3K27ac (one replicate). Briefly, cells were fixed in 1% formaldehyde for 15 minutes and quenched with 0.125 M glycine. Chromatin was isolated by the addition of lysis buffer, followed by disruption with a Dounce homogenizer. Lysates were sonicated and the DNA sheared to an average length of 300-500 bp. Lysate was precleared with protein A agarose bead (Invitrogen, Waltham, USA) and PGR ChIP was performed using antibodies as listed in Appendix 3. Protein-chromatin complexes were washed, eluted from beads and subjected to RNase and proteinase K treatment. Reverse crosslinking was through overnight incubation at 65ºC. DNA was purified by phenol-chloroform extraction and ethanol precipitation. Isolated chromatin was confirmed using qPCR on specific genomic regions with expected PGR and H3K27ac interaction in triplicate using SYBR Green Supermix (Bio-Rad). Illumina sequencing libraries were prepared from the ChIP and input DNA by the standard consecutive enzymatic steps of end-polishing, dA-addition, and adaptor ligation. After a final PCR amplification step, the resulting DNA libraries were quantified and sequenced on Illumina's NextSeq 500 (75 nt reads, single end).

2.2.3.2 Bioinformatics analysis

Bioinformatics analysis was conducted in a combination of R, web-based tools, software and Linux command line as per appropriate for the tool. An overall workflow chart and main bioinformatics tools used for bioinformatics analysis are as described in Figure 2.1 and Table 2.2. Unless otherwise indicated, all analysis was performed using the mm10 assembly as the mouse genome. For all datasets, the quality of raw data was assessed using FASTQC (http://www.bioinformatics.babraham.ac.uk/projects/fastqc). Next, 75-base sequences were aligned using Bowtie2 algorithm [27]. The reproducibility of biological replicates was assessed using Irreproducibility Discovery Rate (IDR) criteria [28]. As the two replicates showed good level of correlation, peaks were called individually for each replicate. Peak calling from read count against input control followed the algorithm for MACS2 [29] with a p-value cut-off = 10^{-10} and a mouse genome size of $1.87x10^9$. Initial analysis showed a high level of overlapping between replicates, with the majority of peaks called in replicate 2 identifiable in replicate 1, thus the overlapped peaks identified via ChIPpeakAnno package [30] in R were used as the consensus data, with overlapped peaks with narrower width chosen to represent a more

conservative dataset. A summary of library size, sequence length, alignment rate and peak count is included in Appendix 4.

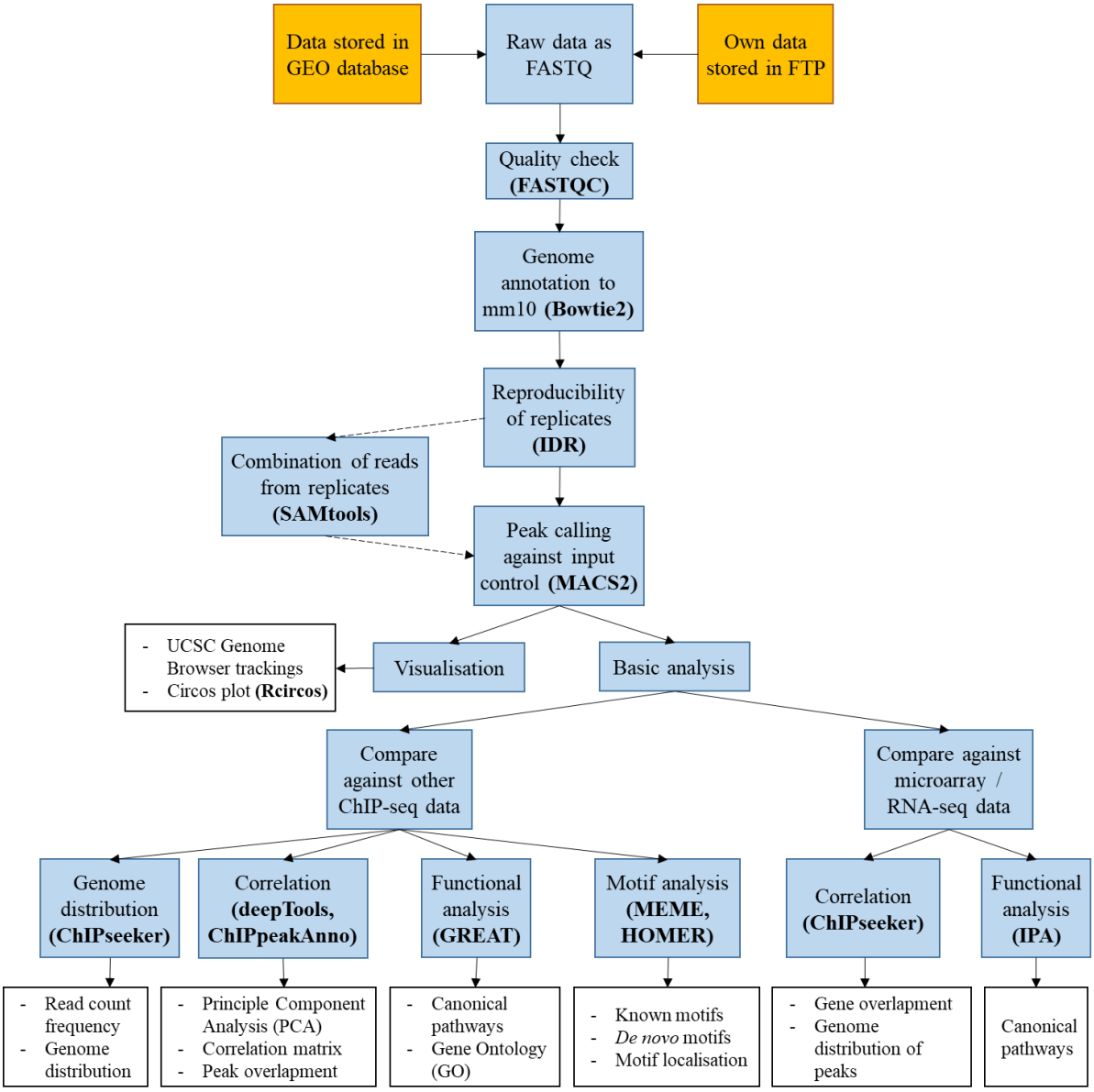

Figure 2.1 Bioinformatics workflow for the analysis of ChP-seq data.

Input sources are indicated in orange boxes. Steps in the analysis are indicated in blue boxes, with output presentation listed in white boxes.

Table 2.2 Tools used for bioinformatics analysis of ChIP-seq data

Goal	Package/tool	Reference
Conversion from SRA to FASTQ format	SRA tools	(http://ncbi.github.io/sra-tools/)
Quality check of FASTQ files	FASTQC	(http://www.bioinformatics.babraham.ac.uk/projects/fastqc/
Genome annotation	Bowtie2	[27]
Reproducibility of data	IDR	[28]
Read combination	samtools	[31]
Peak calling	MACS2	[29]
Peak visualisation on UCSC Genome Browser	UCSC toolkits	[32]
Circos plot plotting	Rcircos	[33]
Correlation via PCA	deepTools	[34]
Correlation via correlation coefficient	deepTools	[34]
Peak/Gene overlapping	ChIPpeakAnno	[30]
Read count frequency against TSS	ChIPseeker	[35]
Genome distribution	ChIPseeker	[35]
Canonical pathway - ChIP-seq	GREAT	[36]
Gene Ontology analysis	GREAT	[36]
Gene Ontology summary and visualisation	REVIGO	[37]
Canonical motif mapping	MEME	[38]
Known motif and *de novo* motif analysis	HOMER	[39]
Motif localisation	HOMER	[39]
Canonical pathway - RNA-seq/microarray	IPA Core Analysis	Qiagen

Correlation of genomic coverage between ChIP-seq datasets was assessed through deeptools commands, with all correlation coefficients passing statistical significance [34]. Genome distribution of peaks was determined using ChIPseeker package [35] in R, with gene boundaries set as ±3 kb of the transcription start site (TSS) / transcription end site (TES) (i.e. TSS - 3 kb assigned as promoter and TES + 3kb assigned as downstream) and regions that did not fall into this range considered to be distal intergenic. Read count frequency plotting was done using the ChIPSeeker package in R for peaks within ±3 kb of the TSS. Functional analysis of peaks, including canonical pathways and Gene Ontology analysis, was through GREAT [36]. Visualisation of Gene Ontology result was through REVIGO [37]. Functional analysis of microarray / RNA-seq identified differentially expressed genes (DEG) was through the IPA software (QIAGEN). For the identification of motif map on the whole mouse genome, the corresponding position weight matrix was obtained from the HOMER Motif Database [39] (Table

2.3) and mapping was conducted using the fimo command in MEME Suite [38]. Motif analysis for known and *de novo* sequence motifs was performed using HOMER motif finding algorithm, with random 200 bp-long sequences from the mouse genome used to estimate motif frequency in random sequence (motif enrichment over background). For visualisation of ChIP-seq data on the UCSC Genome Browser in mm10 genome, output BEDGRAPH files from MACS2 were processed and converted to BIGWIG files using the UCSC toolkit [40]. Files were stored in the public server of Galaxy [41] and uploaded to the UCSC Genome Browser. Visualisation of PRE/NR3C loci are through GFF files generated from the fimo command in MEME Suite on the UCSC Genome Browser [38]. All data are publicly available and both raw and processed data can be accessed from the GEO Database (GEO accession number: GSE115820).

Table 2.3 Position weight matrix for the PRE/NR3C motif from HOMER Motif Database that was used for the identification of the motif map.

Each row corresponds to a nucleotide in the consensus sequence and each column corresponds to nucleotide A, C, G or T. The number represents the probability of each nucleotide to be present at that position.

```
ALPHABET= ACGT

strands: + -

Background letter frequencies (from unknown source):
A 0.250 C 0.250 G 0.250 T 0.250

letter-probability matrix: alength= 4 w= 13 nsites= 1 E= 0e+0

0.000000 0.000000 1.000000 0.000000
0.639000 0.087000 0.117000 0.157000
1.000000 0.000000 0.001000 0.000000
0.000000 1.000000 0.000000 0.000000
0.919000 0.001000 0.001000 0.079000
0.200799 0.171828 0.225774 0.401598
0.383000 0.113000 0.109000 0.395000
0.339339 0.303303 0.146146 0.211211
0.000000 0.000000 0.000000 1.000000
0.000000 0.000000 1.000000 0.000000
0.000000 0.000000 0.000000 1.000000
0.179000 0.146000 0.066000 0.609000
0.000000 1.000000 0.000000 0.000000
```

2.2.4 ChIP-qPCR

Granulosa cells from super-ovulated CBAF1 female mice were collected at 46 h post-eCG or 6 h post-hCG as previously described. Cells were fixed in 1% formaldehyde for 15 minutes at 37^{o}C and quenched with 0.125 M glycine for 10 minutes at room temperate. Cells were washed twice with cold PBS and lysed in lysis buffer (10 mM HEPES, 100 mM KCl, 0.5% NP-40) for 30 minutes at 4^{o}C. Lysate was sonicated using a Bioruptor Plus (Diagenode, Denville, NJ, USA) for 15 minutes at High setting, 30 secs on 30 sec off, then centrifuged at 10000 g for 15 minutes to remove cell debris. To measure protein concentration, Bradford assay using Bio-Rad Protein Assay Dye Reagent Concentrate (Bio-Rad) was performed, with bovine serum albumin (BSA) at concentrations of 40-640 µg/ml were used as protein standards and measurements taken in duplicate for each sample using the Synergy H1 Hybrid Reader (BioTek, Winooski, VT, USA) and the accompanying Gen5 2.00 software.

For immunoprecipitation, Protein A+G magnetic beads (Merck, Burlington, MA, USA) was washed and blocked in BSA (1 mg/ml) and incubated with 4 µg antibodies (PGR or IgG control – Appendix 3) for 30 minutes at room temperature. Lysate was incubated with antibody-bound beads in IP buffer (25 mM Tris (pH 7.4), 5 mM EDTA, 150 mM KCl, 0.5 mM DTT, 0.5% NP-40) for at least 16 h at 4^{o}C, with one volume of lysate retained as lysate input. Beads were washed in IP buffer 5 times for 5 minutes each, then reverse crosslinking was by heating protein-bound beads and lysate input in proteinase K buffer for 30 minutes at 55^{o}C. Lysate was removed from beads and DNA was purified using phenol extraction. Briefly, one volume of phenol:chloroform:isoamyl was added to the bead elute and lysate input, then DNA was precipitated from the aqueous phase at -80^{o}C for at least 2 h by the addition of ammonium acetate and ethanol. Precipitated DNA was washed with 70% ethanol and eluted in 50 µl TEN buffer (0.01 M Tris-HCl pH 8, 1 mM EDTA pH 8, 0.1 M NaCl).

qPCR was performed using SYBR Green Master Mix (Thermo Fisher) and primers specific to target chromatins of PGR as indicated in ChIP-seq. Primers are listed in Appendix 1. qPCR was run on the 7900HT Fast Real-Time PCR System (Applied Biosystems, Thermo Fisher) with the following thermal cycle settings: 50^{o}C for 2 mins, 95^{o}C for 10 mins, [95^{o}C for 15 secs, 60^{o}C for 1 min] x 40 cycles. DNA enrichment result was presented as fold enrichment of PGR to IgG control and to lysate input, using the following formula:

$$Fold\ enriched = \frac{100 * 2^{CT_{input} - CT_{PGR}}}{100 * 2^{CT_{input} - CT_{IgG}}}$$

CT_{input} : C_T value of lysate input

CT_{PGR} : C_T value of PGR elute

CT_{IgG} : C_T value of IgG elute

Statistical significance was determined through one-way ANOVA with Tukey test for multiple comparison.

2.2.5 Microarray data

Gene lists for granulosa cell microarray on PGRKO vs PGR+/± mice were originally from Lisa Akison's thesis [42], now published and publicly available (GEO accession number: GSE92438) [43]. Canonical pathway analysis was performed using IPA software (Qiagen).

2.3 RESULTS

2.3.1 The expression of PGR in peri-ovulatory granulosa cells

The temporal transcriptional pattern of *Pgr* expression during ovulation was confirmed by RT-qPCR on mouse granulosa cells at various hCG-stimulated time points. The expression of *Pgr* was significantly and transiently induced during the pre-ovulatory period, being highest at 4 h post-hCG stimulation compared to later time points (Figure 2.2A). Western blot on protein extracts across the same time-course mimicked the mRNA expression and showed both isoforms – PGR-A (83 kDa) and PGR-B (115 kDa) – induced from 4 h post-hCG, achieving highest intensity at the 6 h time point (Figure 2.2B).

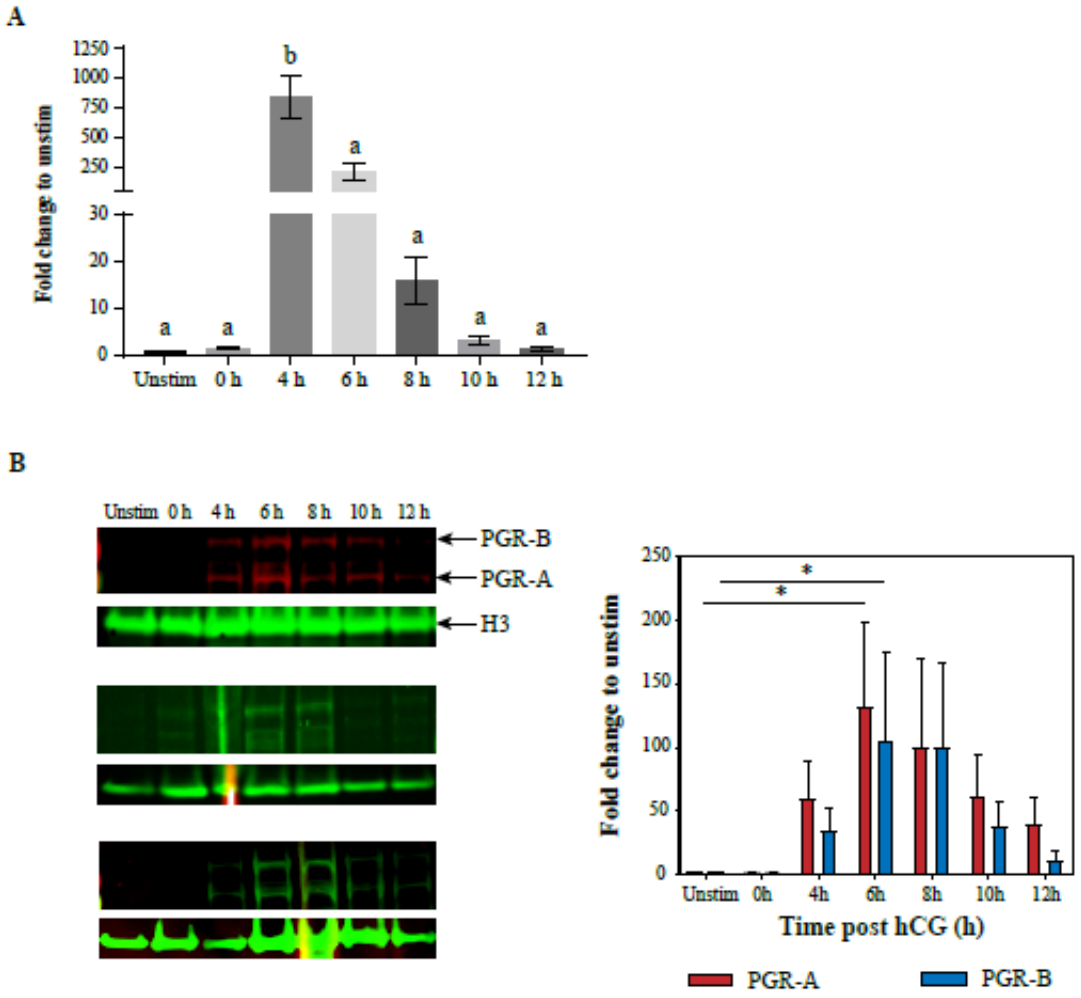

Figure 2.2 PGR mRNA and protein are induced by the LH surge in granulosa cells.

(A) PGR mRNA expression in unstimulated (unstim) or eCG and hCG-primed granulosa cells in eCG 44 h only (0 h) or eCG 44 h + hCG at the indicated times. Fold change is displayed as normalised to the housekeeping *Rpl19* gene and relative to the unstim sample. N = 3 biological replicates, each replicate is from 3-5 mice per time point. Statistical significance was determined through one-way ANOVA with multiple comparison, p-value < 0.0001. Bars with different superscripts are significantly different. **(B)** Western blot of PGR in granulosa cells during ovulation (unstim or eCG + hCG 0-12 h post-hCG). Western blot was performed in N=3 biological replicates, with 3-5 mice per time point per replicate. For each replicate, Western blot was performed for PGR (top panels) and H3 (bottom panel) as the nuclear control. Quantification of Western intensity for PGR-A (red bars) and PGR-B (blue bars) is displayed as fold change to the H3 and to the unstimulated sample. Statistical analysis was through one-way ANOVA with multiple comparison, asterisks indicating statistical significance (p-value < 0.05)

2.3.2 PGR-dependent transcriptome in peri-ovulatory granulosa cells

To identify PGR target genes in granulosa cells, microarray analysis was performed on granulosa cells obtained at 8 h post-hCG stimulated PGRKO and PGR heterozygous female mice. Details for this experiment have been previously published [15]. Selection criteria of p-value ≤ 0.01 and $|\log FC| \geq 1$ were applied in order to determine DEGs from the total gene list and from the more than 20,000 genes originally identified in the microarray, 61 DEGs were selected (Appendix 5). Among these DEGs, almost all (60/61 genes) were downregulated in PGRKO granulosa cells, indicating that their induction is dependent on the presence of PGR, including known PGR target genes *Zbtb16* and *Adamts1* (Figure 2.3A and 2.3B). These DEGs belonged to a number of canonical pathways, including those specific to reproductive tissues such as oestradiol-dependent breast cancer signalling and ovarian cancer signalling (Figure 2.3C). Interestingly, CXCR4 signalling pathway was one of the most enriched pathways, which concurred with the fact that *Cxcr4* was identified as a PGR-dependent gene.

A

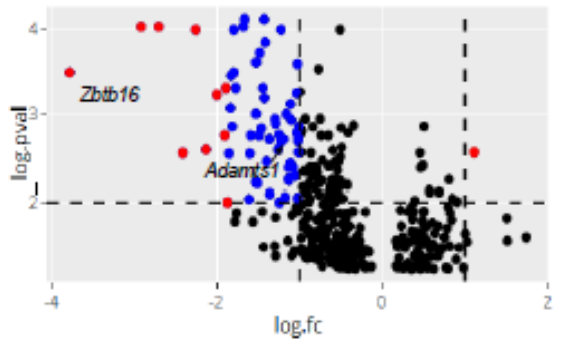

B

Probeset ID	Gene Symbol	RefSeq	stepup p-value	Fold-Change(KO vs. +/-)
10593225	Zbtb16	NM_001033324	0.00032	-13.7345
10498024	Slc7a11	NM_011990	0.00009	-7.5591
10531919	Hsd17b11	NM_053262	0.00009	-6.5212
10380285	Tmem100	NM_026433	0.00277	-5.3345
10573626	Gpt2	NM_173866	0.00010	-4.7675
10381474	Arl4d	NM_025404	0.00254	-4.3798
10493873	Sprr2g	NR_003548	0.00059	-4.0126
10454198	Rnf125	NM_026301	0.00173	-3.7550
10576911	Efnb2	NM_010111	0.00049	-3.7175
10588263	Slco2a1	NM_033314	0.00991	-3.6604
10448081	Rgmb	NM_178615	0.00272	2.1630

C

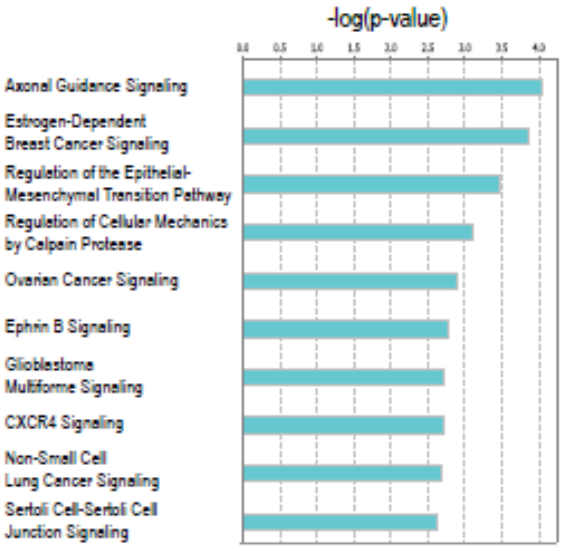

Figure 2.3 PGR-dependent differentially expressed genes in PGRKO vs PGR+/- peri-ovulatory granulosa cells.

(A) Volcano plot of granulosa cell microarray data. The horizontal dashed line indicates p-value cut-off (-log(p-value) ≥ 2). The vertical dashed lines indicate fold change cut-off (|logFC| ≥ 1). Genes that meet these criteria are indicated in blue. Genes that have been selected for panel B are indicated in red. List of DEG is in Appendix 5. **(B)** Examples of genes that are significantly differentially expressed in PGRKO granulosa cells. **(C)** Canonical pathway analysis of PGR-regulated DEG identified in microarray. 61 DEG that were determined from granulosa cell microarray were analysed for enriched pathways using the IPA software. Pathways with a -log(p-value) ≥ 2 were determined to be significantly enriched.

2.3.3 Characteristics of PGR chromatin-binding properties in peri-ovulatory granulosa cells

2.3.3.1 Quality control of PGR ChIP-seq

As seen from Figure 2.2A, the protein level of PGR was highest at 6 h post-hCG stimulation in granulosa cells, which suggested that PGR activity would be the highest at this time point and was thus chosen for investigation of PGR cistrome in granulosa cells. For this, ChIP-seq targeting PGR was performed on granulosa cells harvested at 6 h post-hCG stimulation. Two biological replicates were used for ChIP-seq, each with at least $1x10^7$ cells, with the input control pooled from both replicates. Sequencing quality control for each replicate and the pooled input was conducted using the FASTQC package in R, which judged the quality of sequencing based on sequence quality, sequence content, GC content, length distribution, sequence duplication level and adaptor content. Overall there was no major failed flag in any of the dataset, thus no failed reads were removed and all sequences were included in the subsequent analysis.

2.3.3.2 Assessing robustness and selection of consensus PGR binding sites

To confirm the robustness of the ChIP-seq assay, the reproducibility of the biological replicates was investigated using IDR [28] criteria and the correlation between the two replicates was examined. IDR analysis showed the typical correlation pattern of peaks identified in high-quality ChIP-seq data, including good consistency in peak ranking between the two replicates (Appendix 6A) and a pronounced inflection in the IDR-peak count curve. Further assessment also confirmed the level of correlation between the two replicates. The read count frequency of the two replicates relative to the TSS was highly similar (Appendix 6B), with binding sites from both replicates congregating near the TSS. Pearson correlation coefficient test showed that there was a high correlation between the two replicates, with a 0.95 correlation coefficient (Appendix 6C). An average of 24770 PGR peaks were identified, each duplicate having 31958 and 17582 peaks respectively. Global comparison showed that the majority of binding sites in replicate 2 was in common with replicate 1 (accounting for 15553 binding sites, or 48.67% of replicate 1 and 88.46% of replicate 2) (Appendix 6D). The shared 15553 sites between the two replicates, aligning to 8656 genes, represented the most conservative set of binding sites and were thus chosen as the consensus PGR binding sites for subsequent analyses.

In-house PGR ChIP followed by qPCR also validated the reproducibility of the assay. ChIP was performed on mouse granulosa cells stimulated with eCG followed by 6 h hCG or no hCG, using a PGR antibody targeting a different immunogen from the one used for ChIP-seq (thus validating the specificity to PGR of the antibodies used). Purified chromatins following PGR pull-down were used for qPCR with primers specific to chromatin targets that were observed to have PGR binding or no PGR binding (negative control) via ChIP-seq. ChIP-qPCR results reflected the pattern previously observed and thus validated the ChIP-seq result, with PGR target chromatins being enriched in hCG-stimulated granulosa cells compared to unstimulated and PGR non-target showing no enrichment (Figure 2.4).

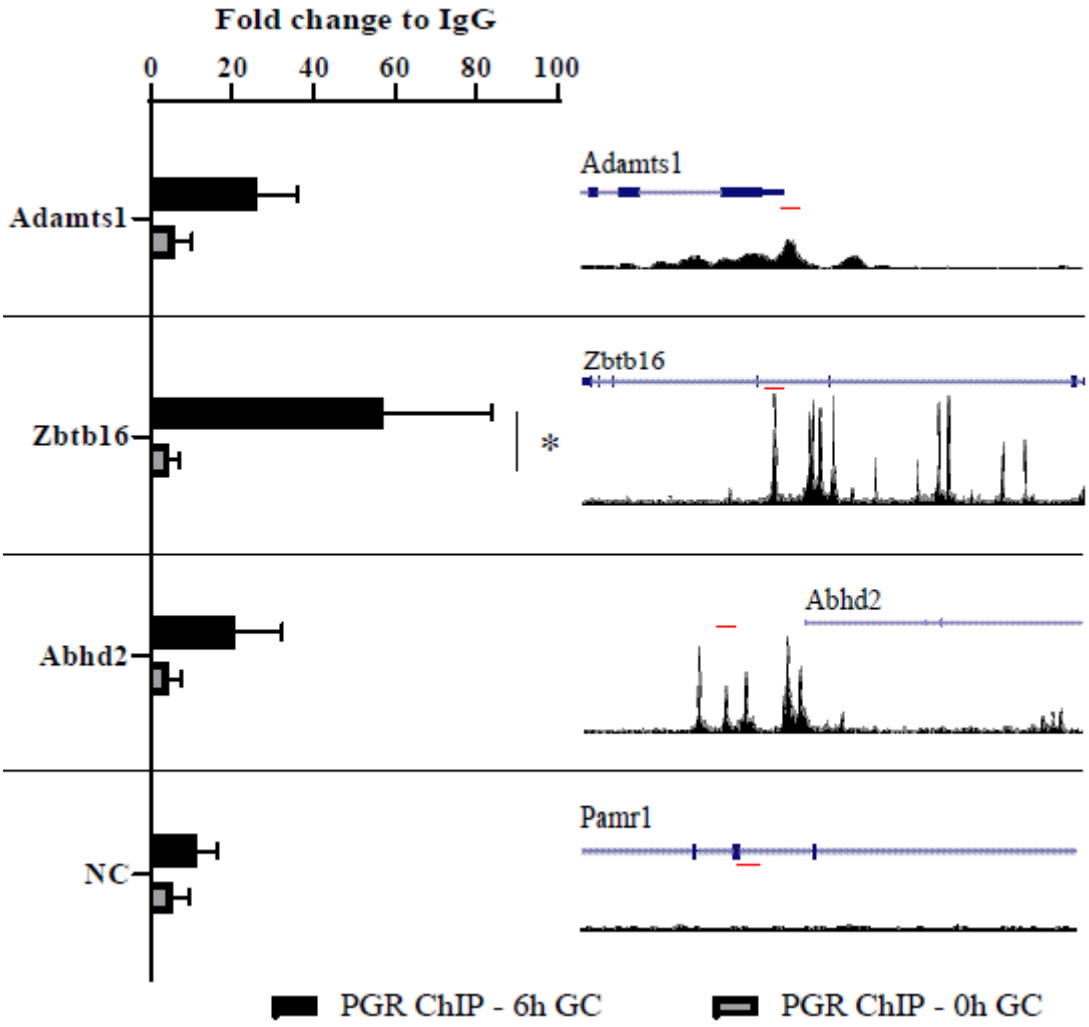

Figure 2.4 Validation of PGR ChIP-seq through ChIP-qPCR.

ChIP-qPCR was performed on mouse granulosa cells obtained with (6 h) or without (0 h) hCG stimulation using antibodies for PGR or IgG negative control. Primers were designed against PGR binding sites according to ChIP-seq data and against a PGR non-binding region (negative control – NC). Data is normalised to IgG pull-down. Black bars are 6 h post-hCG and grey bars are 0 h post-hCG granulosa cells. Statistical difference between 6h and 0h samples was determined using two-way ANOVA test with multiple comparison. Asterisk indicates statistical significance (p-value < 0.05).

2.3.3.1 PGR preference for transcriptionally active promoters in granulosa cells

As seen in the PGR-dependent transcriptome, PGR is responsible for the upregulation of gene expression, thus it is likely that PGR occupancy is enriched at transcriptionally active chromatin sites. To investigate this, PGR and H3K27ac occupancy in granulosa cells were analysed in parallel. Characterisation of TSS-proximal PGR and H3K27ac peaks showed that both were highly enriched very close to TSS; furthermore, the two datasets displayed a commonly observed pattern to previously shown H3K27ac-transcription factor topography, with PGR peaks generally falling into the valley of two flanking H3K27ac peaks (Figure 2.5A). Approximately three-quarters of PGR binding sites overlapped H3K27ac peaks that were associated with 6385 genes (Figure 2.5B), suggesting that PGR indeed mostly binds to transcriptionally active regions. Interestingly, 61.88% of the overlapping PGR and H3K27ac peaks were situated in promoter regions, mostly within 1 kb of a TSS. Conversely, non-overlapping PGR or H3K27ac peaks were relatively randomly distributed in relation to gene structures. In the case of PGR-unique peaks, nearly 40% of identified peaks fell within genebodies, mostly in intergenic and intronic regions. An example of H3K27ac and PGR colocalisation is depicted in a section of chromosome 3, in which the majority of PGR binding sites overlapped with H3K27ac sites, especially in proximity to a genebody (Figure 2.5C). This was also observed in PGR-regulated genes; for example in *Mt2*, a PGR-induced gene in granulosa cells as determined in the PGRKO transcriptome (Figure 2.5D), prominent PGR peaks overlapping with H3K27ac peaks were detected surrounding the TSS of the gene, most notably in the proximal 5' region, suggesting that this region is a PGR-responsive promoter important for *Mt2* transcription.

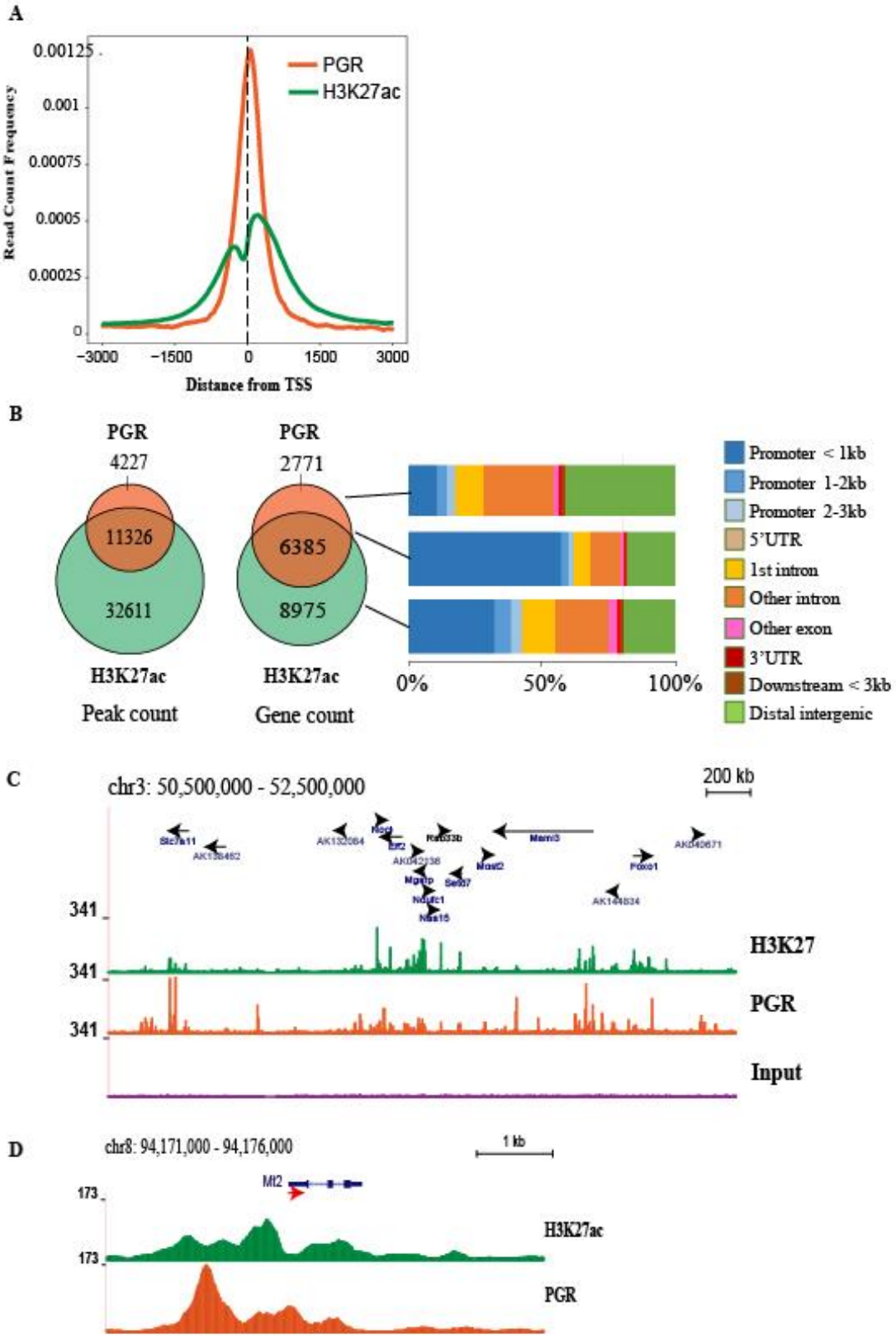
A
0.00125
0.001
0.00075
0.0005
0.00025
0
Read Count Frequency
PGR
H3K27ac
−3000
−1500
0
1500
3000
Distance from TSS
B
PGR
4227
11326
32611
H3K27ac
Peak count
PGR
2771
6385
8975
H3K27ac
Gene count
0%
50%
100%
Promoter < 1kb
Promoter 1-2kb
Promoter 2-3kb
5'UTR
1st intron
Other intron
Other exon
3'UTR
Downstream < 3kb
Distal intergenic
C
chr3: 50,500,000 - 52,500,000
200 kb
341
341
341
H3K27
PGR
Input
D
chr8: 94,171,000 - 94,176,000
1 kb
Mt2
173
173
H3K27ac
PGR

Figure 2.5 PGR associates with transcriptionally active promoters in granulosa cells.
(A) Read count frequency of PGR peaks (orange) and H3K27ac peaks (green) in relation to transcription start sites (TSS). **(B)** Venn diagrams showing the peak count for PGR and H3K27ac and genes with peaks. In each case > 70% of PGR peaks overlap with H3K27ac peaks. Genome distribution of PGR in association with H3K27ac is shown on the right. Genome distribution is displayed as stacked bar graphs and peaks were divided into PGR-unique (top), PGR/H3K27ac overlap (middle) and H3K27ac-unique (bottom). Genomic features include promoters (< 1 kb, 1-2 kb and 2-3 kb), 5' UTR, 1st intron, other introns, exons, 3' UTR and downstream of TES (within 3 kb). Peaks that are not in these features are classified as distal intergenic. **(C)** Example of H3K27ac and PGR binding sites in the mouse genome visualised through UCSC Genome Browser. Tracks are located at chromosome 3 and normalised to the same scale. Genes and direction of transcription are indicated by black arrows. From top to bottom: H3K27ac (green), PGR (orange) and input control (purple). **(D)** Example of H3K27ac and PGR binding sites at the genomic region for *Mt2*. The red arrow indicates the TSS (arrow tail) and direction of transcription.

2.3.3.2 Functional consequences of the PGR cistrome

In order to obtain a scope of the role of PGR chromatin binding in transcription regulation in peri-ovulatory granulosa cells, genes identified in the PGR cistrome were also compared with the ovulation transcriptome, obtained from RNA-seq of granulosa cells from 8 h post-hCG treated mice (Appendix 7). Among the 2179 genes identified in RNA-seq, one-third (or 750 genes) were overlapped with genes annotated to PGR peaks (Figure 2.6A). Interestingly, PGR peaks in association with peri-ovulatory transcriptome were prominently enriched in promoter regions (about 40%). These results suggest that indeed PGR employs interaction with the promoter region to regulate target genes.

The functional impact of PGR cistrome was assessed on a global scale through pathway and Gene Ontology enrichment analysis of PGR peaks in conjunction with H3K27ac peaks. The results showed that PGR and H3K27ac peaks showed functional similarities, with both datasets being enriched for pathways involving cell cycle, transcription and translation regulation (Figure 2.6B) and similar ontological terms identified in both groups (Figure 2.6C). This showed that not only did PGR and H3K27ac shared spatial interaction at the chromatin level but they were also functionally linked in granulosa cells.

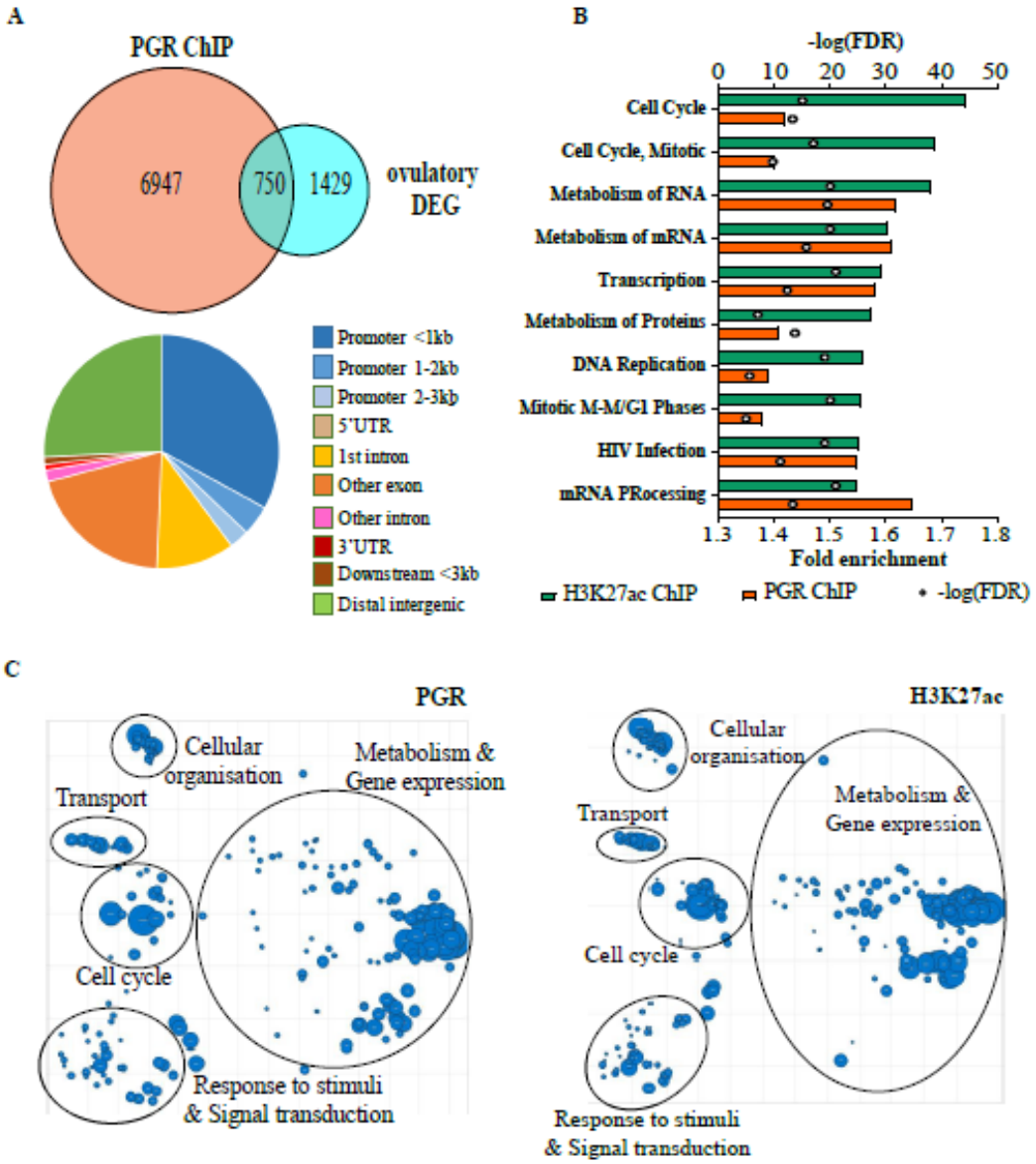

Figure 2.6 Consequence of PGR binding on PGR-dependent gene expression and peri-ovulatory transcriptome.

(A) Venn diagram showing DEG in 8 h post-hCG granulosa cell RNA-seq (ovulatory DEG) in relation to genes with PGR binding sites from ChIP-seq (top) and genome distribution of PGR peaks identified in peri-ovulatory transcriptome (bottom). **(B)** Top ten most enriched pathways associated with binding sites for H3K27ac (green) and PGR (orange). Bars indicate fold enrichment of pathways (bottom x axis). Circles indicate -log(FDR) value (top x axis). **(C)** Gene Ontology analysis of PGR and H3K27ac binding sites. Ontological terms associated with biological processes were obtained from analysis of PGR and H3K27ac ChIP-seq and condensed using REVIGO. Each reduced term is displayed as a circle with the diameter correlating to the -log10(p-value) of said term. Terms of the same umbrella of biological process are grouped together in the XY graph.

2.3.3.3 PGR interacts with PRE as well as non-canonical chromatin motifs

Canonically, PGR is known to interact with the PRE sequence (more generically the NR3C motif, termed PRE/NR3C from now) at target promoters in order to regulate gene expression. However, as PGR shared a response element with other NR3C receptors, such as AR and GR, it is likely that PGR only binds to a selective number of PRE/NR3C loci in the genome. In order to investigate the extent of PGR binding coverage on PRE/NR3C motif, PGR peaks in granulosa cells were compared against global PRE loci in the mouse genome. Using a stringent PRE sequence that is restricted to only full-site PRE (Table 2.3), 37869 loci were identified on the DNA plus strand (or 75607 loci on both strands), among which 642 were bound by PGR, representing 4.43% of PGR binding peaks (Figure 2.7A). As PGR can bind to both transcriptionally active and inactive chromatins, the possible difference in the level of PRE occupancy between chromatins in different active states was also investigated through parallel analysis of PGR and H3K27ac binding sites for overlap with the stringent global PRE map. Approximately half of previously identified PGR binding at PRE loci was shared with H3K27ac (344 sites), which suggested that the chromatin state, while important, was not critical in allowing PGR to bind to PRE and also meant that PGR recruitment to active chromatin is not solely reliant on binding to PRE. Interestingly, H3K27ac could also bind PRE loci independently of PGR binding, suggesting the possibility that other transcription factors, likely other members of the NR3C family, also functioned through the canonical NR3C pathway in peri-ovulatory granulosa cells. Genome distribution analysis showed that PRE loci tended to be found in distal intergenic regions, an understandable result given that the majority of the genome is not defined as genes. In comparison there was an enrichment for proximal promoter-occupied PRE among PGR-H3K27ac shared peaks, supporting the concept that PGR interacts with transcriptionally active promoters and to some extent via interaction with the canonical PRE/NR3C motif (Figure 2.7B).

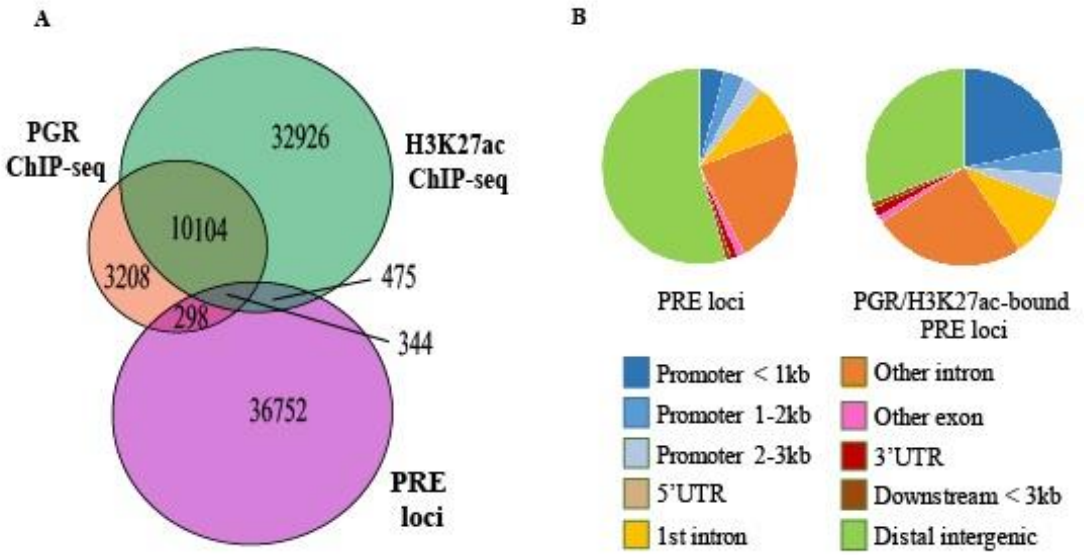

Figure 2.7 PGR binding properties to the canonical PRE motif in granulosa cells.
(A) Venn diagram showing PGR peaks from ChIP-seq in relation to genome-wide consensus PRE locations. PRE sites within the entire mouse genome were identified using FIMO in MEME Suite searching for the consensus PRE sequence. 5% of PGR peaks overlapped with these consensus PRE sites. **(B)** Genome distribution of total PRE loci (left) and PRE loci that had PGR and H3K27ac binding (right), as extracted from (B), convergent area.

Apart from the canonical pathway, PGR binding has also been implied at chromatins without the PRE/NR3C motif. An example of a non-canonical PGR-binding region is shown for the *Adamts1* gene, a well characterised PGR-regulated gene in granulosa cells. Reporter assays have shown that PGR is important for the regulation of *Adamts1* proximal promoter [22] and this was confirmed with identified distinct PGR ChIP peaks in this region (Figure 2.8A); however, the sequence at this site contains no identifiable PRE/NR3C motif. Rather, there were three G/C-rich boxes in the sequence previously determined to be SP1/SP3-binding sites and were critical for the PGR-mediated induction of *Adamts1* [22]. Together with the fact that there is a low level of PRE loci occupied by PGR binding indicates that apart from the known chromatin motif, the majority of PGR-chromatin binding is not restricted to a recognised canonical PRE/NR3C. To determine other sequence motifs through which PGR commonly interacts in granulosa cells, analysis of enriched motifs in the PGR ChIP-seq peak dataset was performed using HOMER. The canonical PRE/NR3C sequence was the most enriched motif (7.2-fold) in the ChIP-seq data compared to the predicted random occurrence of this sequence motif (Figure 2.8B). This motif was also enriched in PGR peaks in association with ovulatory DEGs as identified from peri-ovulatory granulosa cells. Interestingly, a number of other transcription factor binding motifs were also significantly enriched, albeit at lower level than PRE/NR3C. Among the top enriched known motifs were those that were targeted by transcription factors belonging to bZIP (JUN/FOS), GATA, NR5A2 nuclear receptor, bZIP (CEBP) and RUNT families, which were also identified in DEG-binding PGR peaks except for the NR5A motif. *de novo* motif analysis, which identified the actual enriched sequences without presumptive assignment to known motifs, highly reflected the known motif results, with sequences most likely matched to bZIP (JUN/FOS), PRE/NR3C, RUNT, NR5A2, CEBP and GATA motifs being the most enriched in the ChIP-seq dataset (Figure 2.8C). Interestingly, the majority of highly enriched motifs localised near the PGR peak centre, especially within 100 bp of peak centre (Figure 2.8D). More specifically, there was a high enrichment of the canonical PRE/NR3C motif at the peak centre as expected, whereas for other motifs the localisation range was relatively wider, especially in the case of NR5A and RUNT motifs. This was strikingly different to the motif localisation pattern seen in H3K27ac peaks, in which the bZIP (JUN/FOS) and NR5A2 displayed a two-peak pattern flanking approximately 200 bp on either side of H3K27ac peaks and other motifs were much less enriched. Together these findings indicate that PGR selectively binds to a specific subset of PRE/NR3C in this target cell genome and also potentially acts in conjunction with other transcription factors to regulate gene expression, while also alluding to the role of JUN/FOS proteins as a pioneer transcription factor.

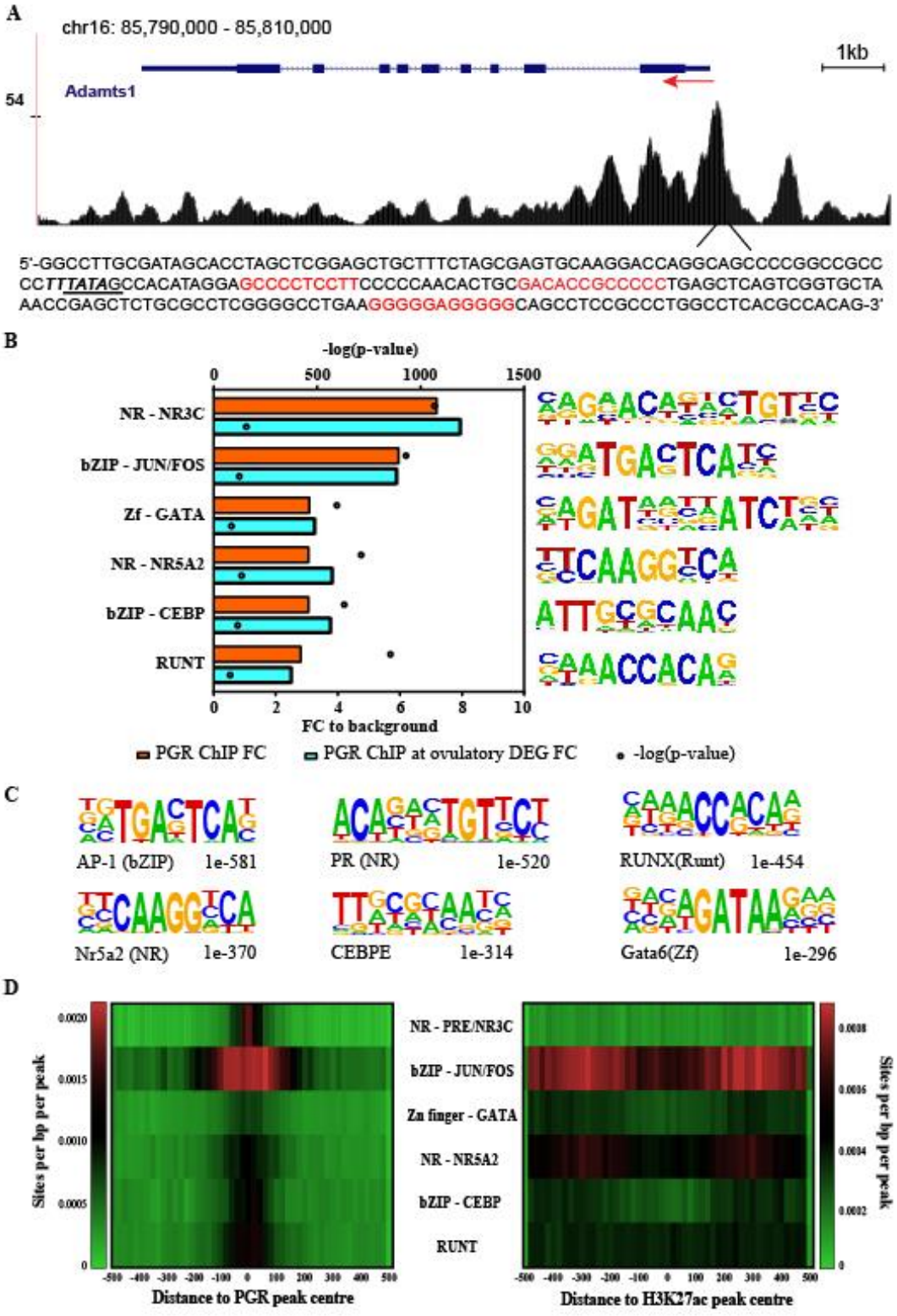
A
chr16: 85,790,000 - 85,810,000
1kb
Adamts1
54
5'-GGCCTTGCGATAGCACCTAGCTCGGAGCTGCTTTCTAGCGAGTGCAAGGACCAGGCAGCCCCGGCCGCC
CCTTTATAGCCACATAGGAGCCCCTCCTTCCCCCAACACTGCGACACCGCCCCCTGAGCTCAGTCGGTGCTA
AACCGAGCTCTGCGCCTCGGGGCCTGAAGGGGGAGGGGGCAGCCTCCGCCCTGGCCTCACGCCACAG-3'
B
-log(p-value)
0
500
1000
1500
NR - NR3C
bZIP - JUN/FOS
Zf - GATA
NR - NR5A2
bZIP - CEBP
RUNT
0
2
4
6
8
10
FC to background
PGR ChIP FC
PGR ChIP at ovulatory DEG FC
-log(p-value)
C
AP-1 (bZIP) 1e-581
PR (NR) 1e-520
RUNX(Runt) 1e-454
Nr5a2 (NR) 1e-370
CEBPE 1e-314
Gata6(Zf) 1e-296
D
Sites per bp per peak
0.0020
0.0015
0.0010
0.0005
0
NR - PRE/NR3C
bZIP - JUN/FOS
Zn finger - GATA
NR - NR5A2
bZIP - CEBP
RUNT
-500 -400 -300 -200 -100 0 100 200 300 400 500
Distance to PGR peak centre
Distance to H3K27ac peak centre
Sites per bp per peak

Figure 2.8 Properties of PGR-binding motifs in granulosa cells.

(A) PGR binding sites in the mouse genome visualised through UCSC Genome Browser. The track shown is located in chromosome 16 at the genomic region for *Adamts1*. The red arrow indicates the TSS (arrow tail) and direction of transcription. The sequence of the most prominent PGR peak is listed below, with the TATA box underlined and previously described PGR-binding G/C-rich sites in red. **(B)** Top most common known sequence motifs found to be enriched at PGR binding sites in granulosa cells (orange) and PGR binding motifs in ovulatory DEG from RNA-seq (aqua). Bars indicate fold enrichment of motif to background (bottom x axis). Circles indicate -log(p-value) (top x axis). Motifs were ranked by -log(p-value). Where multiple motifs belonging to the same transcription factor family were identified, only a representative that was the most enriched by fold-change over background is displayed in the graph. **(C)** *De novo* motifs identified by HOMER from PGR binding cistrome. Motifs selected to display here are based on p-value and the most enrichment from each transcription factor family. **(D)** Heatmap displaying the localisation of motifs in relation to PGR (left) and H3K27ac (right) peak centre. Motifs previously identified in (B) were analysed for distribution within 500 bp upstream and downstream of PGR and H3K27ac peaks.

2.4 DISCUSSION

It is known that PGR plays diverse roles in reproductive tissues, enabling P4-PGR signalling to coordinate various physiological processes in female reproduction. In the ovaries in particular, PGR is induced in granulosa cells of antral follicles by the LH surge and is a key determinant in ovulation, thus is crucial for female fertility. While the physiological effects of PGR and a handful of PGR downstream target genes have been investigated over the years, a full picture of the PGR transcriptome remains unclear. More importantly, as our understanding of context-specific molecular mechanisms of steroid receptor in influencing transcription regulation expands, it is important to characterise the PGR cistrome in peri-ovulatory granulosa cells to gain a full appreciation of the PGR ovulatory roles.

In peri-ovulatory granulosa cells, PGR strongly favours interaction with transcriptionally active promoter regions, with more than half of shared PGR/H3K27ac binding sites found within 3 kb of TSS. Such a phenomenon seems to be specific to granulosa cells, for in other cellular contexts, less than 25% of total PGR binding is in upstream proximity to TSS [20,44]. This is further highlighted in the degree of promoter enrichment in PGR binding sites that are found in proximity to ovulatory genes as indicated through hCG-stimulated granulosa cell RNA-seq, with more than one-third of PGR binding sites found in the proximal promoter regions 3 kb upstream of TSS. This confirms the importance of the classic transcriptional regulatory mechanism of direct promoter binding in PGR ovulatory functions. Apart from the strong enrichment of PGR binding at proximal promoter regions, PGR binding sites can also be distributed elsewhere in the genome, especially within intronic and intergenic regions. This suggests that PGR can exert influence on downstream target genes without binding their promoters and rather through other means, for example enhancer elements that are either distal or intronic. The role of PGR in enhancer actions has been previously described, such as in regulating the uterine expression of *Ihh* [17], *Rankl* and calcitonin genes [45]. In the context of ovulation however, the enhancer role of PGR has not been previously described. The lack of direct PGR promoter binding can be observed in known PGR target genes, such as *Zbtb16, Ereg* and *Pparg*. In these instances, PGR binding can be found within the genebody, especially in introns. Whether such intronic binding is critical for the regulation of these genes or whether PGR actions are via interaction with unidentified enhancer sites that are distal to these target genes through chromatin looping is still unknown. As enhancer actions and chromatin conformation tend to be specific to cellular and temporal contexts, a roadmap of enhancer sites

as well as topologically associating domains (TAD) specific to granulosa cells during ovulation would be required to determine whether PGR is acting in conjunction with any distal regulatory elements to regulate these genes.

Another important discovery in the PGR cistrome is the presence of other non-canonical motifs that are enriched alongside the consensus motif at PGR binding sites. Aside from the PRE/NR3C motif, those that are canonically recognised by other transcription factor families were also enriched at various levels and excitingly, ovulatory functions have previously been indicated in members of these families, which emphasises functional similarities between PGR and other transcription factors in granulosa cells. The range of non-PRE/NR3C motifs enriched in the PGR-bound intervals included those for bZIP (JUN/FOS), GATA, NR5A2 and RUNT families. These findings indicate that unique interactions of PGR with bZIP (JUN/FOS), NR5A2, RUNT and GATA may each contribute to the granulosa-specific PGR action in ovulation. These partner transcription factors potentially regulate granulosa-specific chromatin remodelling to establish accessibility to specific PRE/NR3C as pioneer factors or through direct protein-protein interactions with PGR; suggesting that in granulosa cells, PGR not only utilises direct PRE/NR3C-binding to interact with target chromatin but also that tethering of PGR to target chromatin domains through alternative accessory transcription factors is responsible for the functional diversity in granulosa cells. Supporting this hypothesis, this study demonstrates the previously hypothesised binding of PGR to specific G/C-rich sites in the *Adamts1* gene promoter, which contains no PRE/NR3C motif but has been shown through promoter-reporter analysis to be required for PGR-dependent induction of *Adamts1* transcription [22]. This model of SR-comodulator cooperation has also been previously described for GR and AR. Specifically, GR transcriptional regulation in endometrial cells is also shown to rely on association with pioneer factors, including FOXA1 along with the canonical PRE/NR3C [46] and likewise, the switch in AR action in normal versus malignant prostate cancer is related to context-specific interactions with FOXA1 or JUN/FOS co-regulators [47]. Recent studies of PGR in progesterone-primed uterus have indicated GATA2 as a candidate partner of PGR action in uterine tissue [17] and JUN/FOS proteins to be in contact with PGR in an isoform-specific manner in the myometrium [48]. Taken with these previous reports of steroid receptor tethering to non-canonical motifs through accessory factors, these findings support a mechanism whereby granulosa-specific PGR action is mediated by interaction of PGR with JUN/FOS, NR5A2 and RUNT transcription factors. While the *in silico* analysis can only act as a screening method for potential interacting partners, with this potential binding candidates

for PGR can be selected for future investigations, which will require other protein-protein assays such as immunoprecipitation, mass spectrometry or proximity ligation assay.

Importantly, these findings do not undermine the importance of the canonical pathway of PGR in which binding of PRE/NR3C is employed to recruit PGR to target chromatin sites. In granulosa cells, the consensus PRE/NR3C motif (5'-GnACAnnnTGTnC-3') dominated amongst genome-wide PGR-bound sequences, implying that the main mode of PGR function is through directly binding chromatin via the canonical PRE/NR3C motif. However, as more than 98% of PRE/NR3C loci are not utilised by PGR in granulosa cells, certainly specific regulatory mechanisms are at play in determining the selection of appropriate target sites in the context of peri-ovulatory granulosa cells. Likely that such specificity is determined through the activities of other transcription factors acting in conjunction with PGR, either as pioneer factors or through a role as chromatin remodellers, in order to tether PGR to selective chromatin targets. Thus, future studies into the specificity of PGR in different biological contexts will benefit from taking into account the relevant interactomes.

This chapter is the first to define the genome-wide PGR cistrome in granulosa cells in response to the ovulatory signal, when PGR induction and its response to progesterone are essential for ovulation and hence female fertility. The application of genome-wide microarray in PGRKO, RNA-seq and PGR ChIP-seq in granulosa cells allows us to investigate the impact of PGR chromatin binding events on the PGR-dependent transcriptome as well as the global ovulatory transcriptome. PGR was shown to favourably interact with transcriptionally active promoter regions, with profound importance on the regulation of PGR-dependent as well as the global ovulatory gene profile. Motif analysis of PGR binding sites indicated a role of a transcription complex responsible for the regulation of ovulatory genes with a multitude of specific ovulatory factors acting in conjunction with PGR. This new knowledge of PGR cistromic activities in granulosa cells will be useful in discerning differences in the physiological roles of PGR in the context of different reproductive tissues. These differences will be investigated in the next chapter, where tissue-specific roles of PGR in granulosa cells and the uterus are addressed.

2.5 REFERENCES

1 Taraborrelli, S. Physiology, production and action of progesterone. *Acta Obstetricia et Gynecologica Scandinavica* **94**, 8-16, doi:10.1111/aogs.12771 (2015).

2 Mulac-Jericevic, B., Lydon, J. P., DeMayo, F. J. & Conneely, O. M. Defective mammary gland morphogenesis in mice lacking the progesterone receptor B isoform. *Proceedings of the National Academy of Sciences* **100**, 9744-9749, doi:10.1073/pnas.1732707100 (2003).

3 Mulac-Jericevic, B., Mullinax, R. A., DeMayo, F. J., Lydon, J. P. & Conneely, O. M. Subgroup of Reproductive Functions of Progesterone Mediated by Progesterone Receptor-B Isoform. *Science* **289**, 1751-1754, doi:10.1126/science.289.5485.1751 (2000).

4 Lydon, J. P., DeMayo, F. J., Funk, C. R., Mani, S. K., Hughes, A. R., Montgomery, C. A., Jr., Shyamala, G., Conneely, O. M. & O'Malley, B. W. Mice lacking progesterone receptor exhibit pleiotropic reproductive abnormalities. *Genes Dev* **9**, 2266-2278 (1995).

5 Akison, L. & Robker, R. The Critical Roles of Progesterone Receptor (PGR) in Ovulation, Oocyte Developmental Competence and Oviductal Transport in Mammalian Reproduction. *Reproduction in Domestic Animals* **47**, 288-296, doi:10.1111/j.1439-0531.2012.02088.x (2012).

6 Gaytan, F., Bellido, C., Gaytan, M., Morales, C. & Sanchez-Criado, J. E. Differential effects of RU486 and indomethacin on follicle rupture during the ovulatory process in the rat. *Biol Reprod* **69**, 99-105, doi:10.1095/biolreprod.102.013755 (2003).

7 Loutradis, D., Bletsa, R., Aravantinos, L., Kallianidis, K., Michalas, S. & Psychoyos, A. Preovulatory effects of the progesterone antagonist mifepristone (RU486) in mice. *Human Reproduction* **6**, 1238-1240, doi:10.1093/oxfordjournals.humrep.a137519 (1991).

8 Gemzell-Danielsson, K., Berger, C. & P.G.L, L. Emergency contraception — mechanisms of action. *Contraception* **87**, 300-308, doi:https://doi.org/10.1016/j.contraception.2012.08.021 (2013).

9 Robker, R. L. & Richards, J. S. in *Ovulation* 121-129 (Springer, 2000).

10 Shimada, M., Yamashita, Y., Ito, J., Okazaki, T., Kawahata, K. & Nishibori, M. Expression of two progesterone receptor isoforms in cumulus cells and their roles during meiotic resumption of porcine oocytes. *Journal of Molecular Endocrinology* **33**, 209-225, doi:10.1677/jme.0.0330209 (2004).

11 Bishop, C. V., Hennebold, J. D., Kahl, C. A. & Stouffer, R. L. Knockdown of Progesterone Receptor (PGR) in Macaque Granulosa Cells Disrupts Ovulation and Progesterone Production. *Biol Reprod* **94**, 109, doi:10.1095/biolreprod.115.134981 (2016).

12 Robker, R. L., Russell, D. L., Espey, L. L., Lydon, J. P., O'Malley, B. W. & Richards, J. S. Progesterone-regulated genes in the ovulation process: ADAMTS-1 and cathepsin L proteases. *Proc Natl Acad Sci U S A* **97**, 4689-4694 (2000).

13 Palanisamy, G. S., Cheon, Y.-P., Kim, J., Kannan, A., Li, Q., Sato, M., Mantena, S. R., Sitruk-Ware, R. L., Bagchi, M. K. & Bagchi, I. C. A Novel Pathway Involving Progesterone Receptor, Endothelin-2, and Endothelin Receptor B Controls Ovulation in Mice. *Molecular Endocrinology* **20**, 2784-2795, doi:10.1210/me.2006-0093 (2006).

14 Kim, J., Sato, M., Li, Q., Lydon, J. P., DeMayo, F. J., Bagchi, I. C. & Bagchi, M. K. Peroxisome Proliferator-Activated Receptor γ Is a Target of Progesterone Regulation in the Preovulatory Follicles and Controls Ovulation in Mice. *Molecular and cellular biology* **28**, 1770-1782, doi:10.1128/mcb.01556-07 (2008).

15 Akison, L. K., Boden, M. J., Kennaway, D. J., Russell, D. L. & Robker, R. L. Progesterone receptor-dependent regulation of genes in the oviducts of female mice. *Physiological Genomics* **46**, 583-592, doi:10.1152/physiolgenomics.00044.2014 (2014).

16 Jeong, J.-W., Lee, K. Y., Kwak, I., White, L. D., Hilsenbeck, S. G., Lydon, J. P. & DeMayo, F. J. Identification of Murine Uterine Genes Regulated in a Ligand-Dependent Manner by the Progesterone Receptor. *Endocrinology* **146**, 3490-3505, doi:10.1210/en.2005-0016 (2005).

17 Rubel, C. A., Wu, S.-P., Lin, L., Wang, T., Lanz, R. B., Li, X., Kommagani, R., Franco, H. L., Camper, S. A., Tong, Q., Jeong, J.-W., Lydon, J. P. & DeMayo, F. J. A Gata2-Dependent Transcription Network Regulates Uterine Progesterone Responsiveness and Endometrial Function. *Cell reports* **17**, 1414-1425, doi:10.1016/j.celrep.2016.09.093 (2016).

18 Li, X. & O'Malley, B. W. Unfolding the Action of Progesterone Receptors. *Journal of Biological Chemistry* **278**, 39261-39264, doi:10.1074/jbc.R300024200 (2003).

19 Ceballos-Chávez, M., Subtil-Rodríguez, A., Giannopoulou, E. G., Soronellas, D., Vázquez-Chávez, E., Vicent, G. P., Elemento, O., Beato, M. & Reyes, J. C. The Chromatin Remodeler CHD8 Is Required for Activation of Progesterone Receptor-Dependent Enhancers. *PLOS Genetics* **11**, e1005174, doi:10.1371/journal.pgen.1005174 (2015).

20 Clarke, C. L. & Graham, J. D. Non-Overlapping Progesterone Receptor Cistromes Contribute to Cell-Specific Transcriptional Outcomes. *PLOS ONE* **7**, e35859, doi:10.1371/journal.pone.0035859 (2012).

21 Mohammed, H., Russell, I. A., Stark, R., Rueda, O. M., Hickey, T. E., Tarulli, G. A., Serandour, A. A., Birrell, S. N., Bruna, A., Saadi, A., Menon, S., Hadfield, J., Pugh, M., Raj, G. V., Brown, G. D., D'Santos, C., Robinson, J. L. L., Silva, G., Launchbury, R., Perou, C. M., Stingl, J., Caldas, C., Tilley, W. D. & Carroll, J. S. Progesterone receptor modulates ERα action in breast cancer. *Nature* **523**, 313, doi:10.1038/nature14583 (2015).

22 Doyle, K. M. H., Russell, D. L., Sriraman, V. & Richards, J. S. Coordinate Transcription of the ADAMTS-1 Gene by Luteinizing Hormone and Progesterone Receptor. *Molecular Endocrinology* **18**, 2463-2478, doi:10.1210/me.2003-0380 (2004).

23 Richer, J. K., Jacobsen, B. M., Manning, N. G., Abel, M. G., Wolf, D. M. & Horwitz, K. B. Differential Gene Regulation by the Two Progesterone Receptor Isoforms in Human Breast Cancer Cells. *Journal of Biological Chemistry* **277**, 5209-5218, doi:10.1074/jbc.M110090200 (2002).

24 Takamoto, N., Zhao, B., Tsai, S. Y. & DeMayo, F. J. Identification of Indian Hedgehog as a Progesterone-Responsive Gene in the Murine Uterus. *Molecular Endocrinology* **16**, 2338-2348, doi:10.1210/me.2001-0154 (2002).

25 Rubel, C. A., Lanz, R. B., Kommagani, R., Franco, H. L., Lydon, J. P. & DeMayo, F. J. Research resource: Genome-wide profiling of progesterone receptor binding in the mouse uterus. *Molecular endocrinology* **26**, 1428-1442 (2012).

26 Mazur, E. C., Vasquez, Y. M., Li, X., Kommagani, R., Jiang, L., Chen, R., Lanz, R. B., Kovanci, E., Gibbons, W. E. & DeMayo, F. J. Progesterone Receptor Transcriptome and Cistrome in Decidualized Human Endometrial Stromal Cells. *Endocrinology* **156**, 2239-2253, doi:10.1210/en.2014-1566 (2015).

27 Langmead, B. & Salzberg, S. L. Fast gapped-read alignment with Bowtie 2. *Nature Methods* **9**, 357-359, doi:10.1038/nmeth.1923 (2012).

28 Li, Q., Brown, J. B., Huang, H. & Bickel, P. J. Measuring reproducibility of high-throughput experiments. *The annals of applied statistics* **5**, 1752-1779 (2011).
29 Zhang, Y., Liu, T., Meyer, C. A., Eeckhoute, J., Johnson, D. S., Bernstein, B. E., Nusbaum, C., Myers, R. M., Brown, M., Li, W. & Liu, X. S. Model-based analysis of ChIP-Seq (MACS). *Genome Biol* **9**, R137, doi:10.1186/gb-2008-9-9-r137 (2008).
30 Zhu, L. J., Gazin, C., Lawson, N. D., Pagès, H., Lin, S. M., Lapointe, D. S. & Green, M. R. ChIPpeakAnno: a Bioconductor package to annotate ChIP-seq and ChIP-chip data. *BMC Bioinformatics* **11**, 237, doi:10.1186/1471-2105-11-237 (2010).
31 Li, H., Handsaker, B., Wysoker, A., Fennell, T., Ruan, J., Homer, N., Marth, G., Abecasis, G. & Durbin, R. The Sequence Alignment/Map format and SAMtools. *Bioinformatics* **25**, 2078-2079, doi:10.1093/bioinformatics/btp352 (2009).
32 Kent, W. J., Sugnet, C. W., Furey, T. S., Roskin, K. M., Pringle, T. H., Zahler, A. M. & Haussler, D. The human genome browser at UCSC. *Genome Res* **12**, 996-1006, doi:10.1101/gr.229102 (2002).
33 Zhang, H., Meltzer, P. & Davis, S. RCircos: an R package for Circos 2D track plots. *BMC Bioinformatics* **14**, 244, doi:10.1186/1471-2105-14-244 (2013).
34 Ramírez, F., Ryan, D. P., Grüning, B., Bhardwaj, V., Kilpert, F., Richter, A. S., Heyne, S., Dündar, F. & Manke, T. deepTools2: a next generation web server for deep-sequencing data analysis. *Nucleic Acids Research* **44**, W160-W165, doi:10.1093/nar/gkw257 (2016).
35 Yu, G., Wang, L. G. & He, Q. Y. ChIPseeker: an R/Bioconductor package for ChIP peak annotation, comparison and visualization. *Bioinformatics* **31**, 2382-2383, doi:10.1093/bioinformatics/btv145 (2015).
36 McLean, C. Y., Bristor, D., Hiller, M., Clarke, S. L., Schaar, B. T., Lowe, C. B., Wenger, A. M. & Bejerano, G. GREAT improves functional interpretation of cis-regulatory regions. *Nature biotechnology* **28**, 495 (2010).
37 Supek, F., Bošnjak, M., Škunca, N. & Šmuc, T. REVIGO Summarizes and Visualizes Long Lists of Gene Ontology Terms. *PLOS ONE* **6**, e21800, doi:10.1371/journal.pone.0021800 (2011).
38 Bailey, T. L., Boden, M., Buske, F. A., Frith, M., Grant, C. E., Clementi, L., Ren, J., Li, W. W. & Noble, W. S. MEME SUITE: tools for motif discovery and searching. *Nucleic Acids Res* **37**, W202-208, doi:10.1093/nar/gkp335 (2009).
39 Heinz, S., Benner, C., Spann, N., Bertolino, E., Lin, Y. C., Laslo, P., Cheng, J. X., Murre, C., Singh, H. & Glass, C. K. Simple combinations of lineage-determining transcription factors prime cis-regulatory elements required for macrophage and B cell identities. *Mol Cell* **38**, 576-589, doi:10.1016/j.molcel.2010.05.004 (2010).
40 Kent, W. J., Zweig, A. S., Barber, G., Hinrichs, A. S. & Karolchik, D. BigWig and BigBed: enabling browsing of large distributed datasets. *Bioinformatics* **26**, 2204-2207, doi:10.1093/bioinformatics/btq351 (2010).
41 Afgan, E., Baker, D., Batut, B., van den Beek, M., Bouvier, D., Čech, M., Chilton, J., Clements, D., Coraor, N., Grüning, B. A., Guerler, A., Hillman-Jackson, J., Hiltemann, S., Jalili, V., Rasche, H., Soranzo, N., Goecks, J., Taylor, J., Nekrutenko, A. & Blankenberg, D. The Galaxy platform for accessible, reproducible and collaborative biomedical analyses: 2018 update. *Nucleic Acids Research* **46**, W537-W544, doi:10.1093/nar/gky379 (2018).
42 Akison, L. K. a. *The role of nuclear progesterone receptor (PGR) in regulating gene expression, morphology and function in the ovary and oviduct during the periovulatory period*, (2012).
43 Dinh, D. T., Breen, J., Akison, L. K., DeMayo, F. J., Brown, H. M., Robker, R. L. & Russell, D. L. Tissue-specific progesterone receptor-chromatin binding and the

regulation of progesterone-dependent gene expression. *Scientific reports* **9**, 11966-11966, doi:10.1038/s41598-019-48333-8 (2019).

44 Yin, P., Roqueiro, D., Huang, L., Owen, J. K., Xie, A., Navarro, A., Monsivais, D., Coon V, J. S., Kim, J. J., Dai, Y. & Bulun, S. E. Genome-Wide Progesterone Receptor Binding: Cell Type-Specific and Shared Mechanisms in T47D Breast Cancer Cells and Primary Leiomyoma Cells. *PLOS ONE* **7**, e29021, doi:10.1371/journal.pone.0029021 (2012).

45 Grimm, S. L., Ward, R. D., Obr, A. E., Franco, H. L., Fernandez-Valdivia, R., Kim, J.-S., Roberts, J. M., Jeong, J.-W., DeMayo, F. J., Lydon, J. P., Edwards, D. P. & Weigel, N. L. A Role for Site-Specific Phosphorylation of Mouse Progesterone Receptor at Serine 191 in Vivo. *Molecular Endocrinology* **28**, 2025-2037, doi:10.1210/me.2014-1206 (2014).

46 Whirledge, S., Kisanga, E. P., Taylor, R. N. & Cidlowski, J. A. Pioneer Factors FOXA1 and FOXA2 Assist Selective Glucocorticoid Receptor Signaling in Human Endometrial Cells. *Endocrinology* **158**, 4076-4092, doi:10.1210/en.2017-00361 (2017).

47 Leach, D. A., Panagopoulos, V., Nash, C., Bevan, C., Thomson, A. A., Selth, L. A. & Buchanan, G. Cell-lineage specificity and role of AP-1 in the prostate fibroblast androgen receptor cistrome. *Mol Cell Endocrinol* **439**, 261-272, doi:10.1016/j.mce.2016.09.010 (2017).

48 Nadeem, L., Shynlova, O., Matysiak-Zablocki, E., Mesiano, S., Dong, X. & Lye, S. Molecular evidence of functional progesterone withdrawal in human myometrium. *Nature Communications* **7**, 11565, doi:10.1038/ncomms11565 (2016).

CHAPTER 3 Tissue-specific PGR cistromes and consequences on PGR-regulated transcriptomes in the reproductive tract

3.1 INTRODUCTION

PGR is expressed in various parts of the female reproductive tract and shows distinct functions that are highly dependent on the tissue context, which has been revealed in studies on PGRKO animal models. In the ovary, PGR is transiently expressed in granulosa cells in response to the LH surge [1,2] and is a key factor in ovulation, which is illustrated in an anovulatory phenotype in PGRKO female mice [3]. PGR is also involved in biological processes in other parts of the female reproductive tract in preparation for pregnancy and during parturition. In the oviduct, PGR is involved in the transporting of oocytes and embryos through regulating ciliate movement [4] and in the uterus PGR is involved in preparation for embryo implantation [3] as well as inducing human labour at term [5]. Prior to pregnancy, PGR functions are initiated by progesterone production in response to the LH surge; however, exactly how such diverse roles are achieved through the same endocrine factor is still not well understood.

As PGR is known as a transcription factor that regulates gene expression, differences in PGR functions are likely due to specific gene expression regulation patterns that are PGR-dependent in different tissue contexts. In these various cell types, PGR mediates distinct genes that are critical for tissue-specific functions. For example, PGR modulates genes that are important for ovulation in granulosa cells (*Adamts1* [6], *Areg* and *Ereg* [7]) and importantly also promotes the expression of a number of transcription factors, for instance *Pparg* and *Hif1a* [8,9], defining the role of PGR in initiating the ovulatory transcriptional cascade. In the oviduct, PGR is found to regulate *Myocd* and *Edn3* that are important for muscle contraction and epithelial cell secretion [10], whereas in the progesterone-responsive uterus PGR modulates the expression of *Gata2* and *Ihh* [11]. While the PGR-derived transcriptome has been profiled in different reproductive contexts, there has been no consolidation of these data in an attempt to explain the tissue specificity of PGR functions.

PGR exerts its transcriptional regulatory role mainly through the canonical molecular mechanism, which involves the activation of PGR through ligand binding, nuclear translocation, dimerisation and interaction with the canonical PRE/NR3C motif at target DNA. Genes without the PRE/NR3C motif in their regulatory regions can also be indirectly influenced by PGR through an interaction with intermediate transcription factors. An example of this is shown in the PGR-induced *Adamts1* gene in granulosa cells which possesses SP1/SP3 binding sites that are critical for PGR regulation of this gene [12]. Instances of PGR binding at non-canonical DNA targets have also been identified in the uterus, especially in the regulation of *Zbtb16* [11,13]. However, it is unknown whether such mechanism is also employed by PGR in granulosa cells.

Due to the highly selective roles of PGR in different tissue contexts, it is vital that differences in the PGR transcriptional regulatory pathways are clarified. The specific roles of PGR in different tissue contexts have been previously examined in normal vs cancerous human mammary cell lines [14] as well as between human breast cancer and uterine leimyoma that are positive for PGR [15]. In all of these comparisons, PGR has been shown to hold distinct cistromic properties. However, such comparisons were made in the context of cancers where PGR actions are of particular interest, yet in the normal reproductive tract where PGR has prominent but different functions, no studies have yet investigated how the specialised physiological roles in different reproductive organs are achieved through the same receptor signalling mechanism. Thus, such characteristics cannot be implied for PGR action in the reproductive tract, making it valuable to actively investigate these contrasting regulatory mechanisms in the context of female reproduction, which is crucial in understanding the mechanisms that are responsible for the diversity in PGR action between different target tissues.

The PGR cistrome and transcriptome in peri-ovulatory granulosa cells have been established in Chapter 2, in which direct PGR binding at transcriptionally active promoters was found to be crucial for PGR-regulated gene expression. Furthermore, potential co-modulators of PGR were identified that might play a role in modulating the ovulatory role of PGR in granulosa cells. In following that, this chapter investigated the diverse reproductive roles of PGR on a genomic level. First, tissue-specific PGR-dependent transcriptomes were defined from microarray analysis of PGRKO granulosa cells, the oviduct and uterus, followed by comparative analysis of PGR cistromes in progesterone-responsive granulosa cells versus the

uterus in order to determine unique context-specific molecular mechanisms involved in PGR action in reproduction.

3.2 MATERIALS & METHODS

3.2.1 Animals

CBFA1 mice were obtained from The University of Adelaide, Laboratory Animal Services. All mice were maintained in 12 h light /12 h dark conditions and given water and rodent chow *ad libitum*. All experiments were approved by The University of Adelaide Animal Ethics Committee and were conducted in accordance with the Australian Code of Practice for the Care and Use of Animals for Scientific Purposes (ethics no m/2015/075).

3.2.2 ChIP-seq

3.2.2.1 Experiment

PGR ChIP-seq on granulosa cells was performed as part of the experiments described in Chapter 2 (section 2.2.3.1). Briefly, super-ovulation in 21-day old CBAF1 female mice was hormonally stimulated with eCG and hCG, then culled and dissected at 6h post-hCG for whole ovary extraction. PGR ChIP-seq was performed by Active Motif on two biological replicates of granulosa cells from at least 5 mice each with a minimum of $1x10^7$ cells. Briefly, cells were fixed in formaldehyde and lysed in lysis buffer, then chromatin was sonicated and precleared with agarose beads. PGR pull-down was through an antibody for PGR as indicated in Appendix 3. PGR-associated chromatin was washed, eluted from beads, treated with proteinase K and RNase. DNA was purified through phenol-chloroform extraction and ethanol precipitation. Illumina sequencing libraries were prepared from the ChIP and input DNA by the standard consecutive enzymatic steps of end-polishing, dA-addition, and adaptor ligation. After a final PCR amplification step, the resulting DNA libraries were quantified and sequenced on Illumina's NextSeq 500 (75 nt reads, single end). PGR ChIP-seq on progesterone-treated uterus has been published [13]; briefly, 6-week old ovariectomised female C57BL/6 mice were administered subcutaneously with vehicle (oil) or 1 mg P4 and the uterus was dissected 1 h after injection. Sample processing and ChIP-seq was as described above. The raw sequencing data was obtained from GEO (GSE34927).

3.2.2.2 Bioinformatics analysis

Bioinformatics analysis was conducted using appropriate tools as described in Section 2.2.3.2. Quality check of sequencing data for all samples showed no warnings. Genomic alignment and peak calling from read count against input was as previously described. A summary of library size, sequence length, alignment rate and peak count is shown in Appendix 5. Downstream analysis of peaks was as previously described in section 2.2.3.2. The obtainment of the global PRE/NR3C map was as described in section 2.2.3.2.

3.2.3 Microarray analysis

Gene lists for oviduct and uterus microarray on PGRKO vs PGR+/± mice were from previously published datasets [10,11,16]. Gene lists for granulosa cell microarray on PGRKO vs PGR+/± mice were originally from Lisa K Akison's PhD thesis [17], now published and publicly available (GEO accession number: GSE92438) [18]. Upstream regulator analysis was performed using IPA software (Qiagen) and regulators belonging to category 'ligand-dependent nuclear receptor' and 'transcription regulator' were selected. P-value ≤ 0.01 and $|\log FC| \geq 1$ criteria were applied to obtain significant DEG for subsequent comparisons. Gene Ontology analysis was performed using R packages and canonical pathway analysis was performed using IPA software as listed in Figure 2.1 and Table 2.2.

3.3 RESULTS

3.3.1 PGR regulates specific transcriptomes in granulosa cells, oviduct and uterus

PGR exhibits tissue-specific functions in the reproductive tract, most likely due to the different PGR-regulated transcriptome profile in these tissues. In order to confirm this hypothesis the difference in PGR target genes in reproductive tissues was demonstrated by comparing PGR-dependent DEGs identified by microarray analysis of PGRKO mouse uterus and oviduct with those in granulosa cells. Gene lists were obtained from the original analysis done for each tissue type and the uniform DEG selection criteria were applied as previously described. Through this, 41 and 81 DEGs were identified in the uterus and oviduct, respectively, which are listed in Appendix 8 and Appendix 9. Comparison between the three tissues showed few overlaps between PGR-dependent gene sets – only 7 genes were differentially expressed in more than one tissue and none was found to be shared in all three (Figure 3.1A). Intriguingly, one of these

genes, *Efnb2*, was regulated in the inverse manner between granulosa cells and uterus, being significantly upregulated (2.2-fold) in PGRKO uterus yet downregulated (3.7-fold) in granulosa cells. Upstream regulator analysis via IPA for each tissue showed that for all three, PGR was confirmed within the top 10 candidates and regulating the same number of genes in each tissue (5-7 genes), alongside other potential transcription factors (Figure 3.1B). Gene Ontology and pathway analysis also showed a wide range of unique ontological terminologies and molecular pathways enriched in each tissue (Figure 3.1C, Figure 3.2). These confirm that PGR transcriptional regulation is highly diverse, specialised and tissue-dependent.

A

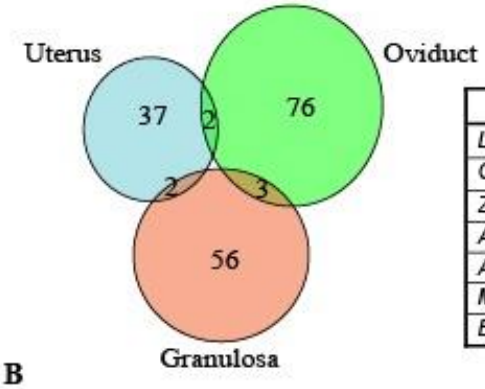

Gene	Uterus	Oviduct	Granulosa cell
Lrp2	-5.49834	-3.316	
Cited2	-2.31345	-2.258	
Zbtb16		-4.326	-13.7345
Adamts1		-3.18	-2.5762
Arl4d		-3.52	-4.37976
Mt2	-2.04277		-2.87657
Efnb2	2.18312		-3.71747

B

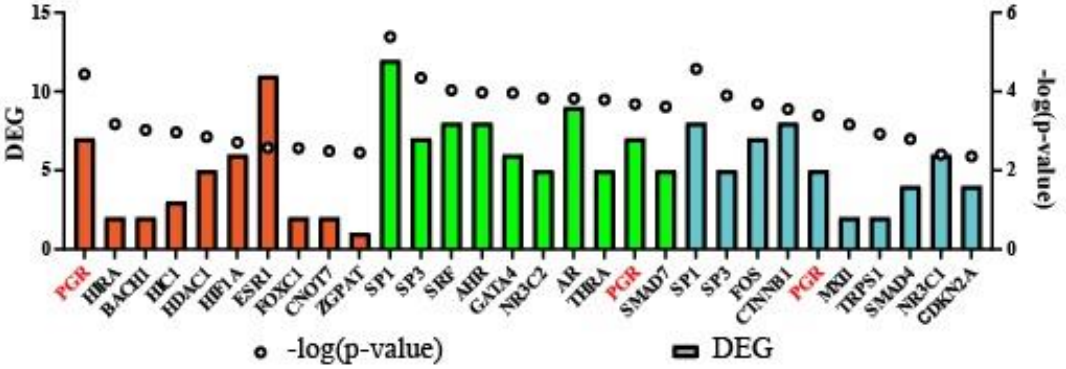

C

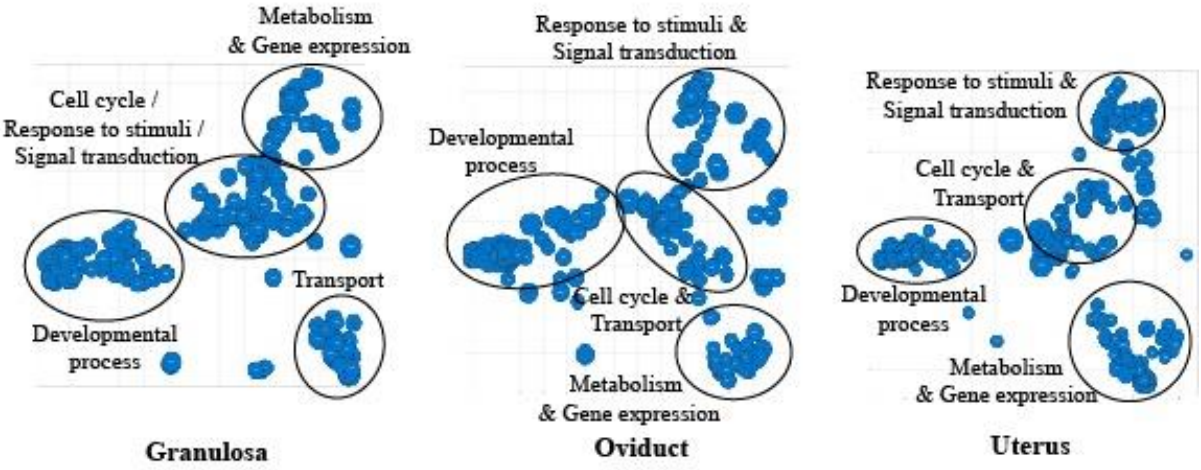

Figure 3.1 Differences in PGR-regulated transcriptome in granulosa cells, oviduct and uterus.

(A) Venn diagram of DEG identified in PGRKO vs PGR+/± granulosa cells (orange), oviduct (green) and uterus (blue). DEG was compiled from independent microarrays performed on PGRKO vs PGR+/± uterus, oviduct and granulosa cells with full gene lists available in Appendix 5, 8 and 9. Overlapped genes that were identified in more than one tissue type, with accompanied PGRKO to PGR+/± fold change are listed in the table. **(B)** Upstream regulators of DEG in granulosa cells (orange), oviduct (green) and uterus (blue) as identified through IPA, showing the top 10 identified regulators (p-value cut-off = 0.05). **(C)** Gene Ontology analysis of DEG in granulosa, oviduct and uterus. Ontological terms associated with biological processes were obtained from analysis of DEG in granulosa cells, oviduct and uterus and condensed using REVIGO. Each reduced term is displayed as a circle with the diameter correlating to the -log10(p-value) of said term. Terms of the same umbrella of biological process are grouped together in the XY graph.

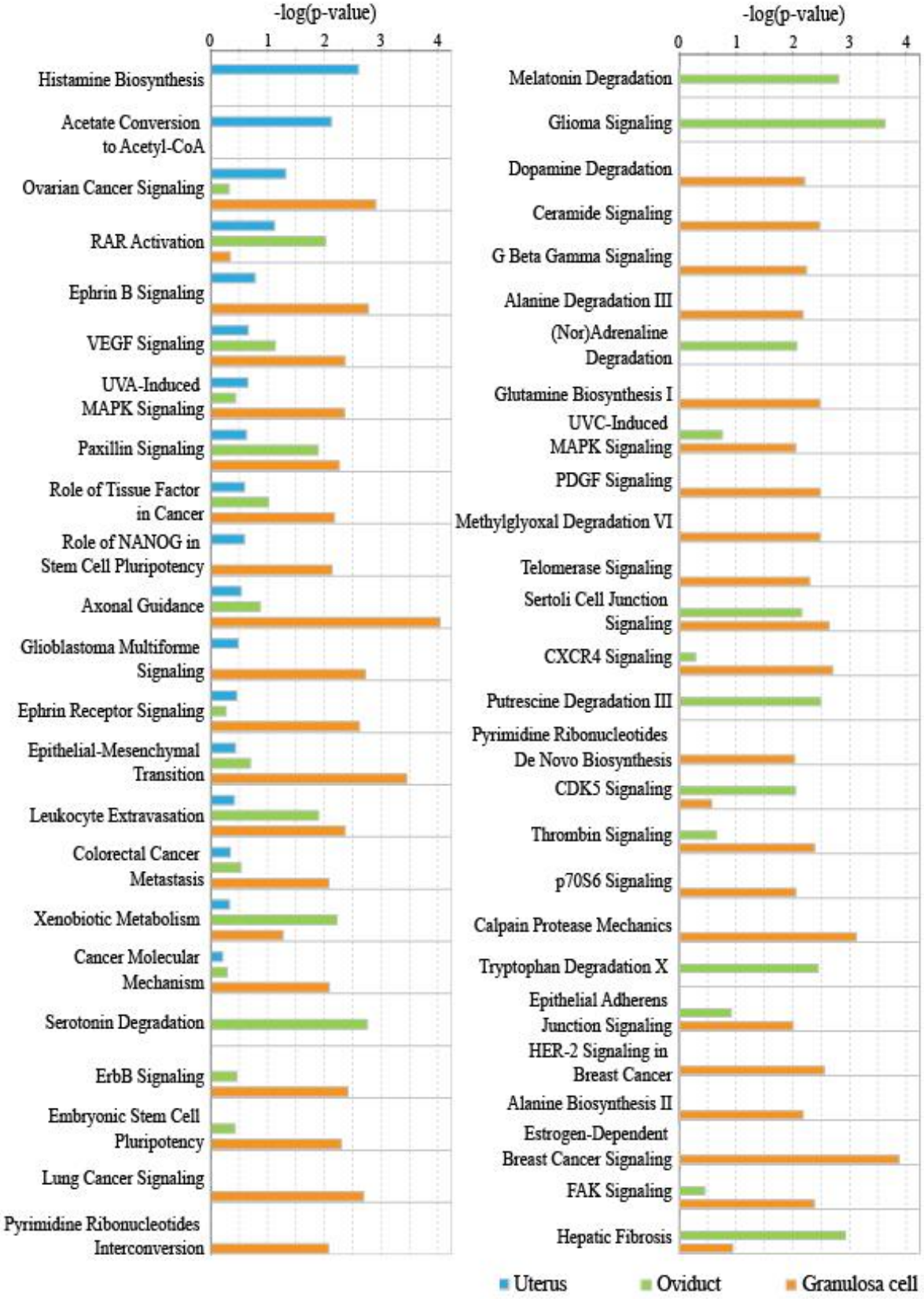
-log(p-value)
0
1
2
3
4
Histamine Biosynthesis
Acetate Conversion to Acetyl-CoA
Ovarian Cancer Signaling
RAR Activation
Ephrin B Signaling
VEGF Signaling
UVA-Induced MAPK Signaling
Paxillin Signaling
Role of Tissue Factor in Cancer
Role of NANOG in Stem Cell Pluripotency
Axonal Guidance
Glioblastoma Multiforme Signaling
Ephrin Receptor Signaling
Epithelial-Mesenchymal Transition
Leukocyte Extravasation
Colorectal Cancer Metastasis
Xenobiotic Metabolism
Cancer Molecular Mechanism
Serotonin Degradation
ErbB Signaling
Embryonic Stem Cell Pluripotency
Lung Cancer Signaling
Pyrimidine Ribonucleotides Interconversion
-log(p-value)
0
1
2
3
4
Melatonin Degradation
Glioma Signaling
Dopamine Degradation
Ceramide Signaling
G Beta Gamma Signaling
Alanine Degradation III
(Nor)Adrenaline Degradation
Glutamine Biosynthesis I
UVC-Induced MAPK Signaling
PDGF Signaling
Methylglyoxal Degradation VI
Telomerase Signaling
Sertoli Cell Junction Signaling
CXCR4 Signaling
Putrescine Degradation III
Pyrimidine Ribonucleotides De Novo Biosynthesis
CDK5 Signaling
Thrombin Signaling
p70S6 Signaling
Calpain Protease Mechanics
Tryptophan Degradation X
Epithelial Adherens Junction Signaling
HER-2 Signaling in Breast Cancer
Alanine Biosynthesis II
Estrogen-Dependent Breast Cancer Signaling
FAK Signaling
Hepatic Fibrosis
Uterus
Oviduct
Granulosa cell

Figure 3.2 Canonical pathway analysis of DEG in the uterus, oviduct and granulosa cells. DEG were subjected to analysis using IPA software with core analysis on default setting. Pathways were selected for those with -log(p-value) ≥ 2 in at least one tissue. -log(p-value) is shown for each tissue type – uterus (blue), oviduct (green), granulosa cells (orange). When a pathway is not identified in the tissue, the -log(p-value) bar is absent.

3.3.2 Characteristics of PGR chromatin-binding properties in progesterone-responsive uterus

In order to discern the difference in progesterone-responsive PGR cistrome in granulosa cells versus uterus, first the PGR cistrome in uterus in response to P4 or vehicle (oil) treatment at 4 h post-stimulation was investigated which has been previously described [13]. To reduce bias that might occur due to differences in analysis and make it more comparable to the granulosa cell ChIP-seq data, the uterus ChIP-seq data was re-analysed in parallel to granulosa cell ChIP-seq, using the latest mouse genome assembly (mm10). This analysis was also helpful in validating the bioinformatics workflow that was created for granulosa cell ChIP-seq.

Characterisation of TSS-proximal PGR peaks in both treatments showed a similar topographical pattern of chromatin binding in each treatment (Figure 3.3A). Overall 13240 binding sites were identified in P4-treated uterus and 3004 in oil treatment (Figure 3.3B), among which 2218 sites (or 74% of oil-identified peaks and 16% of P4 peaks) were shared between the two treatments. This indicates that while there was a basal level of PGR-chromatin occupancy in the absence of PGR ligand, treatment of P4 not only sustained the majority of basal binding but also led to an increase in PGR chromatin occupancy. Interestingly, PGR peaks in the uterus showed a strong inclination for intergenic region binding regardless of the treatment, with a minimum of 40% of peaks unique to each treatment as well as peaks shared in both being found in distal intergenic regions (Figure 3.3C). In comparison, occupancy in the promoter region was remarkably low, with less than 20% of peaks found in the proximal promoter region. An example of PGR occupancy with and without ligand is shown for two PGR-regulated genes in the uterus as identified through microarray. *Mthfd2*, which is upregulated in P4-treated uterus, possessed intense PGR binding signals that were not observed in oil-treated uterus (Figure 3.3C). *Klf6*, a gene downregulated in P4 treatment, exhibited prominent PGR binding in its proximity in and oil treatment that were also found in P4 treatment (Figure 3.3D). These confirm that PGR is capable of binding chromatins despite the lack of P4, however the significance of this phenomenon on PGR-regulated transcription is still unclear.

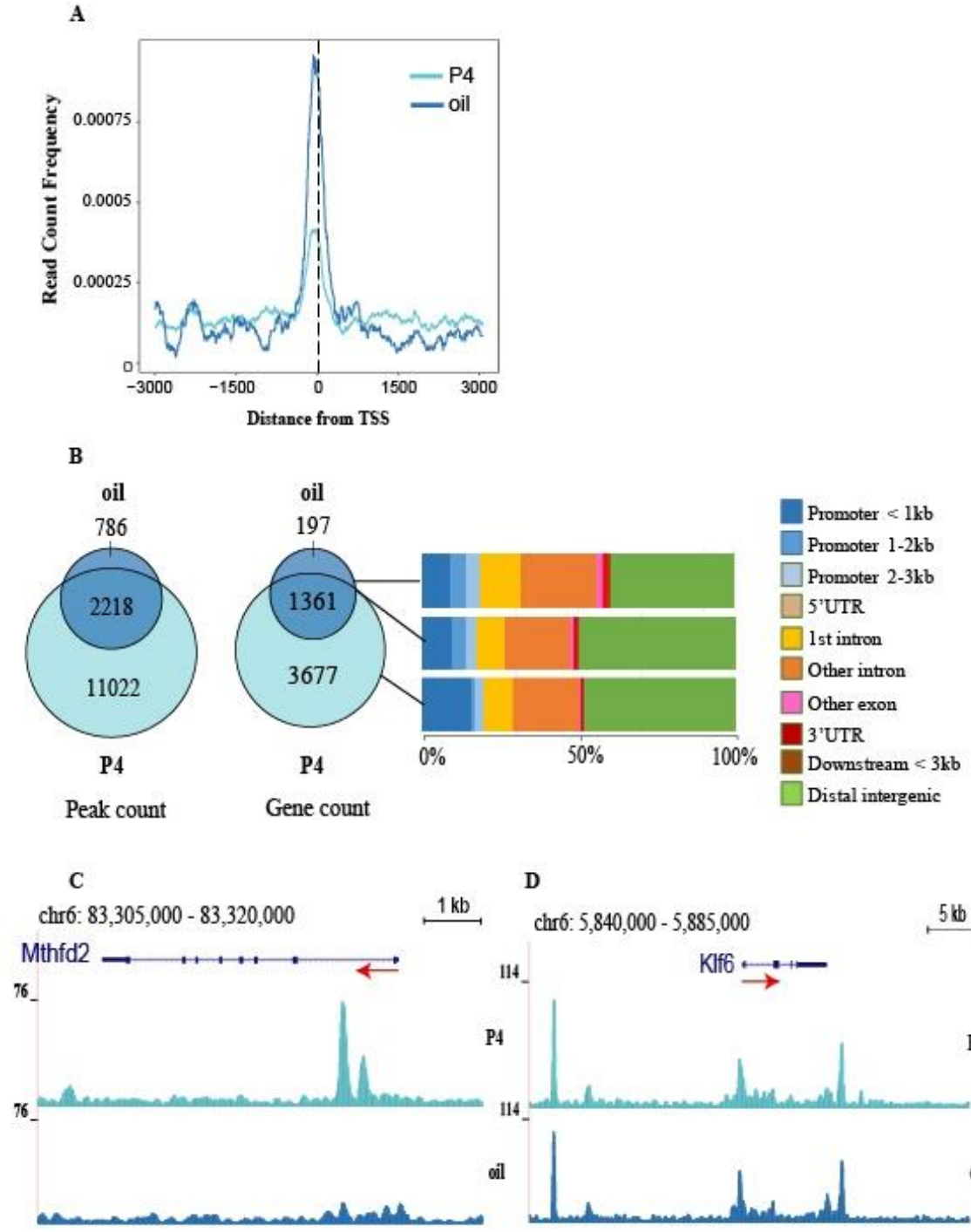
A
P4
oil
Read Count Frequency
0.00075
0.0005
0.00025
0
−3000
−1500
0
1500
3000
Distance from TSS
B
oil
786
2218
11022
P4
Peak count
oil
197
1361
3677
P4
Gene count
0%
50%
100%
Promoter < 1kb
Promoter 1-2kb
Promoter 2-3kb
5'UTR
1st intron
Other intron
Other exon
3'UTR
Downstream < 3kb
Distal intergenic
C
chr6: 83,305,000 - 83,320,000
1 kb
Mthfd2
76
76
P4
oil
D
chr6: 5,840,000 - 5,885,000
5 kb
Klf6
114
114
P4
P4
oil
oil

Figure 3.3 Correlation between PGR binding sites in uteri treated with P4 or vehicle control.

(A) Read count frequency of PGR ChIP-seq peaks in P4 treatment (light blue) or oil treatment (dark blue) in relation to the TSS. **(B)** Venn diagrams showing the peak count for P4 and oil treatments (left) and gene with peaks (right). Peaks were divided into oil-unique (top), treatment overlap (middle) and P4-unique (bottom) for genomic distribution analysis. Genome distribution is displayed as stacked bar graphs and includes promoters (< 1 kb, 1-2 kb and 2-3 kb), 5' UTR, 1st intron, other introns, exons, 3' UTR and downstream of TES (within 3 kb). Peaks that are not in these features are classified as distal intergenic. **(C)** Example of P4-specific PGR binding sites at the genomic region for *Mthfd2*. Tracks are normalised to the same scale, with signal track for P4 treatment (light blue) and oil treatment (dark blue). The red arrow indicates the TSS (arrow tail) and direction of transcription. **(D)** Example of PGR binding sites at the genomic region for *Klf6* in which there was binding of PGR in both treatment conditions.

Distinctions in PGR binding properties in the uterus might be due to differences in PRE loci preference in the presence or absence of ligand. To investigate this, PGR cistrome in P4 and oil treatment was compared against global PRE map. P4-induced as well as basal (oil) binding sites showed a relatively high level of PRE occupancy (approximately 11% in each treatment) (Figure 3.4A). However, the majority of occupied loci in the oil treated were also found in the P4 condition (98% of sites), once again showing that PGR binding is independent of the presence of P4. Among PGR-occupied PRE/NR3C loci, there was a slight increase in promoter enrichment, however the majority of loci was still found in the intergenic region (Figure 3.4B). To further investigate the nature of PGR-bound chromatins in the uterus, enriched motifs were discovered in PGR peaks with and without P4 treatment. The canonical PRE/NR3C motif was very highly enriched in both treatments (18.6-fold in P4 and 17.3-fold in oil) (Figure 3.4C). Other transcription factor binding motifs, including GATA, Homeobox, ERE and bZIP, were also enriched albeit at a much lower relative level, which was also supported by *de novo* motif analysis (Figure 3.4D-E). This showed that in the uterus, PGR binding of PRE/NR3C was highly preferential regardless of the presence of P4.

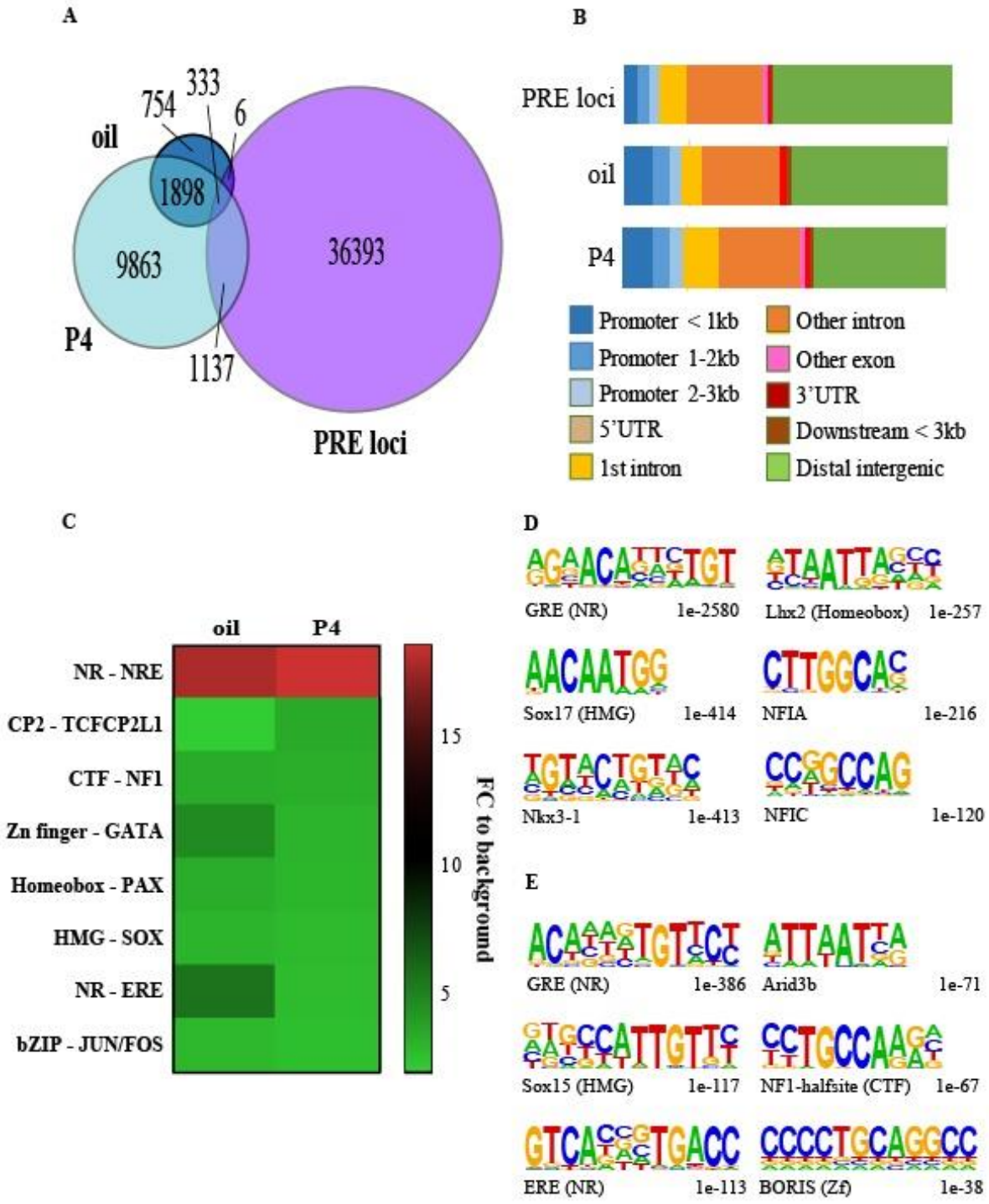
A
754
333
6
oil
1898
9863
36393
P4
1137
PRE loci
B
PRE loci
oil
P4
Promoter < 1kb
Promoter 1-2kb
Promoter 2-3kb
5'UTR
1st intron
Other intron
Other exon
3'UTR
Downstream < 3kb
Distal intergenic
C
oil
P4
NR - NRE
CP2 - TCFCP2L1
CTF - NF1
Zn finger - GATA
Homeobox - PAX
HMG - SOX
NR - ERE
bZIP - JUN/FOS
15
10
5
FC to background
D
GRE (NR) 1e-2580
Lhx2 (Homeobox) 1e-257
Sox17 (HMG) 1e-414
NFIA 1e-216
Nkx3-1 1e-413
NFIC 1e-120
E
GRE (NR) 1e-386
Arid3b 1e-71
Sox15 (HMG) 1e-117
NF1-halfsite (CTF) 1e-67
ERE (NR) 1e-113
BORIS (Zf) 1e-38

Figure 3.4 Properties of PGR-binding motifs the uterus.

(A) Venn diagram showing PGR peaks from P4 and oil ChIP-seq in relation to global PRE loci. 13% of PGR-bound peaks in presence of P4 overlap with PRE sites. **(B)** Genome distribution of total PRE loci (top) and PRE loci that had PGR binding with oil treatment (middle) and P4 treatment (bottom), as extracted from (A), convergent areas. **(C)** Heatmap showing most common known transcription factor recognition motifs found to be enriched at PGR binding sites in the uterus in P4 or oil treatment. Motifs were ranked by -log(p-value) and among motifs from the same transcription factor family, the one that was most enriched by fold enrichment to background frequency is displayed in the graph. **(D)** *De novo* sequences identified by HOMER enriched in PGR-bound peaks after P4 treatment. Motifs presented are those from each transcription factor family with the most significant p-value and the most enrichment. **(E)** *De novo* motifs identified by HOMER for PGR binding sites in oil treatment.

3.3.3 Distinctions between PGR cistrome in granulosa cells vs uterus

PGR resulted in different transcriptomes and functional profiles in different reproductive tissues, for which it was hypothesised that differences in the cistromic properties were responsible. The difference between PGR chromatin binding properties between granulosa cells and uterus was confirmed through examining the correlation between the two PGR cistromes, with the Pearson correlation coefficient between 0.63-0.68 for granulosa cells/uterus data pairs (Figure 3.5A). Plotting of the read count frequency in relation to TSS for progesterone-responsive PGR binding sites in granulosa cells and uterus showed that while PGR was enriched in close proximity to the TSS in both tissues, this was much more pronounced in granulosa cells than in the uterus (Figure 3.5B). Overall there were 1206 binding sites shared between granulosa cells and uterus, accounting for approximately 810 annotated genes or 9% of all peaks in each tissue (Figure 3.5C). Analysis of genome distribution highlighted significant differences between the two tissue types, with peaks found only in the uterus being most enriched in the distal intergenic regions (42%). Granulosa-unique peaks however were most likely to be found in the proximal promoter regions (51%), especially within 1 kb of the TSS. Instances of differential PGR binding in granulosa cells and uterus could be seen in Figure 3.5D, in which PGR-dependent genes in each tissue, such as *Wnt11* in the uterus and *Abhd2* in granulosa cells, possessed tissue-unique PGR binding sites. PGR also bound to introns of many genes, such as in *Zbtb16*, a PGR-dependent gene in mouse granulosa cells which has also been reported as PGR-induced in human and mouse endometrial stromal cells[19]. Despite *Zbtb16* being PGR-regulated in both tissues, the PGR interaction profile between the uterus and ovary was distinctive. While there were shared peaks between the two tissues, granulosa cells also exhibited a number of specific peaks and interestingly, only half of the discovered peaks had the consensus NR3C/PRE sequence. These intronic PGR-binding sites have been shown to be key regulatory elements in the uterine response to progesterone. Genes associated with PGR binding in the two tissue types also belonged to different pathways, with granulosa cell binding sites being involved in transcriptional and translational regulation of gene expression, whereas uterus-patterned binding sites were more important in cellular functions, including angiogenesis, cell adhesion and migration (Figure 3.6A). Different functional classifications were also enriched in the two datasets, further confirming that there were differences in functional consequences for PGR binding in the two tissue contexts (Figure 3.6B).

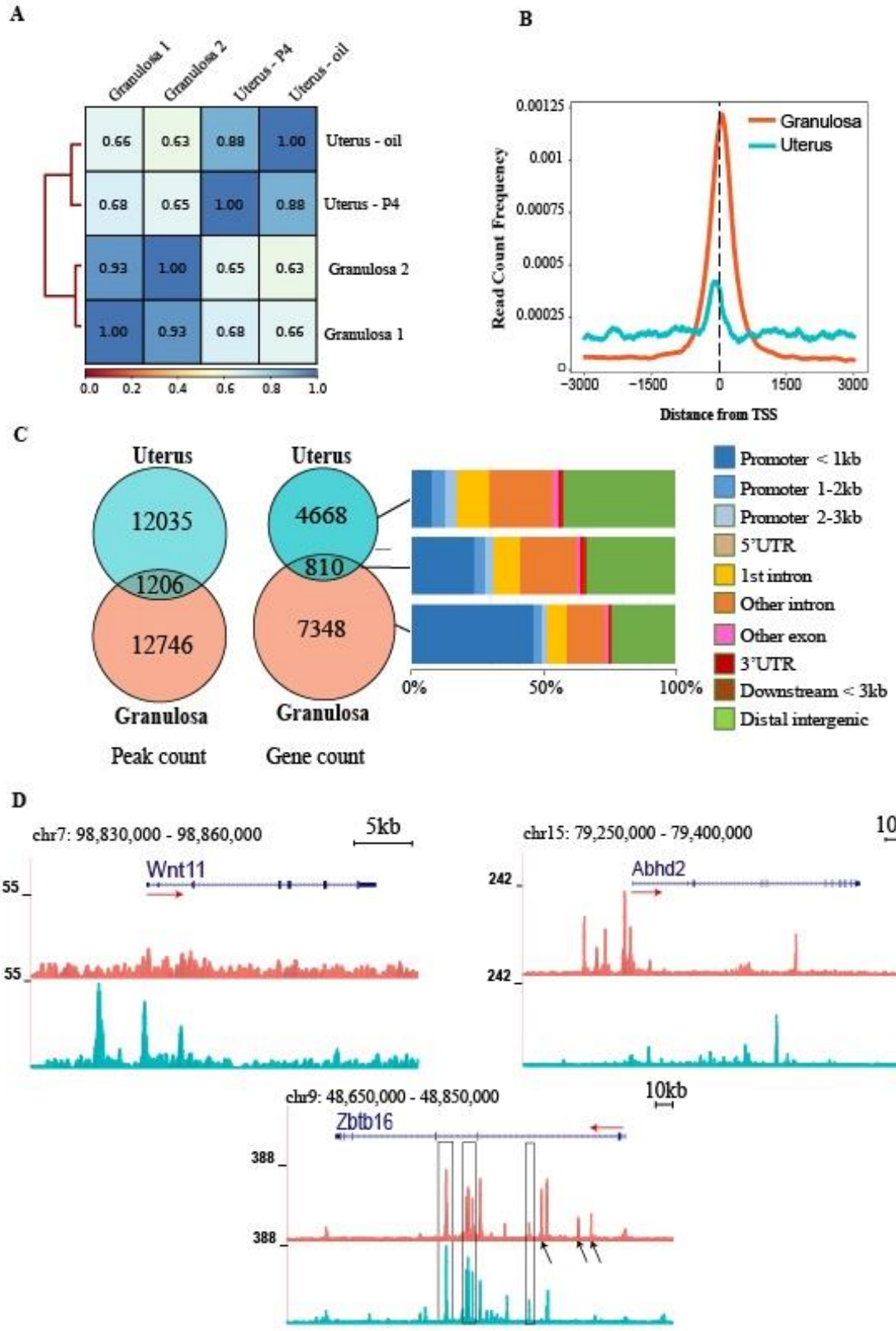
A
Granulosa 1
Granulosa 2
Uterus - P4
Uterus - oil
0.66 0.63 0.88 1.00 Uterus - oil
0.68 0.65 1.00 0.88 Uterus - P4
0.93 1.00 0.65 0.63 Granulosa 2
1.00 0.93 0.68 0.66 Granulosa 1
0.0 0.2 0.4 0.6 0.8 1.0
B
Granulosa
Uterus
Read Count Frequency
0.00125
0.001
0.00075
0.0005
0.00025
0
−3000 −1500 0 1500 3000
Distance from TSS
C
Uterus
12035
1206
12746
Granulosa
Peak count
Uterus
4668
810
7348
Granulosa
Gene count
0% 50% 100%
Promoter < 1kb
Promoter 1-2kb
Promoter 2-3kb
5'UTR
1st intron
Other intron
Other exon
3'UTR
Downstream < 3kb
Distal intergenic
D
chr7: 98,830,000 - 98,860,000
5kb
Wnt11
55
55
chr15: 79,250,000 - 79,400,000
10kb
Abhd2
242
242
chr9: 48,650,000 - 48,850,000
10kb
Zbtb16
388
388

Figure 3.5 Correlation between PGR binding sites in granulosa cells vs uterus.

(A) Pearson correlation matrix for granulosa cells ChIP-seq replicate 1 and replicate 2 and uterus ChIP-seq with P4 and oil treatment. The correlation in genomic coverage between all datasets was analysed and organised in hierarchical order. **(B)** Read count frequency of PGR ChIP-seq peaks in granulosa cells (pink) and progesterone-responsive uterus (blue) in relation to the TSS. **(C)** Venn diagrams showing the peak count for uterus and granulosa cells (top) and gene with peaks (bottom). Genome distribution of PGR peaks in uterus and granulosa cells is shown below. Genome distribution is displayed as stacked bar graphs and peaks were divided into uterus-unique (top), overlap (middle) and granulosa-unique (bottom). Genomic features include promoters (< 1 kb, 1-2 kb and 2-3 kb), 5' UTR, 1st intron, other introns, exons, 3' UTR and downstream of TES (within 3 kb). Peaks that are not in these features are classified as distal intergenic. **(D)** Example of tissue-specific PGR binding patterns on the genome. PGR binding sites are shown for granulosa cells (pink) and uterus (blue) at the genomic region for *Wnt11* (uterus-specific), *Abhd2* (granulosa-specific) and *Zbtb16* (tissue-specificity within a gene). Tracks are normalised to the same scale, the red arrow indicates the TSS (arrow tail) and direction of transcription. Black arrows indicate granulosa-specific peaks and black outline indicates peaks with PRE/NR3C motif.

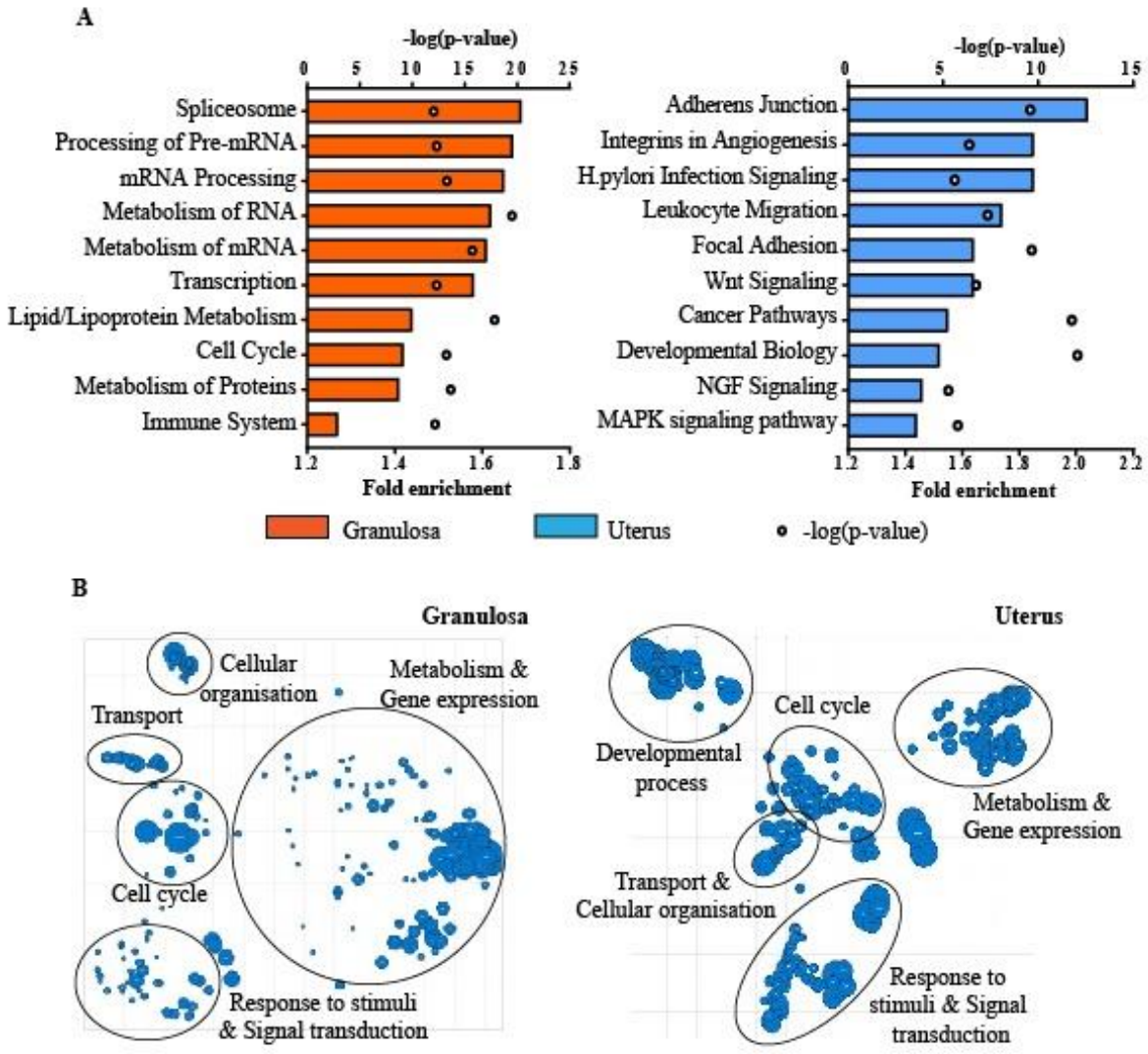

Figure 3.6 Functional consequence of PGR cistrome in uterus and granulosa cells.

(A) Top ten most enriched pathways of genes associated with PGR binding sites for granulosa cells (orange) and uterus (pink). Bars indicate fold enrichment of pathways and circles indicate -log(p-value) value. **(B)** Gene Ontology analysis of PGR ChIP-seq peaks in granulosa and uterus. Enriched ontological terms for PGR ChIP-seq data were obtained and reduced. Each reduced term is displayed as a circle with the diameter correlating to the -log10(p-value) of said term. Terms of the same umbrella of biological process are grouped together in the XY graph.

To elucidate the sequential difference in target chromatins between granulosa cells and uterus, motif analysis was performed for tissue-specific PGR binding sites. While PRE/NR3C was highly enriched in both tissues in comparison to background signals, it was the obvious preferred target for PGR in the uterus more so than in granulosa cells (Figure 3.7A). Again, while other transcription factor binding motifs were also discovered at uterus binding sites, these were much less enriched in relation to PRE/NR3C, whereas non-canonical motifs were enriched to a comparable degree to the canonical PRE/NR3C motif in granulosa cells. Interestingly, additional differences were also evident in non-PRE/NR3C motifs enriched in PGR cistrome from either tissue type, in which peaks specific to the uterus interacted with motifs belong to CP2, Homeobox and SOX families while peaks in granulosa cells included strongly enriched motifs for bZIP, RUNT, NR5A and CEBP transcription factor families. When the localisation of PRE/NR3C motif was examined in more detail, the degree of PRE/NR3C centricity in PGR-targeted chromatins in the uterus was very clear, with a high level of the canonical motif found in the centre of uterus-unique and tissue-shared PGR peaks (Figure 3.7B), whereas in contrast there was lower PRE/NR3C motif occupancy in granulosa-unique binding sites. These results demonstrate fundamental differences in the chromatin targets of PGR in different tissues, in which the canonical motif was significantly more preferred in the uterus, while in granulosa cells occupancy of other motifs (and hence interaction with other transcription factors) seemed to play a bigger role.

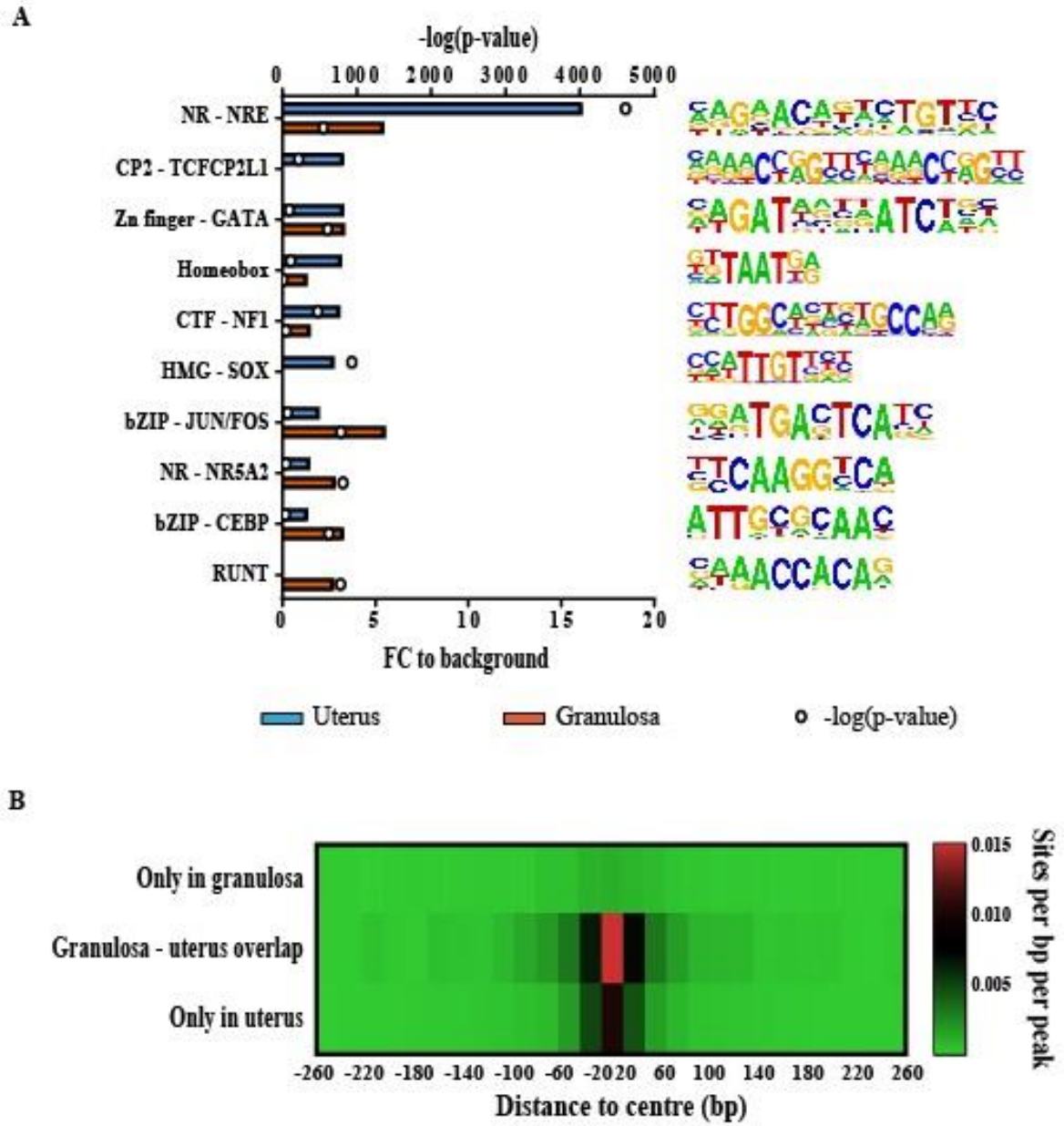

Figure 3.7 Properties of PGR-binding sequences in tissue-specific binding sites.

(A) Top most common known TF-binding motifs found to be enriched at PGR binding sites in granulosa cells (orange) and uterus (blue). The top 5 motifs from each tissue are shown. Bars indicate fold enrichment of motif to background (bottom x axis) and circles indicate -log(p-value) (top x axis). Motifs were ranked by -log(p-value) and among motifs from the same transcription factor family, the one that was most enriched by fold enrichment to background frequency is selected. **(B)** Heatmap displaying the localisation of the PRE/NR3C canonical motif in relation to the centre of peaks in only granulosa cells (top), overlap (middle) and only in the uterus (bottom). The frequency of PRE/NR3C was analysed for distribution within 520 bp upstream and downstream of PGR peaks.

3.4 DISCUSSION

The various physiological phenotypes associated with PGR functions in different parts of the female reproductive tract leading up to pregnancy have been well-defined. However, few attempts have been made to describe the molecular mechanisms that allow PGR to achieve pleiotropic actions in the reproductive tract. This study is the first to consolidate PGR-dependent transcriptomes obtained from different reproductive tissues and contrast PGR cistromes in progesterone-responsive granulosa cells and the uterus to show that PGR is responsible for the regulation of tissue-specific genes through selective interaction with distinct PRE/NR3C motifs in the genome of each cell type and with novel accessory transcription factors.

The results confirm that the tissue specificity of PGR action has a transcriptomic basis which involves PGR exerting diverse physiological roles in different target organs through the regulation of widely different sets of genes. The lack of mutual genes, major differences in known upstream regulators of these genes, and distinctly enriched canonical pathways point to variances in the underlying transcriptional regulatory mechanisms employed by PGR in different tissue contexts. The transcriptomes used in this analysis are somewhat limited in their coverage and sensitivity to transcripts of low abundance, which is likely why relatively low numbers of genes (41-81 genes) were identified in each tissue type. With advances in current technology, most relevantly as RNA-seq becomes more established and well-used, future studies taking advantage of such technology will be able to achieve wider coverage of these transcriptomes. To date, there has been no report of similar experiment using a more comprehensive technique, apart from the PGR-dependent granulosa transcriptome (to be covered in Chapter 7).

As PGR controls vastly different sets of genes in different reproductive tissues, it is reasonable to suggest that unique PGR chromatin targeting patterns are responsible for such drastic differences in downstream targets. Indeed, PGR possesses a remarkable tissue-specific inclination for binding to specific gene regions depending on the tissue type. Less than 10% of PGR binding sites was found to be mutually bound in granulosa cells and the uterus. Consistent with these findings, a similar study comparing PGR cistromes between T47D breast cancer cell line versus primary leiomyoma found less than 15% overlap in PGR-binding sites [15]. In addition to minimal overlap, the characteristics of preferential PGR targets in each tissue type

were also strikingly different. In granulosa cells PGR favoured binding to very proximal gene promoter regions, with over 50% of granulosa specific PGR-binding sites within 3 kb upstream of a TSS. PGR is only transiently present in granulosa cells, which may bias chromatin binding towards the most accessible chromatin regions in key granulosa cell target genes, likely primed through binding pioneer transcription factors. In comparison, in the uterus where PGR is constitutively present, progesterone-activated PGR more commonly bound distal intergenic regions, alluding to PGR role in enhancers, which has been previously seen in other biological contexts [11,20]. Thus in the uterus, PGR may contribute to the formation of TADs and segmenting the genome into a permissive 3-dimensional functional structure (chromatin looping), primed for a specific response to ligands which are provided by ovarian granulosa cells at ovulation [21]. Most exciting is the discovery of possible cell-specific mechanisms through which PGR interacts with target genomes. In both target tissues, PGR, like all NR3C receptors including GR and AR, binds to the core PRE/NR3C motif. However, the degree of PRE/NR3C occupancy was strikingly different between the two tissues of enquiry. In PGR binding intervals unique to the uterus, or shared between uterus and granulosa cells, the NR3C/PRE binding motif and NR3C/PRE half sites were highly represented while in comparison these motifs were far less common in granulosa-specific intervals. As different subsets of PRE/NR3C were utilised in granulosa cells and in the uterus, this suggests that PGR chromatin occupancy of PRE/NR3C is highly selective in the genome of different tissues, which requires precise regulation. Cell-specific PGR actions in carcinoma have been shown to rely on context-specific accessory factors [15]. In the context of reproduction, this study shows that not only was the consensus PRE/NR3C motif targeted at different levels, PGR also interacted with non-canonical motifs in a tissue-specific manner. Some transcription factor families were equally targeted in both tissues, such as GATA transcription factors, whereas for others the level of enrichment was highly specific. In granulosa cells, the RUNT motif was uniquely targeted, whereas uterine PGR tended to bind members of the SOX family. RUNX transcription factors, including RUNX1 and RUNX2, are key regulators of gene expression in granulosa cells during ovulation [22,23]. Interestingly, SOX2 was also identified to be an upstream modulator of uterine genes. Although the exact roles of SOX2 on normal uterine functions are still not well explored, SOX2 expression independent of progesterone has been shown in the normal mouse uterus [24] and SOX2 also plays a role in endometrial cancer [25]. As distinct groups of transcription factor families are involved in PGR action in granulosa cells vs the uterus, it is possible that they are also responsible for the regulation PRE/NR3C motif targeting of PGR in these tissue contexts,

in which distinct groups of modulators recruit PGR to different chromatin sites through tethering or through remodelling chromatin compactment.

Following the description of PGR cistrome in peri-ovulatory granulosa cells in which PGR was vital for the regulation of ovulation, this chapter characterised the distinction in PGR roles in different reproductive tissues, including transcriptomic and cistromic differences. PGR-specific gene expression patterns were identified in progesterone-responsive granulosa cells, oviduct and uterus and PGR showed striking dissimilarities in PGR cistromic properties in progesterone-responsive granulosa cells and uterus. These results show that PGR employs distinctive molecular pathways in different reproductive tissues, especially through the coordination with tissue-specific groups of co-factors, in order to modulate separate groups of genes that result in specific PGR-regulated physiology. Through common motif analysis, a number of such prospective transcription factors were selected for subsequent studies. In the next chapters, the physical interaction between PGR and these binding candidates in ovulatory granulosa cells was explored and thus shed light on the specific underlying molecular mechanism(s) employed by PGR in ovulation.

3.5 REFERENCES

1 Park, O.-K. & Mayo, K. E. Transient Expression of Progesterone Receptor Messenger RNA in Ovarian Granuiosa Cells after the Preovulatory Luteinizing Hormone Surge. *Molecular Endocrinology* **5**, 967-978, doi:doi:10.1210/mend-5-7-967 (1991).

2 Natraj, U. & Richards, J. S. Hormonal regulation, localization, and functional activity of the progesterone receptor in granulosa cells of rat preovulatory follicles. *Endocrinology* **133**, 761-769, doi:10.1210/en.133.2.761 (1993).

3 Lydon, J. P., DeMayo, F. J., Funk, C. R., Mani, S. K., Hughes, A. R., Montgomery, C. A., Jr., Shyamala, G., Conneely, O. M. & O'Malley, B. W. Mice lacking progesterone receptor exhibit pleiotropic reproductive abnormalities. *Genes Dev* **9**, 2266-2278 (1995).

4 Vinijsanun, A. & Martin, L. Effects of progesterone antagonists RU486 and ZK98734 on embryo transport, development and implantation in laboratory mice. *Reprod Fertil Dev* **2**, 713-727, doi:10.1071/rd9900713 (1990).

5 Pabona, J. M. P., Zhang, D., Ginsburg, D. S., Simmen, F. A. & Simmen, R. C. M. Prolonged Pregnancy in Women Is Associated With Attenuated Myometrial Expression of Progesterone Receptor Co-Regulator Krüppel-Like Factor 9. *The Journal of Clinical Endocrinology & Metabolism* **100**, 166-174, doi:10.1210/jc.2014-2846 (2015).

6 Brown, H. M., Dunning, K. R., Robker, R. L., Boerboom, D., Pritchard, M., Lane, M. & Russell, D. L. ADAMTS1 Cleavage of Versican Mediates Essential Structural Remodeling of the Ovarian Follicle and Cumulus-Oocyte Matrix During Ovulation in Mice1. *Biology of Reproduction* **83**, 549-557, doi:10.1095/biolreprod.110.084434 (2010).

7 Hsieh, M., Lee, D., Panigone, S., Horner, K., Chen, R., Theologis, A., Lee, D. C., Threadgill, D. W. & Conti, M. Luteinizing Hormone-Dependent Activation of the Epidermal Growth Factor Network Is Essential for Ovulation. *Molecular and cellular biology* **27**, 1914-1924, doi:10.1128/mcb.01919-06 (2007).

8 Kim, J., Bagchi, I. C. & Bagchi, M. K. Signaling by hypoxia-inducible factors is critical for ovulation in mice. *Endocrinology* **150**, 3392-3400, doi:10.1210/en.2008-0948 (2009).

9 Kim, J., Sato, M., Li, Q., Lydon, J. P., DeMayo, F. J., Bagchi, I. C. & Bagchi, M. K. Peroxisome Proliferator-Activated Receptor γ Is a Target of Progesterone Regulation in the Preovulatory Follicles and Controls Ovulation in Mice. *Molecular and cellular biology* **28**, 1770-1782, doi:10.1128/mcb.01556-07 (2008).

10 Akison, L. K., Boden, M. J., Kennaway, D. J., Russell, D. L. & Robker, R. L. Progesterone receptor-dependent regulation of genes in the oviducts of female mice. *Physiological Genomics* **46**, 583-592, doi:10.1152/physiolgenomics.00044.2014 (2014).

11 Rubel, C. A., Wu, S.-P., Lin, L., Wang, T., Lanz, R. B., Li, X., Kommagani, R., Franco, H. L., Camper, S. A., Tong, Q., Jeong, J.-W., Lydon, J. P. & DeMayo, F. J. A Gata2-Dependent Transcription Network Regulates Uterine Progesterone Responsiveness and Endometrial Function. *Cell reports* **17**, 1414-1425, doi:10.1016/j.celrep.2016.09.093 (2016).

12 Doyle, K. M. H., Russell, D. L., Sriraman, V. & Richards, J. S. Coordinate Transcription of the ADAMTS-1 Gene by Luteinizing Hormone and Progesterone Receptor. *Molecular Endocrinology* **18**, 2463-2478, doi:10.1210/me.2003-0380 (2004).

13 Rubel, C. A., Lanz, R. B., Kommagani, R., Franco, H. L., Lydon, J. P. & DeMayo, F. J. Research resource: Genome-wide profiling of progesterone receptor binding in the mouse uterus. *Molecular endocrinology* **26**, 1428-1442 (2012).

14 Clarke, C. L. & Graham, J. D. Non-Overlapping Progesterone Receptor Cistromes Contribute to Cell-Specific Transcriptional Outcomes. *PLOS ONE* **7**, e35859, doi:10.1371/journal.pone.0035859 (2012).

15 Yin, P., Roqueiro, D., Huang, L., Owen, J. K., Xie, A., Navarro, A., Monsivais, D., Coon V, J. S., Kim, J. J., Dai, Y. & Bulun, S. E. Genome-Wide Progesterone Receptor Binding: Cell Type-Specific and Shared Mechanisms in T47D Breast Cancer Cells and Primary Leiomyoma Cells. *PLOS ONE* **7**, e29021, doi:10.1371/journal.pone.0029021 (2012).

16 Jeong, J.-W., Lee, K. Y., Kwak, I., White, L. D., Hilsenbeck, S. G., Lydon, J. P. & DeMayo, F. J. Identification of Murine Uterine Genes Regulated in a Ligand-Dependent Manner by the Progesterone Receptor. *Endocrinology* **146**, 3490-3505, doi:10.1210/en.2005-0016 (2005).

17 Akison, L. K. a. *The role of nuclear progesterone receptor (PGR) in regulating gene expression, morphology and function in the ovary and oviduct during the periovulatory period*, (2012).

18 Dinh, D. T., Breen, J., Akison, L. K., DeMayo, F. J., Brown, H. M., Robker, R. L. & Russell, D. L. Tissue-specific progesterone receptor-chromatin binding and the regulation of progesterone-dependent gene expression. *Scientific reports* **9**, 11966-11966, doi:10.1038/s41598-019-48333-8 (2019).

19 Kommagani, R., Szwarc, M. M., Vasquez, Y. M., Peavey, M. C., Mazur, E. C., Gibbons, W. E., Lanz, R. B., DeMayo, F. J. & Lydon, J. P. The Promyelocytic Leukemia Zinc Finger Transcription Factor Is Critical for Human Endometrial Stromal Cell Decidualization. *PLoS genetics* **12**, e1005937-e1005937, doi:10.1371/journal.pgen.1005937 (2016).

20 Ceballos-Chávez, M., Subtil-Rodríguez, A., Giannopoulou, E. G., Soronellas, D., Vázquez-Chávez, E., Vicent, G. P., Elemento, O., Beato, M. & Reyes, J. C. The Chromatin Remodeler CHD8 Is Required for Activation of Progesterone Receptor-Dependent Enhancers. *PLOS Genetics* **11**, e1005174, doi:10.1371/journal.pgen.1005174 (2015).

21 de Laat, W. & Duboule, D. Topology of mammalian developmental enhancers and their regulatory landscapes. *Nature* **502**, 499, doi:10.1038/nature12753 (2013).

22 Jo, M. & Curry, T. E., Jr. Luteinizing Hormone-Induced RUNX1 Regulates the Expression of Genes in Granulosa Cells of Rat Periovulatory Follicles. *Molecular Endocrinology* **20**, 2156-2172, doi:10.1210/me.2005-0512 (2006).

23 Park, E.-S., Lind, A.-K., Dahm-Kähler, P., Brännström, M., Carletti, M. Z., Christenson, L. K., Curry, T. E., Jr. & Jo, M. RUNX2 Transcription Factor Regulates Gene Expression in Luteinizing Granulosa Cells of Rat Ovaries. *Molecular Endocrinology* **24**, 846-858, doi:10.1210/me.2009-0392 (2010).

24 Davoudi, M., Zavareh, S., Ghorbanian, M. T., Paylakhi, S. H. & Mohebbi, S. R. The effect of steroid hormones on the mRNA expression of oct4 and sox2 in uterine tissue of the ovariectomized mice model of menopause. *Int J Reprod Biomed (Yazd)* **14**, 471-476 (2016).

25 Yamawaki, K., Ishiguro, T., Mori, Y., Yoshihara, K., Suda, K., Tamura, R., Yamaguchi, M., Sekine, M., Kashima, K., Higuchi, M., Fujii, M., Okamoto, K. & Enomoto, T. Sox2-dependent inhibition of p21 is associated with poor prognosis of endometrial cancer. *Cancer Science* **108**, 632-640, doi:10.1111/cas.13196 (2017).

CHAPTER 4 Potential co-regulators of PGR in granulosa cells

4.1 INTRODUCTION

The process of ovulation involves the complex interplay of multiple physiological events under the control of an array of regulatory factors, encoded by a myriad of genes. Regulating these genes are a cast of transcription factors, including PGR, likely acting in conjunction with each other to mutually co-regulate target genes. While the role of PGR in ovulation has been extensively studied, the involvement of co-modulators in this biological context has been overlooked. Aside from PGR, a number of transcription factors have been accredited with ovulatory roles in granulosa cells and are herein hypothesised to act as co-regulators of PGR in this context. Indeed, analysis of motifs enriched at granulosa cell PGR binding sites confirmed that PGR did not solely rely on the canonical mechanism but indeed predominantly targeted other non-canonical motifs across the genome in order to access regulatory control of genes without dependence on PRE/NR3C that are invariable in their position in the genome of all PGR-responsive tissues. Such interaction was also specific to the tissue context, with different groups of motifs being enriched in PGR binding cistromes in granulosa cells versus the uterus, indicating divergent molecular mechanisms being utilised by PGR depending on the presence of other transcription factors. From this analysis, potential binding candidates of PGR have been identified, including transcription factors with known roles in granulosa cells during ovulation.

Included in these potential PGR partners are members of the RUNT, NR5A and JUN/FOS family, each of which plays a role in granulosa cells in response to the LH surge. The RUNT motif is recognised by the RUNX transcription factor family and members of this group, in particular RUNX1 and RUNX2, are upregulated in granulosa cells by ovulatory cues [1,2]. In peri-ovulatory granulosa cells, RUNX1 and RUNX2 are known to regulate the expression of a number of genes, including those involved in prostaglandin synthesis (*Ptgs2*, *Ptgds*) [2,3], metabolism (*Fabp6*) [2] and steroidogenesis (*Cyp11a1*) [1], suggesting functional similarities with PGR [4]. The physiological impact of RUNX has been indirectly investigated through KO mouse models for CBFβ, the canonical dimerising partner of RUNX, in which CBFβ KO female mice have a significantly lower ovulation rate and reduced expression of *Edn2*, *Ptgs1* and *Lhcgr* in

granulosa cells [5]. The TGATCA motif is recognised by members of the JUN/FOS protein family which share a common basic Leucine zipper DNA-binding tertiary structure. JUN/FOS proteins play important roles in the ovary, especially in steroidogenesis [6]. While the effect of JUN/FOS on follicular rupture in vertebrate species has not been demonstrated, in *C. elegans* JUN/FOS are shown to be important for ovulation [7]. NR5A2, also known as liver receptor homolog 1 (LRH1), is an orphan (ligand-less) receptor that is important in the regulation of steroidogenesis as well as cytoskeletal remodelling prior to ovulation [8,9]. The ablation of LRH1 in granulosa cell-specific knockout mouse models results in an anovulatory phenotype, including entrapped mature oocytes in follicles that become atretic and the lack of corpus luteum formation [10-12]. While LRH1 is present in granulosa cells at different stages of development [13], the LRH1 cistromes are shown to be highly dynamic in response to LH signalling, with LRH1 chromatin binding events shifting to open chromatin spaces that are made available after the LH surge [8].

While PGR and other granulosa cell transcription factors regulate similar functional outcomes, it is unknown whether PGR forms direct complexes with any of these transcription factors in granulosa cells. However, an interaction between PGR and JUN/FOS proteins have been previously described in human myometrial cells in which the physical interaction between various JUN/FOS proteins and specific PGR isoforms has an impact on the intricate regulation of genes that are important for the induction of labour [14]. Furthermore, RUNX members have been shown to interact with AR and GR to regulate their transactivation efficiency [15-17]. Other candidate binding partners of PGR as suggested in PGR ChIP-seq have also been linked to ovarian development and ovulation (GATA4, GATA6 [18]) or have been shown to interact with PGR in other tissue contexts (GATA2 [19]). In general, an interaction between these candidates and PGR has never been described in the context of granulosa cells. More importantly, even though many of such transcription factors are highly active in peri-ovulatory granulosa cells, the functional association between these transcription modulators and PGR during ovulation has not been previously explored.

Apart from other transcription factors, PGR action can also be modulated by RNA components, especially lncRNA. The classic RNA regulator of PGR and other steroid receptors is *Sra1*, a lncRNA that forms a physical interaction with steroid receptors and promotes the activity of the AF-1 domain [20]. Curiously, *Sra1* can also exhibit steroid receptor regulatory function in the form of a protein, named SRAP [21]. With the roles of *Sra1* and SRAP being mainly examined

in the context of tumorigenesis, their relevance in female reproduction remain poorly understood. However, transgenic mice with overexpressed *Sra1* are shown to be subfertile and the presence of *Sra1* and its protein counterpart has been linked to reproductive disorders that affect the ovary and uterus [22-25]. Another lncRNA that has been attributed to steroid receptor regulation is *Gas5*. The genomic structure of *Gas5* is complex, with 12 exons and snoRNA-encoding intronic regions that result in various combination of isoforms due to alternative splicing and intronic retention [26]. *Gas5* isoforms are shown to be differentially regulated, alluding to possible functional differences between variants. Furthermore, snoRNA encoded in the *Gas5* introns are also known to be functional [27]. Unlike *Sra1* where a functional protein has been identified, so far there has been no protein products found for *Gas5*. Originally linked to cellular response to stress conditions, *Gas5* also plays prominent roles in the modulation of steroid receptor activity, especially GR [28]. In this context, *Gas5* forms a physical interaction with the DBD domain of GR, thereby competes with target DNA for GR occupancy and inhibits GR transactivation functions. In the same vein, *Gas5* is shown to be capable of PGR binding [29]; however, whether such interaction is also possible in tissues with normal PGR actions and results in changes in PGR activities is still unknown. The roles of *Gas5* on reproductive physiology, especially ovarian functions, remain unknown. However, evidence from our lab has shown that *Gas5* is present in human cumulus cells and is associated with pregnancy outcomes [30] and other studies have indicated the presence of *Gas5* in oocytes and granulosa cells [31,32]. Both lncRNA and other short ncRNA including miRNA have been shown to play various roles in ovarian functions, such as oocyte development [33] and ovulation [34]. This highlights the importance of lncRNA and other poorly-described ncRNA in the ovary, especially in the ovulation process. The fact that ncRNA are usually present in low abundance also makes them easily overlooked.

While enriched motif analysis of the PGR ChIP-seq data has indicated a number of transcription factor families with potential interaction with PGR, this conclusion is inferred from the motif sequences and is not direct proof of transcription factor interactions. It is also unable to differentiate between members of a transcription factor family with shared DNA binding motif and thus cannot conclude the exact protein partner to PGR. Hence, it is necessary to confirm such interactions using other *in vitro* and *in vivo* methods. The aim of this chapter was to confirm the physical interaction between potential protein partners and PGR in the context of peri-ovulatory granulosa cells. To do this, proximity ligation assay (PLA) was utilised, which is an immunofluorescence technique that takes advantage of the highly specific

recognition of antibodies to their target proteins and coordinated fluorescent markers that requires very close (within 40 nm) proximity of the two target proteins. Cultured granulosa cells responding to an ovulatory stimulus were used to demonstrate physical interactions between proteins at an *in vivo* cellular level. For each of the transcription factor families, hypothesised PGR-interacting candidates were selected based on previous knowledge of their roles in ovulatory granulosa cells, and most importantly, evidence from PGR ChIP-seq indicating enrichment of motifs for these factors in PGR binding sites. Additionally, in order to comprehensively address potential PGR interacting partners, ncRNA that are known to interact with steroid receptors in other biological contexts were also assessed for possible interaction with PGR in peri-ovulatory granulosa cells using RNA co-immunoprecipitation (RIP).

4.2 MATERIALS & METHODS

4.2.1 Animals

CBAF1 mice were obtained from The University of Adelaide, Laboratory Animal Services. All mice were maintained in 12 h light /12 h dark conditions and given water and rodent chow *ad libitum*. All experiments were approved by The University of Adelaide Animal Ethics Committee and were conducted in accordance with the Australian Code of Practice for the Care and Use of Animals for Scientific Purposes (ethics no m/2015/075).

4.2.2 Tissue collection

Super-ovulation in 21-day old CBAF1 female mice was induced by injecting mice i.p with 5 IU eCG and 5 IU hCG 46 h post-eCG. Mice were culled and dissected at 0, 4, 6 or 8 h post-hCG for intact ovaries. Tissues were fixed in 4% formaldehyde overnight at 4^{o}C, then on the next day were washed in PBS and stored in 70% ethanol at 4^{o}C. Tissues were embedded in paraffin and sectioned using the microtome into sections of 5 µm thickness, then placed on polylysine-coated positively-charged slides.

4.2.3 Granulosa cell culture and treatment

For granulosa cell collection, 21-day old CBAF1 female mice were stimulated with 5 IU eCG and culled at 46 h post-eCG. Ovaries were dissected from the tract and punctured using a 26G needle to release granulosa cells into a dish containing DMEM:F12 media. COCs were

removed from the dish and granulosa cells were counted before being seeded into an 8-well chamber slide (minimum 100,000 cells/well) previously coated with fibronectin to promote cell adhesion by incubating for 1 h with 5 µg/ml recombinant fibronectin in PBS. Cells were incubated at 37ºC, 5% CO_2 for 90 minutes then washed with PBS in order to remove any dead cells and remaining tissue debris and then cells were incubated overnight. The next day, cells were treated with hCG (final concentration 2 IU/ml) and R5020 (final concentration 100 nM) for 6 h at 37ºC, 5% CO_2.

4.2.4 Cell line culture and treatment

T47D human breast cancer cells were maintained in RPMI 1640 media (Sigma) supplemented with 10% foetal calf serum (FCS, Sigma), 10 µg/ml insulin (Sigma), 0.5 U/ml penicillin (Sigma), 50 µg/ml streptomycin (Sigma), 1X non-essential amino acid (Thermo Fisher) and 1X GlutaMAX (Thermo Fisher) at 37ºC, 5% CO_2. Prior to treatment, cells were seeded at 50,000 – 200,000 cells/well into an 8-well chamber slide in the above standard RPMI 1640 media and left overnight to adhere to the well surface. Cells were treated with R5020 diluted in ethanol (final concentration 100 nM) or vehicle (ethanol) at 37ºC, the length of treatment depending on the assay.

4.2.5 Immunofluorescence

4.2.5.1 Tissue sections

Sections were dewaxed and rehydrated with xylene and ethanol, then antigen retrieval was by boiling slides in citrate buffer (pH 6) or basic buffer (pH 9) in a pressure cooker for 20 minutes, with the buffer condition determined after empirical testing for each antibody. Sections were blocked with 9% normal goat serum and 1% BSA in TBS for 1 h at room temperature. Sections were incubated with primary antibodies (listed in Appendix 10) diluted to 1:500 in 1% serum for 1 h at room temperature or overnight at 4ºC and with corresponding secondary antibodies diluted to 1:2000 in 1% serum for 1 h at room temperature. Hoechst 33342 at 1:1000 dilution was included in the secondary incubation to stain nuclei. Slides were then mounted with mounting media (Dako, Agilent, Santa Clara, CA, USA) and coverslips, and sections imaged using the Olympus FV3000 confocal laser scanning microscope (Olympus, Tokyo, Japan).

4.2.5.2 Cell cultures

Cells were cultured on coverslips in a 6-well plate or cultured directly in an 8-well chamber slide and underwent treatment according to the assay and cell type. The dosage of hCG is standard in the lab for granulosa cell culture and the dosage of R5020 was determined after testing of different dosages. After treatment, media was aspirated and cells were gently washed twice with PBS. Cells were fixed in 4% formaldehyde for 10 minutes at room temperature, washed three times with PBS and permeabilised with 0.01% Triton X-100 in PBS for 1 h at room temperature. After washing three times with PBS, cells were blocked using 9% normal goat serum and 1% BSA in PBS for 1 h at room temperature. Cells were incubated with primary antibodies diluted to 1:500 in 1% serum for 1 h at room temperature or overnight at 4^{o}C and with corresponding secondary antibodies diluted to 1:2000 in 1% serum for 1 h at room temperature. Hoechst 33342 at 1:1000 dilution was included in the secondary incubation to stain nuclei. Slides were then mounted with mounting media and coverslips, and imaged using the Olympus FV3000 confocal laser scanning microscope.

4.2.6 Proximity Ligation Assay

PLA was performed using the Duolink PLA Probes and PLA Fluorescence *in situ* Detection Kit Red (Sigma) and followed the manufacturer's protocol. For ovarian tissues, sections in paraffin were processed as for IF, including dewaxing, antigen retrieval and permeabilisation. For cultured cells, cells were fixed and permeabilised as described for IF. For blocking, the provided Blocking Buffer was used for blocking for 1 h at 37^{o}C. Samples were incubated with primary antibody couples raised in distinct species that recognise each of the target proteins, diluted in Antibody Diluent, for 2 h at room temperature or overnight at 4^{o}C (see list of antibodies in Appendix 10). Cells were then incubated with secondary antibody PLA probes of appropriate species modified with oligonucleotide for 1 h at 37^{o}C, then probes were ligated for 30 minutes at 37^{o}C, followed by the amplification and fluorescent nucleotide incorporation reaction at 37^{o}C for a minimum of 100 minutes. Between steps, slides were washed using the provided wash buffers following the manufacturer instructions. Slides were mounted with Prolong Gold Mounting Media with DAPI (Thermo Fisher), cured for at least 1 h at room temperature in the dark and then stored at -20^{o}C prior to imaging. Slide imaging was performed using an Olympus confocal microscope at a minimum of 60x magnification. Specific positive signals from this method require that the two proteins of interest are within 40 nm and indicate that they either directly interact or are part of the same protein complex. PLA of cultured cells

was performed in triplicates and PLA signals were identified as fluorescent puncta using the 'Count Maxima' function in ImageJ [35].

4.2.7 RNA co-immunoprecipitation

Granulosa cells from super-ovulated CBAF1 female mice were collected at 6 h post-hCG as previously described. Cells were fixed in 1% formaldehyde for 15 minutes at 37ºC and quenched with 0.125 M glycine for 10 minutes at room temperate. Cells were washed twice with cold PBS and lysed in lysis buffer for 30 minutes at 4ºC. Lysate was sonicated using a Bioruptor Plus (Diagenode, Denville, NJ, USA) for 15 minutes at High setting, 30 secs on/ 30 sec off, then centrifuged at 10,000 g for 15 minutes to remove cell debris. To measure protein concentration, Bradford assay using Bio-Rad Protein Assay Dye Reagent Concentrate (Bio-Rad) was performed, with BSA at concentrations of 40-640 µg/ml used as protein standards and measurements taken in duplicate for each sample using the Synergy H1 Hybrid Reader (BioTek, Winooski, VT, USA) and the accompanying Gen5 2.00 software. For immunoprecipitation, Protein A+G magnetic beads (Merck, Burlington, MA, USA) were incubated with 4 µg antibodies (as indicated in Appendix 3) for 30 minutes at room temperature. Lysate was incubated with antibody-bound beads in IP buffer (25 mM Tris (pH 7.4), 5 mM EDTA, 150 mM KCl, 0.5 mM DTT, 0.5% NP-40) for at least 16 h at 4ºC, with one volume of lysate retained as lysate input. Beads were washed in IP buffer 5 times for 5 min each, then reverse crosslinking was by heating protein-bound beads and lysate input in proteinase K buffer (Sigma) for 30 minutes at 55ºC. Lysate was then isolated from magnetic beads. RNA was isolated from immunoprecipitated extracts using Trizol extraction method. Briefly, bead elute and lysate input were incubated with 250 µl of Trizol (Thermo Fisher), then 50 µl chloroform was added. RNA was precipitated from the aqueous phase by the addition of isopropanol and freezing at -80ºC for at least 2 h, followed by centrifugation. Precipitated RNA pellets were washed with 75% ethanol, dissolved in 100 µl water and treated with rDNase I (Ambion, Thermo Fisher) for 30 minutes at 37ºC. cDNA from purified RNA was synthesised using Superscript III kit and accompanying protocol (Thermo Fisher) as described in section 2.2.2.2. 500 ng of purified RNA was used per reaction. qPCR was performed as described in section 2.2.2.2 using SYBR Green Master Mix with primers designed for specific RNA targets, or commercial Taqman assays whenever available. Primers are listed in Appendix 1.

4.3 RESULTS

4.3.1 Expression of PGR and other transcription factors in peri-ovulatory follicles

The *in situ* expression of PGR in the ovaries during the peri-ovulatory window was confirmed using immunofluorescence with PGR antibody on ovarian sections obtained from female mice stimulated with eCG + hCG for 0-8 h. PGR was not observed without hCG treatment (0 h) and was detectable from 4 h post-hCG, remaining high until 8 h post-hCG, with PGR expressed specifically in granulosa cells of antral follicles (Figure 4.1A). Negative controls (IgG control and no primary antibody control) showed low to undetectable nonspecific fluorescent signals. The specificity of hCG induction was confirmed in immunofluorescence for H3K27ac specific antibody. This mark of active chromatin was constitutively present, shown in pre- and post-hCG ovaries which displayed prominent staining signals (Figure 4.1B). The acetylation of the transcription factor CBP, previously shown to enhance CBP transactivation functions [36], was also shown to be induced by hCG treatment.

From PGR ChIP-seq motif analysis, a number of potential co-factors were identified. Among these non-canonical motifs, the RUNT motif, recognised by the RUNX transcription factor family, was specifically targeted by PGR in granulosa cells yet not in the uterus. To confirm the presence and localisation of RUNX members, ovarian sections were stained with antibodies against RUNX1, RUNX2 and their dimerising partner CBFβ. Both RUNX proteins showed no signals in antral follicles pre-hCG while CBFβ showed some staining in granulosa cells (Figure 4.2). All proteins were induced in antral follicles after hCG stimulation, with the highest intensity observed for RUNX1 and RUNX2 at 6 h post-hCG.

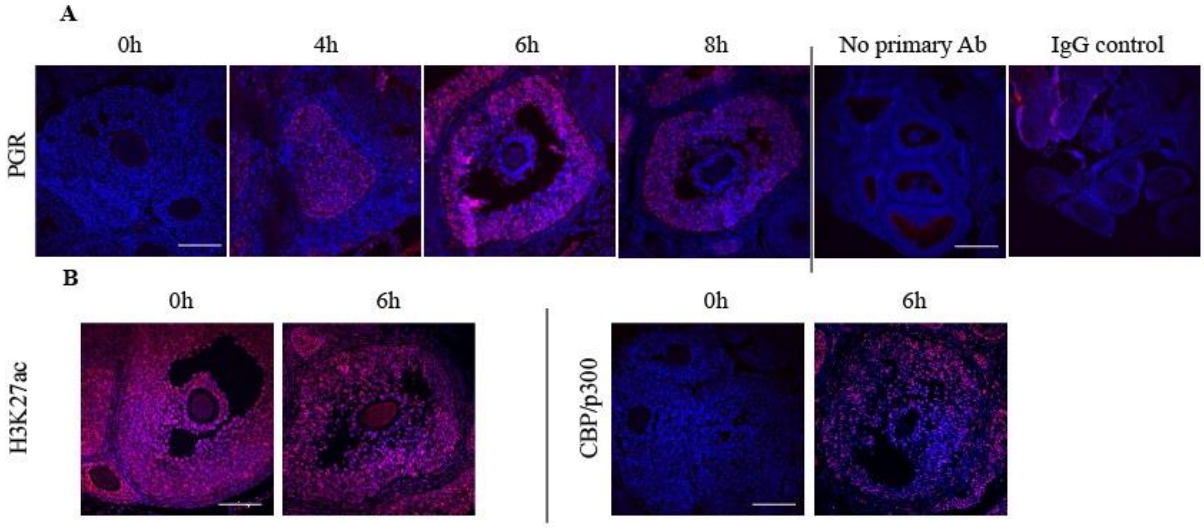

Figure 4.1 Immunofluorescent detection of PGR and transcription markers in ovarian sections.

(A) Immunofluorescent detection of PGR in ovarian sections. Ovaries were obtained from mice stimulated for 46h with eCG and 0, 4, 6 or 8 h with hCG. Ovarian sections were stained for PGR (red) and nucleus using Hoechst 33342 (blue). Negative controls included species (mouse) IgG isotype (IgG control) and secondary antibody only (No primary Ab). Scale bar for PGR staining = 100 µm, for No primary Ab control = 300 µm. **(B)** Immunofluorescent detection of H3K27ac and acetyl-CBP/p300 in ovarian sections. Ovaries were obtained from mice stimulated with eCG for 44 h or eCG followed by hCG for 6 h. Red fluorescence indicates positivity for H3K27ac (left panels) or acetyl-CBP (right panels). Images are representative of three biological replicates. Scale bar for H3K27ac and CBP staining = 100 µm.

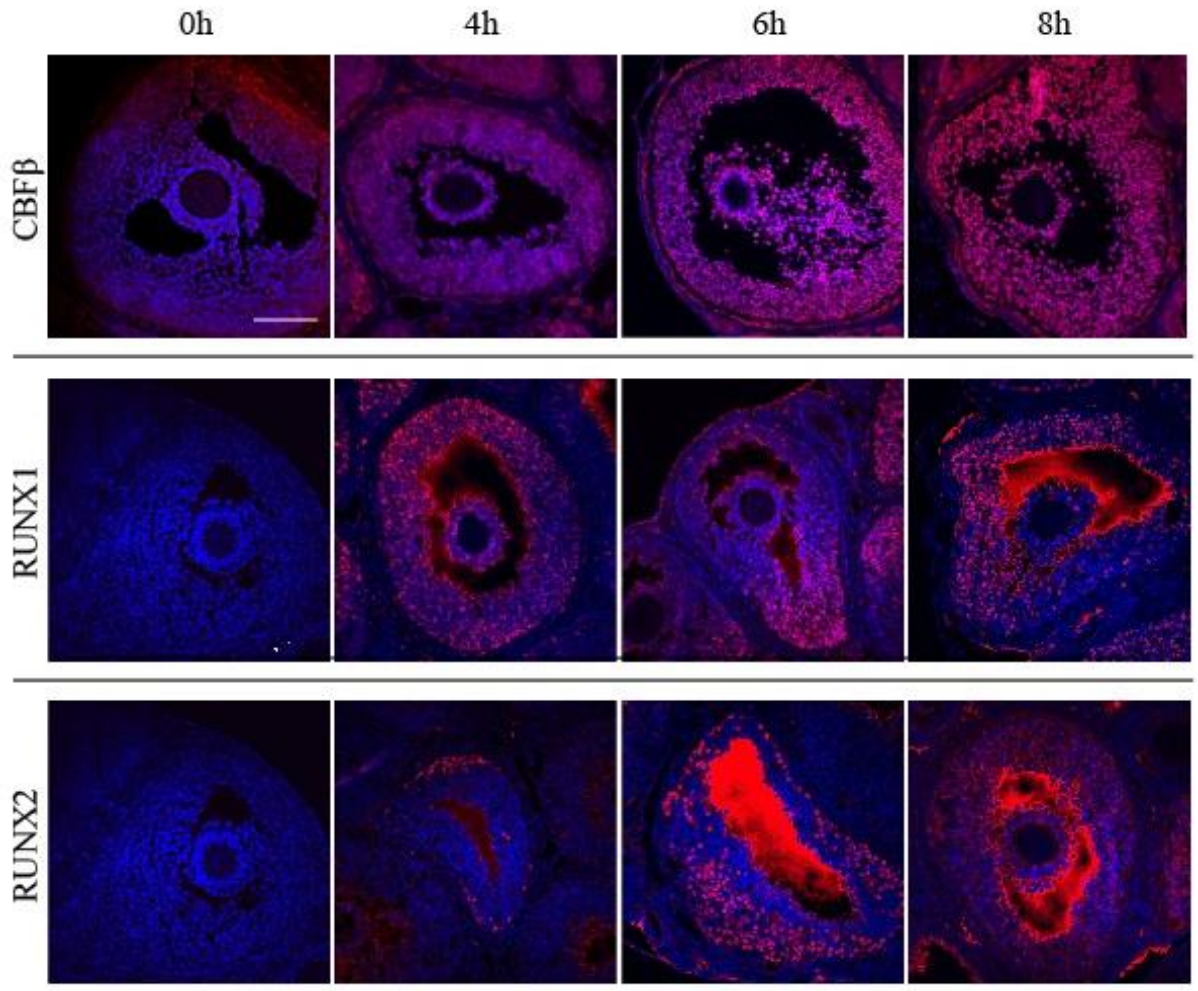

Figure 4.2 Immunofluorescent detection CBFβ, RUNX1 and RUNX2 in ovarian sections.

Ovaries obtained from mice stimulated for 46 h with eCG and 0, 4, 6 or 8 h with hCG were processed for immunohistochemical detection of CBFβ (row 1), RUNX1 (row 2) and RUNX2 (row 3). Antibody labelling is in red and nuclear staining in blue. Staining in antrum is due to nonspecific binding of mouse-raised antibodies. Scale bar = 100 µm.

4.3.2 Validation of the PLA methodology in tissues and cell culture

The PLA technique was validated in the human breast cancer cell line T47D which has high level of endogenous PGR that could rapidly respond to progesterone treatment. This was confirmed through immunofluorescence of T47D cells treated with the PGR agonist R5020, where the nuclear localisation of PGR was displayed in T47D as soon as 1 h after R5020 treatment, as opposed to the lack of nuclear PGR signal in the vehicle-treated control (Figure 4.3A). With R5020 treatment there was a co-localisation between PGR and H3K27ac in immunofluorescence (IF) and PLA signal was detected in cell nuclei 90 min after R5020 treatment, suggesting that PGR is in close proximity to H3K27ac and thus transcriptionally active chromatin (Figure 4.3B). To validate the efficiency of the PLA method in detecting protein-protein interactions in different cellular compartments, the nuclear PGR/H3K27ac interaction as well as the cytoplasmic/membrane interaction between beta-catenin and e-cadherin were examined using PLA, in which abundant PLA puncta signifying the expected complexes were detected. PLA also showed that the physical PGR/H3K27ac interaction was present only after 90 minutes of treatment, although PGR localisation to the nucleus was already observed at 60 minutes post-treatment, showing the highly dynamic nature of PGR nuclear complex formation, enzymatic activation and transcriptional induction.

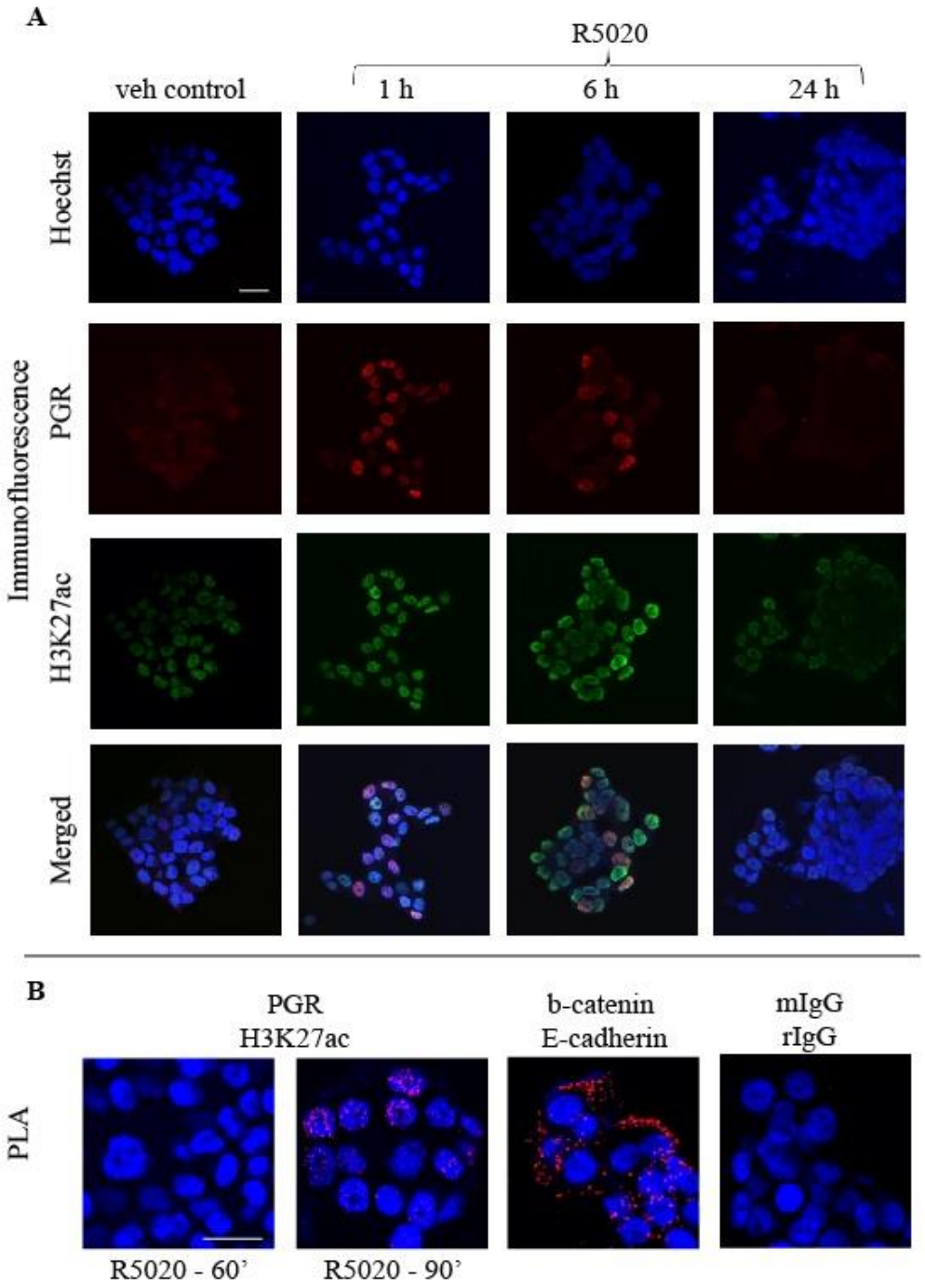

Figure 4.3 Dynamics of PGR/H3K27ac interaction in R5020-treated T47D cells.

(A) Immunofluorescent detection of PGR and H3K27ac in R5020-treated T47D cells. T47D cells were treated with vehicle control for 1 h or 100 nM R5020 for 1, 6 or 24 h. From top to bottom: Hoechst (blue), PGR (red), H3K27ac staining (green) and merged. **(B)** Proximity ligation assay in T47D cells treated with R5020. T47D cells were treated with 100 nM R5020 for 60 or 90 minutes and PLA was performed for PGR/H3K27ac (left), b-catenin/e-cadherin (middle) or IgG control (right). Scale bar = 20 μm.

4.3.3 Interaction of PGR and co-partners in peri-ovulatory granulosa cells

As the PLA protocol was confirmed on cultured T47D cells, PLA was attempted on paraffin-embedded ovarian sections from 6 h post-hCG ovaries. For confirmation of the method, protein pairs chosen were for RUNX1/RUNX1 (using antibodies targeting different regions of the RUNX1 protein, presumably nuclear interaction), b-catenin/e-cadherin (cytoplasmic interaction) and mIgG/rIgG (negative control). However, the commonly observed PLA puncta were not specifically observed and instead ubiquitous fluorescence signal was observed in all samples, including nuclear, cytoplasmic interactions and negative control (Figure 4.4). Optimising protocols using different antigen retrieval, antibody incubation and washing conditions had no effect on the nonspecific fluorescent signal.

To overcome the non-specific labelling in fixed whole tissue, the interaction between PGR and potential TF partners was subsequently investigated in cultured peri-ovulatory granulosa cells treated with hCG and progestin. To confirm that the cell culture system mimicked the phenotype of *in vivo* granulosa cells, granulosa cells obtained from eCG-stimulated mice were cultured and immunofluorescence was performed after hCG + R5020 treatment for 6 h. The treatment resulted in the expected pattern of expression for target proteins in the nucleus, in which PGR is specifically induced by the treatment regime whereas H3K27ac is constitutively present. Other transcription factors such as RUNX1, RUNX2 and CBFβ were also present in treated granulosa cells, showing that the *in vitro* system could closely portray the biology observed *in vivo* (Figure 4.5).

The interaction between PGR and RUNX members in a transcription complex was examined using PLA targeting different protein-protein interactions. PLA of progestin-treated cells showed positive signals for interaction between PGR and H3K27ac and acetyl-CBP/p300 in the nucleus of granulosa cells, as expected since these complexes are known as part of the transcription machinery (Figure 4.6). Positive interaction was also observed between both RUNX1 and RUNX2 and their dimerising partner CBFβ in the nucleus, confirming that RUNX proteins were active in granulosa cells, as well as between RUNX proteins and CBP/p300. Excitingly an interaction between RUNX transcription factors and PGR was observed. PGR/CBFβ PLA signals were also observed, not only in the nucleus but also in the cytoplasm of granulosa cells, a cellular localisation which was not shown in any other protein-protein pairs.

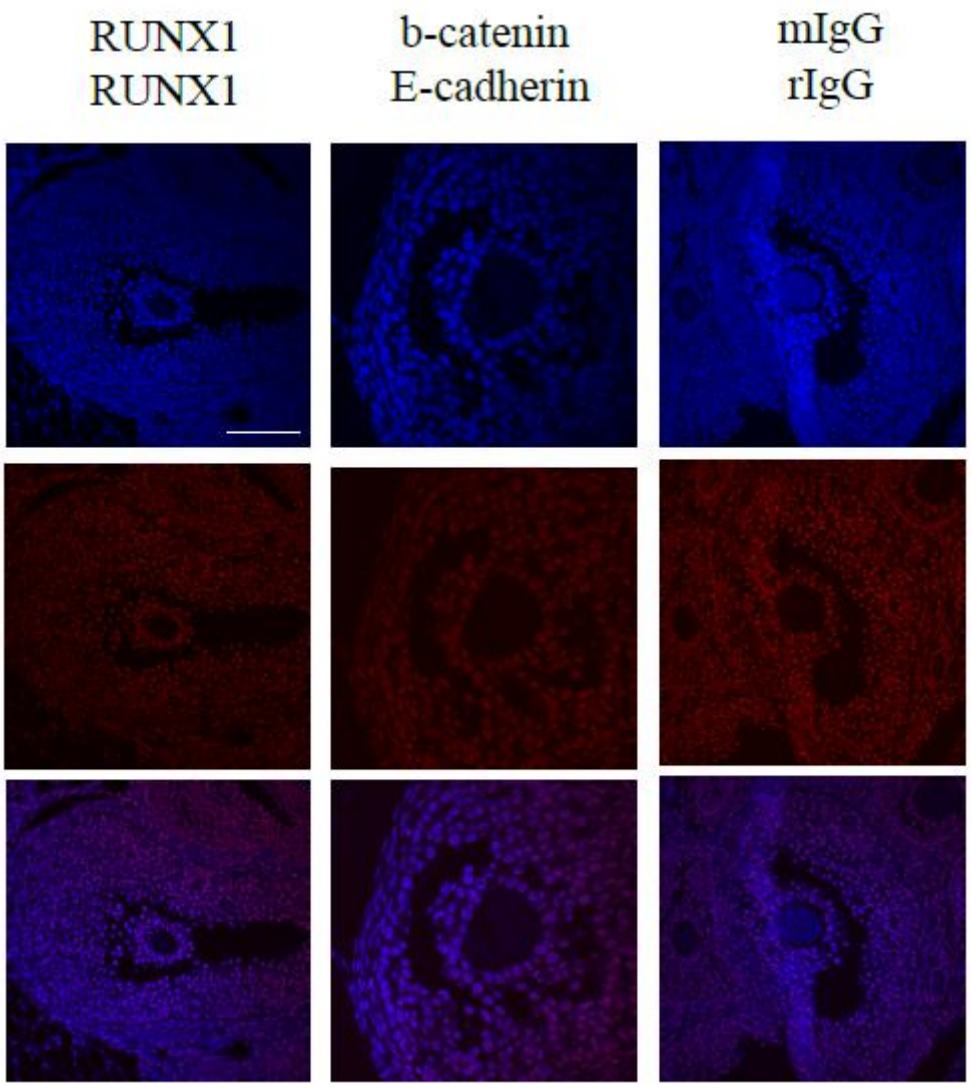

Figure 4.4 Proximity ligation assay in ovarian sections.

Ovarian sections were obtained at 6 h post-hCG stimulation and subjected to PLA protocol. Protein pairs include RUNX1 (rabbit antibody)/RUNX1 (mouse antibody) and b-catenin (rabbit antibody)/E-cadherin (mouse antibody). Negative control includes mIgG (mIgG) (mouse antibody)/rIgG (rabbit antibody). From top to bottom: Hoechst (blue), PLA signal (red) and merged. Scale bar = 100 µm.

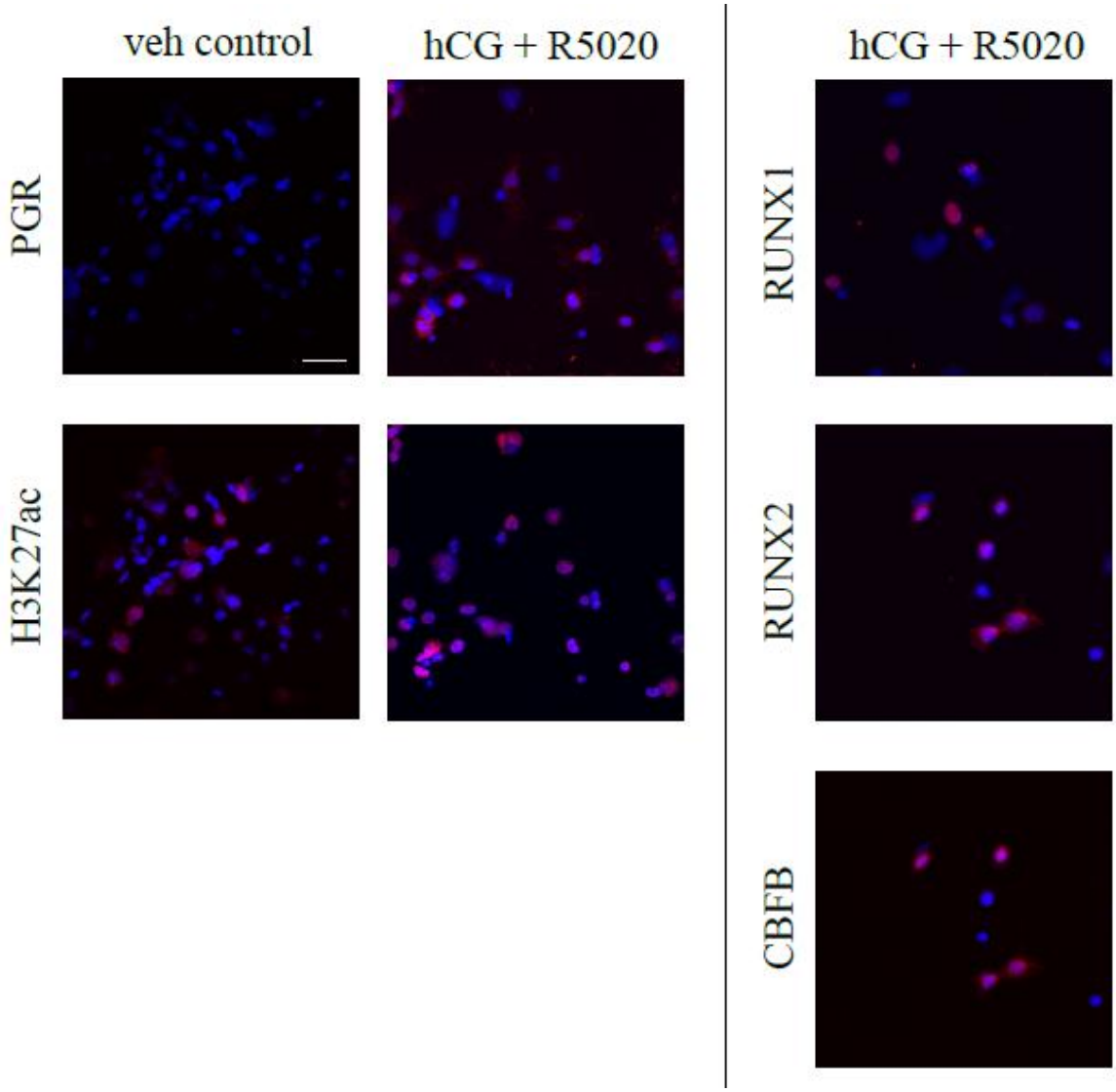

Figure 4.5 Immunofluorescent detection of PGR and associated transcriptional markers in cultured granulosa cells treated with hCG and R5020.

Granulosa cells were harvested from ovaries at 44 h post-eCG and treated with vehicle control or 2 IU/ml hCG and 100nM R5020 for 6 h. Immunohistochemistry was performed for H3K27ac and PGR in untreated/treated cells (column 1-2), RUNX1, RUNX2 and CBFβ in treated cells (column 3). Antibody labelling is in red and nuclear staining in blue. Scale bar = 30 µm.

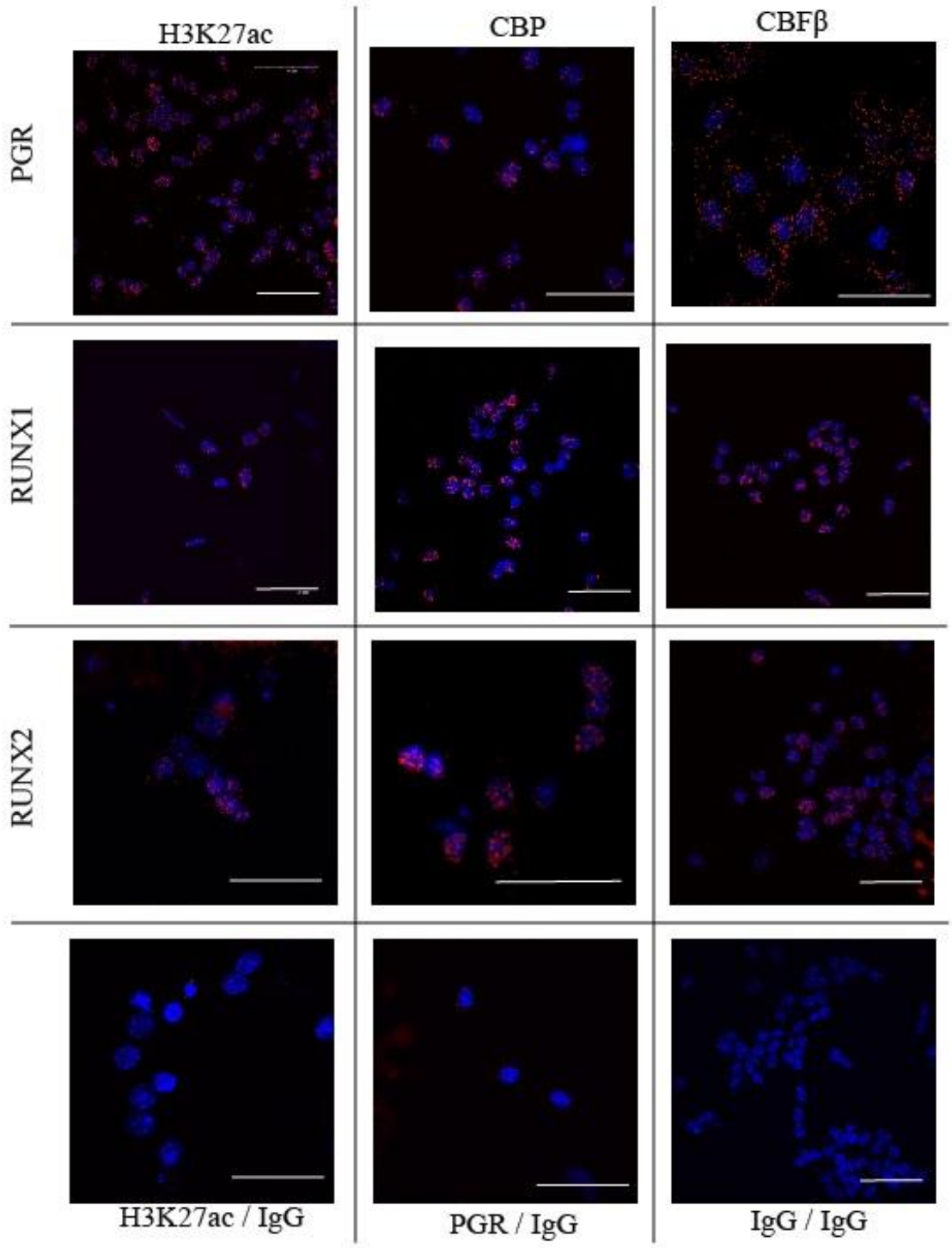

Figure 4.6 Interaction between PGR and RUNX members in granulosa cells treated with hCG and R5020.

Granulosa cells were harvested from ovaries at 44 h post-eCG and treated with hCG and R5020 for 6 h *in vitro*. PLA was performed for antibody combinations (PGR, H3K27ac, CBP/p300, CBFβ, RUNX1 and RUNX2) as indicated or IgG negative controls (H3K27ac/IgG, PGR/ IgG or IgG/IgG). Red indicates protein interactions. Blue is Hoechst nuclear stain. Scale bar = 50 μm.

Since the canonical motifs for the bZIP (JUN/FOS) transcription factor family and for NR5A2/LRH1 were also highly enriched at PGR binding sites in granulosa cells, the potential interaction between PGR and members of these families was also investigated. The expression of cJUN, JUNB and JUND, which are members of the bZIP family, were determined in *in vitro* granulosa cells treated with hCG and R5020, of which only JUND showed prominent signals (Figure 4.7). Correspondingly, PLA signal was only observed with PGR/JUND antibody pairs. LRH1 and PGR/LRH1 interactions were also detected in hormone-treated cultured granulosa cells, confirming close spatial interactions between PGR and JUND as well as LRH1 in peri-ovulatory granulosa cells.

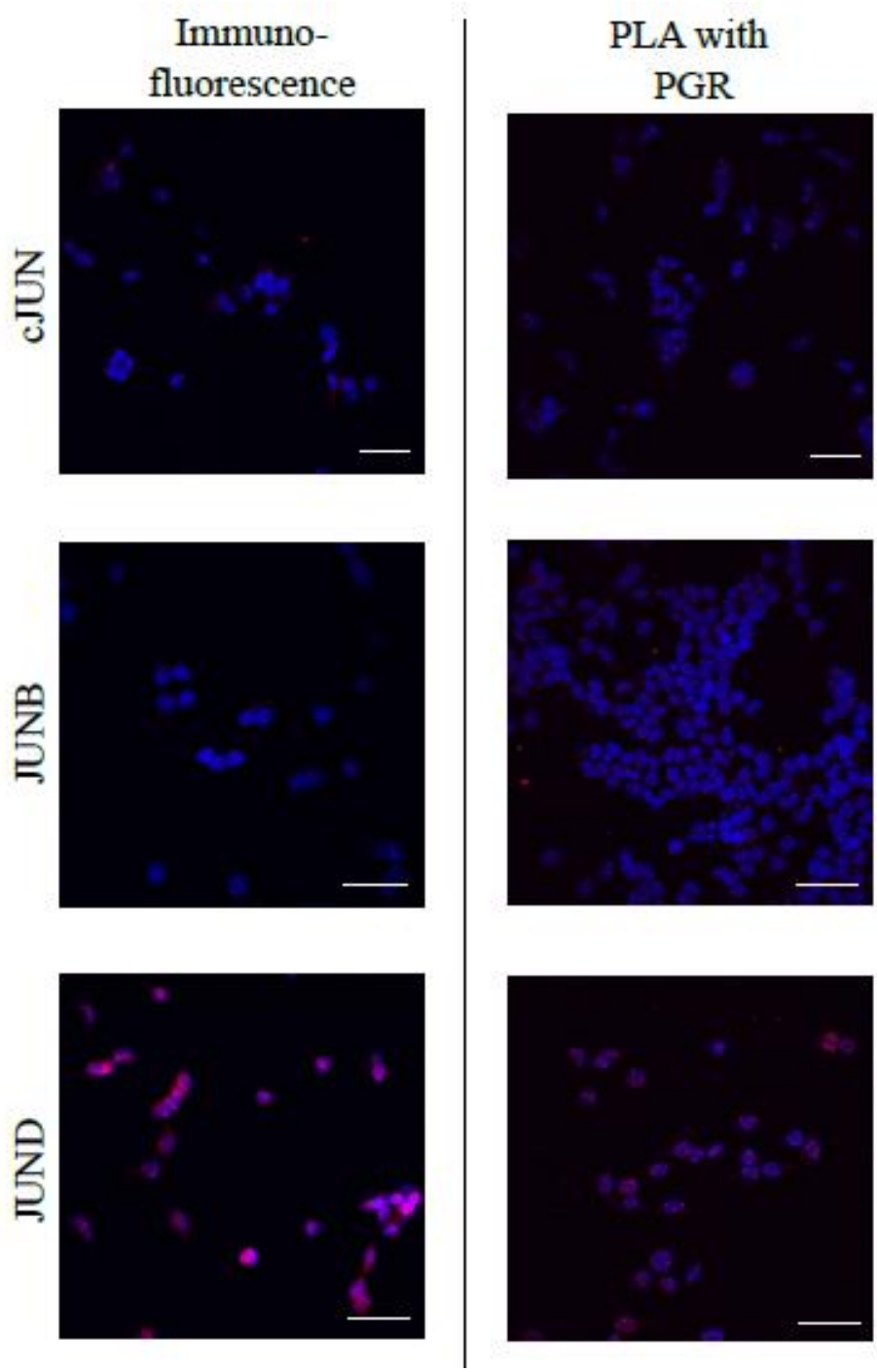

Figure 4.7 Interaction between PGR and bZIP (JUN/FOS) members and LRH1 in granulosa cells treated with hCG and R5020.

Granulosa cells were harvested from ovaries at 44 h post-eCG and treated with hCG and R5020 for 6 h. Antibodies against c-JUN, JUNB, JUND or LRH1 were used for immunofluorescence (left) or PLA (right). Red indicates protein presence (IF) or protein interactions (PLA). Blue is Hoechst nuclear stain. Scale bar = 50 µm.

4.3.4 Interaction of PGR and non-coding RNA in peri-ovulatory granulosa cells

In order to investigate the potential role of RNA binding in PGR transcriptional regulation, PGR-RNA interaction was investigated using RIP. To validate the RIP methodology, RIP-qPCR was performed on granulosa cells with or without hCG stimulation using an antibody targeting the splicing complex protein SNRNP70 that binds the U1 snRNA. U1 expression was confirmed in granulosa cells through qPCR which showed U1 to slightly increase at 6 h compared to 0 h hCG stimulation (Figure 4.8A). RIP-qPCR showed that in relation to the IgG pull-down negative control there was an enrichment of U1 snRNA in granulosa cells at 6 h post-hCG compared to 0 h (Figure 4.9A). As SNRNP70-U1 are involved in alternative splicing and thus would naturally be found in a complex with immature mRNA, a gene with a single exon was selected as the biological negative control, which should not be spliced and thus not involved with the splicing complex. Indeed, *Oxct2*, a single exon gene, was not enriched in SNRNP70 pull-down in comparison to IgG pull-down, confirming that the RIP methodology was consistent in enriching protein-bound RNA.

To investigate PGR-bound RNA in granulosa cells during ovulation, PGR-pull down was performed on granulosa cells at 0 or 6 h post-hCG and qPCR was performed on PGR-bound RNA isolated from the lysate. *Sra1* was induced in granulosa cells during ovulation, peaking at 8 h post-hCG stimulation (Figure 4.8B). RIP-qPCR showed that *Sra1* was enriched in immunoprecipitates using PGR antibody compared to IgG and more enriched in 6 h post-hCG granulosa cells in comparison to 0 h (Figure 4.9B). Alongside *Sra1*, *Gas5*, a lncRNA repressor of steroid receptors and another potential RNA regulator of PGR, was investigated as a binding partner. *Gas5* includes 12 described exons and there is a high level of alternative splicing as well as intron retention in *Gas5*. As spliced isoforms of *Gas5* have been shown to be important in various *Gas5* activities, three primer assays targeting different *Gas5* exons were examined for enrichment in PGR pull-down. All three assays showed a decrease in expression in peri-ovulatory granulosa cells (Figure 4.8C-E). *Gas5* expression reached the lowest level at 8 h post-hCG in assay 22 (exon 11-12), assay 23 (exon 6-7) showing a more subtle trend in downregulation. In RIP-qPCR, assay 22 showed a tendency for enrichment in PGR pulldowns compared to IgG which was highest after 6 h compared to 0 h hCG stimulation. However, qPCR with assay 21 showed high Gas5 enrichment with PGR pulldown at both 0 h and 6 h post hCG and little enrichment was seen with assay 23 (Figure 4.9B). This showed that *Sra1*

is a potential interactor with PGR in granulosa cells while the evidence is less definitive for *Gas5*.

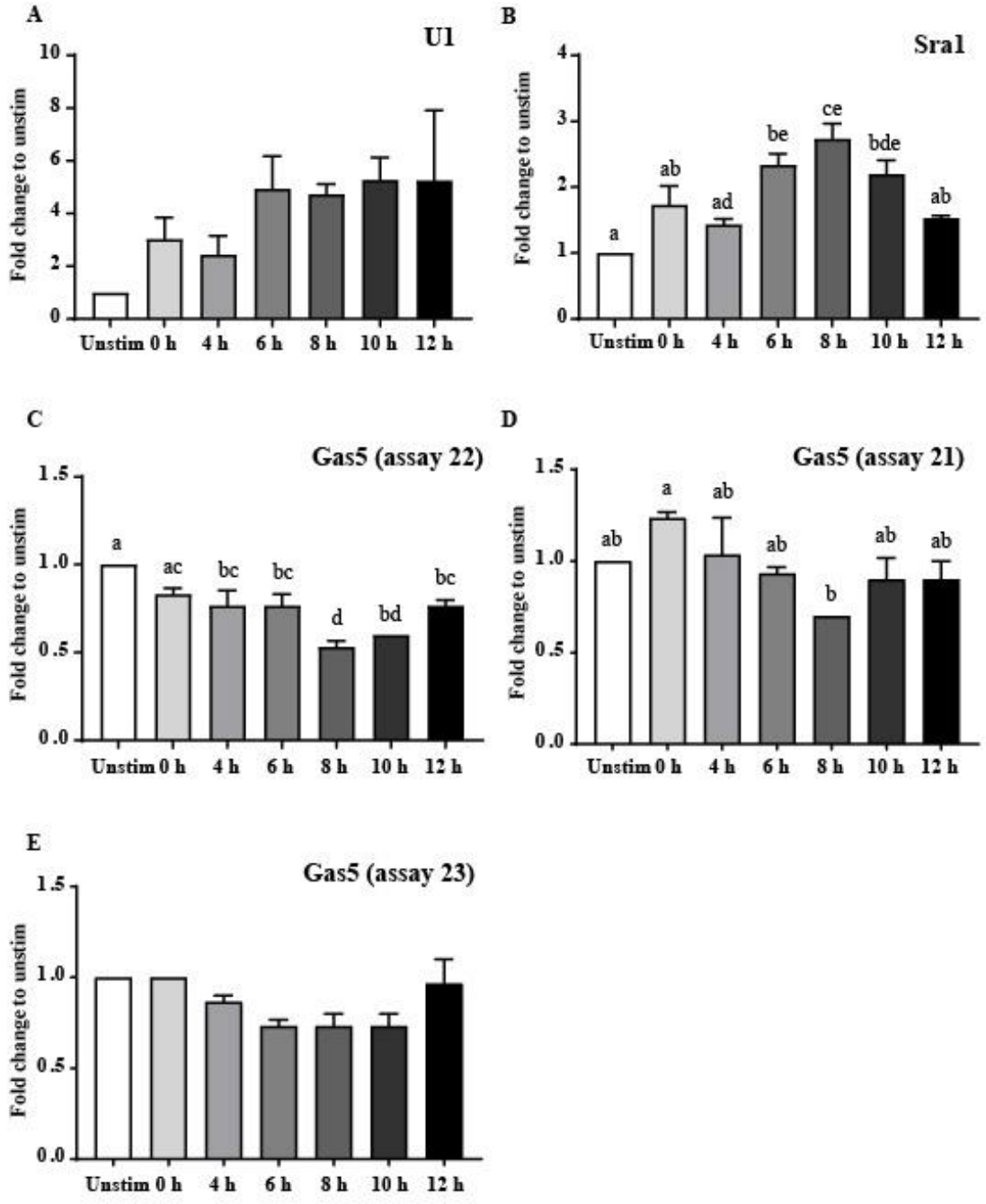

Figure 4.8 The expression of non-coding RNA and in peri-ovulatory granulosa cells.

RT-qPCR was performed on granulosa cells from mice not treated with eCG/hCG (unstim) or treated with eCG + hCG for the indicated time (0-12 h). Primers targeting *U1* **(A)**, *Sra1* **(B)** and *Gas5* using three different assays **(C-E)** were used. *Rpl19* was used as housekeeping gene and gene expression is displayed as fold change to unstim. N = 3 biological replicates, each replicate is from 3-5 mice per time point. Statistical significance was determined through one-way ANOVA with multiple comparison. p = 0.0497 (*U1*), p = 0.0001 (*Sra1*), p = 0.0002 (*Gas5* assay 22), p = 0.0557 (*Gas5* assay 21), p = 0.0155 (*Gas5* assay 23). Bars with different superscripts are significantly different.

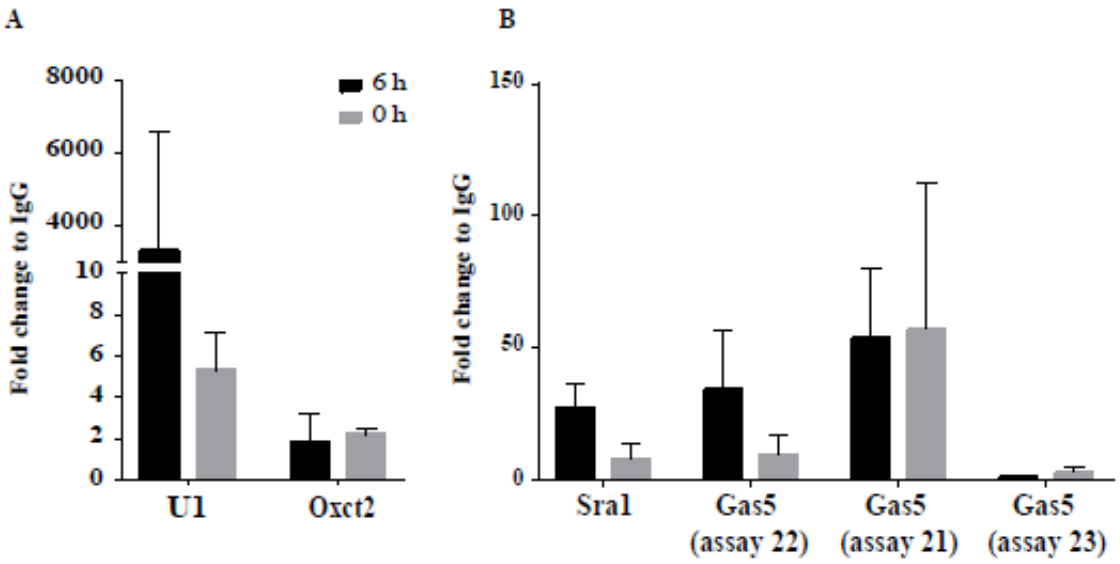

Figure 4.9 Interaction between PGR and RNA partners in granulosa cells.

(A) RIP of SNRNP70 in granulosa cells from ovaries that were eCG-primed (0h) or eCG + hCG-primed (6 h). Purified SNRNP70-bound RNA was assayed for the interaction with *U1* and *Oxct2* by RT-qPCR. (B) RIP of PGR in granulosa cells as in (A). Purified PGR-bound RNA was assayed by RT-qPCR for the interaction with *Sra1* and *Gas5* (using three specific assays targeting different genomic regions). Statistical analysis was performed using two-way ANOVA test. N = 3 independent experiments. Black bars are 6 h post-hCG granulosa cells and grey bars are 0 h post-hCG. Data is normalised to IgG pull-down.

4.4 DISCUSSION

The PGR cistromes in reproductive tissues have highlighted a number of transcription factor binding motifs enriched in PGR bound intervals, suggesting a potential interaction with the relevant transcription factor recruits PGR-binding in a mutual transcription complex. Here this study confirms the expression and interaction between PGR and a number of candidate transcriptional modulators in mouse granulosa cells in response to the LH surge, with potential implications for ovulatory functions. From the granulosa cell PGR ChIP-seq data, members from the most highly enriched transcription factor families were selected for investigation of potential interactions with PGR. These include members of the RUNX family (RUNX1, RUNX2, CBFβ), JUN/FOS family (c-JUN, JUNB, JUND) and NR5A (LRH1), which all have previously been indicated to play a role in the ovary, especially in granulosa cells during ovulation [1,2,5,6,10]. Almost all of these candidate proteins were found to be expressed in cultured granulosa cells in response to the ovulatory cues, with the exception of c-JUN and JUNB. Excitingly, physical interactions with PGR and each of these expressed transcription factor proteins was demonstrated through PLA. These results support the hypothesis that PGR binds chromatin in granulosa cells in complexes that include RUNX1 and RUNX2 as well as LRH1 and JUND. The disparity in c-JUN and JUNB expression *in vitro* vs *in vivo* granulosa cells has been previously reported [6], thus it remains to be determined whether c-JUN and JUNB in fact do interact with PGR in the *in vivo* setting. For the majority of candidate proteins, the interaction with PGR was found to be in the nucleus of hCG-stimulated granulosa cells, indicating the presence of the PGR transcription complex in the nucleus where it exhibits actions at the genomic level.

Transcription factors are known to have vastly different windows of expression during ovulation, with the expression of some proteins maintained throughout different stages of development and sustained in the ovary during ovulation (i.e. LRH1 [37]) whereas others have a much shorter expression window (i.e. PGR). Not only that, within the peri-ovulatory window these transcription factors might also display optimal activity at different time points; for example, investigation into the LRH1 cistrome has shown LRH1 to be active and occupying transcriptionally active chromatin by 4 h post-hCG stimulation in granulosa cells [8], which is before the peak of PGR activity. Coupled with the highly transient nature of protein-protein interactions in the transcription complex [38], this means that it is difficult to capture the PGR/co-modulator complex at the precise time when the transcription complex is active. Furthermore,

while DNA-binding transcription factor families can be implied as candidate PGR partners through motif analysis of the PGR ChIP-seq data, other co-modulators that do not bind DNA cannot be identified using this method. This includes transcription adaptors that act as linkages for components of the transcription complex without direct interaction with DNA [39]. The most well-known example of an SR-binding adaptor is the SRC family, consisting of SRC-1, SRC-2 and SRC-3, each of which can interact with various steroid receptors including AR, GR and PGR [40]. SRC proteins do not directly bind DNA but maintain the integrity of the transcription complex by acting as a bridge between different DNA-binding factors and the general transcription machinery. Future experiments involving PLA as well as immunoprecipitation and mass spectrometry will be able to explore other potential components of the ovarian PGR transcription complex. The temporal pattern of protein-protein expression is not the only critical aspect as the order of interaction between different components is also decisive in the formation of the protein complex. Using various *in vitro* and *in vivo* methods, a model for the SR/SRC complex has been generated, with SRC-3 units acting as a physical linkage between ER-α and CBP/p300, making SRC-3 essential for the ER-α transcription complex [41]. Thus, it is essential to take into consideration the temporal and sequential dynamics of PGR/co-modulator interactions when investigating the PGR-inclusive transcription complex, which is yet to be studies in such detail.

H3K27ac, being a generic marker for transcriptionally active chromatin regions, was shown with immunofluorescence to be present in ovarian sections regardless of treatment conditions. Acetyl CBP/p300 was only detected post-LH using a specific antibody that only detects the acetylated Lys1499 amino acid of CBP/p300 and not total CBP/p300. It is known that the HAT activity of CBP/p300 can result in auto-acetylation at specific sites, which enhances the HAT function of CBP/p300 [36]. While the acetylation state of CBP/p300 has never been examined in the context of its action in granulosa cells, this new data suggests that together with phosphorylation, acetylation might be another way through which CBP/p300 becomes activated in response to the LH-induced signalling cascade.

The potential involvement of ncRNA on PGR activities in peri-ovulatory granulosa cells was also implicated in this study. Through RIP, *Sra1*, a classic RNA modulator of steroid receptors in general and PGR in particular, was found to bind PGR specifically after hCG stimulation. *Gas5*, another known steroid receptor interactor, was also found to bind PGR after hCG stimulation on a exon-specific basis. Among the three *Gas5* primer assays being used, each

targeting a different exonic region of the *Gas5* gene, the only one that was enriched for PGR binding was for exon 11-12. Interestingly, this is also the *Gas5* region with known interactions with SR; specifically, *Gas5* exon 12 has been shown to form a hairpin folding structure that mimics the conformation of the PRE/NR3C DNA motif and thus can compete against target DNA in binding with GR, thereby sequestering GR away from target genes and suppressing its transactivation functions [28]. The roles of either *Sra1* or *Gas5* in ovulation are virtually unknown; but the discovery that these lncRNA interact with PGR in a LH-inductive manner suggests that they exert regulatory functions on PGR in granulosa cells. Intriguingly, *Gas5* transcripts bearing the PGR-interacting region are found to be downregulated during ovulation in granulosa cells, whereas *Sra1* is upregulated after the LH surge, suggesting that these lncRNA are engaged in different regulatory mechanisms. Both *Sra1* and *Gas5* are also known to interact with a wide range of NR3C receptors [25,29], including AR, GR and MR that are also present in the ovary with important functions, especially in luteinisation [42-44]; thus it will be important to also investigate the role of these lncRNA on the regulation of these SR. Some evidence has also linked *Gas5* abundance to the anovulatory condition PCOS [45], suggesting that this may have an important role in regulating ovarian hormone responsiveness. The roles of other lncRNA in the ovary have also been implied, including *Neat1* [46], *Xist* and *Zfas1* [47]. In addition, a growing number of transcriptomic studies have identified specific subsets of lncRNA that are upregulated in a cell-specific manner in the ovary [47-49]. Whether any of these lncRNA acts upon regulating ovulatory transcription factors, especially PGR, is still unknown and would require further investigations.

As the complexities of transcriptional regulation are revealed, it is apparent that the participation of non-promoter sequences such as enhancers and distal intergenic regions also play a vital role in modulating transcription of distal genes. In addition, modulating interactions between transcriptional regulators and protein or nucleotide (i.e. ncRNA) co-factors, is critical. Thus, it is important to investigate the transcriptional complex as a whole in order to gain a full comprehension of how gene expression is regulated uniquely in each cell context. Through investigating potential protein partners derived from the granulosa PGR ChIP-seq data, the interaction between PGR and a number of transcription factors have been determined. Among the confirmed physical partners of PGR are members of the RUNX family, including RUNX1, which were found to be exclusively enriched with PGR ChIP in peri-ovulatory granulosa cells and not in the uterus. RUNX1 is involved in diverse processes in granulosa cells in a developmental context-specific manner and is especially important for transcriptional

regulation in ovulation. Despite this, the ovulatory role of RUNX1 has never been put into context with other transcription mediators in granulosa cells. Thus, the next chapters further interrogated the contextual cistromic properties of RUNX1 in granulosa cells and the functional interaction between RUNX1 and PGR. This chapter also explored the potential role of lncRNA, in particular *Sra1* and *Gas5*, in PGR action and further studies in the RNA interactome could lead to novel regulatory mechanisms of PGR action in ovulation and other biological contexts.

4.5 REFERENCES

1 Jo, M. & Curry, T. E., Jr. Luteinizing Hormone-Induced RUNX1 Regulates the Expression of Genes in Granulosa Cells of Rat Periovulatory Follicles. *Molecular Endocrinology* **20**, 2156-2172, doi:10.1210/me.2005-0512 (2006).

2 Park, E.-S., Lind, A.-K., Dahm-Kähler, P., Brännström, M., Carletti, M. Z., Christenson, L. K., Curry, T. E., Jr. & Jo, M. RUNX2 Transcription Factor Regulates Gene Expression in Luteinizing Granulosa Cells of Rat Ovaries. *Molecular Endocrinology* **24**, 846-858, doi:10.1210/me.2009-0392 (2010).

3 Liu, J., Park, E.-S. & Jo, M. Runt-related transcription factor 1 regulates luteinized hormone-induced prostaglandin-endoperoxide synthase 2 expression in rat periovulatory granulosa cells. *Endocrinology* **150**, 3291-3300 (2009).

4 Liu, D. T., Brewer, M. S., Chen, S., Hong, W. & Zhu, Y. Transcriptomic signatures for ovulation in vertebrates. *General and Comparative Endocrinology* **247**, 74-86, doi:https://doi.org/10.1016/j.ygcen.2017.01.019 (2017).

5 Lee-Thacker, S., Choi, Y., Taniuchi, I., Takarada, T., Yoneda, Y., Ko, C. & Jo, M. Core binding factor β expression in ovarian granulosa cells is essential for female fertility. *Endocrinology* **159**, 2094-2109 (2018).

6 Choi, Y., Rosewell, K. L., Brännström, M., Akin, J. W., Curry Jr, T. E. & Jo, M. FOS, a Critical Downstream Mediator of PGR and EGF Signaling Necessary for Ovulatory Prostaglandins in the Human Ovary. *The Journal of Clinical Endocrinology & Metabolism* **103**, 4241-4252 (2018).

7 Hiatt, S. M., Duren, H. M., Shyu, Y. J., Ellis, R. E., Hisamoto, N., Matsumoto, K., Kariya, K.-i., Kerppola, T. K. & Hu, C.-D. Caenorhabditis elegans FOS-1 and JUN-1 Regulate plc-1 Expression in the Spermatheca to Control Ovulation. *Molecular Biology of the Cell* **20**, 3888-3895, doi:10.1091/mbc.e08-08-0833 (2009).

8 Bianco, S., Bellefleur, A.-M., Beaulieu, É., Beauparlant, C. J., Bertolin, K., Droit, A., Schoonjans, K., Murphy, B. D. & Gévry, N. The Ovulatory Signal Precipitates LRH-1 Transcriptional Switching Mediated by Differential Chromatin Accessibility. *Cell Reports* **28**, 2443-2454.e2444, doi:https://doi.org/10.1016/j.celrep.2019.07.088 (2019).

9 Zhang, C., Large, M. J., Duggavathi, R., DeMayo, F. J., Lydon, J. P., Schoonjans, K., Kovanci, E. & Murphy, B. D. Liver receptor homolog-1 is essential for pregnancy. *Nature Medicine* **19**, 1061-1066, doi:10.1038/nm.3192 (2013).

10 Duggavathi, R., Volle, D. H., Mataki, C., Antal, M. C., Messaddeq, N., Auwerx, J., Murphy, B. D. & Schoonjans, K. Liver receptor homolog 1 is essential for ovulation. *Genes Dev* **22**, 1871-1876, doi:10.1101/gad.472008 (2008).

11 Bertolin, K., Gossen, J., Schoonjans, K. & Murphy, B. D. The Orphan Nuclear Receptor Nr5a2 Is Essential for Luteinization in the Female Mouse Ovary. *Endocrinology* **155**, 1931-1943, doi:10.1210/en.2013-1765 (2014).

12 Gerrits, H., Paradé, M. C. B. C., Koonen-Reemst, A. M. C. B., Bakker, N. E. C., Timmer-Hellings, L., Sollewijn Gelpke, M. D. & Gossen, J. A. Reversible infertility in a liver receptor homologue-1 (LRH-1)-knockdown mouse model. *Reproduction, Fertility and Development* **26**, 293-306, doi:https://doi.org/10.1071/RD12131 (2014).

13 Liu, D. L., Liu, W. Z., Li, Q. L., Wang, H. M., Qian, D., Treuter, E. & Zhu, C. Expression and Functional Analysis of Liver Receptor Homologue 1 as a Potential Steroidogenic Factor in Rat Ovary1. *Biology of Reproduction* **69**, 508-517, doi:10.1095/biolreprod.102.011767 (2003).

14 Nadeem, L., Shynlova, O., Matysiak-Zablocki, E., Mesiano, S., Dong, X. & Lye, S. Molecular evidence of functional progesterone withdrawal in human myometrium. *Nature Communications* **7**, 11565, doi:10.1038/ncomms11565 (2016).

15 Little, G. H., Baniwal, S. K., Adisetiyo, H., Groshen, S., Chimge, N.-O., Kim, S. Y., Khalid, O., Hawes, D., Jones, J. O., Pinski, J., Schones, D. E. & Frenkel, B. Differential Effects of RUNX2 on the Androgen Receptor in Prostate Cancer: Synergistic Stimulation of a Gene Set Exemplified by SNAI2 and Subsequent Invasiveness. *Cancer Research* **74**, 2857-2868, doi:10.1158/0008-5472.can-13-2003 (2014).

16 Yang, R., Browne, J. A., Eggener, S. E., Leir, S.-H. & Harris, A. A novel transcriptional network for the androgen receptor in human epididymis epithelial cells. *Molecular Human Reproduction* **24**, 433-443, doi:10.1093/molehr/gay029 (2018).

17 Ning, Y.-M. & Robins, D. M. AML3/CBFα1 Is Required for Androgen-specific Activation of the Enhancer of the Mouse Sex-limited Protein (Slp) Gene. *Journal of Biological Chemistry* **274**, 30624-30630, doi:10.1074/jbc.274.43.30624 (1999).

18 Bennett, J., Wu, Y.-G., Gossen, J., Zhou, P. & Stocco, C. Loss of GATA-6 and GATA-4 in Granulosa Cells Blocks Folliculogenesis, Ovulation, and Follicle Stimulating Hormone Receptor Expression Leading to Female Infertility. *Endocrinology* **153**, 2474-2485, doi:10.1210/en.2011-1969 (2012).

19 Rubel, C. A., Wu, S.-P., Lin, L., Wang, T., Lanz, R. B., Li, X., Kommagani, R., Franco, H. L., Camper, S. A., Tong, Q., Jeong, J.-W., Lydon, J. P. & DeMayo, F. J. A Gata2-Dependent Transcription Network Regulates Uterine Progesterone Responsiveness and Endometrial Function. *Cell reports* **17**, 1414-1425, doi:10.1016/j.celrep.2016.09.093 (2016).

20 Beato, M. & Vicent, G. P. A new role for an old player. *Transcription* **4**, 167-171, doi:10.4161/trns.25777 (2013).

21 Cooper, C., Vincett, D., Yan, Y., Hamedani, M. K., Myal, Y. & Leygue, E. Steroid receptor RNA activator bi-faceted genetic system: Heads or Tails? *Biochimie* **93**, 1973-1980, doi:https://doi.org/10.1016/j.biochi.2011.07.002 (2011).

22 Eoh, K. J., Paek, J., Kim, S. W., Kim, H. J., Lee, H. Y., Lee, S. K. & Kim, Y. T. Long non-coding RNA, steroid receptor RNA activator (SRA), induces tumor proliferation and invasion through the NOTCH pathway in cervical cancer cell lines. *Oncol Rep* **38**, 3481-3488, doi:10.3892/or.2017.6023 (2017).

23 Lin, K., Zhan, H., Ma, J., Xu, K., Wu, R., Zhou, C. & Lin, J. Silencing of SRA1 Regulates ER Expression and Attenuates the Growth of Stromal Cells in Ovarian Endometriosis. *Reproductive Sciences* **24**, 836-843, doi:10.1177/1933719116670036 (2017).

24 Li, Y., Zhao, W., Wang, H., Chen, C., Zhou, D., Li, S., Zhang, X., Zhao, H., Zhou, D. & Chen, B. Silencing of LncRNA steroid receptor RNA activator attenuates polycystic ovary syndrome in mice. *Biochimie* **157**, 48-56, doi:https://doi.org/10.1016/j.biochi.2018.10.021 (2019).

25 Lanz, R. B., Chua, S. S., Barron, N., Söder, B. M., DeMayo, F. & O'Malley, B. W. Steroid receptor RNA activator stimulates proliferation as well as apoptosis in vivo. *Molecular and cellular biology* **23**, 7163-7176 (2003).

26 Smith, C. M. & Steitz, J. A. Classification of gas5 as a multi-small-nucleolar-RNA (snoRNA) host gene and a member of the 5'-terminal oligopyrimidine gene family reveals common features of snoRNA host genes. *Molecular and cellular biology* **18**, 6897-6909 (1998).

27 Pickard, M. R. & Williams, G. T. Molecular and Cellular Mechanisms of Action of Tumour Suppressor GAS5 LncRNA. *Genes* **6**, 484-499 (2015).

28 Hudson, W. H., Pickard, M. R., de Vera, I. M., Kuiper, E. G., Mourtada-Maarabouni, M., Conn, G. L., Kojetin, D. J., Williams, G. T. & Ortlund, E. A. Conserved sequence-specific lincRNA-steroid receptor interactions drive transcriptional repression and direct cell fate. *Nat Commun* **5**, 5395, doi:10.1038/ncomms6395 (2014).

29 Kino, T., Hurt, D. E., Ichijo, T., Nader, N. & Chrousos, G. P. Noncoding RNA gas5 is a growth arrest- and starvation-associated repressor of the glucocorticoid receptor. *Sci Signal* **3**, 2000568 (2010).
30 Gebhardt, K. M., Feil, D. K., Dunning, K. R., Lane, M. & Russell, D. L. Human cumulus cell gene expression as a biomarker of pregnancy outcome after single embryo transfer. *Fertility and Sterility* **96**, 47-52.e42, doi:http://dx.doi.org/10.1016/j.fertnstert.2011.04.033 (2011).
31 Cheng, Y., Kim, J., Li, X. X. & Hsueh, A. J. Promotion of Ovarian Follicle Growth following mTOR Activation: Synergistic Effects of AKT Stimulators. *PLoS ONE* **10**, e0117769, doi:10.1371/journal.pone.0117769 (2015).
32 Lee, S.-E., Sun, S.-C., Choi, H.-Y., Uhm, S.-J. & Kim, N.-H. mTOR is required for asymmetric division through small GTPases in mouse oocytes. *Molecular reproduction and development* **79**, 356-366, doi:10.1002/mrd.22035 (2012).
33 Robles, V., Valcarce, D. G. & Riesco, M. F. Non-coding RNA regulation in reproduction: Their potential use as biomarkers. *Non-coding RNA Research* **4**, 54-62, doi:https://doi.org/10.1016/j.ncrna.2019.04.001 (2019).
34 Liu, K.-S., Li, T.-P., Ton, H., Mao, X.-D. & Chen, Y.-J. Advances of Long Noncoding RNAs-mediated Regulation in Reproduction. *Chin Med J (Engl)* **131**, 226-234, doi:10.4103/0366-6999.222337 (2018).
35 Schneider, C. A., Rasband, W. S. & Eliceiri, K. W. NIH Image to ImageJ: 25 years of image analysis. *Nature Methods* **9**, 671-675, doi:10.1038/nmeth.2089 (2012).
36 Karukurichi, K. R., Wang, L., Uzasci, L., Manlandro, C. M., Wang, Q. & Cole, P. A. Analysis of p300/CBP histone acetyltransferase regulation using circular permutation and semisynthesis. *J Am Chem Soc* **132**, 1222-1223, doi:10.1021/ja909466d (2010).
37 Falender, A. E., Lanz, R., Malenfant, D., Belanger, L. & Richards, J. S. Differential Expression of Steroidogenic Factor-1 and FTF/LRH-1 in the Rodent Ovary. *Endocrinology* **144**, 3598-3610, doi:10.1210/en.2002-0137 (2003).
38 Swift, J. & Coruzzi, G. M. A matter of time - How transient transcription factor interactions create dynamic gene regulatory networks. *Biochim Biophys Acta Gene Regul Mech* **1860**, 75-83, doi:10.1016/j.bbagrm.2016.08.007 (2017).
39 Martin, K. J. The interactions of transcription factors and their adaptors, coactivators and accessory proteins. *Bioessays* **13**, 499-503, doi:10.1002/bies.950131003 (1991).
40 York, B. & O'Malley, B. W. Steroid Receptor Coactivator (SRC) Family: Masters of Systems Biology. *Journal of Biological Chemistry* **285**, 38743-38750, doi:10.1074/jbc.R110.193367 (2010).
41 Yi, P., Wang, Z., Feng, Q., Chou, C. K., Pintilie, G. D., Shen, H., Foulds, C. E., Fan, G., Serysheva, I., Ludtke, S. J., Schmid, M. F., Hung, M. C., Chiu, W. & O'Malley, B. W. Structural and Functional Impacts of ER Coactivator Sequential Recruitment. *Mol Cell* **67**, 733-743 e734, doi:10.1016/j.molcel.2017.07.026 (2017).
42 Fru, K. N., VandeVoort, C. A. & Chaffin, C. L. Mineralocorticoid Synthesis During the Periovulatory Interval in Macaques1. *Biology of Reproduction* **75**, 568-574, doi:10.1095/biolreprod.106.053470 (2006).
43 Rae, M. T., Price, D., Harlow, C. R., Critchley, H. O. D. & Hillier, S. G. Glucocorticoid receptor-mediated regulation of MMP9 gene expression in human ovarian surface epithelial cells. *Fertility and Sterility* **92**, 703-708, doi:https://doi.org/10.1016/j.fertnstert.2008.06.040 (2009).
44 Walters, K. A., Middleton, L. J., Joseph, S. R., Hazra, R., Jimenez, M., Simanainen, U., Allan, C. M. & Handelsman, D. J. Targeted Loss of Androgen Receptor Signaling in Murine Granulosa Cells of Preantral and Antral Follicles Causes Female Subfertility1. *Biology of Reproduction* **87**, doi:10.1095/biolreprod.112.102012 (2012).

45 Lin, H., Xing, W., Li, Y., Xie, Y., Tang, X. & Zhang, Q. Downregulation of serum long noncoding RNA GAS5 may contribute to insulin resistance in PCOS patients. *Gynecological Endocrinology* **34**, 784-788 (2018).

46 Nakagawa, S., Shimada, M., Yanaka, K., Mito, M., Arai, T., Takahashi, E., Fujita, Y., Fujimori, T., Standaert, L., Marine, J.-C. & Hirose, T. The lncRNA Neat1 is required for corpus luteum formation and the establishment of pregnancy in a subpopulation of mice. *Development* **141**, 4618-4627, doi:10.1242/dev.110544 (2014).

47 Ernst, E. H., Nielsen, J., Ipsen, M. B., Villesen, P. & Lykke-Hartmann, K. Transcriptome Analysis of Long Non-coding RNAs and Genes Encoding Paraspeckle Proteins During Human Ovarian Follicle Development. *Frontiers in Cell and Developmental Biology* **6**, doi:10.3389/fcell.2018.00078 (2018).

48 Xu, X.-F., Li, J., Cao, Y.-X., Chen, D.-W., Zhang, Z.-G., He, X.-J., Ji, D.-M. & Chen, B.-L. Differential Expression of Long Noncoding RNAs in Human Cumulus Cells Related to Embryo Developmental Potential:A Microarray Analysis. *Reproductive Sciences* **22**, 672-678, doi:10.1177/1933719114561562 (2015).

49 Bouckenheimer, J., Fauque, P., Lecellier, C.-H., Bruno, C., Commes, T., Lemaître, J.-M., De Vos, J. & Assou, S. Differential long non-coding RNA expression profiles in human oocytes and cumulus cells. *Scientific Reports* **8**, 2202, doi:10.1038/s41598-018-20727-0 (2018).

CHAPTER 5 RUNX1 chromatin interaction in granulosa cells specialisation and regulation of follicle functions during pre- and peri-ovulation

5.1 INTRODUCTION

RUNX1 belongs to the RUNX transcription factor family together with two other members RUNX2 and RUNX3, all of which recognise the canonical RUNT sequence (5′-PuACCPuCA-3′) [1]. The transcriptional activity of RUNX transcription factors involves the formation of a heterodimer with CBFβ, which by itself does not directly interact with target DNA but can promote RUNX DNA binding efficiency. Traditionally known as an important tumorigenesis factor in acute myeloid leukaemia, members of the RUNX family are also involved in developmental processes in various organ systems, such as haematopoiesis in the liver and ossification of cartilage in skeletal formation [2,3]. Within the last 10 years, RUNX members have been shown to be expressed in the reproductive tract, indicating the potential role of RUNX in a range of female reproductive processes. RUNX1 in particular has been detected in both the ovary and uterus of rodents [4,5] as well as in human granulosa cells [6]. In the ovary, RUNX1 is present in granulosa cells during foetal development and at adulthood, where it plays different important roles in each context [4,5].

In the adult rat ovary, RUNX1 expression is induced by the LH surge and is upregulated during the peri-ovulatory window [4]. Studies in *in vitro* cultured rat granulosa cells have shown that RUNX1 expression is responsive to ovulatory cues, including stimulation by hCG, forskolin and phorbol myristate acetate [4]. RUNX1 ablation using siRNA in cultured goat granulosa cells leads to a decrease in progesterone and oestradiol production through downregulation of genes that are involved in progesterone synthesis [7]. RUNX1 also acts as a transcriptional regulator of other genes in granulosa cells, including *Mt1a, Hapln1* and *Rgcc*, through direct binding at their promoter sites, [4]. RUNX1 has been demonstrated to be vital for foetal development since global RUNX1 KO leads to foetal death [2]; and thus this mouse model cannot be used to investigate female fertility. However, a granulosa cell-specific KO model targeting CBFβ, the heterodimer partner of RUNX1, exhibited altered expression of ovulatory genes, ovulation

failure and subfertility in the female KO mice [8]. Of note, this phenotype is very similar to what observed in the PGRKO mouse model [9], albeit with lesser severity, suggesting a possible functional cooperation between RUNX1 (and other RUNX transcription factor) and PGR in the context of ovulation. Currently this concept has remained unexplored due to the lack of a fully-described RUNX1-dependent transcriptome in granulosa cells as well as the lack of an inducible tissue-specific RUNX1 KO animal model.

Apart from its role in ovulation, RUNX1 is also reported to be important in the feminisation of gonadal somatic cells in female foetuses. RUNX1 is highly upregulated specifically in the female gonad especially during early foetal development, which has been observed in multiple vertebrate species including human, suggesting a high level of conservation of RUNX1 function [10]. In mouse foetal gonads, RUNX1 colocalises with FOXL2, a transcription factor well-defined as a female-patterned determinant in granulosa cells [10]. Furthermore, RUNX1 and FOXL2 share many mutual target chromatin regions and downstream genes. Double RUNX1/FOXL2 KO female gonads express the Sertoli cell marker DMRT1 and show the development of testis cords, which does not fully manifest in single RUNX1 KO or FOXL2 KO female gonads. This suggests an important role of RUNX1, in conjunction with FOXL2, in driving the differentiation of bipotential somatic cells to granulosa cells.

Other members of the RUNX transcription family, namely RUNX2 and RUNX3, are also found to be expressed in the reproductive tract and involved in female fertility. Like RUNX1, RUNX2 is also upregulated in granulosa cells after the LH surge [11]. A cre-lox transgenic mouse model with complete ablation of CBFβ but only partial deletion of RUNX2 (CBFβ -/- RUNX2 +/-) shows reduced ovulation rate and sterility in female mice [8]. In peri-ovulatory granulosa cells, RUNX2 is responsible for the transcriptional regulation of genes important in ovulation, including *Ptgs2, Ptgds* and *Mmp13,* though direct binding at RUNT motifs in their promoter regions [11,12]. RUNX3, also expressed in the ovary, is involved in transcriptional regulation of inhibins and aromatase in granulosa cells; yet is not critical for ovulation, as shown in a global RUNX3 KO mouse model [13]. Instead RUNX3 appears to play a more vital role in regulating the gonadotrophin feedback loop through acting on kisspeptin neurons in the hypothalamus [13,14]. All three RUNX members have also been identified in mouse endometrial stromal cells and are involved in decidualisation and embryo implantation [5,15,16].

It is clear that RUNX1 plays various important roles in granulosa cells, from granulosa cell specialisation to ovulatory regulation. Because of this, studies on RUNX1 function in fertility in an *in vivo* context is made difficult due to potential confounding effects from the influence of RUNX1 on ovarian development. A granulosa cell- and ovulation-specific RUNX1 KO model would be crucial in revealing the specific role of RUNX1 in ovulation. Furthermore, as RUNX1 canonically acts as a transcription factor with important roles in development and function of several different tissues, it is likely that RUNX1 can target different chromatin regions in a context-specific manner to achieve specific roles. Thus, a full description of the RUNX1 cistrome in granulosa cells in different biological contexts is also necessary to determine the differentiation-dependent characteristics of RUNX1 chromatin binding properties. Thus, the primary aim of this chapter is to characterise the chromatin binding properties of RUNX1 in granulosa cells in different biological contexts. Granulosa cells were obtained from prenatal ovaries, where RUNX1 acts as a determinant for granulosa cell differentiation from the bipotential somatic cells, and from adult granulosa cells after eCG stimulation (pre-LH) or after eCG/hCG stimulation for 6 h (post-LH). The latter time point corresponds to the time when PGR ChIP-seq was performed and when RUNX1 expression is highest during the peri-ovulatory window. RUNX1 target chromatin regions were characterised to determine basal and time point-specific RUNX1/chromatin interactions. Specifically, the effect of the LH surge on RUNX1 cistrome was investigated in detail.

5.2 MATERIALS & METHODS

5.2.1 Animals

For peri-ovulatory granulosa cell experiments, CBAF1 mice were obtained from The University of Adelaide, Laboratory Animal Services. All mice were maintained in 12 h light /12 h dark conditions and given water and rodent chow *ad libitum*. All experiments were approved by The University of Adelaide Animal Ethics Committee and were conducted in accordance with the Australian Code of Practice for the Care and Use of Animals for Scientific Purposes (ethics no m/2015/075).

For foetal granulosa cell experiments, CD-1 mice were purchased from Charles River Laboratories (Wilmington, MA, USA) and maintained at the NIEHS Animal Facility as previously described [10].

5.2.2 Peri-ovulatory time course experiment

5.2.2.1 mRNA level quantification

COC/GC samples from CBAF1 female mice at different eCG/hCG stimulation time points were obtained and RNA extraction and cDNA synthesis were as described in section 2.2.2.2. RNA from COC/GC collected from one ovary per time point per replicate was used for cDNA synthesis and RT-qPCR. RT-qPCR was performed on *Runx1*, *Runx2*, *Runx3* and *Cbfb* as well as the housekeeper gene *Rpl19* using Taqman assays as listed in Appendix 1. Presentation of data and statistical analysis were as previously described in section 2.2.2.2.

5.2.2.2 Protein level quantification

Lysate from COC/GC pooled from ovaries of 3-5 mice per time point per replicate from the eCG/hCG time course was prepared as described in section 2.2.2.3. Western blot was performed on denatured lysate, with primary antibodies for RUNX1, RUNX2, CBFβ and H3 listed in Appendix 2. Protein quantification was as previously described in section 2.2.2.3.

5.2.3 ChIP-seq experiments

5.2.3.1 Adult mouse granulosa cell collection

Super-ovulation in 21-day old CBAF1 female mice was induced by injecting mice i.p with 5 IU eCG and 5 IU hCG 46 h post-eCG. Mice were killed by cervical dislocation and ovaries dissected at either 46 h post-eCG (termed RUNX1 0h) or after 46 h eCG plus 6 h -hCG (termed RUNX1 6h). Granulosa cells were collected from punctured ovaries, snap frozen in liquid nitrogen and shipped in liquid nitrogen to Active Motif (Carlsbad, CA, USA) for ChIP-seq. Two samples from at least 5 mice with a minimum of $1x10^7$ cells were used for RUNX1 ChIP. Details of this experiment are similar to as previously described in section 2.2.3.1. Briefly, cells were fixed, lysed, sonicated and precleared prior to immunoprecipitation. 20 µg of chromatin from each replicate was used for ChIP-seq with 10 µl RUNX1 antibody (provided by Dr Yoram Groner and Dr Ditsa Levanon [17], the Weizmann Institute of Science, Israel – Appendix 3). Bound chromatins were isolated and sequencing libraries were prepared for ChIP and input DNA. Sequencing was performed on Illumina's NextSeq 500 (75 nt reads, single end).

5.2.3.2 Foetal granulosa cells

ChIP-seq was performed on ovaries that were separated from the mesonephros of E14.5 CD-1 mouse embryos and snap frozen in liquid nitrogen (from now termed RUNX1 E14.5). Full details of the experiment can be found in the according publication [10]. Briefly, two independent ChIP-seq experiments were performed by Active Motif using 20-30 μg of sheared chromatin from pooled embryonic ovaries (100-120 ovaries per ChIP) and 10 μl of RUNX1 antibody. ChIP-seq libraries were sequenced as single-end 75-mers by Illumina NextSeq 500, then filtered to retain only reads with average base quality score > 20.

5.2.3.3 Bioinformatics analysis

Bioinformatics analysis was conducted using appropriate tools as described in section 2.2.3.2. Quality check of sequencing data for all samples showed no warnings. For consensus peak selection of RUNX1 6h data, as the two replicates showed good correlation, peaks were called individually for each replicate. For RUNX1 0h and RUNX1 E14.5 data, as quality control showed variation between the two replicates, reads were combined for both replicates and for input controls from both replicates using samtools [18]. Peak calling from read count against input was as previously described. Initial analysis showed a high level of overlap between replicates from RUNX1 6h samples, with the majority (99.1%) of peaks called in replicate 2 also identifiable in replicate 1, thus the overlapped peaks identified via ChIPpeakAnno [19] package were used as the consensus data. Downstream analysis of peaks was as previously described in section 2.2.3.2. For the identification of the RUNT motif map on the whole mouse genome, the corresponding position weight matrix was obtained from the HOMER Motif Database (Table 5.1) and mapping was conducted using the MEME Suite. Enriched motif analysis was as previously described in section 2.2.3.2. RUNX1 E14.5 ChIP-seq data is publicly available and can be accessed from the GEO Database (GEO accession number GSE128767).

Table 5.1 Position weight matrix for the RUNT motif HOMER Motif Database that was used for the identification of the motif map.

Each row corresponds to a nucleotide in the consensus sequence and each column corresponds to nucleotide A, C, G or T. The number represents the probability of each nucleotide to be present at that position.

```
ALPHABET= ACGT

strands: + -

Background letter frequencies (from unknown source):
A 0.250 C 0.250 G 0.250 T 0.250

MOTIF 1 HAACCACADV

letter-probability matrix: alength= 4 w= 10 nsites= 1 E= 0e+0
0.574000 0.159000 0.031000 0.236000
0.895000 0.001000 0.103000 0.001000
0.870000 0.029000 0.100000 0.001000
0.001000 0.997000 0.001000 0.001000
0.001000 0.997000 0.001000 0.001000
0.885000 0.001000 0.066000 0.048000
0.001000 0.997000 0.001000 0.001000
0.913000 0.057000 0.001000 0.029000
0.398000 0.067000 0.339000 0.196000
0.359640 0.355644 0.161838 0.122877
```

5.3 RESULTS

5.3.1 RUNX transcription factors are induced in granulosa cells during ovulation

Since each of the RUNX family members (*Runx1*, *Runx2* and *Runx3*) have been shown to play a role in the ovary, the temporal pattern of expression of all three RUNX mRNA transcripts and proteins, plus their dimerising partner CBFβ, was examined in granulosa cells through RT-qPCR and Western blot. Among the three RUNX transcription factors, only RUNX1 and RUNX2 showed significant upregulation during the peri-ovulatory window. For RUNX1, the mRNA and protein levels were low but detectable in granulosa cells from unstimulated and 0h-hCG granulosa cells but were rapidly induced (20-40 fold respectively) within 4 h and peaking 6 h post-hCG (Figure 5.1A). *Runx2* mRNA was also induced up to 600-fold and reached highest level at 8 h post-hCG, however RUNX2 protein level was induced by 6 h and continued

to rise, reaching 60-fold over unstimulated granulosa cell level by 12 h post-hCG (Figure 5.1B). *Runx3* was not significantly upregulated in response to hCG (Figure 5.1C) and thus protein expression was not investigated. The mRNA expression of *Cbfb*, the dimerising partner for RUNX proteins, was only slightly upregulated during the peri-ovulatory window however protein levels were more dramatically induced by hCG (Figure 5.1D).

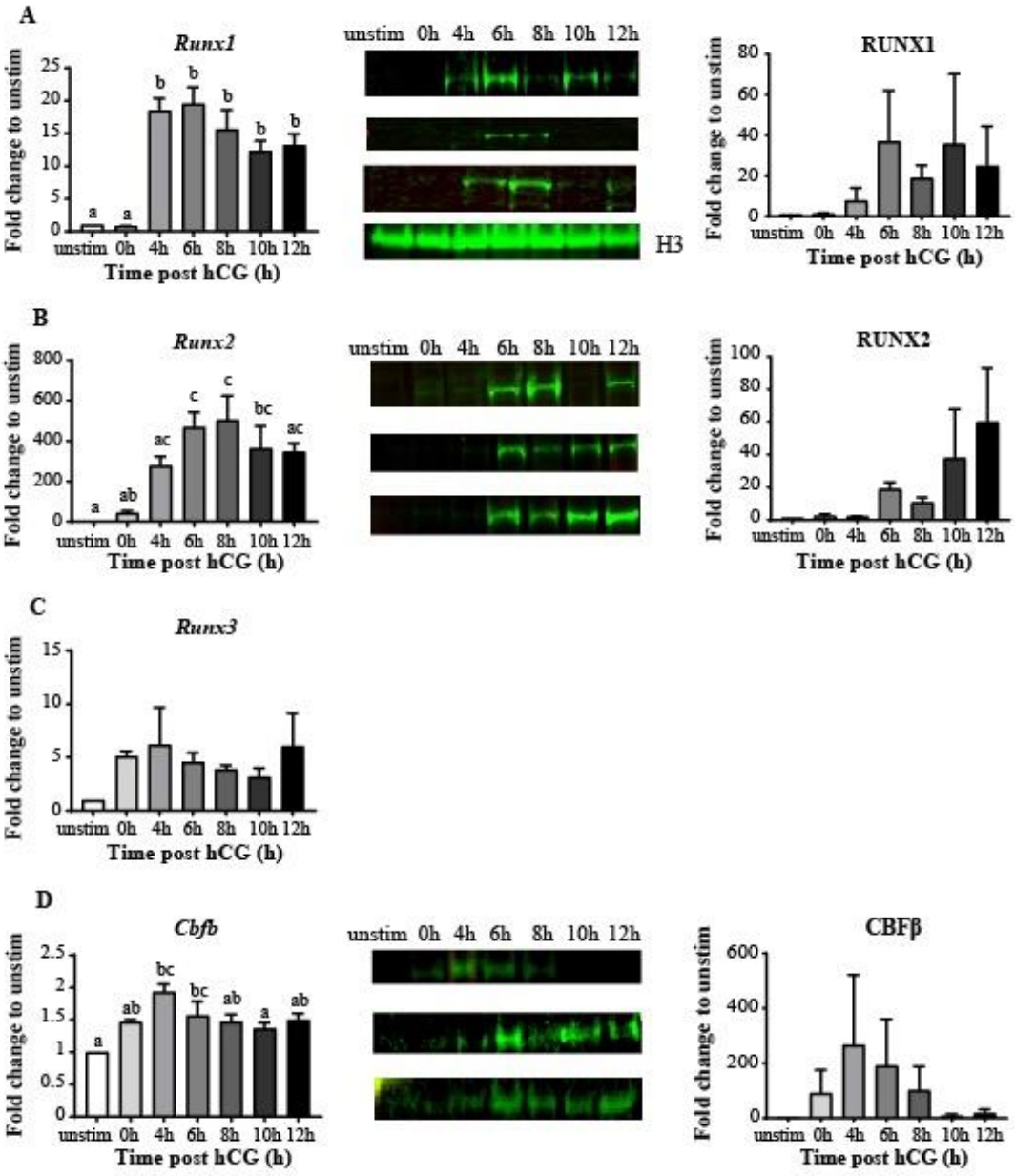
A
Runx1
Fold change to unstim
Time post hCG (h)
unstim 0h 4h 6h 8h 10h 12h
H3
RUNX1
B
Runx2
RUNX2
C
Runx3
D
Cbfb
CBFβ

Figure 5.1 RUNX / CBFβ mRNA and protein are induced by the LH surge in granulosa cells.

Expression of RUNX1 (A), RUNX2 (B), RUNX3 (C) and CBFβ (D) was determined through RT-qPCR quantification of mRNA (left panel), Western blot (middle panel) and protein quantification (right panel). For mRNA expression, RT-qPCR was performed on granulosa cells obtained either without eCG or hCG (unstim) or eCG + hCG 0-12 h stimulation. Fold change is displayed as normalised to the housekeeping *Rpl19* gene and relative to the unstim sample. N = 3 biological replicates, each replicate is from 3-5 mice per time point. Statistical significance was determined through one-way ANOVA with multiple comparison, $p < 0.0001$ (*Runx1*), $p = 0.0011$ (*Runx2*), $p = 0.4742$ (*Runx3*), $p = 0.0039$ *(Cbfb)*. Bars with different superscripts are significantly different. For Western blot, granulosa cells from ovaries treated in the same way were used, with n = 3 biological replicates and each replicate consisting of ovaries from 3-5 mice per time point. Quantification of Western intensity is displayed as fold change normalised to the housekeeping nuclear protein H3 and relative to unstim. Statistical analysis was through one-way ANOVA with multiple comparison.

5.3.2 Characteristics of RUNX1 cistromes in granulosa cells in different developmental contexts

5.3.2.1 Assessing robustness and selection of consensus RUNX1 binding sites

The induction of RUNX1 protein in granulosa cells peaked at 6 h post-hCG suggests that RUNX1 activity would be the highest at this time point; this coincides with the peak PGR protein abundance and thus was chosen for ChIP-seq analysis. This time point also allowed for compatible comparison with the existing PGR and H3K27ac ChIP-seq datasets. To investigate the chromatin binding properties of RUNX1 in response to the LH surge, RUNX1 ChIP-seq was performed on eCG-stimulated mouse granulosa cells with and without further hCG treatment (termed RUNX1 6h and RUNX1 0h respectively). RUNX1 is not only present in adult granulosa cells but is also expressed in foetal granulosa cells and has demonstrated important roles in the female-oriented differentiation of supporting cells in the ovary. To determine whether the characteristics of RUNX1 cistrome are conserved through different developmental stages, the RUNX1 cistrome in foetal granulosa cells was also examined (referred to as RUNX1 E14.5). Two biological replicates from foetal ovary pools were used for ChIP-seq with a separate input control for each replicate [10]. For all three sample groups, the sequencing quality control for each replicate and input control was conducted using the FASTQC package in R prior to analysis, which showed no major inconsistency.

To confirm the robustness of RUNX1 ChIP-seq, the reproducibility of each pair of replicates was assessed using IDR and correlation parameters. The two biological replicates of RUNX1 0h displayed a higher level of variation, shown in the number of peaks passing IDR correlation criteria and the Pearson correlation coefficient value (correlation coefficient = 0.93) (Appendix 11A). The pattern of RUNX1 0h binding sites between replicates were comparable to one another, despite a difference in the total number of peaks per replicate, with 854 peaks shared between the two replicates (or 90.18% of replicate 1 and 27.25% of replicate 2. The high concordance of replicate 1 with replicate 2 and higher number of peaks in replicate 2 indicate that the variation was likely due to a lower ChIP-seq efficiency in replicate 1, hence in order to mitigate the potential for false negatives (i.e. actual RUNX1 binding sites not represented in this dataset) the two replicates were combined for peak calling and the resulting combined 2383 peaks were considered to be consensus RUNX1 binding sites in RUNX1 0h.

As seen previously with PGR ChIP-seq, IDR analysis of 6h RUNX1 showed a correlation pattern of peaks identified in high-quality ChIP-seq data, such as good consistency in peak ranking between the two replicates and a pronounced inflection in the IDR curve (Appendix 11B). The two replicates were highly correlated, as seen in the overall pattern of RUNX1 binding and the Pearson correlation coefficient test (correlation coefficient = 0.96). In total, 28671 binding sites were identified in replicate 1 and 18761 binding sites were in replicate 2. Global comparison showed that the majority of binding sites in replicate 2 was in common with replicate 1 (accounting for 18594 binding sites, or 64.85% of replicate 1 and 99.11% of replicate 2). The shared 18594 sites between the two replicates represented the highest confidence set of binding sites and were thus chosen as the RUNX1 6h dataset for subsequent analyses.

While there was correlation between the two RUNX1 E14.5 replicates, peak ranking exhibited less consistency between two replicates (Appendix 11C). Furthermore, while the peak pattern from both replicates showed a strong inclination for TSS binding, there was a slight shift in peak summit between the two replicates and there was also a slightly weaker correlation between the two replicates than previously seen in other ChIP-seq replicates (Pearson correlation coefficient = 0.92). In total, there was a 3-fold difference in the number of identified peaks between the two replicates (1561 and 4941 peaks in replicate 1 and 2 respectively), with 1028 peaks shared between the two replicates (65% of replicate 1 and 20% of replicate 2). All of this indicates a moderate difference between the two biological replicates, which from experience is commonly observed in pooled embryonic samples. Again, in order to mitigate the potential for false negatives, reads from both replicates were combined and peaks called from the pooled reads were treated as the consensus RUNX1 binding site list. By combining the two replicates 6538 peaks were identified. The high overlap among each of the RUNX1 ChIP-Seq datasets in subsequent analysis suggests that false positives are rare in the datasets.

5.3.2.2 Mutual and context-specific RUNX1 binding sites in granulosa cells

RUNX1 ChIP-seq from adult (RUNX1 6h, RUNX1 0h) and foetal (RUNX1 E14.5) granulosa cells were comparatively analysed. PCA analysis of the three read coverage datasets showed two distinct clusters, with RUNX1 0h and RUNX1 E14.5 grouping together away from RUNX1 6h (Figure 5.2A). This was confirmed with a correlation matrix which showed that there was a higher correlation between RUNX1 0h and RUNX1 E14.5 (Pearson correlation

coefficient = 0.88), which was greater than the correlation between either dataset to RUNX1 6h (Figure 5.2B). However, regardless of the biological context, RUNX1 peaks in both adult and foetal granulosa cells congregated in close proximity to the TSS (Figure 5.2C).

Among the 18504 binding sites in post-hCG granulosa cells 5128 sites were shared with foetal granulosa cells (78% of total foetal binding sites or 28% of total RUNX1 6h sites) (Figure 5.2D). 1169 binding sites (or 49% and 18% of total RUNX1 0h and RUNX1 E14.5 binding sites respectively) were shared between RUNX1 0h and RUNX1 E14.5. Interestingly, 1161 of 1169 sites were also shared with RUNX1 6h, indicating that not only was there a basal maintenance level of RUNX1 chromatin binding in granulosa cells but also a large number of inducible RUNX1 binding events that are conserved in different developmental contexts.

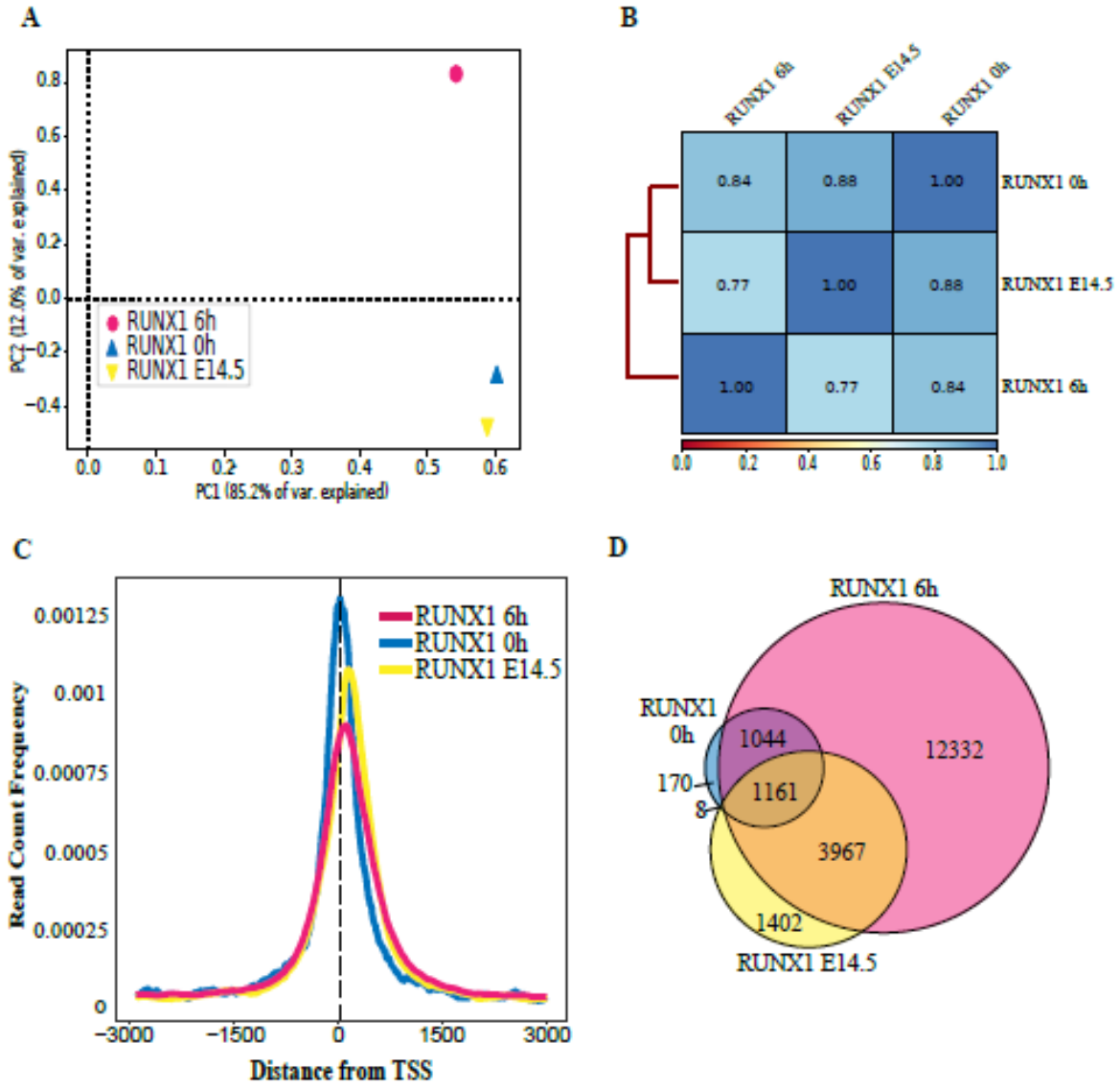

Figure 5.2 Correlation between RUNX1 binding sites in different biological contexts

(A) Principle component analysis (PCA) of RUNX1 ChIP-seq in E14.5 ovary or granulosa cells from eCG + HCG 0 h or 6 h. **(B)** Pearson correlation coefficient between RUNX1 0 h, RUNX1 6 h and RUNX1 E14.5 datasets. The correlation in genomic coverage between all datasets was analysed and organised in hierarchical order. **(C)** Read count frequency of RUNX1 0 h, RUNX1 6 h and RUNX1 E14.5 ChIP-seq peaks in relation to the TSS. **(D)** Venn diagram showing the peak count for RUNX1 6h, RUNX1 0h and RUNX1 E14.5 cistrome.

5.3.2.3 RUNX1 regulates different pathways in a context-specific manner

Figure 5.2D shows that RUNX1 targets different subsets of chromatin regions depending on the biological context in granulosa cells. To explore the context-specific roles of RUNX1 activity, RUNX1 binding sites from the three datasets were divided into further subcategories of interest based on the timing of RUNX1 occupancy: foetal-specific (binding sites found only in RUNX1 E14.5), constitutive (binding sites found in all three contexts), adult-specific (binding sites found only in RUNX1 6h and RUNX 0h), LH-specific (binding sites found only in RUNX1 6h) (Figure 5.3A-D). An example of chromatin binding pattern was shown for each subcategory, which showed context-specific RUNX1 binding events.

In foetal-specific RUNX1 binding sites (Figure 5.3A), there was a strong enrichment for binding at promoters (73% occupancy in proximal promoter regions), especially within 1 kb upstream from a TSS. A similar pattern was also observed in constitutively bound sites, with more than 85% binding sites being enriched in promoter regions (Figure 5.3B). In RUNX1 binding sites found in adult granulosa cells, this pattern was not as strong: 30% of adult-specific RUNX1 sites were present within 3 kb of TSS (Figure 5.3C) and more than half of hCG-induced sites occupied promoters (Figure 5.3D). This showed that in biological contexts where RUNX1 is functionally active, such as in foetal granulosa cells or in peri-ovulatory granulosa cells, RUNX1 binding is purposely promoter-centric and is likely involved directly in transcriptional regulation.

To explore the consequences of RUNX1 on specific biological pathway regulation, Gene Ontology enrichment of each subcategory was examined. Common biological pathways enriched in all four datasets mostly belonged to normal cellular functions, such as metabolism, gene expression regulation and cellular response to external stimuli pathways. Between foetal- and adult-patterned binding sites, an enrichment of different groups of pathways was observed. In the foetal-specific RUNX1 cistrome, pathways that were important in developmental processes, including differentiation and embryonic development, were highly abundant (Figure 5.3A); however, in adult-patterned cistromes RUNX1 binding sites were associated more with cell cycle/apoptosis and cellular organisation (Figure 5.3B-D).

The impact of RUNX1 binding in adult granulosa cells on gene expression regulation during ovulation was confirmed by comparison between RUNX1-bound genes and the set of genes

regulated by an ovulatory stimulus (DEGs in granulosa cells 0h vs 8h hCG-stimulation identified through RNA-seq) (Figure 5.3E). RUNX1 interaction at ovulatory genes were largely LH-specific and not from constitutive RUNX1 binding (790 DEGs to 74 DEGs, respectively), suggesting that *de novo* RUNX1 binding specifically induced due to the LH surge is highly functionally important to the resultant gene expression changes. However, there were also 74 DEGs that were found with RUNX1 binding in all biological context and 45 DEGs with RUNX1 binding at both 0h and 6h post-hCG, indicating that the maintenance of basal RUNX1 chromatin binding may also play a part in gene regulation during ovulation. Remarkably RUNX1-bound genes constituted more than one-third of all identified ovulatory DEGs, which further confirmed the importance of RUNX1 binding on consequential gene regulation during ovulation.

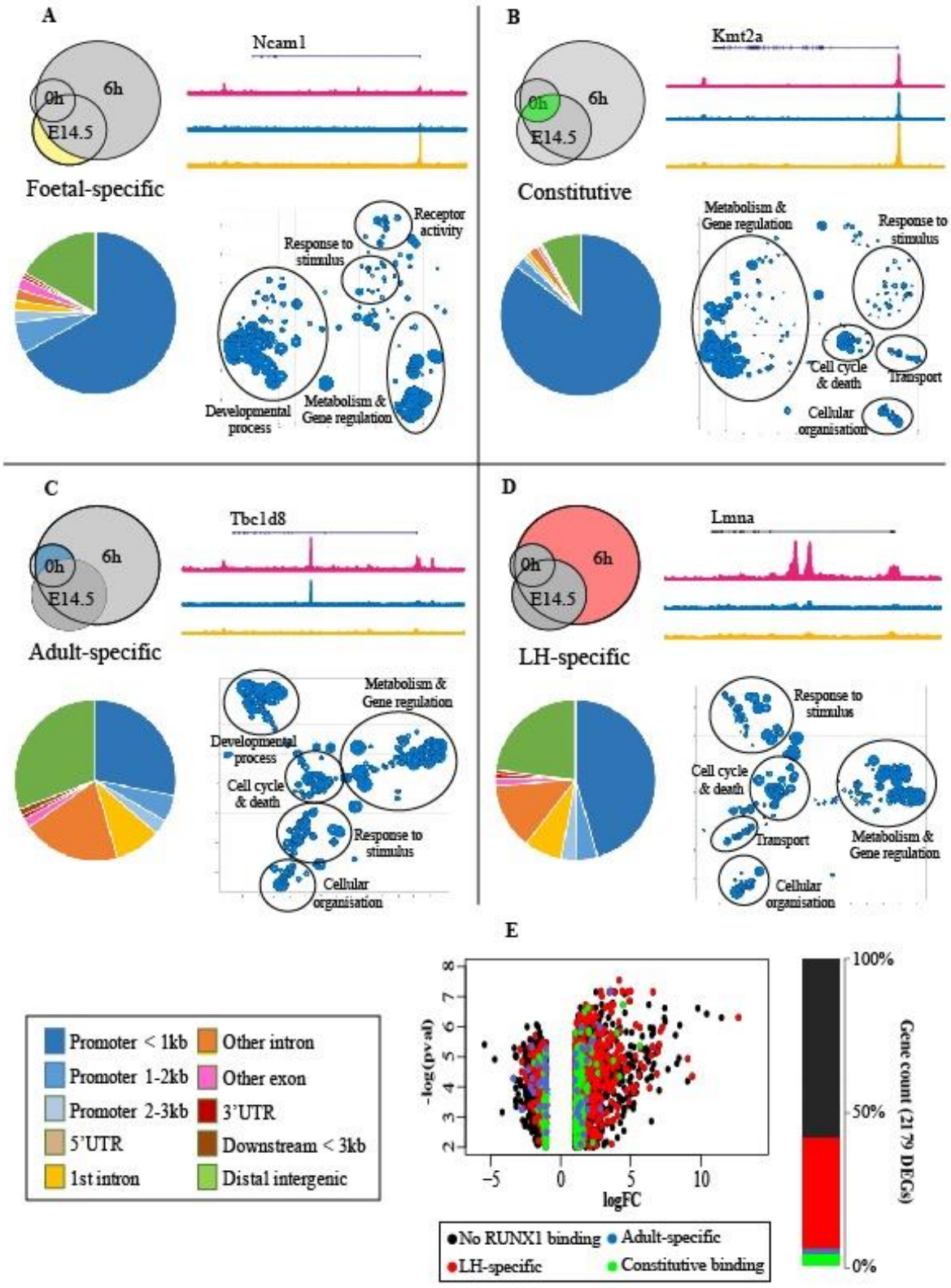
A
Ncam1
0h
6h
E14.5
Foetal-specific
Receptor activity
Response to stimulus
Developmental process
Metabolism & Gene regulation
B
Kmt2a
0h
6h
E14.5
Constitutive
Metabolism & Gene regulation
Response to stimulus
Cell cycle & death
Transport
Cellular organisation
C
Tbc1d8
0h
6h
E14.5
Adult-specific
Metabolism & Gene regulation
Developmental process
Cell cycle & death
Response to stimulus
Cellular organisation
D
Lmna
0h
6h
E14.5
LH-specific
Response to stimulus
Cell cycle & death
Transport
Metabolism & Gene regulation
Cellular organisation
E
Promoter < 1kb
Promoter 1-2kb
Promoter 2-3kb
5'UTR
1st intron
Other intron
Other exon
3'UTR
Downstream < 3kb
Distal intergenic
-log(pval)
logFC
No RUNX1 binding
Adult-specific
LH-specific
Constitutive binding
100%
50%
0%
Gene count (2179 DEGs)

Figure 5.3 Gene categories associated with RUNX1 binding throughout ovarian folliculogenesis.

(A-D) Subcategories of RUNX1 ChIP-seq datasets divided into groups according to the presence of peaks unique to early granulosa cell differentiation E14.5 (A), constitutively present at all developmental stages (B), adult-specific (C) or LH-specific (D). In panels A-D clockwise from top left corner: Venn diagram with coloured areas illustrating the subcategory of RUNX1-bound peaks. Example genes with RUNX1 peaks in E14.5 ovaries (yellow), in granulosa cells after eCG stimulation (blue) or hCG (pink). Gene ontological terms enriched in each subcategory of RUNX1 bound genes showing major clusters of ontological terms (circled and labelled accordingly). Distribution of peaks among genomic features including promoters (< 1 kb, 1-2 kb and 2-3 kb), 5' UTR, 1st intron, other introns, exons, 3' UTR and downstream of TES (within 3 kb). Peaks that are not in these features are classified as distal intergenic. **(E)** Volcano plot of all ovulatory DEGs with RUNX1 binding. DEGs were identified through RNA-seq comparison of granulosa cells following eCG only vs eCG + hCG 8 h stimulation. DEGs that met statistical criteria ($|\log FC| \geq 1$ and $-\log(\text{p-value}) \geq 2$) are graphed. DEGs with no RUNX1 binding at any stage are in black, with LH-induced RUNX1 binding in red, with adult-patterned RUNX1 binding in blue and constitutive RUNX1 binding in green. Gene counts for each fraction are summarised in stacked bar chart.

5.3.2.4 RUNX1 binds to different motifs in foetal and adult granulosa cells

RUNX1 canonically binds to the RUNT motif. The global RUNT motif was mapped in the mouse genome, of which there were 41840 loci. To determine the level of RUNX1 coverage on the canonical RUNT map, RUNX1 binding sites in the three different granulosa cell contexts were compared against global RUNT loci. In adult granulosa cells, 431 of RUNX1 6h and 70 of RUNX1 0h binding sites were found to be at a RUNT locus, with 54 sites shared between the two time points (Figure 5.4A), indicating that there was an increase in RUNX1-RUNT binding after the LH surge. In foetal granulosa cells, 73 binding peaks were located at a RUNT locus, with the majority of these RUNT loci also found in the RUNX1 6h dataset.

While RUNX1 in both adult and foetal granulosa cells bound to the consensus RUNT motif, a large number of RUNX1 peaks were not found to be located a canonical RUNT site. Furthermore, as RUNX1 clearly had different roles and targeted different genomic regions in different biological contexts, it was hypothesised that RUNX1 also interacted with different non-canonical motifs in adult versus foetal granulosa cells. To investigate this, enriched motif analysis was performed on RUNX1 peaks that were adult-specific (found only in RUNX1 6h and RUNX1 0h), shared (found in all three biological contexts) or foetal-specific (Figure 5.4B). In all three groups, the canonical RUNT motif was the most highly enriched (3.8- to 5.6-fold over background). In adult-specific binding sites, a number of non-canonical motifs were identified, including motifs for NR5A2, PRE/NR3C, GATA and JUN/FOS families. Each of these were also previously found enriched at PGR ChIP-seq binding sites. In foetal-specific RUNX1 peaks however, such motifs were not highly enriched or were not at all identified; instead motifs such as that for CTCF, HMG and Homeobox transcription factor families were found. This suggests potential different transcription factor partners to RUNX1 in adult and foetal granulosa cells.

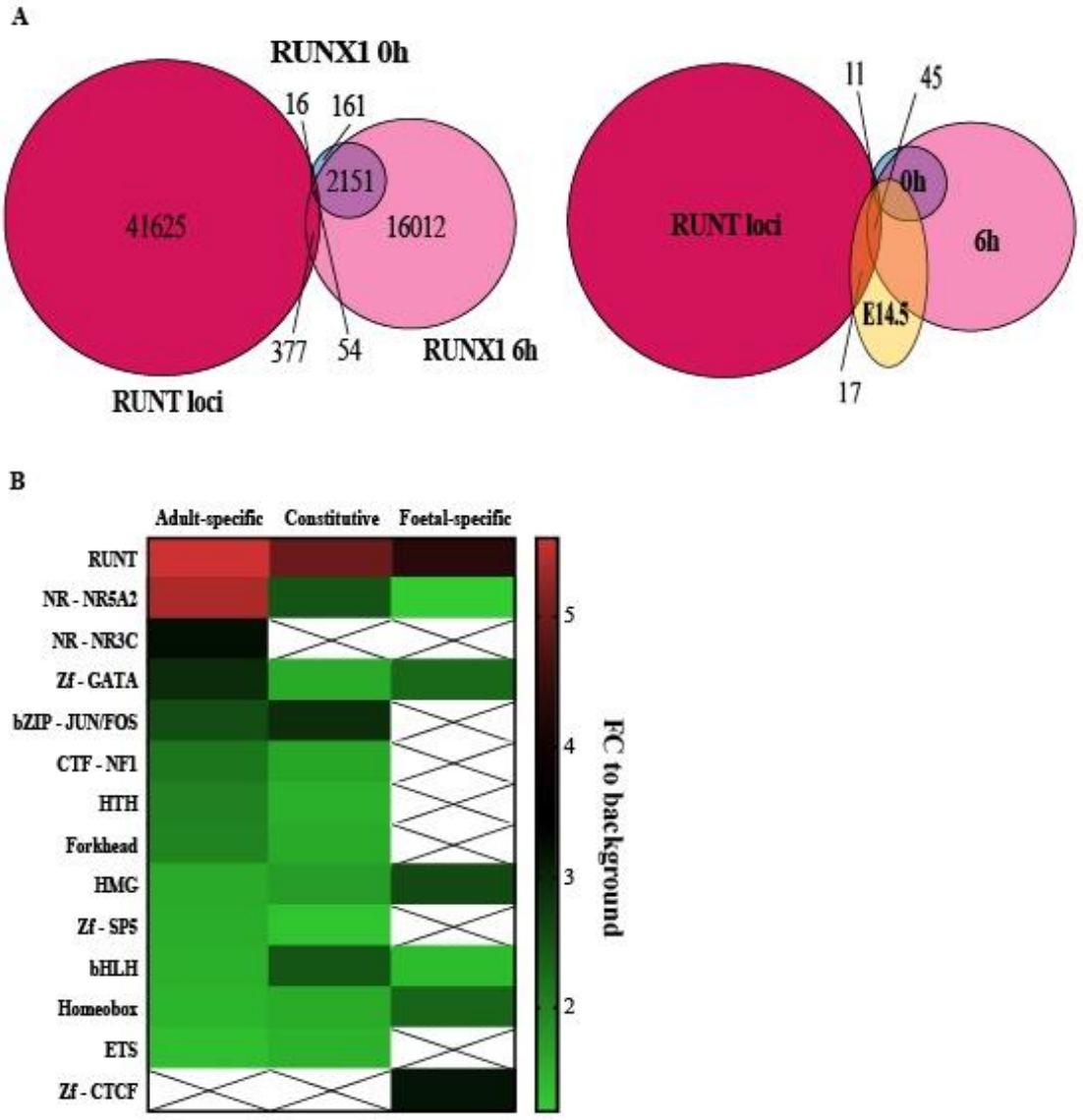

Figure 5.4 Identity of context-specific RUNX1-binding motifs.

(A) Venn diagram showing overlap of all RUNT loci within the mouse genome sequence (red) with RUNX1-bound peaks in eCG only (RUNX1 0 h – blue) or eCG + hCG 6 h (RUNX1 6h – pink), with additional RUNX1 E14.5 ChIP-seq overlay (orange). **(B)** Top most common known motifs found to be enriched at RUNX1 binding sites, displayed as heatmap of fold enrichment over background. From left to right: adult-specific, adult-foetal constitutive and foetal-specific binding sites. Heatmap colours indicate fold enrichment of motif at peaks and crossed blank cells mean the motif was not enriched in the dataset.

5.3.3 Distinct RUNX1 cistromes in granulosa cells in response to the LH surge

5.3.3.1 RUNX1 preferably binds transcriptionally active promoters before and after the LH surge

There were significant differences in adult versus foetal-patterned RUNX1 binding preferences and a large induction of RUNX1 regulatory activity in adult granulosa cells in response to the LH surge. To dissect the specificity of RUNX1 activity during the peri-ovulatory period, RUNX1 cistromes before and after hCG stimulation were examined alongside the active chromatin marker H3K27ac in 6 h hCG granulosa cells. As expected, the hierarchical relationship between datasets showed that there was a considerably higher level of correlation between RUNX1 6h and H3K27ac cistrome than between RUNX1 0h and H3K27ac (Pearson correlation coefficient = 0.78 and 0.62, respectively) (Figure 5.5A). Indeed, this was confirmed through a global comparison between binding sites for RUNX1 at the two time points, which showed a high level of overlapping (2205 peaks, accounting for 11.86% of RUNX1 6h and 92.53% of RUNX1 0h peaks) (Figure 5.5B). Among the 2205 shared sites, 87% were also found to overlap with H3K27ac sites, suggesting that there was a basal level of RUNX1 occupancy at potential open chromatin sites prior to the LH surge; however this was markedly increased after the LH surge, with three-quarters of total RUNX1 6h peaks overlapped with H3K27ac peaks (13745 out of 18594 peaks). Analysis of the genomic distribution of RUNX1 ChIP-seq at transcriptionally active sites showed that promoter occupancy was highly enriched at RUNX1 peaks regardless of the time point, showing that even prior to the LH surge RUNX1 has the potential to target transcriptionally active promoters (Figure 5.5C). An example of LH-induced RUNX1 binding can be seen in the promoter region of *Adamts1* where prominent the RUNX1 peak was seen only in RUNX1 6h (Figure 5.5D). Furthermore, when binding sites were divided into shared and time point-specific subsets, the overall binding patterns of data subsets showed prominent RUNX1 6h binding signals compared to RUNX1 0h, especially at shared peaks. As seen previously, the majority of peaks were specific to RUNX1 6h and even among shared binding sites, peak intensity was on average higher in RUNX1 6h compared to RUNX1 0h (Figure 5.5E-F). Detailed analysis of the genomic distribution of each subset confirmed the previous observation of promoter binding preference, with a slight increase seen in shared peaks (Figure 5.5G).

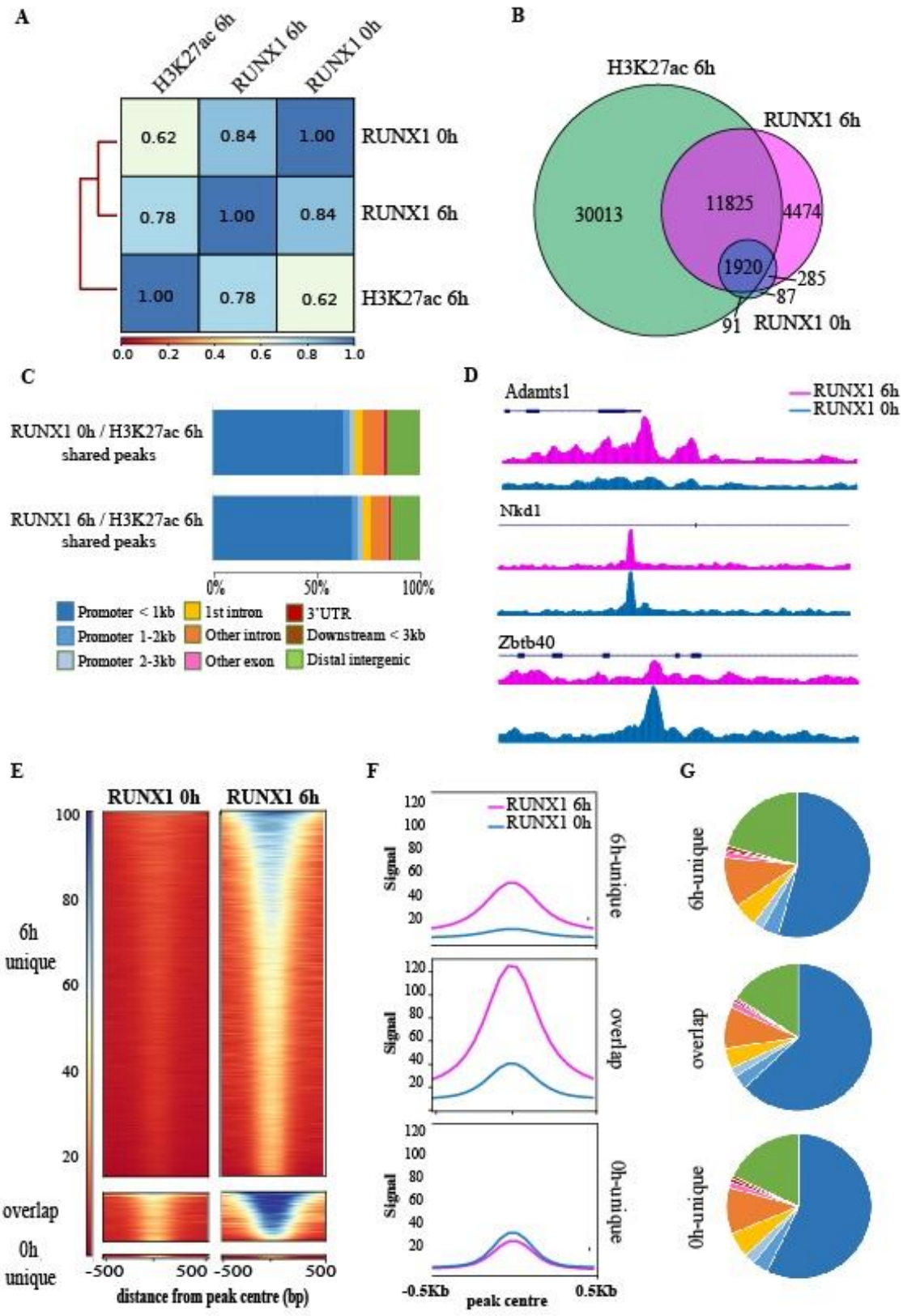
A
H3K27ac 6h
RUNX1 6h
RUNX1 0h
0.62
0.84
1.00
0.78
1.00
0.84
1.00
0.78
0.62
0.0 0.2 0.4 0.6 0.8 1.0
B
H3K27ac 6h
RUNX1 6h
RUNX1 0h
30013
11825
4474
1920
285
87
91
C
RUNX1 0h / H3K27ac 6h shared peaks
RUNX1 6h / H3K27ac 6h shared peaks
0%
50%
100%
Promoter < 1kb
Promoter 1-2kb
Promoter 2-3kb
1st intron
Other intron
Other exon
3'UTR
Downstream < 3kb
Distal intergenic
D
Adamts1
Nkd1
Zbtb40
RUNX1 6h
RUNX1 0h
E
RUNX1 0h
RUNX1 6h
6h unique
overlap
0h unique
-500
500
distance from peak centre (bp)
F
RUNX1 6h
RUNX1 0h
Signal
6h-unique
overlap
0h-unique
-0.5Kb
peak centre
0.5Kb
G
6h-unique
overlap
0h-unique

Figure 5.5 LH-dependent RUNX1 chromatin binding properties.

(A) Pearson correlation coefficient comparisons of the RUNX1 cistromes in granulosa cells at eCG (RUNX1 0h) or 6 h (RUNX1 6h) versus H3K27ac ChIP-seq peaks after hCG 6 h. The correlation in genomic coverage between all datasets was analysed and organised in hierarchical order. **(B)** Venn diagram showing shared and factor-unique peak counts for RUNX1 6h, RUNX1 0h and H3K27ac cistromes. **(C)** Genome distribution of the overlapped RUNX1 0h/H3K27ac and RUNX1 6h/H3K27ac binding sites. Genomic features include promoters (< 1 kb, 1-2 kb and 2-3 kb), 5' UTR, 1st intron, other introns, exons, 3' UTR and downstream of TES (within 3 kb). Peaks that are not in these features are classified as distal intergenic. **(D)** Examples of context-specific RUNX1 binding sites in the genome, showing loci with binding specifically at 6h post-hCG (top), 0h post-hCG (bottom) and at both time points (middle). Binding intensity of RUNX1 6h is displayed in pink and RUNX1 0h in blue. **(E)** Heatmap of RUNX1 read frequency and visualisation of the pattern of signal intensity **(F)**, divided into peaks specific to hCG treatment (6h unique), shared (overlap) and eCG only (0h unique) subgroups. Read intensity is displayed in relation to peak centre and the flanking 500 bp region. **(G)** Genomic distribution of 6h-specific (top), shared (middle) or 0h-specific (bottom) RUNX1 binding sites. Genomic features are as in (C).

5.3.3.2 RUNX1 interacts with RUNT as well as non-canonical sequence motifs

Not all RUNX1 binding in granulosa cells occurs at a canonical RUNT loci. To identify all sequences recognised by RUNX1 in adult granulosa cells, motif enrichment analysis was performed on RUNX1 0h and RUNX1 6h datasets (Figure 5.6A). As expected, the canonical RUNT motif was highly enriched in RUNX1 ChIP-seq in both 0 h and 6 h hCG-treated granulosa cells (5.3- and 3.5-fold enrichment to background, respectively). A number of non-canonical motifs also showed enrichment in the RUNX1 cistromes. For example, apart from the canonical RUNT motif, in pre-LH granulosa cells RUNX1 preferably bound motifs for NR5A2 (3.7-fold) and GATA (3-fold), whereas post-LH RUNX1 most strongly bound to the bZIP (JUN/FOS) motif (4.2-fold enrichment). Other motifs, such as that for CEBP and PRE/NR3C motifs were also enriched in both datasets. A similar hierarchy of motifs enriched in the RUNX1 6h dataset was found at RUNX1 6h binding sites at ovulatory DEGs identified via RNA-seq, in which the motif for JUN/FOS was the most highly enriched (5.4-fold enriched), following by RUNT (4-fold) and NR5A2 (3.3-fold). HOMER *de novo* motif analysis supported this result by identifying enriched sequences in ChIP-seq peaks that corresponded to the same transcription factor families, as well as other motifs, such as that similar to the ETS and CCAAT motifs (Figure 5.6B). Overall, RUNX1 was shown to interact with the RUNT motif as well as non-canonical DNA motifs, suggesting an interaction between RUNX1 and other transcriptional modulators, possibly as a pioneer factor to other ovulatory transcription factors.

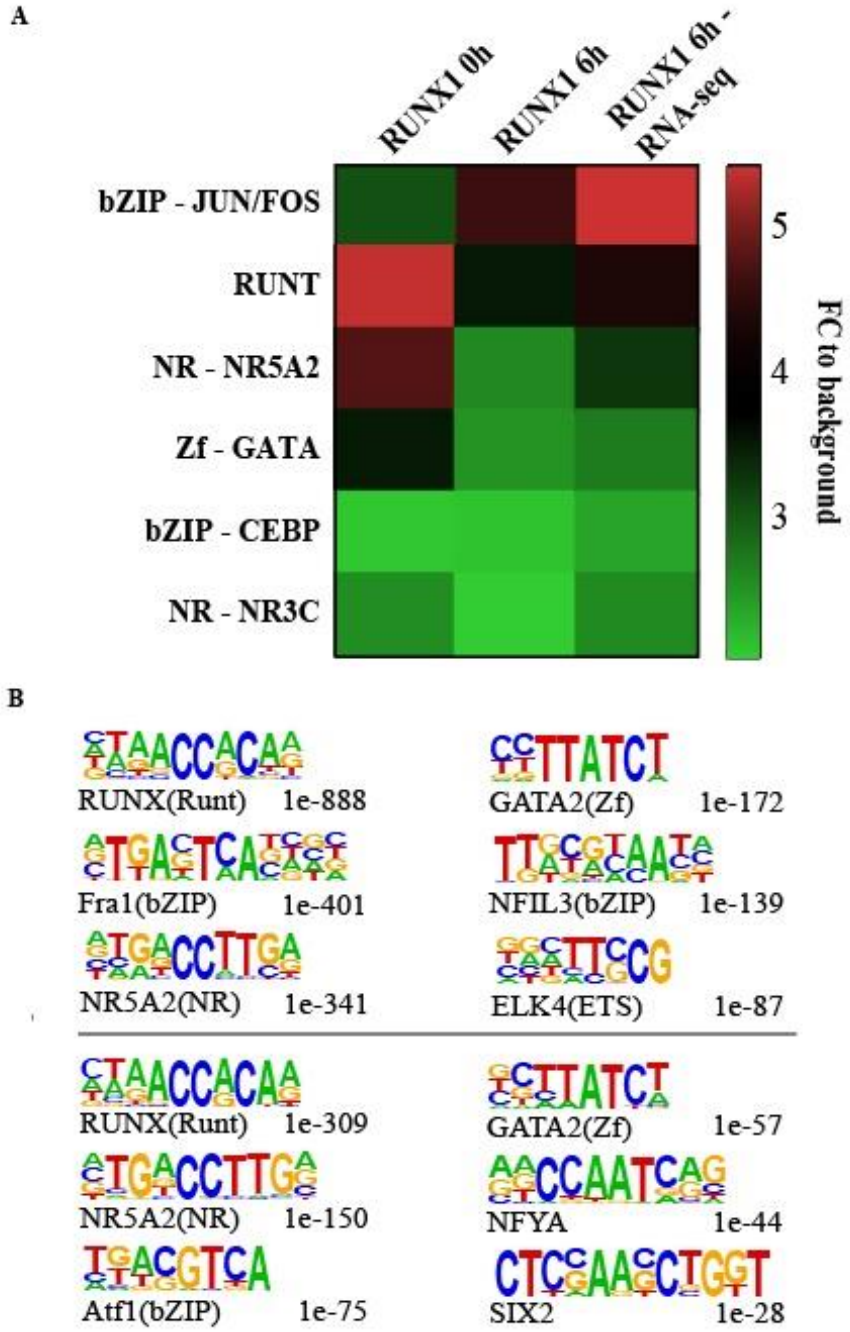

Figure 5.6 Changing identity of RUNX1 binding motifs in response to LH ovulatory signal.

(A) Heatmap showing most common known motifs enriched at RUNX1 0h and RUNX1 6h binding sites or RUNX1 bound genes shown in RNA-seq data to be regulated by hCG-stimulation of ovulation. Motifs were ranked by -log(p-value) and among motifs from the same transcription factor family. **(B)** *De novo* motifs identified by HOMER for RUNX1 6h (top) and RUNX1 0h (bottom) binding sites. Motifs are selected based on p-value and the most significantly enriched motif from each transcription factor family is display.

5.4 DISCUSSION

RUNX1 and other members of the RUNX family are associated with the regulation of gene expression during ovulation. However, not unlike PGR, the ovulatory role of RUNX1 has never been investigated on a global scale or in the context of other ovulatory factors in a regulatory system. RUNX1 being a key factor in granulosa cell specification during foetal development complicates studies on the ovulatory effect of RUNX1. Thus, it is necessary to separate the specific roles of RUNX1 in granulosa cells at different developmental stages in order to fully appreciate its impact on ovulation. This study provides first description of RUNX1 activity in granulosa cells at the genome-wide level in foetal granulosa cells, where RUNX1 is involved in the differentiation of the bipotential gonadal somatic cells, compared to adult granulosa cells in response to ovulatory cues, where RUNX1 plays a role in ovulation regulation. Specific cistromic patterns were drawn in each biological contexts that had an effect on RUNX1 functions at these time points.

RUNX1 ChIP-seq in granulosa cells at three developmental time points of interest revealed a basal level of chromatin binding from the time of ovarian divergence from the unspecified gonad and in adult granulosa cells and an overwhelming increase in peri-ovulatory granulosa cells. Almost all constitutively present RUNX1 binding sites were located in proximal promoter regions of genes, and included genes that encode histone components of the nucleosome (*Hist1h2ao, Hist1h4m, Hist1h4n*), metabolism (*Gapdh*), DNA polymerases (*Poll, Pole4*) and ubiquitination process (*Ube2m, Ube2f, Ubc*), indicating a role of RUNX1 in basic cellular functions. Intriguingly, the gene encoding for RUNX1 itself had constitutive RUNX1 binding in its promoter and introns regardless of time point, suggesting a level of auto-regulation in RUNX1, perhaps in order to sustain basal level of RUNX1 expression prior to ovulatory cues. On the same note, RUNX1 also bound the promoter of RUNX2 in an LH-inducible manner, implying a role of RUNX1 in regulating RUNX2 expression. The cross-regulation of RUNX members have previously been described in rat granulosa cells, in which RUNX2 was found to bind *Runx1* promoter and *in vitro* RUNX2 ablation via siRNA led to an increase in *Runx1* expression [12]. Knockdown of the RUNX dimerising partner CBFβ in granulosa cells also leads to an increase in RUNX1 level whilst RUNX2 level remains unaltered [8], which suggests possible compensation mechanisms involved in RUNX regulation. Further studies using a viable tissue-specific RUNX1 KO model will be useful in clarifying such trans-regulatory effects. Genes encoding various transcription factors were also

constitutively bound by RUNX1 in granulosa cells, such as *Jund, Fos, Klf16, Sox12* and *Zbtb1*. However, while some of these transcription factors have been previously described in the context of ovarian functions (JUN/FOS proteins), the majority of these genes have not been previously studied in granulosa cells and thus requiring further investigations.

After hCG treatment, there was a significant induction in RUNX1 mRNA and protein expression in granulosa cells, leading to an increase in RUNX1 chromatin binding activities, which was illustrated by an increase in RUNX1 binding sites after hCG stimulation. Such LH-induced pattern of cistromic activity in preparation for ovulation has previously been seen in other transcriptional regulatory factors [20]. The role of RUNX1 in regulatory ovulatory genes is shown in comparison between RUNX1-bound genes and genes that are regulated in peri-ovulatory granulosa cells. RUNX1 bound more than 40% of all identified DEGs which stresses the importance of RUNX1 as a master transcription regulator in ovulation. However, LH-induced RUNX1 binding sites do not solely target proximal promoter regions; rather, following hCG there was an increase in intergenic binding incidents compared to constitutive RUNX1 binding sites. This suggests additional RUNX1 function upon the LH surge, in which RUNX1 also activates intergenic chromatin targets, likely to be enhancer elements. The role of RUNX1 at enhancer sites has been previously indicated in other cellular contexts [21-24]. Further investigations into the role of RUNX1 in the enhancer landscape of peri-ovulatory granulosa cells is necessary. Analysis of enriched motifs at RUNX1 binding sites has given us a snapshot of the dynamics of the transcription complex in which RUNX1 is involved during ovulation, displayed as a clear shift in non-canonical motif binding of RUNX1 that is induced by the LH surge. Specifically, there was a striking enrichment of the motif for the bZIP (JUN/FOS) transcription factor family at RUNX1 bound DNA at 6 h post-hCG and especially at RUNX1 binding sites associated with genes regulated by hCG ovulatory trigger. This motif is specifically recognised by JUN and FOS transcription factors, including c-JUN, JUNB, JUND and c-FOS. In the ovary, JUN/FOS members play an important role in granulosa cell gene expression, in particular genes involved in steroidogenesis [25]. The same motif was also found to be highly enriched at PGR binding sites in the same biological context. This further highlights the presence of JUN/FOS transcription factors in granulosa cells during ovulation, most likely in association with PGR as well as RUNX1. While an interaction between JUN/FOS proteins and RUNX1 has not been previously indicated, JUN/FOS are known to interact with PGR in human uterine myometrium [26]. The results have also shown genes encoding for JUN/FOS to be occupied by RUNX1 binding in peri-ovulatory granulosa cells,

implying another role of RUNX1 in their regulation. Further studies into the relationship between PGR, RUNX1 and JUN/FOS in the context of ovulation is required.

RUNX1 was expressed at low level in granulosa cells prior to the LH surge and was not detectable through microscopy. However, while there was minimal activity of RUNX1 prior to the LH surge, in granulosa cells without hCG stimulation RUNX1 was shown to be capable of chromatin binding, particularly proximal promoters, that were later marked as being transcriptionally active after the LH surge. Indeed, in the majority of RUNX1 0h/H3K27ac peaks, such binding events were maintained through the peri-ovulatory window and was present in the RUNX 6h dataset. Interestingly, many non-canonical motifs were enriched at RUNX1 binding sites before and after the LH surge, such as PRE/NR3C and GATA motifs that are recognised by LH-induced transcription factors (PGR [27], GATA4 and GATA6 [28]). RUNX1 and GATA1 have been previously shown to form a physical interaction and share mutual DNA targets that are important for megakaryocyte differentiation [29]. Other motifs, such as NR5A2, are canonically bound by LRH1, which is present in granulosa cells both before and after the LH surge [20]. This illustrates a potential role of RUNX1 in 'priming' potential target chromatins for future activation during the peri-ovulatory window by other factors. RUNX1 is not present in abundance in early-staged follicles [4], meaning that between the process of granulosa cell specification in foetal ovaries and ovulation RUNX1 activity in the ovary was switched off. In zebrafish such a switch was shown to be regulated by CTCF and cohesin [30], however whether the same also happens in mammals is still unknown. It would be of interest to further explore the role of RUNX1 during later stages of granulosa cell differentiation during folliculogenesis but prior to ovulation, and what mechanism regulates the silencing of RUNX1 in early life.

Apart from its role in adult ovarian functions, RUNX1 is also involved in the transition of undifferentiated gonadal somatic cells to granulosa cells in the bipotential gonad [10]. Using ChIP-seq targeting RUNX1 binding in foetal ovaries, the global RUNX1 chromatin binding landscape was identified with a level of binding specifically found in foetal granulosa cells and a large proportion of this shared with that found in adult granulosa cells. Such foetal-specific binding pattern was reflected in the canonical pathways that were enriched in the dataset, with many involved in developmental processes, such as cell fate commitment, cell differentiation and organ morphogenesis. The RUNX1-dependent transcriptome of foetal granulosa cells has been reported [10], however, the relationship between direct RUNX1 binding and consequential

gene expression regulation has not been investigated in detail. In addition, a number of non-RUNT motifs were identified to be specifically targeted by RUNX1 in foetal and not adult granulosa cells, which indicates potential binding partners of RUNX1 at this distinct developmental stage. Included among these is the motif for CTCF, which is uniquely enriched in RUNX1 binding sites in prenatal granulosa cells. CTCF is a key factor in chromatin looping and the formation of TADs, thus allowing for clusters of genes to be regulated by distal enhancer elements within the TAD boundary [31]. Understandably, the expression of CTCF is crucial for normal gene regulation and physiology and in particular, the role of CTCF in foetal development has been implicated in the eye [32], limb [33] and neurons [34]. Although the physical interaction between CTCF and RUNX1 remains unexplored, as previously mentioned, CTCF can regulate the spatial expression of *Runx1* in zebrafish embryos [30]. Separately, RUNX1 has been shown to regulate the activity of enhancer elements in order to regulate target genes in other cellular contexts [22-24], for this the initiation and maintenance of specific chromosomal conformation would be required. Thus CTCF would be crucial for RUNX1 action and is likely in close proximity to RUNX1 binding sites. Conversely, the PRE/NR3C motif was only found at RUNX1 binding sites in adult and not foetal granulosa cells. As PGR and RUNX1 also had a similar pattern of regulation during the peri-ovulatory window and formed physical interaction in granulosa cells, this shows that an interaction between PGR and RUNX1 is specific for the context of ovulatory granulosa cells. The interaction between RUNX1 and various co-modulators have been shown to be critical to RUNX1 activities in different biological contexts [35]. In prenatal granulosa cells in particular, RUNX1 has been shown to form functional interaction with FOXL2 in order to drive feminisation of gonadal somatic cells [10], and in this instance the canonical binding motif for FOXL2 was also identified in foetal RUNX1 binding sites. Therefore, future studies on the role of RUNX1 in granulosa cell specification would benefit from investigating the relationship between RUNX1 and co-factors in this biological context.

To conclude, this chapter offers the first insight into RUNX1 activities in granulosa cells on a genomic level in foetal granulosa cells, where RUNX1 is involved in the differentiation of the bipotential gonadal cells, and in adult granulosa cells in response to ovulatory cues, where RUNX1 plays a role in ovulation regulation. ChIP-seq indicates distinctive RUNX1 cistromes in different biological contexts with a basal level of chromatin occupancy found at all time points. In the context of adult granulosa cells, RUNX1 mRNA, protein and chromatin binding action was massively induced by the LH surge and was reflected by its role in the regulation

of ovulatory genes in granulosa cells, which highlights the importance of RUNX1 in peri-ovulatory granulosa cells. As RUNX1 can form a physical interaction with PGR, the next chapter investigated the similarities between PGR and RUNX1 cistromes in granulosa cells and the functional consequences of such interaction on the ovulatory gene profile.

5.5 REFERENCES

1 Mevel, R., Draper, J. E., Lie-a-Ling, M., Kouskoff, V. & Lacaud, G. RUNX transcription factors: orchestrators of development. *Development* **146**, dev148296 (2019).

2 Okuda, T., van Deursen, J., Hiebert, S. W., Grosveld, G. & Downing, J. R. AML1, the Target of Multiple Chromosomal Translocations in Human Leukemia, Is Essential for Normal Fetal Liver Hematopoiesis. *Cell* **84**, 321-330, doi:https://doi.org/10.1016/S0092-8674(00)80986-1 (1996).

3 Takarada, T., Hinoi, E., Nakazato, R., Ochi, H., Xu, C., Tsuchikane, A., Takeda, S., Karsenty, G., Abe, T., Kiyonari, H. & Yoneda, Y. An analysis of skeletal development in osteoblast-specific and chondrocyte-specific runt-related transcription factor-2 (Runx2) knockout mice. *Journal of Bone and Mineral Research* **28**, 2064-2069, doi:10.1002/jbmr.1945 (2013).

4 Jo, M. & Curry, T. E., Jr. Luteinizing Hormone-Induced RUNX1 Regulates the Expression of Genes in Granulosa Cells of Rat Periovulatory Follicles. *Molecular Endocrinology* **20**, 2156-2172, doi:10.1210/me.2005-0512 (2006).

5 Bai, Z.-K., Li, D.-D., Guo, C.-H., Yang, Z.-Q., Cao, H., Guo, B. & Yue, Z.-P. Differential expression and regulation of Runx1 in mouse uterus during the peri-implantation period. *Cell and Tissue Research* **362**, 231-240, doi:10.1007/s00441-015-2174-z (2015).

6 Wissing, M. L., Kristensen, S. G., Andersen, C. Y., Mikkelsen, A. L., Høst, T., Borup, R. & Grøndahl, M. L. Identification of new ovulation-related genes in humans by comparing the transcriptome of granulosa cells before and after ovulation triggering in the same controlled ovarian stimulation cycle. *Human Reproduction* **29**, 997-1010, doi:10.1093/humrep/deu008 (2014).

7 Gao, K., Wang, P., Peng, J., Xue, J., Chen, K., Song, Y., Wang, J., Li, G., An, X. & Cao, B. Regulation and function of runt-related transcription factors (RUNX1 and RUNX2) in goat granulosa cells. *The Journal of Steroid Biochemistry and Molecular Biology* **181**, 98-108, doi:https://doi.org/10.1016/j.jsbmb.2018.04.002 (2018).

8 Lee-Thacker, S., Choi, Y., Taniuchi, I., Takarada, T., Yoneda, Y., Ko, C. & Jo, M. Core binding factor β expression in ovarian granulosa cells is essential for female fertility. *Endocrinology* **159**, 2094-2109 (2018).

9 Lydon, J. P., DeMayo, F. J., Funk, C. R., Mani, S. K., Hughes, A. R., Montgomery, C. A., Jr., Shyamala, G., Conneely, O. M. & O'Malley, B. W. Mice lacking progesterone receptor exhibit pleiotropic reproductive abnormalities. *Genes Dev* **9**, 2266-2278 (1995).

10 Nicol, B., Grimm, S. A., Chalmel, F., Lecluze, E., Pannetier, M., Pailhoux, E., Dupin-De-Beyssat, E., Guiguen, Y., Capel, B. & Yao, H. H. C. RUNX1 maintains the identity of the fetal ovary through an interplay with FOXL2. *Nature communications* **10**, 5116 (2019). <https://doi.org/10.1038/s41467-019-13060-1>.

11 Park, E.-S., Lind, A.-K., Dahm-Kähler, P., Brännström, M., Carletti, M. Z., Christenson, L. K., Curry, T. E., Jr. & Jo, M. RUNX2 Transcription Factor Regulates Gene Expression in Luteinizing Granulosa Cells of Rat Ovaries. *Molecular Endocrinology* **24**, 846-858, doi:10.1210/me.2009-0392 (2010).

12 Park, E.-S., Park, J., Franceschi, R. T. & Jo, M. The role for runt related transcription factor 2 (RUNX2) as a transcriptional repressor in luteinizing granulosa cells. *Molecular and Cellular Endocrinology* **362**, 165-175, doi:https://doi.org/10.1016/j.mce.2012.06.005 (2012).

13 Ojima, F., Saito, Y., Tsuchiya, Y., Ogoshi, M., Fukamachi, H., Inagaki, K., Otsuka, F., Takeuchi, S. & Takahashi, S. Runx3 regulates folliculogenesis and steroidogenesis in granulosa cells of immature mice. *Cell and Tissue Research* **375**, 743-754, doi:10.1007/s00441-018-2947-2 (2019).

14 Ojima, F., Saito, Y., Tsuchiya, Y., Kayo, D., Taniuchi, S., Ogoshi, M., Fukamachi, H., Takeuchi, S. & Takahashi, S. Runx3 transcription factor regulates ovarian functions and ovulation in female mice. *J Reprod Dev* **62**, 479-486, doi:10.1262/jrd.2016-005 (2016).

15 Bai, Z.-K., Guo, B., Tian, X.-C., Li, D.-D., Wang, S.-T., Cao, H., Wang, Q.-Y. & Yue, Z.-P. Expression and regulation of Runx3 in mouse uterus during the peri-implantation period. *Journal of Molecular Histology* **44**, 519-526, doi:10.1007/s10735-013-9501-z (2013).

16 Guo, C.-H., Yue, Z.-P., Bai, Z.-K., Li, D.-D., Yang, Z.-Q. & Guo, B. Runx2 acts downstream of C/EBPβ to regulate the differentiation of uterine stromal cells in mice. *Cell and Tissue Research* **366**, 393-401, doi:10.1007/s00441-016-2412-z (2016).

17 Umansky, K. B., Gruenbaum-Cohen, Y., Tsoory, M., Feldmesser, E., Goldenberg, D., Brenner, O. & Groner, Y. Runx1 Transcription Factor Is Required for Myoblasts Proliferation during Muscle Regeneration. *PLOS Genetics* **11**, e1005457, doi:10.1371/journal.pgen.1005457 (2015).

18 Li, H., Handsaker, B., Wysoker, A., Fennell, T., Ruan, J., Homer, N., Marth, G., Abecasis, G. & Durbin, R. The Sequence Alignment/Map format and SAMtools. *Bioinformatics* **25**, 2078-2079, doi:10.1093/bioinformatics/btp352 (2009).

19 Zhu, L. J., Gazin, C., Lawson, N. D., Pagès, H., Lin, S. M., Lapointe, D. S. & Green, M. R. ChIPpeakAnno: a Bioconductor package to annotate ChIP-seq and ChIP-chip data. *BMC Bioinformatics* **11**, 237, doi:10.1186/1471-2105-11-237 (2010).

20 Bianco, S., Bellefleur, A.-M., Beaulieu, É., Beauparlant, C. J., Bertolin, K., Droit, A., Schoonjans, K., Murphy, B. D. & Gévry, N. The Ovulatory Signal Precipitates LRH-1 Transcriptional Switching Mediated by Differential Chromatin Accessibility. *Cell Reports* **28**, 2443-2454.e2444, doi:https://doi.org/10.1016/j.celrep.2019.07.088 (2019).

21 Huang, G., Zhang, P., Hirai, H., Elf, S., Yan, X., Chen, Z., Koschmieder, S., Okuno, Y., Dayaram, T., Growney, J. D., Shivdasani, R. A., Gilliland, D. G., Speck, N. A., Nimer, S. D. & Tenen, D. G. PU.1 is a major downstream target of AML1 (RUNX1) in adult mouse hematopoiesis. *Nature Genetics* **40**, 51-60, doi:10.1038/ng.2007.7 (2008).

22 Guo, H., Ma, O., Speck, N. A. & Friedman, A. D. Runx1 deletion or dominant inhibition reduces Cebpa transcription via conserved promoter and distal enhancer sites to favor monopoiesis over granulopoiesis. *Blood* **119**, 4408-4418, doi:10.1182/blood-2011-12-397091 (2012).

23 Mao, A.-P., Ishizuka, I. E., Kasal, D. N., Mandal, M. & Bendelac, A. A shared Runx1-bound Zbtb16 enhancer directs innate and innate-like lymphoid lineage development. *Nature Communications* **8**, 863, doi:10.1038/s41467-017-00882-0 (2017).

24 Choi, A., Illendula, A., Pulikkan, J. A., Roderick, J. E., Tesell, J., Yu, J., Hermance, N., Zhu, L. J., Castilla, L. H., Bushweller, J. H. & Kelliher, M. A. RUNX1 is required for oncogenic Myb and Myc enhancer activity in T-cell acute lymphoblastic leukemia. *Blood* **130**, 1722-1733, doi:10.1182/blood-2017-03-775536 (2017).

25 Choi, Y., Rosewell, K. L., Brännström, M., Akin, J. W., Curry Jr, T. E. & Jo, M. FOS, a Critical Downstream Mediator of PGR and EGF Signaling Necessary for Ovulatory Prostaglandins in the Human Ovary. *The Journal of Clinical Endocrinology & Metabolism* **103**, 4241-4252 (2018).

26 Nadeem, L., Shynlova, O., Matysiak-Zablocki, E., Mesiano, S., Dong, X. & Lye, S. Molecular evidence of functional progesterone withdrawal in human myometrium. *Nature Communications* **7**, 11565, doi:10.1038/ncomms11565 (2016).

27 Robker, R. L., Russell, D. L., Espey, L. L., Lydon, J. P., O'Malley, B. W. & Richards, J. S. Progesterone-regulated genes in the ovulation process: ADAMTS-1 and cathepsin L proteases. *Proc Natl Acad Sci U S A* **97**, 4689-4694 (2000).

28 Bennett, J., Wu, Y.-G., Gossen, J., Zhou, P. & Stocco, C. Loss of GATA-6 and GATA-4 in Granulosa Cells Blocks Folliculogenesis, Ovulation, and Follicle Stimulating Hormone Receptor Expression Leading to Female Infertility. *Endocrinology* **153**, 2474-2485, doi:10.1210/en.2011-1969 (2012).

29 Tijssen, Marloes R., Cvejic, A., Joshi, A., Hannah, Rebecca L., Ferreira, R., Forrai, A., Bellissimo, Dana C., Oram, S. H., Smethurst, Peter A., Wilson, Nicola K., Wang, X., Ottersbach, K., Stemple, Derek L., Green, Anthony R., Ouwehand, Willem H. & Göttgens, B. Genome-wide Analysis of Simultaneous GATA1/2, RUNX1, FLI1, and SCL Binding in Megakaryocytes Identifies Hematopoietic Regulators. *Developmental Cell* **20**, 597-609, doi:https://doi.org/10.1016/j.devcel.2011.04.008 (2011).

30 Marsman, J., O'Neill, A. C., Kao, B. R.-Y., Rhodes, J. M., Meier, M., Antony, J., Mönnich, M. & Horsfield, J. A. Cohesin and CTCF differentially regulate spatiotemporal runx1 expression during zebrafish development. *Biochimica et Biophysica Acta (BBA) - Gene Regulatory Mechanisms* **1839**, 50-61, doi:https://doi.org/10.1016/j.bbagrm.2013.11.007 (2014).

31 Nora, E. P., Goloborodko, A., Valton, A.-L., Gibcus, J. H., Uebersohn, A., Abdennur, N., Dekker, J., Mirny, L. A. & Bruneau, B. G. Targeted Degradation of CTCF Decouples Local Insulation of Chromosome Domains from Genomic Compartmentalization. *Cell* **169**, 930-944.e922, doi:https://doi.org/10.1016/j.cell.2017.05.004 (2017).

32 Li, T., Lu, Z. & Lu, L. Regulation of Eye Development by Transcription Control of CCCTC Binding Factor (CTCF). *Journal of Biological Chemistry* **279**, 27575-27583, doi:10.1074/jbc.M313942200 (2004).

33 Soshnikova, N., Montavon, T., Leleu, M., Galjart, N. & Duboule, D. Functional Analysis of CTCF During Mammalian Limb Development. *Developmental Cell* **19**, 819-830, doi:https://doi.org/10.1016/j.devcel.2010.11.009 (2010).

34 Hirayama, T., Tarusawa, E., Yoshimura, Y., Galjart, N. & Yagi, T. CTCF Is Required for Neural Development and Stochastic Expression of Clustered Pcdh Genes in Neurons. *Cell Reports* **2**, 345-357, doi:https://doi.org/10.1016/j.celrep.2012.06.014 (2012).

35 Lichtinger, M., Hoogenkamp, M., Krysinska, H., Ingram, R. & Bonifer, C. Chromatin regulation by RUNX1. *Blood Cells, Molecules, and Diseases* **44**, 287-290, doi:https://doi.org/10.1016/j.bcmd.2010.02.009 (2010).

CHAPTER 6 The functional and physical interaction between PGR and RUNX1 in ovulatory gene regulation

6.1 INTRODUCTION

PGR is widely expressed throughout the female reproductive tract and is involved in the coordination of biological processes required for the establishment of pregnancy. In the ovary, it is specifically induced in peri-ovulatory granulosa cells in response to the LH surge and is a major determining factor in ovulation, with PGRKO female mice being anovulatory and completely infertile [1]. In the oviduct, PGR is involved in the active transport of oocytes and embryos [2,3], and in the uterus PGR promotes decidualisation and embryo implantation [1]. These PGR functions are achieved through PGR-dependent gene regulation, including distinct gene sets that are critical for ovulation in granulosa cells [4], ciliate function and motility in the oviduct [3] and decidualisation factors in the uterus [5]. To fully comprehend the influence of PGR on tissue-specific gene expression profile, PGR-regulated tissue-specific transcriptomes from different reproductive tissues were compared. PGR was confirmed to be responsible for the regulation of highly distinct groups of genes in ovary, oviduct and uterus. To further explore the tissue-specific roles of PGR in different reproductive tissues, the PGR cistrome in progesterone-responsive granulosa cells was also compared to PGR cistrome in the uterus. In response to the LH surge in granulosa cells, there was a massive increase in PGR expression and function, with PGR targeting transcriptionally active promoter regions. In describing the non-canonical targets of PGR in granulosa cells, the RUNT motif was identified to be one of the most highly enriched motifs, which is canonically bound by the RUNX transcription factor family. Interestingly, RUNT was only implicated as a PGR target in granulosa cells and was not enriched in uterine PGR ChIP-seq in progesterone-responsive uterus, implying the RUNX transcription factors to be potential co-modulators to PGR in a granulosa-specific context.

The RUNX transcription factor family consists of three members that share a common DNA binding domain which recognises the RUNT sequence motif. A heterodimer partner, named CBFβ, is required for efficient RUNX-DNA interaction. RUNX1, which is upregulated in granulosa cells during ovulation in rodent ovaries, functions as a transcription mediator of gene

expression [6]. While a global RUNX1 KO mouse model is not viable, female mice that are CBFβ KO specifically in granulosa cells experience ovulation failure and are subfertile [7]. Outside of the ovulation context, the importance of RUNX1 in granulosa cells has also been demonstrated in the earliest stages of granulosa cell differentiation in female gonads during foetal development [8].

Both PGR and RUNX1 are known to cooperate with other transcriptional co-activators in different cellular contexts. PGR can interact with both co-activators and co-repressors depending on the biological contexts and result in specific regulation of PGR activities [9]. Notably, PGR is capable of interacting with other ovulatory transcription factors, including members of the JUN/FOS family in human myometrial cells [10] and SP1/SP3 in regulation ovulatory genes in granulosa cells [11]. RUNX1 and other RUNX transcription factors require dimerisation with CBFβ to efficiently bind target genes. RUNX1 has also been found to interact with the chromatin remodeller SWI/SNF complex and co-repressors such as HDAC proteins and the Groucho/TLE family, as well as various transcription factors [12]. RUNX proteins can interact with SR, as indicated in osteoblasts and prostate cancer cells where RUNX-steroid receptor binding leads to mutual repression of the transactivation function of each other [13,14]. However, the involvement of PGR and RUNX1 in the same transcription complex and consequences on the regulation of ovulatory genes have not been investigated.

With the availability of newly emerging knowledge on the chromatin binding properties of ovulatory transcription factors in granulosa cells [15], in which the potential interaction with other modulators is crucial for their functions, it is informative that such cistromes are analysed alongside one another to gain a full understanding of the transcriptional regulatory interactome and how that affects downstream gene expression. In Chapter 5, the context-specific properties of RUNX1 cistromes in granulosa cells were demonstrated, in which it was found that RUNX1 DNA binding was markedly increased upon the LH surge, with the majority of binding sites located in proximal promoter regions, which are all features in common with the PGR cistrome. Furthermore, an enrichment of the PRE/NR3C motif, canonically targeted by PGR, was also found at RUNX1 binding sites, which supports the hypothesis that PGR and RUNX1 interact on a chromatin level. In addition, direct RUNX1 binding was localised to the regulatory regions of ovulatory genes. Cumulatively, these new findings indicate that PGR and RUNX1 may be part of the same transcription complex responsible for the regulation of gene expression in granulosa cells during ovulation. The physical interaction between PGR and RUNX1 in

granulosa cells in response to ovulatory cues was confirmed by PLA, as well the interaction between PGR and RUNX2 and CBFβ. Documented PGR and RUNX1 transcriptional activities in peri-ovulatory granulosa cells further point to a functional cooperation between PGR and RUNX1 in the regulation of ovulatory genes. To test the hypothesis that there is cooperative action of PGR and RUNX1 on a genome-wide level, comparisons were made between the PGR and RUNX1 cistromes, as indicated via ChIP-seq. The dynamics of the physical interaction between PGR and RUNX transcription factors in peri-ovulatory granulosa cells was also investigated.

6.2 MATERIALS & METHODS

6.2.1 Animals

For peri-ovulatory granulosa cell experiments, CBAF1 mice were obtained from Laboratory Animal Services and maintained as in section 2.2.1.

6.2.2 ChIP-seq experiments

PGR and RUNX1 ChIP-seq experiments were conducted as described in section 2.2.3 and 5.2.3. Briefly, granulosa cells were collected from super-ovulated CBAF1 female mice at 6 h after hCG injection and used for ChIP-seq targeting PGR or RUNX1. Bioinformatics analysis for ChIP-seq datasets was conducted using appropriate tools as described in section 2.2.3.

6.2.3 Proximity ligation assay

PLA was performed on granulosa cells for PGR/RUNX protein-protein interactions as described in section 4.2.6. Briefly, granulosa cells were obtained from ovaries of super-ovulated female CBAF1 mice at 44 h post-eCG stimulation. Granulosa cells were plated in fibronectin-coated chamber slides and cultured in DMEM:F12 media before being treated with 2 IU/ml hCG and 100 nM R5020 for 0-8 h. After treatment, cells were fixed with formaldehyde and permeabilised. PLA followed the protocol as previously described, using antibodies targeting PGR and RUNX1/RUNX2, and corresponding IgG antibodies were used as negative control. Slides were imaged using confocal microscope. Quantification of PLA signal was by ImageJ [16]. For each replicate of each sample, three microscopy images at 120x magnification

were used for quantification. The nuclear boundary for each cell was determined through DAPI staining, with cytoplasmic region defined as the area outside of the nuclear boundary. PLA signals were identified as fluorescent puncta and quantified in using the 'Count Maxima' function in ImageJ for each cellular compartment. Significantly differences between time points were determined through two-way ANOVA with Tukey test for multiple comparison for row factor (difference between time points) and column factor (difference between cellular compartments). The p-values reported in the results are for row factor to indicate changes over time.

6.3 RESULTS

6.3.1 Interaction between RUNX1 and the PGR transcription machinery on a chromatin level

6.3.1.1 RUNX1 shares occupancy of promoters with PGR

RUNX1 binding properties were compared with that of PGR at 6h post-hCG in order to determine the relationship between RUNX1 and PGR cistromes. PGR showed a high correlation with RUNX1 6h (Pearson correlation coefficient = 0.87) and both transcription factors showing equal correlation to the active chromatin marker H3K27ac (correlation coefficient = 0.76-0.78) (Figure 6.1A). Overall the chromatin binding patterns of PGR and RUNX1 were relatively similar, as seen in a circos plot of all binding sites in the genome (Figure 6.1B) and in the read count frequency plot where both PGR and RUNX1 peaks overlapped with TSS and were flanked by H3K27ac double peaks (Figure 6.1C). PGR shared a remarkable number of mutual binding sites with RUNX1 both prior and after the LH surge, with 9704 binding sites identified to have both PGR and RUNX1 binding at 6h post-hCG (Figure 6.1D). Among these shared PGR/RUNX1 binding sites, more than 80% were located at transcriptionally active chromatin defined H3K27ac ChIP-seq peaks.

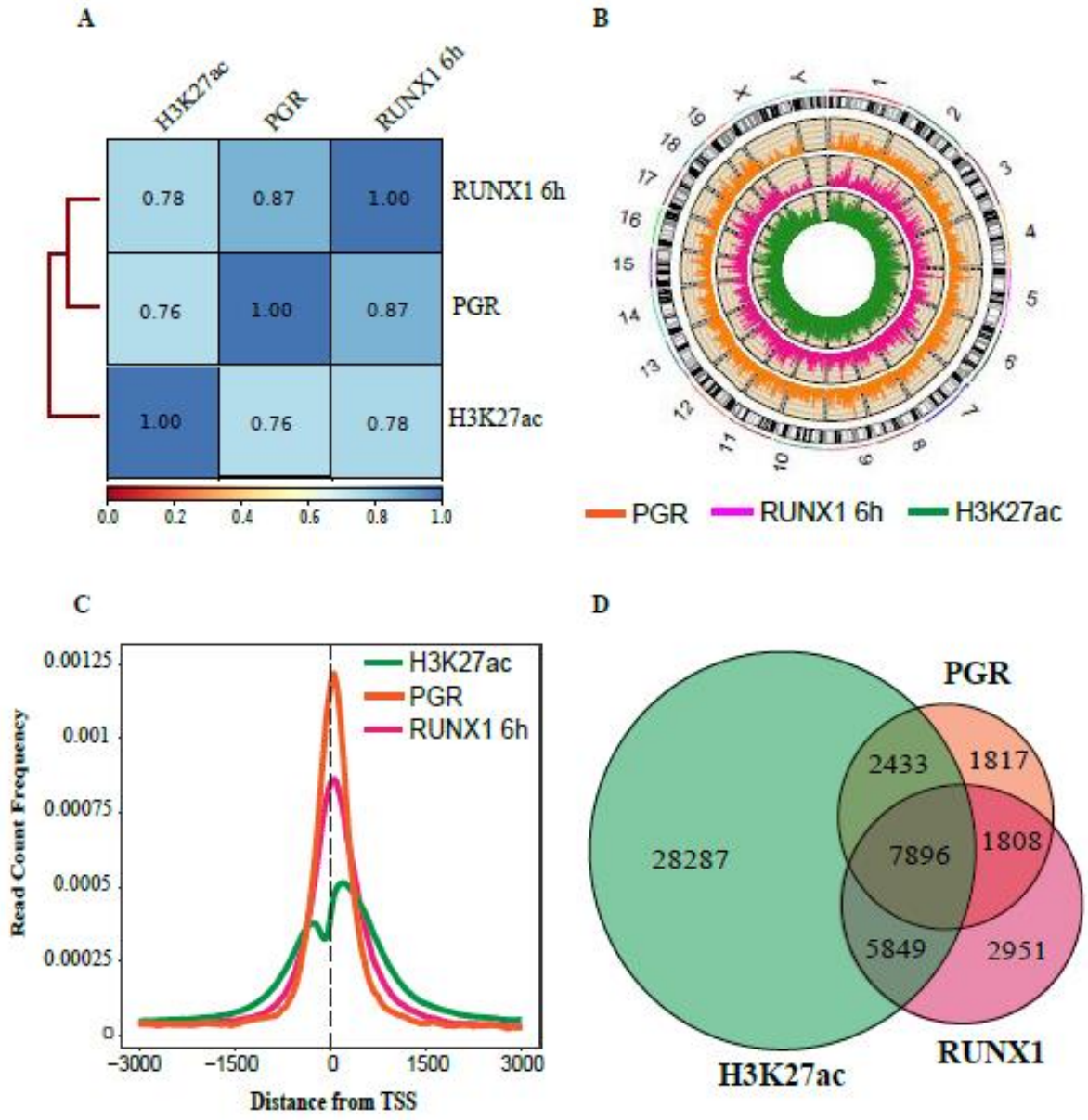

Figure 6.1 PGR and RUNX1 shared mutual chromatin targets in peri-ovulatory granulosa cells.

(A) Pearson correlation coefficient showing relationships between RUNX1, PGR and H3K27ac binding sites at 6 h after hCG stimulation. The correlation in genomic coverage between all datasets was analysed and organised in hierarchical order. **(B)** Circos plot showing binding sites for PGR (orange), RUNX1 6h (pink), RUNX1 0h (blue) and H3K27ac (green) on the whole mouse genome. **(C)** Read count frequency of PGR, RUNX1 6h, RUNX1 0h and H3K27ac ChIP-seq peaks in relation to the TSS. **(D)** Venn diagram showing shared and factor-unique peak counts for RUNX1 6h, PGR and H3K27ac cistromes.

Separating RUNX1 and PGR cistromes at 6h post-hCG into those that were shared or uniquely bound by each transcription factor showed that the strong preference for binding close (≤ 1 kb) to gene TSS was a predominant characteristic of RUNX1 bound intervals (Figure 6.2A-B). Binding sites that were found to have RUNX1 binding, either uniquely-bound by RUNX1 or with both PGR/RUNX1 binding, were remarkably highly enriched at proximal promoter regions (Figure 6.2C). On the other hand, PGR-unique intervals did not exhibit such a dramatic enrichment at promoters, which is not reflective of the genomic distribution of total PGR ChIP-seq data described earlier in Figure 2.5. These results suggest that the prevalence for proximal promoter occupancy by PGR is determined by the presence of RUNX1 at these binding sites. Together with the fact that RUNX1 preferably bound transcriptionally active chromatins, these imply a possible role of RUNX1 as a pioneer factor for PGR-associated transcription in which RUNX1 promotes PGR binding at transcriptionally available promoters. Examples of PGR and RUNX1 binding at target chromatin sites can be seen in Figure 6.2D. PGR and RUNX1 were also found to bind the promoter and introns of *Runx1* and *Runx2*, suggesting a degree of PGR- and RUNX1-regulated activation of these genes (Figure 6.2E).

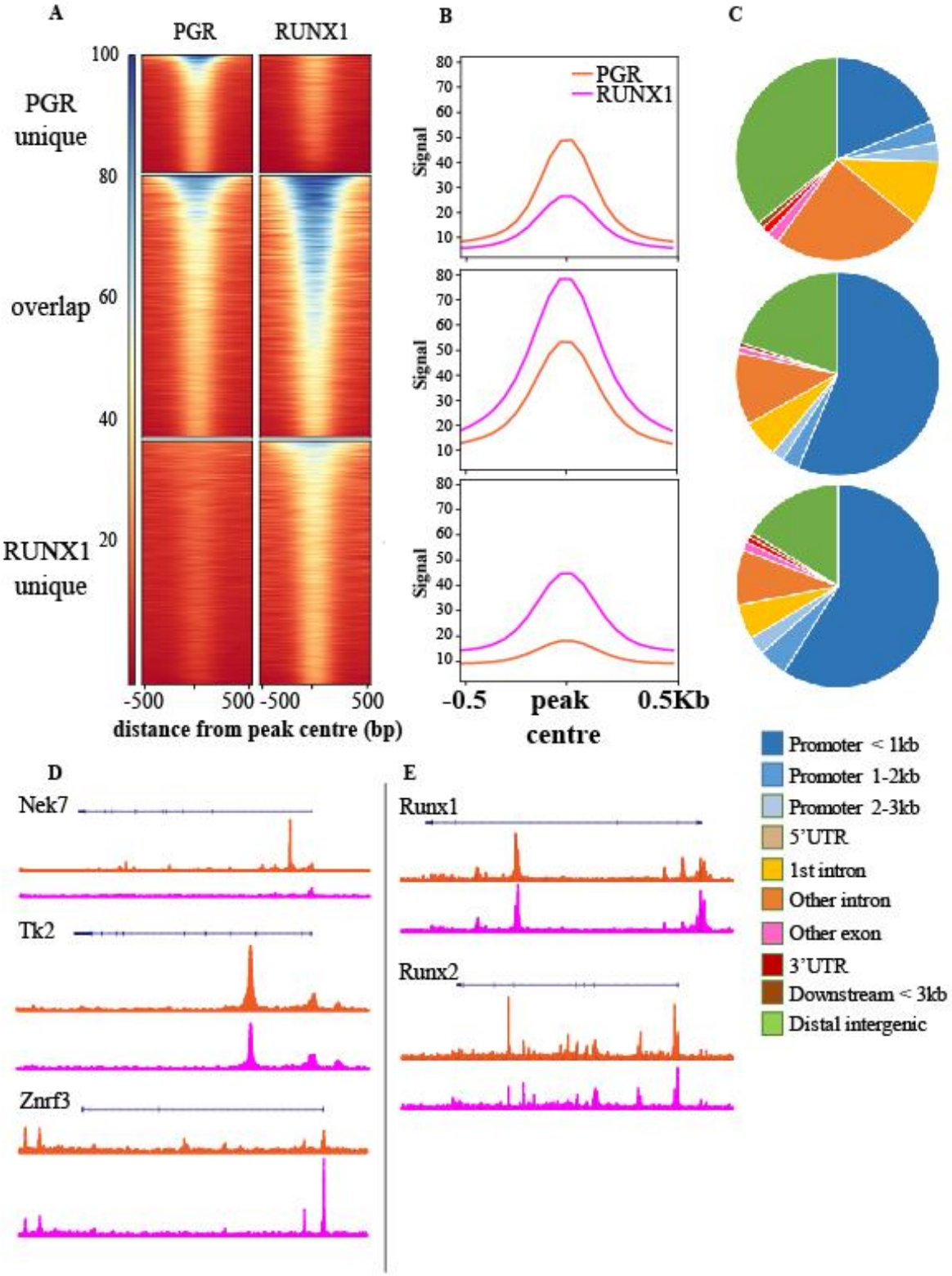
A
PGR
RUNX1
PGR unique
overlap
RUNX1 unique
100
80
60
40
20
-500
500
-500
500
distance from peak centre (bp)
B
PGR
RUNX1
Signal
-0.5
peak centre
0.5Kb
C
Promoter < 1kb
Promoter 1-2kb
Promoter 2-3kb
5'UTR
1st intron
Other intron
Other exon
3'UTR
Downstream < 3kb
Distal intergenic
D
Nek7
Tk2
Znrf3
E
Runx1
Runx2

Figure 6.2 Transcription factor-specific chromatin binding properties of PGR and RUNX1 cistrome.

(A-B) Heatmap of PGR and RUNX1 6h read frequency (A) and visualisation of the pattern of signal intensity (B), divided into peaks specific to PGR (PGR unique), shared (overlap) and specific to RUNX1 (RUNX1 unique) subgroups. Read intensity is displayed in relation to peak centre and the flanking 500 bp regions. **(C)** Genomic distribution of PGR-specific (top), shared (middle) or RUNX1-specific (bottom) binding sites. Genomic features include promoters (< 1 kb, 1-2 kb and 2-3 kb), 5' UTR, 1st intron, other introns, exons, 3' UTR and downstream of TES (within 3 kb). Peaks that are not in these features are classified as distal intergenic. **(D)** Example of factor-specific binding sites in the genome, showing loci with binding specifically to PGR (top), RUNX1 (bottom) and shared between PGR and RUNX1 (middle). **(E)** Example of PGR and RUNX1 binding at *Runx1* and *Runx2*. Binding intensity of PGR is displayed in orange and RUNX1 in pink.

6.3.1.2 RUNX1 and PGR functional similarities in peri-ovulatory granulosa cells

To determine whether RUNX1 and PGR shared similar functions in peri-ovulatory granulosa cells, canonical pathways enriched by RUNX1 peaks pre- and post-LH were annotated using GREAT analysis. Gene Ontology analysis showed that RUNX1 peaks in granulosa cell post-hCG 6 h were enriched for pathways similar to those found for PGR, mostly those that are important for normal cellular functions, such as metabolism, gene expression and response to external stimulus (Figure 6.3A). To identify the extent of PGR and RUNX1 cooperation on gene regulation at a genome-wide level, PGR-binding and RUNX1-binding genes were compared against ovulatory genes identified through RNA-seq of 8h post-hCG granulosa cells. Among the 2179 identified DEGs, 788 (36%) DEGs were found to be bound by both RUNX1 and PGR (Figure 6.3B), while 101 (4.6%) were bound only by PGR or 266 (12%) bound only by RUNX1. This means that the majority of RUNX1- (75%) and PGR-bound (89%) DEGs in fact shared binding by both transcription factors, implying that simultaneous interaction of both PGR and RUNX1 to target chromatin is important for ovulatory gene regulation. As previously shown, a slight tendency for promoter occupancy was observed in PGR binding at DEG. Interestingly, RUNX1 binding at DEGs exhibited an even greater preference for promoters, with more than half of RUNX1 binding sites found to be within 3 kb upstream of a TSS, especially within 1 kb of the TSS (Figure 6.3C), again highlighting the importance of RUNX1 in promoter targeting. As expected, many hCG-regulated genes (i.e. 1024 DEGs) were not bound by PGR nor RUNX1 (Figure 6.3B) and these likely represent genes controlled by other mediators of LH action (CREB, CEBPβ, MAPK etc.).

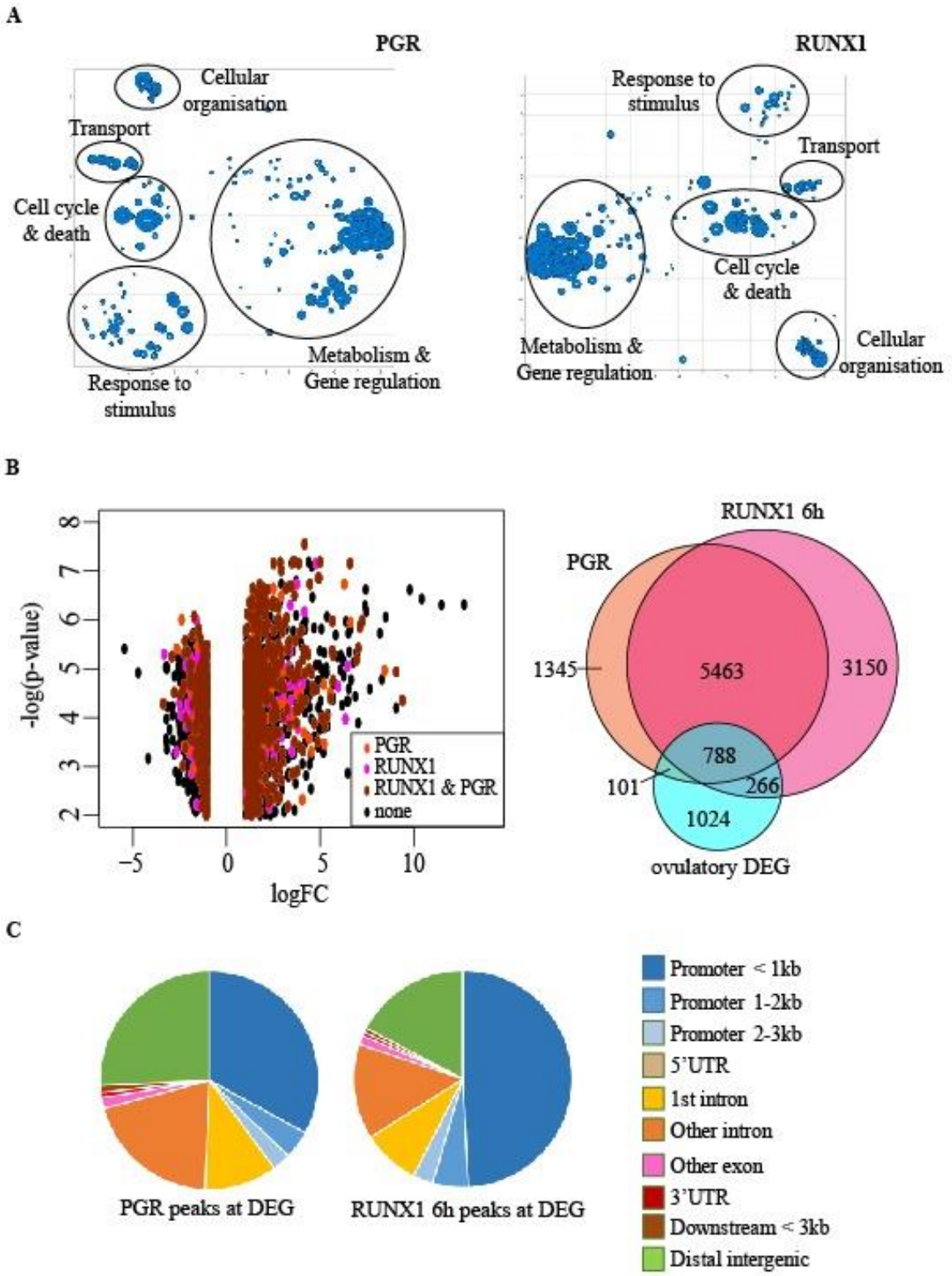
A
PGR
Cellular organisation
Transport
Cell cycle & death
Metabolism & Gene regulation
Response to stimulus
RUNX1
Response to stimulus
Transport
Cell cycle & death
Metabolism & Gene regulation
Cellular organisation
B
-log(p-value)
logFC
PGR
RUNX1
RUNX1 & PGR
none
RUNX1 6h
PGR
1345
5463
3150
788
101
266
1024
ovulatory DEG
C
PGR peaks at DEG
RUNX1 6h peaks at DEG
Promoter < 1kb
Promoter 1-2kb
Promoter 2-3kb
5'UTR
1st intron
Other intron
Other exon
3'UTR
Downstream < 3kb
Distal intergenic

Figure 6.3 Consequences of RUNX1 binding on gene expression.

(A) Gene Ontology analysis of PGR and RUNX1 binding sites. Ontological terms associated with biological processes were obtained from analysis of PGR and RUNX1 ChIP-seq and condensed using REVIGO. **(B)** Volcano plot of ovulatory DEGs with PGR or RUNX1 binding at 6h post-hCG treatment. DEGs were identified through RNA-seq of peri-ovulatory granulosa cells and only DEGs that met statistical criteria ($|\log FC| \geq 1$ and $-\log(\text{p-value}) \geq 2$) are graphed (black dots). DEGs with PGR binding are orange, with RUNX1 binding are pink and with both PGR and RUNX1 binding are brown. Gene counts for each fraction are summarised in Venn diagram. **(C)** Genome distribution of PGR and RUNX1 6h peaks identified in peri-ovulatory transcriptome. From (B), PGR and RUNX1 peaks that were found to bind RNA-seq identified DEGs were separately extracted for genome distribution analysis.

6.3.2 The physical interaction between RUNX1 and PGR is highly dynamic in the peri-ovulatory window

A very close spatial association of PGR with members of the RUNX family was demonstrated in mouse granulosa cells *in vitro* at 6 h post-progestin treatment, suggesting a direct physical interaction between these two transcription factors. To further investigate the dynamics of these interactions, PLA targeting PGR interaction with RUNX1 or RUNX2 was performed on granulosa cells treated with hCG + progestin for up to 8h to mimic the *in vivo* ovulatory stimulus. Both RUNX1 and RUNX2 showed positive interaction with PGR that was highly induced by hCG + progestin treatment (Figure 6.4). PGR/RUNX1 interaction was absent (similar to IgG-only negative controls) before hormone treatment and was increased by 4-6 h after treatment after which there was a decrease in signals. PGR/RUNX2 showed a slightly different pattern, with the strongest interaction with PGR observed at 5-7 h post-treatment and with the protein-protein interaction retained up to 8 h post-treatment. In both PGR/RUNX1 and PGR/RUNX2 interactions, the protein pairs were largely found in the nuclear compartment of the cell, confirming that PGR and RUNX transcription factors were concurrently interacting with chromatin after the addition of ovulatory cues. These results indicate an LH-dependent interaction between PGR and RUNX members.

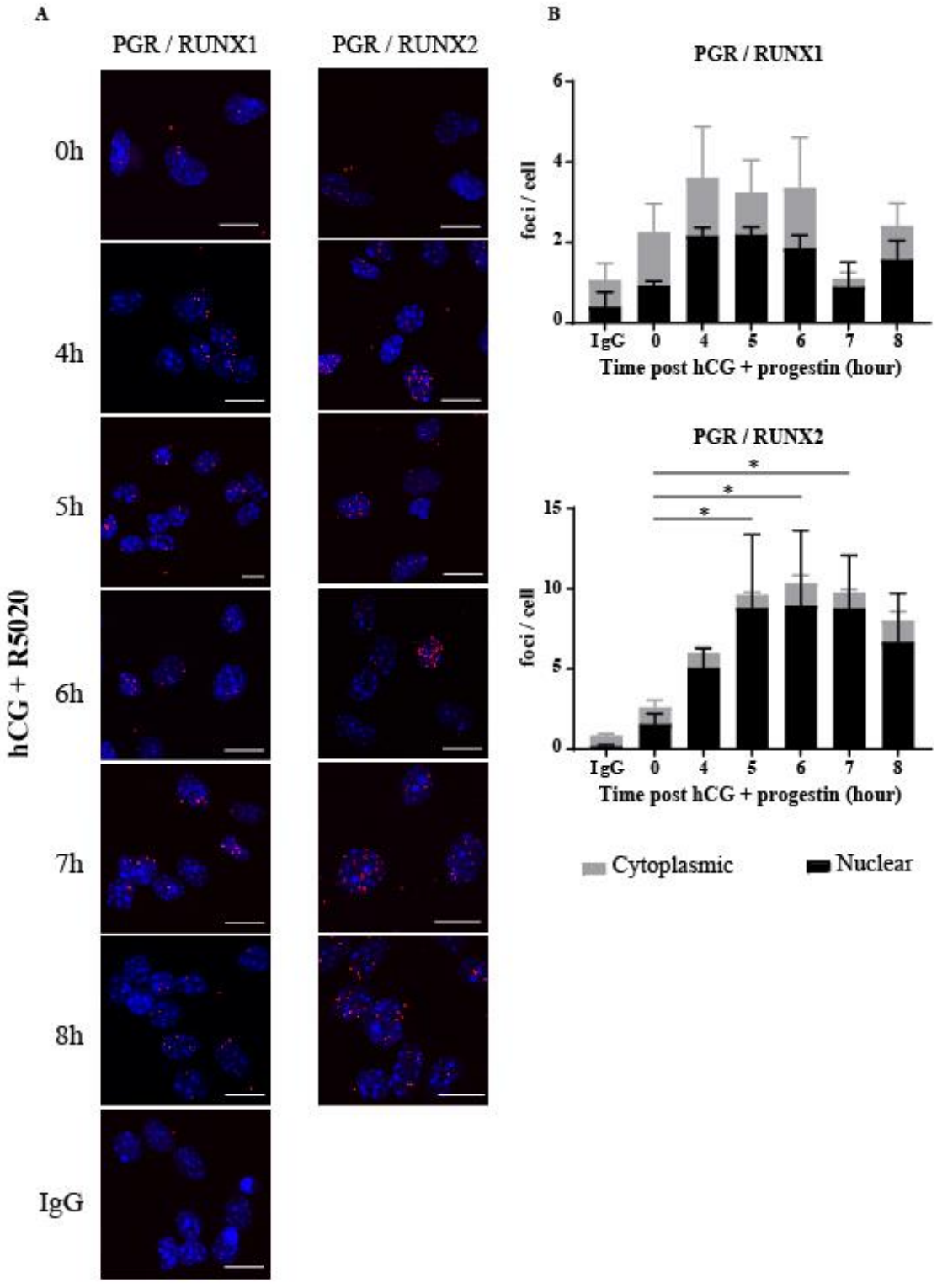
A
PGR / RUNX1
PGR / RUNX2
0h
4h
5h
6h
7h
8h
IgG
hCG + R5020
B
PGR / RUNX1
foci / cell
IgG 0 4 5 6 7 8
Time post hCG + progestin (hour)
PGR / RUNX2
foci / cell
IgG 0 4 5 6 7 8
Time post hCG + progestin (hour)
Cytoplasmic
Nuclear

Figure 6.4 LH-dependent dynamic PGR / RUNX interactions in response to ovulatory stimulus.

Granulosa cells were treated *in vitro* with hCG and R5020 for the duration indicated. **(A)** Representative images of PLA showing the interaction between PGR and RUNX1 (left column) and RUNX2 (right column) or IgG control (bottom row). PLA signals are red puncta and nuclei were stained with DAPI in blue. Scale bar = 10 µm. **(B)** Quantification of PLA signals, displayed as the number of foci per cell. PLA was performed in 3 biological replicates (4 mice per replicate) and quantification was through ImageJ 'Find Maxima' function on at least three images per condition per replicate. P-value indicates two-way ANOVA statistical analysis for row factor (time factor), p = 0.0737 (PGR/RUNX1), p = 0.0251 (PGR/RUNX2). Asterisk indicates statistically different samples.

6.4 DISCUSSION

Both PGR and RUNX1 are transcription factors that are known to regulate ovulatory genes in peri-ovulatory granulosa cells. In the ovary, the temporal and spatial pattern of expression for PGR and RUNX1 are highly similar, with both being rapidly and transiently expressed in response to the LH surge [6,17]. The detailed analysis of the PGR cistrome led to the hypothesis that PGR and RUNX potentially cooperate in peri-ovulatory granulosa cells and are involved in the regulation of ovulatory gene expression, with a possible direct interaction between the two transcription factors. As a physical interaction between PGR and RUNX1 in granulosa cells in response to ovulatory cues was also demonstrated, it became imperative that the relationship between these two transcription factors on a functional level be explored. To investigate this, combined analysis of PGR and RUNX1 cistromes as well as comparison of their genome-wide interaction with genes regulated by ovulatory stimulus were performed.

The findings of this chapter showed that PGR and RUNX1 shared a remarkably high number of mutual DNA targets, especially within transcriptionally active regions. One remarkable observation was the very high prevalence of RUNX1 in promoter-centric PGR binding at a level well beyond random chance. PGR chromatin binding is specifically enriched at transcriptionally active promoter regions in granulosa cells but not in the uterus. Here it was found that PGR-bound sites in the absence of RUNX1 co-binding were dramatically less likely to bind to promoter regions, whereas shared PGR/RUNX1 binding sites were as highly enriched in proximal promoter regions as RUNX-only bound regions. These results indicate that the promoter selective targeting of PGR is dependent on RUNX1. On the other hand, in the absence of PGR, RUNX1 still preferentially bound promoter regions, suggesting that the co-dependence for promoter targeting was not reciprocal. While the temporal dynamics of RUNX1 and PGR chromatin binding was not directly determined, these results lead to the implication that RUNX1 may act as a pioneer factor in directing PGR to target chromatin regions. The fact that RUNX1-bound sites were enriched for the canonical motif for PGR (PRE/NR3C motif) even before the LH surge, supports the conclusions that RUNX1 binds chromatin before PGR and that RUNX1 has a role in the granulosa-specific PGR-chromatin binding pattern. Consistent with this conclusion, RUNX1 and RUNX3 have been previously reported to behave as pioneer factors through the recruitment of chromatin modifiers to open up chromatin for the access of other transcription factors [18,19]. In addition to the canonical binding partner CBFβ, RUNX proteins are also known to interact with other transcription

modulators, including both activators and repressors, in various biological contexts [20]. Further studies using a granulosa cell-specific RUNX1 KO mouse model or *in vitro* RUNX1 knockdown granulosa cells will be able to test the theory that RUNX1 is necessary for PGR to bind its target cistrome.

Functional analysis of PGR and RUNX1 cistromes in combination with ovulatory gene profile in granulosa cells showed that PGR and RUNX1 interact on a functional level during ovulatory gene regulation. A striking number of hCG-responsive DEGs were found to have both PGR and RUNX1 binding in their proximity, indicating a partnership between PGR and RUNX1 in regulating downstream gene expression. These mutual target genes underlie the highly similar corresponding enriched pathway profiles of PGR and RUNX1 cistromes, as indicated in the analysis of Gene Ontology and canonical pathways in PGR and RUNX1 ChIP-seq data. Thus, both transcription factors co-ordinately regulate gene expression during ovulation and the cooperation between both factors is likely critical for this tissue specific regulation. Among mutual PGR/RUNX1 target ovulatory genes are a number of genes identified as PGR-dependent in previous studies. ADAMTS1, a member of the ADAMTS family, is involved in matrix remodelling and morphology of the cumulus-oocyte complex through cleavage of versican and a lack of ADAMTS1 can affect ovulation and lead to subfertility in female mice [21,22]. Reporter assays have shown that PGR regulates *Adamts1* expression via interaction with G/C-box SP1/SP3-binding sites in the *Adamts1* proximal promoter region [11]. Data from this study now shows that both PGR and RUNX1 shared the same binding site at the *Adamts1* promoter, which is not bound by RUNX1 prior to the LH surge. Another mutual target of PGR and RUNX1 identified in this study is CXCR4. CXCR4 and its ligand, CXCL12, are induced by hCG in granulosa cells in humans and mouse and in sheep these factors have been shown to promote cumulus expansion and oocyte maturation [23-25]. Other genes that are known PGR targets, including *Zbtb16*, a zinc finger-domain transcription factor shown to be progesterone-responsive in human endometrial stromal cells [26], and *Edn2*, a vasoactive growth factor implicated in the follicular rupture process [27], are also bound by both PGR and RUNX1. Genes that were previously linked to RUNX1 activity are also found to be in fact mutual PGR/RUNX1 targets, including *Hapln1* and *Rgcc* [28,29]. Interestingly, PGR and RUNX1 binding was found in open chromatin regions in the gene boundary of both *Runx1* and *Runx2*, implying a role of PGR in regulation of *Runx1* and *Runx2* as well as an auto-regulatory role of RUNX1 and of RUNX1 to *Runx2*. Such cross-regulatory function has previously been described for the CBFβ- and RUNX2-mediated expression of *Runx1* [7].

The cooperation between PGR and specific interactomes in different biological contexts is important for the regulation of PGR transactivation functions, as has been well illustrated in the context of PGR action in mammary and uterine tissues [9]. Direct interaction between PGR and RUNX transcription factors was observed in cultured granulosa cells upon stimulation with hCG and progestin. The interaction between PGR and RUNX1 or RUNX2 in cultured granulosa cells is shown to be dynamically regulated by these ovulatory hormones and predominantly in the nuclear compartment, indicating that PGR and RUNX1/2 are likely to be involved in the same transcription complex that is activated by the ovulatory LH surge stimulus *in vivo*. These PGR/RUNX interactions highlight the role of RUNX1 and RUNX2 in partnership with PGR in granulosa cells to mediate follicular rupture. RUNX1 was selected for ChIP-seq analysis because it has been shown to be important for granulosa cell functions through promoting important gene expression [6]. However, RUNX2 is also known to be induced by the ovulatory stimulus and is involved in both transcription induction and repression in granulosa cells [30,31]. A more thorough investigation into the RUNX2 cistrome and RUNX2-dependent transcriptome in peri-ovulatory granulosa cells would be illuminating in fully characterising the role of RUNX2 in ovulation. An interaction between RUNX members and other SR, namely AR and GR, have also been reported [13,14,32]. Intriguingly, these interactions involve binding of RUNX to the DBD of steroid receptors, which results in the mutual sequestering of steroid receptors and RUNX from target genes and thereby having a repressive role on steroid receptors and RUNX activities [33]. In certain contexts however, co-binding of RUNX and steroid receptors at target genes can have an additive effect on transcription induction [14]. Such a mechanism does not seem to be the case in PGR/RUNX interactions in granulosa cells where there is a positive impact on the transactivation function of PGR; and thus it is likely that a different regulatory mechanism is at play, perhaps involving interactions with other secondary modulators.

In summary, the relationship between PGR and RUNX1 has been illustrated in the context of ovulation. PGR and RUNX1 formed a physical interaction at target chromatin sites in response to ovulatory cues and this had consequences on downstream gene expression. As an interaction between PGR and other transcription factors has also been confirmed (RUNX2, JUND and LRH1) or implied (GATA, CEBP transcription factors), it is possible that these transcription factors are also parts of the mutual transcription complex with PGR and RUNX1. Whether this is the case requires further investigation. The role of other transcription mediators that do not

directly interact with DNA, such as HDAC and SRC, in modulating PGR transcriptional regulatory functions also needs to be determined.

6.5 REFERENCES

1 Lydon, J. P., DeMayo, F. J., Funk, C. R., Mani, S. K., Hughes, A. R., Montgomery, C. A., Jr., Shyamala, G., Conneely, O. M. & O'Malley, B. W. Mice lacking progesterone receptor exhibit pleiotropic reproductive abnormalities. *Genes Dev* **9**, 2266-2278 (1995).

2 Akison, L. & Robker, R. The Critical Roles of Progesterone Receptor (PGR) in Ovulation, Oocyte Developmental Competence and Oviductal Transport in Mammalian Reproduction. *Reproduction in Domestic Animals* **47**, 288-296, doi:10.1111/j.1439-0531.2012.02088.x (2012).

3 Akison, L. K., Boden, M. J., Kennaway, D. J., Russell, D. L. & Robker, R. L. Progesterone receptor-dependent regulation of genes in the oviducts of female mice. *Physiological Genomics* **46**, 583-592, doi:10.1152/physiolgenomics.00044.2014 (2014).

4 Robker, R. L., Russell, D. L., Espey, L. L., Lydon, J. P., O'Malley, B. W. & Richards, J. S. Progesterone-regulated genes in the ovulation process: ADAMTS-1 and cathepsin L proteases. *Proc Natl Acad Sci U S A* **97**, 4689-4694 (2000).

5 Mazur, E. C., Vasquez, Y. M., Li, X., Kommagani, R., Jiang, L., Chen, R., Lanz, R. B., Kovanci, E., Gibbons, W. E. & DeMayo, F. J. Progesterone Receptor Transcriptome and Cistrome in Decidualized Human Endometrial Stromal Cells. *Endocrinology* **156**, 2239-2253, doi:10.1210/en.2014-1566 (2015).

6 Jo, M. & Curry, T. E., Jr. Luteinizing Hormone-Induced RUNX1 Regulates the Expression of Genes in Granulosa Cells of Rat Periovulatory Follicles. *Molecular Endocrinology* **20**, 2156-2172, doi:10.1210/me.2005-0512 (2006).

7 Lee-Thacker, S., Choi, Y., Taniuchi, I., Takarada, T., Yoneda, Y., Ko, C. & Jo, M. Core binding factor β expression in ovarian granulosa cells is essential for female fertility. *Endocrinology* **159**, 2094-2109 (2018).

8 Nicol, B., Grimm, S. A., Chalmel, F., Lecluze, E., Pannetier, M., Pailhoux, E., Dupin-De-Beyssat, E., Guiguen, Y., Capel, B. & Yao, H. H. C. RUNX1 maintains the identity of the fetal ovary through an interplay with FOXL2. *Nature communications* **10**, 5116 (2019). <https://doi.org/10.1038/s41467-019-13060-1>.

9 Grimm, S. L., Hartig, S. M. & Edwards, D. P. Progesterone Receptor Signaling Mechanisms. *Journal of Molecular Biology* **428**, 3831-3849, doi:https://doi.org/10.1016/j.jmb.2016.06.020 (2016).

10 Nadeem, L., Shynlova, O., Matysiak-Zablocki, E., Mesiano, S., Dong, X. & Lye, S. Molecular evidence of functional progesterone withdrawal in human myometrium. *Nature Communications* **7**, 11565, doi:10.1038/ncomms11565 (2016).

11 Doyle, K. M. H., Russell, D. L., Sriraman, V. & Richards, J. S. Coordinate Transcription of the ADAMTS-1 Gene by Luteinizing Hormone and Progesterone Receptor. *Molecular Endocrinology* **18**, 2463-2478, doi:10.1210/me.2003-0380 (2004).

12 Chuang, L. S. H., Ito, K. & Ito, Y. RUNX family: Regulation and diversification of roles through interacting proteins. *International Journal of Cancer* **132**, 1260-1271, doi:10.1002/ijc.27964 (2013).

13 Kawate, H., Wu, Y., Ohnaka, K. & Takayanagi, R. Mutual transactivational repression of Runx2 and the androgen receptor by an impairment of their normal compartmentalization. *The Journal of Steroid Biochemistry and Molecular Biology* **105**, 46-56, doi:https://doi.org/10.1016/j.jsbmb.2006.11.020 (2007).

14 Little, G. H., Baniwal, S. K., Adisetiyo, H., Groshen, S., Chimge, N.-O., Kim, S. Y., Khalid, O., Hawes, D., Jones, J. O., Pinski, J., Schones, D. E. & Frenkel, B. Differential

Effects of RUNX2 on the Androgen Receptor in Prostate Cancer: Synergistic Stimulation of a Gene Set Exemplified by SNAI2 and Subsequent Invasiveness. *Cancer Research* **74**, 2857-2868, doi:10.1158/0008-5472.can-13-2003 (2014).

15 Bianco, S., Bellefleur, A.-M., Beaulieu, É., Beauparlant, C. J., Bertolin, K., Droit, A., Schoonjans, K., Murphy, B. D. & Gévry, N. The Ovulatory Signal Precipitates LRH-1 Transcriptional Switching Mediated by Differential Chromatin Accessibility. *Cell Reports* **28**, 2443-2454.e2444, doi:https://doi.org/10.1016/j.celrep.2019.07.088 (2019).

16 Schneider, C. A., Rasband, W. S. & Eliceiri, K. W. NIH Image to ImageJ: 25 years of image analysis. *Nature Methods* **9**, 671-675, doi:10.1038/nmeth.2089 (2012).

17 Park, O.-K. & Mayo, K. E. Transient Expression of Progesterone Receptor Messenger RNA in Ovarian Granuiosa Cells after the Preovulatory Luteinizing Hormone Surge. *Molecular Endocrinology* **5**, 967-978, doi:doi:10.1210/mend-5-7-967 (1991).

18 Oakford, P. C., James, S. R., Qadi, A., West, A. C., Ray, S. N., Bert, A. G., Cockerill, P. N. & Holloway, A. F. Transcriptional and epigenetic regulation of the GM-CSF promoter by RUNX1. *Leukemia Research* **34**, 1203-1213, doi:https://doi.org/10.1016/j.leukres.2010.03.029 (2010).

19 Lee, J.-W., Kim, D.-M., Jang, J.-W., Park, T.-G., Song, S.-H., Lee, Y.-S., Chi, X.-Z., Park, I. Y., Hyun, J.-W., Ito, Y. & Bae, S.-C. RUNX3 regulates cell cycle-dependent chromatin dynamics by functioning as a pioneer factor of the restriction-point. *Nature Communications* **10**, 1897, doi:10.1038/s41467-019-09810-w (2019).

20 Lichtinger, M., Hoogenkamp, M., Krysinska, H., Ingram, R. & Bonifer, C. Chromatin regulation by RUNX1. *Blood Cells, Molecules, and Diseases* **44**, 287-290, doi:https://doi.org/10.1016/j.bcmd.2010.02.009 (2010).

21 Mittaz, L., Russell, D. L., Wilson, T., Brasted, M., Tkalcevic, J., Salamonsen, L. A., Hertzog, P. J. & Pritchard, M. A. Adamts-1 Is Essential for the Development and Function of the Urogenital System1. *Biology of Reproduction* **70**, 1096-1105, doi:10.1095/biolreprod.103.023911 (2004).

22 Brown, H. M., Dunning, K. R., Robker, R. L., Boerboom, D., Pritchard, M., Lane, M. & Russell, D. L. ADAMTS1 Cleavage of Versican Mediates Essential Structural Remodeling of the Ovarian Follicle and Cumulus-Oocyte Matrix During Ovulation in Mice1. *Biology of Reproduction* **83**, 549-557, doi:10.1095/biolreprod.110.084434 (2010).

23 Choi, Y., Park, J. Y., Wilson, K., Rosewell, K. L., Brännström, M., Akin, J. W., Curry, T. E., Jr. & Jo, M. The expression of CXCR4 is induced by the luteinizing hormone surge and mediated by progesterone receptors in human preovulatory granulosa cells. *Biology of reproduction* **96**, 1256-1266, doi:10.1093/biolre/iox054 (2017).

24 Zhang, R.-N., Pang, B., Xu, S.-R., Wan, P.-C., Guo, S.-C., Ji, H.-Z., Jia, G.-X., Hu, L.-Y., Zhao, X.-Q. & Yang, Q.-E. The CXCL12-CXCR4 signaling promotes oocyte maturation by regulating cumulus expansion in sheep. *Theriogenology* **107**, 85-94, doi:https://doi.org/10.1016/j.theriogenology.2017.10.039 (2018).

25 Hernandez-Gonzalez, I., Gonzalez-Robayna, I., Shimada, M., Wayne, C. M., Ochsner, S. A., White, L. & Richards, J. S. Gene Expression Profiles of Cumulus Cell Oocyte Complexes during Ovulation Reveal Cumulus Cells Express Neuronal and Immune-Related Genes: Does this Expand Their Role in the Ovulation Process? *Molecular Endocrinology* **20**, 1300-1321, doi:10.1210/me.2005-0420 (2006).

26 Kommagani, R., Szwarc, M. M., Vasquez, Y. M., Peavey, M. C., Mazur, E. C., Gibbons, W. E., Lanz, R. B., DeMayo, F. J. & Lydon, J. P. The Promyelocytic Leukemia Zinc Finger Transcription Factor Is Critical for Human Endometrial Stromal Cell Decidualization. *PLoS genetics* **12**, e1005937-e1005937, doi:10.1371/journal.pgen.1005937 (2016).

27 Palanisamy, G. S., Cheon, Y.-P., Kim, J., Kannan, A., Li, Q., Sato, M., Mantena, S. R., Sitruk-Ware, R. L., Bagchi, M. K. & Bagchi, I. C. A Novel Pathway Involving Progesterone Receptor, Endothelin-2, and Endothelin Receptor B Controls Ovulation in Mice. *Molecular Endocrinology* **20**, 2784-2795, doi:10.1210/me.2006-0093 (2006).

28 Park, E.-S., Choi, S., Muse, K. N., Curry, T. E., Jr. & Jo, M. Response Gene to Complement 32 Expression Is Induced by the Luteinizing Hormone (LH) Surge and Regulated by LH-Induced Mediators in the Rodent Ovary. *Endocrinology* **149**, 3025-3036, doi:10.1210/en.2007-1129 (2008).

29 Liu, J., Park, E.-S., Curry, T. E., Jr. & Jo, M. Periovulatory expression of hyaluronan and proteoglycan link protein 1 (Hapln1) in the rat ovary: hormonal regulation and potential function. *Mol Endocrinol* **24**, 1203-1217, doi:10.1210/me.2009-0325 (2010).

30 Park, E.-S., Lind, A.-K., Dahm-Kähler, P., Brännström, M., Carletti, M. Z., Christenson, L. K., Curry, T. E., Jr. & Jo, M. RUNX2 Transcription Factor Regulates Gene Expression in Luteinizing Granulosa Cells of Rat Ovaries. *Molecular Endocrinology* **24**, 846-858, doi:10.1210/me.2009-0392 (2010).

31 Park, E.-S., Park, J., Franceschi, R. T. & Jo, M. The role for runt related transcription factor 2 (RUNX2) as a transcriptional repressor in luteinizing granulosa cells. *Molecular and Cellular Endocrinology* **362**, 165-175, doi:https://doi.org/10.1016/j.mce.2012.06.005 (2012).

32 Ning, Y.-M. & Robins, D. M. AML3/CBFα1 Is Required for Androgen-specific Activation of the Enhancer of the Mouse Sex-limited Protein (Slp) Gene. *Journal of Biological Chemistry* **274**, 30624-30630, doi:10.1074/jbc.274.43.30624 (1999).

33 Baniwal, S. K., Khalid, O., Sir, D., Buchanan, G., Coetzee, G. A. & Frenkel, B. Repression of Runx2 by Androgen Receptor (AR) in Osteoblasts and Prostate Cancer Cells: AR Binds Runx2 and Abrogates Its Recruitment to DNA. *Molecular Endocrinology* **23**, 1203-1214, doi:10.1210/me.2008-0470 (2009).

CHAPTER 7 PGR regulates isoform-specific transcriptomes in granulosa cells

7.1 INTRODUCTION

Progesterone receptor consists of two major isoforms (PGR-A and PGR-B) that are transcribed from two distinct TSS. While the two isoforms share almost all important structural domains for ligand response and transcriptional activation, PGR-B possesses an extra 164 amino acids at the N-terminus, giving it an additional AF-3 domain that allows for unique interactions with a host of coactivators which enhances its transactivation functions [1]. While other PGR isoforms have also been described, PGR-A and B remain the most prominent isoforms with important implications on PGR functions in the reproductive tract and in mammary tissues, both in normal physiology and in tumour development.

In the ovary, both PGR isoforms are induced by the LH surge; however, the ratio between isoforms (PGR-A:PGR-B) is approximately 2:1 in mouse granulosa cells [2]. Even though both isoforms are expressed in granulosa cells of pre-ovulatory follicles, PGR-A is accredited as the more essential isoform in ovulation. This was determined from studies on KO mouse models that are specific to each PGR isoform. As the two isoforms are translated from two distinct start codons, SNP mutation at these sites allows for the specific knockout of the A-isoform (AKO) [3] or B-isoform (BKO) [4]. A similar reproductive phenotype was observed in both total PGRKO and AKO [3,5]. Specifically, female mice that are null for PGR or mice that have a mutation which prevents production of functional PGR-A exhibit a specific failure of follicle rupture, but not luteinisation, even after gonadotropin stimulation and are thus infertile (PGRKO) or subfertile (AKO) [3,6]. Phenotypical similarities between total PGRKO and specific AKO mutants are also observed in other reproductive tissues, such as in the uterus where the ablation of total PGR or just PGR-A results in a disrupted decidualisation response. However, in mammary tissues, the role of PGR-A is not as prominent as PGR-B [3,4]. While a number of PGR-driven ovulatory genes have been identified in granulosa cells, specific actions of the two PGR isoforms have not been investigated. Known PGR-regulated genes in ovary include classic PGR targets, such as *Adamts1*, *Pparg* and *Edn2* [7-9]; however, a confirmation of genes

with exclusive regulation by PGR-A has yet to be elucidated, which would solidify the importance of PGR-A in the mechanism of ovulation.

The B-isoform, on the other hand, has been largely overlooked in the context of ovarian functions due to the lack of abnormal ovarian physiology observed in the BKO mouse model. Unlike PGRKO and AKO, female mice lacking PGR-B do not experience anovulation and have normal fertility in comparison with WT cohorts [4]. However, as AKO female mice are not completely infertile, PGR-B potentially has a role that can functionally compensate, albeit only partially, in the absence of PGR-A. Since the ablation of PGR-B has no effect on female fertility, PGR-A by itself seems to be sufficient in ovulation and other female reproductive functions. In the uterus, PGR-B plays little role before implantation, as seen in the normal progesterone-dependent epithelial proliferation in BKO mice [4]. In humans, the suppression of PGR during labour is important for inducing parturition [10]. However, PGR-B female mice are fertile, suggesting that there is redundancy in the uterine role of PGR-B in the establishment and maintenance of pregnancy [4]. In other tissue types, the role of PGR-B is more prominent. In mammary tissues, PGR-B is the main factor at play in mammary development, as seen in defective alveologenesis and ductal development in mice that have aberrant PGR-B overexpression or are PGR-B deficient, respectively [4,11].

While each PGR isoform seems to have discrete tissue-specific functions, the interplay between the two PGR isoforms is in fact rather complex and is precisely regulated in a spatiotemporal pattern and tissue-specific manner. In tissues that are PGR-positive, both PGR-A and PGR-B tend to be present; however, they are often not expressed at equal levels. In the context of cancer, changes in the PGR-A:PGR-B ratio can lead to abnormal cellular responses and the elevation of tumour development [12]. Interestingly, in both of these tissue contexts, PGR-A displays trans-repressive functions, not only on the auto-regulation of PGR-B but also other steroid receptors including GR and ER [13]. In these cases, PGR-A is identified as a suppressor of PGR-B activity without affecting PGR-B expression level [1]. The peptide sequence IKEE at the N-terminus of PGR-B is shown to be important in the PGR-A regulated inhibition of PGR-B [13], although the exact nature of the inhibitory process, such as the involvement of other co-repressors or the effect on PGR-B stability, is still poorly understood. In the uterus, this auto-inhibitory function plays an important role during parturition in which uterine progesterone withdrawal induces PGR-A trans-repression function, leading to a suppression of PGR-B and an increase in contraction and inflammation genes that are required for labour [10]. In the context

of granulosa cells, it is reasonable to suggest that a similar cross-regulatory relationship is possible, and since both isoforms are present in peri-ovulatory granulosa cells, it is valid to take a further look at the differences in PGR-A and PGR-B activities in granulosa cells.

Chapter 2 previously described the PGR-dependent transcriptome in mouse peri-ovulatory granulosa cells. Such transcriptome was obtained from microarray analysis, a relatively insensitive approach where only known transcripts of high abundance were identified, thus low expressed or novel transcript variants associated with ovulation are not accounted for in the microarray dataset. Microarray also fails to capture transcripts that are not well-defined such as lncRNA. Furthermore, the specific role of each isoform cannot be dissected from a total PGRKO model. With the current advances in transcriptomic analysis and the establishment of well-described isoform-specific KO animal models, many of the deficiencies in our knowledge of PGR regulation in ovulation can be circumvented, which allows for the establishment the specific PGR-A and PGR-B roles. Thus, in order to fully determine the effect of PGR and each of its isoforms, isoform-specific transcriptomes were obtained from hCG-stimulated granulosa cells from mice that were WT or KO for total PGR, PGR-A only or PGR-B only, using RNA-seq from total RNA extract. By individually examining the transcriptome-wide consequences of individual mutants of PGR-A and PGR-B, the specific contribution of each isoform is determined in full detail, which allows for the identification of novel PGR-A and PGR-B functions. As PGRKO and AKO female mice have the closest matched phenotypes, it was hypothesised that genes regulated by PGR-A would most closely mirror total PGR. Furthermore, identifying the genes regulated by PGR-A versus PGR-B using RNA-seq would enable a deeper interpretation of the modes of action of each isoform and their potential interaction with other transcription factors in granulosa cells. Finally, comparing dysregulated transcriptomes in PGRKO to those in the PGR-A and PGR-B specific KOs will refine current insights into the genes that may be critical for ovulation.

7.2 MATERIALS & METHODS

7.2.1 Animals and breeding strategy

Three transgenic mouse models were used in this chapter, consisting of knock-out strains for PGR, PGR-A only or PGR-B only.

C.129S7(B6)-Pgr^{tm1Bwo}/OmcJ (PGRKO) mice are a targeted mutation strain with the Jackson Laboratory designation Pgr^{tm1Bwo} (targeted mutation 1, Bert W O'Malley, JAX stock #030883). In this model, the *Pgr* gene was disrupted by the insertion of a neomycin cassette into exon 1, which is downstream to the TSS of both isoform A and B. The genetic background for this strain is 129S7/SvEvBrd-Hprt^{+}. B6;129S7-Pgr^{tm1Omc}/J (PGR-A KO) mice are a targeted mutation strain with the Jackson Laboratory designation Pgr^{tm1Omc} (targeted mutation 1, Orla M Conneely, JAX stock #022464). In order to knockout PGR isoform A without disrupting isoform B, the translational start site at codon 166 (specific to isoform A) was modified to encode alanine. The genetic background for this strain is 129S7/SvEvBrd-Hprt^{b-m2}. B6;129S7-Pgr^{tm2Omc}/J (PGR-B KO) mice are a targeted mutation strain with the Jackson Laboratory designation Pgr^{tm2Omc} (targeted mutation 2, Orla M Conneely, JAX stock #022465). In order to knockout PGR isoform B without disrupting isoform A, the start codon of isoform B was modified to encode leucine (ATG to CTG). The genetic background for this strain is 129S7/SvEvBrd-Hprt^{b-m2}. See Figure 7.1A for a schematic of the gene knockout strategy for each strain. All three mouse strains were originated from the Baylor College of Medicine and the expression of PGR in each strain has been confirmed using Western blot, described in the respective publication [3-5]. Mice that are null for PGR are hereafter referred to as PGRKO, and mice null for one of the isoforms are AKO or BKO; while their WT littermates are referred to as PGRWT, AWT or BWT, respectively.

Founder mice were obtained from the Jackson Laboratory at 9 weeks old. Breeding colonies were maintained at the Laboratory Animal Services (University of Adelaide, Australia) SPF facility. All mice were maintained in 12 h light /12 h dark conditions and given water and rodent chow *ad libitum*. All experiments were approved by The University of Adelaide Animal Ethics Committee and were conducted in accordance with the Australian Code of Practice for the Care and Use of Animals for Scientific Purposes (ethics numbers m/2018/100 and m/2018/122) and guidelines from the Office of the Gene Technology Regulator (OGTR) (IBC dealings 14797, 14798 and 14799). In order to establish the breeding colonies from the given stock, het/het pairs were established to generate a mixture of WT and KO mice (for experiments) and heterozygotes (for future breeding pairs). Animals used in experiments were generated from at least 6 breeding pairs.

7.2.2 Genotyping of PGRKO mouse strains

Mice from each strain were genotyped from DNA extracted from ear biopsies at weaning and tail tips at culling. Genomic DNA was obtained by digesting tissue in 250 µl Digestion Solution (20 mM EDTA, 40 mM Tris, 120 mM NaCl, 1% SDS, pH 8.0) and 5 µl of 10 mg/ml Proteinase K (Sigma) at 55ºC for at least 4 h with constant shaking. Cellular debris was precipitated by adding 250 µl of 4 M ammonium acetate and incubating at room temperature for 15 minutes with mixing. DNA was precipitated using 100% ethanol, washed with 70% ethanol and resuspended in water.

7.2.2.1 PGRKO genotyping

For PGRKO mice, genotyping was through PCR and gel electrophoresis analysis as described by JAX. DNA was amplified using primers specific for either the WT *Pgr* gene or the neomycin insert. Genotyping was accomplished by a two-way PCR strategy. The antisense mut primer was used with a sense primer from the *Pgr* gene to amplify a 200 bp product from the mutant allele. The antisense WT primer was used with the same sense primer to produce a 262 bp WT sequence. For the PCR reaction, GoTaq Flexi DNA Polymerase and accompanied buffer was used (Promega, Annandale, NSW, Australia). The components for the 20 µl reaction are: 4 µl GoTaq Green Master Mix, 1.2 µl $MgCl_2$, 0.2 µl dNTPs, 0.1 µl sense primer, 0.1 µl antisense primer, 0.1 µl DNA Polymerase, 2.5 µl genomic DNA template and 11.8 µl H_2O. The thermal cycle for this PCR was: 95ºC for 2 mins, 40 cycles x [95ºC for 1 min, 60ºC for 30 secs, 72ºC for 1 min], then 72ºC for 5 minutes and hold at 4ºC; using an Applied Biosystems GeneAmp PCR System 9700 Thermal Cycler (Applied Biosystems, Thermo Fisher). Amplified products were visualised by agarose gel electrophoresis. Primer sequences were:

PGR sense	5'– GAGGTGGAAGAGGACAGTGG – 3'
PGR antisense (WT)	5'– TGGGCACATGGATGAAATC – 3'
Neo antisense (mut)	5'– GCCAGAGGCCACTTGTGTAG – 3'

The genotype of PGRKO animals was determined based on PCR specific to the WT or neo-containing mutant alleles. Examples with the presence of the WT band (262 bp) and the mut band (200 bp), with heterozygous animals showing both bands, are shown in Figure 7.1B.

7.2.2.2 AKO genotyping

Genotyping of the PRAKO mouse strain was through real-time PCR followed by end-point analysis as described by JAX. DNA was amplified using sense and antisense primers targeting the *Pgr* gene. For the detection of the PGR-A SNP mutation, genotype-specific primers were designed with a fluorescence tag at the 5' end (VIC dye for WT primer and FAM dye for mut primer) and MGB quencher conjugated at the 3' end. Each primer probe detects either the WT sequence or mutated SNP sequence. The component for the 10 µl reaction are as follow: 5 µl Taqman ProAmp MasterMix (Thermo Fisher), 0.25 µl SNP Taqman assay, 1 µl genomic DNA and 3.75 µl H_2O. The thermal cycle for this reaction was: 60ºC for 30 secs, 95ºC for 10 mins, 40 cycles x [95ºC for 15 secs, 60ºC for 1 min], 60ºC for 30 secs and hold at 4ºC; using a QuantStudio12K Flex System (Thermo Fisher). Allelic detection was determined through analysis using the corresponding Genotyping function of the QuantStudio System.

Sequences of the primers and probes are:

PGR-A sense	5'– GCCATCACTTCCTGGTGTCT – 3'
PGR-A antisense	5'– TGGGTGGTGACAGTCCTTTG – 3'
PGR-A WT	VIC 5'– CCCGCTCATGAGTCGGC– 3'
PGR-A mut SNP	FAM 5'– CCCGCTCGCTAGTCGGC – 3'

The genotype of AKO animals was determined based on the ratio of KO-specific and WT-specific fluorescent probe from Taqman assays designed specifically for each mutation. An example of allelic discrimination plots is shown in Figure 7.1C, in which WT animals show high WT:KO ratio, KO animals with low WT:KO ratio and het animals in between. A negative control is included (H_2O control) in which neither of the fluorophores was detected.

7.2.2.3 BKO strain

Genotyping for the BKO strain is as described above for the AKO mouse strain. Sequences of the primers and probes are:

PGR-B sense	5'– AGACAGGGGAGGAGAAAAGG – 3'
PGR-B antisense	5'– GCGAGACTACAGACGACACG – 3'
PGR-B WT	VIC 5'– CGTCATGACTGAGCTGCA G– 3'
PGR-B mut SNP	FAM 5'– CGTCCTGACTGAGCTCCAG – 3'

The genotype of BKO animals was determined based on the ratio of KO-specific and WT-specific fluorescent probe from Taqman assays designed specifically for each mutation. An example of allelic discrimination plots is shown in Figure 7.1D, in which WT animals show high WT:KO ratio, KO animals with low WT:KO ratio and het animals in between.

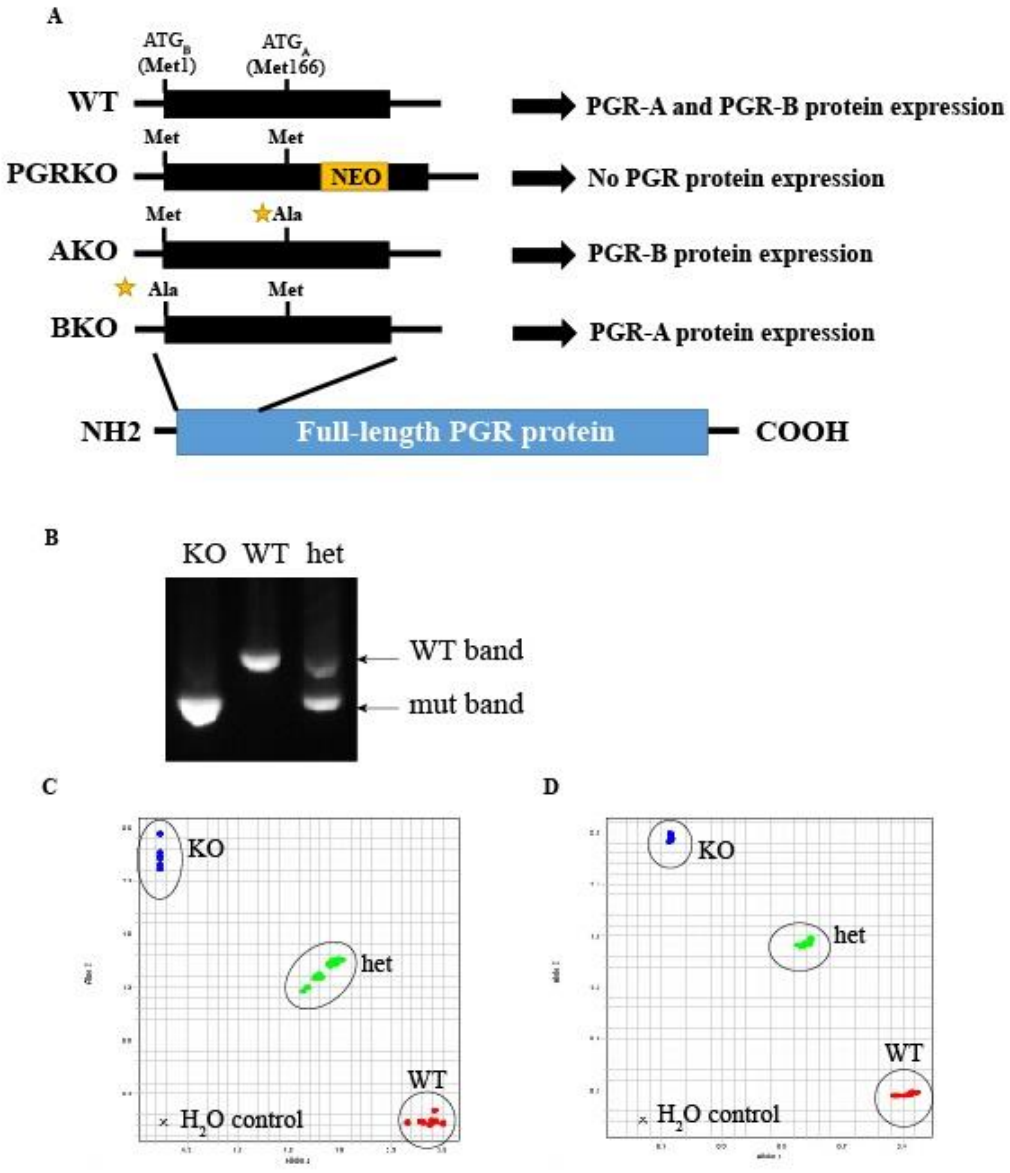

Figure 7.1 Strategies for KO generation.

(A) The targeted mutation strategies for all three KO strains involving genetic modification of exon 1 of the *Pgr* gene (encoding the N-terminus of PGR). ATG_A and ATG_B are the translation start sites for PGR-A and PGR-B respectively. For total PGRKO, a *Neo* cassette was inserted into exon 1 downstream of both TSS causing a frameshift mutation to disrupt both isoforms. For AKO, the ATG sequence specific for PGR-A was mutated to encode Alanine. The BKO, the ATG sequence for PGR-B was mutated to Leucine. **(B)** Representative gel electrophoresis image for genotyping of the PGRKO colony. WT, het and KO genotypes identification was based on the presence of the WT band (262 bp) and the mut band (200 bp). **(C-D)** Allelic discrimination plot for genotyping of the AKO colony (C) and BKO colony (D). For each strain, isoform-specific SNP are detected by fluorescent Taqman probes and genotype is determined based on the ratio of WT:KO fluorophore.

7.2.3 Western blot

WT and KO 3-4 weeks old female mice were stimulated for superovulation by 5 IU eCG followed 46 h later by 5 IU hCG. Mice were killed by cervical dislocation at 6 h post-hCG stimulation and ovaries dissected and punctured with a 26G needle for COC/GC isolation. Lysate was prepared from COC/GC pooled from 2 ovaries by adding 100 µl LDS Sample Buffer, 1 µl β-mercaptoethanol and 1 µl benzonase, then incubation for 10 minutes at 65^{o}C for cell lysis and protein denaturation. Western blot was performed and quantified as described in section 2.2.2.3. Antibodies for PGR and H3 are as listed in Appendix 2.

7.2.4 RNA-sequencing

7.2.4.1 Tissue sample collection and RNA extraction

21-27 days old female mice that were WT or KO were injected with 5 IU eCG and 5IU hCG 46 h post-eCG injection. Mice were sacrificed 8 h post-hCG stimulation and ovaries were punctured to collect granulosa cells, which were snap frozen in liquid nitrogen upon collection. For each knockout strain, 12 female mice of each genotype were used (24 mice per strain). For each knockout strain, a total of 4 biological replicates of each genotype were obtained, with each biological replicate generated from ovarian material pooled from 3 animals. RNA extraction was performed using the RNeasy Mini Kit (Qiagen) as per the manufacturer's protocol, including DNase treatment, and the RNA pellet was resuspended in 15 µl RNase-free water. RNA concentration was assessed using the Nanodrop One UV-Vis Spectrophotometer (Thermo Fisher).

7.2.4.2 Sequencing

Library preparation and sequencing were conducted at the SAHMRI Genomics Facility (Adelaide, Australia). Prior to library prep, RNA quality was assessed using the RNA ScreenTape System (Agilent, Santa Clara, CA, USA). The Universal RNA-Seq with NuQuant, Mouse AnyDeplete kit (Nugen, Redwood City, CA, USA) was used for total RNA library prep. Sequencing was performed on the NovaSeq 6000 S1 Sequencing System (Illumina).

7.2.4.3 Bioinformatics analysis

Bioinformatics analysis was conducted using the public server of Galaxy [14]. An overall workflow is shown in Figure 7.2 and Table 7.1. All analysis was performed using the mm10

mouse assembly [15]. Datasets from each mouse model were processed together in batch. For all datasets, sequencing data was assessed using FASTQC. Next, 101-base sequences were aligned to the mouse genome using HISAT2 [16]. Alignment was filtered using samtools [17] with MAPQ 30 cut-off. For each alignment, novel transcriptome was assembled and merged together using StringTie tools [18] to take into account *de novo* transcripts. The novel transcriptome assembly was annotated using the mm10 genome assembly (GENCODE project, V23 version) using GffCompare [19]. Read count was performed in relation to the annotated novel assembly using featureCounts [20] . Read counts were normalised to the geometric mean calculated for each gene across all samples using DESeq2 [21]. Differential expression analysis and correlation analysis between replicates were performed using DESeq2, using the generalised DESeq2 linear model as described in the original publication [21]:

$$K_{ij} \sim NB(\mu_{ij}, \alpha_i)$$

With counts K_{ij} for gene i, sample j modelled using a negative binomial distribution with fitted mean μ_{ij} and a gene-specific dispersion parameter α_i. The fitted mean is composed of a sample-specific size factor s_j and a parameter q_{ij} proportional to the expected true concentration of fragments for sample j. The coefficients β_i give the log2 fold changes for gene i for each column of the model matrix X.

Independent filtering was performed as part of the DESeq2 function and genes with low counts were removed prior to differential analysis. Differential expression was defined as a fold-change ≥ 2 ($|\log FC| \geq 1$) and Benjamini-Hochberg adjusted p-value ≤ 0.01. The enrichment of Gene Ontology Biological Process terms was identified using GO::TermFinder [22,23]. Upstream regulator analysis of DEGs was through the IPA software (QIAGEN). Correlation of samples between different strains was through transcriptomic alignment via Salmon [24] and DESeq2. Visualisation of RNA-seq data on UCSC Genome Browser was through bigWig files generated from merged alignment BAM files using deepTools [25], with reads normalised to 1x depth of coverage.

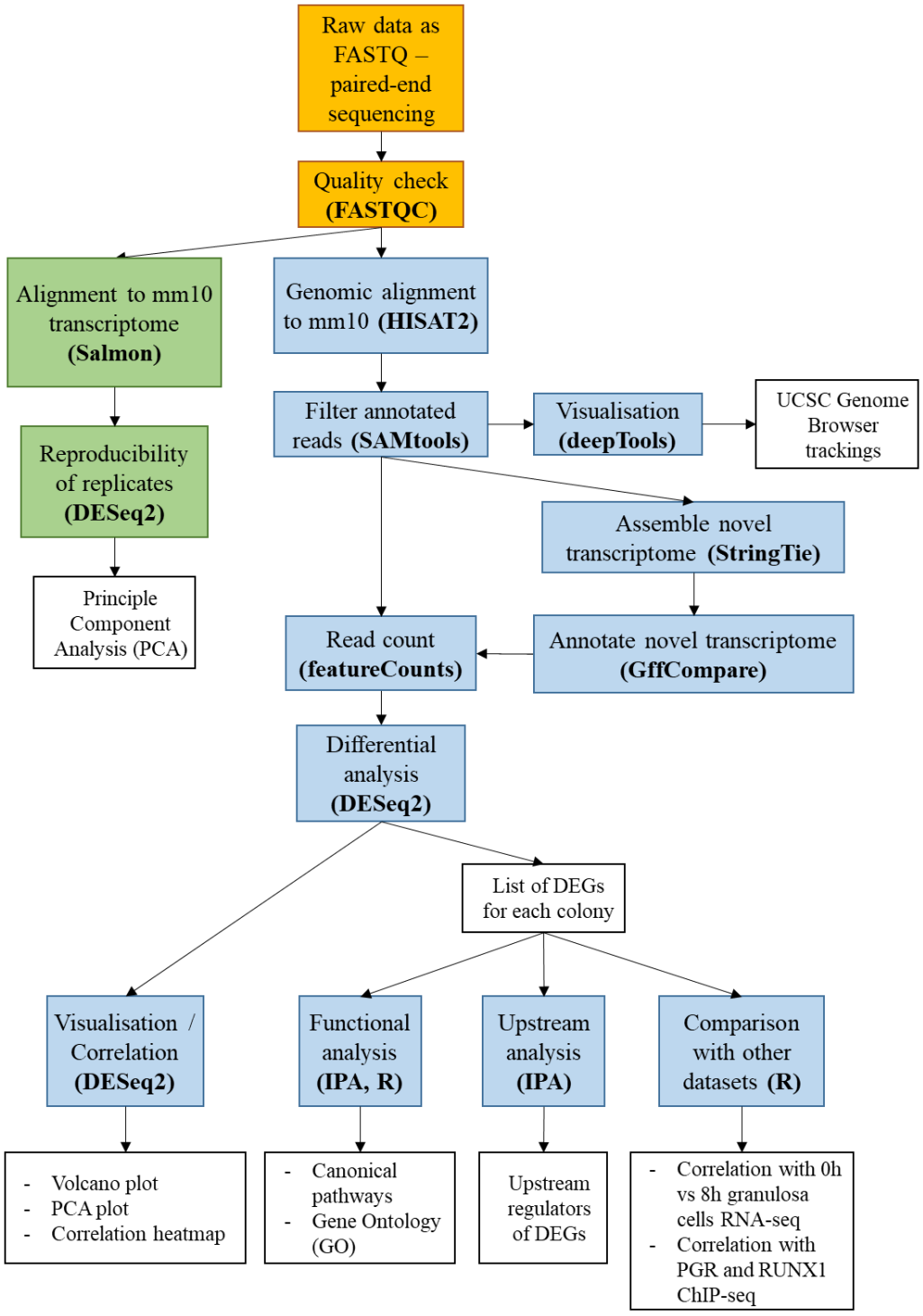

Figure 7.2 Bioinformatics workflow for RNA-seq analysis.

Orange boxes indicate input and pre-alignment quality control. Blue boxes are the main workflow, in which genomic alignment and transcriptome building were performed. Green boxes are the workflow for cross-strain comparison, in which no *de novo* transcriptome building was required. White boxes are output. Each step is listed with the tools used for the task in brackets. The analysis was performed on the public server of Galaxy and R when appropriate.

Table 7.1 Tools used for bioinformatics analysis of RNA-seq data.

Goal	Package/tool	Reference
Quality check of FASTQ files	FASTQC	(http://www.bioinformatics.babraham.ac.uk/projects/fastqc/
Genomic alignment	HISAT2	[16]
Alignment filtering	samtools	[17]
Novel transcriptome assembly	StringTie	[18]
Annotation of novel assembly	GffCompare	[19]
Read counting	featureCounts	[20]
Differential analysis	DESeq2	[21]
Gene Ontology analysis / correlation analysis	GO::TermFinder	[23]
Transcriptomic alignment	Salmon	[24]
Generating genomic coverage of reads	deepTools	[25]
Upstream regulator analysis	IPA Core Analysis	QIAGEN
Peak visualisation on UCSC Genome Browser	UCSC toolkits	[26]

7.3 RESULTS

7.3.1 PGR protein expression in PGRKO, AKO and BKO ovaries

To confirm the expression of PGR isoforms in peri-ovulatory granulosa cells from different strains, the abundance of each isoform from each of the different PGR mutant mouse strains was examined by Western blot using an antibody that could detect both isoforms of PGR (Figure 7.3). WT and KO female mice were stimulated for superovulation and COC/GC were collected from ovaries at 6 h post-hCG stimulation, the time during the peri-ovulatory window when PGR protein levels are highest. In general, as expected, strong bands corresponding to PGR-A and PGR-B were evident in granulosa cell extracts of WT mice in each line. These bands were not evident in the PGRKO samples and quantitation of fluorescence showed a highly significant and equal decrease in both A- and B-isoforms in cells from PGRKO animals in comparison to PGRWT. Unexpectedly, both isoforms were also undetectable in AKO animals compared to AWT. In the BKO strain, there was the expected loss of visible band for the PGR-B isoform and significant reduction in quantifiable B-isoform level; however, there was also a 1.8-fold increase in the abundance of the A-isoform.

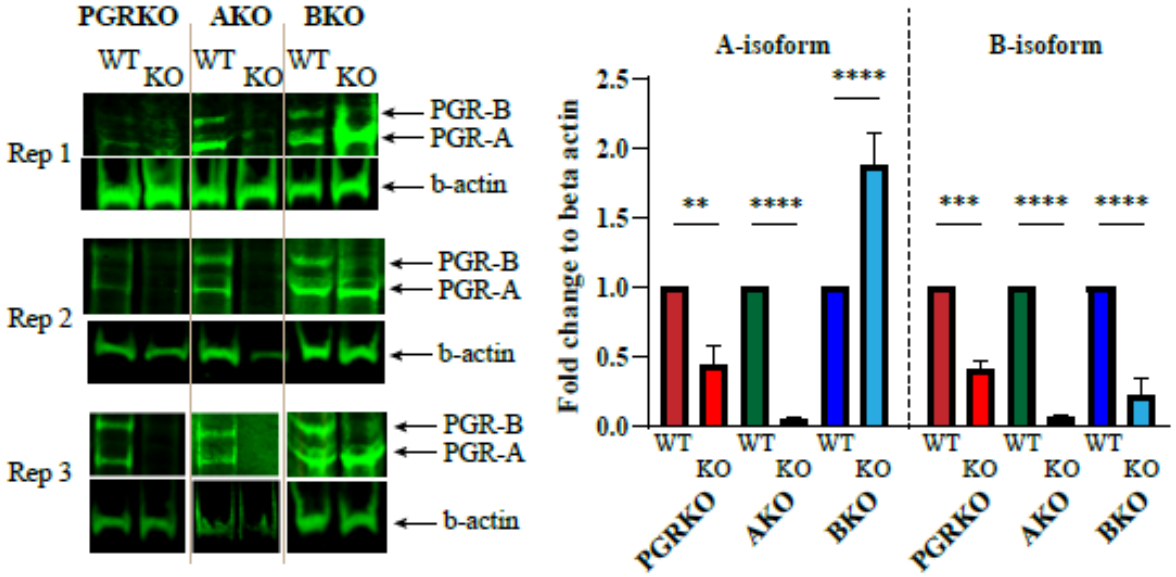

Figure 7.3 Expression of PGR-A and PGR-B proteins in granulosa cells of animals from each strain.

Western blot of WT and KO granulosa cells obtained from female mice at 6 h after hCG treatment. From left to right: PGRWT, PGRKO, AWT, AKO, BWT and BKO. Western membranes were probed with antibodies specific to PGR (both isoforms) and beta-actin (housekeeping control). Fluorescence signals for each PGR isoform were quantified and normalised to housekeeping and to its respective WT sample. N = 3, statistical significance was through two-way ANOVA with multiple comparison, asterisks signifying statistical significance: * = 0.0332, ** = 0.0021, *** = 0.0002, **** ≤ 0.0001.

7.3.2 PGR isoform-specific transcriptomes

As PGR protein level peaks at 6 h post-hCG, it is also reasonable to expect a strong influence on target transcriptional regulation occurs shortly after this peak. Accordingly, previous experiments have shown that at 8 h post-hCG injection the majority of ovulatory gene expression is altered compared to levels prior to hCG treatment (Appendix 7). Thus, the isoform-specific PGR-dependent transcriptomes of peri-ovulatory granulosa cells were examined at 8 h post hCG. Four biological replicates were used per genotype per mutant strain. FASTQC was performed for each file to assess the quality of sequencing. The quality check outcome was appropriate for RNA-seq data and no major concerns were identified. A summary for each sequencing files, including library size, sequence length, genomic alignment rate and gene counts is included in Appendix 12. Prior to differential expression analysis, the correlation between replicates was assessed.

7.3.2.1 Granulosa cell gene expression changes in PGRKO mice

Correlation analysis showed that in both WT and KO samples from the PGRKO line, replicates 1-3 were highly similar, as shown by a tight clustering pattern of genomic coverage of reads from each sample in the PCA plot and short Euclidean distances between samples of the same genotype (Figure 7.4A-B). Samples WT4 and KO4 were not as closely correlated to their respective cohorts. These samples were determined to be affected by inefficient library preparation and thus were excluded from downstream analysis. Differential expression analysis identified a total of 611 DEGs that passed the selection criteria of Benjamini-Hochberg adjusted p-value ≤ 0.01 and $|\text{logFC}| \geq 1$ cut-off (Appendix 13). Among these 611 DEGs, the clear majority were downregulated in PGRKO versus PGRWT samples (434 DEGs downregulated in PGRKO as opposed to 177 upregulated), indicating a prominent role of PGR in transcriptional induction (Figure 7.4C-D). Included in these differentially expressed genes were many that have been previously demonstrated to be downstream target genes of PGR and in some cases play key roles in ovulation, including *Adamts1, Il6, Edn2* and *Pparg*, all of which are significantly downregulated in PGRKO in comparison to PGRWT. Apart from these classic PGR targets, however, the majority of identified DEGs have not been previously associated with PGR. For instance, the top 10 most upregulated and top 10 most downregulated DEGs were all novel downstream targets of PGR (Figure 7.4D). The PGRKO DEGs were associated with a number of biological processes, including adhesion, morphogenesis and cellular development, as shown through Gene Ontology analysis (Figure 7.4E).

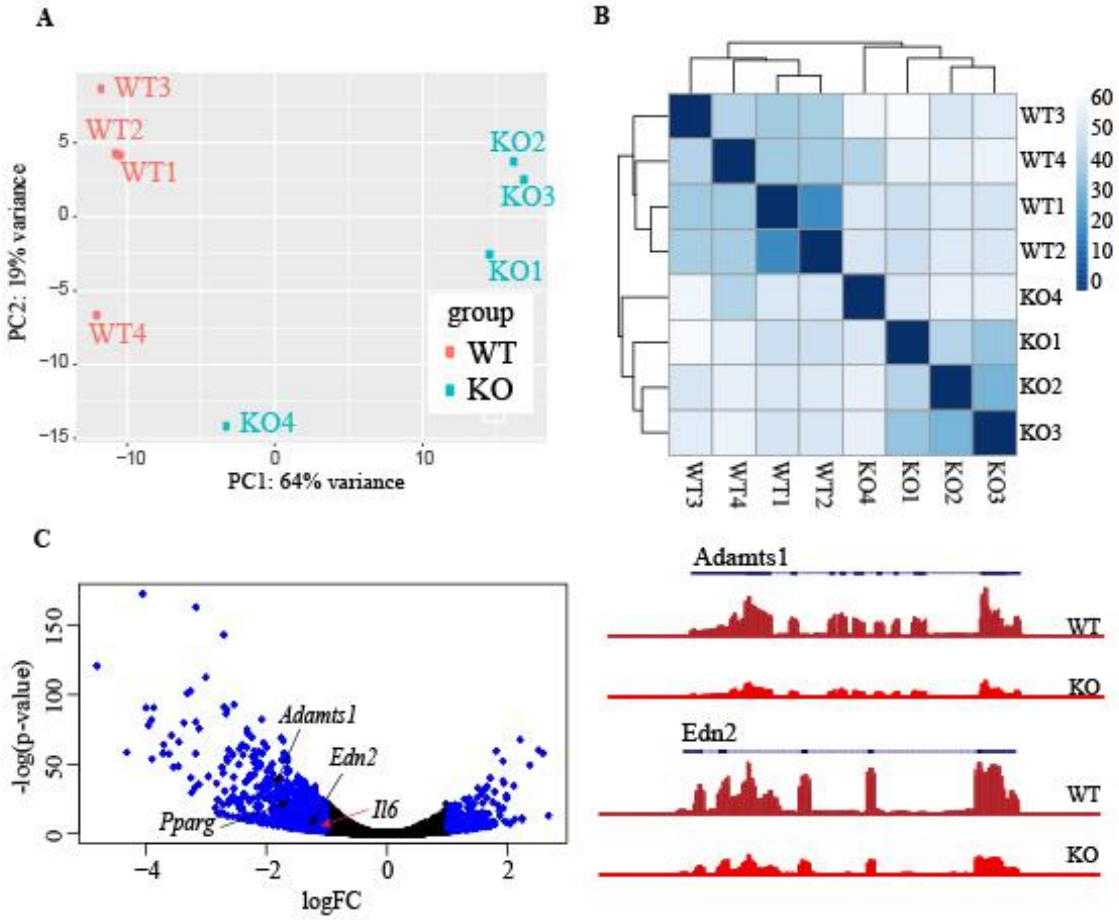

D

Gene	LogFC	Adj p-value
LYVE1	-4.81	1.27E-121
CLDN1	-4.05	1.19E-173
Gm34549	-3.90	1.92E-54
Cyp2j11/Cyp2j8	-3.46	2.9E-49
L3MBTL4	-3.37	1.64E-80
HSD17B11	-3.31	9.05E-102
SCARA5	-3.26	1.57E-103
Gm12637	-3.19	8.22E-34
GLP2R	-3.17	5.18E-164
Gm33677	-3.12	3.24E-36
NPR3	1.98	7.13E-26
CT025533.1	2.03	4.24E-08
Sprr2b	2.04	4.38E-08
CNR1	2.10	4.55E-35
MYH6	2.12	4.52E-11
CLCA1	2.23	4.7E-12
CHI3L1	2.24	7.9E-11
Gm26771	2.51	7.86E-61
SFRP2	2.58	1.17E-58
Sprr2d	2.67	1.16E-13

E

GO ID	GO term	p-val
GO:0007155	cell adhesion	2.22E-10
GO:0022610	biological adhesion	2.51E-10
GO:0000902	cell morphogenesis	9.75E-08
GO:0032989	cellular component morphogenesis	1.50E-07
GO:0051960	regulation of nervous system development	4.20E-07
GO:0022008	neurogenesis	6.92E-07
GO:0048699	generation of neurons	6.93E-07
GO:0060284	regulation of cell development	8.29E-07
GO:0048468	cell development	1.71E-06
GO:2000026	regulation of multicellular organismal development	3.10E-06

Figure 7.4 Genes differentially regulated in the absence of both PGR isoforms in ovulatory granulosa cells.

(A) PCA plot of RNA-seq replicates for PGRKO and PGRWT granulosa cells collected after 8 h hCG stimulation. **(B)** Correlation heatmap for PGRKO and WT replicates. The colour of matrix squares indicates sample-to-sample distance as calculated using normalised read counts by DESeq2, noted in the bar on the right. **(C)** Volcano plot of genes identified in PGRKO RNA-seq. Genes that are upregulated in PGRKO have a positive logFC value and vice versa. All genes with Benjamini-Hochberg adjusted p-value ≤ 0.01 are plotted (black) and genes passing the $|\text{logFC}| \geq 1$ criteria are determined as DEG (blue). Full list of DEG is in Appendix 13. Selective DEG with known ovulatory functions are labelled in the plot. Examples of the pattern of expression for *Adamts1* and *Edn2* are visualised on the right through the UCSC Genome Browser, showing read count build-up for PGR WT (dark red) and KO (red). Tracks are normalised to the same scale. **(D)** Top ten most upregulated and ten most downregulated DEGs from PGRKO vs WT RNA-seq, displayed together with logFC and p-value. **(E)** Biological processes enriched in PGKO DEGs, as indicated from Gene Ontology analysis. Only significantly enriched pathways (p-value ≤ 0.05) were displayed.

7.3.2.2 Granulosa cell gene expression changes in AKO mice

Correlation analysis of samples from the AKO strain showed a close resemblance between replicates of the same genotype, as shown in PCA plot and the sample-to-sample distance matrix (Figure 7.5A-B). The exception was sample KO1, which appeared as an outlier to the other KO samples and was thus not included in any further downstream analysis. In total, 686 DEGs satisfied the $|\log FC| \geq 1$ and adjusted p-value ≤ 0.01 criteria and were identified to be differentially expressed in AKO versus AWT granulosa cells, with about three-quarters of DEGs (515 DEGs) downregulated in AKO samples, indicating a preference for gene induction by PGR-A (Figure 7.5C, Appendix 14). Similar to PGRKO RNA-seq, a number of known ovulatory factors were found to be dysregulated in the AKO samples, such as *Pparg* and *Edn2*. Other genes that are known PGR targets, such as *Zbtb16* and *Mt2*, were also identified to be specifically regulated by PGR-A. Among the most differentially expressed DEGs, the gene encoding for PGR itself was the most highly upregulated gene in AKO, suggesting a role of the PGR A-isoform in auto-inhibition (Figure 7.5D). Similar to the PGRKO dataset, DEGs found in AKO were mostly enriched for pathways involved in cellular development, morphogenesis and adhesion (Figure 7.5E).

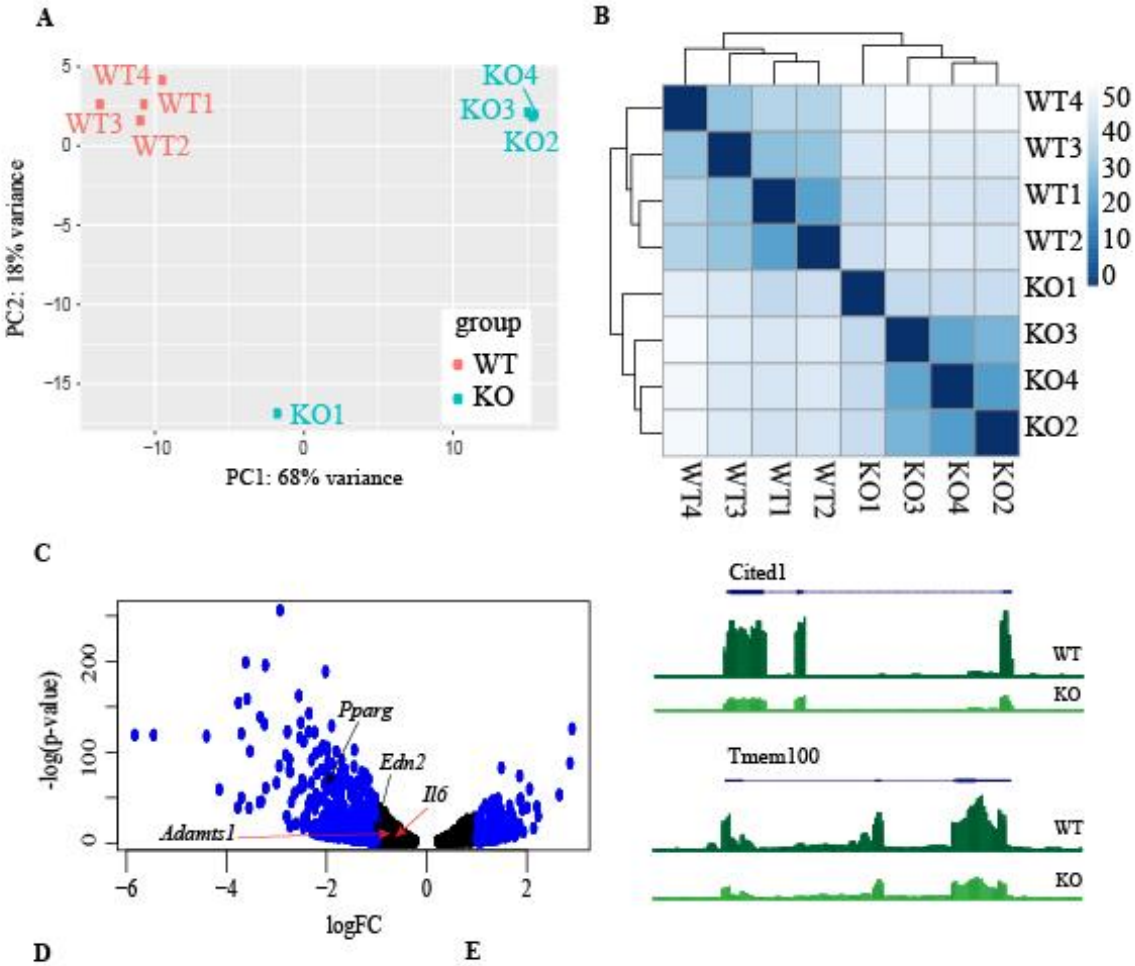

D

Gene	LogFC	Adj p-value
LYVE1	-5.83	0
Spnr2g	-5.46	1.87E-119
Cyp2j11/Cyp2j8	-4.40	3.1E-118
ZIC2	-4.14	1.28E-59
HAND2	-3.77	7.86E-40
CLDN1	-3.76	8.62E-155
KCNV2	-3.70	6.09E-121
1700040D17Rik	-3.70	1.52E-50
CITED1	-3.62	2.26E-199
MYH13	-3.59	3.95E-159
NPR3	1.91	1.4E-37
SFRP2	1.93	5.27E-13
C4orf17	2.00	1.35E-39
OLFML2B	2.05	4.41E-60
Gm15749	2.14	5.01E-17
CTXN3	2.20	1.31E-40
Gm26771	2.22	3.27E-30
Gm16485	2.65	1.15E-53
CYP26B1	2.86	1.31E-88
PGR	2.90	2.51E-126

E

GO ID	GO term	p-val
GO:0048699	generation of neurons	1.54E-06
GO:0022008	neurogenesis	6.37E-06
GO:0051960	regulation of nervous system development	2.49E-05
GO:0048468	cell development	2.92E-05
GO:0007399	nervous system development	3.87E-05
GO:0032879	regulation of localization	8.74E-05
GO:0060284	regulation of cell development	9.90E-05
GO:0031175	neuron projection development	0.000119835
GO:0009653	anatomical structure morphogenesis	0.000196768
GO:0007155	cell adhesion	0.000224383

Figure 7.5 Genes differentially regulated in the absence of PGR-A in ovulatory granulosa cells.

(A) PCA plot of RNA-seq replicates for AKO and AWT granulosa cells collected after 8 h hCG stimulation. **(B)** Correlation heatmap for AKO and AWT replicates. The colour of matrix squares indicates sample-to-sample distance as calculated using normalised read counts by DESeq2, noted in the bar on the right. **(C)** Volcano plot of genes identified in AKO RNA-seq. Genes that are upregulated in AKO have a positive logFC value and vice versa. All genes with p-value ≤ 0.01 are plotted (black) and genes passing the |logFC| ≥ 1 criteria are determined as DEG (blue). Full list of DEG is in Appendix 14. Selective DEG with known ovulatory functions are labelled in the plot. Examples of the pattern of expression for *Cited1* and *Tmem100* are visualised on the right through the UCSC Genome Browser, showing read count build-up for AWT (dark green) and KO (green). Tracks are normalised to the same scale. **(D)** Top ten most upregulated and ten most downregulated DEGs from AKO vs WT RNA-seq, displayed together with logFC and p-value. **(E)** Biological processes enriched in AKO DEGs, as indicated from Gene Ontology analysis. Only significantly enriched pathways (p-value ≤ 0.05) were displayed.

7.3.2.3 Granulosa cell gene expression changes in BKO mice

PCA plot of BKO samples and BWT controls showed that while there was a degree of clustering within each genotype group there was far less variance between BWT versus BKO (Figure 7.6A). Likewise, sample-to-sample Euclidean distances calculated from normalised read count indicates that the lack of an obvious clustering pattern is potentially due to the high correlation between all samples regardless of genotype (Figure 7.6B). This lack of separation in transcriptome identity is observed after differential expression analysis, which identified only 143 DEGs, or a quarter of the number of DEGs identified in PGRKO or AKO samples (Figure 7.6C-D, Appendix 15). Surprisingly, almost all of these DEGs (138/143 DEGs) were upregulated in BKO, suggesting that PGR-B is playing a predominant role as a transcriptional repressor in granulosa cells. Due to the low number of DEGs, few enriched pathways were identified to be associated with PGR-B regulated DEGs, with the most significantly enriched pathway being involved in cell-cell adhesion (Figure 7.6E).

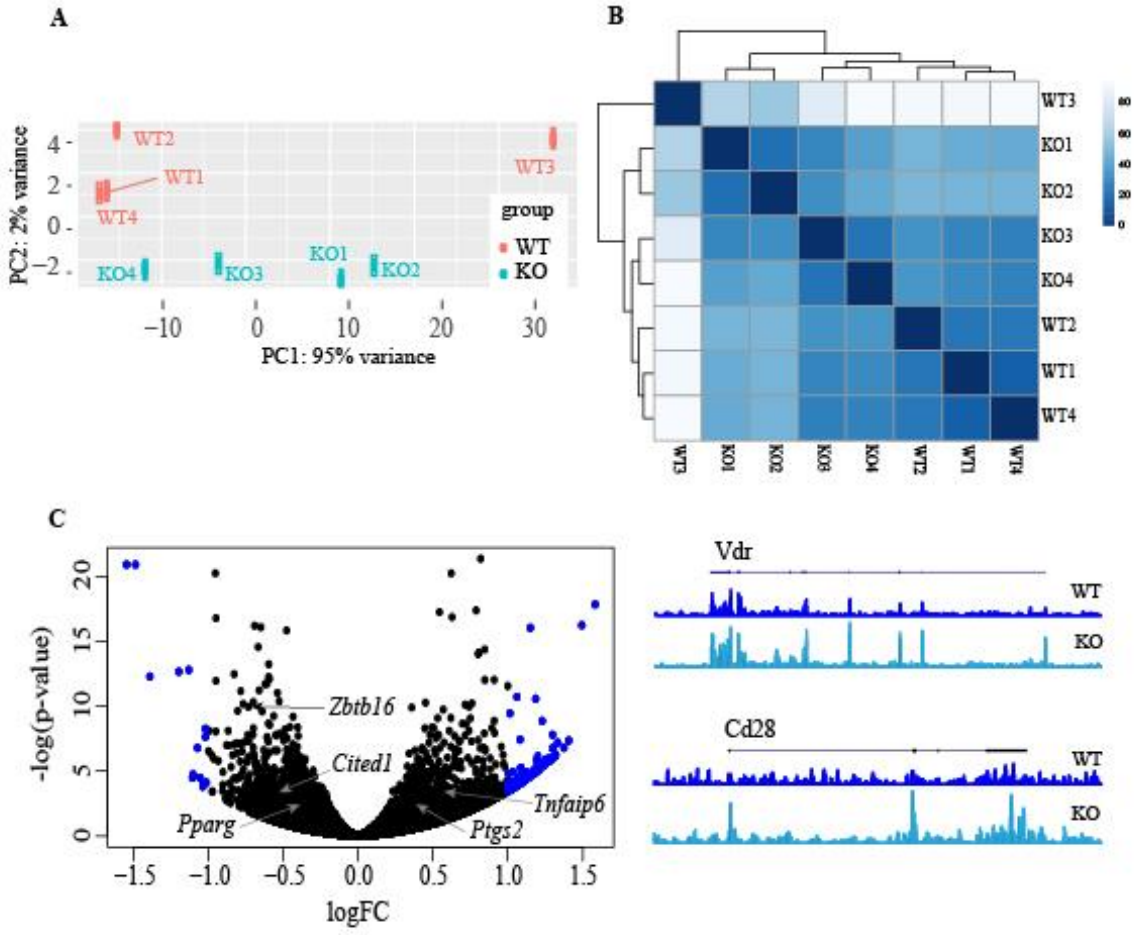

D

Gene	LogFC	Adj p-value
KCNV2	-1.49	1.21E-21
Cyp2j11/Cyp2j8	-1.20	2.15E-13
Gm25395	-1.10	0.000018
HAND2	-1.03	0.0000889
Gm34609	1.00	0.000206
CD86	1.00	0.000063
ST8SIA6	1.00	0.0000812
4930432E11Rik	1.00	0.000269
TSPEAR	1.00	0.000322
C6	1.00	0.000172
DNAH3	1.30	1.58E-08
WDR63	1.30	0.000000173
A330069K06Rik	1.30	0.000000929
AGMO	1.32	0.000000618
ZBBX	1.32	0.000000693
4930474G06Rik	1.32	0.000000535
RP1	1.33	6.38E-08
RP1L1	1.38	0.000000161
3100003L05Rik	1.41	4.37E-08
AC134577.1	1.49	5.7E-17

E

GO ID	GO term	p-val
GO:0098742	cell-cell adhesion via plasma-membrane adhesion molecules	0.001475
GO:0051932	synaptic transmission, GABAergic	0.016433
GO:1902476	chloride transmembrane transport	0.03227
GO:0001505	regulation of neurotransmitter levels	0.0338

Figure 7.6 Genes differentially regulated in the absence of PGR-B in ovulatory granulosa cells.

(A) PCA plot of RNA-seq replicates for BKO and BWT granulosa cells collected after 8 h hCG stimulation. **(B)** Correlation heatmap for BKO and WT replicates. The colour of matrix squares indicates sample-to-sample distance as calculated using normalised read counts by DESeq2, noted in the bar on the right. **(C)** Volcano plot of genes identified in AKO RNA-seq. Genes that are upregulated in AKO have a positive logFC value and vice versa. All genes with p-value ≤ 0.01 are plotted (black) and genes passing the $|\text{logFC}| \geq 1$ criteria are determined as DEG (blue). Full list of DEG is in Appendix 15. Selective DEG with known ovulatory functions are labelled in the plot. Examples of the pattern of expression for *Vdr* and *Cd28* are visualised below through the UCSC Genome Browser, showing read count build-up for BWT (dark blue) and KO (light blue). Tracks are normalised to the same scale. **(D)** Top ten most upregulated and ten most downregulated DEGs from BKO vs WT RNA-seq, displayed together with logFC and p-value. **(E)** Biological processes enriched in BKO DEGs, as indicated from Gene Ontology analysis. Only significantly enriched pathways (p-value ≤ 0.05) were displayed.

7.3.2.4 Unique patterns of gene regulation that are isoform-specific

To further determine the level of difference between the identified transcriptomes, DEGs that are reliant on the presence of either or both of PGR isoforms were compared against each other. PCA plot of all datasets displayed a number of clustering patterns (Figure 7.7A). The PGRKO samples and their PGRWT controls both clustered separately from the isoform specific groups, consistent with the difference between background strains. Variation between WT samples from the three strains might have resulted from the genetic differences in the mouse strains used to generate KO colonies. The PGRKO line was maintained in the BALB/cJ mouse strain, while AKO and BKO animals were crossed into the C57BL/6 line, and different embryonic stem cell lines were used for each strain (129S7/SvEvBrd-Hprt^{+} for PGRKO and 129S7/SvEvBrd-Hprt$^{b\text{-}m2}$ for AKO and BKO) (JAX). Such variations in the genetic background of PGRKO versus the AKO and BKO mouse lines can be expected to cause differences between WT controls at the transcriptome-wide level while also yielding the high level of similarity between AWT and BWT animals that are nearly genetically identical. More importantly, and also as expected, the PGRKO and AKO groups both formed clusters separate from their WT controls (with the exception of the described outliers). There was no distinction between BWT and BKO samples, which also overlapped the AWT samples, confirming the comparatively limited disruption to gene expression pattern from the absence of PGR-B in granulosa cells.

Comparisons of DEGs between the three datasets showed that 289 DEGs were found in both PGRKO and AKO datasets (equivalent to 42-47% of total DEGs in either datasets) (Figure 7.7B-D). All of these DEGs shared the same direction of change relative to WT controls and many have been previously identified to be regulated by PGR in granulosa cells (Figure 7.7C). On the other hand, very few genes were shared between BKO and the other two transcriptomes (10 shared DEGs between PGRKO/BKO and 16 between AKO/BKO) or shared between all three datasets (7 DEGs). Among these shared genes, however, there was also an inverse pattern of expression observed in BKO, with DEGs upregulated in BKO tending to be downregulated in PGRKO and AKO. Examples of shared DEGs between different strains can be seen in Figure 7.7D.

A

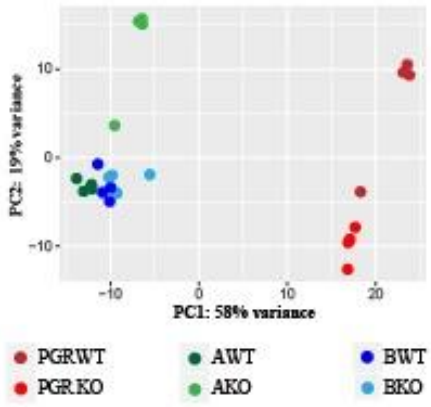

B

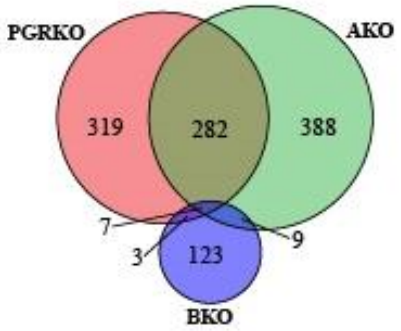

C

	Gene	PRKO	AKO	BKO
PRKO - AKO - BKO	KCNV2	-2.96	-3.702	-1.488
	Cyp2j11/Cyp2j8	-3.459	-4.398	-1.199
	Gm20642	1.638	1.699	1.014
	Gm7019	1.088	1.336	1.014
	HELT	-2.054	-2.326	1.076
	AC155634.2	1.634	1.399	1.082
	Nrg3os	1.404	1.655	1.15
PRKO - AKO	CITED1	-2.436	-3.617	
	EDN2	-1.315	-1.061	
	FABP4	-1.629	-3.529	
	PPARG	-1.876	-1.912	
	SRA1	-1.152	-1.152	
PRKO - BKO	Arhgef38	1.202		1.019
	CDHR3	1.061		1.034
	Uox	1.543		1.134
AKO - BKO	HAND2		-3.774	-1.034
	DNAI1		-1.022	1.261
	DNAH3		-1.173	1.298
	ZBBX		-1.314	1.317
	RP1		-1.132	1.332
	Gm45321		-1.204	1.024
	Gm19303		-1.342	1.036
	3100003L05Rik		-1.115	1.407
	AC134577.1		1.117	1.494

D

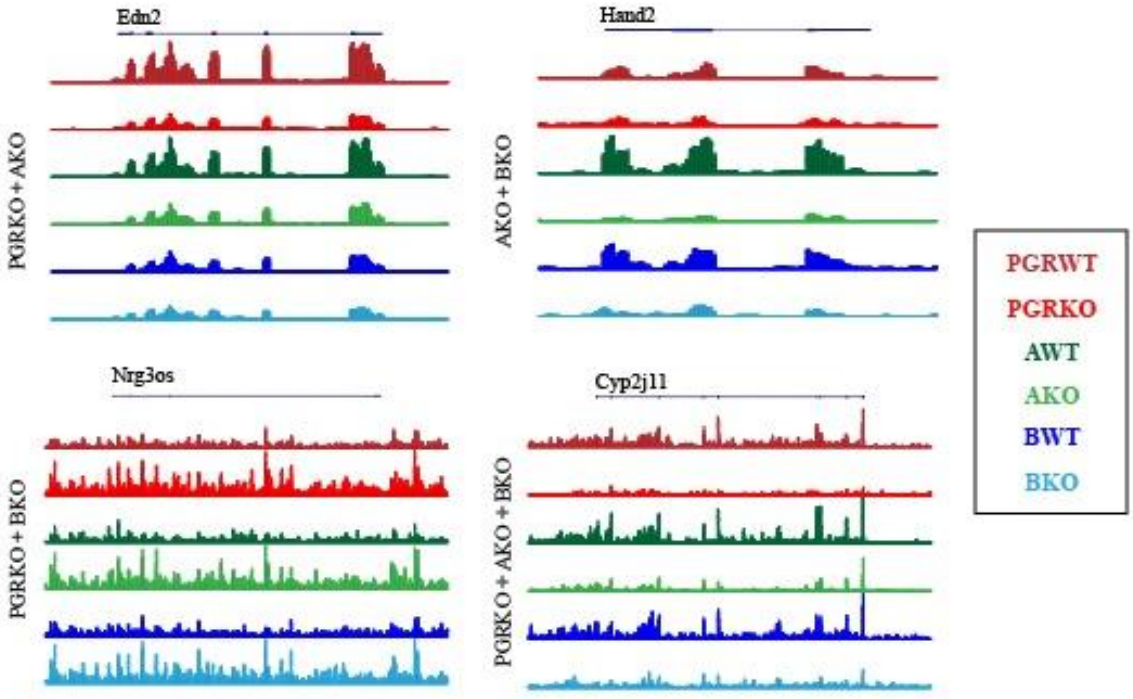

Figure 7.7 Correlation between PGR isoform-specific transcriptomes.
(A) PCA plot of all RNA-seq samples, including PGRKO, AKO and BKO strains (4 replicates per sample) **(B)** Venn diagram of DEG identified in PGRKO vs WT (red), AKO vs WT (green) and BKO vs WT (blue) granulosa cells. DEGs were compiled from independent RNA-seq with full gene lists available in Appendix 7 **(C)** Overlapped genes of each comparison, with accompanying KO vs WT logFC from corresponding dataset displayed. **(D)** Examples of shared DEGs between transcriptomes, visualised using the UCSC Genome Browser. Tracks are normalised to the same scale. For each gene, custom tracks showing read count build-up for PGR WT (dark red), PGR KO (red), AWT (dark green), AKO (light green), BWT (dark blue), BKO (light blue) are shown. All tracks are normalised to the same scale.

To determine whether different PGR isoforms have unique functional co-modulator partners in peri-ovulatory granulosa cells, upstream regulators of PGR isoform-dependent transcriptomes were assessed using IPA. In PGRKO and AKO, many transcription regulators were shown to have a significant association with these differentially expressed genesets, with many shared between the two datasets (Table 7.2). Reassuringly, PGR was identified as one of the most highly enriched regulators in both datasets. Additionally, a number of transcription factors that are known to be downstream targets of PGR, such as ZBTB16 (Zinc finger and BTB domain containing 16), as well as other transcription regulators with roles in ovulatory granulosa cells, including PPARG, NR5A2 (LRH1), GATA4, SP1, CEBP/p300 and JUN/FOS were also identified. Conversely, very few transcription regulators were found to be associated with PGR-B regulated DEGs. Concurrent with the previous observation of PGR-B inhibiting downstream gene expression, other transcription repressors were found to be enriched in this dataset, including REST and RCOR1.

Table 7.2 Upstream regulators of PGRKO / AKO / BKO DEGs.

Upstream regulators associated with DEG sets in PGRKO vs PGRWT, AKO vs AWT and BKO vs BWT were identified via IPA. Only transcription regulators and ligand-dependent nuclear receptor are shown in this table. A p-value = 0.01 cut-off was applied. Molecules are ranked by p-value and are shown with the number of DEGs under their regulation.

PGRKO	p-value	# of genes	AKO	p-value	# of genes	BKO	p-value	# of genes
KLF4	0.0000	15	PGR	0.0000	17	RCOR1	0.00128	2
TCF7	0.0001	6	HDAC1	0.0000	16	DLX6	0.00163	2
GATA3	0.0001	13	FEV	0.0000	9	DLX2	0.00222	2
FOXA2	0.0001	12	ESR2	0.0000	23	CRX	0.00314	2
CEBPA	0.0001	18	FOXO3	0.0001	17	DLX5	0.0034	2
HTT	0.0001	24	KLF4	0.0001	15	LHX5	0.00999	1
NR1I2	0.0001	10	NFE2L2	0.0001	20	NKAP	0.00999	1
NFE2L2	0.0002	17	EZH2	0.0001	18			
THRB	0.0003	11	RORC	0.0001	11			
CEBPB	0.0004	16	SMARCA4	0.0001	25			
RORC	0.0004	9	FOXA2	0.0001	13			
HIF1A	0.0004	16	HTT	0.0001	27			
CEBPD	0.0005	7	PPARG	0.0002	21			
GATA4	0.0007	10	GATA2	0.0002	18			
AHR	0.0007	14	HNF1B	0.0002	9			
PGR	0.0007	12	RXRG	0.0002	5			
SQSTM1	0.0007	5	RXRB	0.0003	7			
FOXO3	0.0009	13	CDX2	0.0003	10			
SOX10	0.0009	4	NFKBIA	0.0003	19			
EZH2	0.0009	14	SIX5	0.0007	4			
NR1I3	0.0009	7	RXRA	0.0009	14			
TBX5	0.0011	6	LMO4	0.0010	3			
SP7	0.0011	3	CEBPD	0.0017	7			
RUNX1	0.0013	9	HIRA	0.0017	3			
RXRA	0.0013	12	PPARD	0.0018	11			
EPAS1	0.0014	10	CDX1	0.0019	5			
NOTCH1	0.0014	11	EPAS1	0.0019	11			
HNF1B	0.0015	7	PLAGL1	0.0021	3			
FOXC2	0.0015	5	ESR1	0.0021	38			
HDAC1	0.0015	11	NR1I2	0.0023	9			
PDX1	0.0016	9	NKX3-1	0.0025	5			
NFKBIA	0.0017	15	ZFPM2	0.0025	3			
PPARG	0.0018	16	HDAC2	0.0026	8			
RORA	0.0019	9	CREB1	0.0027	20			
BRD8	0.0020	2	NR1I3	0.0030	7			

PGRKO	p-value	# of genes	AKO	p-value	# of genes
YY2	0.0020	3	HIF1A	0.0035	16
PAX3	0.0021	9	PIAS1	0.0038	4
EHF	0.0022	6	AIRE	0.0039	5
TLX3	0.0023	3	HOXA9	0.0041	9
ETV5	0.0028	6	AHR	0.0045	14
MEF2C	0.0028	7	STAT5B	0.0046	12
CCAR1	0.0029	2	FOS	0.0048	19
RARB	0.0029	7	NAB2	0.0048	3
SOX9	0.0030	5	THRB	0.0049	10
MAFK	0.0031	3	SMAD3	0.0055	11
NR3C2	0.0033	7	FOXA1	0.0059	8
GATA2	0.0038	13	SMARCA2	0.0063	5
RAX	0.0040	2	SOX9	0.0071	5
ZNF521	0.0040	2	RORA	0.0072	9
EGR3	0.0041	4	GATA6	0.0072	9
HNF1A	0.0042	15	Foxp1	0.0083	4
ZBTB16	0.0044	7	NR3C1	0.0085	21
POU4F1	0.0049	6	RARB	0.0089	7
CDX2	0.0053	7	TCF7	0.0090	4
SIRT1	0.0054	13	NR1H4	0.0091	8
PRDM1	0.0058	9	GATA4	0.0095	9
CDX1	0.0059	4	ESRRG	0.0097	4
ESR2	0.0066	15	LHX1	0.0098	6
GATA6	0.0067	8			
FOS	0.0067	16			
NR1D2	0.0068	2			
BRMS1	0.0068	2			
BACH2	0.0077	4			
SP1	0.0078	16			
FEV	0.0080	5			
STAT5B	0.0080	10			
CREB1	0.0081	16			
SOX2	0.0083	14			
RARG	0.0084	5			
TP53	0.0084	40			
ZNF281	0.0087	3			
TWIST1	0.0094	7			

7.3.3 Combined analysis of transcriptomes regulated by ovulatory stimulus, PGR-regulated transcriptomes and PGR bound cistromes

To determine the influence of PGR on the whole ovulatory transcriptome in granulosa cells, transcriptomes from PGRKO, AKO and BKO were assessed alongside genes regulated by ovulatory stimulus (identified through RNA-seq of mouse granulosa cell transcriptomes before vs 8 h after hCG treatment (Appendix 7). Among the 2179 ovulatory DEGs in granulosa cells, 151 (or 7%) were found to be differentially expressed in PGR transcriptome (25% of PGRKO DEGs, Figure 7.8A). Within these DEGs, almost all (146 DEGs) were found to be upregulated and only 5 were found to be downregulated in ovulation. Similarly, 144 ovulatory DEGs were found in the AKO transcriptome, 139 (97%) of which were upregulated in peri-ovulatory granulosa cells. 88 ovulatory DEGs were found in both PGRKO and AKO datasets, confirming the predominant role of PGR-A in the overall PGR effect during ovulation. Only 2 ovulatory DEGs were found to be exclusively regulated by BKO in granulosa cells.

Nearly half of all ovulatory DEGs have associated PGR or RUNX1 bound ChIP-seq peaks, with the majority of DEGs bound by both transcription factors during ovulation. To determine the direct impact of PGR and RUNX1 binding on PGR-dependent gene expression, PGR isoform-specific transcriptomes were compared against PGR and RUNX1 cistromes (Figure 7.8B). Surprisingly, despite the previous finding of a very high proportion of PGR and RUNX1 binding in close proximity to gene bodies or TSS, only a quarter of PGRKO or AKO DEGs were found to have PGR or RUNX1 binding in their proximity. The majority of these DEGs had both PGR and RUNX1 binding, indicating a close relationship between RUNX1 and PGR in the regulation of mutual target genes. However, about three-quarters of PGR-dependent DEGs were found to not have direct PGR binding within the gene proximity, suggesting possible regulatory actions via distal enhancer units of PGR or intermediate transcription factors. Few DEGs in BKO, however, showed evidence of PGR or RUNX1 direct binding, with only 20 DEGs found in common with the ChIP targets of either transcription factors. Analysing the genomic distribution of binding sites found at DEGs from different datasets showed no remarkable differences from the known binding pattern of PGR and RUNX1, with RUNX1 favouring interactions at proximal promoter regions (Figure 7.8C). Cumulatively these results indicate that PGR-A is important in the induction of gene expression in ovulation, with direct PGR and RUNX1 binding within the gene boundary as well as interaction through distal enhancer elements being of import in the regulation of these genes.

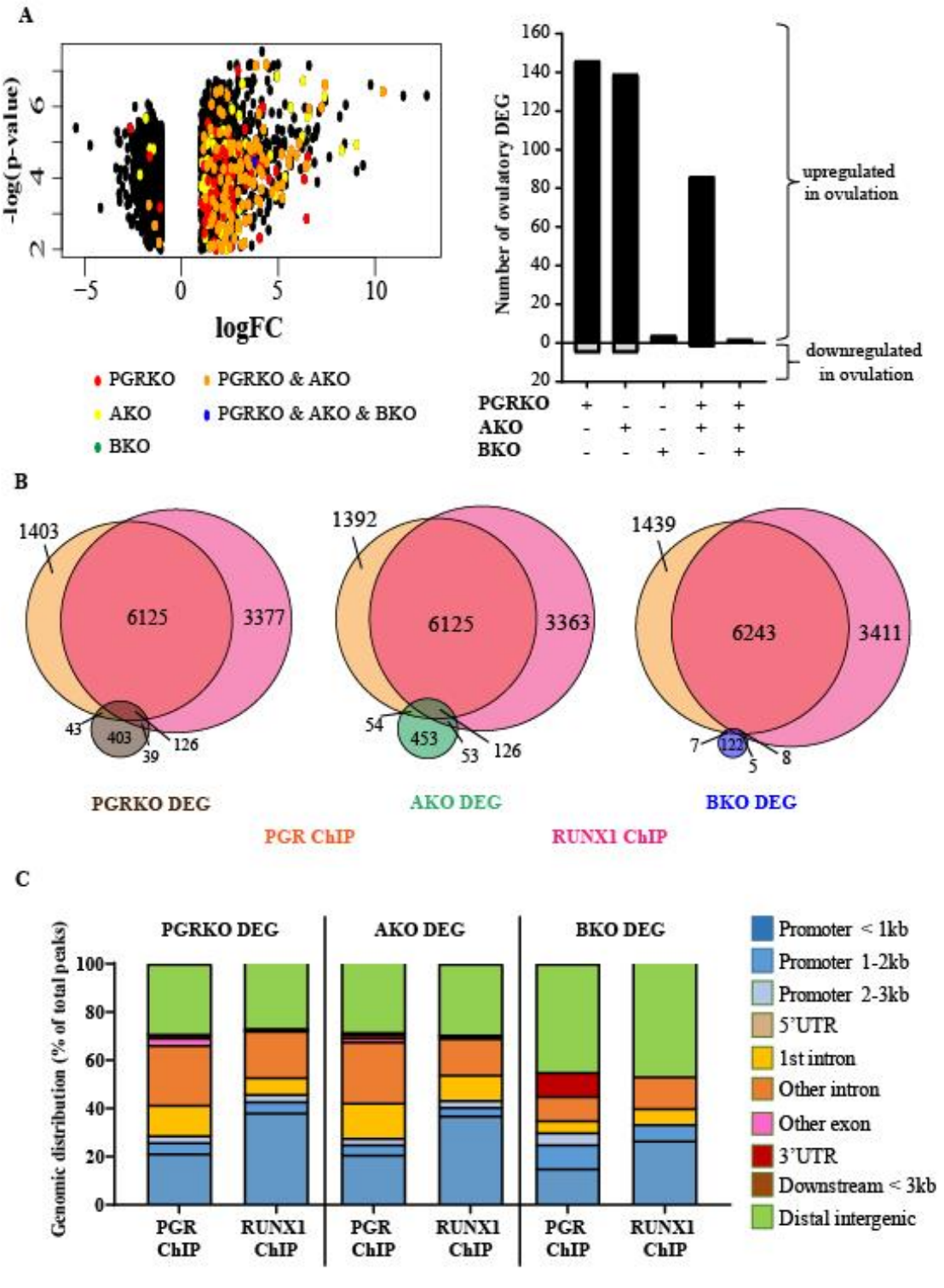
A
-log(p-value)
logFC
PGRKO
PGRKO & AKO
AKO
PGRKO & AKO & BKO
BKO
Number of ovulatory DEG
upregulated in ovulation
downregulated in ovulation
PGRKO
AKO
BKO
B
1403
6125
3377
43
403
39
126
1392
6125
3363
54
453
53
126
1439
6243
3411
7
122
5
8
PGRKO DEG
AKO DEG
BKO DEG
PGR ChIP
RUNX1 ChIP
C
PGRKO DEG
AKO DEG
BKO DEG
Genomic distribution (% of total peaks)
PGR ChIP
RUNX1 ChIP
Promoter < 1kb
Promoter 1-2kb
Promoter 2-3kb
5'UTR
1st intron
Other intron
Other exon
3'UTR
Downstream < 3kb
Distal intergenic

Figure 7.8 Isoform-specific transcriptome in relation to ovulatory genes and ovulatory transcription factors.

(A) Volcano plot displaying ovulatory DEGs from RNA-seq in 8 h vs 0 h hCG-stimulated granulosa cells that are in common with PGR isoform-specific RNA-seq datasets. hCG-regulated genes found in PGRKO RNA-seq datasets are labelled red, in AKO RNA-seq in yellow, in BKO RNA-seq in green, in both PGRKO and AKO RNA-seq in orange and in all three PGR datasets in blue. Quantification of each overlapping subset is displayed in the bar graph on the right, with DEG that are upregulated or downregulated during ovulation indicated. **(B)** Venn diagrams showing the overlap between genes associated with a peak in PGR and RUNX1 ChIP-seq in relation to PGRKO RNA-seq (left), AKO RNA-seq (middle) and BKO RNA-seq (right). **(C)** Genomic distribution of PGR and RUNX1 binding sites that are found in PGR DEG, AKO DEG or BKO DEG. Genome distribution is displayed as stacked bar graphs and peaks were divided into PGR peaks and RUNX1 in PGRKO RNA-seq (left), in AKO RNA-seq (middle) and BKO RNA-seq (right). Genomic features include promoters (< 1 kb, 1-2 kb and 2-3 kb), 5' UTR, 1st intron, other introns, exons, 3' UTR and downstream of TES (within 3 kb). Peaks that are not in these features are classified as distal intergenic.

7.4 DISCUSSION

While the important roles of PGR-A and PGR-B on general reproductive physiology has been described, the underlying mechanisms by which they can achieve profoundly tissue-specific actions differences is still not well understood and no studies have investigated the distinct roles of PGR-A and PGR-B in granulosa cell functions. Thus, this study embarked on describing the ovulatory transcriptomes that are dependent on each PGR isoform, taking advantage of isoform-specific knockout mouse strains and high throughput RNA sequencing, and have illustrated isoform-specific gene expression profiles with consequences to ovulation.

A high degree of similarities between transcriptomes that were under the influence of PGR-A and total PGR was observed. As expected, many ovulatory genes that are PGR-regulated in granulosa cells were indicated in these datasets, such as *Edn2*, *Mt1*, *Mt2* and *Pparg* [7,9,27]. Some of these genes, such as *Adamts1*, while shown to be statistically downregulated only in PGRKO, was also reduced in AKO (logFC = -0.768 with p-value = 2.73E-13). A handful of these genes have been shown to be associated with PGR functions in other biological contexts, such as *Alox12e* [28] and *Efnb2* [29]in the uterus. Of particular interest is *Zbtb16*, which encodes for a zinc-fingered transcription factor that has both transcriptional activating and repressing roles. *Zbtb16* plays a role in mediating the expression of *Egr1* in the uterus and PGR has previously been shown to regulate *Zbtb16* expression through binding sites within its intronic body[30]. Through microarray *Zbtb16* was shown as a target gene of PGR in granulosa cells during ovulation, which is confirmed with the AKO RNA-seq data. *Zbtb16* is also targeted by RUNX1 in cells of lymphoid lineage, where the intronic binding of RUNX1 is shown to be important for *Zbtb16* expression [31] and these same intronic binding sites were also observed for PGR and RUNX1 in granulosa cells. Many of these genes remain unfamiliar in the context of granulosa cell biology or in relation to PGR functions and require further investigation. Conversely, there were also genes previously identified in granulosa cells but which have never been linked to PGR, such as *Serpina1* [32]. However, it is clear that the PGR- and PGR-A dependent transcriptomes were highly reflective of the global ovulatory transcriptome in granulosa cells, the majority of such genes were upregulated during ovulation, indicative of the transcriptional activating role of PGR and PGR-A in particular.

Approximately a quarter of genes identified in PGRKO and AKO possessed PGR binding in their proximity, suggesting that while direct PGR binding plays a major role in the regulation

of these genes, it is likely that other mechanisms such as indirect regulation via intermediate transcription factors as well as PGR binding distal enhancer regions maybe important for PGR action in the majority of genes. Indeed, upstream regulators for PGR-dependent genes identified not only PGR as expected, but also a number of transcription factors with potential to be regulators of subsets of the PGR-regulated genes. These included CTNNB1, SP1 and CEBPα and CEBPβ, which are known to play a role in transcriptional regulation in ovulation [33-35]. RUNX1 was also identified as a likely regulator of the PGR-dependent genes, which supports the proposed functional cooperation between RUNX1 and PGR in peri-ovulatory granulosa cells. Also in support of this, over a quarter of PGRKO and AKO genes were found to have RUNX1 binding in their proximity, with more than 70% of such binding occurring in conjunction with PGR binding. As the RUNX1-modulated gene expression pattern in peri-ovulatory granulosa cells remains unexplored, a better description of this transcriptome would help elucidate the degree of functional similarities between these two transcription factors. A number of identified upstream regulators were also downstream targets of PGR with known roles in ovulation, such as PPARγ and HIF1α [9,36], indicating the role of PGR as a master transcription factor that facilitates a signalling cascade by promoting the expression of additional intermediary transcriptional regulators.

While there was a large level of overlap between the PGR and AKO transcriptomes, they were not completely alike. To explain this, the dimer nature of PGR needs to be considered. Active PGR usually exists in a dimerised form of either heterodimer (PGR-A/PGR-B) or homodimer (PGR-A/PGR-A or PGR-B/PGR-B). Studies have shown that each PGR isoform has distinct co-regulator binding properties that are conveyed to dimers; for example, BTEB1 is found to enhance PGR-B transactivation through stronger interaction with the PGR-B homodimer, yet has no effect on the PGR-A homodimer and even promotes PGR-A trans-repression of PGR-B when it binds the PGR-A/PGR-B heterodimer [37]. Similarly, PGR-B shows a higher binding affinity to SRC-1 and SRC-2 than PGR-A [38]. The functional consequences of these different dimer forms, however, has not been explored in detail. Although PGR-A is found to have a higher expression level than PGR-B in granulosa cells, it is unknown which of the dimer forms is the dominant; thus, by selectively removing one isoform in these KO mouse models, PGR is almost certainly forced to form homodimers in AKO and BKO, which might lead to consequences on the PGR-dependent transcriptome beyond the effect of loss of a single isoform.

Unlike for PGRKO and AKO, the BKO transcriptome does not seem to be crucial for ovulation. The absence of PGR-B led to far less prominent changes in the gene expression pattern during ovulation and very little overlap with either PGRKO or AKO RNA-seq datasets. Interestingly, less than 10% of identified genes were downregulated in the absence of PGR-B, suggesting a repressive function is the major role of PGR-B in granulosa cells. In support of this, upstream regulators associated with PGR-B dependent genes included co-repressors, such as RCOR1 and REST, which are members of the REST repressor family with important roles in gene silencing [39]. Such divergent effects on transcriptional regulation has previously been described in breast cancer where cells expressing only either PGR isoform have unique transcriptional profiles [12]. Thus, the transcriptomic pattern of PGR-B confirms the previously observed lack of reproductive defects in BKO female mice, as PGR-B appears to be relatively uninvolved in crucial gene regulation in ovulation and may have some roles in transcriptional inhibition.

Intriguingly, Western blot showed that in AKO peri-ovulatory granulosa cells, an absence of both isoforms and not just PGR-A was observed. The opposite was not the case in BKO granulosa cells in which PGR-A was still present in BKO samples. This hints at a role of PGR-A in regulating the expression of PGR-B through means that are yet unknown. Curiously enough, PGR-A is known to have a repressive effect on PGR-B transactivation in mammary and uterine tissues [10,13], and thus cannot explain the ablation of PGR-B in the absence of PGR-A in this case. Another possibility is that PGR-A has a protective role on PGR-B in granulosa cells that prevents PGR-B degradation. Ligand-dependent protein degradation has been previously described in multiple steroid receptors including PGR [40,41] and there is evidence of PGR isoforms having specific protein stability that is dependent on MAPK-triggered phosphorylation [42]. These speculations will have to be addressed in more details in future studies. If that is indeed the case, this can explain the similarities between PGRKO and AKO reproductive phenotypes as AKO reproductive tissues are essentially PGRKO. Despite this, transcriptomic differences between PGRKO and AKO colonies suggests that KO of specific PGR isoforms can have additional effects on downstream pathways, the nature of which is still unknown. Furthermore, it is also likely that this resultant KO effect might be specific only to granulosa cells, as B-isoform is still observed in oestrogen-treated AKO uterus [3]. More detailed studies of the dynamics of PGR-B independent of PGR-A during the peri-ovulatory window will also be required.

Due to the depth of the sequencing effort, transcripts of low abundance were also captured in these RNA-seq experiments, including ncRNA which can manifest profound physiological effects even at low quantity. However, the workflow described for the current analysis, which did not separate ncRNA from highly abundant mRNA, would not be able to identify differentially expressed ncRNA due to bias to mRNA enrichment. Thus, while the role of ncRNA has not been investigated in detail in the current study, the data is available for future in-depth studies on the subject and will be helpful for the further understanding of the effect of PGR isoforms on the expression of ncRNA and whether there is a subsequent impact on granulosa cell functions during ovulation.

Considering that both PGRKO and AKO mutants are anovulatory while BKO mice ovulate normally, these new in-depth sets of genes that are regulated in each context provide detailed information about the genes that are critical for the mechanism of ovulation. While a number of the genes identified as dysregulated in both PGRKO and AKO mice have been studied in ovulation, a detailed set of other genes was also uncovered which remain to be investigated to determine their roles. To this end, it is important that a number of gene ontological pathways are conserved between total PGR and PGR-A regulated genesets including Cell Adhesion, Cell Development and Neurogenesis. Further investigation into the pathways and their constituent genes is likely to discover new aspects of the ovulatory mechanism.

Overall, this is the first description of the PGR isoform-specific transcriptomes in granulosa cells, where PGR plays a crucial role in the regulation of ovulation. The transcriptome results agree with the previously described ovarian phenotype of AKO and BKO mouse models and highlight a number of genes with potential novel roles in ovulation that invite further investigation. Stark contrasts between isoform-dependent gene expression profiles confirmed the prominence of PGR-A in ovulatory functions and that PGR-B had little involvement in the regulation of ovulatory genes and is likely involved in other roles, possibly repressing transcriptional expression of certain genes. These results once again corroborate previous findings on differences in PGR isoform properties and functions that have been observed in other cellular contexts and indicate that a distinction between PGR isoforms is highly important in investigating PGR actions. The findings support an interaction between PGR and RUNX1 in many, but not all PGR regulated genes indicating that PGR action in granulosa cells is complex and involves RUNX1 interaction, as well as independent actions and the induction of

intermediate transcription factors including PPARγ and HIF. Possible additional interactions of PGR-A with β-catenin, SP1 and CEBP transcription factors also warrant further study.

7.5 REFERENCES

1 Dong, X., Challis & Lye, S. Intramolecular interactions between the AF3 domain and the C-terminus of the human progesterone receptor are mediated through two LXXLL motifs. **32**, 843, doi:10.1677/jme.0.0320843 (2004).

2 Teilmann, S. C., Clement, C. A., Thorup, J., Byskov, A. G. & Christensen, S. T. Expression and localization of the progesterone receptor in mouse and human reproductive organs. *J Endocrinol* **191**, 525-535, doi:10.1677/joe.1.06565 (2006).

3 Mulac-Jericevic, B., Mullinax, R. A., DeMayo, F. J., Lydon, J. P. & Conneely, O. M. Subgroup of Reproductive Functions of Progesterone Mediated by Progesterone Receptor-B Isoform. *Science* **289**, 1751-1754, doi:10.1126/science.289.5485.1751 (2000).

4 Mulac-Jericevic, B., Lydon, J. P., DeMayo, F. J. & Conneely, O. M. Defective mammary gland morphogenesis in mice lacking the progesterone receptor B isoform. *Proceedings of the National Academy of Sciences* **100**, 9744-9749, doi:10.1073/pnas.1732707100 (2003).

5 Lydon, J. P., DeMayo, F. J., Funk, C. R., Mani, S. K., Hughes, A. R., Montgomery, C. A., Jr., Shyamala, G., Conneely, O. M. & O'Malley, B. W. Mice lacking progesterone receptor exhibit pleiotropic reproductive abnormalities. *Genes Dev* **9**, 2266-2278 (1995).

6 Robker, R. L., Russell, D. L., Espey, L. L., Lydon, J. P., O'Malley, B. W. & Richards, J. S. Progesterone-regulated genes in the ovulation process: ADAMTS-1 and cathepsin L proteases. *Proc Natl Acad Sci U S A* **97**, 4689-4694 (2000).

7 Ko, C., Gieske, M. C., Al-Alem, L., Hahn, Y., Su, W., Gong, M. C., Iglarz, M. & Koo, Y. Endothelin-2 in Ovarian Follicle Rupture. *Endocrinology* **147**, 1770-1779, doi:10.1210/en.2005-1228 (2006).

8 Brown, H. M., Dunning, K. R., Robker, R. L., Boerboom, D., Pritchard, M., Lane, M. & Russell, D. L. ADAMTS1 Cleavage of Versican Mediates Essential Structural Remodeling of the Ovarian Follicle and Cumulus-Oocyte Matrix During Ovulation in Mice1. *Biology of Reproduction* **83**, 549-557, doi:10.1095/biolreprod.110.084434 (2010).

9 Kim, J., Sato, M., Li, Q., Lydon, J. P., DeMayo, F. J., Bagchi, I. C. & Bagchi, M. K. Peroxisome Proliferator-Activated Receptor γ Is a Target of Progesterone Regulation in the Preovulatory Follicles and Controls Ovulation in Mice. *Molecular and cellular biology* **28**, 1770-1782, doi:10.1128/mcb.01556-07 (2008).

10 Pabona, J. M. P., Zhang, D., Ginsburg, D. S., Simmen, F. A. & Simmen, R. C. M. Prolonged Pregnancy in Women Is Associated With Attenuated Myometrial Expression of Progesterone Receptor Co-Regulator Krüppel-Like Factor 9. *The Journal of Clinical Endocrinology & Metabolism* **100**, 166-174, doi:10.1210/jc.2014-2846 (2015).

11 Aupperlee, M. D., Smith, K. T., Kariagina, A. & Haslam, S. Z. Progesterone Receptor Isoforms A and B: Temporal and Spatial Differences in Expression during Murine Mammary Gland Development. *Endocrinology* **146**, 3577-3588, doi:10.1210/en.2005-0346 (2005).

12 Singhal, H., Greene, M. E., Zarnke, A. L., Laine, M., Al Abosy, R., Chang, Y.-F., Dembo, A. G., Schoenfelt, K., Vadhi, R., Qiu, X., Rao, P., Santhamma, B., Nair, H. B., Nickisch, K. J., Long, H. W., Becker, L., Brown, M. & Greene, G. L. Progesterone receptor isoforms, agonists and antagonists differentially reprogram estrogen signaling. *Oncotarget* **9**, 4282-4300, doi:10.18632/oncotarget.21378 (2017).

13 Abdel-Hafiz, H., Takimoto, G. S., Tung, L. & Horwitz, K. B. The Inhibitory Function in Human Progesterone Receptor N Termini Binds SUMO-1 Protein to Regulate Autoinhibition and Transrepression. *Journal of Biological Chemistry* **277**, 33950-33956, doi:10.1074/jbc.M204573200 (2002).

14 Afgan, E., Baker, D., Batut, B., van den Beek, M., Bouvier, D., Čech, M., Chilton, J., Clements, D., Coraor, N., Grüning, B. A., Guerler, A., Hillman-Jackson, J., Hiltemann, S., Jalili, V., Rasche, H., Soranzo, N., Goecks, J., Taylor, J., Nekrutenko, A. & Blankenberg, D. The Galaxy platform for accessible, reproducible and collaborative biomedical analyses: 2018 update. *Nucleic Acids Research* **46**, W537-W544, doi:10.1093/nar/gky379 (2018).

15 Schneider, V. A., Graves-Lindsay, T., Howe, K., Bouk, N., Chen, H.-C., Kitts, P. A., Murphy, T. D., Pruitt, K. D., Thibaud-Nissen, F., Albracht, D., Fulton, R. S., Kremitzki, M., Magrini, V., Markovic, C., McGrath, S., Steinberg, K. M., Auger, K., Chow, W., Collins, J., Harden, G., Hubbard, T., Pelan, S., Simpson, J. T., Threadgold, G., Torrance, J., Wood, J. M., Clarke, L., Koren, S., Boitano, M., Peluso, P., Li, H., Chin, C.-S., Phillippy, A. M., Durbin, R., Wilson, R. K., Flicek, P., Eichler, E. E. & Church, D. M. Evaluation of GRCh38 and de novo haploid genome assemblies demonstrates the enduring quality of the reference assembly. *Genome Research* **27**, 849-864, doi:10.1101/gr.213611.116 (2017).

16 Kim, D., Langmead, B. & Salzberg, S. L. HISAT: a fast spliced aligner with low memory requirements. *Nature Methods* **12**, 357-360, doi:10.1038/nmeth.3317 (2015).

17 Li, H., Handsaker, B., Wysoker, A., Fennell, T., Ruan, J., Homer, N., Marth, G., Abecasis, G. & Durbin, R. The Sequence Alignment/Map format and SAMtools. *Bioinformatics* **25**, 2078-2079, doi:10.1093/bioinformatics/btp352 (2009).

18 Pertea, M., Pertea, G. M., Antonescu, C. M., Chang, T.-C., Mendell, J. T. & Salzberg, S. L. StringTie enables improved reconstruction of a transcriptome from RNA-seq reads. *Nature Biotechnology* **33**, 290-295, doi:10.1038/nbt.3122 (2015).

19 Trapnell, C., Williams, B. A., Pertea, G., Mortazavi, A., Kwan, G., van Baren, M. J., Salzberg, S. L., Wold, B. J. & Pachter, L. Transcript assembly and quantification by RNA-Seq reveals unannotated transcripts and isoform switching during cell differentiation. *Nature Biotechnology* **28**, 511-515, doi:10.1038/nbt.1621 (2010).

20 Liao, Y., Smyth, G. K. & Shi, W. featureCounts: an efficient general purpose program for assigning sequence reads to genomic features. *Bioinformatics* **30**, 923-930, doi:10.1093/bioinformatics/btt656 (2013).

21 Love, M. I., Huber, W. & Anders, S. Moderated estimation of fold change and dispersion for RNA-seq data with DESeq2. *Genome Biology* **15**, 550, doi:10.1186/s13059-014-0550-8 (2014).

22 The Gene Ontology Consortium. The Gene Ontology Resource: 20 years and still GOing strong. *Nucleic Acids Research* **47**, D330-D338, doi:10.1093/nar/gky1055 (2018).

23 Boyle, E. I., Weng, S., Gollub, J., Jin, H., Botstein, D., Cherry, J. M. & Sherlock, G. GO::TermFinder--open source software for accessing Gene Ontology information and finding significantly enriched Gene Ontology terms associated with a list of genes. *Bioinformatics* **20**, 3710-3715, doi:10.1093/bioinformatics/bth456 (2004).

24 Patro, R., Duggal, G., Love, M. I., Irizarry, R. A. & Kingsford, C. Salmon provides fast and bias-aware quantification of transcript expression. *Nature methods* **14**, 417 (2017).

25 Ramírez, F., Ryan, D. P., Grüning, B., Bhardwaj, V., Kilpert, F., Richter, A. S., Heyne, S., Dündar, F. & Manke, T. deepTools2: a next generation web server for deep-sequencing data analysis. *Nucleic Acids Research* **44**, W160-W165, doi:10.1093/nar/gkw257 (2016).

26 Kent, W. J., Sugnet, C. W., Furey, T. S., Roskin, K. M., Pringle, T. H., Zahler, A. M. & Haussler, D. The human genome browser at UCSC. *Genome Res* **12**, 996-1006, doi:10.1101/gr.229102 (2002).

27 Ogiwara, K., Takano, N., Shinohara, M., Murakami, M. & Takahashi, T. Gelatinase A and membrane-type matrix metalloproteinases 1 and 2 are responsible for follicle rupture during ovulation in the medaka. *Proceedings of the National Academy of Sciences of the United States of America* **102**, 8442-8447, doi:10.1073/pnas.0502423102 (2005).

28 Li, Q., Cheon, Y. P., Kannan, A., Shanker, S., Bagchi, I. C. & Bagchi, M. K. A novel pathway involving progesterone receptor, 12/15-lipoxygenase-derived eicosanoids, and peroxisome proliferator-activated receptor gamma regulates implantation in mice. *J Biol Chem* **279**, 11570-11581, doi:10.1074/jbc.M311773200 (2004).

29 Jeong, J.-W., Lee, K. Y., Kwak, I., White, L. D., Hilsenbeck, S. G., Lydon, J. P. & DeMayo, F. J. Identification of Murine Uterine Genes Regulated in a Ligand-Dependent Manner by the Progesterone Receptor. *Endocrinology* **146**, 3490-3505, doi:10.1210/en.2005-0016 (2005).

30 Kommagani, R., Szwarc, M. M., Vasquez, Y. M., Peavey, M. C., Mazur, E. C., Gibbons, W. E., Lanz, R. B., DeMayo, F. J. & Lydon, J. P. The Promyelocytic Leukemia Zinc Finger Transcription Factor Is Critical for Human Endometrial Stromal Cell Decidualization. *PLoS genetics* **12**, e1005937-e1005937, doi:10.1371/journal.pgen.1005937 (2016).

31 Mao, A.-P., Ishizuka, I. E., Kasal, D. N., Mandal, M. & Bendelac, A. A shared Runx1-bound Zbtb16 enhancer directs innate and innate-like lymphoid lineage development. *Nature Communications* **8**, 863, doi:10.1038/s41467-017-00882-0 (2017).

32 Poulsen, L. l. C., Englund, A. L. M., Wissing, M. L. M., Yding Andersen, C., Borup, R. & Grøndahl, M. L. Human granulosa cells function as innate immune cells executing an inflammatory reaction during ovulation: a microarray analysis. *Molecular and Cellular Endocrinology* **486**, 34-46, doi:https://doi.org/10.1016/j.mce.2019.02.014 (2019).

33 Fan, H.-Y., Liu, Z., Johnson, P. F. & Richards, J. S. CCAAT/Enhancer-Binding Proteins (C/EBP)-α and -β Are Essential for Ovulation, Luteinization, and the Expression of Key Target Genes. *Molecular Endocrinology* **25**, 253-268, doi:10.1210/me.2010-0318 (2011).

34 Fan, H.-Y., O'Connor, A., Shitanaka, M., Shimada, M., Liu, Z. & Richards, J. S. β-Catenin (CTNNB1) Promotes Preovulatory Follicular Development but Represses LH-Mediated Ovulation and Luteinization. *Molecular Endocrinology* **24**, 1529-1542, doi:10.1210/me.2010-0141 (2010).

35 Doyle, K. M. H., Russell, D. L., Sriraman, V. & Richards, J. S. Coordinate Transcription of the ADAMTS-1 Gene by Luteinizing Hormone and Progesterone Receptor. *Molecular Endocrinology* **18**, 2463-2478, doi:10.1210/me.2003-0380 (2004).

36 Kim, J., Bagchi, I. C. & Bagchi, M. K. Signaling by hypoxia-inducible factors is critical for ovulation in mice. *Endocrinology* **150**, 3392-3400, doi:10.1210/en.2008-0948 (2009).

37 Zhang, X.-L., Zhang, D., Michel, F. J., Blum, J. L., Simmen, F. A. & Simmen, R. C. M. Selective Interactions of Krüppel-like Factor 9/Basic Transcription Element-binding Protein with Progesterone Receptor Isoforms A and B Determine Transcriptional Activity of Progesterone-responsive Genes in Endometrial Epithelial Cells. *Journal of Biological Chemistry* **278**, 21474-21482, doi:10.1074/jbc.M212098200 (2003).

38 Scarpin, K. M., Graham, J. D., Mote, P. A. & Clarke, C. L. Progesterone Action in Human Tissues: Regulation by Progesterone Receptor (PR) Isoform Expression, Nuclear Positioning and Coregulator Expression. *Nuclear Receptor Signaling* **7**, nrs.07009, doi:10.1621/nrs.07009 (2009).

39 Hwang, J.-Y. & Zukin, R. S. REST, a master transcriptional regulator in neurodegenerative disease. *Current Opinion in Neurobiology* **48**, 193-200, doi:https://doi.org/10.1016/j.conb.2017.12.008 (2018).

40 Zhang, P.-J., Zhao, J., Li, H.-Y., Man, J.-H., He, K., Zhou, T., Pan, X., Li, A.-L., Gong, W.-L., Jin, B.-F., Xia, Q., Yu, M., Shen, B.-F. & Zhang, X.-M. CUE domain containing 2 regulates degradation of progesterone receptor by ubiquitin-proteasome. *The EMBO journal* **26**, 1831-1842, doi:10.1038/sj.emboj.7601602 (2007).

41 Bellance, C., Khan, J. A., Meduri, G., Guiochon-Mantel, A., Lombès, M. & Loosfelt, H. Progesterone receptor isoforms PRA and PRB differentially contribute to breast cancer cell migration through interaction with focal adhesion kinase complexes. *Molecular biology of the cell* **24**, 1363-1374, doi:10.1091/mbc.E12-11-0807 (2013).

42 Khan, J. A., Amazit, L., Bellance, C., Guiochon-Mantel, A., Lombès, M. & Loosfelt, H. p38 and p42/44 MAPKs Differentially Regulate Progesterone Receptor A and B Isoform Stabilization. *Molecular Endocrinology* **25**, 1710-1724, doi:10.1210/me.2011-1042 (2011).

CHAPTER 8 Conclusions & future directions

8.1 INTRODUCTION

Ovulation is a complex process in which many cellular and biochemical factors are acting in coordination to ultimately result in the release of the mature oocyte into the oviduct for fertilisation. A key ovarian hormone that is essential for this process is progesterone, which acts through its receptor PGR to regulate numerous downstream target genes that are in turn involved in various aspects of ovulation. The undisputable importance of PGR on ovulation has been illustrated on a physiological level in the PGRKO mouse model and also in humans through the demonstration that PGR antagonists block ovulation. The disruption of PGR by either means results in an anovulatory and sterile phenotype in female mice due to failure in follicle rupture despite normal oocyte maturation [1,2]. Not only is PGR crucial for ovulation but it also plays an important role in other tissues throughout the female reproductive tract as a coordinator of various biological processes in preparation for pregnancy. PGR is important for modulating ciliate movements in the oviduct and therefore the transportation of oocytes and embryos through the reproductive tract [3]. In the uterus, PGR has a role in decidualisation and embryo implantation [1]. While it is understood that PGR is a key factor in many aspects of female reproduction, it is still unclear how these diverse processes are synchronised by a single transcription factor. The goal of this thesis was thus to address the following broad questions:

How can PGR, in response to progesterone, coordinate diverse biological processes in different tissue contexts? In the case of ovulation in particular, what are the underlying molecular mechanisms that set apart PGR actions in granulosa cells in comparison to other reproductive tissue types?

The hypothesis is that unique aspects of the PGR transcription complex different tissue contexts allow for PGR actions in granulosa cells to be set apart and enable the coordination of diverse biological processes in distinct reproductive tissues. To build the model for PGR transcription complex in peri-ovulatory granulosa cells, key aspects of the PGR cistrome, transcriptome and interactome were explored in each of the six chapters. A pictorial summary of the thesis structure is shown in Figure 8.1.

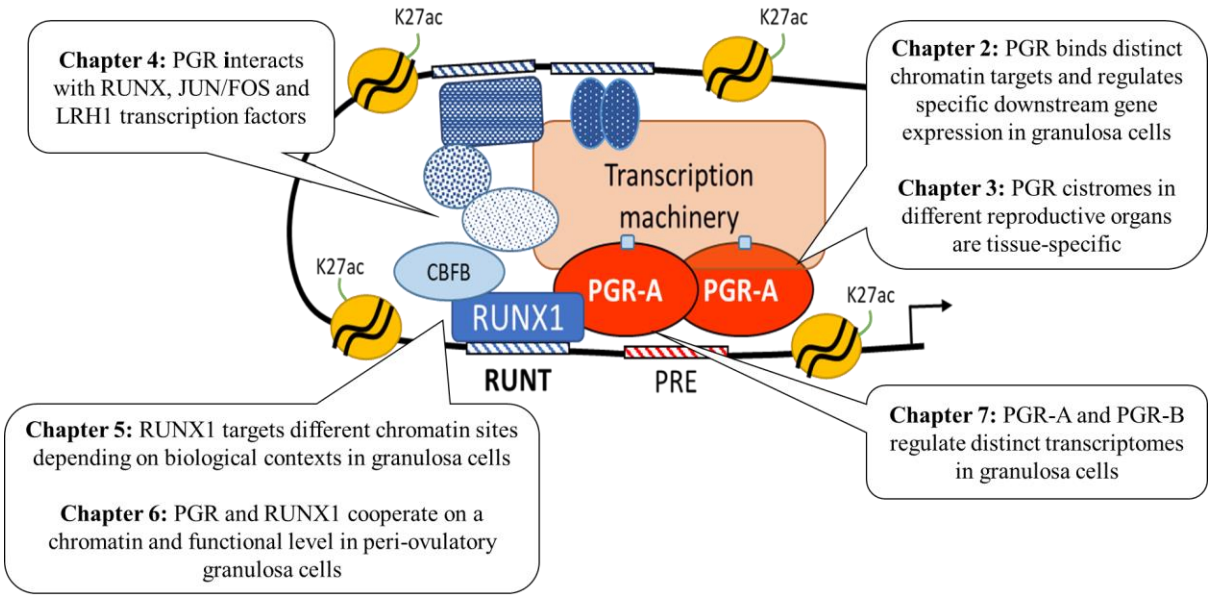

Figure 8.1 Summary of the thesis.

Different aspects of the transcription complex involving PGR in peri-ovulatory granulosa cells were investigated in each chapter of this thesis, as indicated in the schematic.

8.2 MAIN FINDINGS

The goal of the thesis and questions that arose throughout the study were addressed in six chapters, with the following main conclusions reached:

8.2.1 PGR binds chromatin and regulates downstream gene expression in a tissue-specific manner

The main function of PGR is to regulate gene expression through directly binding target DNA, canonically at the consensus PRE motif. However, it has been shown that PGR can regulate target genes without the PRE motif through tethering by other transcription factors [4]. To determine whether this is the preferred mechanism in granulosa cells in general, Chapter 2 explored the PGR cistrome in peri-ovulatory granulosa cells. PGR was found to mostly occupy transcriptionally active promoter regions and remarkably, PGR was found to not only interact with its canonical PRE motif but also with a number of non-canonical motifs usually bound by other transcription factor families. The significance of these PGR chromatin binding events was also demonstrated by the integration with PGR-dependent and LH-stimulated granulosa cell transcriptomes.

As PGR coordinates distinct biological events in the ovary, oviduct and uterus, it is possible that the chromatin binding properties of PGR in different reproductive tissues are also unique, resulting in specific PGR-regulated gene expression profiles with consequences on the distinct physiological roles of PGR. To confirm this, in Chapter 3, comparisons were made between three PGR-dependent transcriptomes in the progesterone-stimulated mouse granulosa cells, oviduct and uterus, for which three highly unique groups of genes were identified. Such striking differences are likely due to distinct molecular mechanisms employed by PGR in cells from different tissues in the reproductive tract. To identify these distinct molecular mechanisms, comparative analysis of PGR chromatin binding properties were made in two progesterone-responsive tissue types – granulosa cells and the uterus. PGR was shown to have highly specialised chromatin binding properties – granulosa PGR preferably bound proximal promoter regions, which was not observed in uterine PGR, and consequentially leads to the enrichment of distinct molecular pathways. Interestingly, PGR not only showed different levels of PRE binding but also interaction with distinct groups of non-canonical motifs, indicating that the interactome of PGR in different tissues is important in determining tissue-specific transcriptional functions and biological functions.

8.2.2 PGR interacts with a selective group of co-regulators in peri-ovulatory granulosa cells especially RUNX1

Based on the results of Chapter 3, a number of transcription factor families were hypothesised to interact with chromatin-bound PGR through motif analysis. However, it is unknown whether these transcription factors form a physical interaction with PGR in granulosa cells. As each motif tends to be recognised by multiple transcription factors of the same family, candidates were selected based on the level of motif enrichment at PGR binding sites as well as on their known precedence as an ovarian transcription factor. These included RUNX (RUNX1, RUNX2, CBFβ), JUN/FOS (c-JUN, JUNB, JUND) and NR5A (LRH1), all of which are known to regulate gene expression in granulosa cells during ovulation [5-10]. In particular the RUNX binding motif was significantly enriched only in granulosa cells and not the uterus. In Chapter 4, the physical interaction between PGR and members of the RUNX, JUN/FOS and NR5A families was investigated through proximity ligation assay of cultured granulosa cells stimulated with hCG and progestin to mimic the earliest responses of the LH surge. Apart from c-JUN and JUNB, all candidate proteins were induced and formed a physical interaction with PGR in the nucleus of granulosa cells in response to these ovulatory cues, indicating that these transcription factors are involved in the PGR-inclusive transcription complex. Also importantly, the dynamics of the interactions between PGR and RUNX1 / RUNX2 was also investigated in Chapter 6, in which these interactions were shown to be induced within 4-6 h after hCG treatment. These results together suggest that PGR-chromatin binding in granulosa cells involves a cooperative mechanism forming transcriptional complexes with RUNX, LRH1 and JUN/FOS families.

RUNX1 is expressed in granulosa cells at different stages of ovarian development and has been shown to regulate gene expression in granulosa cells during ovulation [5] and to also be important in granulosa specification in the foetal ovary [11]. Thus it is important to define the distinct RUNX1 cistromes in these biological contexts. Chapter 5 addressed the differences in RUNX1 cistromes in foetal granulosa cells vs adult granulosa cells before and after the LH surge through comparative analysis of RUNX1 ChIP-seq at different biological stages. The results highlighted the high level of promoter occupancy by RUNX1 in all biological contexts and illustrated an induction of novel RUNX1 chromatin binding sites in response to the LH surge. Subsequently, Chapter 6 demonstrated the similarities between PGR and RUNX1 bound sites through comparative analysis of PGR and RUNX1 ChIP-seq in hCG-stimulated granulosa

cells. RUNX1 and PGR cistromes showed remarkably high overlap in granulosa cells and the two transcription factors also shared the same repertoire of enriched non-canonical motifs, indicating potential members of the PGR/RUNX1 transcription complex. Such interaction also explains the functional similarities between the two transcription factors.

Aside from other transcription factors, PGR action can also be mediated by interaction with lncRNA, such as *Sra1* [12] and *Gas5* [13]. Various lncRNA have also attributed to ovarian functions [14]; however, the regulatory role of lncRNA on PGR during ovulation has never been addressed. The relationship between PGR and its known ncRNA regulators, addressed through RIP, showed evidence that *Sra1* and *Gas5* indeed bound PGR in granulosa cells in response to the LH surge; suggesting a possible role for these lncRNA, as well as ncRNA generally, in regulating transcriptional complex formation during ovulation.

Overall, these chapters confirm that PGR interacts with a selective group of co-regulators in peri-ovulatory granulosa cells, including both other transcription factors and lncRNA. In particular, PGR/RUNX1 interaction results in striking similarities between the PGR and RUNX1 cistromes. However, RUNX1 bound chromatin in granulosa cells at various developmental stages. Most interestingly, the RUNT motif was enriched in PGR cistrome while the PRE/NR3C motif was not as enriched in the RUNX1 cistrome. All of these suggest that RUNX1 likely plays the role of a pioneer factor to recruit PGR to its granulosa-specific target sites. Such an interaction results in important consequences for the downstream ovulation-specific gene expression profile.

8.2.3 PGR-A and PGR-B regulate different transcriptomes in granulosa cells

Another aspect of specific PGR functions is its multiple isoforms, especially the two main isoforms PGR-A and PGR-B. While PGR-B has an additional AF domain that generally enhances its transactivation properties compared to PGR-A [15], PGR-A has also been shown to have a trans-repressive role on PGR-B [16]. Furthermore, PGR usually acts as a dimer made up of either the same monomer (PGR-A and PGR-B homodimers) or a mix of the two isoforms (PGR-A/PGR-B heterodimer) [17]. This results in a complex interplay between the two transcription factors and distinctive gene expression profiles driven by the presence of the two isoforms. Both isoforms are expressed in PGR-positive tissues, with PGR-A being the dominant isoform in reproductive tissues whereas PGR-B is more essential for mammary

tissues [18,19]. However, while PGR-A has been shown to be more important in determining the female reproductive phenotype, this has not been defined by transcriptomic evidence. Thus, to determine the isoform-specific transcriptomes, in Chapter 7, RNA-seq was performed on peri-ovulatory granulosa cells obtained from three KO mouse models – PGRKO, AKO and BKO. PGRKO and AKO transcriptomes were shown to be highly similar, with both KO models exhibiting suppression of the majority of identified genes as well as many ovulatory genes being identified in both datasets, reflected in the high overlap between PGRKO and AKO genes and global ovulatory genes in granulosa cells. In contrast, PGR-B seemed to play a lesser transactivation function in granulosa cells, with few differentially expressed genes identified in BKO. Finally, co-binding of PGR and RUNX1 in proximity to the gene boundary was found to be important for the regulation of PGRKO and AKO genes. This suggests that PGR-A and RUNX1 may form a specific interaction leading to granulosa-specific PGR-mediated transcriptional regulation.

8.2.4 Overall conclusion of thesis

A unique cooperation between PGR-A and specific transcription factors, including RUNX1, JUND and LRH1 forms a mutual transcriptional complex. Ultimately, such cooperation results in the regulation of genes that are important for ovulation.

A summary of this conclusion is shown in Figure 8.2.

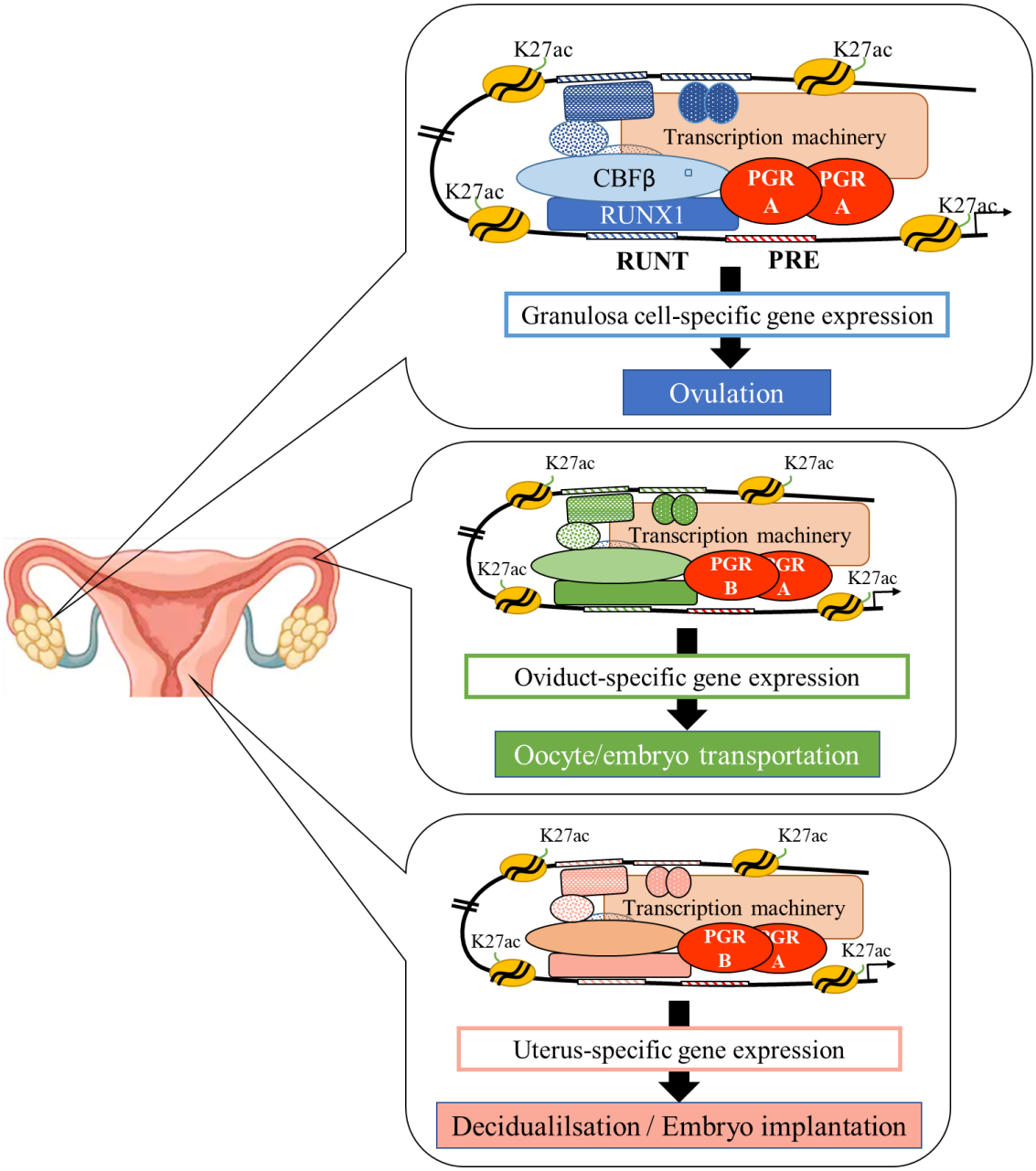

Figure 8.2 Schematic conclusion to the thesis, in regards to specialised PGR action in the ovary and the female reproductive tract.

8.3 REMAINING QUESTIONS & FUTURE STUDIES

This study serves at the first step in building the identity of the transcription complex of PGR and at the same time also distinguishing it from PGR mechanisms in other reproductive tissues and explaining the tissue-specific roles of PGR in the context of reproduction. In answering these questions, a combination of high-throughput techniques (such as ChIP-seq and RNA-seq) have been utilised for one of the first times in granulosa cells to identify the cistromic and transcriptomic properties of PGR. Such methods naturally generate a massive amount of data, and while the overall landscape of PGR action in granulosa cells has been characterised, as was intended to answer the questions being raised, this data remains to be further explored in detail. Characterisation of PGR chromatin binding properties have indicated a preference for non-promoter target sites for PGR in both tissue types, but more significantly in the uterus, implying that PGR can both interact with proximal promoters as well as more distal enhancer elements in a tissue-specific manner. In the context of breast tissues, PGR has been shown to exert influence on the transcription of target genes through interaction with specific enhancer sites [20,21]. However, such activity has not been previously described in the context of reproduction. For distally binding PGR to influence target genes requires reshaping the chromosomal conformation and involves a number of chromatin remodellers, including CTCF and Cohesin [22]. The function of these proteins has been linked to various transcription factors, such as FOXA1 and FOXA2 [23]. Whether the involvement of PGR is only a downstream effect of precedent chromatin conformational changes or PGR actively plays a role in chromatin restructure is still unknown. To look at this in further detail, the spatial organisation of chromatin in peri-ovulatory granulosa cells needs to first be characterised, for instance through chromatin conformation capture using Hi-C; alternatively, mapping of chromatin remodellers, such as CTCF sites, on the genome through immuno-based methods, can be utilised. This type of analysis will also be beneficial for understanding the roles of other transcription mediators as well as for constructing the transcription machinery in granulosa cells. Subsequently, the contribution of PGR on such chromatin landscape can be investigated utilising PGRKO mouse models.

Analysis of the PGR and RUNX1 cistromes has shown a high level of conformity between PGR and RUNX1 on a chromatin and functional level, with PGR action at target promoters predicted to be reliant on the presence of RUNX1. Furthermore, RUNX1 exhibited a basal level of chromatin occupancy on the genome prior to the LH, which was retained and co-bound

by PGR post-LH. This suggests that RUNX1 acts as a pioneer factor by binding potential PGR target chromatin and tethers PGR to non-traditional target sites during ovulation. Exactly how this is achieved is still unknown. Perhaps RUNX1 promotes the 'loosening' of the tightly-packed nucleosome structure by facilitating the recruiting chromatin remodelling factors such as SRC and CBP/p300 and thereby making the chromatin site accessible to PGR. Such a process has been illustrated in other contexts [24,25]; however, whether RUNX1 can similarly coordinate this in granulosa cells is thus far unknown. Alternatively, RUNX1 might act as a 'bait' to PGR and form direct interaction with PGR during the random scanning process, in which transcription factors scan the chromatin for accessible binding sites [26]. Such a model has been previously described in CEBPβ tethering of steroid receptors [27,28] and PGR is known to interact with SP1/SP3 binding sites to regulate *Adamts1* expression [4]. Studies into the interaction between RUNX1 and chromatin remodellers using immunoprecipitation or microscopy methods are vital in testing these hypotheses. Furthermore, tissue-specific conditional RUNX1 KO models will be helpful in determining the degree of PGR dependence on RUNX1.

Aside from RUNX1, RUNX2 and members of the JUN/FOS and NR5A transcription factor families were also shown to form a physical interaction with PGR that was mediated by ovulatory stimulation. These are by no means an exhaustive list, since motifs for other transcription factor families like CEBP and GATA were also found to be enriched at PGR binding sites. These transcription factors have also been linked to the regulation of ovulatory genes in granulosa cells [6,9], suggesting possible functional interactions between PGR and these co-modulators that require further investigation. In particular, the order in which these proteins are recruited to target chromatin sites would be of interest in unravelling the significance of each transcription factor in the ovulatory transcription complex. Another component of this transcription complex that has not been investigated in this study is the involvement of non-DNA binding transcription adaptors, such as SRC and HDAC, which could not be identified through motif analysis. A full description of the PGR interactome in granulosa cells through IP-MS would be able to identify all protein components of the transcription complex involving PGR.

From these cistromic and transcriptomic results, a large number of target genes for PGR-A and PGR-B have been identified, many of which are novel genes or have never been described in ovulation. Noteworthy among these PGR-regulated genes is *Zbtb16*, which is found to be

differentially expression in AKO granulosa cells and encodes for the transcription factor PLZF. While a role of PLZF in granulosa cells has not been characterised, it is found to be a PGR target gene in the endometrial stromal cell where it plays a role in regulating decidualisation [29]. Here, PGR binding at enhancer-like elements within the first intron of *Zbtb16* is proven to be vital for the induction of this gene. Similarly, RUNX1 binding of these *Zbtb16* intronic sites is important for the regulation of this gene [30]. In this current study, both PGR and RUNX1 were found to bind these locations in granulosa cells. Further investigations into the expression and function of *Zbtb16* in ovulation might identify it as a novel ovarian transcription factor.

Analysis of the differences in isoform-specific transcriptomes have clearly shown that PGR-A and PGR-B regulated two isoform-specific interactomes, implying the existence of distinct mechanisms employed by the two isoforms. So far, the lack of ChIP-grade antibodies that are specific to either isoform means that differences in the chromatin binding properties of PGR-A and PGR-B cannot be detected through conventional ChIP. However, with the availability of isoform-specific knockout mouse models, such barriers can be overcome. Other indirect approaches, such as investigating the effect of PGR isoforms on chromatin accessibility through ATAC-seq, FAIRE-seq or ChIP-seq with histone markers, can also be utilised to further discern the significance of each isoform on a chromatin level. However, in support of the idea of isoform-specific transcription regulation, PGR-A and PGR-B have previously shown clear differences in binding preferences to other transcription factors, such as BTEB1 and SRC [31], with consequences on downstream gene expression *in vitro* [32]. However, such characteristics have not been portrayed *in vivo*; thus, experiments designed to explore isoform-specific interactions in an *in vivo* settings using immuno-based protein capture or proximity ligation assays on granulosa cells expressing specific isoforms will be crucial in determining any differences in PGR-A and PGR-B co-binding partners. As each of PGR isoforms does not solely act independently from one another but can act cooperatively in the form of a heterodimer to regulate gene expression, it is also important to consider differences in the characteristics of PGR heterodimer vs homodimers and their implications on downstream gene expression. In such cases, a transgenic model in which heterodimerisation or homodimerisation is enforced, for example through the transfection of a chimeric construct bearing the sequence for both PGR-A and PGR-B on the same construct, would help in dissecting the role of each dimer form.

While the importance of lncRNA is the focus for many recent exciting studies, there is still very little known about their roles in ovulation and only a handful of lncRNA has been characterised in detail. Many ncRNA, including lncRNA, are transcribed from introns or the complementary strand of a protein-coding gene [33] and are thus often overlooked as a by-product of the transcription or splicing events. As ncRNA are often lowly transcribed in cells, yet at the same time can still exert important regulatory roles, the conventional method of RNA-seq analysis is often unable to discern differential expression patterns of ncRNA. Despite this, a number of ncRNA-encoded genes were identified in these datasets. This includes several antisense transcripts as well as *Rny1* and *Rmst*, which are virtually unknown to the ovulation process. Since none of these ncRNA has been described in detail, especially in the ovary, it is unknown whether they play a role in ovulation. The scope of lncRNA involvement in ovulation will need to be investigated in further detail, specifically through RNA-seq analysis using specific ncRNA-oriented workflow. Conversely, PGR was also found to interact with lncRNA (i.e. *Sra1, Gas5*) in response to the LH surge, suggesting that lncRNA plays a role in regulating PGR function in granulosa cells. As this was largely an exploratory study limited to ncRNA with known PGR binding capability, the breadth of the PGR ncRNA interactome largely remains a mystery. Experimental designs that are more high-throughput, such as RIP-seq, would be necessary to uncover the degree of ncRNA action in regulating PGR as well as other transcription factors during ovulation.

Overall, through detailed investigation into different aspects of PGR action, including the PGR-regulated cistrome and transcriptome as well as PGR interactome, a model for the PGR transcriptional complex has begun to be described. However, this is unlikely the complete picture of the PGR transcription complex in granulosa cells, with many other elements remains to be explored. To name a few – what other transcriptional modulators are components of this complex, including chromatin-binding transcription factors and non-chromatin binding regulators? What is the extent of lncRNA involvement in the regulation of PGR functions? Are there differences in the interactome of different PGR isoforms? The answering of these questions will require mixed approaches, such as high-throughput techniques looking at protein/RNA interactions (immunoprecipitation-mass spectrometry/sequencing) and chromatin conformation (ATAC-seq, Hi-C), as well as the utilisation of specific KO models of PGR, RUNX1 and other target genes. The generation of a large body of data also provides the opportunity for future studies into specific downstream target genes of PGR as well as PGR-regulated enhancer elements in the context of ovulation.

8.4 SIGNIFICANCE OF THIS STUDY

In the ovary, PGR is an important key transcription factor that determines ovulation, the dysregulation of which is likely to contribute to the aetiology of anovulatory infertility, observed in various KO mouse models [1,18,19] as well as in human [34]. In addition, PGR is also present throughout the female reproductive tract as well as non-reproductive tissues such as the brain [35], breast [36] and bone [37], where it plays various roles that are specific to the tissue context in response to hormones. As PGR acts in diverse organs throughout the body, alterations into PGR activities, either pathologically or artificially in hormone therapies for contraceptive or therapeutic purposes, can lead to unwanted, perhaps even dangerous, effects on other tissues. The effect of unphysiological hormone actions is most prevalent in the field of female contraception, where synthetic oestrogens and progestins are administered as a means to repress gonadotropin production and thereby follicle development and ovulation [38]. Such artificially elevated state of progestin level not only affects the target hypothalamic-pituitary-ovarian axis and steroidogenesis pathway but can also affect other tissues that are highly responsive to progesterone, leading to an array of unwanted side-effects, including thrombosis, depression and an increased risk of breast [39] and cervical cancer [40]. Progestins and oestrogens are also widely used in other therapeutic contexts, especially in the treatment of hormone-responsive cancers, including breast and endometrial cancer, and also in managing menopausal symptoms. While reports on the correlation between hormone therapies and side-effects are largely inconclusive [41,42], a number of adverse effects such as thrombosis and breast cancer have been found to be associated with prolonged or high dosage of progestin usage in endometrial cancer treatment [43] and in menopausal hormone replacement therapy [44,45], respectively. Thus, it is important that different therapeutic approaches with minimised adverse effects can be devised, for which an understanding in the tissue-specific PGR pathways is required.

This study presents the first description of the potential molecular mechanism employed by PGR in regulating gene expression that allows for specific functions in granulosa cells during ovulation. These insights into PGR action in granulosa cells deepen our understanding of tissue-specific mechanisms of PGR in ovulation, which can lead to novel replacements for current contraceptive methods, especially the development of contraceptives that can specifically block ovulation without these side-effects that often arise with hormone therapies. Concurrently, by adding to the landscape of PGR responsiveness in reproductive tissues, our

findings provide insight into new and efficient cancer therapeutics targeting specific reproductive organs with mitigated side effects on other PGR-dependent tissues.

8.5 REFERENCES

1 Lydon, J. P., DeMayo, F. J., Funk, C. R., Mani, S. K., Hughes, A. R., Montgomery, C. A., Jr., Shyamala, G., Conneely, O. M. & O'Malley, B. W. Mice lacking progesterone receptor exhibit pleiotropic reproductive abnormalities. *Genes Dev* **9**, 2266-2278 (1995).

2 Gemzell-Danielsson, K., Berger, C. & P.G.L, L. Emergency contraception — mechanisms of action. *Contraception* **87**, 300-308, doi:https://doi.org/10.1016/j.contraception.2012.08.021 (2013).

3 Akison, L. & Robker, R. The Critical Roles of Progesterone Receptor (PGR) in Ovulation, Oocyte Developmental Competence and Oviductal Transport in Mammalian Reproduction. *Reproduction in Domestic Animals* **47**, 288-296, doi:10.1111/j.1439-0531.2012.02088.x (2012).

4 Doyle, K. M. H., Russell, D. L., Sriraman, V. & Richards, J. S. Coordinate Transcription of the ADAMTS-1 Gene by Luteinizing Hormone and Progesterone Receptor. *Molecular Endocrinology* **18**, 2463-2478, doi:10.1210/me.2003-0380 (2004).

5 Jo, M. & Curry, T. E., Jr. Luteinizing Hormone-Induced RUNX1 Regulates the Expression of Genes in Granulosa Cells of Rat Periovulatory Follicles. *Molecular Endocrinology* **20**, 2156-2172, doi:10.1210/me.2005-0512 (2006).

6 Choi, Y., Rosewell, K. L., Brännström, M., Akin, J. W., Curry Jr, T. E. & Jo, M. FOS, a Critical Downstream Mediator of PGR and EGF Signaling Necessary for Ovulatory Prostaglandins in the Human Ovary. *The Journal of Clinical Endocrinology & Metabolism* **103**, 4241-4252 (2018).

7 Park, E.-S., Lind, A.-K., Dahm-Kähler, P., Brännström, M., Carletti, M. Z., Christenson, L. K., Curry, T. E., Jr. & Jo, M. RUNX2 Transcription Factor Regulates Gene Expression in Luteinizing Granulosa Cells of Rat Ovaries. *Molecular Endocrinology* **24**, 846-858, doi:10.1210/me.2009-0392 (2010).

8 Lee-Thacker, S., Choi, Y., Taniuchi, I., Takarada, T., Yoneda, Y., Ko, C. & Jo, M. Core binding factor β expression in ovarian granulosa cells is essential for female fertility. *Endocrinology* **159**, 2094-2109 (2018).

9 Duggavathi, R., Volle, D. H., Mataki, C., Antal, M. C., Messaddeq, N., Auwerx, J., Murphy, B. D. & Schoonjans, K. Liver receptor homolog 1 is essential for ovulation. *Genes Dev* **22**, 1871-1876, doi:10.1101/gad.472008 (2008).

10 Battaglia, R., Vento, M. E., Borzì, P., Ragusa, M., Barbagallo, D., Arena, D., Purrello, M. & Di Pietro, C. Non-coding RNAs in the Ovarian Follicle. *Frontiers in Genetics* **8**, doi:10.3389/fgene.2017.00057 (2017).

11 Nicol, B., Grimm, S. A., Chalmel, F., Lecluze, E., Pannetier, M., Pailhoux, E., Dupin-De-Beyssat, E., Guiguen, Y., Capel, B. & Yao, H. H. C. RUNX1 maintains the identity of the fetal ovary through an interplay with FOXL2. *Nature communications* **10**, 5116 (2019). <https://doi.org/10.1038/s41467-019-13060-1>.

12 Lanz, R. B., Razani, B., Goldberg, A. D. & O'Malley, B. W. Distinct RNA motifs are important for coactivation of steroid hormone receptors by steroid receptor RNA activator (SRA). *Proceedings of the National Academy of Sciences* **99**, 16081-16086, doi:10.1073/pnas.192571399 (2002).

13 Kino, T., Hurt, D. E., Ichijo, T., Nader, N. & Chrousos, G. P. Noncoding RNA gas5 is a growth arrest- and starvation-associated repressor of the glucocorticoid receptor. *Sci Signal* **3**, 2000568 (2010).

14 Yerushalmi, G. M., Salmon-Divon, M., Yung, Y., Maman, E., Kedem, A., Ophir, L., Elemento, O., Coticchio, G., Dal Canto, M., Mignini Renzinu, M., Fadini, R. &

Hourvitz, A. Characterization of the human cumulus cell transcriptome during final follicular maturation and ovulation. *Molecular Human Reproduction* **20**, 719-735, doi:10.1093/molehr/gau031 (2014).

15 Kastner, P., Krust, A., Turcotte, B., Stropp, U., Tora, L., Gronemeyer, H. & Chambon, P. Two distinct estrogen-regulated promoters generate transcripts encoding the two functionally different human progesterone receptor forms A and B. *The EMBO Journal* **9**, 1603-1614, doi:10.1002/j.1460-2075.1990.tb08280.x (1990).

16 Abdel-Hafiz, H., Takimoto, G. S., Tung, L. & Horwitz, K. B. The Inhibitory Function in Human Progesterone Receptor N Termini Binds SUMO-1 Protein to Regulate Autoinhibition and Transrepression. *Journal of Biological Chemistry* **277**, 33950-33956, doi:10.1074/jbc.M204573200 (2002).

17 Li, X. & O'Malley, B. W. Unfolding the Action of Progesterone Receptors. *Journal of Biological Chemistry* **278**, 39261-39264, doi:10.1074/jbc.R300024200 (2003).

18 Mulac-Jericevic, B., Lydon, J. P., DeMayo, F. J. & Conneely, O. M. Defective mammary gland morphogenesis in mice lacking the progesterone receptor B isoform. *Proceedings of the National Academy of Sciences* **100**, 9744-9749, doi:10.1073/pnas.1732707100 (2003).

19 Mulac-Jericevic, B., Mullinax, R. A., DeMayo, F. J., Lydon, J. P. & Conneely, O. M. Subgroup of Reproductive Functions of Progesterone Mediated by Progesterone Receptor-B Isoform. *Science* **289**, 1751-1754, doi:10.1126/science.289.5485.1751 (2000).

20 Subtil-Rodríguez, A., Millán-Ariño, L., Quiles, I., Ballaré, C., Beato, M. & Jordan, A. Progesterone Induction of the 11β-Hydroxysteroid Dehydrogenase Type 2 Promoter in Breast Cancer Cells Involves Coordinated Recruitment of STAT5A and Progesterone Receptor to a Distal Enhancer and Polymerase Tracking. *Molecular and cellular biology* **28**, 3830-3849, doi:10.1128/mcb.01217-07 (2008).

21 Buser, A. C., Obr, A. E., Kabotyanski, E. B., Grimm, S. L., Rosen, J. M. & Edwards, D. P. Progesterone Receptor Directly Inhibits β-Casein Gene Transcription in Mammary Epithelial Cells Through Promoting Promoter and Enhancer Repressive Chromatin Modifications. *Molecular Endocrinology* **25**, 955-968, doi:10.1210/me.2011-0064 (2011).

22 Nora, E. P., Goloborodko, A., Valton, A.-L., Gibcus, J. H., Uebersohn, A., Abdennur, N., Dekker, J., Mirny, L. A. & Bruneau, B. G. Targeted Degradation of CTCF Decouples Local Insulation of Chromosome Domains from Genomic Compartmentalization. *Cell* **169**, 930-944.e922, doi:https://doi.org/10.1016/j.cell.2017.05.004 (2017).

23 Fournier, M., Bourriquen, G., Lamaze, F. C., Côté, M. C., Fournier, É., Joly-Beauparlant, C., Caron, V., Gobeil, S., Droit, A. & Bilodeau, S. FOXA and master transcription factors recruit Mediator and Cohesin to the core transcriptional regulatory circuitry of cancer cells. *Scientific Reports* **6**, 34962, doi:10.1038/srep34962 (2016).

24 Oakford, P. C., James, S. R., Qadi, A., West, A. C., Ray, S. N., Bert, A. G., Cockerill, P. N. & Holloway, A. F. Transcriptional and epigenetic regulation of the GM-CSF promoter by RUNX1. *Leukemia Research* **34**, 1203-1213, doi:https://doi.org/10.1016/j.leukres.2010.03.029 (2010).

25 Aikawa, Y., Nguyen, L. A., Isono, K., Takakura, N., Tagata, Y., Schmitz, M. L., Koseki, H. & Kitabayashi, I. Roles of HIPK1 and HIPK2 in AML1- and p300-dependent transcription, hematopoiesis and blood vessel formation. *The EMBO journal* **25**, 3955-3965, doi:10.1038/sj.emboj.7601273 (2006).

26 Hager, G. L., McNally, J. G. & Misteli, T. Transcription Dynamics. *Molecular Cell* **35**, 741-753, doi:https://doi.org/10.1016/j.molcel.2009.09.005 (2009).

27 Johansson-Haque, K., Palanichamy, E. & Okret, S. Stimulation of MAPK-phosphatase 1 gene expression by glucocorticoids occurs through a tethering mechanism involving C/EBP. *J Mol Endocrinol* **41**, 239-249 (2008).

28 Sivakumaran, S., Zhang, J., Kelley, K. M. M., Gonit, M., Hao, H. & Ratnam, M. Androgen activation of the folate receptor α gene through partial tethering of the androgen receptor by C/EBPα. *The Journal of Steroid Biochemistry and Molecular Biology* **122**, 333-340, doi:https://doi.org/10.1016/j.jsbmb.2010.08.008 (2010).

29 Kommagani, R., Szwarc, M. M., Vasquez, Y. M., Peavey, M. C., Mazur, E. C., Gibbons, W. E., Lanz, R. B., DeMayo, F. J. & Lydon, J. P. The Promyelocytic Leukemia Zinc Finger Transcription Factor Is Critical for Human Endometrial Stromal Cell Decidualization. *PLoS genetics* **12**, e1005937-e1005937, doi:10.1371/journal.pgen.1005937 (2016).

30 Mao, A.-P., Ishizuka, I. E., Kasal, D. N., Mandal, M. & Bendelac, A. A shared Runx1-bound Zbtb16 enhancer directs innate and innate-like lymphoid lineage development. *Nature Communications* **8**, 863, doi:10.1038/s41467-017-00882-0 (2017).

31 Scarpin, K. M., Graham, J. D., Mote, P. A. & Clarke, C. L. Progesterone Action in Human Tissues: Regulation by Progesterone Receptor (PR) Isoform Expression, Nuclear Positioning and Coregulator Expression. *Nuclear Receptor Signaling* **7**, nrs.07009, doi:10.1621/nrs.07009 (2009).

32 Zhang, X.-L., Zhang, D., Michel, F. J., Blum, J. L., Simmen, F. A. & Simmen, R. C. M. Selective Interactions of Krüppel-like Factor 9/Basic Transcription Element-binding Protein with Progesterone Receptor Isoforms A and B Determine Transcriptional Activity of Progesterone-responsive Genes in Endometrial Epithelial Cells. *Journal of Biological Chemistry* **278**, 21474-21482, doi:10.1074/jbc.M212098200 (2003).

33 Rearick, D., Prakash, A., McSweeny, A., Shepard, S. S., Fedorova, L. & Fedorov, A. Critical association of ncRNA with introns. *Nucleic acids research* **39**, 2357-2366, doi:10.1093/nar/gkq1080 (2011).

34 Pisarska, M. D., Carson, S. A., Casson, P. R., Tong, X., Buster, J. E. & Kieback, D. G. A mutated progesterone receptor allele is more prevalent in unexplained infertility. *Fertility and Sterility* **80**, 651-653, doi:10.1016/S0015-0282(03)00755-6 (2003).

35 Acharya, K. D., Nettles, S. A., Sellers, K. J., Im, D. D., Harling, M., Pattanayak, C., Vardar-Ulu, D., Lichti, C. F., Huang, S., Edwards, D. P., Srivastava, D. P., Denner, L. & Tetel, M. J. The Progestin Receptor Interactome in the Female Mouse Hypothalamus: Interactions with Synaptic Proteins Are Isoform Specific and Ligand Dependent. *eNeuro* **4**, ENEURO.0272-0217.2017, doi:10.1523/ENEURO.0272-17.2017 (2017).

36 Obr, A. E. & Edwards, D. P. The biology of progesterone receptor in the normal mammary gland and in breast cancer. *Molecular and cellular endocrinology* **357**, 4-17, doi:10.1016/j.mce.2011.10.030 (2012).

37 Rickard, D. J., Iwaniec, U. T., Evans, G., Hefferan, T. E., Hunter, J. C., Waters, K. M., Lydon, J. P., O'Malley, B. W., Khosla, S., Spelsberg, T. C. & Turner, R. T. Bone Growth and Turnover in Progesterone Receptor Knockout Mice. *Endocrinology* **149**, 2383-2390, doi:10.1210/en.2007-1247 (2008).

38 Frye, C. A. An overview of oral contraceptives: mechanism of action and clinical use. *Neurology* **66**, S29-36, doi:10.1212/wnl.66.66_suppl_3.s29 (2006).

39 Beaber, E. F., Buist, D. S. M., Barlow, W. E., Malone, K. E., Reed, S. D. & Li, C. I. Recent Oral Contraceptive Use by Formulation and Breast Cancer Risk among Women 20 to 49 Years of Age. *Cancer Research* **74**, 4078-4089, doi:10.1158/0008-5472.can-13-3400 (2014).

40 Vessey, M. & Painter, R. Oral contraceptive use and cancer. Findings in a large cohort study, 1968–2004. *British Journal of Cancer* **95**, 385-389, doi:10.1038/sj.bjc.6603260 (2006).

41 Stanczyk, F. Z. & Bhavnani, B. R. Use of medroxyprogesterone acetate for hormone therapy in postmenopausal women: Is it safe? *The Journal of Steroid Biochemistry and Molecular Biology* **142**, 30-38, doi:https://doi.org/10.1016/j.jsbmb.2013.11.011 (2014).

42 Hays, J., Ockene, J. K., Brunner, R. L., Kotchen, J. M., Manson, J. E., Patterson, R. E., Aragaki, A. K., Shumaker, S. A., Brzyski, R. G. & LaCroix, A. Z. Effects of estrogen plus progestin on health-related quality of life. *New England Journal of Medicine* **348**, 1839-1854 (2003).

43 Lee, W.-L., Lee, F.-K., Su, W.-H., Tsui, K.-H., Kuo, C.-D., Hsieh, S.-L. E. & Wang, P.-H. Hormone therapy for younger patients with endometrial cancer. *Taiwanese Journal of Obstetrics and Gynecology* **51**, 495-505, doi:https://doi.org/10.1016/j.tjog.2012.09.003 (2012).

44 Rossouw, J. E., Anderson, G. L., Prentice, R. L., LaCroix, A. Z., Kooperberg, C., Stefanick, M. L., Jackson, R. D., Beresford, S. A. A., Howard, B. V., Johnson, K. C., Kotchen, J. M. & Ockene, J. Risks and benefits of estrogen plus progestin in healthy postmenopausal women: Principal results from the women's health initiative randomized controlled trial. *Journal of the American Medical Association* **288**, 321-333 (2002).

45 Collaborators, M. W. S. Breast cancer and hormone-replacement therapy in the Million Women Study. *The Lancet* **362**, 419-427 (2003).

APPENDIX

Appendix 1 List of primers used for qPCR, ChIP-qPCR and RIP-qPCR.

Experiment	Target	qPCR chemistry	Assay # / Primer sequence
qPCR	Cbfb	Taqman	Mm01251026_g1
	Pgr	Taqman	Mm00435628_m1
	Rpl19	Taqman	Mm02601633_g1
	Runx1	Taqman	Mm01213405_m1
	Runx2	Taqman	Mm00501584_m1
	Runx3	Taqman	Mm00490666_m1
ChIP-qPCR	Abhd2	SYBR Green	Forward: TTG ACA CTC TGC CTC AGC AC Reverse: CAC CTT CCT GTG GAC TTC GT
	Adamts1	SYBR Green	Forward: TGA GCT CAG TCG GTG CTA AA Reverse: CGC TGT ACA AAG TGC TGG TC
	Zbtb16	SYBR Green	Forward: GCC AGA ACA ATG CGT ACA GA Reverse: ACA CAG CTC CTT GAG GGA AG
	Chr2 (negative control)	SYBR Green	Forward: CCA GGG TTT GAC CTT CTG GAC A Reverse: AAG CAG AAG CTT CCT GTG GA
qPCR / RIP-qPCR	Gas5 (assay 21)	Taqman	Mm00657321_g1
	Gas5 (assay 22)	Taqman	Mm00657322_g1
	Gas5 (assay 23)	Taqman	Mm03456223_g1
	Oxct2	Taqman	Mm00499041_s1
	Sra1	Taqman	Mm00491756_m1
	U1	SYBR Green	Forward: GGG AGA TAC CAT GAT CAC GAA GGT Reverse: CCA CAA ATT ATG CAG TCG AGT TTC CC

Appendix 2 List of primary and secondary antibodies used in Western blot.

Target	Brand	Catalogue #	Dilution	Antigen (primary) Detection method (secondary)	Host	
CBFβ	Cell Signaling	62184	1/1000	Synthetic human CBFβ (residues surrounding Asn14)	Rabbit mAb	
PGR	Thermo Fisher	MA5-12568	1/1000	Human endometrial carcinoma grown in mice	Mouse mAb	Primary antibody
RUNX1	Abcam	ab23980	1/500	Synthetic human Runx1 (amino acid 200-300)	Rabbit pAb	
RUNX2	Jomar Life Research	D130-3	1/500	Recombinant Runx2	Mouse mAb	
Beta-actin	Sigma	a3854	1/5000	Slightly modified β-cytoplasmic actin N-terminal	Mouse mAb	
H3	Cell Signaling	9715	1/1000	Synthetic human histone H (C-terminal domain)	Rabbit pAb	
Mouse	LiCor	926-68020	1/10000	Fluorescence	Goat	Secondary antibody
Rabbit	LiCor	926-32211	1/10000	Fluorescence	Goat	

Appendix 3 List of antibodies used in ChIP and RIP.

Experiment	Target	Brand	Catalogue #
ChIP-seq	PGR	Santa Cruz Biotechnology	Sc-7209
	H3K27ac	Active Motif	39133
	RUNX1	In-house	-
ChIP-qPCR	PGR	Thermo Fisher	MA5-12568
	IgG	Millipore	CS200621
RIP-qPCR	SNRNP70	Millipore	CS203216
	PGR	Thermo Fisher	MA5-12568
	IgG	Millipore	CS200621

Appendix 4 Summary of ChIP-seq datasets, including library size, sequence length, alignment stats and peak counts

Dataset	Library size	Sequence length	Overall alignment rate (%)	Number of alignments pre-filtering	Number of alignments post-filtering	% of alignment retained post-filtering	Total peaks
GC_PR1	42021574	75	95.18	40046280	30069719	75.09	31958
GC_PR2	41045366	75	95.63	39298828	26271714	66.85	17582
GC_H3K27ac	39025317	75	97.97	38279931	33628664	87.85	43937
GC_input	45504914	75	97.61	44496459	40601755	91.25	
Uterus_oil	31584817	36	93.36	29492429	20987521	71.16	3004
Uterus_p4	31419572	36	95.36	29965710	22856529	76.28	13240
Uterus_input	36668321	36	99.17	36367487	34028853	93.57	
RUNX1_6h_1	37295205	75	95.54	35668132	25813506	72.37	18761
RUNX1_6h_2	33899014	75	95.75	32487968	19944795	61.39	28671
RUNX1_6h_input	35409268	75	97.71	34637522	32122534	92.74	
RUNX1_0h_1	34218195	75	95.25	33451268	20615995	61.63	3134
RUNX1_0h_2	37130050	75	95.27	35652131	26013416	72.96	947
RUNX1_0h_input	39783773	75	96.03	36916375	30169512	81.72	
RUNX1_E14.5_1	26252832	75	95.27	25063418	11532018	46.01	1561
RUNX1_E14.5_2	29540852	75	95	28109185	18502338	65.82	4941
RUNX1_E14.5_input_1	22604270	75	96.63	21899919	20730920	94.66	
RUNX1_E14.5_input_2	37418469	75	96.83	36315937	32910035	90.62	

Appendix 5 List of differentially expressed genes in PGRKO vs PGR+/- granulosa cells identified through microarray.

Genes that had |logFC| ≥ 1 and a p-value cut-off of 0.01 were selected as DEG. LogFC is displayed as PGRKO vs PGR+/-.

Gene Symbol	logFC	p-value	Gene Symbol	logFC	p-value
Zbtb16	-13.7345	0.0003	Cd34	-2.6770	0.0001
Slc7a11	-7.5591	0.0001	Ldhd	-2.6442	0.0035
Hsd17b11	-6.5212	0.0001	Adamts1	-2.5762	0.0019
Tmem100	-5.3345	0.0028	Rbm35b	-2.5681	0.0081
Gpt2	-4.7675	0.0001	Stxbp6	-2.4634	0.0011
Arl4d	-4.3798	0.0025	Stard5	-2.4531	0.0013
Sprr2g	-4.0126	0.0006	9430020K01Rik	-2.3975	0.0025
Rnf125	-3.7550	0.0017	Susd3	-2.3737	0.0017
Efnb2	-3.7175	0.0005	Lba1	-2.3663	0.0100
Slco2a1	-3.6604	0.0099	Rras2	-2.3339	0.0001
Gnao1	-3.6084	0.0028	Gstm1	-2.3326	0.0020
Gas7	-3.5699	0.0008	Porcn	-2.2888	0.0019
Tbc1d8	-3.5541	0.0004	Lrp8	-2.2629	0.0088
Cgn	-3.5274	0.0014	Crispld2	-2.2351	0.0010
Adam8	-3.4781	0.0001	Syne1	-2.1899	0.0055
Cxcr4	-3.4756	0.0003	Pdlim1	-2.1859	0.0057
Tdrkh	-3.4170	0.0005	Pitpnc1	-2.1853	0.0041
Snap25	-3.2078	0.0001	Rnf180	-2.1572	0.0036
Entpd1	-3.1707	0.0001	Vps26a	-2.1556	0.0008
Lepr	-3.0562	0.0091	Actn3	-2.1455	0.0011
Maml3	-3.0398	0.0028	Hrbl	-2.1182	0.0041
Cldn1	-3.0150	0.0017	Dysf	-2.0700	0.0051
Kl	-2.8830	0.0010	Fzd1	-2.0453	0.0006
Glul	-2.8799	0.0002	Apol7b	-2.0430	0.0016
Mt2	-2.8766	0.0060	Ccrk	-2.0308	0.0003
Nudt9	-2.8589	0.0062	Etl4	-2.0301	0.0089
Mkx	-2.8130	0.0017	Egfr	-2.0191	0.0020
Sphk1	-2.7980	0.0002	Dclre1b	-2.0147	0.0027
A230067G21Rik	-2.7570	0.0014	Slc16a6	-2.0131	0.0019
Abhd2	-2.7182	0.0005	Apol7b	-2.0047	0.0014
Glul	-2.6955	0.0001	Rgmb	2.1630	0.0027
Tsc22d3	-2.6920	0.0006			

Appendix 6 Reproducibility and correlation of PGR ChIP-seq replicates.

(A) Scatter plot of signal scores, peak ranks and peak count based on estimated IDR for granulosa PGR ChIP-seq biological replicates. Log(signal) and peak rank are displayed as replicate 1 vs replicate 2. Peaks with IDR > 0.01 are in red and peaks with IDR ≤ 0.01 are in black. **(B)** Read count frequency of PGR ChIP-seq peaks in replicate 1 (dark orange) and replicate 2 (light orange) in relation to the TSS. **(C)** Pearson correlation matrix for replicate 1 and replicate 2. The colour of matrix squares indicates correlation coefficient, noted in the bar at the bottom. **(D)** Venn diagram of peak count in both replicates, showing peaks that are overlapped in both.

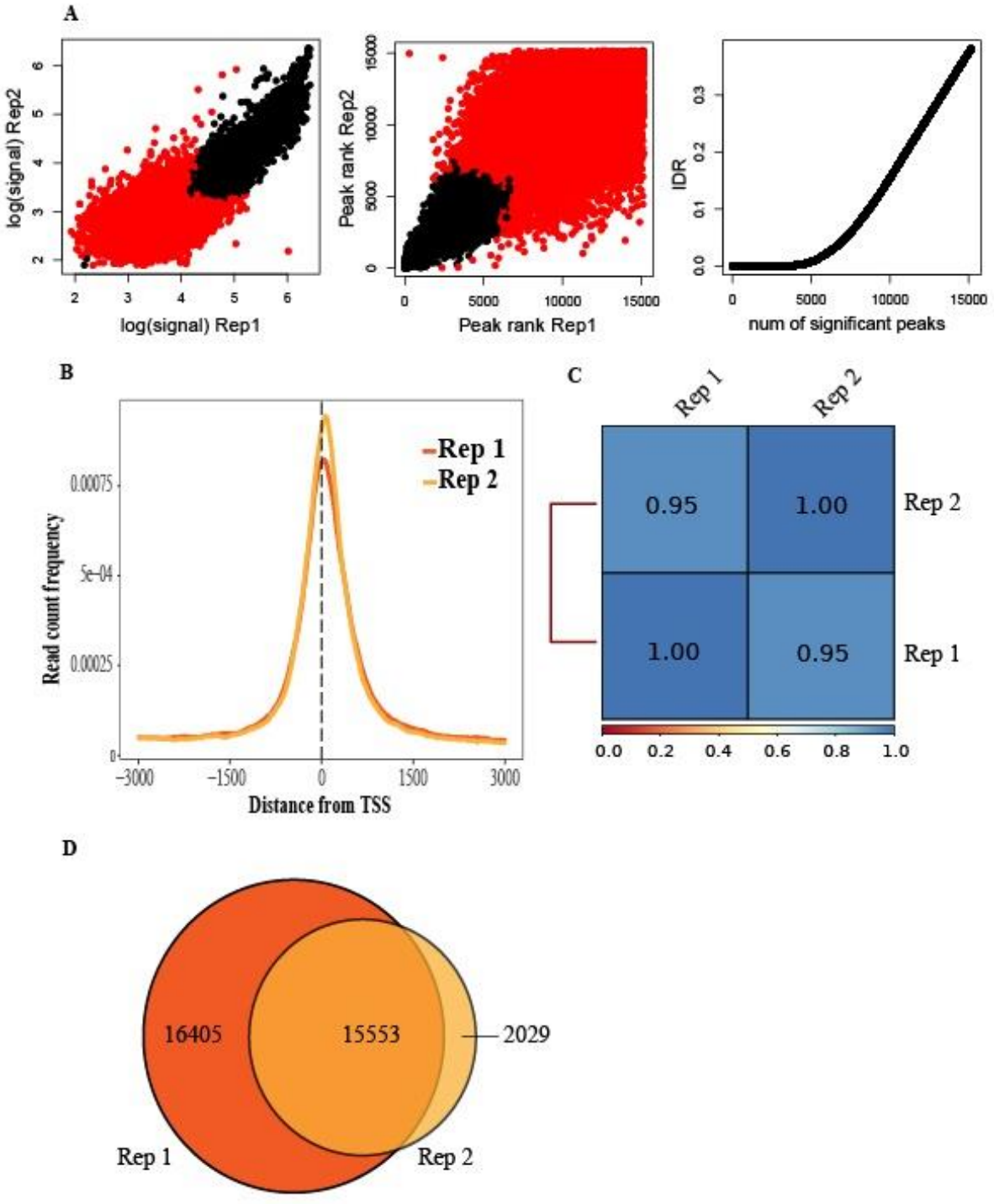
A
log(signal) Rep2
log(signal) Rep1
Peak rank Rep2
Peak rank Rep1
IDR
num of significant peaks
B
Rep 1
Rep 2
Read count frequency
Distance from TSS
C
Rep 1
Rep 2
0.95
1.00
1.00
0.95
0.0 0.2 0.4 0.6 0.8 1.0
D
16405
15553
2029
Rep 1
Rep 2

Appendix 7 List of differentially expressed genes in 8h vs 0h post-hCG granulosa cells identified through RNA-seq.

Genes that had |logFC| ≥ 1 and a p-value cut-off of 0.01 were selected as DEG. LogFC is displayed as 8h vs 0h.

Gene	logFC	Adj p-value	Gene	logFC	Adj p-value
Pgr15L	-5.45	3.91E-06	Tspan2	1.16	3.79E-04
Atp4B	-4.71	1.21E-05	Plcd1	1.17	2.71E-04
1810053B23Rik	-4.18	6.86E-04	Gem	1.17	2.58E-05
Kcne2	-3.37	5.20E-05	Fras1	1.17	4.58E-04
Ogdhl	-3.32	5.08E-06	Klf15	1.17	6.95E-06
Slco2B1	-3.25	9.36E-06	Pip5K1A	1.17	1.05E-05
Gm830	-3.22	2.73E-04	Vim	1.17	3.96E-05
Gm15635	-3.21	1.07E-04	Lrrc75A	1.17	7.27E-06
Ccdc3	-3.19	8.97E-06	Frat1	1.17	1.16E-05
4933436F18Rik	-3.19	3.18E-04	Wdfy2	1.17	1.82E-04
Serpina3C	-3.18	4.46E-04	Tmem62	1.18	1.47E-05
Gm26776	-3.18	1.01E-05	Sat1	1.18	8.18E-05
Gm9515	-3.14	5.97E-05	Coch	1.18	1.74E-04
Serpina3A	-3.04	1.74E-04	Qpct	1.18	6.45E-04
Tmem25	-2.91	5.65E-06	Phactr1	1.18	0.007539284
Prph2	-2.89	5.93E-05	Ifrd1	1.18	1.54E-05
Tmprss13	-2.88	8.83E-05	Gm5820	1.18	1.70E-05
Mylk4	-2.87	2.89E-04	Ubtd1	1.18	7.01E-05
St8Sia1	-2.79	5.59E-04	A330041J22Rik	1.18	1.51E-05
Gpr179	-2.78	3.07E-05	Klhl2	1.18	7.05E-05
P2Rx2	-2.78	1.41E-05	Pcdh18	1.18	9.08E-04
1700030I03Rik	-2.72	0.001285065	Fgf2	1.19	6.86E-05
Adra2A	-2.68	4.01E-06	Nfkbia	1.19	1.51E-05
Ism2	-2.67	5.04E-04	Apbb3	1.19	1.64E-05
Mug-Ps1	-2.66	3.90E-04	Mapk13	1.19	0.004468639
Gm14085	-2.64	3.97E-06	Ptpn9	1.19	1.76E-05
Large2	-2.63	5.59E-06	Setd7	1.19	3.59E-04
Gm17641	-2.60	1.00E-04	4933425L06Rik	1.20	0.002847759
Gprc6A	-2.57	0.00194785	Tmem38B	1.20	4.16E-04
Mmd2	-2.57	8.95E-06	Plau	1.20	0.003489281
Asic4	-2.55	1.11E-05	Rundc3B	1.20	0.001290571
Sybu	-2.52	1.37E-04	Chst1	1.20	0.001824497
Slfn4	-2.51	3.60E-04	Ston1	1.21	3.17E-04
Tmem221	-2.51	5.11E-05	4931440P22Rik	1.21	7.25E-05
Clec1A	-2.50	1.30E-05	Mrfap1	1.21	5.83E-05
1110032F04Rik	-2.50	1.88E-04	Pcdh19	1.21	0.002794548

Aifm3	-2.50	1.00E-05	Abtb2	1.21	1.03E-04
Defb20	-2.50	0.001411865	Cdyl2	1.21	0.001574878
Bc035044	-2.49	1.80E-05	Klhl36	1.21	8.78E-04
Phyhip	-2.47	3.52E-05	Vat1	1.21	1.02E-05
Dock8	-2.45	7.41E-06	Fam83F	1.21	0.001689579
Fndc5	-2.43	8.95E-05	Rnu2-10	1.21	0.001279607
Nphs2	-2.43	1.47E-05	Cbr3	1.22	0.002981693
Adgrg7	-2.43	2.63E-04	Heyl	1.22	2.77E-05
Scgb3A1	-2.41	6.68E-05	Pip4K2A	1.22	0.001157224
Gm37264	-2.41	9.64E-05	Fam78B	1.23	3.27E-05
Ccbe1	-2.39	1.00E-06	Bfar	1.23	3.46E-06
Gm45540	-2.39	3.57E-04	Arid3A	1.23	5.59E-04
Emilin3	-2.38	1.52E-04	Bex1	1.23	1.33E-05
Clec9A	-2.37	5.15E-05	Ezr	1.23	3.52E-05
Pipox	-2.36	1.61E-05	Ugdh	1.23	4.45E-07
Gm15816	-2.34	1.85E-05	Deptor	1.23	1.63E-04
Gm4926	-2.33	3.72E-04	Fam110B	1.23	7.14E-04
Olfm1	-2.32	1.07E-05	Gstm1	1.23	2.16E-04
Dock2	-2.32	2.74E-05	B4Galt6	1.23	0.004769457
Fam183B	-2.32	6.13E-05	Arntl	1.23	1.08E-04
Nppc	-2.31	9.66E-04	Pygm	1.23	5.57E-04
Gm10319	-2.31	2.88E-04	Map4K3	1.24	1.02E-04
Gm12065	-2.31	5.43E-05	Spint1	1.24	1.50E-04
Dapl1	-2.30	9.31E-04	Atp13A3	1.24	4.31E-04
Fam178B	-2.29	4.63E-04	Bcl6B	1.25	0.001854321
Oca2	-2.29	3.89E-04	Gpr35	1.25	1.60E-04
Cox4I2	-2.28	8.56E-05	Slc6A8	1.25	6.54E-06
Fam196B	-2.27	0.002117816	Map7D1	1.25	3.86E-05
Tmem130	-2.27	3.29E-04	Actn1	1.25	1.48E-05
Tmem52	-2.27	5.22E-06	Gpr153	1.25	0.005101659
Gm18609	-2.27	1.76E-04	Add3	1.25	3.65E-04
Ano1	-2.26	2.12E-05	Phip	1.25	8.78E-06
Srcin1	-2.25	5.76E-06	2210408F21Rik	1.25	0.00850106
Gja6	-2.25	1.25E-04	Ptn	1.25	0.00426192
Ptges	-2.24	4.82E-06	Spats2L	1.25	5.30E-05
Hbegf	-2.23	3.21E-05	Hspb8	1.25	1.54E-04
Cbs	-2.21	2.68E-06	Coq10B	1.25	4.25E-06
Dnah2	-2.21	6.72E-05	Kcng3	1.26	0.003272843
Car14	-2.21	6.04E-05	Tgfbr2	1.26	1.32E-05
Gm45060	-2.21	1.10E-04	Slc41A2	1.26	1.93E-05
Fam81A	-2.21	5.39E-05	Serpinb1A	1.27	1.70E-05
Gm7168	-2.20	4.11E-04	Gfpt2	1.27	3.26E-05

Bb365896	-2.20	1.70E-04	Rhbdf2	1.27	5.22E-06
Ank1	-2.19	8.59E-06	Nrn1	1.27	5.04E-05
Gm13944	-2.18	4.03E-04	Man2A1	1.27	4.12E-06
Cela2A	-2.17	6.39E-04	Lrrc4	1.27	2.80E-04
Slc28A1	-2.17	3.13E-05	Zc3H12C	1.27	2.94E-06
Efcab1	-2.17	1.01E-04	Vav2	1.27	3.02E-06
Ankrd35	-2.17	8.14E-05	Itga7	1.28	0.006632074
Slc13A4	-2.16	4.06E-04	Glis3	1.28	2.31E-04
Alms1-Ps2	-2.16	2.56E-04	Cc2D1A	1.28	1.79E-04
Adam5	-2.15	6.48E-05	Idi1	1.28	4.17E-06
Slc5A4B	-2.15	1.03E-04	Top1	1.29	2.76E-06
Mybpc3	-2.15	1.53E-04	St6Gal1	1.29	8.56E-05
Upk3A	-2.14	3.80E-04	Cfap45	1.29	0.001504323
Fxyd6	-2.14	9.76E-05	Fam214B	1.29	2.86E-04
Serpina5	-2.14	8.06E-05	Fdps	1.29	2.55E-05
H60B	-2.13	4.34E-04	Chrd	1.29	0.002025125
Rapsn	-2.12	7.40E-05	Prkcdbp	1.29	0.001612037
Hsd11B2	-2.12	4.71E-06	Epb41L3	1.29	0.003313947
Paqr6	-2.10	1.41E-05	Midn	1.29	1.51E-05
Drd4	-2.08	1.51E-04	H2-Q10	1.29	0.005738259
Gm11638	-2.07	1.74E-05	Tns1	1.30	6.46E-04
Nr0B1	-2.06	1.15E-04	Rhou	1.30	2.80E-04
Cfap70	-2.06	9.42E-05	Zcchc16	1.30	2.51E-05
Dhh	-2.06	5.12E-05	Npas3	1.30	0.007655035
1110002J07Rik	-2.06	2.33E-04	1810011O10Rik	1.30	0.001367197
Limch1	-2.06	7.82E-06	Prkx	1.30	4.91E-07
March10	-2.05	1.11E-05	Rusc2	1.30	0.002839731
Pik3Cg	-2.05	0.003123826	Zyx	1.30	4.31E-04
Cnnm1	-2.05	4.53E-06	Avpi1	1.30	0.001283998
Fabp3	-2.05	2.39E-05	Bcat1	1.31	8.71E-04
March1	-2.04	0.001509433	S1Pr1	1.31	0.004015118
Gm36670	-2.04	0.002049851	Stk17B	1.31	4.22E-06
Atp2A3	-2.03	1.71E-04	Dgkh	1.31	1.43E-05
Ihh	-2.03	4.52E-04	Ywhaz	1.31	1.05E-05
Adam3	-2.03	4.72E-04	Hephl1	1.31	2.00E-05
Gjc3	-2.03	0.001228419	Slc7A3	1.31	0.001937097
Adhfe1	-2.03	2.60E-05	Spock3	1.32	4.64E-05
Slc19A3	-2.02	3.08E-05	Aacs	1.32	1.82E-05
Gm11611	-2.01	2.09E-05	Cnga1	1.32	9.32E-04
Raet1D	-2.00	5.39E-04	Pgap2	1.32	1.12E-05
Mtcl1	-1.99	5.08E-06	Fndc1	1.32	9.36E-05
A230065N10Rik	-1.99	4.04E-05	Mir6244	1.32	9.31E-05

Rassf2	-1.99	1.33E-04	Jazf1	1.32	0.001156616
Tcp11X2	-1.99	7.97E-04	Camk4	1.32	8.19E-05
1700007K13Rik	-1.99	3.50E-04	1500017E21Rik	1.33	2.39E-04
Flt4	-1.98	1.43E-05	Bzw1	1.33	9.16E-07
Plxdc1	-1.98	5.35E-04	Trim46	1.33	0.002975589
Mfsd7C	-1.98	6.35E-06	Colec12	1.33	8.89E-04
Bb218582	-1.98	1.59E-04	Epha4	1.33	0.0015131
Aldh1A7	-1.98	1.26E-04	Inpp1	1.33	3.78E-06
Scrn2	-1.98	2.88E-06	Itgb3	1.33	1.66E-04
Smim10L2A	-1.97	4.77E-05	Slc37A2	1.33	5.49E-05
Alms1-Ps1	-1.97	0.001097512	Alpl	1.33	0.002431242
Me3	-1.97	7.91E-06	Anxa2	1.33	2.31E-04
Ciart	-1.97	1.49E-04	Kdm4D	1.33	2.35E-04
Icam4	-1.96	2.35E-04	Cd47	1.33	1.38E-05
Gm10129	-1.96	5.47E-06	Gpc4	1.34	6.00E-05
Apof	-1.96	0.001001805	Pitrm1	1.34	5.24E-07
Glb1L2	-1.96	7.67E-05	Vcl	1.34	4.71E-06
Slc47A2	-1.95	9.36E-06	Tnfrsf21	1.34	9.73E-04
Adamts5	-1.95	9.99E-06	Nin	1.34	4.22E-06
Shisa6	-1.95	2.02E-05	Appl2	1.34	2.11E-05
Dppa1	-1.94	8.18E-04	Kcnk5	1.34	2.65E-05
Txk	-1.94	1.77E-05	Usp18	1.34	0.006173675
Aif1L	-1.94	3.86E-05	Mvd	1.34	4.87E-05
Sspn	-1.93	1.35E-05	Dcaf4	1.34	0.00193989
Gm15958	-1.93	1.16E-04	Tacc1	1.35	4.64E-05
Dsp	-1.93	6.40E-06	Ripk2	1.35	4.20E-06
Myo15B	-1.93	5.59E-06	Slc39A14	1.35	1.64E-05
Nat8F3	-1.92	3.05E-04	Rhbdf1	1.35	7.91E-06
Aldh3B1	-1.92	1.58E-05	Pde4B	1.35	2.18E-04
Tex15	-1.92	1.64E-05	Sox11	1.35	3.15E-04
D330045A20Rik	-1.91	9.99E-05	Pla2G15	1.35	3.12E-05
Trpv4	-1.91	4.10E-05	Dnajc6	1.35	0.001188876
Fam234B	-1.90	1.31E-05	Ate1	1.35	0.001129948
Abca4	-1.89	2.84E-04	Endod1	1.35	3.50E-05
Capn5	-1.89	5.91E-05	Plk2	1.35	9.29E-05
Prss23Os	-1.89	3.54E-05	Lgi2	1.35	0.0010021
Gm13619	-1.89	5.26E-04	Tes	1.36	3.63E-06
Csdc2	-1.89	4.47E-06	Slc3A2	1.36	3.02E-06
Pm20D1	-1.88	9.02E-05	Tbl1Xr1	1.36	5.72E-06
Gm38034	-1.87	1.46E-04	Pdlim5	1.36	9.18E-06
Psd	-1.87	0.001379085	Jarid2	1.36	8.67E-07
Xkr5	-1.87	7.61E-05	Sos2	1.36	3.90E-07

Fkbp6	-1.87	1.99E-04	Zfp462	1.37	4.57E-06
Gm30292	-1.87	5.93E-05	Dnah7A	1.37	3.92E-04
Mro	-1.87	2.30E-05	Ier5	1.37	1.48E-05
Hsf3	-1.86	3.54E-05	A930001C03Rik	1.37	0.002196057
P2Ry6	-1.86	1.38E-04	Tceal7	1.37	1.15E-04
Efcab12	-1.86	1.70E-05	Msmo1	1.37	6.35E-06
Apoc3	-1.86	3.08E-05	Tmeff1	1.37	3.44E-05
Gm13442	-1.85	4.93E-05	Sorcs1	1.37	5.45E-04
Adgrg1	-1.85	1.04E-04	Fam189A2	1.37	7.43E-04
Hpgd	-1.85	8.48E-06	Nhsl1	1.37	2.73E-04
Tmem171	-1.85	3.11E-05	Tnip2	1.37	7.27E-06
Lyrm9	-1.85	6.78E-05	Hk2	1.37	2.85E-06
Prss23	-1.85	5.48E-05	Hmgcs1	1.37	2.14E-05
G6Pc2	-1.85	0.005466033	Cnn3	1.37	5.33E-06
B130011K05Rik	-1.85	2.73E-04	Fzd9	1.37	0.005360215
Ces2G	-1.84	6.74E-04	Fam198B	1.38	3.65E-04
Rec8	-1.84	2.09E-04	E130308A19Rik	1.38	2.06E-04
Art4	-1.84	2.09E-06	Foxp1	1.38	5.18E-05
Gm2044	-1.83	3.68E-04	Abi3	1.38	0.001158614
Nat8	-1.83	0.001964124	Tmem144	1.38	9.92E-06
Aox4	-1.83	8.36E-04	Map3K2	1.38	1.36E-06
Thbs2	-1.82	9.65E-05	Cited2	1.38	3.48E-06
Colgalt2	-1.81	0.001116162	Stxbp6	1.38	1.18E-04
Syt13	-1.81	3.59E-04	Il10Ra	1.38	0.003684575
Gm15512	-1.81	6.61E-05	Adam19	1.38	3.19E-05
Carmil3	-1.81	2.54E-06	Cd24A	1.39	1.98E-04
9330102E08Rik	-1.81	5.95E-06	Rab6B	1.39	5.81E-04
Dok2	-1.80	7.83E-05	Atf5	1.39	2.39E-05
Gabra4	-1.80	0.00132886	Fam84A	1.39	1.77E-04
Slc47A1	-1.80	4.30E-05	Map1A	1.40	7.21E-06
Gm38059	-1.80	0.003001613	Fam131B	1.40	8.56E-05
Sarm1	-1.80	3.52E-04	Hpse	1.40	2.47E-05
Omd	-1.80	6.30E-05	Ppcs	1.40	4.82E-06
Fxyd1	-1.80	7.87E-05	Tjp2	1.40	3.83E-06
Foxl2Os	-1.80	1.03E-05	Cyp51	1.40	7.11E-06
Gm9560	-1.80	1.66E-04	Ier2	1.40	0.00393738
Aldh1B1	-1.79	4.34E-05	Cpne3	1.40	2.29E-07
Arhgap22	-1.79	2.24E-05	Tmem198B	1.40	3.17E-05
Gpr155	-1.79	1.61E-04	Il1R1	1.41	4.65E-06
C230038L03Rik	-1.79	8.39E-06	Mxi1	1.41	1.51E-05
Rgs11	-1.79	2.06E-05	Cd63	1.41	9.66E-06
Eda2R	-1.79	3.62E-06	Dclre1B	1.41	1.32E-04

Gm44913	-1.78	0.002885691	Arpc1B	1.41	6.81E-06
Gm9801	-1.78	2.71E-04	Odc1	1.41	1.00E-05
Cadm3	-1.78	4.39E-04	Pde4Dip	1.42	5.87E-06
9530059O14Rik	-1.78	7.28E-05	Rnu1A1	1.42	0.007897724
Gm16282	-1.78	2.98E-04	Slc16A10	1.42	3.15E-05
Gm26580	-1.77	0.002479011	Furin	1.42	5.35E-05
Aqp8	-1.77	1.74E-04	Pcdh9	1.42	0.001954522
Gm44386	-1.77	4.65E-04	Gm15471	1.43	3.60E-04
Cacna1A	-1.77	3.37E-04	Msantd3	1.43	3.26E-05
4930452B06Rik	-1.77	3.85E-05	Epb41L1	1.43	1.46E-06
Grin2C	-1.77	1.89E-06	Gm36569	1.43	6.98E-04
Itih5	-1.77	0.001135826	Bicd1	1.43	9.18E-06
Gm9961	-1.76	1.50E-04	Klhl29	1.43	0.001891385
Phex	-1.76	1.69E-04	Mlh1	1.43	1.60E-05
Inhbb	-1.76	6.72E-04	Dach2	1.43	8.27E-04
Kcnq5	-1.76	1.61E-05	Rin1	1.44	0.002804753
Gm2155	-1.76	8.35E-05	E130307A14Rik	1.44	2.40E-04
Sec31B	-1.76	3.30E-05	Pcdh11X	1.45	3.96E-04
Cyp2S1	-1.75	1.32E-04	Kcnab1	1.45	1.35E-04
Klf1	-1.75	8.56E-05	Hira	1.45	2.36E-05
Cxxc4	-1.75	4.78E-05	Sorbs3	1.45	6.42E-05
Ankrd63	-1.75	4.81E-04	Zdhhc23	1.45	1.25E-05
Gm11653	-1.75	8.52E-04	Sorbs2	1.45	0.008490469
Gper1	-1.75	2.03E-05	Vmp1	1.46	4.17E-06
Cadps	-1.75	1.68E-04	Rhoj	1.46	6.07E-04
3110080E11Rik	-1.75	0.005064643	Hs6St2	1.46	8.74E-06
Il15	-1.74	6.30E-05	Rwdd2A	1.46	5.20E-04
Tmie	-1.74	1.57E-05	Dusp5	1.46	3.26E-05
Sema7A	-1.74	7.38E-05	Dgkk	1.46	4.64E-04
Gm44409	-1.74	0.007386999	Brsk1	1.47	8.98E-05
Derl3	-1.73	8.57E-07	Agpat9	1.47	3.82E-05
Maneal	-1.73	3.68E-04	Lrrc8C	1.47	0.001213797
Gm5134	-1.73	8.12E-05	Tuba1C	1.47	4.20E-06
Tenm4	-1.72	1.57E-05	Nkx6-2	1.47	4.44E-04
Plxnc1	-1.72	3.11E-04	Slc16A13	1.47	7.11E-06
Gm26660	-1.71	2.31E-04	Zfand5	1.48	1.04E-06
Plin1	-1.71	3.00E-04	Tspan5	1.48	3.01E-05
Gm36948	-1.71	0.001503974	Plekhg2	1.48	1.21E-05
Rbm20	-1.71	1.24E-05	Lpin3	1.48	7.11E-06
Pclo	-1.71	9.89E-05	Cers6	1.48	1.45E-06
Zfp185	-1.70	1.09E-05	Palld	1.48	2.94E-04
Aldh1A1	-1.70	9.66E-05	Pgap1	1.48	3.59E-05

Adam18	-1.70	1.13E-04	Tnr	1.48	0.002030627
Dnph1	-1.70	6.51E-05	Myrf	1.48	2.51E-04
Greb1L	-1.70	6.24E-05	Asgr2	1.48	2.30E-04
Aoc3	-1.69	0.004085145	Rnf19A	1.48	7.15E-06
Epb41L4B	-1.69	2.13E-05	Hectd2	1.48	2.44E-05
Mycbpap	-1.69	4.34E-05	Vapa	1.48	1.04E-06
1810065E05Rik	-1.68	5.38E-04	Tmem150B	1.49	3.25E-04
Gm43088	-1.68	9.13E-05	Rhob	1.49	1.99E-04
Gm10010	-1.68	0.001496503	Kdr	1.49	0.004719172
9030617O03Rik	-1.68	4.27E-06	Gda	1.50	2.10E-06
Chst8	-1.68	1.83E-04	Cacnb2	1.50	0.00279867
Akr1C14	-1.68	9.79E-04	Fcgr3	1.50	0.003462478
Rgs3	-1.67	1.44E-05	Sh3Bp4	1.50	4.12E-06
Prrg3	-1.67	7.26E-05	Pdlim1	1.50	3.58E-05
Tnni3	-1.67	1.48E-04	Slc4A4	1.50	1.31E-04
Spef2	-1.67	0.002854909	Zswim4	1.51	8.21E-05
Grap2	-1.67	0.001139595	Casc1	1.51	7.39E-05
D430019H16Rik	-1.66	3.71E-05	6030408B16Rik	1.51	0.002364239
Dnah2Os	-1.66	1.59E-04	Mbnl1	1.51	4.13E-06
Strip2	-1.66	1.56E-05	Arhgap32	1.51	8.65E-06
Sspnos	-1.66	2.04E-05	Nabp1	1.51	5.08E-06
Gm45061	-1.66	1.52E-04	Bcl6	1.51	1.73E-05
Nckap5	-1.66	6.25E-05	Aw551984	1.51	0.001066339
Kirrel3Os	-1.66	6.05E-04	Cntnap5B	1.51	3.24E-04
Acacb	-1.66	4.02E-05	Nfe2	1.51	0.001552375
Gulo	-1.65	2.74E-05	1500009L16Rik	1.51	4.77E-05
Atp1B2	-1.65	2.94E-05	Lss	1.51	3.83E-06
Angptl2	-1.65	7.11E-06	Nab1	1.51	4.39E-06
Zfp385B	-1.65	1.85E-05	Il17Ra	1.51	2.99E-06
Sptbn5	-1.65	2.18E-04	Creb5	1.52	8.42E-04
Gm16183	-1.64	0.002188914	Zfp36L1	1.52	1.13E-05
Gm11652	-1.64	0.008315402	Aloxe3	1.52	0.007891551
Tppp3	-1.64	5.32E-05	Pmepa1	1.52	2.01E-05
Trib2	-1.64	9.57E-04	S1Pr3	1.52	2.75E-04
Chrdl1	-1.64	1.20E-04	Hs3St1	1.52	2.05E-06
Fam180A	-1.64	1.07E-04	Spred2	1.53	4.12E-06
Cyp27A1	-1.64	1.33E-04	Slco5A1	1.53	1.63E-04
Grik3	-1.64	5.62E-06	Plcb4	1.53	6.68E-04
Rgs6	-1.63	2.45E-05	4930483K19Rik	1.53	2.14E-05
Eldr	-1.63	1.49E-05	Tifa	1.53	2.11E-04
Sct	-1.62	0.002081995	Iah1	1.53	3.06E-06
Cspg4	-1.62	2.92E-05	Tspan12	1.54	8.64E-07

Siae	-1.62	4.44E-05	Adgrv1	1.54	8.67E-05
Rgs13	-1.62	1.28E-04	Shisa5	1.54	4.32E-06
Alpk3	-1.61	1.01E-06	Cdc73	1.54	7.98E-05
Ephx1	-1.61	4.11E-04	Echdc2	1.55	1.41E-04
Abca9	-1.61	2.26E-04	Insig1	1.55	2.62E-06
Glrb	-1.61	4.43E-05	Ang	1.55	0.001321952
Ly6G6D	-1.61	0.001041243	Hmgn3	1.55	3.66E-05
Dock9	-1.61	1.27E-04	Pawr	1.56	1.58E-05
Cd59B	-1.61	3.40E-04	Mocs1	1.56	0.0017965
Kctd14	-1.60	4.34E-05	Kcnab3	1.56	0.001228253
Fam13A	-1.60	5.86E-04	Tcp11L2	1.56	0.003090432
Smoc1	-1.60	1.41E-04	Fam129B	1.56	0.004635882
Ddah1	-1.60	5.78E-05	Cln5	1.56	8.67E-07
Gm15740	-1.60	0.002762767	Tle3	1.56	2.39E-05
Fam19A4	-1.59	9.82E-04	Klf6	1.56	1.35E-04
Tulp2	-1.59	0.001100992	Vgll3	1.56	3.58E-04
Grem2	-1.59	0.006014387	Hr	1.57	8.45E-04
2810030D12Rik	-1.59	1.12E-04	Cfap69	1.57	5.75E-05
Scn2A	-1.59	4.35E-04	Id2	1.57	1.57E-04
Rbfox3	-1.59	3.03E-04	Reep1	1.57	5.59E-06
Efhc1	-1.59	4.48E-05	Rora	1.57	0.002647898
Gm25837	-1.59	3.50E-05	Itga4	1.57	4.03E-04
Hey2	-1.59	7.83E-05	Cyr61	1.57	0.001021827
Eya2	-1.58	3.69E-05	Anxa11	1.57	4.78E-04
Gm26892	-1.58	0.007774682	Dnah7C	1.57	3.06E-06
Nme4	-1.58	9.64E-05	Mical1	1.58	1.03E-05
Sugct	-1.58	0.002390684	Dchs1	1.58	2.47E-04
Foxo1	-1.57	2.58E-05	Rnf152	1.59	0.002018111
Gm9747	-1.57	1.02E-04	Plpp3	1.59	2.03E-05
Tmem231	-1.57	3.51E-06	Creb3	1.59	3.48E-06
Slc25A35	-1.57	1.01E-05	Dlk1	1.59	6.07E-04
Lgr6	-1.57	5.17E-04	Tead1	1.59	9.18E-06
Fancd2Os	-1.56	0.001203405	Gnao1	1.59	0.001342406
A330094K24Rik	-1.56	6.36E-05	Epas1	1.59	0.003346671
Kank1	-1.56	2.39E-05	Sik1	1.59	1.79E-05
D3Ertd751E	-1.56	3.00E-05	Dyrk2	1.60	2.65E-05
Syt7	-1.56	5.54E-04	Lsm11	1.60	3.62E-06
Gm10489	-1.56	8.64E-04	Acy3	1.60	3.15E-04
St3Gal4	-1.55	4.76E-04	Tuba8	1.61	0.002905168
E330023G01Rik	-1.55	9.46E-04	Cadm1	1.61	1.13E-05
Lmntd2	-1.55	1.43E-04	Eva1C	1.61	8.38E-04
Gm25262	-1.55	3.07E-04	Klf3	1.61	3.48E-06

Acad12	-1.55	1.91E-05	Kbtbd11	1.61	4.21E-04
Tmem182	-1.55	1.10E-04	Shb	1.62	3.26E-04
Gm39090	-1.55	0.005131948	Milr1	1.62	2.43E-04
H3F3Aos	-1.55	1.54E-04	Cpeb2	1.62	1.09E-05
Fam198A	-1.55	4.34E-04	Luzp2	1.62	2.98E-04
Cyp19A1	-1.55	0.006189017	Fkbp1A	1.63	1.81E-06
Pde11A	-1.55	6.34E-05	Hdc	1.63	0.002582809
Iigp1	-1.54	2.76E-04	9430020K01Rik	1.63	0.001376125
Dcc	-1.54	0.001223486	Pdlim7	1.63	5.14E-05
Paqr8	-1.54	1.46E-04	Gm8216	1.63	0.004186573
Rragb	-1.54	8.22E-06	Ephx2	1.63	2.57E-06
Gstt1	-1.54	3.24E-04	Pde10A	1.63	6.04E-05
Bc064078	-1.54	1.26E-04	Nrp1	1.64	0.001160945
Dsc2	-1.53	4.55E-04	Gm11427	1.64	1.15E-04
Ifit2	-1.53	6.84E-05	Dusp1	1.64	0.00375423
Dagla	-1.53	1.01E-05	Ddx28	1.64	3.96E-06
Gm26576	-1.53	0.001308271	Filip1	1.64	0.001552902
Fam162B	-1.53	0.005826405	Gm29054	1.64	6.19E-04
Tmem45A	-1.53	9.49E-04	Gm2427	1.65	2.10E-04
Mctp1	-1.53	5.01E-05	Aa414768	1.65	2.39E-05
Rmi2	-1.52	1.19E-04	Acly	1.65	5.12E-07
Mylk3	-1.52	0.001658965	Ctps	1.65	1.08E-06
Lrrc10B	-1.52	8.79E-05	Atf3	1.65	8.60E-04
Ntng1	-1.52	5.99E-04	Rab11Fip1	1.65	1.13E-05
Dhrs3	-1.52	5.59E-06	Plekhh3	1.66	3.06E-06
Gm2447	-1.52	7.16E-04	Cotl1	1.66	7.02E-06
Slc25A18	-1.52	3.03E-06	Peak1Os	1.66	3.08E-04
Aph1A	-1.52	3.11E-05	Gm37784	1.66	2.08E-05
Enpp5	-1.52	6.36E-05	Coro2B	1.66	0.003967384
Sez6	-1.51	8.60E-04	Ddit4	1.66	4.21E-06
Gm26794	-1.51	1.39E-04	Jdp2	1.66	1.49E-04
Otof	-1.51	5.12E-05	Mfsd6	1.67	1.04E-05
Sdf2L1	-1.51	7.88E-05	Sh2B2	1.67	6.50E-04
Gpha2	-1.51	2.07E-04	Sorl1	1.67	9.29E-05
Slc17A9	-1.51	3.96E-05	Iqck	1.67	1.50E-04
2610203C22Rik	-1.50	0.003319656	Mast4	1.67	4.82E-05
Hcn2	-1.50	1.15E-04	Kctd11	1.67	1.00E-06
Gm15941	-1.50	8.51E-04	Nab2	1.67	4.18E-06
Lims2	-1.50	9.54E-04	Gas7	1.68	0.001223972
Magee2	-1.50	6.85E-04	Lncpint	1.68	0.007954862
Ly6G6E	-1.50	2.47E-04	Igsf3	1.68	1.95E-06
Gm10125	-1.50	4.26E-04	Capg	1.68	4.61E-05

Gm45607	-1.50	1.37E-04	Cd180	1.68	7.44E-05
Steap3	-1.50	1.95E-05	Card19	1.68	3.99E-04
Cyp2J9	-1.49	2.58E-05	Mis18A	1.68	4.17E-06
Zdhhc1	-1.49	1.54E-06	Tpm4	1.68	2.75E-07
Dpyd	-1.49	1.81E-06	Sorbs2Os	1.68	0.007786702
Otor	-1.49	8.82E-04	Gm21814	1.69	1.36E-04
Ccdc158	-1.49	1.51E-05	Pcdh17	1.69	1.52E-04
Nrm	-1.49	1.04E-05	Notch2	1.69	1.51E-05
Kifc2	-1.49	6.81E-05	Zfp53	1.69	1.80E-05
Gm29444	-1.48	1.68E-04	Eid2	1.69	4.06E-06
Itpr2	-1.48	1.82E-06	Arf6	1.69	3.23E-07
Cacna1D	-1.48	1.49E-04	Sema3D	1.69	0.001293607
Rhpn1	-1.48	6.60E-05	Gm13068	1.69	5.24E-05
Kcnj3	-1.47	1.67E-04	Hspb1	1.70	0.006242778
Irs1	-1.47	1.03E-04	1700108F19Rik	1.70	1.86E-04
Sytl4	-1.47	3.96E-05	Akap2	1.70	0.00123745
Gm37270	-1.47	0.00121693	Arhgef12	1.70	1.51E-05
Adck5	-1.47	7.67E-05	Mgst1	1.70	6.74E-07
Nceh1	-1.47	1.49E-05	Peak1	1.70	6.06E-06
Nox4	-1.47	9.08E-04	Lgmn	1.70	1.32E-04
Pcyt1B	-1.47	5.44E-05	Gm45667	1.70	0.001642782
3632451O06Rik	-1.47	0.003431754	Sfrp4	1.70	6.39E-04
Plcb2	-1.47	0.001871964	Rbm47	1.71	5.44E-05
Nrep	-1.46	1.21E-05	Hey1	1.71	5.88E-04
9630013D21Rik	-1.46	9.41E-04	Maff	1.72	3.06E-06
Rimklb	-1.46	8.22E-05	Slc25A30	1.72	1.51E-05
Slc9A3	-1.46	6.11E-04	Gm42538	1.72	3.91E-06
Dhtkd1	-1.45	2.03E-05	Angptl4	1.72	1.25E-04
Tspan18	-1.45	6.35E-06	A530013C23Rik	1.72	9.13E-05
Tmtc4	-1.45	1.65E-05	Zcchc12	1.72	2.03E-04
Pdk1	-1.45	5.83E-05	Gfra1	1.72	3.07E-05
Dok7	-1.44	1.54E-05	Dock10	1.73	1.38E-05
Zbtb8B	-1.44	1.33E-05	Gpr85	1.73	5.44E-05
Agbl3	-1.44	1.51E-05	Luzp1	1.73	1.19E-06
Gm28175	-1.44	3.07E-04	Rgs2	1.73	5.27E-07
Clmp	-1.44	2.93E-04	Sntb1	1.74	5.56E-04
Hnmt	-1.44	2.88E-04	Ptpro	1.74	0.001474322
Tram2	-1.44	1.10E-04	Ndrg1	1.74	1.04E-04
D130017N08Rik	-1.44	2.22E-04	Ggct	1.74	7.50E-06
Atp5S	-1.44	5.89E-05	Epha2	1.74	0.004694183
Gpr165	-1.44	4.78E-04	Ptk2B	1.75	2.62E-04
Angpt1	-1.44	0.001874545	Hes1	1.75	1.49E-05

Gm28221	-1.44	3.03E-04	S100A10	1.75	1.64E-05
Slc2A5	-1.43	6.43E-04	Col4A1	1.75	2.05E-04
Evc	-1.43	3.96E-06	Zfp189	1.75	6.74E-07
Atf7Ip2	-1.43	2.95E-04	Edn1	1.76	0.00520389
Epha8	-1.43	0.001221517	Zfp948	1.76	3.21E-06
Gm26859	-1.43	2.50E-04	Gm37335	1.76	8.58E-06
Akr1C13	-1.43	1.23E-04	Tgfb1	1.76	5.08E-06
Neu3	-1.43	4.17E-06	Rras2	1.76	2.55E-05
Bmpr1B	-1.43	2.71E-04	Rnf128	1.76	1.46E-06
Gm45650	-1.42	0.004907226	Dram1	1.76	4.47E-05
Fuca2	-1.42	1.92E-04	Irf2Bpl	1.76	7.97E-06
Neurl1B	-1.42	1.88E-04	Prox1	1.77	1.21E-04
Cd82	-1.42	3.92E-05	Zfp13	1.77	1.60E-05
Cd7	-1.42	5.93E-04	Cd44	1.77	7.99E-05
Echdc3	-1.42	8.93E-06	Gm15511	1.77	0.008071149
Stra6	-1.42	1.77E-04	Nudt9	1.77	1.52E-04
A430018G15Rik	-1.42	2.57E-04	Camk2N2	1.77	1.90E-04
Mccc2	-1.42	4.12E-06	4930517G19Rik	1.77	0.001217213
Amdhd1	-1.42	3.65E-04	Pde4D	1.78	2.59E-05
Osr2	-1.42	9.20E-04	Fetub	1.78	1.90E-07
Vmn2R9	-1.41	0.005067543	Gm33023	1.78	5.56E-05
Nat8F4	-1.41	4.20E-06	Mrgpre	1.78	2.35E-04
Gm13571	-1.41	0.001109251	Itgax	1.78	1.29E-04
Cryl1	-1.41	1.40E-05	Dnaja4	1.78	1.10E-05
Gsg1L	-1.41	1.21E-04	Kif5A	1.79	1.60E-04
Tmem220	-1.41	2.21E-04	Igfbp3	1.79	0.001756423
Isoc2B	-1.41	7.38E-05	Itgb1Bp1	1.79	1.58E-05
Syt9	-1.41	0.00123148	Klf13	1.79	1.22E-05
Slc38A5	-1.41	1.88E-04	Rubcnl	1.79	6.08E-04
Mansc1	-1.40	3.81E-06	Efhd1Os	1.79	0.009932081
Kcnh2	-1.40	1.98E-04	Arid5A	1.79	2.33E-04
Lzts1	-1.40	1.29E-04	Gm20186	1.80	1.01E-05
Spata18	-1.40	5.50E-04	Zfp354B	1.80	7.05E-05
Clybl	-1.40	1.85E-05	Gm15645	1.80	2.41E-04
Gm12473	-1.40	6.23E-05	Wnk4	1.80	2.53E-04
Aire	-1.40	1.96E-04	Lrrfip1	1.80	6.78E-05
Khk	-1.40	4.29E-05	Slc25A33	1.80	5.08E-06
Mycl	-1.40	3.04E-04	Arid5B	1.81	1.19E-05
Bc067074	-1.39	7.59E-04	Boc	1.81	1.63E-05
Caskin1	-1.39	3.05E-05	Mgp	1.81	1.25E-04
Slc27A1	-1.39	8.93E-06	Gclc	1.81	3.90E-07
Tmem35B	-1.39	8.61E-05	Ppp1R3C	1.81	2.66E-04

Wdr31	-1.39	1.05E-04	Syt12	1.81	5.93E-04
Plekhd1Os	-1.38	2.37E-04	Hs6St1	1.81	5.59E-06
Aw549542	-1.38	5.17E-04	Slc35E4	1.82	3.50E-05
Npr2	-1.38	1.97E-04	Kcnk6	1.82	5.71E-04
Gm37459	-1.38	0.005861513	Lpar1	1.82	1.51E-05
Folr1	-1.38	4.68E-04	Lypd6B	1.83	1.76E-04
Dcaf12L1	-1.38	2.14E-05	Gm26586	1.83	2.29E-07
Gm20402	-1.38	1.70E-05	Chsy3	1.83	4.10E-05
Fshr	-1.38	2.68E-06	Sertad1	1.83	6.35E-06
Eri3	-1.38	9.36E-06	Frat2	1.83	1.88E-05
Cep83Os	-1.38	6.74E-05	D430041D05Rik	1.84	0.008437018
Duox2	-1.38	0.001829747	Cytip	1.84	0.001776843
4930480K23Rik	-1.38	7.94E-05	Rnu5G	1.84	1.85E-04
Zmym6	-1.38	2.52E-06	Smarca1	1.84	1.31E-05
Cyfip2	-1.37	3.59E-05	Sav1	1.84	9.63E-06
Csrnp3	-1.37	1.26E-04	Sipa1L2	1.84	6.14E-06
Naglu	-1.37	0.001534467	Gm16192	1.85	4.11E-04
Adamts12	-1.37	6.04E-04	Gli3	1.85	7.29E-06
Astn1	-1.37	0.002140513	Sstr3	1.85	0.0033641
Syp	-1.37	1.51E-04	Enpp1	1.85	5.28E-06
Arhgef28	-1.37	3.70E-05	Klf12	1.85	0.001653798
Stox1	-1.37	9.65E-04	Gtdc1	1.85	7.11E-06
Tln2	-1.37	1.19E-05	Aqp11	1.86	0.00289988
Myo5C	-1.36	4.53E-06	1700099I09Rik	1.86	2.68E-04
Abhd3	-1.36	2.16E-04	Ybx1	1.86	6.74E-07
Kirrel3	-1.36	0.002731864	Anxa11Os	1.86	0.001202137
Tmem14A	-1.36	7.03E-05	Dusp8	1.87	1.10E-04
Prkdc	-1.36	6.27E-06	Cobll1	1.87	3.19E-07
Fam234A	-1.36	0.001063501	Mb	1.87	0.007263376
Katnal2	-1.36	4.45E-04	Abca1	1.87	7.97E-06
Dixdc1	-1.36	8.68E-05	Osgin1	1.87	1.07E-04
4930581F22Rik	-1.36	2.73E-04	Zfp423	1.88	9.89E-05
Gm26723	-1.35	3.27E-05	Gadd45B	1.88	2.62E-05
Slc12A7	-1.35	3.53E-05	Napepld	1.88	5.08E-06
Ncald	-1.35	8.74E-06	Gm16229	1.88	6.54E-06
Pde8B	-1.35	6.39E-05	Fignl2	1.88	1.46E-04
Zdhhc15	-1.35	3.80E-05	Stard5	1.89	0.002648517
Tanc2	-1.35	5.62E-05	Slc6A6	1.89	2.18E-06
Fcgr2B	-1.35	0.001269966	Gm38484	1.89	3.00E-05
Gm15735	-1.35	8.64E-05	Galnt3	1.90	4.38E-04
Npb	-1.35	1.98E-04	Gm14052	1.90	0.003841943
P4Htm	-1.35	9.10E-06	Fam19A2	1.90	0.003016598

Bc043934	-1.35	5.45E-05	Nrxn1	1.90	4.43E-04
Psd4	-1.35	5.65E-05	Tnfrsf23	1.91	1.21E-04
Tdrd5	-1.35	3.36E-05	Col4A2	1.91	1.04E-04
Rapgef4Os1	-1.34	1.48E-04	Scd1	1.91	5.25E-06
Tmem206	-1.34	5.35E-04	Sgk1	1.91	5.49E-04
Sod3	-1.34	9.67E-04	Adm	1.92	0.002956144
Agtr2	-1.34	3.22E-04	Ncs1	1.92	1.33E-05
Unc93B1	-1.34	1.75E-05	Gprc5B	1.92	1.61E-05
Nav2	-1.34	8.12E-05	Crem	1.92	3.05E-05
Rassf4	-1.34	1.73E-05	Lmna	1.93	8.91E-05
Smpdl3B	-1.34	4.21E-04	Gm45838	1.93	4.32E-04
Dock5	-1.34	0.001871936	Irak2	1.93	7.55E-04
Foxq1	-1.34	0.002310483	Ppp1R13B	1.93	2.29E-07
Nubpl	-1.34	9.73E-05	Junb	1.94	0.001806731
Fhl1	-1.34	5.61E-05	Zfp786	1.94	2.74E-04
Zfr2	-1.34	1.64E-05	Ttc39C	1.95	4.17E-06
Lypd6	-1.33	0.006595882	Parp8	1.95	4.02E-07
Tecta	-1.33	0.002812197	Cblb	1.95	4.91E-07
Syt14	-1.33	1.38E-05	Hgf	1.96	0.004529303
Pak3	-1.33	6.58E-05	Cgn	1.96	1.05E-04
5430419D17Rik	-1.33	0.002394733	Tmem255A	1.96	2.15E-05
Inhba	-1.33	0.002950285	Gm15684	1.96	0.002158475
Rab3Il1	-1.33	2.97E-05	Efs	1.96	6.58E-04
Gm20629	-1.33	0.003528883	Hs3St5	1.97	8.34E-05
Snapc5	-1.33	1.37E-05	Fdx1	1.97	2.29E-07
Slc35G1	-1.33	1.23E-04	Parp16	1.97	1.27E-04
Gstz1	-1.32	1.07E-05	Tubb6	1.97	1.61E-06
Nek10	-1.32	0.001306077	Pla1A	1.97	6.74E-07
Bphl	-1.32	2.24E-05	Dtnb	1.97	1.67E-04
Nemp2	-1.32	1.58E-05	Kcnk2	1.98	3.07E-05
Abcc3	-1.32	2.00E-05	Slc16A11	1.98	2.28E-04
Kif26A	-1.32	1.66E-05	Mt1	1.98	5.33E-06
Pm20D2	-1.32	3.71E-04	Pcsk6	1.98	1.67E-06
Uba7	-1.32	1.34E-04	Ramp2	1.98	1.76E-04
Gas6	-1.32	0.002378226	Entpd7	1.99	1.31E-06
Pde9A	-1.32	5.17E-05	Adamts1	1.99	2.12E-05
Mir130C	-1.32	3.42E-04	Gm15419	1.99	1.05E-04
Mboat1	-1.32	3.59E-05	Gm45719	2.00	0.00236821
Loc102640772	-1.32	3.86E-04	Gabra5	2.00	2.04E-04
Ly75	-1.31	5.64E-05	Lrp8	2.00	5.08E-06
Idua	-1.31	7.11E-06	Synj2	2.00	2.16E-04
Csrp2	-1.31	1.88E-04	Csrnp1	2.00	3.59E-05

Metrn	-1.31	8.96E-06	0610040F04Rik	2.00	1.41E-05
Ctsh	-1.31	3.05E-04	Slc8B1	2.00	1.55E-04
Nlrc5	-1.31	2.97E-05	Slc23A2	2.00	1.82E-06
Sil1	-1.31	5.83E-05	1700017B05Rik	2.01	1.51E-06
Relt	-1.31	1.89E-05	Glp2R	2.01	0.008027756
G0S2	-1.31	6.46E-04	Ccdc160	2.01	1.44E-06
Foxred2	-1.31	3.30E-06	Gm15473	2.01	8.31E-05
4930502E18Rik	-1.30	1.22E-04	Baz1A	2.01	8.67E-07
Gm42600	-1.30	8.00E-04	Ostf1	2.01	1.00E-04
Zfp808	-1.30	7.94E-05	Klc1	2.01	8.93E-06
Pfkm	-1.30	1.31E-05	Gm16092	2.02	1.38E-04
Cd59A	-1.30	0.001622232	Vstm5	2.02	0.002221257
Susd1	-1.29	1.88E-04	Map6	2.03	1.74E-04
Lrrc48	-1.29	6.51E-05	Slit2	2.03	1.10E-04
Myocd	-1.29	3.02E-04	Lrrk2	2.03	7.24E-06
Tmem260	-1.29	6.37E-05	Cd34	2.04	3.44E-07
Mfsd2A	-1.29	0.00100425	Tex30	2.04	4.08E-07
Gm15401	-1.29	3.44E-05	Heg1	2.05	1.86E-04
Gm43581	-1.29	0.002399536	Bc100451	2.06	0.005133448
Kyat3	-1.29	8.39E-05	Rab7B	2.06	4.60E-06
Rab19	-1.29	0.002183685	Gm28592	2.06	1.89E-05
Morn2	-1.29	2.13E-05	Ttc9	2.06	8.95E-06
Cdca7L	-1.29	2.50E-05	Msi1	2.06	1.19E-06
Bbs10	-1.28	9.15E-05	Rbp4	2.06	0.00361678
Gm38402	-1.28	0.001105049	Per1	2.06	1.56E-05
Zfp934	-1.28	3.16E-04	Osmr	2.07	2.63E-04
Tmem229B	-1.28	1.32E-04	Corin	2.07	2.83E-04
Hoga1	-1.28	3.53E-04	Mbp	2.07	0.001014265
Iqgap2	-1.28	2.78E-04	Vcan	2.07	1.81E-06
Sardhos	-1.28	1.25E-04	Wbp1L	2.07	4.36E-06
Vstm4	-1.28	1.36E-04	Sytl5	2.07	5.02E-04
Fbp1	-1.28	3.35E-04	Ramp1	2.07	0.001756966
Gm27196	-1.28	1.57E-04	Gm15543	2.07	5.65E-06
Tmem117	-1.27	7.34E-05	Zpr1	2.08	2.15E-05
Gm6277	-1.27	1.20E-04	Osbpl3	2.08	1.82E-06
Qsox2	-1.27	2.11E-04	Nhsl2	2.08	8.66E-04
Gm14048	-1.27	2.46E-04	Bcl11B	2.10	0.009396127
Pir	-1.27	3.13E-04	Il7	2.10	2.64E-05
Gm4890	-1.27	9.51E-05	6530402F18Rik	2.10	5.16E-04
Acad10	-1.27	1.99E-04	Gm27252	2.10	2.75E-04
Wnt5B	-1.26	3.96E-04	Adgrl2	2.10	3.11E-05
Ctnna2	-1.26	7.58E-04	Frmd6	2.10	7.87E-07

Pak6	-1.26	1.75E-04	Tex16	2.11	9.51E-04
Extl1	-1.26	8.54E-04	Prkar1B	2.11	4.85E-05
Fcgrt	-1.26	4.09E-04	Gas2L1	2.11	1.05E-05
Exoc3L	-1.26	1.18E-04	Gm15475	2.12	7.01E-04
Gm3704	-1.26	0.001113917	Phlda1	2.12	4.59E-05
Dynap	-1.26	5.04E-04	Fgf12	2.12	2.01E-04
Gm37969	-1.26	4.61E-04	Trf	2.12	8.39E-06
Coq8A	-1.26	3.46E-05	Zpld1	2.12	8.25E-07
Gm11832	-1.25	0.004764623	Prr16	2.12	2.34E-04
Rasgrp4	-1.25	8.92E-05	Gm15856	2.12	0.002329315
Tbc1D4	-1.25	4.08E-05	Trpc5	2.12	9.73E-06
Gm38910	-1.25	4.26E-04	D16Ertd472E	2.13	3.83E-06
Hdac11	-1.25	4.00E-04	Dtnbos	2.13	0.002977447
Pik3Ip1	-1.25	2.68E-04	Tnfrsf8	2.14	2.90E-04
Cntln	-1.25	5.59E-06	Gm16897	2.14	1.58E-06
Sh3D21	-1.25	0.001233457	Mgam	2.14	2.66E-04
Arsg	-1.25	1.55E-05	Stc1	2.15	0.00338419
Gng7	-1.25	9.66E-04	Aqp2	2.15	0.002492321
Ptprd	-1.25	2.39E-05	Sytl3	2.15	1.63E-05
Mef2C	-1.25	6.13E-05	Gm13477	2.15	0.001346394
Lrrc8D	-1.25	1.55E-05	Agfg2	2.16	4.60E-06
Plekhd1	-1.24	1.72E-05	Pfkfb4	2.16	1.51E-05
Pomt1	-1.24	2.28E-04	Gm11560	2.17	5.12E-05
Spice1	-1.24	6.37E-05	Atp4A	2.17	3.38E-04
Gm44238	-1.24	9.21E-04	Arhgdib	2.17	0.00119038
Epn2	-1.24	9.18E-06	Gm43031	2.17	6.40E-06
Gm43189	-1.24	0.006799834	Clec10A	2.17	8.64E-04
Antxr1	-1.24	2.55E-05	Hmgcll1	2.17	1.81E-04
Phactr2	-1.24	2.39E-05	Tbc1D8	2.19	5.61E-05
Sardh	-1.24	4.08E-05	Klf9	2.19	4.08E-05
Slc38A3	-1.24	7.79E-04	Piezo2	2.19	1.61E-05
Map3K5	-1.24	8.97E-05	Prkca	2.19	2.40E-07
1700020G17Rik	-1.24	4.74E-04	Bhlhe40	2.19	4.62E-06
Fggy	-1.24	9.29E-05	Tmsb4X	2.20	4.00E-05
Gm42303	-1.23	1.65E-04	Frmd5	2.21	1.22E-06
Gm16425	-1.23	0.003990649	Vcpkmt	2.21	4.84E-07
Mfsd7A	-1.23	6.48E-05	Nr4A1	2.21	7.11E-06
Slc16A1	-1.23	0.00246134	Sgtb	2.21	9.99E-07
Clec2L	-1.23	7.06E-04	9330132A10Rik	2.22	0.0010472
Ahr	-1.23	5.31E-04	Flnc	2.22	1.01E-04
Ift88	-1.23	8.75E-06	Abcb1B	2.22	4.88E-04
Plcxd2	-1.23	3.96E-05	Gm9887	2.22	7.20E-06

Bc026585	-1.23	4.06E-05	Mtnr1A	2.22	0.007095108
Gdf1	-1.23	1.14E-04	Tfpi2	2.23	8.06E-05
Galnt10	-1.23	4.74E-05	Scin	2.23	0.001007151
Sh3Tc1	-1.23	0.002122786	Gm15425	2.23	0.002529404
Pick1	-1.23	1.55E-05	Scrn1	2.23	0.005463749
Ebpl	-1.22	1.35E-05	9130017K11Rik	2.24	4.36E-04
Ankle1	-1.22	3.31E-05	Hmga2	2.24	4.81E-05
2310001H17Rik	-1.22	0.005169347	Cebpb	2.25	3.05E-06
Bcan	-1.22	0.006421506	Scn1B	2.25	7.13E-04
Cd200	-1.22	2.12E-05	Mob3B	2.25	3.45E-04
Cyb5R1	-1.22	5.11E-05	Dok1	2.25	2.53E-05
Ptprt	-1.22	2.35E-04	Col17A1	2.25	2.88E-05
Lect1	-1.22	4.34E-05	Dysf	2.26	3.32E-04
Il13Ra2	-1.22	6.38E-04	Gm12843	2.26	1.15E-05
Ctso	-1.22	9.29E-05	Trib1	2.27	3.07E-04
Lhpp	-1.21	1.00E-05	Parm1	2.27	3.79E-05
Spata33	-1.21	7.39E-05	Aplnr	2.27	0.001326376
Dync2Li1	-1.21	4.34E-05	Gfod1	2.27	2.01E-05
Angpt2	-1.21	0.002897483	Tmem200B	2.28	3.78E-04
Dscc1	-1.21	4.55E-05	Gm5294	2.28	2.54E-04
Fcho1	-1.21	9.93E-05	Basp1	2.28	1.08E-05
Kdelc2	-1.21	1.11E-04	Grhl3	2.28	0.00704362
Sgcb	-1.21	1.07E-04	Rprm	2.28	3.78E-04
Esr1	-1.21	4.06E-05	Stx11	2.29	9.39E-04
Gpr135	-1.21	4.61E-04	Cited1	2.29	0.005175098
Hlcs	-1.21	4.21E-06	Acot4	2.29	0.004609852
Rapgef4	-1.21	6.13E-05	Bean1	2.29	1.98E-04
Fgfr4	-1.21	8.28E-04	Gm11655	2.29	0.003329534
Cables1	-1.20	2.14E-05	Kcnmb4Os1	2.30	9.93E-05
Slc35F2	-1.20	4.43E-05	Akr1B8	2.30	5.08E-06
Adamts2	-1.20	8.92E-05	Ppp1R14A	2.30	4.27E-04
Dhrs7	-1.20	1.39E-04	Gm45892	2.31	1.67E-04
Myo7A	-1.20	6.13E-05	Pcyt1A	2.31	2.37E-06
Sema3G	-1.20	0.001033531	4833422C13Rik	2.32	3.58E-04
Tnfsf10	-1.20	0.001152183	Tmem100	2.32	2.08E-05
Ubash3A	-1.20	7.52E-04	Adcyap1R1	2.32	8.93E-06
Sept4	-1.19	3.44E-05	Gm17087	2.32	9.66E-04
Chaf1B	-1.19	1.62E-04	Trim9	2.33	0.002674948
Dnase1L1	-1.19	2.99E-05	Slc7A8	2.33	8.67E-07
Gca	-1.19	5.93E-04	Cthrc1	2.33	3.56E-04
Osbpl1A	-1.19	1.64E-05	Lbh	2.34	1.70E-05
Frzb	-1.19	0.002796118	Gm45457	2.34	0.009889059

Dap	-1.19	3.11E-05	Kcnmb4	2.35	3.15E-05
9530077C05Rik	-1.19	1.81E-04	Cav2	2.35	2.57E-04
Bst2	-1.19	1.48E-04	Gm16318	2.35	7.19E-04
Ank3	-1.19	7.99E-05	Gm5106	2.35	9.37E-04
Rai2	-1.18	2.91E-04	Nrcam	2.36	3.96E-05
Myo6	-1.18	3.69E-04	Unc79	2.36	2.63E-04
Cabp1	-1.18	1.85E-04	Cav1	2.37	1.16E-05
Arhgdig	-1.18	0.001363223	Adh1	2.37	3.07E-05
Khdrbs3	-1.18	6.64E-05	Adamts20	2.38	0.004782395
Ccdc40	-1.18	9.30E-04	Kcnmb4Os2	2.38	1.05E-05
Ivns1Abp	-1.18	1.55E-04	Pde6H	2.38	0.003116105
Loxl1	-1.18	4.27E-04	Fam210B	2.39	5.38E-05
Wfdc10	-1.17	0.003228031	Vldlr	2.39	4.97E-07
Xxylt1	-1.17	3.46E-05	Itpk1	2.39	1.77E-05
Nmral1	-1.17	4.20E-05	Entpd1	2.40	5.08E-06
Jak3	-1.17	1.54E-04	Msx1	2.40	1.76E-05
Gcdh	-1.17	8.58E-06	Robo2	2.40	5.59E-06
Nipal3	-1.16	1.55E-04	Prrx1	2.41	1.00E-04
Kcnh7	-1.16	0.001278282	Gm44043	2.41	1.71E-04
1810062G17Rik	-1.16	0.001175	Gm20540	2.41	5.47E-04
Brca2	-1.16	3.52E-06	Sv2C	2.43	1.64E-05
Snhg11	-1.16	5.34E-04	Aldh1A3	2.43	1.13E-04
Slc2A9	-1.16	6.19E-04	Bcl3	2.43	8.56E-05
Fam3A	-1.16	3.89E-05	Gm16559	2.43	1.13E-04
Tgfb3	-1.16	8.93E-05	Satb2	2.44	4.53E-06
St3Gal5	-1.16	0.002641644	Smco3	2.44	7.55E-05
Psmb9	-1.16	8.45E-05	Mmp19	2.44	1.41E-04
4930550L24Rik	-1.16	0.006973818	Slurp1	2.44	2.75E-04
Fndc9	-1.16	2.71E-04	Gsta2	2.45	8.06E-05
Slc39A11	-1.16	6.97E-05	Rrad	2.45	6.36E-06
Tnfsf11	-1.15	0.006525566	Il23A	2.45	3.69E-05
Etfbkmt	-1.15	3.68E-04	9330136K24Rik	2.46	6.22E-06
Dnah11	-1.15	2.89E-05	Ret	2.46	1.87E-04
Glt28D2	-1.15	8.12E-04	Sbsn	2.47	1.59E-04
Fmn1	-1.15	0.00434045	Far1Os	2.47	1.57E-06
Id3	-1.15	1.56E-05	Rims4	2.47	4.58E-07
Sft2D2	-1.15	8.93E-06	Krt79	2.48	4.01E-06
Ankrd24	-1.15	6.57E-06	Cdkn1A	2.48	1.87E-04
Cryz	-1.15	1.66E-05	Gm44981	2.48	0.001122528
Zkscan2	-1.15	1.74E-04	Klf2	2.48	1.72E-04
Utrn	-1.15	4.22E-06	Gm13889	2.49	4.14E-07
Aldoc	-1.15	2.69E-04	Gpr68	2.49	1.85E-05

Zbtb40	-1.15	1.58E-05	Mid1	2.49	1.35E-05
Ddx60	-1.14	5.66E-04	Aard	2.49	2.09E-06
Dact2	-1.14	3.52E-04	Fgl2	2.49	1.23E-04
Rgs7Bp	-1.14	2.75E-04	Rgs4	2.50	1.77E-04
Anxa6	-1.14	1.10E-05	Itga5	2.50	3.83E-06
Prkag2	-1.14	8.16E-06	L3Mbtl4	2.50	0.008509516
Alg6	-1.14	4.01E-05	Gpt2	2.51	2.29E-07
Slc9A5	-1.14	3.22E-04	Hsd17B11	2.51	1.15E-05
2310040G24Rik	-1.14	0.004086668	Far1	2.51	7.00E-08
Masp1	-1.14	4.58E-04	Klf4	2.51	6.72E-05
Pmp22	-1.13	9.98E-05	Mical2	2.51	1.16E-05
Tmem106C	-1.13	1.11E-05	C230034O21Rik	2.51	2.08E-04
Naaladl2	-1.13	0.008898488	Zfp36	2.51	8.29E-04
Egflam	-1.13	0.007759296	Dmd	2.52	1.15E-05
Dnajb14	-1.13	3.32E-05	Tll1	2.52	4.70E-06
Hacl1	-1.13	1.48E-05	Lrp8Os2	2.52	4.04E-04
Fbxo41	-1.13	0.00505215	Itga2	2.52	1.70E-06
Zeb1	-1.13	1.13E-05	Cldn3	2.53	5.06E-05
Lgals3Bp	-1.13	0.001003305	Synm	2.53	7.76E-06
Gprasp2	-1.13	1.22E-04	Gm44763	2.53	9.78E-04
C1Qtnf1	-1.13	4.55E-04	Acsl4	2.53	5.24E-07
Rph3Al	-1.13	1.76E-05	Gm14021	2.53	0.002645975
Nap1L5	-1.12	5.00E-04	Rufy4	2.53	0.002773969
Gm16432	-1.12	8.46E-04	Sdc1	2.53	4.45E-06
1700024F13Rik	-1.12	8.36E-04	Twist1	2.55	2.32E-04
Crb1	-1.12	4.46E-04	Prss30	2.55	6.46E-04
Omp	-1.12	0.002823069	Thsd7A	2.56	8.54E-05
Kcnb2	-1.12	9.36E-04	Teddm2	2.56	1.76E-05
Rtn2	-1.12	5.38E-04	Cnr1	2.56	0.002648547
Tlr5	-1.12	5.55E-04	Rgcc	2.56	9.91E-06
Gm1673	-1.12	1.62E-04	Them6	2.56	5.24E-05
Raet1E	-1.12	0.001789585	Six4	2.57	2.15E-04
Mcm8	-1.11	3.61E-04	Egr2	2.58	5.19E-04
Itga11	-1.11	2.08E-04	Pdzph1	2.58	3.53E-04
Ppargc1B	-1.11	8.20E-04	Phf20L1	2.58	4.45E-07
Unc119	-1.11	5.88E-05	Pla2G7	2.58	1.46E-04
Ppp1R3G	-1.11	2.41E-04	Gm24224	2.58	0.00116217
Alms1	-1.11	1.22E-05	St3Gal1	2.59	3.79E-06
6430573F11Rik	-1.11	0.004897859	Apol6	2.59	0.001387809
Kntc1	-1.11	1.03E-04	Gm45102	2.59	1.49E-04
Angpt4	-1.11	0.005823352	Sec14L2	2.61	3.07E-04
9330179D12Rik	-1.11	0.002510511	Gm38055	2.61	0.008299913

Pcbd2	-1.11	2.82E-04	Sh3Gl2	2.62	8.80E-05
Slfn9	-1.11	2.30E-04	C130089K02Rik	2.62	0.004013595
5730405O15Rik	-1.11	0.001488596	Fblim1	2.62	9.06E-05
Mpp3	-1.11	2.63E-05	Nxf3	2.63	1.19E-06
Socs1	-1.11	0.007249503	Peg10	2.64	1.53E-06
Xrcc2	-1.11	1.07E-04	Ssbp2	2.64	4.65E-06
Gcnt4	-1.11	1.13E-04	Creb3L1	2.64	3.46E-05
Spin2C	-1.11	4.07E-04	Srgap1	2.64	9.26E-05
Raver2	-1.11	5.59E-06	Jph2	2.64	7.76E-06
Rin2	-1.11	1.02E-04	Nt5E	2.64	2.44E-04
Tbata	-1.10	6.70E-04	Fat4	2.65	7.43E-05
Tmem255B	-1.10	0.001212454	Tpd52L1	2.65	1.41E-05
Map2K6	-1.10	2.22E-04	A830012C17Rik	2.65	3.33E-04
Tanc1	-1.10	2.77E-05	Wnt2	2.66	6.48E-05
Sppl3	-1.10	4.34E-05	Srgn	2.66	2.14E-05
3830406C13Rik	-1.10	5.64E-05	Lrrc6	2.67	8.55E-05
Comp	-1.10	0.003537276	Abcb1A	2.67	1.35E-04
Cfap61	-1.10	0.002355756	Tdrkh	2.67	4.03E-04
Trappc9	-1.10	6.91E-05	Stk32A	2.69	1.60E-04
Per3	-1.10	3.46E-05	E030018B13Rik	2.69	0.004173691
Arsb	-1.10	5.95E-05	Grik2	2.69	2.03E-04
Carhsp1	-1.10	1.10E-05	Glul	2.69	1.04E-06
Mme	-1.10	0.001671519	Nbl1	2.69	1.15E-05
Nr1D2	-1.09	1.76E-05	Gm42939	2.69	0.00431983
Tert	-1.09	4.81E-05	Ccdc30	2.70	1.22E-05
Ano4	-1.09	6.50E-04	Fes	2.71	6.55E-04
C920021L13Rik	-1.09	4.96E-04	Adamts4	2.72	2.41E-05
Scg5	-1.09	0.003625438	Col24A1	2.72	2.44E-06
1810058I24Rik	-1.09	3.09E-05	Gm37019	2.73	0.001997097
Iqgap3	-1.09	6.98E-05	Gm20089	2.74	0.004963092
Arhgap27	-1.09	1.13E-04	Bdnf	2.75	1.06E-04
Arg1	-1.09	0.001605079	Hapln1	2.76	8.50E-05
P2Ry1	-1.09	2.69E-04	Sema3A	2.77	1.60E-06
Trim34A	-1.09	0.001007151	Thsd7B	2.77	0.001109731
Tmeff2	-1.09	3.52E-04	Adamts9	2.77	3.06E-06
H2-M3	-1.09	1.41E-04	Kctd12	2.77	5.48E-07
Azin2	-1.09	1.31E-04	Gm26778	2.78	9.16E-07
Il27Ra	-1.09	2.79E-04	Srxn1	2.78	1.29E-06
Arsa	-1.09	9.05E-05	Mreg	2.78	1.00E-06
Agpat5	-1.09	9.88E-05	Etv4	2.79	4.64E-05
1700112E06Rik	-1.09	0.007376284	Lrmp	2.80	2.01E-04
Ddt	-1.08	3.85E-04	Nfatc2	2.80	0.001041752

Slc5A3	-1.08	2.44E-04	Gm43672	2.82	1.61E-05
Nek8	-1.08	3.65E-05	Hal	2.82	0.004417755
Chchd6	-1.08	1.52E-04	Frmpd1	2.82	5.48E-05
4933416I08Rik	-1.08	9.97E-04	Tsc22D3	2.83	1.90E-05
Pbxip1	-1.08	2.14E-05	Cyp4F18	2.86	5.28E-04
Adam22	-1.08	4.24E-04	Gm28373	2.86	0.001384637
Nrip1	-1.08	4.44E-04	Gm15737	2.87	3.37E-05
Prkag2Os1	-1.08	0.00344755	Ncoa7	2.87	6.70E-08
Slc25A42	-1.08	2.04E-05	Ier3	2.87	8.30E-06
Gm15663	-1.08	9.46E-04	Plk3	2.88	9.72E-06
Cbfa2T3	-1.08	1.02E-04	Prune2	2.88	2.38E-05
Fbxo47	-1.08	4.96E-04	Lynx1	2.88	4.05E-07
Cln6	-1.07	2.83E-05	Htr1D	2.89	1.03E-05
Fancd2	-1.07	1.04E-04	Traf3Ip2	2.90	1.51E-05
Ecm2	-1.07	6.69E-04	Il6Ra	2.90	7.60E-05
Tmem241	-1.07	5.04E-05	Bin1	2.91	3.29E-07
Ai464131	-1.07	4.06E-05	Gm45194	2.91	1.11E-05
Mcm6	-1.07	1.35E-04	Adgrf5	2.91	4.13E-06
6720489N17Rik	-1.07	1.13E-04	Zfp52	2.92	1.86E-07
Ppp1R26	-1.07	6.57E-05	Dtx1	2.93	2.49E-04
Lockd	-1.07	1.26E-04	Abhd2	2.93	9.74E-08
Card14	-1.07	3.12E-04	Npr3	2.93	0.002256233
Kcnn1	-1.07	5.32E-04	Gm11651	2.94	5.78E-05
Agrn	-1.07	7.81E-05	Actn3	2.94	0.001918996
Prelid2	-1.07	6.92E-04	Tspan11	2.95	2.29E-05
Slc26A1	-1.07	6.55E-05	Gm14020	2.95	0.002967125
Gstm7	-1.07	1.75E-05	Nupr1	2.95	6.54E-06
Igf2R	-1.07	0.002428026	Gm5834	2.95	2.24E-04
Epm2A	-1.07	7.57E-04	Pdzrn3	2.96	1.83E-05
Uevld	-1.06	6.67E-05	Sema3E	2.97	4.64E-05
Catsper2	-1.06	9.60E-05	Col12A1	2.97	1.88E-05
Grem1	-1.06	0.005802864	Usp43	2.97	5.36E-04
Abhd14A	-1.06	7.53E-06	Cyp4B1	2.98	4.69E-04
Kitl	-1.06	0.009855361	Dok6	2.98	7.67E-04
Gm15201	-1.06	2.02E-04	Mdga2	2.99	1.25E-05
Synpo	-1.06	2.11E-05	Ahsg	2.99	1.74E-06
Plbd1	-1.06	2.62E-05	Gm15247	3.00	2.00E-04
Sned1	-1.06	4.47E-05	Fhl3	3.00	9.52E-05
C130074G19Rik	-1.06	9.94E-05	Nr4A3	3.01	2.75E-05
Sox12	-1.06	8.92E-05	Ptpn5	3.01	5.49E-05
Abca7	-1.06	9.96E-06	Chgb	3.02	4.92E-06
Shisa9	-1.06	0.002507969	Hspa2	3.03	9.63E-05

Dnajb13	-1.06	9.97E-05	Cdh17	3.03	1.97E-05
Mgst3	-1.06	3.69E-05	A330015K06Rik	3.04	1.88E-05
Cpa2	-1.06	0.009422558	Tac1	3.05	3.86E-05
Stac	-1.06	2.51E-05	Gm8251	3.05	4.63E-05
Proser2	-1.06	2.15E-04	Ace	3.05	4.99E-06
Nnt	-1.06	9.98E-05	Csf2Rb	3.05	9.52E-05
Inca1	-1.06	6.50E-04	Rassf9	3.07	1.61E-05
Vwa8	-1.05	1.85E-05	5430420F09Rik	3.07	0.008320271
Gja1	-1.05	0.003929781	Nfil3	3.08	2.48E-05
Tbc1D32	-1.05	1.74E-05	Nsun7	3.09	1.06E-04
Chid1	-1.05	7.15E-06	Gm15328	3.09	4.85E-05
Trpc3	-1.05	1.15E-04	Gm16332	3.09	7.59E-04
Tmem72	-1.05	1.72E-04	Adarb1	3.10	1.19E-06
Tmem143	-1.05	6.57E-06	Gm17509	3.11	1.55E-05
Impa2	-1.05	6.02E-05	Cyp11B1	3.12	2.22E-05
Ccdc159	-1.05	4.43E-04	Ppp1R36	3.13	0.007227887
Tlcd2	-1.05	5.59E-05	Enpp2	3.13	2.02E-04
Osbpl5	-1.05	1.75E-05	Gm15726	3.14	1.06E-04
Nxpe4	-1.05	0.002025125	Gm11870	3.15	1.27E-04
Dtd1	-1.05	1.40E-04	Adam8	3.15	2.29E-07
Dym	-1.05	1.35E-05	Gldc	3.16	5.71E-04
A930005H10Rik	-1.05	4.46E-04	Rhox5	3.19	1.53E-06
E130311K13Rik	-1.05	2.79E-05	Timp1	3.20	4.14E-06
Bhlhe41	-1.05	4.71E-04	Bmper	3.20	9.03E-07
Hmgcs2	-1.05	8.86E-06	Dusp4	3.24	6.74E-05
Atrnl1	-1.05	1.82E-04	Eno2	3.25	9.96E-06
Mettl22	-1.05	4.17E-06	St8Sia4	3.27	5.81E-05
Abhd14B	-1.04	5.94E-05	Adam2	3.27	1.99E-04
Xylb	-1.04	4.21E-04	Edn2	3.27	0.006615751
Gm11747	-1.04	5.60E-04	#N/A	3.27	2.08E-04
Gstm6	-1.04	6.52E-05	Gm11843	3.28	5.33E-06
Ccdc125	-1.04	4.58E-05	Sh3Gl3	3.28	1.03E-04
Ccnd2	-1.04	0.005124334	Npr1	3.29	4.25E-06
Best1	-1.04	0.002872209	Gm37265	3.29	0.001569914
Col4A6	-1.04	7.04E-04	M1Ap	3.29	6.67E-04
Mut	-1.04	8.09E-05	Dusp6	3.30	3.02E-06
Tpk1	-1.04	1.17E-04	5330416C01Rik	3.30	2.15E-05
Adora1	-1.04	3.83E-05	Gm16048	3.30	3.34E-05
Tmed3	-1.04	5.82E-05	Unc5D	3.31	0.001361167
B4Gat1	-1.04	8.16E-05	Cdh6	3.31	0.001605079
Gpx7	-1.04	1.74E-04	Gm44639	3.32	9.99E-05
Gm684	-1.04	0.001515292	Klrb1F	3.32	3.65E-05

Slfn8	-1.04	0.001145989	Procr	3.32	1.13E-05
Tmem8B	-1.04	1.88E-05	Apcdd1	3.32	1.10E-05
Txndc16	-1.04	1.43E-04	Adamts3	3.33	9.18E-06
Gimap8	-1.04	0.004882311	Penk	3.34	9.26E-06
3632454L22Rik	-1.04	0.003929781	Zbtb16	3.35	1.44E-04
Mybph	-1.04	2.76E-04	Emb	3.35	2.76E-06
Hsd17B1	-1.04	0.002580545	Errfi1	3.38	2.06E-07
Tlr3	-1.04	8.82E-04	Mpzl2	3.39	2.24E-05
1110019D14Rik	-1.04	7.10E-04	Rab20	3.39	8.56E-05
Arxes2	-1.03	2.48E-04	Gm26771	3.40	3.05E-05
Pcca	-1.03	3.33E-06	Olfr1250	3.41	1.39E-04
Gstm4	-1.03	6.96E-04	Etv5	3.41	4.97E-07
Klc2	-1.03	5.33E-06	Steap1	3.42	4.22E-06
Au040320	-1.03	9.63E-06	Pxdc1	3.44	4.42E-05
Nkd2	-1.03	0.004311282	Syne1	3.45	1.02E-05
Dlec1	-1.03	5.99E-04	Osgin2	3.47	2.06E-07
Rida	-1.03	2.44E-04	Spry3	3.47	1.66E-05
Hacd4	-1.03	3.25E-05	Nr1H4	3.47	1.27E-04
Ralb	-1.03	4.44E-04	Gm39041	3.48	5.54E-04
Spint2	-1.03	0.003009829	Fam110C	3.48	7.00E-08
Med9Os	-1.02	0.003227886	Myh13	3.49	0.001496503
Prkaa2	-1.02	3.64E-04	Clcf1	3.49	4.92E-04
Msh2	-1.02	1.41E-05	Avil	3.50	1.30E-05
Mcm3	-1.02	7.52E-04	Sec1	3.51	4.30E-05
Tmtc2	-1.02	0.001963737	Gm3716	3.51	1.20E-04
Fgf13	-1.02	0.001543796	Kcnv2	3.52	0.001382912
Cenpm	-1.02	2.24E-04	Mrap	3.53	6.55E-08
Sgsh	-1.02	2.73E-04	Popdc3	3.54	4.32E-06
Stbd1	-1.02	3.27E-05	Slco1A1	3.55	4.32E-04
Pcyox1L	-1.02	3.80E-05	Tnfrsf12A	3.57	1.69E-06
Aasdh	-1.02	1.38E-05	Dhrs9	3.58	9.20E-05
Lrp3	-1.02	1.16E-05	Gm10584	3.59	3.54E-05
Sspo	-1.02	0.001139708	Gimap5	3.59	5.59E-04
Fsbp	-1.02	3.42E-04	Sfrp2	3.61	1.66E-05
Pbld2	-1.02	0.001118867	Cited4	3.62	7.65E-05
Lyplal1	-1.01	7.84E-05	Gm6614	3.62	3.12E-04
Tet1	-1.01	3.96E-05	Pcsk5	3.62	6.55E-08
Trappc6A	-1.01	3.01E-05	Zfp365	3.63	3.23E-07
Tarsl2	-1.01	1.25E-05	S100A3	3.64	0.007824676
Nupr1L	-1.01	0.003350471	Plaur	3.64	1.99E-05
Foxl2	-1.01	5.18E-05	Rpp25	3.64	1.47E-05
Rnft2	-1.01	2.16E-04	Oit3	3.68	2.65E-06

B230217C12Rik	-1.01	7.04E-04	Areg	3.69	0.00222647
Apoa1Bp	-1.01	6.30E-05	Met	3.70	7.21E-05
Ext1	-1.01	0.002002691	Abi3Bp	3.71	1.61E-07
Acat1	-1.01	1.23E-04	Zfp949	3.71	8.12E-07
D930048N14Rik	-1.01	1.84E-04	Cldn1	3.72	1.43E-04
Dirc2	-1.01	5.33E-06	Snap91	3.73	2.40E-05
Cyp2J6	-1.01	4.73E-04	Tmem37	3.74	1.30E-04
Zfp950	-1.01	1.15E-04	Dll3	3.74	5.13E-05
Ppm1K	-1.01	3.86E-04	Enpp3	3.75	1.86E-07
Dnah7B	-1.01	9.09E-04	Klrb1C	3.75	1.35E-05
Mir1901	-1.01	3.69E-04	Vdr	3.77	3.44E-05
Esrrg	-1.00	0.003097381	Fosl1	3.77	0.001255833
Ephb6	-1.00	9.81E-06	Egln3	3.78	1.42E-05
Fgfrl1	-1.00	4.21E-04	Lif	3.78	3.69E-04
Dpp10	-1.00	0.002887231	Olfr1251	3.79	5.23E-05
Mlxipl	-1.00	1.66E-04	Rhox8	3.80	1.09E-05
Tmem218	-1.00	1.15E-04	Nptx1	3.80	1.67E-04
Slc6A15	-1.00	0.001647002	Baat	3.82	6.30E-05
Pccb	-1.00	2.53E-05	Pappa2	3.84	7.03E-05
Col4A3	-1.00	9.66E-04	Fzd1	3.86	7.00E-08
Amhr2	-1.00	9.60E-04	F3	3.86	8.76E-06
Ror1	-1.00	0.001042393	Gm19463	3.86	7.00E-08
Hmgcr	1.00	2.11E-05	Slco2A1	3.87	9.36E-06
Gse1	1.00	9.55E-04	Creg2	3.91	4.03E-04
Prss35	1.00	4.58E-05	Igdcc3	3.91	1.48E-05
Sgms1	1.00	8.58E-06	Hmga1	3.94	1.82E-06
Chmp4C	1.00	1.85E-04	A730049H05Rik	3.97	4.10E-05
Cdc42Se1	1.01	2.06E-05	Cxcl5	3.98	3.07E-05
Cbarp	1.01	1.13E-05	Gm45774	3.98	3.04E-06
Osbpl6	1.01	1.44E-05	A730020M07Rik	4.00	5.70E-05
Galnt18	1.01	0.009621887	Gm27820	4.00	2.96E-05
Rnaseh2A	1.01	9.19E-04	Mt2	4.01	1.59E-06
Clip3	1.01	0.005157006	Vnn3	4.04	1.51E-05
Tmem189	1.01	1.93E-05	Dusp2	4.05	0.004792905
Ahi1	1.01	1.21E-05	Nrg3	4.05	5.82E-05
Tusc1	1.02	5.82E-05	F2Rl2	4.05	8.82E-04
Usp53	1.02	4.41E-05	Arl4D	4.06	1.28E-06
Rassf8	1.02	2.58E-05	Kcne4	4.07	4.77E-04
Ell2	1.02	8.74E-06	Lox	4.08	6.35E-06
Rtkn2	1.02	2.16E-05	Pnoc	4.08	2.01E-05
Epha7	1.02	1.01E-05	Lrrc4C	4.08	1.68E-05
Tln1	1.02	4.48E-06	Pitpnc1	4.09	4.01E-06

Chd7	1.03	1.01E-05	Trpa1	4.13	2.06E-04
Stxbp1	1.03	1.82E-04	Bves	4.15	6.87E-07
Bc005537	1.03	1.97E-05	Tagln2	4.17	2.83E-08
Arhgap24	1.03	0.005961878	Star	4.17	1.25E-05
Pkdcc	1.03	5.08E-04	Il33	4.18	3.33E-04
Cdkn2D	1.03	0.001395849	Gm45073	4.18	7.76E-05
Hspa4L	1.03	5.49E-05	Scg2	4.19	2.67E-05
Me1	1.03	6.27E-06	Hmga1-Rs1	4.19	1.58E-06
Tnfaip8	1.03	9.03E-04	Il1Rl2	4.19	1.38E-06
Ppp3Ca	1.03	1.78E-06	Vsig8	4.21	4.42E-05
Rnase4	1.03	0.003204444	Hhip	4.21	1.04E-06
Rap1A	1.03	3.91E-06	Efnb2	4.24	4.29E-06
Btg3	1.03	2.08E-05	Gm26626	4.24	2.48E-05
Hipk1	1.03	2.10E-04	Runx2Os2	4.25	0.001531121
Maml2	1.04	9.18E-05	Trbc2	4.27	2.40E-04
Gm12500	1.04	9.76E-05	Gm19610	4.34	2.13E-05
Rdh5	1.04	9.36E-04	Rasal1	4.34	5.08E-06
Baiap2	1.04	1.14E-04	Trac	4.38	1.01E-05
Leng9	1.04	3.27E-05	Slc7A11	4.38	6.55E-08
L3Mbtl3	1.04	7.87E-06	Rgs1	4.41	2.70E-04
Zbtb1	1.04	1.60E-06	Rasef	4.42	3.59E-05
Lonrf3	1.04	4.29E-05	Runx2	4.42	1.03E-05
Slc9A3R1	1.04	8.16E-06	Serpinb9B	4.43	9.00E-04
Tchh	1.04	3.72E-05	Ifi202B	4.43	6.13E-05
Camk2N1	1.04	3.63E-04	Runx1	4.45	1.86E-07
Fbxo33	1.04	4.28E-06	Runx2Os1	4.51	0.002864274
Xpnpep1	1.04	1.69E-04	Esm1	4.53	6.16E-04
Nyap1	1.05	0.003375358	Gm11714	4.53	5.17E-04
Pcdh7	1.05	5.12E-05	Gm15482	4.53	1.06E-04
Pdgfa	1.05	1.53E-04	Fmo2	4.54	1.26E-05
Col18A1	1.05	2.03E-04	Camp	4.54	4.93E-04
Zfp516	1.05	2.44E-05	Alcam	4.54	8.06E-08
Zfp251	1.05	7.27E-06	Gpr83	4.58	3.44E-07
Amigo2	1.05	3.05E-05	Lrrn3	4.60	2.33E-05
E130012A19Rik	1.06	3.42E-04	Wnt11	4.60	2.78E-05
Cars	1.06	3.83E-06	Ly6D	4.67	1.46E-06
Mob3A	1.06	4.64E-04	Calml3	4.67	1.30E-04
Smarcd3	1.06	1.99E-05	E230020D15Rik	4.69	2.42E-04
Kcnt1	1.06	4.92E-04	Pcdh10	4.77	7.00E-08
Dgka	1.06	0.004087961	Arc	4.77	2.65E-05
Msn	1.06	4.18E-06	Cntnap5A	4.77	8.48E-06
Dlg4	1.06	0.003908498	Tmem71	4.80	2.64E-05

Nyx	1.06	1.01E-04	Ptgs1	4.86	3.10E-04
Nr3C1	1.06	2.52E-06	Tac2	4.87	1.74E-05
Etl4	1.07	2.67E-04	Svet1	4.89	4.01E-04
Fbxl22	1.07	3.35E-05	Gm12349	4.89	6.24E-05
Slc38A4	1.07	3.71E-05	Rnf180	4.90	1.40E-07
Ttpal	1.07	4.21E-04	Has2Os	4.94	8.48E-06
Gm7008	1.07	3.79E-04	Cxcr4	4.94	1.40E-07
Palm2	1.07	0.005045637	Gm13857	4.95	1.93E-05
Gss	1.07	1.67E-05	Gm43621	4.97	1.67E-04
Rerg	1.07	7.68E-04	1700027H10Rik	4.98	4.32E-06
Akr1C18	1.07	0.007721588	Gm45652	4.98	1.69E-04
Dhcr7	1.07	3.61E-05	Rragd	5.00	6.55E-08
Tk2	1.08	1.69E-04	Slc10A5	5.02	4.55E-05
5830432E09Rik	1.08	0.005002862	0610031O16Rik	5.03	8.86E-05
Vasn	1.08	8.00E-05	Slc22A22	5.06	1.01E-05
Pdgfd	1.08	6.88E-04	Galnt16	5.06	1.54E-06
Gm6225	1.08	0.001509433	Asgr1	5.08	1.02E-04
Snapc1	1.08	1.75E-05	Fabp7	5.10	4.17E-04
Psat1	1.08	4.57E-06	Dmbt1	5.14	1.22E-05
Tiparp	1.09	4.95E-06	Tchhl1	5.17	5.22E-04
Ehbp1L1	1.09	0.001245528	Havcr2	5.19	2.08E-05
Tiam1	1.09	3.48E-06	Vstm2A	5.20	1.65E-04
Il20Rb	1.09	0.008741556	Fabp4	5.22	3.49E-04
Cyb561	1.09	1.02E-04	Akr1B7	5.22	4.71E-06
Txndc2	1.09	2.90E-04	Kl	5.23	1.54E-04
Cadm4	1.09	0.003442728	Slc5A7	5.33	9.47E-06
Icosl	1.09	8.35E-05	Apela	5.34	1.23E-05
Gcnt2	1.09	0.006747813	Il6	5.35	9.50E-05
Gm10768	1.09	4.21E-04	Zfp804A	5.36	8.57E-07
Mex3B	1.09	2.11E-05	Gm42793	5.40	1.50E-04
Bin3	1.09	8.68E-05	Pthlh	5.41	8.60E-05
Dner	1.09	0.002924715	Lyve1	5.54	3.07E-05
Eaf1	1.09	2.18E-05	Sphk1	5.56	4.08E-05
Rdh10	1.10	1.86E-05	Egr3	5.65	4.32E-06
Sdcbp	1.10	7.53E-07	Rnd3	5.65	1.06E-06
Car2	1.10	0.004027136	Gm12648	5.66	4.38E-05
Bbc3	1.10	0.005768878	A230059L01Rik	5.67	2.02E-05
Maf	1.10	2.04E-04	Ereg	5.67	3.85E-05
Tcf24	1.10	3.35E-04	Trank1	5.68	5.28E-06
Cntnap2	1.10	0.009384629	Rnf125	5.69	1.74E-05
Nudt4	1.11	9.70E-06	Ptprn	5.73	2.08E-05
Nmrk1	1.11	0.002574091	Has2	5.82	2.05E-06

Msantd1	1.11	0.00592378	Gm15767	5.92	5.68E-06
Ncbp1	1.11	2.01E-05	Msc	5.96	2.30E-05
Ramp3	1.11	0.006955385	Gm9947	6.08	1.05E-05
Gm10941	1.11	0.001280177	4930432L08Rik	6.11	5.28E-06
Wt1	1.12	8.39E-04	Gm28294	6.17	5.58E-05
Cela1	1.12	0.003376208	Klrb1A	6.18	6.42E-06
Bloc1S4	1.12	1.35E-04	Lingo4	6.24	6.95E-06
Epm2Aip1	1.12	1.56E-05	Nmu	6.25	1.41E-05
Ndrg4	1.12	0.001326376	Aldob	6.29	1.86E-07
Slc9A3R2	1.12	0.001628078	Pgr	6.35	1.07E-04
Cecr2	1.12	2.14E-05	Kdm4Dl	6.38	1.08E-06
Spsb2	1.12	6.49E-05	Gm37498	6.42	4.64E-05
Gadd45A	1.12	5.98E-04	Adh7	6.45	8.93E-06
Cntn3	1.12	0.005642239	Gm16485	6.47	0.001371218
Fam102B	1.12	4.22E-06	Brinp3	6.49	4.59E-05
Ckb	1.12	4.88E-04	Trdv5	6.50	1.88E-06
Sesn2	1.13	4.97E-05	Npy	6.53	2.56E-05
Mir22Hg	1.13	6.06E-06	Ptgs2Os2	6.55	4.53E-06
Bend7	1.13	1.38E-05	Lepr	6.59	7.00E-08
Slc7A1	1.13	4.02E-04	Helt	6.61	1.13E-06
Ednra	1.13	1.42E-05	Btc	6.61	1.55E-06
Erf	1.13	1.07E-05	Olr1	6.65	1.70E-05
Nedd9	1.13	1.46E-06	Gm29398	6.78	7.45E-06
Hdac7	1.13	4.78E-04	Sema4F	6.88	3.70E-05
F8A	1.13	1.19E-05	Epgn	6.93	6.59E-06
Map6D1	1.13	6.46E-04	Gm37630	6.94	4.74E-06
Ank2	1.14	1.77E-04	Retn	6.98	4.57E-06
Hccs	1.14	3.62E-06	Gm20125	7.03	1.29E-04
Slc44A1	1.14	3.91E-06	Spp1	7.03	3.83E-06
Nr2F6	1.14	1.64E-05	Tnfaip6	7.12	1.38E-06
Jag1	1.14	3.17E-06	Prkg2	7.25	1.04E-06
Wdfy1	1.14	5.08E-06	Ripply1	7.39	5.13E-07
Atp2B1	1.14	1.99E-05	Kcnk10	7.42	2.40E-07
Tle1	1.14	1.51E-05	Ptgs2	7.46	6.74E-07
Chrna2	1.14	7.47E-04	Krt23	7.65	2.59E-05
Vps26A	1.14	4.19E-04	Gm38189	8.19	1.88E-06
Borcs6	1.15	5.28E-05	Gm43434	8.29	1.66E-05
Pcsk9	1.15	1.09E-04	2010109I03Rik	8.44	1.09E-05
Fads6	1.15	7.40E-04	Gcg	8.49	8.83E-07
Bex4	1.15	1.52E-06	Trdc	9.05	6.37E-05
Tsc22D4	1.15	1.83E-04	Snap25	9.06	1.15E-05
Ccnd3	1.15	0.00280665	Adcyap1	9.39	4.41E-05

Inpp5A	1.15	3.32E-05	Ptx3	9.78	2.42E-07
4932441J04Rik	1.16	3.82E-05	Sprr2G	10.42	3.72E-07
Lrrc8B	1.16	1.33E-04	Nts	11.47	4.97E-07
Rev3L	1.16	4.47E-05	Sult1E1	12.68	4.87E-07
Epor	1.16	2.11E-04			

Appendix 8 List of differentially expressed genes in PGRKO vs PGR+/- oviduct identified through microarray.

Genes that had |logFC| ≥ 1 and a p-value cut-off of 0.01 were selected as DEG. LogFC is displayed as PGRKO vs PGR+/-.

Gene	logFC	p-value	Gene	logFC	p-value
Itga8	-9.866	1.52E-06	Osr2	-2.38	6.82E-03
Hmgcs2	-5.812	3.06E-04	Pgr	-2.374	9.92E-04
Maob	-5.481	3.37E-04	Galntl2	-2.362	9.41E-04
Gm106	-4.506	1.46E-03	Pde5a	-2.348	5.69E-04
Zbtb16	-4.326	5.69E-04	Rasl11b	-2.338	3.38E-03
Dpep1	-4.019	4.73E-03	Wfdc1	-2.323	1.55E-03
Cyp1b1	-3.877	5.85E-03	Slc41a3	-2.31	7.65E-04
Slc7a8	-3.765	9.12E-03	Ptgfr	-2.279	1.32E-02
Rgs2	-3.644	5.78E-04	Adcy5	-2.272	3.37E-04
Tcf23	-3.564	9.41E-04	Myocd	-2.267	2.86E-03
Des	-3.548	3.37E-04	Cited2	-2.258	1.26E-02
Arl4d	-3.52	1.79E-03	Itgbl1	-2.204	3.37E-04
Edn3	-3.431	1.15E-03	Adamts9	-2.195	1.38E-02
Prlr	-3.388	1.61E-03	Spock2	-2.19	4.47E-04
Lrp2	-3.316	6.02E-04	Synpo2	-2.188	1.02E-02
Adamts1	-3.18	7.65E-04	Ctgf	-2.182	1.50E-03
Kcnj8	-3.149	5.72E-04	Crispld1	-2.177	7.65E-04
Gria3	-3.145	3.32E-03	Lama1	-2.166	1.48E-02
Cpxm2	-3.117	4.92E-04	Fgf7	-2.152	8.75E-03
Ppap2b	-2.895	4.47E-04	Tgfbi	-2.133	4.73E-04
Postn	-2.865	1.04E-03	Cldn3	-2.128	9.28E-03
Fxyd4	-2.85	5.46E-04	Hoxa3	-2.128	5.11E-03
Errfi1	-2.779	4.47E-04	Adamts5	-2.117	9.42E-03
Sult1a1	-2.708	4.47E-04	Chrdl1	-2.109	1.70E-03
Tmem204	-2.707	4.65E-03	Aspn	-2.093	1.63E-02
Fkbp5	-2.683	4.53E-03	Hoxa6	-2.088	1.67E-02
Col12a1	-2.667	9.92E-04	Gpr124	-2.087	2.12E-03
Abca8a	-2.66	7.29E-03	Slc2a4	-2.063	3.58E-03
Col11a1	-2.642	6.27E-05	Pgm5	-2.05	8.55E-04
Penk1	-2.64	5.72E-04	Stk17b	-2.045	8.04E-03
Figf	-2.629	2.04E-03	Tgfbr3	-2.036	4.73E-04
Rasd2	-2.533	4.93E-03	Aldh1l1	-2.031	1.85E-03
Actg2	-2.522	6.27E-05	Timp3	-2.029	5.76E-03
Klf15	-2.508	9.60E-04	Cdkn1c	-2.026	9.47E-04
Hif3a	-2.505	7.65E-04	C7	-2.024	7.54E-03
Mamdc2	-2.488	9.10E-04	Pi15	-2.014	9.35E-04
Mapk11	-2.47	7.65E-04	Pln	2.033	3.07E-03
Sectm1a	-2.464	3.12E-03	Padi4	2.147	6.83E-03

Pdlim3	-2.426	1.81E-03	Agtr2	2.183	2.60E-03
Kcnip2	-2.418	3.22E-03	Slc26a4	2.685	5.46E-04
Wfdc15b	-2.396	1.69E-03			

Appendix 9 List of differentially expressed genes in PGRKO vs PGR+/+ uterus identified through microarray.

Genes that had |logFC| ≥ 1 and a p-value cut-off of 0.01 were selected as DEG. LogFC is displayed as PGRKO vs PGR+/+.

Gene	**logFC**	**p-value**	**Gene**	**logFC**	**p-value**
Cyp26a1	-9.64	0.00018	Ccng1	-2.24	0.00011
Lrp2	-5.50	0.00041	Enpp1	-2.24	0.00262
Npl	-5.28	0.00039	Slain1	-2.22	0.00843
Acot7	-4.88	0.00011	Ctla2a	-2.17	0.00207
Hdc	-4.83	0.0002	Etnk1	-2.05	0.00368
Mthfd2	-4.40	0.00062	Mt2	-2.04	0.00759
Nfil3	-3.49	0.00345	Tnfrsf21	-2.02	0.00066
Myd88	-3.13	0.00099	Acss1	-2.01	0.00405
Pla2g10	-2.92	0.00033	Ptk2b	-2.01	0.00217
Ggct	-2.83	9.91E-05	Tiparp	-2.00	0.00334
Pdk3	-2.76	0.00439	Ckmt1	-2.00	0.00922
Sgk1	-2.73	4.33E-05	Pip5k1b	-2.00	0.0026
Caprin2	-2.53	6.94E-05	Cdh16	2.02	0.00895
Pdzk1ip1	-2.52	0.00037	Sox7	2.04	0.0005
Ptgs1	-2.49	0.00237	Emb	2.07	0.00085
Wnt11	-2.43	0.0052	Mycn	2.10	0.0066
Alpl	-2.43	0.00984	Car8	2.12	0.0075
Slc25a48	-2.37	5.31E-05	Efnb2	2.18	0.00051
Cited2	-2.31	0.00276	St6galnac5	2.26	0.00282
Gars	-2.28	0.00705	Gjb2	2.89	0.00385
Clcn5	-2.25	0.00594			

Appendix 10 List of antibodies used for immunofluorescence and PLA

Target	Brand	Catalogue #	Host	Antigen
PGR	Thermo Fisher	MA5-12658	Mouse mAb	PGR from a human endometrial carcinoma (EnCa 101) grown in athymic mice
	Cell Signaling	8757	Rabbit mAb	Residues surrounding Tyr541 of human PGR
H3K27ac	Active Motif	39133	Rabbit pAb	Peptide including acetyl-lysine 27 of H3
Acetyl-CBP/p300	Cell Signalling	7389	Rabbit pAb	Recombinant CBP specific to the amino terminus of human CBP
RUNX1	Cell Signaling	4334	Rabbit mAb	Amino acid near the N-terminal of human RUNX1
	Santa Cruz	Sc-365644	Mouse mAb	Amino acid 186-250 of human RUNX1
RUNX2	Jomar Life Research	D130-3	Mouse mAb	Recombinant RUNX2
	Santa Cruz	Sc-390715	Mouse mAb	Amino acid 294-363 of mouse RUNX2
CBFβ	Cell Signalling	62184	Rabbit mAb	Residue surrounding Asn14 of human CBFβ
c-JUN	Santa Cruz	sc-376488	Mouse mAb	Amino acid 237-273 of mouse c-JUN
JUNB	Santa Cruz	sc-8051	Mouse mAb	Amino acid 210-222 of mouse JUNB
JUND	Santa Cruz	sc-271938	Mouse mAb	Amino acid 316-341 of mouse JUND
LRH1	Perseus Proteomics	PP-H2325-00	Mouse mAb	Amino acid 161-280 of human LRH1

Appendix 11 RUNX1 ChIP-seq reproducibility and correlation of biological replicates for RUNX1 0h, RUNX1 6h and RUNX1 E14.5.

Sections are divided into RUNX1 0h (A), RUNX1 6h (B) and RUNX1 E14.5 (C). In each section: Scatter plot of signal scores, peak ranks and peak count based on estimated IDR for RUNX1 ChIP-seq biological replicates (left). Log(signal) and peak rank are displayed as replicate 1 vs replicate 2. Peaks with IDR > 0.01 are in red and peaks with IDR ≤ 0.01 are in black. Read count frequency of RUNX1 ChIP-seq peaks in replicate 1 and replicate 2 in relation to the TSS (middle). Pearson correlation matrix for replicate 1 and replicate 2 (right). The colour of matrix squares indicates correlation coefficient, noted in the bar at the bottom. Venn diagram of peak count in both replicates, showing peaks that are overlapped in both

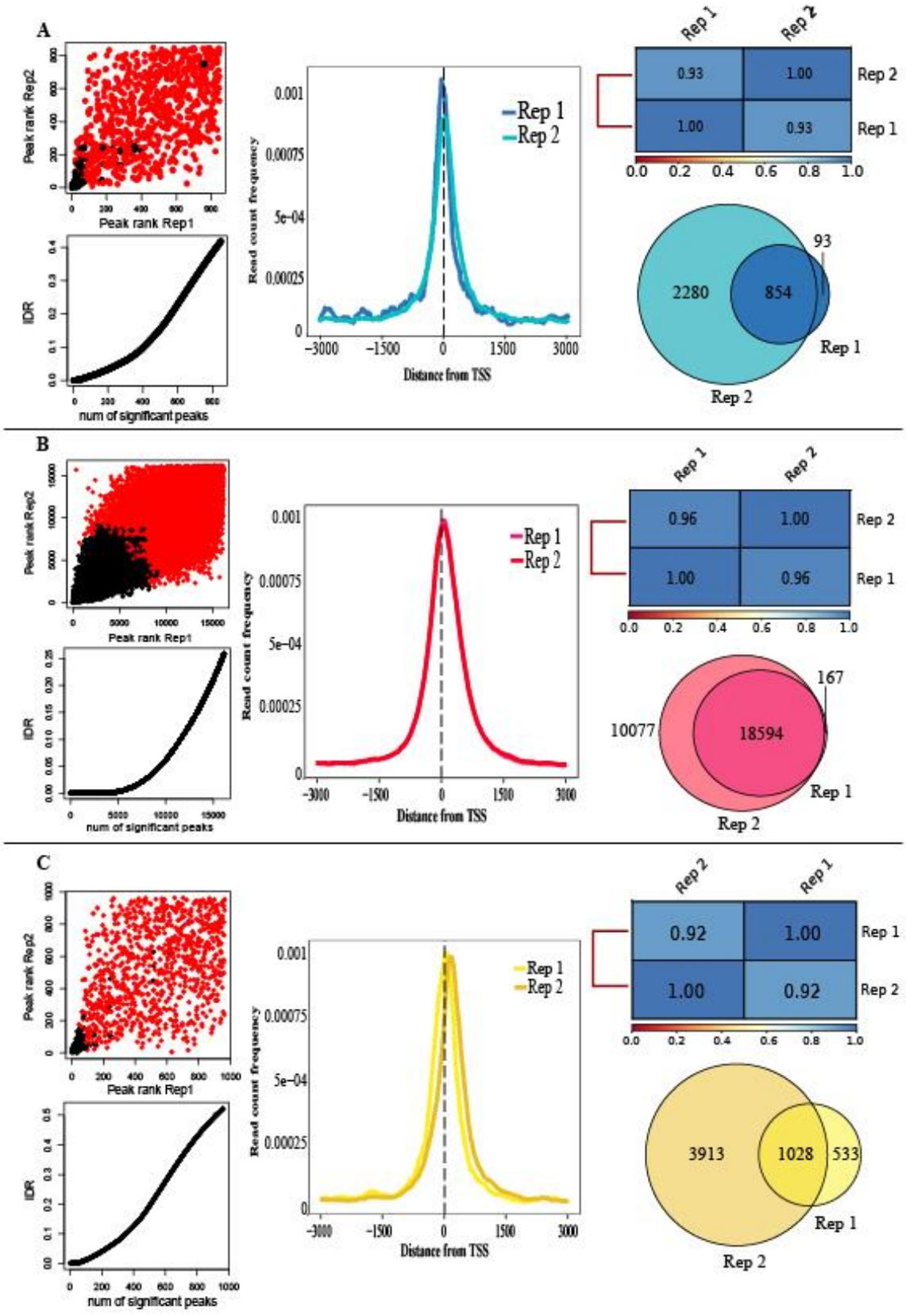
A
Peak rank Rep2
Peak rank Rep1
IDR
num of significant peaks
Read count frequency
Rep 1
Rep 2
Distance from TSS
Rep 1
Rep 2
0.93
1.00
1.00
0.93
Rep 2
Rep 1
0.0 0.2 0.4 0.6 0.8 1.0
2280
854
93
Rep 1
Rep 2
B
Peak rank Rep2
Peak rank Rep1
IDR
num of significant peaks
Read count frequency
Rep 1
Rep 2
Distance from TSS
Rep 1
Rep 2
0.96
1.00
1.00
0.96
Rep 2
Rep 1
0.0 0.2 0.4 0.6 0.8 1.0
10077
18594
167
Rep 1
Rep 2
C
Peak rank Rep2
Peak rank Rep1
IDR
num of significant peaks
Read count frequency
Rep 1
Rep 2
Distance from TSS
Rep 2
Rep 1
0.92
1.00
1.00
0.92
Rep 1
Rep 2
0.0 0.2 0.4 0.6 0.8 1.0
3913
1028
533
Rep 1
Rep 2

Appendix 12 Summary of RNA-seq-seq datasets, including library size, sequence length, alignment stats, gene count and DEG count

Dataset	Library size	Sequence length	Overall alignment rate	Number of alignments pre-filtering	Number of alignnments post-filtering	% of alignment retained post-filtering	Number of expressed genes	Mean count cut-off	Number of genes post-filter	DEG (KO vs WT)
PR_WT1_R1	98646766	101	89.29	219652387	161499585	73.53	48083	11	32389	611 DEGs (434 downregulated, 177 upregulated)
PR_WT1_R2	98646766	101								
PR_WT2_R1	86097747	101	89.65	191411670	141827067	74.10				
PR_WT2_R2	86097747	101								
PR_WT3_R1	91499775	101	89.95	205975628	149821093	72.74				
PR_WT3_R2	91499775	101								
PR_WT4_R1	91481539	101	89.56	204544043	150230837	73.45				
PR_WT4_R2	91481539	101								
PR_KO1_R1	85913413	101	90.11	191698835	142028359	74.09				
PR_KO1_R2	85913413	101								
PR_KO2_R1	82837909	101	89.02	186884096	133122561	71.23				
PR_KO2_R2	82837909	101								
PR_KO3_R1	84211516	101	89.63	189420543	136964226	72.31				
PR_KO3_R2	84211516	101								
PR_KO4_R1	87996436	101	88.61	195431490	143504392	73.43				
PR_KO4_R2	87996436	101								
A_WT1_R1	91164449	101	90.66	204596707	150270954	73.45	48113	23	28705	686 DEGs (515 downregulated, 171 upregulated)
A_WT1_R2	91164449	101								
A_WT2_R1	88859348	101	88.68	199384188	142744907	71.59				
A_WT2_R2	88859348	101								
A_WT3_R1	88543261	101	91.01	196100419	148333038	75.64				
A_WT3_R2	88543261	101								
A_WT4_R1	87666250	101	90.69	194780631	146005569	74.96				

A_WT4_R2	87666250	101								
A_KO1_R1	94385408	101	90.5	208570243	157941605	75.73				
A_KO1_R2	94385408	101								
A_KO2_R1	92141186	101	89.95	205324175	151654876	73.86				
A_KO2_R2	92141186	101								
A_KO3_R1	97537594	101	90.33	217188872	161311718	74.27				
A_KO3_R2	97537594	101								
A_KO4_R1	83720240	101	90.49	184923926	140017075	75.72				
A_KO4_R2	83720240	101								
B_WT1_R1	93517712	101	89.52	206903424	154461178	74.65	51771	2	43782	142 DEGs (4 downregulated, 138 upregulated)
B_WT1_R2	93517712	101								
B_WT2_R1	94588459	101	90.59	208013215	159246040	76.56				
B_WT2_R2	94588459	101								
B_WT3_R1	87752248	101	89.45	194832357	145127282	74.49				
B_WT3_R2	87752248	101								
B_WT4_R1	88197326	101	89.46	194662277	146128992	75.07				
B_WT4_R2	88197326	101								
B_KO1_R1	90133697	101	87.46	200226516	145259269	72.55				
B_KO1_R2	90133697	101								
B_KO2_R1	88558420	101	89.67	194495485	148225066	76.21				
B_KO2_R2	88558420	101								
B_KO3_R1	95930056	101	87.78	210532927	157098322	74.62				
B_KO3_R2	95930056	101								
B_KO4_R1	92601256	101	86.48	204126836	147926625	72.47				
B_KO4_R2	92601256	101								

Appendix 13 List of differentially expressed genes identified in RNA-seq PGRKO vs WT granulosa cells identified through RNA-seq.

Genes that had |logFC| ≥ 1 and an adjusted p-value cut-off of 0.01 were selected as DEG. LogFC is displayed as KO vs WT.

Gene	LogFC	Adj p-value	Gene	LogFC	Adj p-value
Lyve1	-4.81	1.27e-121	Armc12	-1.20	0.00344
Cldn1	-4.05	1.19e-173	4931415c17rik	-1.20	0.000283
Gm34549	-3.90	1.92E-54	Mbnl1	-1.20	9.61E-35
Cyp2j11/cyp2j8	-3.46	2.9e-49	Gclc	-1.19	1.22e-31
L3mbtl4	-3.37	1.64e-80	Rp23-337k17.1	-1.19	0.000708
Hsd17b11	-3.31	9.05e-102	Nxf3	-1.19	5.42e-12
Scara5	-3.26	1.57e-103	Ate1	-1.19	4.05e-22
Gm12637	-3.19	8.22E-34	Cln5	-1.19	9.97E-21
Glp2r	-3.17	5.18e-164	Rp23-357o17.2	-1.19	0.00498
Gm33677	-3.12	3.24E-36	Agfg2	-1.18	3.26E-28
4930467D21Rik	-3.11	1.89E-76	Iqck	-1.18	1.56E-17
Kcnv2	-2.96	6.27e-42	Gm43791	-1.18	4.22e-17
Sctr	-2.81	4.7e-25	Loc728392	-1.17	0.000138
Zic2	-2.74	1.03e-15	Ac134576.3	-1.17	0.00262
Havcr2	-2.73	1.84e-48	Gm44769	-1.17	0.0000287
Creg2	-2.72	2.65e-44	Gm45708	-1.17	0.0000659
Gas7	-2.71	5.6e-144	Trim9	-1.17	3.18e-17
Tbc1d8	-2.70	5.34e-92	Gm6382	-1.17	1.28e-08
Ac096777.1	-2.69	2.07e-31	Kcnh6	-1.17	0.00639
Scg2	-2.67	3.56e-87	Rp23-469k15.2	-1.17	0.00304
Myh3	-2.65	2.21e-55	Gm10706	-1.17	0.00298
Sphk1	-2.64	3.27e-53	Gm28516	-1.17	0.00605
Ppp1r36	-2.63	2.58e-22	Elovl2	-1.16	4.94e-18
Lingo4	-2.63	4.07e-61	Gm40318	-1.16	0.00599
Hopxos	-2.62	1.1E-24	Stmn4	-1.15	0.0000305
C10orf71	-2.56	7.34E-28	Dok7	-1.15	6.94E-12
Rcvrn	-2.54	8.06e-25	Entpd7	-1.15	4.92e-25
Gm38411	-2.54	1.42E-41	Sra1	-1.15	4.82E-21
Itgb6	-2.54	3.65e-33	Rufy4	-1.15	0.000000127
Hopx	-2.47	4.41e-25	Ac159006.2	-1.15	0.00396
Vnn3	-2.46	1.52E-50	Xrra1	-1.15	1.75E-12
Sprr2g	-2.45	1.66E-11	4930507D05Rik	-1.15	6.55E-08
A930019D19Rik	-2.44	6.5E-62	Gm12926	-1.15	0.000887
Cited1	-2.44	2.72e-25	Rtbdn	-1.15	0.0000235
Frmpd1os	-2.43	9.35E-21	A830008E24Rik	-1.14	0.000000021
Ntn5	-2.43	6.28e-22	1700011b04rik	-1.14	0.0076
Gm33055	-2.40	2.21E-19	Tfcp2l1	-1.14	7.15E-11
Gm37498	-2.39	6.56E-12	Ifnk	-1.14	0.0000583

Tmem37	-2.38	1.94e-29	Il6	-1.14	6.26e-08
Ac118724.1	-2.34	5.58e-38	Kcna5	-1.14	0.00559
Cdh19	-2.33	8.75e-27	Tcf23	-1.14	0.000316
Helt	-2.33	1.48e-10	Gm12843	-1.14	3.16e-08
Ralgapa2	-2.33	6.15e-63	Icoslg	-1.14	2.07e-16
Cxcr4	-2.31	2.78e-73	Mir6407	-1.14	0.00868
Aldob	-2.29	3.49e-40	Gm7575	-1.13	0.0000187
Jcad	-2.27	5.76e-43	Albfm1	-1.13	1.62e-11
Frmpd1	-2.26	5.2e-41	Naa11	-1.13	1.22e-08
1700040D17Rik	-2.24	6.92E-13	Gm15471	-1.13	8.76E-21
Fzd1	-2.23	2.81e-56	Mir3097	-1.13	0.00679
Gm8200	-2.22	4.1E-10	Ceacam10	-1.13	0.0000156
Ac119998.5	-2.21	3.87e-14	Gm15530	-1.13	0.00000157
Entpd1	-2.20	2.84e-60	Ac113485.1	-1.13	0.00603
Adam8	-2.19	4.45e-57	Gm14167	-1.12	0.0000248
Gm11802	-2.19	1.33E-53	Gm18734	-1.12	0.000106
Gm43545	-2.17	1.84E-47	Xpnpep1	-1.12	8.87E-20
Rnu2-1	-2.16	1.95e-34	Gm30275	-1.12	3.25e-11
Rlbp1	-2.15	7.68e-12	Mt3	-1.12	0.000000445
Ccdc63	-2.15	7.36e-14	A330015k06rik	-1.12	3.52e-13
Gm13583	-2.14	1.58E-27	Olfr1033	-1.12	1.75E-10
Rp23-390f4.1	-2.14	3.58e-18	Ampd3	-1.11	1.58e-11
Ac154639.1	-2.13	1.3e-10	Gm44421	-1.11	0.0109
Kcne4	-2.13	6.28e-22	C2cd4d	-1.11	0.000241
Mir8114	-2.13	2.02E-49	4930522N08Rik	-1.10	0.0089
Gm43401	-2.13	4.37E-22	1010001N08Rik	-1.10	3.57E-25
Myl2	-2.13	6.41e-12	Gm36638	-1.10	0.00135
Gm3716	-2.11	4.29E-21	Gpr68	-1.10	3.33E-17
Cd34	-2.10	3.48e-51	A930028n01rik	-1.10	0.00000371
Klf15	-2.10	2.5e-49	Defb45	-1.10	0.0119
Abcc2	-2.10	3.15e-20	Mir1962	-1.10	0.00829
Teddm2	-2.09	4.55E-35	Wipf3	-1.10	3.22E-16
Adh6b	-2.08	4.53E-12	4931403E22Rik	-1.10	3.57E-15
Gm37265	-2.08	1.07E-10	Bhmt	-1.10	3.67E-08
Kiaa1217	-2.07	9.97e-59	Papss2	-1.10	4.1e-18
Rp23-282m20.5	-2.07	2.97e-08	Dclre1b	-1.09	3.44e-14
Gm38691	-2.07	9.72E-31	A530046M15Rik	-1.09	0.00498
Gm33024	-2.05	4.23E-12	Cryab	-1.09	0.00000288
Gm42463	-2.04	5.5E-14	Gm43672	-1.09	0.0000395
Tsc22d3	-2.03	4.01e-35	Pla2g2f	-1.08	0.0151
Slc7a11	-2.03	4.69e-26	Cep295nl	-1.08	3.76e-11
Gm44079	-2.01	4.67E-39	N-r5s89	-1.08	0.00103
Gm17590	-2.00	5.35E-35	Serpina5	-1.08	0.00412
Gm16897	-2.00	7.44E-63	Pgap2	-1.08	2.42E-16
Rp23-357o17.1	-1.99	6.48e-08	Gm15622	-1.07	0.00214

Actn3	-1.99	1.28E-45	Tle1	-1.07	2.28E-23
Ai463229	-1.98	1.04e-11	Gm5837	-1.07	0.0000186
Kl	-1.98	1.81e-40	Gm43128	-1.06	0.0148
Rp23-98c9.5	-1.96	5.68e-27	Prima1	-1.06	0.000103
Rorc	-1.96	5.32e-35	2200002j24rik	-1.05	0.00000462
Mt2	-1.95	2.89E-27	A630009H07Rik	-1.05	0.0156
Gm16638	-1.94	3.94E-39	Hcn4	-1.05	0.00000778
Adamts1	-1.94	4.95e-35	Pla2g15	-1.05	6.41e-16
Atp4a	-1.93	8.5e-49	Xlr3c	-1.05	0.000421
Rp23-247p3.3	-1.93	1.25e-28	A430088p11rik	-1.05	0.00241
Hspa2	-1.92	2.38e-23	Rp23-182f9.7	-1.04	0.00000766
Ankrd55	-1.91	1.17e-17	Syce2	-1.04	1.2e-11
Gm26638	-1.91	6.83E-12	Gm10635	-1.04	0.00036
Aloxe3	-1.91	1.61e-16	Rnd3	-1.04	7.03e-13
Snap25	-1.90	7.34e-51	Cradd	-1.04	1.37e-13
Dcaf4	-1.90	8.05e-40	Rp23-281m13.1	-1.03	0.0042
4930529N20Rik	-1.90	0.0000005	Col27a1	-1.03	1.6E-11
Gm37342	-1.90	2.06E-19	Add3	-1.03	8.33E-23
Gm36602	-1.89	2.48E-28	Dusp27	-1.03	0.000621
Kcnh4	-1.88	6.02e-21	Eldr	-1.03	0.00000047
Pparg	-1.88	3.75e-29	Ac122251.2	-1.03	0.000678
Gm10728	-1.88	2.6E-14	Apcdd1	-1.03	1.05E-10
Gm44639	-1.87	4.7E-21	Gm28800	-1.03	3.52E-11
Tnfsf11	-1.85	5.28e-31	Plac8l1	-1.03	0.00252
Apol6	-1.85	2.67e-29	Unc79	-1.03	1.28e-08
Pde6h	-1.85	2.51e-14	1700049e15rik	-1.03	0.0185
Ripply1	-1.83	1.45E-08	RP23-243B24.4	-1.02	1.38E-18
Gm20540	-1.81	6.72E-17	E230001N04Rik	-1.02	0.000000863
Cdh13	-1.81	2.21e-35	S100a10	-1.02	1.48e-10
Rubcnl	-1.80	4.02e-31	Clvs2	-1.02	6.92e-09
Art4	-1.80	2.06e-10	Acsbg2	-1.02	0.00081
Gm43434	-1.78	2.42E-26	Gm44069	-1.02	0.0191
Micos10	-1.77	8.71e-26	Gm44284	-1.02	4.16e-11
Mocs1	-1.77	4.57E-41	Cyp2j7	-1.01	0.0124
Gm39041	-1.77	2.8E-26	Gm38248	-1.01	0.000000801
Gm24224	-1.77	1.45E-08	Zyx	-1.01	1.33E-13
Ldhd	-1.77	3.33e-33	Gm25043	-1.01	0.00000537
Efnb2	-1.76	2.48e-33	Apoa1	-1.01	0.00000237
Maml3	-1.75	1.97e-30	Wdfy2	-1.01	2.03e-19
Gldc	-1.75	4.29e-21	Abtb2	-1.01	1.54e-10
Gm13068	-1.75	5.25E-21	Mob3b	-1.00	4.34E-12
Zcchc24	-1.74	1.03e-53	C630043f03rik	-1.00	0.000364
Gm37229	-1.74	9.28E-19	Pyroxd2	-1.00	0.00000907
Gm45073	-1.73	1.37E-10	Ct572985.1	-1.00	0.00000793
D930019O06Rik	-1.73	0.000000847	9130019P16Rik	-1.00	6.91E-12

Mapre2	-1.71	1.01E-58	Btc	1.00	0.0000232
Gm12796	-1.71	1.25E-32	8030423F21Rik	1.01	0.0136
Gm37832	-1.71	0.000000251	4932441J04Rik	1.01	3E-20
Tmc3	-1.70	1.69e-22	Gm45352	1.02	0.00000623
Gk2	-1.70	0.00000537	P2ry14	1.02	2.3e-15
Egfros	-1.70	6.74E-34	Bach2os	1.02	0.00000152
Sh3gl3	-1.69	5.26e-27	Gm15426	1.03	0.0112
Trpa1	-1.69	8.83e-16	Gm43775	1.03	6.1e-11
Gm20089	-1.69	2.01E-22	Vegfc	1.03	0.000000355
Gm2861	-1.69	0.00000388	Gm42486	1.03	0.00232
Gm40910	-1.68	0.00000977	Gm43947	1.03	0.0000539
Kbtbd11	-1.68	1.02e-20	Gm30301	1.04	0.0000966
Gm31510	-1.67	0.0000147	Kctd8	1.04	0.000000582
4930524C18Rik	-1.66	0.000000521	Gm16033	1.04	1.6E-12
Rab11fip1	-1.66	3.02e-38	Gm16057	1.04	0.00134
Bean1	-1.65	1.32e-47	Gm21168	1.04	1.02e-09
Gm42553	-1.65	0.0000204	Astn1	1.04	0.000000113
Stard5	-1.65	2.14e-44	Aw551984	1.04	0.000000164
S100a2	-1.65	2.52e-55	Gm26725	1.04	5.28e-08
Mb	-1.64	2.28e-29	Unc5cl	1.04	0.00602
Gm37673	-1.64	0.00000456	Fcgbp	1.04	0.0152
Gm37844	-1.63	3.97E-08	Gm42536	1.04	0.0178
Gm15475	-1.63	1.77E-21	Rp24-226h19.1	1.04	0.00174
Hsd17b13	-1.63	1.97e-10	Gm26911	1.04	0.000000012
Fabp4	-1.63	0.0000157	9330185c12rik	1.05	0.00000108
Gm42555	-1.63	0.0000299	Gm42676	1.05	0.0157
A930030B08Rik	-1.63	2.83E-09	SIGLEC9	1.05	0.0000851
Cyp2j15-ps	-1.63	0.0000211	1110018n20rik	1.05	0.000787
Prkg2	-1.62	6.46e-46	Coch	1.05	4.39E-09
Hnf4a	-1.62	0.000000104	Ltf	1.05	0.017
Gm9748	-1.62	0.000000228	Gm42478	1.05	0.0000492
Capn6	-1.61	1.92e-13	Gm28096	1.05	0.015
Sec1	-1.61	6.08E-17	Rpp25	1.05	9.14E-09
Gm26807	-1.61	3.22E-08	Gm28893	1.05	0.00803
Gm43621	-1.61	3.2E-16	IGSF10	1.06	2.03E-18
Hkdc1	-1.60	0.00000167	Fras1	1.06	2.17E-20
Apol7e	-1.60	6.29E-08	DOK6	1.06	0.0176
Gm11494	-1.60	0.00000178	Gm17087	1.06	0.000252
Ces1a	-1.59	0.00000847	Rasgrf2	1.06	4.9E-13
Fyb2	-1.59	4.34e-18	Gm13477	1.06	0.0000309
Gm43333	-1.59	0.0000251	Cdhr3	1.06	0.00654
Trdv5	-1.59	1.07E-08	Gm37573	1.07	0.000195
Gm29183	-1.58	1.31E-17	Gm41192	1.07	1.93E-14
Gm4275	-1.58	3.64E-11	Ppp1r1a	1.07	0.00228
Gm30505	-1.58	1.13E-16	Gm5067	1.07	1.07E-11

Pcdh8	-1.57	1.73e-17	Vmn2r23	1.07	0.0151
Tac3	-1.57	6.13e-11	5033403h07rik	1.08	0.00000682
4930452G13Rik	-1.57	0.00006	Gm16559	1.08	4.41E-10
Gm15328	-1.57	4.62E-10	Gm35368	1.08	0.00144
Pdlim1	-1.57	4.04e-33	Gm20703	1.08	0.000596
E230020D15Rik	-1.57	5.4E-14	Rp23-5h4.2	1.09	0.00994
Dysf	-1.56	5.37e-30	Gm7019	1.09	0.00185
Defb119	-1.56	1.36e-20	Hba1/hba2	1.09	0.0056
1810019D21Rik	-1.56	1.76E-23	Satb2	1.09	3.47E-20
Gm15684	-1.56	9.84E-32	Adh1c	1.10	7.33E-10
Gm26843	-1.55	1.32E-15	9530086O07Rik	1.10	0.00000137
Hrct1	-1.55	8.06E-08	Ret	1.10	0.00000569
Aldh3a1	-1.55	8.06e-08	Csf2rb	1.10	4.56E-10
Gm14319	-1.55	2.82E-08	Dpp6	1.11	3.7E-09
Gm42435	-1.53	2.71E-08	Rp23-5h4.1	1.11	0.00307
Ptgs1	-1.53	1.06e-19	Gm12526	1.11	2.85E-09
4933416M07Rik	-1.53	1.96E-11	Ptn	1.11	1.46E-11
Crispld2	-1.52	3.53e-27	Gm14329	1.11	0.00013
6030407O03Rik	-1.52	6.91E-17	Gm15425	1.11	0.000000204
Gm45613	-1.51	1.84E-15	Gm20443	1.11	0.0056
Gstm1	-1.51	3.42e-18	Tmem229a	1.11	0.00634
Bcl11b	-1.51	5.27e-10	9130230l23rik	1.13	0.000000126
Gm45267	-1.51	2.76E-21	Gmnc	1.13	0.00617
Gm27884	-1.49	0.000172	Or2h2	1.13	0.00778
Rnf125	-1.49	2.96E-37	Gm6089	1.13	7.54E-11
Gm38252	-1.48	0.0000026	Gm42675	1.13	0.000387
AC147241.1	-1.48	1.82E-16	Gm16072	1.13	0.00897
PRRT4	-1.48	8.5E-42	Slc22a17	1.13	1.98E-13
Gm45074	-1.48	0.00000452	Speer4a	1.13	8.22E-08
Dkfzp434h168	-1.47	1.76e-40	Rp24-349l11.1	1.14	0.0000499
Gm26833	-1.46	0.000046	Olig3	1.15	0.00101
Gm10631	-1.46	6.78E-20	Bc049352	1.15	0.00125
D630033O11Rik	-1.46	6.18E-12	Olfr1545-ps1	1.15	0.0076
Gm37995	-1.46	0.00000606	Or8d1	1.16	0.0000967
Slc38a4	-1.46	1.27e-17	Gm5144	1.17	0.00317
Gm37675	-1.45	0.000015	Pla2g7	1.17	7.7E-14
Dtna	-1.45	2.77e-38	Dtx1	1.17	2.92E-15
Trpc4	-1.45	3.22e-15	Immp2l	1.17	1.81E-17
Scrn1	-1.44	3.41e-15	Gm42604	1.18	7.76E-09
Vwce	-1.44	8.63e-09	Gm38240	1.19	0.000945
A330049N07Rik	-1.43	0.000000243	Gm35570	1.19	0.00519
Ac113178.1	-1.43	1.94e-33	Cacna2d3	1.20	9.89E-21
Serpina3g	-1.43	0.0000824	Arhgef38	1.20	0.00128
Hgfac	-1.42	2.7e-15	Gm18645	1.20	0.000019
Gnao1	-1.42	7.28e-31	Gm44041	1.22	0.000118

Cyp4f8	-1.42	2.4e-11	Ly6m	1.23	0.000000623
Gstm5	-1.42	2.38e-17	Edil3	1.24	7.22E-15
Rp23-156n5.2	-1.42	0.000463	Hla-dob	1.24	0.0000677
Gm4788	-1.41	1.45E-11	Rsad2	1.24	0.000000741
Gm25631	-1.41	6.42E-09	Gm21655	1.24	3.76E-11
Per2	-1.41	5.18e-19	Gm37941	1.25	0.000534
Gprc5b	-1.40	1.27e-24	Mep1a	1.26	8.19E-08
Slco2a1	-1.40	5.88e-33	Tubb4a	1.26	7.4E-14
Slc16a6	-1.39	2.97e-26	Gm32364	1.26	1.16E-12
Gm34776	-1.39	0.0000724	Gm42639	1.29	1.03E-09
Lpar1	-1.39	1.51e-38	Gm7775	1.30	0.0000494
Ahsg	-1.39	1.08e-10	Ac122355.1	1.30	0.0000017
Gm10729	-1.39	0.00000701	Ac134249.1	1.30	0.00149
Glns-ps1	-1.38	0.0000193	Gm42534	1.31	0.00136
Ca11	-1.38	2.72e-09	Znf804a	1.32	1.16E-11
Gm12801	-1.38	0.000262	Ky	1.32	0.00000854
Rasef	-1.38	9.82e-20	Rbp4	1.33	3.08E-13
E130308A19Rik	-1.38	7.45E-33	Il25	1.33	0.000888
Lamc3	-1.38	9.19e-18	Chrna9	1.33	0.00000283
Esrp2	-1.37	1.07e-18	Gm41031	1.35	1.25E-11
Ac118724.2	-1.37	0.0000264	Prkcb	1.36	1.09E-20
Gm3470	-1.37	0.000277	Cyp26b1	1.36	4.08E-26
Jam3	-1.36	8.74e-38	Dnase2b	1.36	0.000772
Gm807	-1.36	3.57E-10	Lsamp	1.37	7.48E-17
Dmd	-1.36	4.59e-25	Gm10493	1.37	0.0000196
Gstm2-ps1	-1.36	0.000000186	Kcnb1	1.38	3.47E-20
Nipal1	-1.35	1.66e-23	Pgm5	1.38	3.63E-18
Gm6665	-1.35	8.24E-13	NRG3	1.39	3.44E-13
Nt5el	-1.34	0.000000132	Nrg3os	1.40	3.62E-09
Gm45463	-1.34	0.000385	Mir-218	1.41	0.000446
Ac118249.1	-1.34	0.000116	Tmem213	1.41	0.000266
Gm11384	-1.33	1.44E-09	Lpo	1.41	0.000455
Slit1	-1.33	0.00000047	Kel	1.42	1.92E-08
Met	-1.33	1.9e-29	Avil	1.42	5.75E-14
Them6	-1.33	3.92e-13	Brinp3	1.43	9.12E-14
Gm45266	-1.33	3.43E-09	Slit2	1.44	3.56E-22
Ppfia2	-1.32	2.1e-09	Olfr1233	1.44	0.000326
Gm45457	-1.32	3.56E-13	Nsun7	1.44	1.28E-15
Vnn1	-1.32	0.00128	Gm42640	1.45	2.14E-12
Edn2	-1.32	4.98e-08	Tac1	1.46	8.13E-13
Ct030159.2	-1.31	7.29e-12	Gm22513	1.49	1.02E-08
Vldlr	-1.31	3.66e-27	Gm45191	1.49	0.0000034
Gm14020	-1.31	8.33E-10	C4orf17	1.49	4.41E-15
Lrp8os3	-1.31	4.69E-11	4930563J15Rik	1.50	3.77E-08
Gm42464	-1.30	0.00158	Cdh6	1.54	1.48E-11

Gm45615	-1.30	1.14E-10	Uox	1.54	0.0000322
Arhgap31	-1.30	2.06E-32	Spock3	1.56	5.8E-29
Gm37068	-1.30	0.00139	Ac122881.1	1.56	5.06E-12
Cdh18	-1.30	5.78E-08	Gm43426	1.57	6.98E-08
Gm43298	-1.29	0.00164	Stac2	1.57	6.83E-16
Ac132133.3	-1.29	1.09E-10	Sprr2f	1.58	1.02E-08
Sorbs2os	-1.29	1.26E-19	4833427F10Rik	1.58	1.02E-22
Rp24-421p3.9	-1.28	1.23E-21	4933416M06Rik	1.58	1.07E-09
Rbbp7	-1.28	8.19E-19	Ddit4l	1.61	1.99E-32
Phf11	-1.28	0.000000003	Ac155634.2	1.63	0.00000297
Rp24-79i19.5	-1.28	2.01E-21	Spta1	1.63	2.17E-15
Gm39168	-1.28	0.00143	Npy1r	1.64	2.19E-09
Vps26a	-1.27	2.31E-26	Gm20642	1.64	1.97E-10
Gm35041	-1.27	0.000000078	Lingo1	1.64	4.02E-34
Gm29536	-1.27	2.53E-12	Gm15749	1.64	1.5E-26
Sorbs2	-1.27	2.26E-18	Cmtm5	1.66	0.000000847
4833404L02Rik	-1.27	0.00225	Gm9947	1.68	3.81E-15
Gm20616	-1.27	0.0000168	Muc4	1.69	0.0000126
Gm15398	-1.26	0.000000379	Gm7652	1.70	0.00000741
Gm29053	-1.26	0.000104	Gm37877	1.70	3.79E-08
Acss3	-1.26	1.27E-10	Egln3	1.71	8.75E-41
Loc105247277	-1.26	0.00251	4930518C09Rik	1.71	0.000000141
Pfkfb4	-1.26	1.15E-27	Gm20475	1.75	3.97E-08
Gm11250	-1.25	0.000000003	Platr22	1.78	7.49E-31
Gm13441	-1.25	6.33E-11	Mdga2	1.86	4.58E-17
Ear2	-1.25	0.000000102	Msc	1.87	1.33E-13
Gm44129	-1.25	6.38E-09	Kcnk10	1.92	6.09E-53
Gm30606	-1.24	0.0000946	Lrtm1	1.92	1.25E-38
Mt1	-1.24	8.12E-20	Slitrk2	1.93	5.18E-19
E130008D07Rik	-1.24	0.000515	Gm21049	1.94	1.12E-09
Rp23-316f10.1	-1.24	0.00276	Lrrn3	1.97	5.39E-28
Tmem144	-1.24	2.82E-22	Aoc1	1.98	1.47E-08
Mageb18	-1.23	3.22E-15	Npr3	1.98	7.13E-26
Al513022.2	-1.23	1.21E-10	Ct025533.1	2.03	4.24E-08
Reep1	-1.23	1.13E-22	Sprr2b	2.04	4.38E-08
Trhr2	-1.23	0.00301	Cnr1	2.10	4.55E-35
Add2	-1.23	7.65E-16	Myh6	2.12	4.52E-11
Gm16318	-1.22	0.000000423	Clca1	2.23	4.7E-12
Got1l1	-1.22	0.000936	Chi3l1	2.24	7.9E-11
Gm44763	-1.22	0.0000004	Gm26771	2.51	7.86E-61
B4galt6	-1.21	1.2E-15	Sfrp2	2.58	1.17E-58
Gm27177	-1.21	0.00000239	Sprr2d	2.67	1.16E-13
Rps6ka2	-1.21	4.65E-17			

Appendix 14 List of differentially expressed genes identified in RNA-seq AKO vs WT granulosa cells identified through RNA-seq.

Genes that had |logFC| ≥ 1 and an adjusted p-value cut-off of 0.01 were selected as DEG. LogFC is displayed as KO vs WT.

Gene	LogFC	Adj p-value	Gene	LogFC	Adj p-value
Lyve1	-5.83	0	Sox5os4	-1.21	6.68E-26
Sprr2g	-5.46	1.87E-119	Gm45321	-1.20	0.000817
Cyp2j11/cyp2j8	-4.40	3.1e-118	Hsd17b13	-1.20	0.00000251
Zic2	-4.14	1.28e-59	Gm33962	-1.20	2.6E-10
Hand2	-3.77	7.86e-40	Loxl2	-1.20	5.62E-36
Cldn1	-3.76	8.62e-155	Sult1a1	-1.20	1.36E-16
Kcnv2	-3.70	6.09e-121	Sox5os5	-1.19	5.29E-09
1700040D17Rik	-3.70	1.52E-50	Mbnl1	-1.19	5.59E-70
Cited1	-3.62	2.26e-199	Gm12002	-1.19	1.91E-14
Myh13	-3.59	3.95e-159	Mt3	-1.19	1.11E-09
Pla2g2f	-3.55	2.55e-39	Cxcl3	-1.19	0.00134
Fabp4	-3.53	9.66e-102	Cwh43	-1.19	0.00152
Ppp1r36	-3.34	1.66e-45	Hgfac	-1.18	1.9E-14
L3mbtl4	-3.33	2.65e-139	Dtna	-1.18	1.37E-29
Gm45315	-3.30	1.54E-46	Vnn3	-1.18	2.33E-08
Kcne4	-3.24	2.19e-131	A730049h05rik	-1.18	1.96E-43
Itga4	-3.22	3.8e-196	Slc17a8	-1.18	3.92E-11
Sctr	-3.22	3.62e-61	Elovl7	-1.18	1.98E-14
Scg2	-3.00	8.14e-67	Gm3470	-1.17	0.000393
Ntn5	-2.95	2.82e-85	Dnah3	-1.17	0.00148
Jcad	-2.93	9.59e-257	S1pr3	-1.17	8.64E-26
Tmem37	-2.82	3.15e-97	Gm43916	-1.17	1.48E-15
Dusp2	-2.80	2.57e-30	Cfap65	-1.17	0.00203
Rp23-98c9.5	-2.79	2.12e-122	Gm13266	-1.17	0.00246
Hand2os1	-2.78	2.77E-28	Dmd	-1.17	1.35E-53
Mt2	-2.78	1.27E-123	Gm36548	-1.17	0.00139
Havcr2	-2.75	1.52e-80	Tcf23	-1.16	0.00000171
Sphk1	-2.74	2.03e-92	Gm37513	-1.16	0.000537
Rp23-357o17.1	-2.73	5.61e-19	Tmc3	-1.16	2.03E-17
Cdh13	-2.73	7.24e-79	Slc39a4	-1.16	0.000271
Gm3716	-2.70	6.62E-46	Fes	-1.16	1.2E-22
Ac096777.1	-2.64	1.15e-55	Them6	-1.16	7.53E-18
Clec2e/clec2h	-2.61	4.96e-22	Tle1	-1.16	1.25E-70
Slco2a1	-2.55	1.31e-162	Gm9847	-1.16	0.000451
Frmpd1	-2.53	1.72e-116	Smarca2	-1.16	4.62E-54
Trpa1	-2.52	9.79e-61	Luzp2	-1.16	2.37E-12

Hsd17b11	-2.51	4.54e-133	Gria1	-1.16	0.000052
Cerkl	-2.49	2.22e-70	Gm43557	-1.16	0.000664
Scn4a	-2.47	1.09e-17	Drc7	-1.16	0.00291
Krtdap	-2.46	9.96e-28	Gm17831	-1.15	0.000000153
Rp24-421p3.9	-2.46	2.82e-112	Sra1	-1.15	2.77E-25
Sh3gl3	-2.45	3.13e-64	Gm37488	-1.15	4.26E-15
Gm33024	-2.42	1.79E-27	Pifo	-1.15	0.00296
Gm12637	-2.41	8.4E-29	Lrat	-1.15	0.000357
A930030B08Rik	-2.40	2.95E-32	Hspb1	-1.14	1.06E-12
Fam210b	-2.36	5.26e-123	Spock1	-1.14	9.26E-09
Itgb6	-2.36	9.9e-44	Togaram2	-1.14	0.000212
N-R5s89	-2.36	4.56E-20	Gm34549	-1.14	0.00155
Gldc	-2.35	4.07e-143	Gm44442	-1.14	0.00000397
Sec1	-2.33	2.29E-48	Panct2	-1.14	0.00295
Abcc2	-2.31	6.72e-67	Rp23-247p3.2	-1.13	0.0000205
E230020D15Rik	-2.30	9.5E-92	Hla-dob	-1.13	0.00362
Cyp2j15-ps	-2.30	1.19E-14	Igdcc3	-1.13	2.88E-22
Ces1a	-2.30	3.42E-13	Bst1	-1.13	0.0000757
Gm43298	-2.28	6.24E-16	4930419G24Rik	-1.13	0.000000799
Clec2j	-2.27	2.85E-13	Rp1	-1.13	0.00227
Glp2r	-2.24	2.08e-122	Pkdcc	-1.13	6.2E-22
Gm4275	-2.23	6E-38	Tac3	-1.13	0.0000192
4930452G13Rik	-2.22	9.41E-16	Rp23-282m20.5	-1.13	0.00311
Frmpd1os	-2.22	2.66E-21	Slc12a3	-1.13	0.00121
Tbc1d8	-2.22	2.4e-99	Aldh3a1	-1.13	0.0000771
Gm45073	-2.21	1.06E-54	2310039L15Rik	-1.13	3.04E-11
2610035F20Rik	-2.21	5.5E-11	Sox5os3	-1.12	9.95E-22
Rp23-390f4.1	-2.21	2.37e-44	Gm30414	-1.12	0.00386
Gm30771	-2.20	4.61E-13	Ac131329.1	-1.12	0.00149
Gm12796	-2.19	5.4E-77	Fam83f	-1.12	1.34E-09
Gm13068	-2.15	1.89E-50	Gclc	-1.12	1.69E-55
Gm44988	-2.15	3.99E-10	Mageb18	-1.12	2.18E-19
Gstm3	-2.13	4.35E-11	Gm15762	-1.12	0.00224
Pla2r1	-2.12	1.93E-102	Hif3a	-1.12	3.36E-11
Fzd1	-2.10	1.81E-81	Mir6363	-1.12	9.39E-09
Gm27216	-2.10	2.95E-15	Gfi1	-1.12	0.000928
Gm18194	-2.10	2.16E-24	3100003L05Rik	-1.12	0.00412
Gm27884	-2.10	2.34E-10	Xlr3c	-1.11	0.000186
Gm36329	-2.09	2E-21	Gm26717	-1.11	0.000313
4930529N20Rik	-2.09	9.99E-12	4930522N08Rik	-1.11	0.000878
Gm12801	-2.08	8.42E-10	Mob3b	-1.11	4.4E-17
Efnb2	-2.07	1.31e-107	Elmod1	-1.11	0.00443

Bcl11b	-2.07	8.96e-51	Olfr1417	-1.11	0.000887
Arhgdib	-2.07	1.7e-30	Adrb1	-1.10	0.0000175
Tmprss11b	-2.06	1.16E-12	Pygl	-1.10	0.0000244
Helt	-2.05	6.32e-12	Vnn1	-1.10	7.35E-30
Gm45463	-2.05	2.12E-10	Rrm2	-1.10	1.09E-18
Gm15475	-2.05	4.6E-47	Clic6	-1.10	0.00207
Zbtb16	-2.04	1.15e-65	Clec2d	-1.10	2.07E-29
Gm15328	-2.04	9.6E-23	Gm12577	-1.09	0.00000788
Gm39168	-2.03	1.65E-10	Gm43621	-1.09	5.12E-14
Gstm5	-2.02	2.79e-189	Rpl27-ps2	-1.09	0.000104
Kcnh4	-2.01	1.14e-31	Speer4cos	-1.09	0.00559
Vwde	-2.01	3.72e-59	Mgat4c	-1.09	1.91E-14
1500012K07Rik	-2.00	3.34E-09	Rev3l	-1.09	1.8E-41
Gm44079	-2.00	1.4E-78	Pzp	-1.09	0.0000735
Gm37498	-2.00	8.06E-24	Armc4	-1.09	0.000325
Gas7	-1.99	4.93e-106	Rbp7	-1.09	0.00581
Rp23-357o17.2	-1.98	8.36e-09	Crispld2	-1.09	4.69E-36
Vldlr	-1.98	5.85e-103	Gm10997	-1.09	0.000000239
Pde6h	-1.98	4.04e-36	Ces1	-1.09	0.00025
Csgalnact1	-1.97	3.81e-90	C2cd4d	-1.08	0.000221
S100a6	-1.96	3.22e-42	Rny1	-1.08	0.000358
Gm40910	-1.95	1.92E-13	Marco	-1.08	0.00058
Gm13583	-1.94	6.74E-34	Pex5l	-1.08	1.4E-09
Hopxos	-1.94	2.7E-12	Gm37675	-1.08	0.0000518
Gm8834	-1.94	4.23E-18	Gm15573	-1.08	0.00198
5830468F06Rik	-1.94	1.52E-08	SLC28A3	-1.08	0.000014
Ca11	-1.94	1.77e-33	Gm20684	-1.08	0.00133
1700125H03Rik	-1.92	1.07E-12	Plet1	-1.08	0.00303
Pparg	-1.91	7.01e-61	Gm26203	-1.07	0.00104
Gstm2-ps1	-1.90	2.59E-39	Gm38505	-1.07	0.00617
Cd34	-1.90	1.6e-129	C030005k06rik	-1.07	0.000000173
Bean1	-1.90	1.39e-72	Jam3	-1.07	6.04E-30
Hopx	-1.89	5.44e-22	Cdkl1	-1.07	0.0000617
Lpar1	-1.89	1.94e-87	Timp2	-1.07	1.12E-45
Rp23-247p3.3	-1.88	1.97e-37	Atp2b2	-1.07	0.00000101
Gm20540	-1.88	4.2E-41	Cryab	-1.07	0.000000218
Stmn4	-1.87	1.71e-32	Gm37589	-1.06	3.8E-13
Ralgapa2	-1.87	4.46e-57	St14	-1.06	4.81E-08
Mir-434	-1.85	0.00000011	Edn2	-1.06	2.39E-10
Gm22595	-1.84	0.000000014	Plekhs1	-1.06	0.000593
Gm11494	-1.84	8.23E-23	Gm43000	-1.06	9.23E-08
Gm8200	-1.83	2.48E-09	Cbr2	-1.06	0.0000606

RP23-469K15.2	-1.83	1.12E-10	Naip1	-1.06	0.00731
Gm33677	-1.83	3.44E-22	Prkab2	-1.06	4.61E-42
A930019D19Rik	-1.83	9.27E-37	Sox17	-1.06	0.00234
Gm42463	-1.83	3.71E-13	Trpc5os	-1.05	3.35E-12
Gm43545	-1.82	5.14E-54	Ccdc180	-1.05	0.00522
Slc14a1	-1.82	3.73e-13	Smkr-ps	-1.05	4.21E-18
Gm14319	-1.82	1.56E-18	Mir3092	-1.05	0.000243
Ai463229	-1.81	1.11e-14	Strc	-1.05	0.00736
Gm16897	-1.81	2.31E-101	Kcnmb1	-1.05	0.0036
Tnfsf11	-1.81	9.71e-12	Barx2	-1.05	0.000861
Ldhd	-1.81	1.87e-46	Stmnd1	-1.04	0.00728
Gm17590	-1.79	1.12E-42	6030407O03Rik	-1.04	3.4E-14
1700011B04Rik	-1.79	7.77E-09	Gm29183	-1.04	1.33E-09
Tmem100	-1.79	2.34e-67	Gmnc	-1.04	0.00536
Rnf125	-1.79	6.6E-70	KLF5	-1.04	8.64E-13
Hkdc1	-1.78	1.99e-11	Gabra1	-1.04	2.12E-12
Gm44639	-1.77	3.26E-39	Cpn1	-1.04	0.00773
Gm8233	-1.77	0.000000345	Gm37548	-1.04	0.000357
Rubcnl	-1.76	7.11e-36	4930535l15rik	-1.04	0.00545
Gm11917	-1.76	0.00000027	Plin4	-1.04	8.16E-18
Gm14085	-1.75	2.88E-26	Sprr2f	-1.04	0.0000201
Cdh5	-1.75	5.91e-43	Smco3	-1.04	0.00115
Gm45074	-1.74	1.63E-22	Igkc	-1.04	0.00404
Gm38411	-1.72	1.66E-51	1700095J12Rik	-1.04	0.0000163
Npy	-1.72	5.43e-26	Cdh18	-1.03	2.32E-13
Gm10631	-1.72	6.01E-29	Acnat1/Acnat2	-1.03	0.00802
Slc25a33	-1.71	9.02e-79	Gm43539	-1.03	0.000015
Mocs1	-1.71	1.42E-78	Ripk4	-1.03	0.00083
Slc28a2	-1.71	9.63e-31	Gm30211	-1.03	0.0014
Gm18252	-1.71	1.39E-17	Fbxl5	-1.02	3.22E-50
Apoa1	-1.70	8.44e-58	Plet1os	-1.02	0.00594
Gm37832	-1.70	0.000000022	Capn8	-1.02	0.000743
Rras2	-1.70	5.61e-92	Dnai1	-1.02	0.00903
Kl	-1.70	4.92e-62	Gm37651	-1.02	0.00000898
Rp23-337k17.1	-1.69	5.98e-12	Gm24620	-1.02	0.00104
Rapgef5	-1.69	1.21e-65	Dpy19l2	-1.02	0.0029
Gm43401	-1.68	7.9E-43	Ldoc1	-1.02	0.00481
Cntnap3	-1.68	2.46e-11	Dnah12	-1.02	0.00000032
1200007C13Rik	-1.67	6.96E-13	Gm4032	-1.02	0.0000772
Gm39041	-1.67	4.29E-29	Gm17970	-1.02	0.00133
1700073E17Rik	-1.66	0.000000373	Cln5	-1.01	2.04E-35
Gm29536	-1.65	1.6E-41	Tcp10a	-1.01	0.00363

Hhip	-1.64	5.86e-72	Gm19689	-1.01	3.63E-08
Lmntd1	-1.64	1.08e-19	Gm12364	-1.01	0.00000616
Ac154639.1	-1.63	2.53e-18	Gm21814	-1.01	6.55E-16
Stard5	-1.63	7.94e-81	4833423e24rik	-1.01	0.00535
Cys1	-1.63	4.5e-21	Myt1l	-1.01	0.000515
Gm10706	-1.62	2.14E-10	Capsl	-1.01	0.00865
E130008D07Rik	-1.61	7.52E-10	Zcchc24	-1.00	5.43E-28
Xrra1	-1.61	6.33e-31	Fat4	-1.00	2.17E-26
Gm29682	-1.61	1.01E-24	Sdk1	-1.00	2.28E-10
Gm15997	-1.60	0.00000198	Acox2	-1.00	0.00877
Ak3l2-ps	-1.60	1.39E-26	Gm40578	1.00	2.13E-08
Prrt1	-1.60	1.22E-25	Vmn2r88	1.00	0.00445
Arl4d	-1.60	1.17e-32	Gm12860	1.00	0.000123
Plppr5	-1.59	6.06e-18	Efhd1os	1.01	4.07E-14
Gm38378	-1.59	0.000000529	Rbm47	1.01	1.2E-25
Fabp1	-1.59	0.00000809	Cdh10	1.01	2.21E-13
Ac147241.1	-1.58	0.00000153	Slit2	1.01	1.29E-28
Gm45266	-1.57	3.3E-14	Gm12349	1.01	0.00131
Gm37265	-1.57	0.000000691	4933416M06Rik	1.02	1.96E-11
AC087802.4	-1.57	0.00000748	Gm8773	1.02	0.00438
Cd33	-1.57	0.00000036	Gm28721	1.02	0.00545
Gm16318	-1.57	1.76E-15	Epha3	1.02	2.61E-12
Piwil4	-1.57	3.15e-15	Nme8	1.02	0.000029
Rasef	-1.56	3.03e-28	Cish	1.03	5.67E-12
Gm45267	-1.56	5.48E-30	Tspan15	1.03	0.0000321
Add2	-1.56	1.61e-27	Gm26725	1.04	4.37E-14
Entpd1	-1.56	8.85e-68	Gm16048	1.04	7.35E-11
Ampd3	-1.55	5.86e-64	1700126h18rik	1.04	0.0000241
Gm31510	-1.55	0.00000535	Sytl3	1.05	4.74E-13
Ankrd55	-1.54	3.24e-28	Gm43948	1.05	1.17E-12
Glns-ps1	-1.54	1.13E-19	Gm29530	1.05	0.00000553
Gm9748	-1.54	9.18E-15	Plau	1.05	3.49E-17
Gm18911	-1.54	1.28E-10	Hck	1.05	9.91E-08
Gcnt1	-1.53	1.16e-16	Gm29480	1.05	0.000000719
Kbtbd11	-1.53	1.95e-68	Vegfc	1.06	3.2E-13
Ct572985.1	-1.52	1.96e-14	Gm37679	1.06	1.21E-10
Tnfrsf21	-1.52	3.46e-53	4930557b06rik	1.06	0.00756
Fam107a	-1.52	0.000000251	Tac1	1.06	4.28E-11
Bb123696	-1.51	0.000000496	Gm17040	1.06	7.33E-09
Tmem255a	-1.51	1.55e-63	Ptpro	1.07	3.35E-17
4931431B13Rik	-1.51	0.0000335	9530086O07Rik	1.07	0.000000227
Tnn	-1.51	5.89e-08	Gm26911	1.07	9.38E-12

Gm45615	-1.50	4.14E-15	Nsun7	1.07	5.08E-27
Cblif	-1.49	1.26E-08	Loc102633156	1.07	0.00268
4933416M07Rik	-1.49	1.32E-30	Or10v1	1.07	0.00149
Rmst	-1.49	5.63E-19	Kctd19	1.07	0.000603
Rcvrn	-1.49	2.13E-10	Lgi3	1.08	1.28E-31
Gm24224	-1.48	8.02E-10	Tmprss11e	1.08	0.00187
Ac132133.2	-1.48	1.74E-13	Gm13780	1.08	1.87E-11
Ac159006.2	-1.48	0.0000168	Gm17322	1.08	2.3E-11
Gm28651	-1.47	0.00000126	Npr1	1.08	1.32E-13
Serpina11	-1.47	0.0000524	Kcnk10	1.08	4.69E-11
Ccdc63	-1.47	1.18E-17	Arhgap15os	1.09	0.000888
Tmod1	-1.47	1.04E-62	Slc27a6	1.09	3.75E-24
Gm11802	-1.46	4.39E-40	Ccl21	1.09	0.00566
Gm42476	-1.46	0.0000605	Ac120150.1	1.09	0.00174
Aqp11	-1.46	1.79E-27	Kcnk3	1.10	0.0000852
Mapre2	-1.45	1.04E-84	Egr4	1.10	0.0000038
Gm37526	-1.45	0.00000206	Wnt10b	1.10	0.000415
Pdlim1	-1.45	6.15E-103	Ct010447.1	1.10	0.0000175
Mt1	-1.45	2.9E-29	Pdzrn3	1.10	2.03E-13
B020031H02Rik	-1.44	0.0000151	Hk2	1.10	1.47E-24
Plac8l1	-1.44	2.96E-09	Gamt	1.11	5.67E-36
Mir5619	-1.44	0.0000882	RP23-433C10.1	1.11	0.000236
Rbbp7	-1.43	2.28E-65	Gm37941	1.11	0.00349
Gm20616	-1.43	1.52E-08	AC134577.1	1.12	9.86E-19
Gm36070	-1.43	0.000000469	Tmem178a	1.12	1.74E-14
Atp4a	-1.42	1.43E-25	Gm20475	1.12	0.000197
Ankrd45	-1.42	0.0000403	Kcnq4	1.13	1.02E-14
Micos10	-1.42	1.18E-39	Gm17041	1.13	1.55E-14
Teddm2	-1.41	3.19E-42	Gm43057	1.13	0.000331
Gm6382	-1.41	2.5E-26	Gm7775	1.13	0.00182
Mir8114	-1.41	3.5E-45	Nr0b2	1.15	6.84E-09
Defb119	-1.40	3.84E-27	4930584F24Rik	1.15	0.000102
Scara5	-1.40	7.73E-36	Gm15917	1.15	1.48E-19
Kiaa1217	-1.39	4.51E-51	Vsig8	1.16	8.31E-11
Prkg2	-1.39	7.42E-33	Ackr1	1.17	0.00000252
Trpc4	-1.39	4.03E-19	Rrad	1.17	2.75E-17
Ac113178.1	-1.39	1.49E-43	Lsamp	1.17	8.07E-43
Abhd2	-1.38	2.58E-68	Shank1	1.17	1.4E-17
Six4	-1.38	9.2E-09	Gm15584	1.18	1.08E-11
Ifnk	-1.38	0.000000622	Gm45589	1.19	0.000983
F730035M05Rik	-1.37	0.00000265	Ppp1r3c	1.19	0.000000038
Prr29	-1.37	0.00000353	Gm12213	1.19	0.000763

Gm11384	-1.37	5.87E-19	Gm44226	1.20	0.0000456
Actn3	-1.37	1.7E-25	Gm15426	1.20	0.000143
Gm42435	-1.36	0.000000142	Gm43776	1.20	0.00105
Serpina1	-1.36	0.000198	Gm32219	1.21	1.42E-09
Stc2	-1.36	6.99e-22	Gm28053	1.22	1.13E-13
C1orf87	-1.36	0.000263	Gm12214	1.22	0.000194
Gm12505	-1.36	0.00000948	Gm6276	1.23	0.000000967
Cgn	-1.35	2.25e-33	Slc22a17	1.23	7.54E-16
Gm6101	-1.35	0.000273	C11orf86	1.24	0.000582
Igsf5	-1.35	0.00000354	Bc055402	1.24	0.00116
Trim9	-1.35	0.0000757	Gfod1	1.25	3.47E-31
Nrxn3	-1.35	5.09E-14	Sema3d	1.25	2.39E-22
Aloxe3	-1.34	1.28e-10	Tle2	1.25	1.29E-20
Gm25788	-1.34	0.000128	Gm37644	1.26	0.000429
Gm19303	-1.34	0.000169	Gm43947	1.26	1.55E-11
Gm42555	-1.34	0.0000246	Rgs6	1.26	4.3E-15
Nipal1	-1.34	2.76e-45	Gm12526	1.26	2.56E-11
Ryr2	-1.34	1.69e-49	Gm16559	1.26	7.39E-39
Defb45	-1.34	0.000242	Sh3gl2	1.27	4.41E-22
Entpd7	-1.33	3.94e-65	Kcnk15	1.28	6.52E-09
Gm37844	-1.33	3.43E-13	Myh6	1.28	0.0000009
Pcdh8	-1.33	1.31e-24	Gm8439	1.29	1.28E-18
Gm15841	-1.33	0.000385	Gm36569	1.30	1.65E-37
Egfros	-1.32	2.31E-25	Csf2rb	1.30	6.21E-13
Lpar3	-1.32	0.0000013	Map6d1	1.31	3.66E-29
Gm45199	-1.32	0.000382	Adh1c	1.31	7.85E-47
Gm44851	-1.32	9.85E-15	4833403J16Rik	1.32	0.0000262
Gm11250	-1.32	2.01E-26	Plekhg4	1.32	1.2E-14
Gm9959	-1.32	3.62E-19	Gm9947	1.32	4.95E-09
Gm21123	-1.31	0.0000224	Atp1a3	1.32	0.000000351
Zbbx	-1.31	0.000266	Gm9899	1.33	2.37E-10
Slc15a1	-1.31	0.0000378	Lingo1	1.34	6.91E-16
C630043F03Rik	-1.31	1.29E-19	Gm7019	1.34	0.0000098
Gm36447	-1.30	2.19E-09	Brinp2	1.34	5.97E-17
Gm37342	-1.30	4.13E-23	Wnt4	1.35	4.83E-33
Arhgap31	-1.30	2.84e-78	Ly6g6c	1.35	0.0000826
Cxcl6	-1.30	1.63e-08	Avil	1.36	2.49E-20
Myl2	-1.30	0.000000304	Astn1	1.36	8.98E-23
Unc5cl	-1.29	0.000000802	Gm20471	1.36	0.00000088
Parm1	-1.29	6.61e-65	Spock3	1.36	1.03E-46
Gm10728	-1.29	7.84E-10	4833415N18Rik	1.37	0.000137
Slc7a11	-1.29	1.56e-57	Mdga2	1.37	1.45E-29

Stxbp6	-1.29	2.83e-31	Nrg3	1.40	4.6E-25
Hoxd11	-1.29	2.29e-18	Ac155634.2	1.40	0.0000112
4930523O13Rik	-1.29	0.000561	Tbata	1.41	5.66E-14
4921523L03Rik	-1.28	0.000475	Egln3	1.41	8.51E-31
Gm20089	-1.28	4.13E-23	Gabrb3	1.41	8.14E-24
Hnf4a	-1.27	1.3e-11	Rem1	1.41	2.23E-25
Gm15901	-1.27	1.78E-11	Ca12	1.43	2.77E-49
3110080O07Rik	-1.27	1.49E-29	Gm44708	1.43	0.0000174
Cep295nl	-1.27	3.17e-25	Lipg	1.44	2.44E-24
Rhoj	-1.27	1.99e-36	Slc29a4	1.45	3.63E-19
1700019C18Rik	-1.27	0.000398	Brinp3	1.46	1.42E-39
Gm17651	-1.27	3.01E-26	Rpp25	1.47	7.11E-36
Gm5864	-1.27	0.000000679	Gm36757	1.48	1.17E-12
A530021J07Rik	-1.26	0.00000255	Dtx1	1.49	5E-24
Pax3	-1.26	0.0000218	Cntnap5b	1.49	2.85E-83
C10orf53	-1.26	0.000679	Snap91	1.50	2.44E-23
Ttll2	-1.26	0.000205	Gm21655	1.54	2.02E-27
Gm15684	-1.26	3.29E-38	Gm37877	1.54	0.000000195
Gm37229	-1.26	5.42E-41	Gm6089	1.54	8.38E-31
Gm28793	-1.26	0.000159	Cnr1	1.54	3.92E-23
Lamc2	-1.26	1.45e-26	Ccrl2	1.55	4.81E-22
Maml3	-1.25	1.36e-36	Msc	1.55	6.57E-11
Ear2	-1.25	0.000282	Megf10	1.56	1.77E-18
Gm15482	-1.25	0.000000131	Cmtm5	1.58	0.000000242
Apol6	-1.25	3.23E-20	Gm18645	1.59	4.27E-14
Klf15	-1.24	6.93E-28	Gm16057	1.63	2.34E-08
Cd5l	-1.24	0.000532	Gm9962	1.64	8.54E-13
Creg2	-1.24	2.02E-13	Tll2	1.65	4.82E-22
Gm18955	-1.24	0.0011	Nrg3os	1.66	1.07E-41
Pfkfb3	-1.24	9.8E-39	Kcnb1	1.68	1.84E-34
Cdh19	-1.24	4.97E-25	Dpp6	1.70	2.26E-33
Ccdc116	-1.24	3.79E-10	Gm20642	1.70	3.3E-20
Slco4c1	-1.24	0.0000238	Platr22	1.70	1.49E-30
Alox12e	-1.24	0.000748	4930546K05Rik	1.73	6.98E-25
Gm23442	-1.24	9.48E-13	Prrx1	1.74	3.03E-27
A830012C17Rik	-1.24	5.4E-20	Il5	1.74	1.81E-21
Mchr1	-1.23	0.000719	Gm18957	1.74	3.43E-13
Gm16638	-1.23	7.07E-24	Or8d1	1.75	0.000000027
Frmpd2	-1.23	0.000483	Gm7557	1.78	7.97E-12
Fam47e	-1.23	0.000402	Lrtm1	1.80	1.14E-16
Add3	-1.23	3.89E-66	Speer4a	1.81	3.13E-13
Crocc2	-1.23	0.0000352	Cited4	1.85	9.14E-48

Scrn1	-1.23	3.78e-39	Rprm	1.85	3.05E-21
Gm2448	-1.23	0.000121	Ptgfr	1.86	2.45E-74
Gm18997	-1.23	0.00134	Gm43618	1.87	2.17E-49
Sorbs2os	-1.22	1.9E-76	Npr3	1.91	1.4E-37
Gm38055	-1.22	8.83E-17	Sfrp2	1.93	5.27E-13
Ppp2r2c	-1.22	0.00000139	C4orf17	2.00	1.35E-39
Klk3	-1.22	0.0012	Olfml2b	2.05	4.41E-60
Gm43344	-1.22	5.88E-11	Gm15749	2.14	5.01E-17
Ccdc151	-1.22	0.00093	Ctxn3	2.20	1.31E-40
Gm9195	-1.22	0.00065	Gm26771	2.22	3.27E-30
Cyp2j14-ps	-1.22	0.00138	Gm16485	2.65	1.15E-53
Itgb2l	-1.21	0.000715	Cyp26b1	2.86	1.31E-88
Bambi-ps1	-1.21	9.77E-10	Pgr	2.90	2.51E-126

.

Appendix 15 List of differentially expressed genes identified in RNA-seq BKO vs WT granulosa cells identified through RNA-seq.

Genes that had |logFC| ≥ 1 and an adjusted p-value cut-off of 0.01 were selected as DEG. LogFC is displayed as KO vs WT.

Gene	LogFC	Adj p-value	Gene	LogFC	Adj p-value
Kcnv2	-1.49	1.21e-21	Ndst3	1.08	9.03E-05
Cyp2j11/cyp2j8	-1.20	2.15e-13	Ac155634.2	1.08	8.62E-05
Gm25395	-1.10	0.000018	Elfn1	1.08	3.67E-08
Hand2	-1.03	8.89e-05	Gm29865	1.08	5.43E-05
Gm34609	1.00	0.000206	Tmem200a	1.09	5.5E-06
Cd86	1.00	0.000063	Dgki	1.09	6.47E-06
St8sia6	1.00	8.12e-05	Gm2164	1.09	7.91E-05
4930432E11Rik	1.00	0.000269	Dlx6os1	1.09	5.28E-05
Tspear	1.00	0.000322	Gm38256	1.09	7.75E-05
C6	1.00	0.000172	Gm43154	1.09	4.36E-05
Gm11884	1.00	0.000218	Gm11823	1.09	3.52E-05
Prokr2	1.01	0.000016	Otog	1.10	0.00004
1700030F04Rik	1.01	0.000312	Gm26815	1.10	6.88E-05
Rfx4	1.01	0.000095	Kcnq2	1.10	2.57E-05
A530053G22Rik	1.01	0.000214	Gm46329	1.10	5.95E-05
Slc22a16	1.01	0.000149	Gm43122	1.11	5.43E-05
Slc4a10	1.01	0.000303	Ac103362.1	1.11	5.62E-05
Aoah	1.01	0.000249	Arpp21	1.11	5.28E-05
Catspere	1.01	0.000279	C12orf42	1.12	4.13E-05
Gm32884	1.01	0.000253	Crhr2	1.12	4.45E-05
4932414N04Rik	1.01	0.000292	Ovol2	1.12	2.63E-05
Dux	1.01	9.21E-05	Gm26713	1.12	4.36E-05
Siglech	1.01	9.71E-05	4930474H20Rik	1.12	0.00004
Gm20642	1.01	3.51E-10	Gm37971	1.12	1.26E-05
Gm46392	1.01	0.000275	Gm29506	1.13	3.29E-05
Gm7019	1.01	0.00013	Cacng2	1.13	0.000026
Olfm3	1.01	0.000197	Uox	1.13	3.12E-05
Soga3	1.02	0.000205	Ct010475.1	1.14	2.97E-05
Gm35998	1.02	0.000214	Nrg3os	1.15	9.05E-17
Arhgef38	1.02	0.000241	Skint2	1.15	2.33E-05
Serpinb3b/serpinb3c	1.02	0.000249	Adra1a	1.16	2.07E-05
Brinp1	1.02	0.000239	Trpm1	1.16	1.71E-05
Gm45321	1.02	0.00021	Adamts20	1.16	1.28E-05
Enthd1	1.03	0.000171	4930435c17rik	1.17	1.23E-05
Ac163285.1	1.03	0.000232	Fat2	1.17	0.000013
Cnga3	1.03	9.72e-05	Htr2c	1.17	0.000015
Gm281	1.03	0.00022	AC156023.3	1.18	1.51E-05

Lyzl4	1.03	0.000166	Jakmip2	1.18	6.4E-06
Gm19585	1.03	0.000205	Gm21847	1.19	2.67E-11
Gm44613	1.03	0.000208	Wdr64	1.19	0.000012
Ac147639.2	1.03	0.000167	Cd28	1.19	1.46E-06
Cdhr3	1.03	0.000166	Scn9a	1.19	9.57E-06
Gm19303	1.04	0.000161	4921533I20Rik	1.20	4.39E-06
Ac121912.1	1.04	0.000129	Dcdc5	1.20	7.12E-07
Tacr1	1.04	0.000195	Fam135b	1.20	7.38E-06
Vmn2r-ps11	1.04	0.000184	Nol4	1.21	5.99E-06
Dnah6	1.04	6.49e-05	Vmn2r-ps110	1.21	8.35E-06
Gm28694	1.04	7.04E-05	Gm14280	1.21	5.79E-06
Wdr49	1.04	0.000126	Vwa3b	1.22	5.49E-06
Abca15	1.04	0.000136	Gm31698	1.23	4.35E-06
Gm34184	1.05	5.95E-05	Gm13481	1.23	1.36E-09
2310002F09Rik	1.05	0.000161	Gm37093	1.24	3.52E-06
Trpm8	1.05	7.89e-05	Skint5/skint6	1.24	3.68E-06
Srrm3	1.05	0.000133	Gm15083	1.24	3.65E-06
Gm30835	1.05	0.00015	Gm10649	1.24	3.52E-06
Gm16271	1.05	0.000136	Cdh26	1.24	3.01E-06
Trat1	1.05	0.000155	Macc1	1.25	1.51E-06
Ptchd1	1.05	0.000147	Dnai1	1.26	1.17E-06
Cyp2b6	1.05	0.000112	Scn1a	1.28	1.12E-06
Tmem196	1.05	0.000136	Gm11033	1.28	1.56E-06
Gad1	1.05	0.000131	Gm13974	1.29	1.17E-06
Ttll6	1.06	0.000125	Dnah3	1.30	1.58E-08
Ac060761.1	1.06	0.000134	Wdr63	1.30	1.73E-07
Gm13598	1.06	6.11E-05	A330069K06Rik	1.30	9.29E-07
Gm5570	1.06	8.65E-05	Agmo	1.32	6.18E-07
Vdr	1.06	1.89e-11	Zbbx	1.32	6.93E-07
Rgs8	1.06	0.000122	4930474g06rik	1.32	5.35E-07
Gm20752	1.07	0.000109	RP1	1.33	6.38E-08
Cngb3	1.07	0.000105	Rp1l1	1.38	1.61E-07
Mlip	1.08	0.000101	3100003l05rik	1.41	4.37E-08
Helt	1.08	2.63e-05	Ac134577.1	1.49	5.7E-17

Appendix 16 List of PGRKO and AKO DEGs with PGR and/or RUNX1 binding.

Gene	AKO logFC	PGRKO logFC	in PGR ChIP?	in RUNX1 ChIP?	Gene	AKO logFC	PGRKO logFC	in PGR ChIP?	in RUNX1 ChIP?
Lyve1	-5.83	-4.81	+	-	Plac8l1	-1.44	-1.03	-	-
Sprr2g	-5.46	-2.45	-	-	Rbbp7	-1.43	-1.28	+	+
Cyp2j11/cyp2j8	-4.40	-3.46	-	-	Gm20616	-1.43	-1.27	-	-
Zic2	-4.14	-2.74	-	+	Atp4a	-1.42	-1.93	-	-
Cldn1	-3.76	-4.05	+	-	Micos10	-1.42	-1.77	-	-
Kcnv2	-3.70	-2.96	+	+	Teddm2	-1.41	-2.09	-	-
1700040D17Rik	-3.70	-2.24	-	-	Gm6382	-1.41	-1.17	-	-
Cited1	-3.62	-2.44	+	-	Mir8114	-1.41	-2.13	-	-
Pla2g2f	-3.55	-1.08	+	-	Defb119	-1.40	-1.56	-	-
Fabp4	-3.53	-1.63	+	-	Scara5	-1.40	-3.26	+	+
Ppp1r36	-3.34	-2.63	-	-	Kiaa1217	-1.39	-2.07	-	-
L3mbtl4	-3.33	-3.37	+	+	Prkg2	-1.39	-1.62	+	+
Kcne4	-3.24	-2.13	+	+	Trpc4	-1.39	-1.45	+	-
Sctr	-3.22	-2.81	+	-	Ac113178.1	-1.39	-1.43	-	-
Scg2	-3.00	-2.67	-	-	Ifnk	-1.38	-1.14	+	-
Ntn5	-2.95	-2.43	+	+	Gm11384	-1.37	-1.33	-	-
Jcad	-2.93	-2.27	-	+	Actn3	-1.37	-1.99	+	+
Tmem37	-2.82	-2.38	+	+	Gm42435	-1.36	-1.53	-	-
Rp23-98c9.5	-2.79	-1.96	-	-	Trim9	-1.35	-1.17	+	+
Mt2	-2.78	-1.95	+	+	Aloxe3	-1.34	-1.91	-	+
Havcr2	-2.75	-2.73	+	-	Gm42555	-1.34	-1.63	-	-
Sphk1	-2.74	-2.64	+	+	Nipal1	-1.34	-1.35	-	+
Rp23-357o17.1	-2.73	-1.99	-	-	Defb45	-1.34	-1.10	-	+
Cdh13	-2.73	-1.81	+	-	Entpd7	-1.33	-1.15	+	+
Gm3716	-2.70	-2.11	-	-	Gm37844	-1.33	-1.63	-	-

Ac096777.1	-2.64	-2.69	-	-	Pcdh8	-1.33	-1.57	-	+
Slco2a1	-2.55	-1.40	-	+	Egfros	-1.32	-1.70	-	-
Frmpd1	-2.53	-2.26	+	-	Gm11250	-1.32	-1.25	-	-
Trpa1	-2.52	-1.69	+	-	C630043F03Rik	-1.31	-1.00	-	-
Hsd17b11	-2.51	-3.31	+	+	Gm37342	-1.30	-1.90	-	-
Rp24-421p3.9	-2.46	-1.28	-	-	Arhgap31	-1.30	-1.30	-	+
Sh3gl3	-2.45	-1.69	+	-	Myl2	-1.30	-2.13	-	-
Gm33024	-2.42	-2.05	-	-	Unc5cl	-1.29	1.04	-	-
Gm12637	-2.41	-3.19	-	-	Gm10728	-1.29	-1.88	-	-
A930030B08Rik	-2.40	-1.63	-	-	SLC7A11	-1.29	-2.03	+	+
Itgb6	-2.36	-2.54	+	+	Gm20089	-1.28	-1.69	-	-
N-R5s89	-2.36	-1.08	-	-	Hnf4a	-1.27	-1.62	+	+
Gldc	-2.35	-1.75	-	-	Cep295nl	-1.27	-1.08	-	-
Sec1	-2.33	-1.61	-	-	Gm15684	-1.26	-1.56	-	-
Abcc2	-2.31	-2.10	+	-	Gm37229	-1.26	-1.74	-	-
E230020D15Rik	-2.30	-1.57	-	-	Maml3	-1.25	-1.75	+	+
Cyp2j15-ps	-2.30	-1.63	-	-	Ear2	-1.25	-1.25	-	-
Ces1a	-2.30	-1.59	+	-	Apol6	-1.25	-1.85	+	+
Gm43298	-2.28	-1.29	-	-	Klf15	-1.24	-2.10	+	+
Glp2r	-2.24	-3.17	-	-	Creg2	-1.24	-2.72	+	+
Gm4275	-2.23	-1.58	-	-	Cdh19	-1.24	-2.33	+	-
4930452G13Rik	-2.22	-1.57	-	-	Gm16638	-1.23	-1.94	-	-
Frmpd1os	-2.22	-2.43	-	-	Add3	-1.23	-1.03	+	+
Tbc1d8	-2.22	-2.70	+	+	Scrn1	-1.23	-1.44	+	+
Gm45073	-2.21	-1.73	-	-	Sorbs2os	-1.22	-1.29	-	-
Rp23-390f4.1	-2.21	-2.14	-	-	Hsd17b13	-1.20	-1.63	-	-
Gm12796	-2.19	-1.71	-	-	Mbnl1	-1.19	-1.20	+	+
Gm13068	-2.15	-1.75	-	-	Mt3	-1.19	-1.12	-	-
Fzd1	-2.10	-2.23	+	+	Hgfac	-1.18	-1.42	-	-

Gm27884	-2.10	-1.49	-	-	Dtna	-1.18	-1.45	+	-
4930529N20Rik	-2.09	-1.90	-	-	Vnn3	-1.18	-2.46	-	-
Gm12801	-2.08	-1.38	-	-	Gm3470	-1.17	-1.37	-	-
Efnb2	-2.07	-1.76	+	+	Dmd	-1.17	-1.36	+	+
Bcl11b	-2.07	-1.51	+	+	Tcf23	-1.16	-1.14	-	-
Helt	-2.05	-2.33	+	-	Tmc3	-1.16	-1.70	-	-
Gm45463	-2.05	-1.34	-	-	Them6	-1.16	-1.33	+	-
Gm15475	-2.05	-1.63	-	-	Tle1	-1.16	-1.07	+	+
Gm15328	-2.04	-1.57	+	-	Sra1	-1.15	-1.15	-	-
Gm39168	-2.03	-1.28	-	-	Gm34549	-1.14	-3.90	-	-
Gstm5	-2.02	-1.42	-	-	Hla-dob	-1.13	1.24	-	-
Kcnh4	-2.01	-1.88	-	+	Tac3	-1.13	-1.57	-	-
Gm44079	-2.00	-2.01	-	-	Rp23-282m20.5	-1.13	-2.07	-	-
Gm37498	-2.00	-2.39	-	-	Aldh3a1	-1.13	-1.55	+	-
Gas7	-1.99	-2.71	+	+	Gclc	-1.12	-1.19	+	+
Rp23-357o17.2	-1.98	-1.19	-	-	Mageb18	-1.12	-1.23	-	-
Vldlr	-1.98	-1.31	+	+	Xlr3c	-1.11	-1.05	-	-
Pde6h	-1.98	-1.85	+	+	4930522N08Rik	-1.11	-1.10	-	-
Gm40910	-1.95	-1.68	-	-	Mob3b	-1.11	-1.00	-	-
Gm13583	-1.94	-2.14	-	-	Vnn1	-1.10	-1.32	-	-
Hopxos	-1.94	-2.62	-	-	Gm43621	-1.09	-1.61	-	-
Ca11	-1.94	-1.38	-	-	Crispld2	-1.09	-1.52	+	+
Pparg	-1.91	-1.88	+	+	C2cd4d	-1.08	-1.11	-	+
Gstm2-ps1	-1.90	-1.36	-	-	Gm37675	-1.08	-1.45	-	-
Cd34	-1.90	-2.10	+	+	Jam3	-1.07	-1.36	+	+
Bean1	-1.90	-1.65	+	+	Cryab	-1.07	-1.09	-	-
Hopx	-1.89	-2.47	+	+	Edn2	-1.06	-1.32	+	+
Lpar1	-1.89	-1.39	-	-	6030407O03Rik	-1.04	-1.52	-	-
Rp23-247p3.3	-1.88	-1.93	-	-	Gm29183	-1.04	-1.58	-	-

Gm20540	-1.88	-1.81	-	-	Gmnc	-1.04	1.13	-	-
Stmn4	-1.87	-1.15	-	+	Sprr2f	-1.04	1.58	-	-
Ralgapa2	-1.87	-2.33	+	+	Cdh18	-1.03	-1.30	+	-
Gm11494	-1.84	-1.60	+	+	Cln5	-1.01	-1.19	-	-
Gm8200	-1.83	-2.22	-	-	Zcchc24	-1.00	-1.74	+	+
Rp23-469k15.2	-1.83	-1.17	-	-	Slit2	1.01	1.44	-	+
Gm33677	-1.83	-3.12	-	-	4933416M06Rik	1.02	1.58	-	-
A930019D19Rik	-1.83	-2.44	-	-	Gm26725	1.04	1.04	-	-
Gm42463	-1.83	-2.04	-	-	Vegfc	1.06	1.03	-	+
Gm43545	-1.82	-2.17	-	-	Tac1	1.06	1.46	-	+
Gm14319	-1.82	-1.55	-	-	9530086O07Rik	1.07	1.10	-	-
Ai463229	-1.81	-1.98	-	-	Gm26911	1.07	1.04	-	-
Gm16897	-1.81	-2.00	+	-	Nsun7	1.07	1.44	-	+
Tnfsf11	-1.81	-1.85	-	-	Kcnk10	1.08	1.92	-	-
Ldhd	-1.81	-1.77	+	+	Gm37941	1.11	1.25	-	-
Gm17590	-1.79	-2.00	-	-	Gm20475	1.12	1.75	-	-
1700011B04Rik	-1.79	-1.14	-	-	Gm7775	1.13	1.30	-	-
Rnf125	-1.79	-1.49	+	+	Lsamp	1.17	1.37	-	-
Hkdc1	-1.78	-1.60	-	-	Gm15426	1.20	1.03	-	-
Gm44639	-1.77	-1.87	-	-	Slc22a17	1.23	1.13	-	-
Rubcnl	-1.76	-1.80	+	+	Gm43947	1.26	1.03	-	-
Gm45074	-1.74	-1.48	-	-	Gm12526	1.26	1.11	-	-
Gm38411	-1.72	-2.54	-	-	Gm16559	1.26	1.08	-	-
Gm10631	-1.72	-1.46	-	-	Myh6	1.28	2.12	-	-
Mocs1	-1.71	-1.77	+	-	Csf2rb	1.30	1.10	-	-
Apoa1	-1.70	-1.01	-	+	Adh1c	1.31	1.10	-	-
Gm37832	-1.70	-1.71	-	-	Gm9947	1.32	1.68	-	-
Kl	-1.70	-1.98	+	+	Lingo1	1.34	1.64	-	-
Rp23-337k17.1	-1.69	-1.19	-	-	Gm7019	1.34	1.09	-	-

Gm43401	-1.68	-2.13	-	-	Avil	1.36	1.42	+	+
Gm39041	-1.67	-1.77	-	-	Astn1	1.36	1.04	-	-
Gm29536	-1.65	-1.27	-	-	Spock3	1.36	1.56	-	-
Ac154639.1	-1.63	-2.13	-	-	Mdga2	1.37	1.86	+	-
Stard5	-1.63	-1.65	+	-	Nrg3	1.40	1.39	-	-
Gm10706	-1.62	-1.17	-	-	Ac155634.2	1.40	1.63	-	-
E130008D07Rik	-1.61	-1.24	-	-	Egln3	1.41	1.71	+	+
Xrra1	-1.61	-1.15	-	+	Brinp3	1.46	1.43	-	-
Ac147241.1	-1.58	-1.48	-	-	Rpp25	1.47	1.05	+	+
Gm45266	-1.57	-1.33	-	-	Dtx1	1.49	1.17	-	+
Gm37265	-1.57	-2.08	-	-	Gm21655	1.54	1.24	-	-
Gm16318	-1.57	-1.22	-	-	Gm37877	1.54	1.70	-	-
Rasef	-1.56	-1.38	-	-	Gm6089	1.54	1.13	-	-
Gm45267	-1.56	-1.51	-	-	Cnr1	1.54	2.10	-	+
Add2	-1.56	-1.23	+	-	Msc	1.55	1.87	-	+
Entpd1	-1.56	-2.20	+	+	Cmtm5	1.58	1.66	-	-
Ampd3	-1.55	-1.11	+	-	Gm18645	1.59	1.20	-	-
Gm31510	-1.55	-1.67	-	-	Gm16057	1.63	1.04	-	-
Ankrd55	-1.54	-1.91	+	+	Nrg3os	1.66	1.40	-	-
Glns-ps1	-1.54	-1.38	-	-	Kcnb1	1.68	1.38	-	+
Gm9748	-1.54	-1.62	-	-	Dpp6	1.70	1.11	-	+
Kbtbd11	-1.53	-1.68	+	+	Gm20642	1.70	1.64	-	-
Ct572985.1	-1.52	-1.00	-	-	Platr22	1.70	1.78	-	-
Gm45615	-1.50	-1.30	-	-	Or8d1	1.75	1.16	-	-
4933416M07Rik	-1.49	-1.53	-	-	Lrtm1	1.80	1.92	+	+
Rcvrn	-1.49	-2.54	-	-	Speer4a	1.81	1.13	-	-
Gm24224	-1.48	-1.77	-	-	Npr3	1.91	1.98	-	-
Ac159006.2	-1.48	-1.15	-	-	Sfrp2	1.93	2.58	+	+
Ccdc63	-1.47	-2.15	+	+	C4orf17	2.00	1.49	-	-

Gm11802	-1.46	-2.19	-	-	Gm15749	2.14	1.64	-	-
Mapre2	-1.45	-1.71	+	+	Gm26771	2.22	2.51	-	-
Pdlim1	-1.45	-1.57	+	+	Cyp26b1	2.86	1.36	-	+
Mt1	-1.45	-1.24	+	+					

Appendix